Coastal cliff evolution with reference to Staithes, North Yorkshire

Lim, Michael

Coastal cliff evolution with reference to Staithes, North Yorkshire

Michael Lim

Department of Geography

Durham University

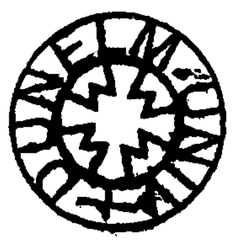

Thesis submitted for the degree of Doctor of Philosophy

2006

Declaration

I confirm that no part of the material presented in this thesis has previously been submitted for a degree in this or any other university. In all cases the work of others, where relevant, has been fully acknowledged.

Michael Lim

Durham University

Abstract

This study investigates the nature of hard rock coastal cliffs. One of the fundamental limitations to improving understanding of such landforms is a lack of accurate quantitative data on the behaviour of the rock slope itself, which is often assumed from recorded changes in the cliffline. High-resolution digital datasets from terrestrial photogrammetry and laser scanning have been analysed, validated, compared and combined to produce a quantitative record of cliff face changes. The approach has been applied to cliff sections at Staithes, North Yorkshire. Following the collection and analysis of field data numerical models have been used to further investigate the mechanisms governing cliff response to environmental controls and the nature of change over time periods extending beyond monitoring records. Care has been exercised throughout the study not to rely on previous notions of slope behaviour, which are often generated from low-resolution or incomplete datasets. The results of this research challenge many of the existing concepts within rock slope studies, promoting a more quantitative reappraisal of landforms which evidently respond to complex and interacting controls, diverging across space and through time.

Acknowledgements

There are many people to whom I owe thanks for the assistance and advice I have received during my thesis. Firstly I would like to acknowledge the role of Cleveland Potash Limited in this research. Their research-led attitude and expertise has made their involvement a key and much valued component of the study. I would particularly like to recognise the working relationships I have had with Mike Keen, Ian Scott and most notably David Pybus.

The role of the three supervisors involved in this project cannot be understated, and without their vision and guidance this thesis would not have been possible. Perhaps my greatest debt of thanks goes to Professor Robert Allison, for his belief in me and constant enthusiasm. Throughout the three years he has always made time for supervision despite his incredibly busy schedule and has provided unfailing support and encouragement. My sincere thanks also go to Professor David Petley for his guidance, particularly in technical aspects of the thesis. I have found his clear focus invaluable and I thank him whole-heartedly for the insightful discussions we have had, always driven by a complete dedication to the research. Additionally I would like to thank Professor Antony Long for his comments during numerous supervisories. The clarity of his judgement and wider perspectives has been essential in realising the implications of my work. Having worked with these three individuals for the last three years it is hard to adequately express my admiration for them, as academics, and as people.

A special mention is reserved for Dr. Nicholas Rosser. This thesis forms part of a wider research project between Durham University and Cleveland Potash Limited, and Nick has been without doubt the single most important component of this team. His contribution to my work has been particularly significant. From assistance in the field to discerning advice on analysis, Nick has devoted a significant portion of his time to the project. I have immense respect for his technical abilities; I thank him sincerely for his intellectual input and value him greatly as a friend.

Sincere thanks to my examiners Professor Brian Whalley and Dr. Danny Donoghue for their pertinent questions and suggestions which have added to the quality of the thesis. I would also like to acknowledge the contributions of Alex Koh and Dr. Jim Chandler during the planning of my fieldwork and the most valued assistance of Melanie Armstrong and Peter Nathan with Elfen programming issues. The positive feedback and alternative perspectives provided by Dr. Mark Lee and the project

steering group including Professor Ian Simmons, David Parrish and Professor Alan Patmore has also been most gratefully received. I am indebted to the technicians and secretarial staff in the department whose help and support has been invaluable. For assistance with the large amounts of field data that had to be collected, often in 'unfavourable' conditions, I would like to thank all who assisted me including Stuart Dunning, David Mould, Simon Nelis, Angel Ng, Mark Smith, Katie Thomson and Sarah Woodroffe. Particular thanks to Ilona Kemeling for making the dingiest office in the world seem a great place to be, to Dr. Patrice Carbonneau for introducing me to Matlab and to Alona Armstrong for all issues stata-related. I must also acknowledge Matthew 'Amadeus' Brain for three years of laughter and entertainment, a truer friend I have never found. The completion of this thesis owes much to the constant and unfailing friendship provided by members of the postgraduate community at Durham University, and for this I sincerely thank them.

Finally it remains for me to thank my family, the greatest influences not just on my thesis, but on my life. The love and support provided my parents and sister has lifted me up and carried me through. I do not have the words to convey what they mean to me, but it is to them that I dedicate this work.

Contents

List of tables

List of equations

Chapter 4

Chapter 6

List of Figures

Chapter 1
Introduction to the study

1.1 Context and justification of the thesis

Rock cliffs form some of the most impressive and widespread coastal landforms, accounting for approximately 75% of the total length of coastlines worldwide (Bird, 2000). Although cliffs form a critical interface between terrestrial and marine environments, understanding of the processes through which they evolve is limited. Inadequate knowledge of the nature of cliff erosion poses a significant threat to coastal communities around the world (Jones and Lee, 1994; Lee, 2001), particularly in the context of increasing coastal populations (Haslett, 2000). Over one billion people live in coastal areas globally (Nicholls and Small, 2002; Small *et al.*, 2000), many in close proximity to the cliffline (Hampton *et al.*, 2004). There is a practical need to understand contemporary coastal cliff systems and how they change in response to controls such as climate and sea-level (Lee, 2005). The IPCC best estimate of sea-level rise suggests a 0.37 m rise is likely over the next one hundred years (Houghton *et al.*, 2001). Such a rise will lead to direct and immediate changes within certain coastal features while inducing more lagged and indirect effects in others. Little is known about the impact of environmental processes on hard rock coastal cliffs.

Scenarios of future climate change for the coastal zone typically predict increases of high energy storm events, both in terms of incidence and magnitude (Lee and Clark, 2002). Several studies have indicated direct links between storm intensity and cliff recession (Kuhn and Shepard, 1979; Sunamura, 1980; Griggs, 1994; Moore *et al.*, 1999; Hapke and Richmond, 2002). The resultant retreat of the cliffline can cause the loss and damage of property, infrastructure, archaeological remains and natural resources, in addition to the threat posed by cliff failures to human life. To reduce these impacts, considerable resources are dedicated to reducing coastal erosion. It is estimated for example that annual UK government spending on coastal and flood

defences reached £564 million in 2005. Coastal protection schemes alone cost £53,700 km^{-1} yr^{-1}, with a maximum effective life of 60 years (DEFRA, 2001). Failure to understand and account for the processes through which rock cliffs evolve means that many coastal protection schemes are poorly designed or inappropriate (Neves and Pereira, 1999; Hall *et al.* 2002).

Quantitative data on cliff evolution are limited by a number of issues, including the slow rates of change; the difficulty of adequately measuring the complete range of rock slope alterations; and the dynamic nature and inaccessibility of the intertidal environment. Cliff forms reflect complex interactions between geological, mechanical and environmental conditions. The effects of antecedent influences on cliff behaviour are complicated by the action of environmental processes.

1.2 An integrated approach to recording and understanding change in coastal rock cliffs

The study of landforms such as cliffs requires three-dimensional change to be recorded. Aspects of cliff retreat, such as area and volume alterations, must all be considered through time to understand the nature of evolution of cliff forms (Sunamura, 1992). In order to predict future development, the geomorphological processes which have led to the contemporary cliff morphology must be understood. The sensitivity of different cliff systems to the processes and mechanisms governing change varies both spatially and temporally. The complexities involved with morphological responses over time have meant that multidisciplinary approaches are increasingly required in the study of landforms (Allison, 1996). Techniques such as geological and geomorphological mapping and monitoring; interpretation of aerial imagery; surface and subsurface analyses; geomechanical classification; laboratory investigations; and numerical modelling have all been applied, in order to gain a more complete understanding of rock slope systems (Crosta and Agliardi, 2003).

The approach of the current study is to investigate the complex behaviour of cliff systems by combining monitoring techniques with models capable of exploring the mechanisms of change. A high-resolution monitoring programme has been established along middle Lias cliffs at Staithes, North Yorkshire. Monthly data has been collected using digital photogrammetry and time-of-flight laser scanning to construct three-dimensional records of cliff recession. The combined approach allows detailed changes across the cliff face to be monitored. The changes recorded have been analysed with a combined finite/discrete element code to offer new insights into the mechanisms and longer-term aspects of slope failure. Ultimately it is through the

integration of monitoring and modelling techniques that significant advances can be made into understanding of coastal cliff behaviour.

1.3 Research aim and objectives

The principal aim of this study is to improve understanding into hard rock coastal cliff evolution through the examination of the key processes and mechanisms governing behaviour. The detailed objectives of the research are:

1. To establish an accurate way to measure changes occurring on hard rock coastal cliffs.
2. To assess the validity of current predictions of coastal cliff retreat rates.
3. To examine in detail the magnitude and frequency of rockfall activity.
4. To investigate the effects of spatial scale on cliff change.
5. To examine the temporal aspects of cliff change.
6. To assess spatial and temporal aspects of rock cliff behaviour with regard to environmental processes.
7. To investigate the material interactions driving rock cliff response.
8. To develop a model to better understand cliff development through time.

1.4 Organisation of the thesis

The structure of the thesis reflects an attempt to progressively build a better understanding of coastal rock cliff change. Chapter 2 introduces the problems associated with coastal rock cliff studies and the extent to which these have been addressed by existing approaches. It reviews the current level of understanding into contemporary rock slope geomorphology and concludes with the identification of four key research questions related to persistent issues concerning the evolution of such landforms.

Chapter 3 describes the study area. The geological, structural, material and morphological characteristics of the cliffed coastline north of Staithes, North Yorkshire, are discussed. The processes operating along the coast are considered. Specific cliff sections are selected for the collection of data on hard rock cliff evolution.

Chapter 4 describes the development of a remote sensing approach, used to provide new high-resolution data on the changes occurring over hard rock coastal cliffs. The relative advantages of both terrestrial digital photogrammetric and laser scanned datasets are explored, evaluated and eventually combined in order to accurately quantify the rates and patterns of change in slope morphology.

Chapter 5 presents the results generated from 20 months of monitoring of selected cliff sections. The data demonstrate the limitations of many current methods used to establish cliff retreat rates and display complex landform responses that vary through space and over time.

Chapter 6 analyses the monitoring results. The dataset reveals much about the nature of the short-term cliff changes. Contributions are made to knowledge of hard rock cliff behaviour, with specific reference to the four key research questions outlined in Chapter 2.

Chapter 7 introduces a combined finite/discrete element numerical modelling code for the analysis of rock slope mechanisms. The Elfen package was selected because of its ability to simulate both discrete body interactions and the internal stress and fracture of material, making it an ideal tool for the investigation of hard rock cliff behaviour. The chapter describes a comparison of model performance against established and validated discrete and finite element simulations enabling the basic mechanisms behind the recorded patterns of change to be better understood.

Chapter 8 is a synthesis of the study findings. The importance of the results is discussed with reference to implications for both site specific and wider scale aspects of research. The chapter revisits the objectives of the thesis before reviewing the original contribution made by the research to the study of coastal rock slopes. In conclusion, recommendations are made for further study.

Chapter 2
Coastal cliff evolution: current understanding

2.1 Introduction

Rock cliff development inevitably involves spatial and temporal change. Data that are representative of rock slope behaviour are limited by both the nature of the cliff environment and the adequacies of approaches used to record and interpret change. Consequently many aspects of hard rock cliff evolution remain poorly understood. This chapter reviews existing approaches to understanding coastal cliffs through the classification and interpretation of the ways in which cliffs develop. Consideration is given to the limited success achieved by both aerial and terrestrial approaches to rock slope monitoring. Terrestrially-based remote sensing holds the potential to combine the spatial coverage and accessibility of aerial techniques with the more relevant and useful perspectives obtained from ground data capture, although until now it has yet to be convincingly applied to coastal cliffs. Interpreting the recorded changes to cliff form can be assisted through the application of numerical models. Appropriate cliff behaviour simulations require the ability to account for both the interaction between discrete elements and the internal material fracture of intact material. The potential of current numerical modelling approaches is reviewed. The chapter concludes with a discussion of the fundamental aspects of cliff geomorphology, culminating in the identification of some key questions that remain about the evolution of coastal rock cliffs, and in particular the processes and mechanisms of change.

2.2 Coastal rock cliffs

Coastal rock cliffs can be defined as the steep-sided exposure of a rock mass that forms the margin between terrestrial and marine environments. The interactions between the rock mass characteristics influenced by material and structural properties on the one hand and external environmental processes on the other generate a wide variety of slope forms (Lee and Clark, 2002). The complexity of the interactions, which vary through time and space, have resulted in difficulties in understanding the behaviour of both cliffs and rock slopes in general. At the coast, studies of rock cliff evolution are further restricted by inter-tidal conditions that limit accessibility and the effectiveness of many conventional techniques for recording and interpreting slope change. Instead, much of the current understanding of coastal rock cliffs is based on attempts to interpret geomorphological response through both general classifications (Varnes, 1978) and more specific considerations of individual processes of change (DeFreitas and Watters, 1973).

2.3 Classification

Coastal cliffs form some of the most widespread and active of all rock slope environments (Robinson, 1974; Kimber, 1998). So dynamic are cliff systems that they have conventionally been defined by rates of change (Agar, 1960; May, 1966; Cambers, 1976; May and Heeps, 1985; Clark and Guest, 1991; Jones and Williams, 1991), although classifications have also been based on the magnitude and frequency of failures (Thornes, 1978; Douglas, 1980), climatic forcing (Grove, 1972; Hutchinson, 1973), hazard potential (Grainger and Kalaugher, 1988; Lee, 1997; Crowell and Leatherman, 1999) and the mechanisms of failure (Jaeger, 1969; Whalley, 1984; Lee and Clark, 2002).

Coastal cliff classifications have long incorporated differences between the behaviour of cliff materials, such as the sliding-dominated development in indurated sandstones or the more gradual and incremental retreat of weak rock and alluvium clifflines (Emery and Kuhn, 1980). Commonly, a distinction is drawn on the basis of the competence of the constituent rock material, with different analyses conducted on the processes associated with 'hard' and 'soft' rock cliffs (Allison, 1989). Lee and Clark (2002) defined a soft rock cliff as that for which recession is considered significant to coastal management. Hard rock cliffs, by contrast, are associated with coasts not prone to rapid erosion (Rees, 2002). It might be easy to infer from such studies that hard rock cliffs do not recede in sufficient volumes to influence contemporary planning strategies. A more accurate description however would be that the rates of retreat in hard rock cliffs have not been recorded in enough resolution and confidence to

determine retreat (Brunsden and Lee, 2004). Indeed the persistence of large relict rockfall scars in hard rock cliffs is testament to the importance of high magnitude failure events, although these are rarely recorded accurately (Hampton *et al.*, 2004). An inability to achieve suitable and accurate datasets on hard rock cliff evolution has limited not just the classification of rock cliffs but also, and more importantly, understanding into the processes and mechanisms governing their behaviour.

In addition to classification schemes based on recession rates or material properties, attempts have been made to interpret the temporal nature of cliff behaviour by defining stages of development. Classifications of the forms assumed by a rock cliff during different phases of development enable landform dynamics to be considered (Hansen, 1984). For example, the activity state indicated by cliff profiles was used by Emery and Kuhn (1980) to identify an 'active' stage in which near-vertical bare rock faces are continually eroded by marine and subaerial processes. Where cliffs are mantled by debris the influence of marine erosion at the base of the slope was reduced substantially and the cliffs were classed as 'inactive'. Finally, cliffs removed from marine activity altogether by uplift or sea-level change were referred to as 'formerly active'. More detailed and useful temporal classifications have promoted stages of initiation, consolidation, readjustment and ultimately abandonment (Brunsden and Lee, 2004), although each stage does not deterministically lead to the next. Rather, individual phases respond to spatially and temporally specific controlling conditions. Although useful in providing a framework through which cliff evolution can be studied, the stages suggested are often simplistic and lack an empirical basis.

The simplistic classification of cliffs by form, recession rate, geotechnical competence or temporal sequence is limited as a result of the complexity of the rock cliff system. In reality, cliffs typically comprise composite sequences of harder and softer materials, subdivided by varied structural weaknesses, and subject to diverse and interrelated internal and external influences. The behaviour of cliffs classified as 'hard' may still be dominated by the presence of a comparatively weak layer (DeFreitas and Watters, 1973). Thus, rock cliff classification schemes simplify interactions between material, form and process. However despite these limitations they remain an important way to order landforms, and they are a valuable tool for geomorphological analysis when viewed within their constraints (Lee and Clark, 2002). Whether characteristic forms, material responses and environmental signals can be reliably deciphered and used to distinguish between cliff types has yet to be determined. Until they are more convincingly established by quantitative methods, questions will remain over much of the way in which we currently perceive cliffs forms to evolve.

2.4 Development

The development of a landform over time is governed by its susceptibility to the drivers of change acting upon it. Environmental factors such as weathering rates, the hydrogeological system, the wave regime and human activity, all of which vary through time and space, may influence the rate and manner of cliff change (Robinson, 1974). The strength of a cliff is derived from the properties of the materials from which it is formed. In most cases, slope-forming materials are broken into unevenly-sized blocks by planes of weakness such as joints, faults or bedding surfaces. The response of *in situ* conditions to environmental influences over time may generate a tendency towards stable or unstable conditions (Hoek and Bray, 1981), with unstable behaviour generally thought to occur through established sets of criteria (Varnes, 1978). Understanding the development of coastal rock cliffs has therefore been dominated by concepts of failure. The main mechanisms of failure in rock masses involve sliding, falling and toppling (DeFreitas, 1972; DeFreitas and Watters, 1973; Pritchard and Savigny, 1989; Hantz *et al.*, 2003), and can be broadly grouped into falling and sliding movements (Figure 2.1).

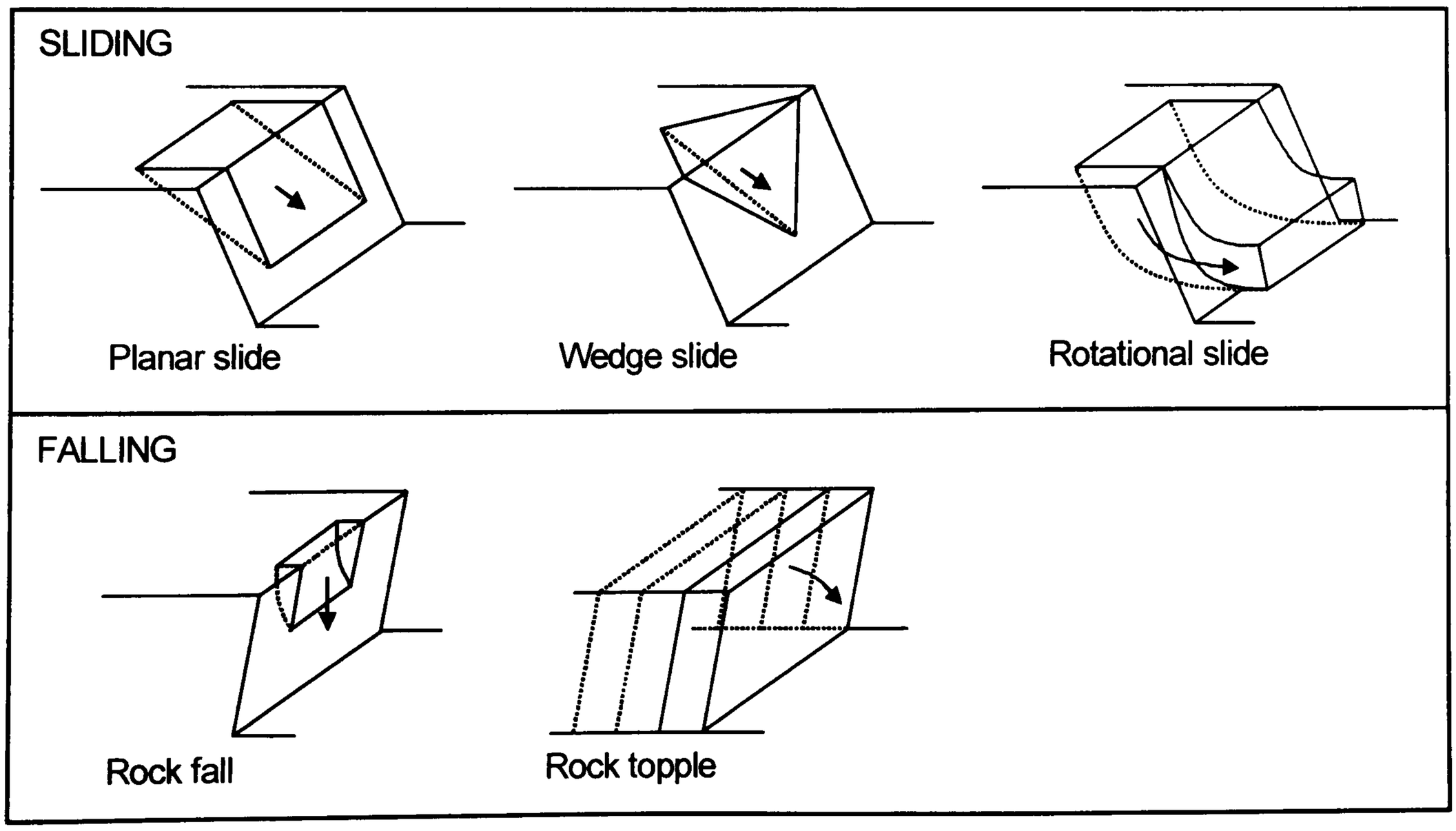

Figure 2.1: Mechanisms of rock failure, divided broadly into sliding and falling failures. Material undergoing failure however may potentially alter from one mode of failure to another, with a slide changing to a fall, or a topple becoming a slide, for example.

2.4.1 Slides

Sliding failure in rock cliffs can be subdivided into plane sliding and wedge sliding (Goodman, 1980). The preconditions for plane sliding, which is sometimes termed slab failure, are such that it is more commonly found in dip slope mountain environments rather than sheer-sided cliffs. The failures occur when certain geometrical conditions are satisfied. When the failure surface strikes sub-parallel (±20° of the strike of the slope face) to the slope and its dip is less than that of the free face, it will daylight in the cliff (Hoek and Bray, 1981). Provided the dip of the failure surface is greater than the angle of fiction of the material, plane sliding is possible. Failure of the material may also be dependent on the presence of lateral scarps that define the dimensions of the released blocks. Wedge failures are more common than planar slides, occurring along the intersection of two or more discontinuities (Hoek *et al.*, 1973). As with plane sliding, failure is most likely to occur if the dip of the line of intersection is greater than the friction angle across the shear surface but less than the dip of the slope face. The occurrence of wedge sliding is therefore commonly limited by the orientation of joint sets in sheer-sided rock cliffs.

The criteria required for failure mean that the necessary conditions for sliding may take time to develop (Goodman, 1980; Sharma *et al.*, 1995). Field monitoring has demonstrated that failure is preceded by the progressive build up of strain, often beginning with tension cracks behind the cliff face or tension zones (Malet *et al.*, 2003). The scale of sliding may range from single rocks sliding along a discontinuity (Figure 2.2) to large intact blocks of material moving over a layer of weakened rock. The subsequent development of the slide depends on the location of the failure surface within the cliff. A shear surface that passes through or beyond the foot of the cliff may cause the failed material to rotate as it meets the cliff platform but if it daylights within the cliff face the material is likely to turn into a falling or flowing failure (Lee and Clark, 2002). Sliding failures are in themselves complex. For example, a sliding event may be episodic, affected internally by the resistance of both asperities on joint faces (Estrin and Brechet, 1996) and intact rock bridges dividing failure surfaces (Scavia, 1995).

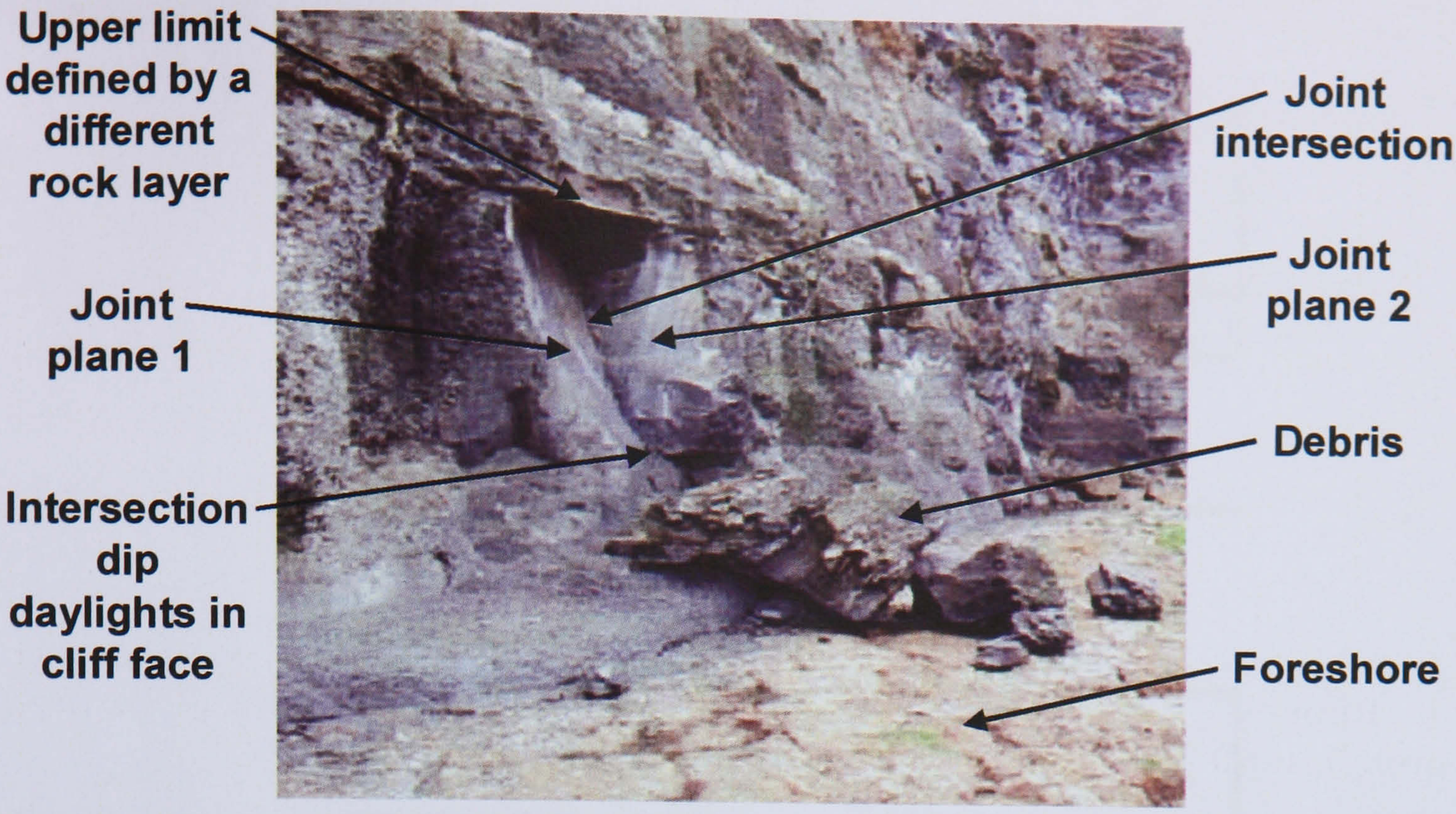

Figure 2.2: An example of a wedge failure in coastal rock cliffs. The intersection of two discontinuities exposed in the slope generated the critical conditions which led to the release of a coherent wedge of material.

2.4.2 Falls

In general, rockfall events are considered to be the detachment and free fall of disintegrated material from the cliff face (Hantz *et al.*, 2003). These are occasionally separated into primary falls, which are released from the rock face, and secondary falls, consisting of previously failed debris (Matznetter, 1956). They may also be subdivided by scale into falls and avalanches (Whalley, 1984). Rock avalanches are formed within very large rock masses. The rock divisions between joints weaken and fracture until a densely packed body of cohesionless angular blocks catastrophically fail from the slope. Where masses with closely spaced jointing are found to be stable with respect to rock avalanches, small blocks and rock fragments may be released from the slope face. Shear stresses build up under gravity and become concentrated within the intact material in the rock mass, leading to fracture controlled detachment (Scavia, 1990).

Overhang failure was included in a recent analysis of typical rock slope failure mechanisms by Hantz *et al.* (2003), and may be of particular concern in the development of coastal cliffs undercut by marine activity (Figure 2.3). Overhang instability can be subdivided into rotational and gravitational detachments. The processes are restricted to the exposed surfaces of the rock mass and failures are consequently shallow seated, characterised by the parallel stripping of rock layers from the cliff face.

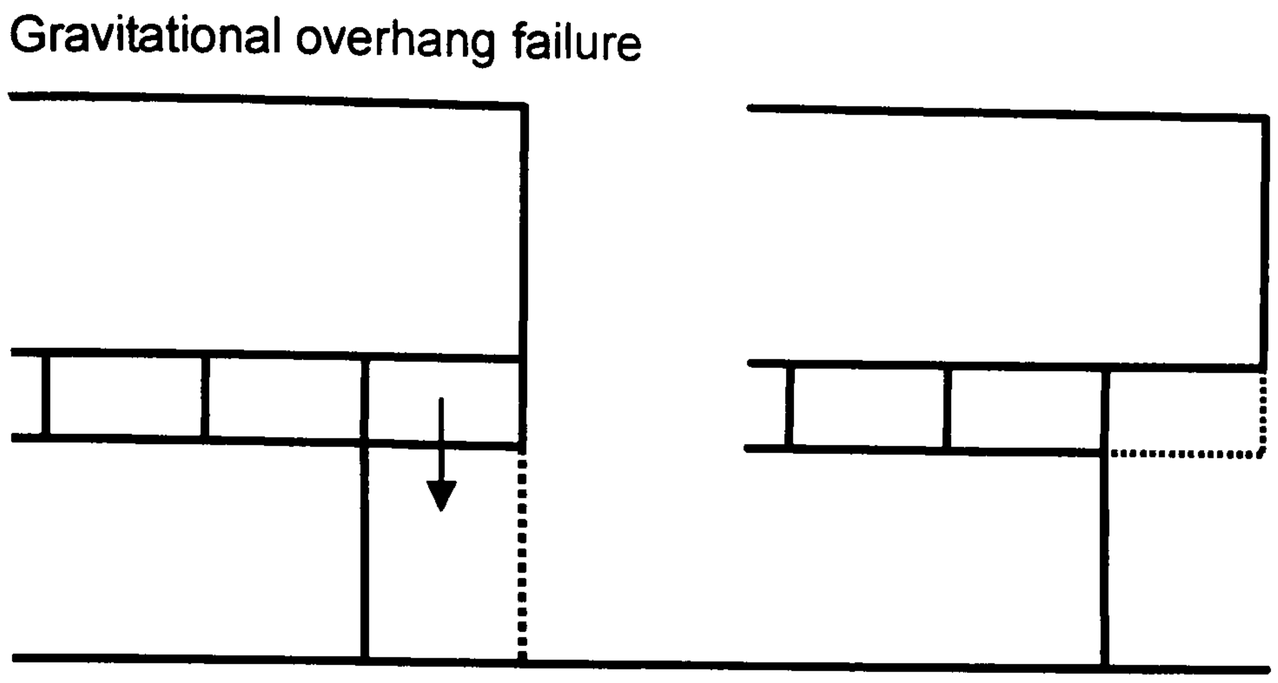

Figure 2.3: Overhang failure in cliff slopes. Gravitational failure involves the loss of support for a block as the layers beneath it are removed. Rotational failure refers to the shearing of a block when the weight of its protruding mass can no longer be maintained by the tensile strength within the material.

Toppling occurs at the boundary of conditions for sliding and falling rock movements. Analysis by DeFreitas and Watters (1973) was subsequently developed to promote toppling as a significant failure mechanism (Goodman and Bray, 1976; Pritchard, 1989; Lanaro, 1997; Nichol *et al.*, 2002). Toppling is now recognised to be an important mechanism of landform evolution, exhibiting unique and complex properties that distinguish it from other modes of failure. Toppling may occur beyond the limiting conditions for sliding failure, where regularly spaced discontinuities strike parallel to the free face and dip into the rock mass (Wyllie, 1980). Conventional analysis states that if the block dimensions and inclination are such that its centre of gravity lies beyond its perimeter then it has the potential to topple.

Toppling involves the rotation of blocks about a pivot point (Prichard and Savigny, 1989) and may be instantaneous, causing catastrophic retreat, or gradual, cambering the slope. Toppling processes have been subdivided into flexural toppling, block toppling and block-flexural toppling (Figure 2.4). Soft rock masses such as schists or slates, or those dominated by one major discontinuity network, typically form columns which bend forward and break in flexure. Stronger materials, such as

limestone and sandstone, exhibit block toppling as surrounding blocks interact to destabilise individual columns. Block-flexure toppling occurs when weaker impurities are interbedded with harder columns, combining natural flexure points with block interactions. Flexural failure has been validated by Pritchard and Savigny (1989) in the Brenda mine, British Colombia, while block topples and block-flexure topples have been identified in several field examples, such as those from Highwood Pass, Alberta, Canada (Cruden and Hu, 1994). The precise toppling mode depends on interrelations between joint spacing, bedding thickness, rock strength and topography, and may also occur as a secondary phase of sliding failure (Evans *et al.*, 1981).

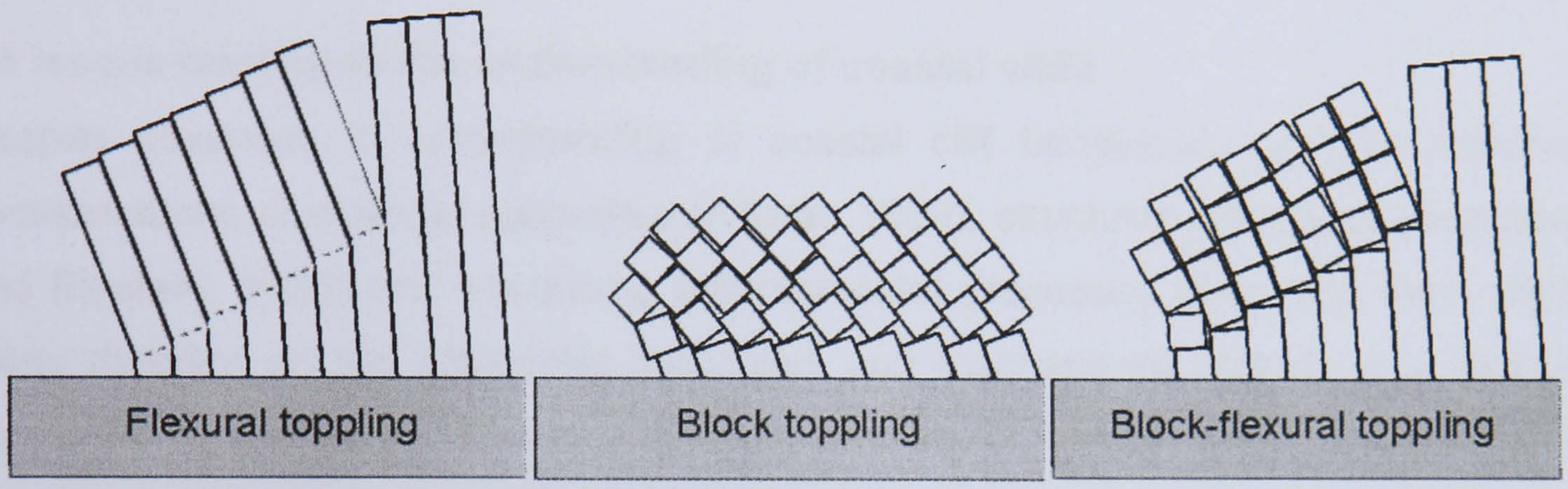

Figure 2.4: Flexural, block and block-flexural toppling failures, as defined by Goodman and Bray (1976). Flexural toppling relies on well-developed discontinuities which form columns that tilt forward during failure. Block toppling relies on the interaction between numerous rock segments to load and destabilise surrounding blocks. Block flexure involves semi-continuous flexure as columns of blocks interact.

2.5 Coastal cliff geomorphology

Although the establishment of boundary conditions for certain types of mechanical response have provided useful analytical tools for rock cliff development, landform behaviour rarely conforms completely to such neat divisions. Failure of cliff material may occur as a consequence of multiple mechanisms. Caution should therefore be exercised over the use of failure criteria developed for idealised scenarios which assume all other variables remain constant over time. In reality, cliffs can be viewed as complex systems in which change, or failure, is influenced by past and present material-form interactions working through space to modify morphology over time.

Geomorphological considerations of the evolution of coastal rock cliffs emphasise the importance of temporal aspects of change. The successive changes to the system further influence and alter the future behaviour of the landform. The concept of cliff 'ripening' has for example been used to link episodes of change to the build up of porewater pressures prior to failure (Brunsden and Lee, 2004). Process-form interactions can therefore be viewed as hierarchical, varying through space and

over time (Brunsden, 1996). Geomorphological change, over any set time frame, is a complex interaction between the agents of change and the sensitivity of a landform (Brunsden, 1999). Controls on coastal cliff development can be considered in terms of the mechanisms by which change or failure can occur and the processes of operation that influence the timing and rate of the event (Brunsden and Thornes, 1979). Whilst landform sensitivity is largely dependent on the *in situ* conditions of the rock slope, the processes of change include climatic, human and, in the case of coastal cliffs, marine agents. The complexities involved mean there are many problems associated with the recording and interpretation of cliff geomorphology.

2.6 Issues relating to the understanding of coastal cliffs

Despite advances in understanding of coastal cliff behaviour, such as enhanced considerations of material properties (Allison, 1989), structural influences (Dershowitz and Einstein, 1988) and interacting environmental processes (Dias and Neal, 1992), many theories on the governing processes and mechanisms remain at a relatively poorly developed level. The lack of understanding of coastal cliff processes can be broadly attributed to three main aspects of rock cliff investigation: the nature of the coastal cliff environment; the ability to adequately record change; and the capacity to account for the mechanics driving change.

2.7 The nature of coastal cliff environments

The coast represents a very challenging environment for the analysis of geomorphological change. There are large variations in processes over relatively small distances, such as above and below the wave impact zone. Furthermore, temporal differences may superimpose short-term variability on longer term patterns of change. For example weather conditions may cause increased rockfall events in a particular year, set within the accelerated retreat of cliffs caused by long-term sea-level rise. The environmental controls on coastal cliff behaviour can be considered on two levels: (1) regional, overriding first order factors such as relative sea-level and climate changes; and (2) local second order influences such as groundwater and rainfall patterns (Bray and Hooke, 1997). Long-term climate changes, such as those experienced throughout the Quaternary, have been linked to distinct phases of cliff development (Gardner, 1977; Griggs and Trenhaile, 1994). It is thought that contemporary coastal cliffs worldwide would have been dominated by subaerial processes during the lower sea-levels of previous glaciations, causing the build up of scree deposits at the slope base (Mottershead, 1997).

Although generic cliff models relating to long-term, first order environmental processes recognise the wider context in which coastal slopes develop (Brunsden and Lee, 2004), and the interaction between marine and terrestrial influences in particular (Emery, 1960), they are often too simplistic to improve understanding of cliff behaviour. A phase of 'initiation' has been used to describe the commencement of marine erosion at the base of the cliff following, for example, the termination of a glaciated period (Davis, 1912; Cotton, 1951, 1969; Fleming, 1965; Bird, 1969), once any accumulated debris has been removed (Jennings *et al.*, 1998). A 'consolidation' phase then reflects the development of a characteristic form that balances the processes operating at that time, reflecting the most stable configuration of prevailing site conditions (Hutchinson, 1984; Jones and Lee, 1994). A 'readjustment' phase involves the transition to a new characteristic cliff form in response to changes either within the system or externally. Finally, an 'abandonment' phase follows the removal of marine activity from the cliff base and return to subaerial controls (Bromhead *et al.*, 2002). Many of the underlying concepts behind the multiphase models are based on assumptions formed from qualitative interpretation of existing landforms, which are therefore subject to question. The existence of a characteristic form for example implies some sort of equilibrium has been reached, although whether such forms are immediate or lagged responses to present or past, extreme or everyday climatic forces is unclear. It could thus be argued that all cliffs are permanently in a phase of readjustment, depending on the temporal scale of interest. Ultimately questions must be raised over the usefulness of such generalised models for systems that evidently vary spatially and often diverge through time. True insight into the processes determining the rate of slope change requires quantitative consideration of the influences created by specific agents of change.

Set within the first order environmental controls are the everyday processes that cause each site to have its own unique response and periodicity, superimposed on the general patterns of change (Dickson *et al.*, 2004). All natural rock slopes are subject to an array of physical, chemical and biological processes that exert multiple effects, both destructive and stabilising. Factors influencing cliff erosion can be divided into internal influences, such as material and structural properties of the slope, combining to determine the resisting force of the rock body, and external influences to the system such as wave pounding and subaerial weathering (Figure 2.5). For convenience the discussion of the contemporary environmental drivers of change in coastal rock masses can be divided into marine and subaerial factors, though it must be remembered that the two are inextricably linked.

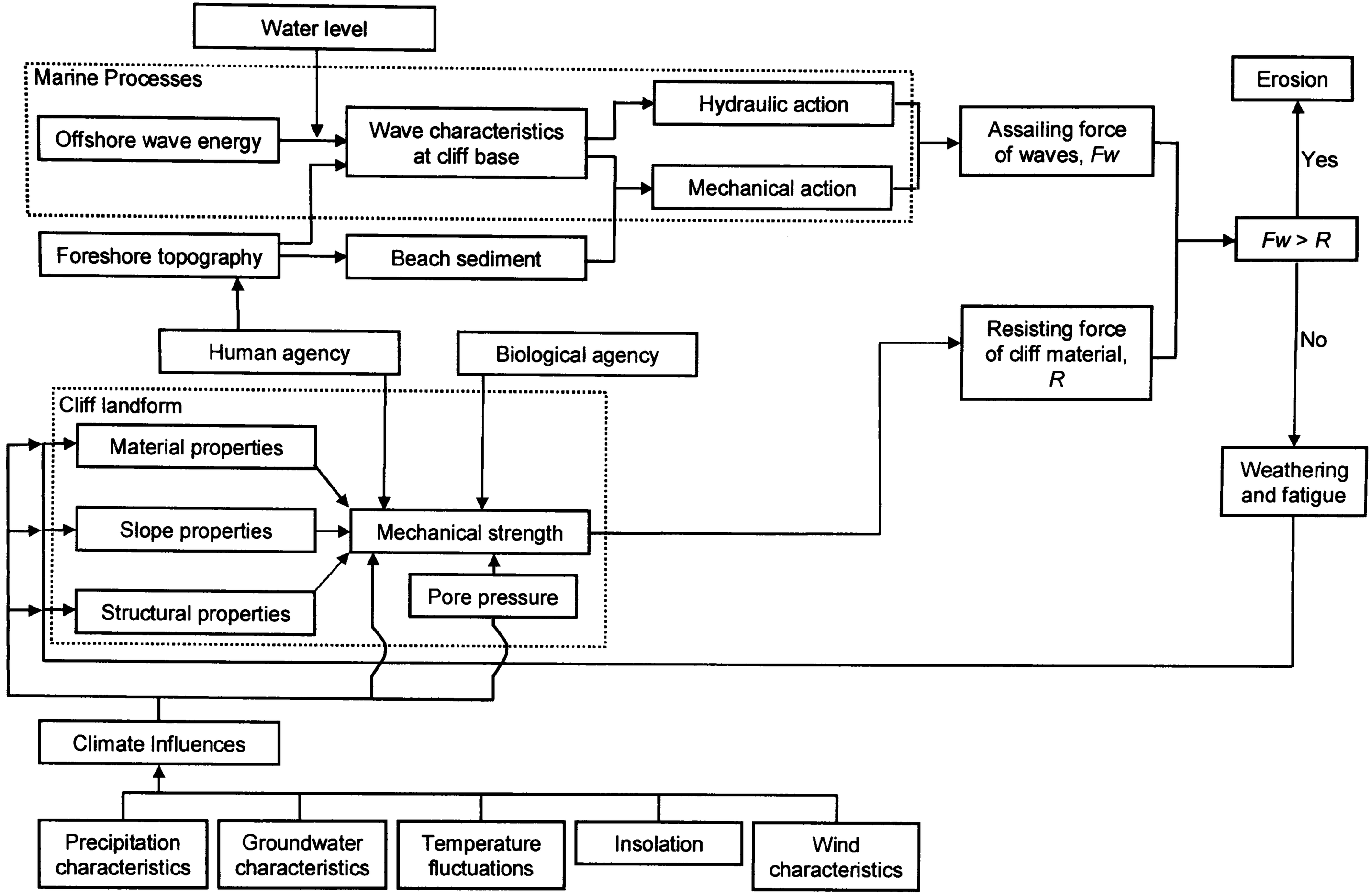

Figure 2.5: Processes affecting cliff erosion. Sunamura's (1992) model of the factors affecting cliff base erosion has been adapted to form a more holistic overview of coastal rock slope behaviour, including subaerial processes in addition to marine influence.

2.7.1 Subaerial processes

All exposed slope faces are subject to subaerial weathering, usually causing the degradation of the rock surface through time. Studies of the processes affecting coastal cliffs have overwhelmingly concentrated on marine factors (Sunamura, 1992), ignoring the sometimes critical inputs from less evident climatic factors (Duperret *et al.*, 2002). The effect of subaerial influences, and indeed all environmental processes, on cliff development is difficult to quantify due to the complexity and variability of the processes involved. Rainfall, for example, is a significant but often overlooked agent of hard rock cliff development. Raindrop impact continually wears down the exposed rock face and, aided by driving winds, can become the main source of detaching particles from the rock material (Lee and Clark, 2002). Drainage of rainwater leads to concentrated flow paths that form rills and gullies (Morgan, 1986). The erosion within these topographic depressions can be relatively high, demonstrating the significance of the pattern of rainfall on cliff behaviour. Consequently, rainfall intensity is an important influence on the nature of subaerial erosion of the cliff, determining whether the water is carried rapidly over the slope face or allowed to infiltrate and flow more gradually into lower sections of material. It is important to consider the timing, intensity and location in addition to the volume of precipitation to determine the overall hydrological influence on cliff form and behaviour.

Water, supplied by precipitation, can be an important control upon rock cliff processes. The flow of water through strata can lead to the direct removal of material from within the cliff, causing weakening through seepage erosion (Howard and McLane, 1988), often concentrated upon lines of structural weakness (Benumof and Griggs, 1999). The chemical effects of water on rock are subtle but can influence sedimentary strata for example, dissolving inter-particle cement (Turner, 1981). Fluctuations in the level of water through sections of rock vary effective stress states, reducing friction (Ritter, 1986; Hutchinson *et al.*, 1985), and cohesion (West, 1996). Elevated porewater pressure may result from the presence of an impermeable layer (Norris and Back, 1990). The fluctuations, although small, act over large areas generating significant forces within the rock mass (Hoek and Bray, 1981). Differences in permeability also commonly lead to concentrated bands of seepage onto the cliff face (Hutchinson *et al.*, 1981). Water flow restricted by impermeable layers can induce mass movements that would not occur in more freely draining bodies of material (Denness, 1971). Groundwater effects may be particularly prevalent at the coast as tidal levels periodically raise local water levels into contact with higher elevations of rock (Grainger and Kalaugher 1987). Groundwater pressures are also known to fluctuate as a direct consequence of cliff recession (Lee and Clark, 2002). Stress relief

resulting from the loss of material from the cliff face may disrupt established seepage patterns, causing suction forces to build up that temporarily stabilise the cliff (Brunsden and Lee, 2004). Water may have little impact on impermeable, continuous rock masses, but where it can enter porous or discontinuous rock, its influence may dramatically alter the behaviour of the material (Attewell and Farmer, 1976; Farmer, 1989).

The coastal setting often means subaerial effects on cliffs are enhanced. The precipitation of salt as sea spray that is deposited and dries on the rock is thought to be a dominant effect in the mechanical disintegration of cliff face material within the zone of marine influence (Bryan and Stephens, 1993). The severe weathering environment has been shown to be dependent on the cliff position, with accelerated erosion rates associated with orientation toward the sun or reduced levels where constant runoff prevents the accumulation of salt crystals (Johannssen *et al.*, 1982). Additional weathering may occur during winter months due to hydrostatic pressures within the cliff as water is drawn towards freezing points (Walder and Hallet, 1985; 1986).

2.7.2 Marine processes

The influence of marine processes in shaping slope form makes the manner and rate at which coastal cliffs change distinct from other rock slope environments. Interpretation of the effects of marine energy on coastal cliff evolution is restricted by the complexity, scale and number of variables involved, such as the offshore wave climate and its landward attenuation; the prevailing wind direction; the orientation of the coast; the foreshore topography; the configuration of the coastline morphology; the entrained sediment content; and many more. Key stages of marine activity are thought to include the formation of a notch at the base of the cliff, the progressive removal of support to material above, the oversteepening and eventual failure of the lower cliff profile and the deposition upon, and subsequent erosion of debris from, the foreshore (Brunsden and Jones, 1980; Vallejo and DeGroot, 1988; Wilcox *et al.*, 1998). The ultimate control on marine erosion is the degree of exposure of the coast to marine influences. Coasts with large tidal ranges are thought likely to be subject to a more limited period of maximum erosion as the zone of breaking waves is continuously shifted up and down the foreshore (Brunsden and Lee, 2002). However, such analyses may prove overly simplistic if the associated stronger tidal currents cause wave energy to become more effective at erosion. The force of wave impacts on the cliff depends on the deep-water climate and wave characteristics. The delivery of energy varies with wave type, ranging from low impacts of standing waves that can be reflected prior to breaking, to the elevated force of plunging waves that break at the cliff

toe (Hampton *et al.*, 2004). The depth of water across the foreshore is critical in determining the amount and nature of marine energy delivered to the cliff.

The episodic nature of coastal cliff behaviour has often been attributed to the irregular occurrence of storms (Bacon and Carter, 1991; Flick, 1998; Hapke and Richmond, 2002). Allan and Komar (2002) found occasional storm surges had the potential to raise average monthly sea-levels by 0.6 m above the long-term average along the Pacific Northwest coast. The effect of storms on wave climate and therefore cliff weakening commonly generates seasonal signals, particularly in temperate regions where winter months result in increased storminess and reduced beach cover (Hampton, 2002). During a storm, the compressive forces from wave impacts are high, particularly when the waves reach the critical height that causes them to break at or near the cliff base, generating a quarrying effect (Trenhaile, 1987; Sunamura, 1992). Set against the high magnitude, low frequency storm impacts is the continual abrasion of the intertidal zone by hydraulic action. Coarse entrained material continually wears down the cliff strata (Robinson, 1977; Kamphuis, 1987; Nairn, 1997). The interaction between the continual degradation of material and localised quarrying remains unquantified, although Kuhn and Shepard (1979) suggested that infrequent storm events were more significant to coastal erosion patterns in San Diego County, California, than much longer periods of relatively calmer conditions.

In addition to direct influences on the cliff, long-term marine effects have the potential to influence recession indirectly, through the lowering of the foreshore for example. Rock platforms provide a natural barrier to wave energy, regulating basal cliff erosion according to specific topographic features (Trenhaile, 1987). This results in the removal of foreshore material through wave-induced shear stresses (Philpott, 1984), turbulent flow plucking (Sunamura, 1992), abrasion (Sunamura, 1976), wetting and drying cycles and the strain softening caused by the repeated loading and unloading associated with the tidal cycle (Davidson and Arnott, 1986). Unless the rate of rock platform lowering equals that of cliff recession, the widening platform will dissipate increasing amounts of energy, causing a negative feedback until it has been lowered sufficiently to allow further recession (Robinson, 1974; Kamphuis, 1987).

The orientation of the slope face relative to the incoming tide is of particular relevance in the study of coastal cliffs, determining the impact of wave attack (Carter, 1988). Waves are thought to exert proportionately less influence on straight cliff sections compared to asymmetric coastlines, which focus energy on certain areas. Often such concentrations are on headlands due to nearshore bathymetry (Shepard

and Grant, 1947). The importance of slope properties extends beyond those of the cliff face itself, to the foreshore, which influences the transfer of marine energy to the base of the cliff. Beaches have long been seen as fundamental in actively absorbing the impact of breaking waves through kinetic and frictional diffusion of marine energies (Bird, 2000). The nature of the foreshore, its composition and topography and the overall geometrical alignment of the coastline with respect to dominant wave directions and heights may therefore influence the rate of change across different cliff sections (Trenhaile, 2002).

Sea-level rise is an important factor in the long-term evolution of coastal cliffs. Since the last glaciation global sea-levels have risen due to the mass melting of ice sheets and the thermal expansion of water bodies. The worldwide eustatic rise is thought to have reached an average rate of 10 mm a^{-1}, declining to 1 mm a^{-1} some 5000 years ago (Emery and Kuhn, 1982), although measured rates for many parts of the British coastline over the last century have been 3 mm a^{-1} (Woodworth *et al.*, 1999). The magnitudes involved appear relatively small but their effect on coastal cliffs may be significant. The 130 m total sea-level rise over the last 18 000 years is estimated to have caused up to 130 km of coastal retreat globally, or 1 m for every millimetre of sea-level rise (Hampton *et al.*, 2004). Although such claims are useful in highlighting how comparatively small process changes can potentially exert large scale impacts on landform response, the actual behaviour of the slope will overwhelmingly reflect site specific influences (Komar and Shih, 1993).

The variable nature of interactions between the different coastal processes influencing rates of activity in cliffs means they are poorly understood. Models of specific coastal process interactions have been developed in an attempt to relate shoreline retreat to variables such as sediment supply and local sea-levels (Bruun, 1988). Although such models attempt to define linkages to better understand the development of coastal systems, many of the assumptions made, such as a clear bounding extremity for the seaward exchange of sediment, no dissipative beach effects and no lag times, raise questions over their validity (Sunamura, 1988; 1992; Healy, 1991; Wood *et al.*, 1994). Other models of coastal variables have focused on significant wave height distributions (Ferreira and Guedes Soares, 2000; Prevosto *et al.*, 2000), geostrophic wind effects (Teixeira *et al.*, 1995), wave spectra (Nieto *et al.*, 1995), tidal currents (Paillard *et al.*, 2000) and storm severity (Elsinghorst *et al.*, 1998) but all involve uncertainty over the interplay with additional elements of the coastal environment. Recently, more holistic approaches have attempted to combine multiple models into coherent simulations of climatic interchange. Lee *et al.*, (2002) presented

CLIFFPLAN, which links models of slope stability, beach profile erosion, sediment transport and wave energies. Random sampling from weighted probability distributions is used to represent the uncertainty in both input parameters and the cliff recession process itself. Realisation of the simulation is then used to form a histogram of probability distribution from numerous model runs of the randomly selected variables. Such approaches, although useful for management and planning, fail to account for the mechanisms causing cliff evolution and caution should be exercised when assuming that a cause and effect relationship can be reliably predicted. Failure in certain slopes may leave recognisable signatures in the landscape, generating repetitive forms (Brunsden and Thornes, 1979), but to assume such profiles can be expected to occur regularly or with any constancy, reflecting equilibrium conditions over time, is questionable (Pilkey *et al.*, 1993).

2.7.3 Human influence

An additional factor in determining the evolution of coastal cliffs is anthropogenic influence. The development of infrastructure for example can increase loading on the crest of the cliff and it can produce concentrated releases of water onto and into cliff material, making it more susceptible to failure (Emery and Kuhn, 1982). Kuhn and Shepard (1984) suggested that irrigation and cliff top septic systems in San Diego County may add as much as 1.5 m to groundwater levels. The significance of artificial water sources on cliff erosion was noted in a study by Hapke and Richmond (2002), who found that retreat rates over a three month period were much lower for undeveloped and naturally drained slopes. As coastal cliff faces may also provide access to valued geological commodities, they have often been the site of mining and quarrying activities that by definition alter cliff retreat processes and rates.

Much of the effects of the human agency on cliffs concerns measures to stabilise and protect against future erosion. Stabilisation approaches include the regrading, anchoring and draining of the slope (Hutchinson *et al.*, 1985; Clark and Guest, 1991); cliff top protection with impermeable barriers to runoff (Byrne, 1963); and armouring of the slope toe (Komar and McDougal, 1988). Attempts to 'fix' the coastline or limit its retreat in certain areas have implications for the patterns of coastal processes (Kraus, 1988). For example, relationships have been identified between the length of defence structures and enhancements in flanking erosion (McDougal *et al.*, 1987). Preventing marine effects at the cliff base may also limit the supply of sediment into the coastal system (Runyan and Griggs, 2003). In the case of hard rock cliffs, the contribution to the sediment budget from cliff failures is considered insignificant. It has been estimated that if 50,000 km of cliff-fronted coastlines worldwide were to retreat by

0.05 m a^{-1} the sediments generated would account for only about 0.04% of that produced by streams (Emery and Milliman, 1978), although the validity of such a comparison remains questionable. The restrictions on understanding of cliff evolution imposed by the inability to quantify the effects of processes operating within the cliff environment are compounded by the difficulties of recording in detail the resultant landform changes.

2.8 Recording rock cliff changes

The geomorphological study of landforms attempts to improve understanding of the interaction between materials and processes that govern changes in form over time (Sunamura, 1992). Exploring the nature of the material-process-form relationship that determines rock cliff behaviour requires current volumes, rates and patterns of change to be established at appropriate spatial and temporal scales. Near-vertical, active and often overhanging slope faces, and tidally-exposed bases, make coastal cliff sections particularly problematic landforms to study. The challenges posed by coastal cliffs have limited the success of monitoring approaches and led to specific interpretations of cliff behaviour based on compromised datasets. The data collected to study the contemporary patterns of cliff development can be divided into attempts to measure cliff change from a planimetric perspective and from a terrestrial viewpoint.

2.8.1 Planimetric records of cliff change

Historic maps are used to provide information on the long-term evolution of coastlines with rock cliffs (Agar, 1960). Alterations in the cliff top and/or cliff toe are compared over time to analyse cliff retreat rates. The limitations associated with such data are often ignored in interpretation, raising significant questions over the validity of the findings. The apparently episodic nature of cliff failures and increasing pressure for the management and development of many coastal environments has lead to a greater emphasis on measuring the position of the cliffline (Hutchinson, 1973; Quigley *et al.*, 1977; Everts, 1991; van Rijn, 1998), although the cumulative errors within the source documents and images are often several orders of magnitude larger than the rate of retreat being measured.

Rock slope behaviour patterns determined from historic maps are influenced by errors associated with the shrinkage and stretching of the physical document over time, in addition to issues of accuracy and precision associated with map production (Snyder, 1987). In 1985 the U.S. Army Corp of Engineers recorded error ranges of ±12 m in recession rates along the southern Californian coast, based on the difference between National Oceanographic Service topographic sheets conducted in 1852, with

claimed accuracies of 6 m for the 1:20,000 scale sheets, and aerial photography collected in 1982 (Hampton *et al.*, 2004). The large uncertainties were caused by an inability to accurately locate the cliff base in the historic surveys. The omission of ground control in earlier surveys, and sketching between points, may generate additional errors of ±10 m or more for map scales of between 1:10,000 and 1:20,000 (Shalowitz, 1964). As a result, measurements typically lack comparability both between separate surveys and within each mapping project (Crowell *et al.*, 1991).

Issues of comparability between separate rock slope studies are enhanced by the use of maps from different periods which are often based upon different scales, projections, ellipsoids and datum that require conversion to a common system before comparisons can be made (Anders and Byrnes 1991; Moore, 2000). Improvements have been made to historical map and image data with stereo zoom transfer scopes and by digitising the locations of known control points, cross referenced with the use of geographical imaging software (Evenden, 1990, 1991; McBride, 1989), although the potential errors remain compounded by the range of techniques used (Moore, 2000). The inherent errors in the use of historical records raise questions over the accuracy of detected patterns of rock cliff position, and therefore the subdivision of long-term averages into annual retreat rates.

Aerial surveys are the most common method for monitoring cliff recession. Generally these approaches record alterations in the position of the cliff through time (Gelinas and Quigley, 1973; Graham and Mills, 2000; Hua and Fairbairn, 2000). The flexibility of the collection and analysis of aerial data means that large stretches of coastline can be recorded in a single epoch. Thus, it is often the most cost effective way to account for wide scale variability found along the coast. However, although they form the basis for several important concepts of coastal cliff behaviour, there are many documented problems arising from aerial datasets that limit both their accuracy and the ability to interpret cliff change using such data (Moore, 2000). The limitations involve aspects of both data collection and analysis.

For recent shoreline positions, digitised aerial photography offers a more reliable method of locating the cliff through time (Crowell *et al.*, 1991). Modern aerial imagery is available at increasingly high resolution, and is often referenced accurately with global positioning systems or GPS (Byrnes and Hilland, 1994; Gorman *et al.*, 1998). Photographs are however affected by distortions and displacements that alter the relationship between the representation of an object in an image and its true position and geometry (Slama, 1980). The cumulative effects of elevation and radial

displacements cause the accurate location of near-vertical cliff sections to be particularly problematic. A 30 m high cliff edge located 0.04 m from the image centre of a 1:12,000 scale photograph was found to be displaced by 7.9 m in true ground coordinates (Hampton *et al.*, 2004). The accuracy of photographs is further limited by the variable orientation of the camera during image capture from a moving aircraft. When a camera is not truly vertical the image scale is perturbed, reduced on the upward side of the tilted axis and increased on the downward side (Moore, 2000). The tilt is typically within 3° in aerial projects (Leatherman, 1983), although a 1° offset can cause up to 13.6 m ground error in a point 0.1 m from the image centre of a 1:20,000 scale photo (Anders and Byrnes, 1991).

The application of aerial imagery for cliff monitoring depends on the ability to accurately locate the position of the cliff top and occasionally the toe. This has proven to be one of the most problematic aspects of cliff studies. Cliff erosion studies have used uncorrected (Griggs and Savoy, 1985; Guy, 1999), partially corrected (Thornton *et al.*, 1987; Griggs, 1994) and fully corrected images (Moore *et al.*, 1999; Priest, 1999) to characterise retreat through measurement of the cliffline. The most accurate studies have used digital photogrammetry to generate three-dimensional models that allow the cliff position to be viewed in stereo (Hapke and Richmond, 2002). This process however still requires the cliff edge to be digitised onto two-dimensional orthorectified images. In a recent study, the placement errors associated with the precise location of the cliff top in the aerial images ranged from 2.5 m to 6.3 m on 1:7,500 orthophotographs (Hampton *et al.*, 2004). The ambiguities are caused when the cliff top cannot be defined by a clear linear datum, identifiable from a planimetric perspective (Zviely and Klein, 2004). Tonal contrasts in the division between the rock mass and overlying material are blurred by overhanging and face vegetation; algal growth; groundwater seepage; staining from soil and till layers above; and shadowing (Figure 2.6). Other aerial methods of monitoring cliffs have been similarly limited when locating the topographic break of slope that defines the cliff edge. Grids of Light Detection and Ranging (LiDAR) data have been successfully used to monitor extensive shallow angle soft rock cliffs to sub-metre height accuracies, although the planimetric resolution of the grid is often 2 or more metres (Mikhail *et al.*, 2001), incurring additional errors when the cliff top lies between survey points (Figure 2.7).

The problems of establishing the position of the cliff top in aerial images are less pronounced when the slope is sub-vertical. Differential synthetic aperture radar (SAR) has been used to quantify landslide displacement over large areas (Fruneau *et al.*, 1996; Massonnet and Feigl, 1998; Rott *et al.*, 1999; Vietmeier *et al.*, 1999),

although detection is restricted to the direction of the SAR antenna illumination (Hervás *et al.*, 2003). Adams and Chandler (2002) evaluated the accuracy of LiDAR and medium scale photogrammetry to detect change over the Black Ven landslide complex in Dorset. The overall root mean square error for LiDAR and photogrammetry were found to be 0.26 m and 0.43 m respectively for the 1:7,500 scale models. Such aerial techniques have typically proven effective at quantifying change over low angled coastal slopes prone to rapid change caused by extreme weather phenomena. Hapke and Richmond (2002), for example, used aerial digital photogrammetry to record three-dimensional variations in the magnitude and spatial extent of episodic cliff failures caused by the 1989 Loma Prieta earthquake and the 1997-1998 El Niño storms, although little consideration was given to the errors involved. Hapke and Griggs (2002) used stereo images taken in 1942, at 1:30,000 scale, and 1994, at 1:24,000 scale, to generate digital terrain models (DTMs) of the steep-sided slopes along the Big Sur Coast, California. The DTMs were subtracted to calculate a total volumetric retreat, which was then averaged to estimate yearly rates of change. The volumetric errors were estimated to be between 3% and 5% meaning reliable detection was restricted to the rarer, larger events which may not be described well by annual rates of change. Furthermore, when geomorphological change is more subtle, and the coastal environment less prone to catastrophic events, aerial surveys become limited and are rarely able to capture the frequent and often small-scale iterations that characterise short-term rock slope behaviour.

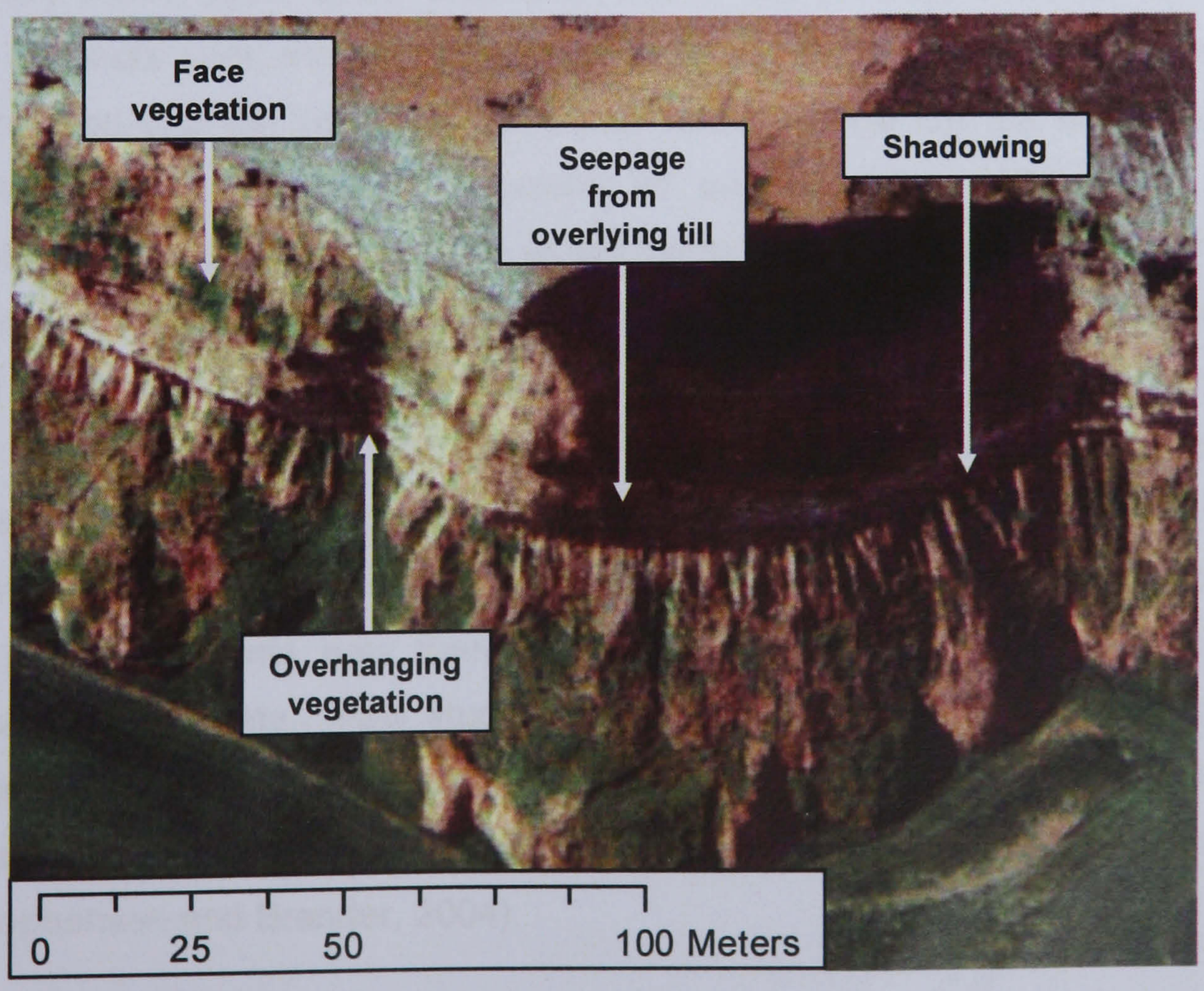

Figure 2.6: Example of an aerial photo of rock cliffs. The position of the cliffline is obscured by tonal and light contrasts and material interactions.

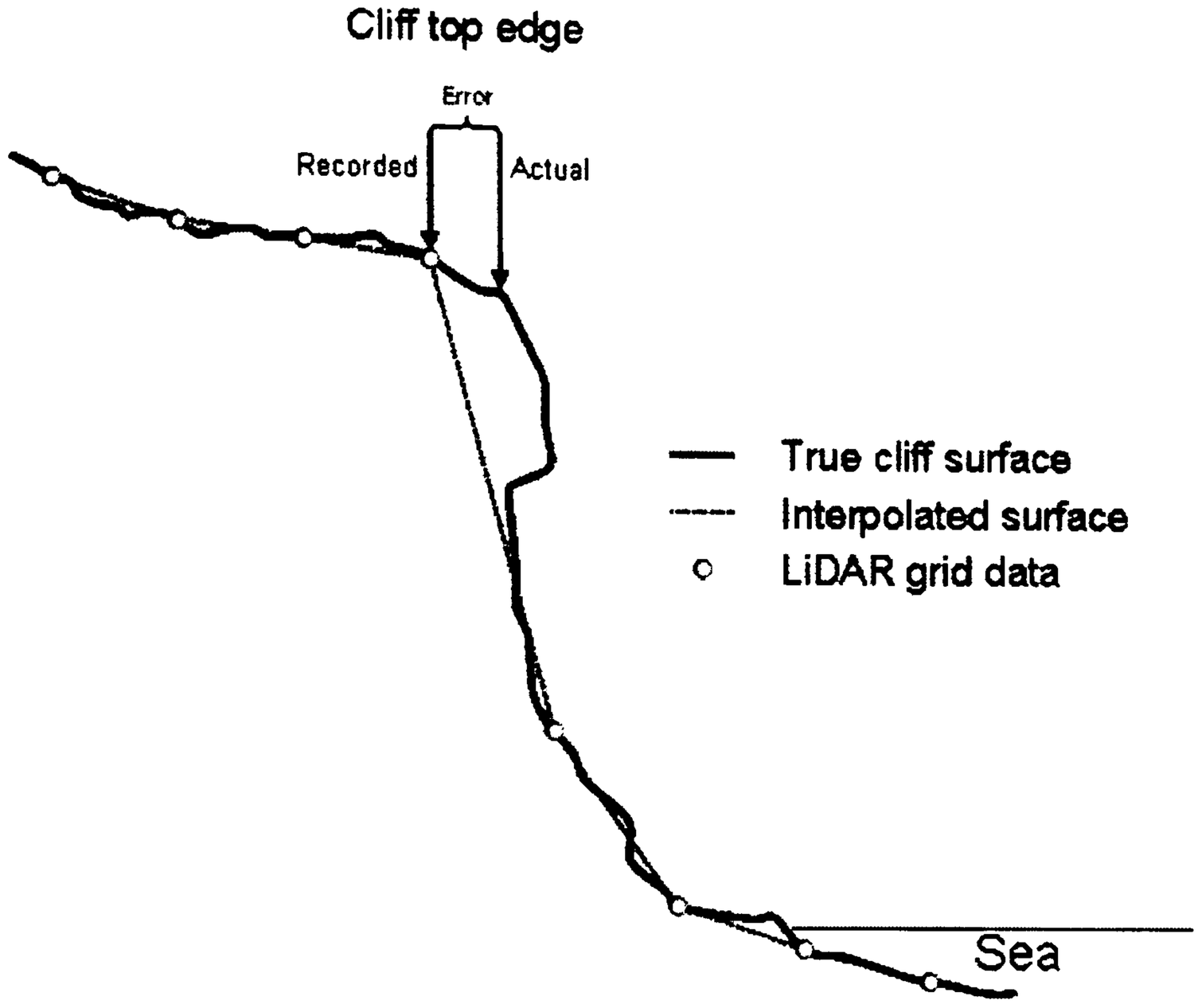

Figure 2.7: The problematic nature of LiDAR grid data in cliffline studies. Despite the accuracy of the grid data obtained with LiDAR the location of the cliff top edge remains problematic, incurring errors between the interpolated surface and the true cliff position; an important consideration because most cliffs retreat at sub-metre annual rates (after Mikhail *et al.*, 2001).

Data derived from aerial surveys have dominated investigations of cliff evolution (Emery and Kuhn, 1980; Zviely and Klein, 2004), and provided evidence for many of the key concepts upon which understanding of coastal cliff behaviour is based. The errors involved and the limited frequency at which change can be monitored cause questions to be raised over the validity of such theories, which have become embedded in rock cliff studies. Even yearly flights to record cliffline positions are rare and difficult to sustain in the long-term, often requiring comparisons of the slope across different seasons or times of the day (Hervás *et al.*, 2003). Oka (1998) relied on imagery captured in 1968, 1969, 1978, 1983 and 1988 to measure active slopes in northwest Nagano Prefecture, Japan, restricting analysis to patchy and sporadic developments in mountain slope erosion. The apparently episodic behaviour of recorded rockfall events may therefore be an artefact of the infrequent temporal resolution of aerial data. Few studies have been able to satisfactorily quantify the spatial and temporal episodicity indicated by many aerial approaches (Hampton *et al.*, 2004), although episodic behaviour is often assumed to apply generically to coastal cliffs (Stephenson and Brander, 2004).

The most important limitation on the improvement of knowledge on hard rock coastal cliff evolution provided by aerial approaches is that they fail to account for any

of the changes occurring over the cliff face itself. The assumption that the cliff top and/or cliff toe positions may be used as a proxy for the behaviour of the overall landform is logical in the long-term, particularly for near-vertical cliffs, but gives no indication of how cliffs evolve. There is little empirical evidence to suggest that hard rock cliffs retreat uniformly through time or that planimetric changes in the cliffline correspond to slope-wide responses. Thus, many rock cliff studies to date have remained fundamentally restricted by a technique and data driven emphasis on retreat rates. The omission of data on the changes across the cliff face has meant that investigations into coastal cliff geomorphology have formed views of development based upon qualitative observations constrained by general retreat rates of the cliffline. Ultimately it is not the overall rate at which landforms retreat but the manner in which change takes place that should provide the primary concern of studies seeking to understand cliff behaviour. To achieve this, more appropriate perspectives such as those provided by ground based approaches are required. Terrestrial techniques for recording cliff change can be divided into manual and remote sensing approaches.

2.8.2 Manually collected records of cliff change

The majority of terrestrial approaches to cliff monitoring rely on manual measurements of subsections of rock face, considered to be representative of the wider area being analysed. Fixed ground control points can be used to conduct surveys over shallow angled cliff faces (Miller and Aubrey, 1985). Vaughan (1932) collected repeat surveys from the cliff base to fixed points on the shore platform, recording an erosion rate of 0.18-0.36 m a^{-1} in cliffs in southern California. Differences in erosion rates were detected, with higher cliffs taking longer to erode back in the long-term as a result of significant volumes of debris that protected the toe following failures. The data suggested that large magnitude events may exert a scale effect on the long-term development of the cliffline, although the usefulness of a single erosion rate for any cliff section based on manual point surveys is questionable (Robinson, 1974). More recently, the development of differential GPS has enabled the location of cliff top positions to be achieved to sub-centimetre accuracies (Buckley and Mills, 2000). However, this technique cannot record cliff face changes and is of limited use in locating the position of the toe of high near-vertical cliffs, which restrict satellite coverage.

Approaches to recording change over rock cliffs themselves are generally limited by inaccessibility to studies of the cliff toe. There are many problems associated with the physical measurement of rock surfaces, most notably in obtaining representative spatial coverage. The varying lifespan of 3 mm deep graffiti on cliff

faces has for example been relied upon to estimate the rate of surface retreat, attributing the temporal differences to the prevalence of storm events between inscribed dates (Emery, 1941). More controlled approaches have been used to establish an average erosion rate of approximately 0.03 m a^{-1} along the southern Californian coastline between 1971 and 1973, using 0.25 m nails driven 1 m above the base of sandstone cliffs (Pinckney and Lee, 1973). Later Lee *et al.* (1976), further recorded recession ranges between 0 m a^{-1} and 0.04 m a^{-1} across 31 sites in the same area. The data collected using such approaches are restricted to measurements of abrasion, excluding larger rock failures that typically result in the loss of the nail. It has also been suggested that the act of driving the nails into the rock may weaken the cliff material, causing artificially high rates of retreat (Emery and Kuhn, 1980).

Thus, a range of questions remain unanswered about the diversity of change within rock cliffs because of the inability of manual measurements to achieve satisfactory coverage and resolution. In some cases it is simply impossible to establish any change from photographs (Shepard and Grant, 1947), even where they have been collected specifically to record landform development. Even studies over 35 years or more have failed to report little more than qualitative aspects of change, such as the growth of biological communities, the downwearing of surfaces, and the rounding of edges (Emery and Kuhn, 1980).

The near-vertical profile, large scale and inter-tidal exposure of hard rock coastal cliffs make them inaccessible, dangerous features to work on. The resultant need to assume that two-dimensional alterations in the selected cliff positions can be used as an effective measure of slope retreat has restricted the interpretation of coastal cliff behaviour. The importance of volumetric considerations in rock slope analyses is now recognised (Hantz *et al.*, 2003; Hapke and Griggs, 2002), although there remains a notable absence of data to accurately quantify both large scale events and small scale iterative change across slope faces (Brunsden, 1996).

2.8.3 Remotely sensed terrestrial records of cliff change

The primary requirement for the characterisation of landform behaviour is the ability to record change at every significant scale, within known error margins. Advances in remote sensing have begun to address the challenges of deriving data from inaccessible environments such as rock cliffs (Chandler and Moore, 1989). Remotely captured data helps to circumvent the problems that have limited manual data collection for inaccessible landforms such as steep slopes. Remote data capture enables features to be classified, digitised and extracted for further analysis. Despite

the omission of datasets on the changes across near-vertical rock slopes, the potential of terrestrial digital photogrammetry (Chandler, 1999) and terrestrial laser scanning (Nagihara *et al.*, 2004) to record high-resolution change across wide areas has been acknowledged in other landform studies.

Photogrammetry is a technique whereby stereo images are rectified of distortions, co-registered and used to extract digital elevation models (DEMs) and three-dimensional orthoimages, providing both planimetric and topographic data. The reconstructed surfaces can be used to measure, quantify and analyse landforms over successively monitored time intervals (Figure 2.8). In recent years, the availability of increasingly sophisticated, cost-effective and automated digital systems has facilitated the use of photogrammetric techniques in a wide variety of landform studies, from fluvial (Pyle *et al.*, 1997) and hillslope (Oka, 1998) to desert (Livingstone *et al.*, 1999) and glacial environments (Baltsavias *et al.*, 2001). With regard to rock slope investigations, the potential of photogrammetry to remotely record qualitative and quantitative data on morphological change has long been recognised (Wickens and Barton, 1971; Hoek and Bray, 1981).

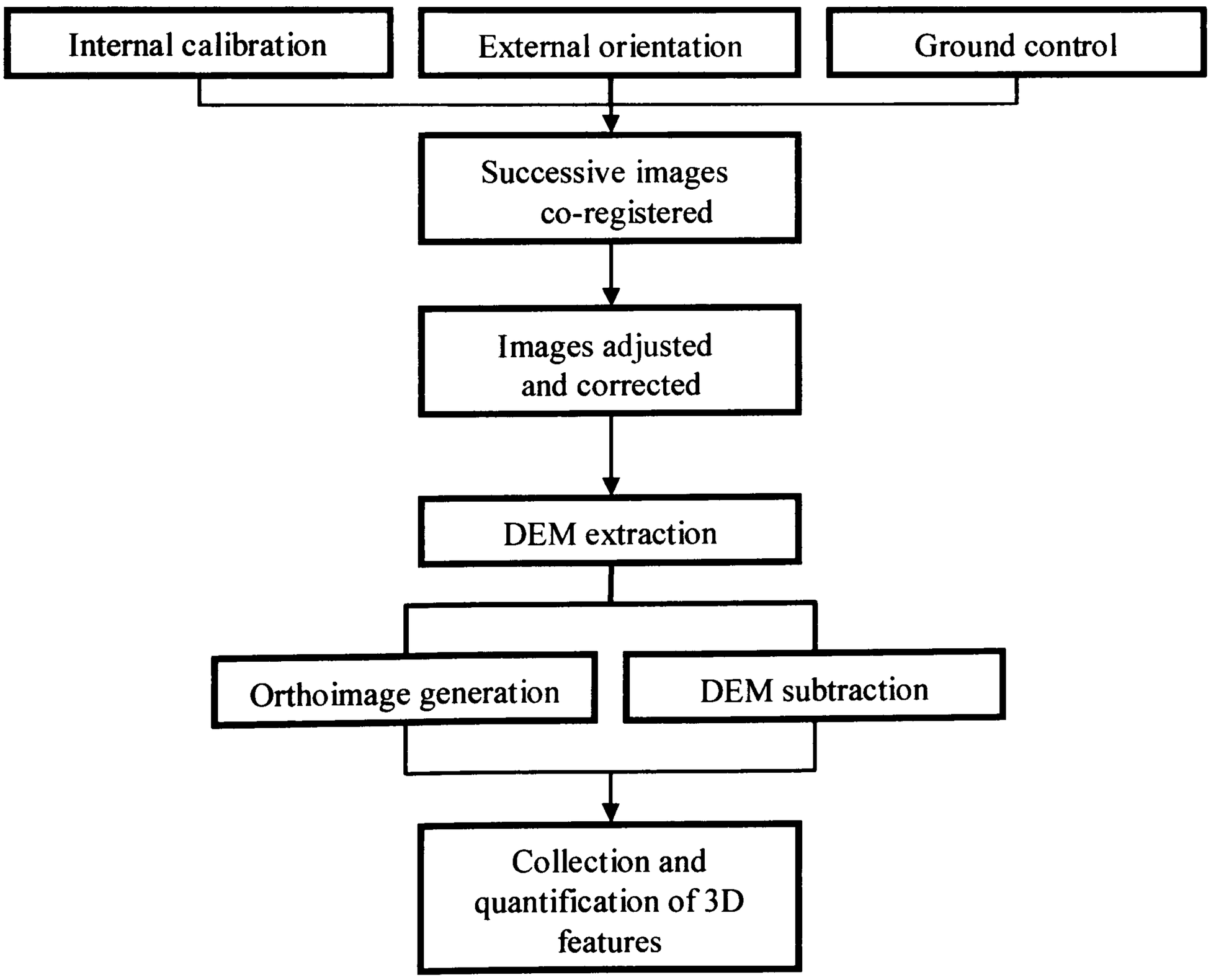

Figure 2.8: Photogrammetric workflow. The diagram describes the process of deriving three-dimensional data on subject terrain from the triangulation and adjustment of stereo images. The extracted elevation data may then be used for the three-dimensional investigation of landforms.

Although the potential exists for terrestrial photogrammetry to record the distances, areas, volumes and orientations of rock slope change, the challenges of applying such a precise and controlled science to an environment as dynamic as coastal cliffs however have severely restricted such studies. Attempts to analyse photogrammetric performance over 15 m^2 patches of rock face found significant information loss across reconstructed surfaces (Huang, 2000). A limited number of terrestrial studies have been successfully applied where small scale landforms enable sufficient access for adequate ground control to be established. River bank erosion calculations were made for a 60 m section of the River Yarty in Devon by physically positioning circular targets on the banks (Barker *et al.*, 1997). The scale of these applications has remained limited by the need to manually locate artificial control points on the reconstructed surface (Pyle and Richards, 1997), proving a hindrance to the use of photogrammetry on sheer-sided rock faces unless accessibility can be gained with the use of a costly hydraulic platform for example (Cheffins and Rushton, 1970). The quality of photogrammetric monitoring across cliff faces is further degraded by the oblique perspective, weather conditions and rapidly changing natural topography (Lim *et al.*, 2005).

The limitations associated with matching images captured with visible light have prompted the development of sensors that function with wavelengths beyond the optical spectrum. The development of increasingly sophisticated and versatile terrestrial laser scanning technologies now offers a new method of remote sensing for geomorphological applications (Nagihara *et al.*, 2004). Although a wide variety of scanning systems now exist, the majority fall within two broad concepts of data collection. Triangulating laser scanners emit a concentrated pulse of light onto a surface which is captured by a fixed digital sensor, enabling highly precise triangulations to be made of recorded surfaces (Ahmon, 2004). The limitations associated with triangulating systems in terms of geomorphological applications are the size and weight of the devices, their fragility, the excessive data sets generated and most importantly their limited range, which is typically within 10 m. The second category of terrestrial laser scanner uses time-of-flight data capture techniques. Time-of-flight technology assumes the speed of an emitted laser pulse to be constant, therefore using the time taken for the light pulse to return to calculate the distance to the target. When fitted to a motorised head, the laser emitter can be passed back and forth over surfaces to form a detailed impression of elevation changes. This approach allows for the increments between passes and within pulse emissions to determine the resolution of data collected.

The datasets produced by laser scanning offer effective solutions to many of the issues limiting photogrammetric performance for reconstructing cliff faces. The point clouds generated offer consistent three-dimensional representations of the cliff face, which can be triangulated or sub-sampled for further analysis of the landform. Laser scans are not significantly influenced by light contrasts, shadowing or perspective variations, reducing the potential errors caused by the ambient conditions at the time of data collection. The raw form of the information in laser scanning can also be the DEM itself, avoiding issues of processing performance in the final model produced and eliminating the uncertainties associated with matching algorithms in photogrammetric DEM generation.

The use of terrestrial laser scanners in geomorphological applications remains limited at present (Kersten *et al.*, 2004). The absence of a precisely calibrated reflector introduces numerous variables into the distance measurement. The characteristics of the surface, its roughness, its distance from the scanner, the reflectivity of the material and its angle towards the incident beam all influence the strength of the return signal (Lichti and Harvey, 2002). The band widths used (750 – 1500 nm) function on the periphery of atmospheric wavelengths, allowing certain portions of the radiation to be absorbed into the atmosphere. This causes wet surfaces such as wave-soaked rock material to have a lower reflectance, degrading the signal strength of the reflected beam. When analysing scanned models the lack of colour data also limits the qualitative assessment of data recorded, restricting interpretation of the circumstances under which geomorphological change has occurred; although recently developed camera and scanner systems have begun to capture coloured point clouds. Despite these issues, the point cloud data produced over the ranges concerning the monitoring of cliff faces up to 100 m high are capable of producing accuracies within ±0.06 m, offering enormous potential for geomorphological applications.

The range of monitoring approaches now available requires researchers to select the most appropriate technique for each specific application (Moore, 2002). The inability to satisfactorily resolve rock cliff change from all but the most regularly eroding coastlines has raised serious questions over the use of general retreat rates (Robinson, 1977). Whether or not extrapolated annual recession rates can be effectively used to characterise the patterns of rock slope behaviour has yet to be detailed. Little is known about the dominant frequencies, scales and patterns at which the changes in rock cliffs are governed, and whether these alter over time. The most important aspect to monitoring coastal slopes remains the resolution at which change can be reliably recorded within clearly identified and quantified errors (Lane *et al.*,

1998), which has largely been ignored in geomorphological literature (Hampton *et al.*, 2004).

2.9 The mechanisms driving rock cliff change

Understanding hard rock coastal cliff behaviour is limited not just by an inability to accurately record the alterations in slope form but also by the mechanisms driving the changes. Change in rock cliffs generally involves interacting pieces of rock, from small fragments to large coherent blocks, all with different material and structural properties and subject to diverse environmental influences that vary spatially and over time. Although they form an essential component of the overall response of the cliff, direct measurement of the mechanisms of change in rock cliffs is rarely achievable. Investigations into the mechanics driving the frequency, magnitude and duration of cliff processes have therefore led to many different approaches for evaluating rock mass behaviour (Lanaro *et al.*, 1997).

The mechanisms of rock cliff change develop in response to the forces acting on specific *in situ* conditions within the slope. Lithology, stratigraphy and geological structure all combine to provide controls on the nature of failure (Emery and Kuhn, 1982). The manner of retreat is therefore strongly influenced by site specific differences in slope-forming materials (Prior and Renwick, 1980; Brunsden, 1984). At the coast, attempts have been made to attribute cliff change to dominant controls such as morphology (Agar, 1960), joint structure (Davies *et al.*, 1998), face geometry (Williams *et al.*, 1993) and geology (Dickson *et al.*, 2004). Bray and Hooke (1997) directly link the proportions of clay material within the cliff to sensitivity to change, suggesting that cliffs with higher clay contents display a more seasonal recession signal. The effects of more subtle or complex variations in rock properties are poorly understood and are often restricted to qualitative assessments.

The dominant control on the stability of a rock slope is often the presence and nature of discontinuities in the rock mass (Priest and Hudson, 1981). In such cases it is not the intact strength of the rock but the cohesive and frictional characteristics of the discontinuities that are thought to determine rock mass properties under stress (Hoek, 1983). Investigations into the effect of mechanical weaknesses on slope behaviour have demonstrated the significance of discontinuity characteristics such as spacing, orientation, aperture, infilling material and continuity on rock mass strength (Jiang *et al.*, 1995). Spacing influences the effect of discontinuities on rock mass strength, with closer, more dense jointing causing a destabilising effect as behaviour becomes increasingly dominated by joint properties rather than intact material strength (Pritchard

and Savigny, 1989). The orientation of joints also has implications for the kinematics within the cliff. Randomly orientated joints commonly form interlocking rock sections with high friction angles, while uniform orientations may provide a fundamental control on the mechanisms of failure (Kimber *et al.*, 1998). Sedimentary rocks are often divided by horizontal bedding planes, generating near-vertical slope faces when the dip is less than the angle of friction (Selby, 1987), although failures may also occur as a result of additional joint networks. The aperture or width of joints determines the contact between the wall rocks and hence frictional resistance to applied stresses (Dong and Pan, 1996). Open joints also provide routes for weathering agents and infilling material to permeate beyond the exposed rock face, further weakening the constituent material (DeToledo and DeFreitas, 1993).

The persistence of discontinuities is a critical but poorly understood element of rock mass behaviour (Jing, 2003). On a simplistic level, vertically- or horizontally-aligned discontinuities within the rock mass do not permit simple sliding movement (Hoek and Bray, 1981), so yielding along discontinuities and internal fracture of rock bridges are required before failure can occur. Discontinuities play an important role in concentrating stress within the cohesive elements of the rock mass. Attempts have been made to establish the influence exerted by fracture and discontinuity growth by simulating random joint distributions in rock mass analyses through probabilistic methods (Dershowitz and Einstein, 1988). More mechanically-based approaches have illustrated that the factor of safety for a given slope may be over-estimated if the process of joint propagation as stresses concentrate at crack tips is ignored (Scavia, 1995). Small alterations to discontinuity persistence may also result in large changes to the factor of safety (Scavia, 1990). The progressive nature of failure was theorised into general model guidelines by Bjerrum (1967) where a shear surface is propagated, developing a continuous sliding surface before failure can occur. In such a scenario, failure will progress though a rock mass as the shear strength of consecutive intact portions of rock within the active zone is exceeded.

The multiple and interacting factors involved with rock mass behaviour means that the mechanisms driving rock cliff change must ultimately be simplified in order to be studied. Attempts to consider the mechanisms behind rock cliff responses can be broadly divided into two approaches: investigation of the relevant influences on failure through the identification and weighting of the relevant parameters (Deere *et al.*, 1969; Bieniawski, 1978; Goodman, 1980); and the recreation of the mechanical conditions within the landform with the use of numerical model simulations (Dershowitz and Einstein, 1988; Ramamurthy and Arora, 1994).

2.9.1 Rock cliff parameterisation

One approach to understanding landforms is to parameterise the contribution of the various components that influence the nature of the change. Detailed quantitative information on rock mass properties is difficult to acquire, rendering the measurement of internal stresses and strengths within the rock impractical for many assessments. Engineering approaches have sought to gauge the stability of diverse rock forms by rating the different influences on slope response based on sample data (Terzaghi, 1946; 1950; Barton *et al.*, 1974; Bieniawski, 1986). In many rock slopes the information is based on extrapolations of slope face measurements but in the case of steep-sided cliffs, where the face exposures are inaccessible, sample data is generally further restricted to measurements and observations made from the slope toe.

Many attempts have been made to characterise, order and extrapolate the contribution of rock mass parameters to the mechanisms governing behaviour (Cameron-Clarke and Budvari, 1981; Dershowitz and Einstein, 1988; Hoek, 1983; Price, 1993; Ramamurthy and Arora, 1994). All rating systems are limited by their simplicity and the nature of their weighting, placing significant emphasis on the ability to obtain data 'representative' of the whole landform. The relation of limited measurements to the mechanisms of cliff change depends on how consistent the wider rock mass properties are with respect to the sample used. In general, engineering parameterisations of rock mass behaviour require the characterisation of geological and geometrical factors, although some also include process conditions such as the presence of groundwater (Barton *et al.*, 1974). For example, the Rock Quality Designation (RQD) developed by Deere (1989) attempts to quantify the degree of weakening within the overall mass. The designation associates the loss of mechanical strength with the amount of fracturing caused by jointing. Discontinuities within the rock mass have been estimated from the number of joints within a representative unit volume (Palmström, 1982), the number of sections within a standard core size (Deere, 1989) or the variation in the velocity of seismic waves caused by the elastic properties of the rock (Sen and Kazai, 1984; Singh and Goel, 1999). Modern engineering systems relate the RQD with other variables such as uniaxial compressive strength (Serafim and Pereira, 1983) and joint roughness measurements (Cording and Deere, 1972) to form a cumulative rating for the ability of the rock slope to resist stress.

Analyses of the contribution of different parameters within classifications have shown the importance of the placement and orientation of planes of weakness in controlling form and failure (Hutchinson, 1973; May and Heeps, 1985; Williams, 1987;

Dershowitz, 1988; Gerrard, 1988; Cundall, 1992; Dias and Neal, 1992; Allison, 1993; May and Hansom, 2003). Engineering classifications such as the Rock Mass Rating system (Bieniawski, 1973) and the Rock Mass Quality system (Barton *et al.*, 1974) are limited to types of rock mass similar to the empirical case histories from which they were designed (Emery and Kuhn, 1982). The emphasis of different parameters within specific schemes means that at least two are generally required for initial site classifications to obtain a representative impression of the stability conditions (Hoek *et al.*, 1995). Rating schemes should also therefore be performed separately for subsections of larger rock masses, due to the heterogeneous nature of many rock masses.

Generic parameterisations have typically been restricted to divisions based on a few landform controls, such as morphology, geomechanical material properties and behaviour (Robertson, 1970; Hutchinson, 1973; Barton, 1974). Geomorphologists have modified engineering classifications to study rock slope forms with respect to processes (Allison, 1996). The Selby (1980) Rock Mass Strength classification scheme uses the flow of water through the rock mass; its intact strength and weathering state; and discontinuity properties such as width, continuity, filling material, spacing and orientation to categorise rock slope competence from very strong through to very weak (Table 2.1). These criteria have been used to develop theories on the interactions that determine geomorphic form, but remain semi-quantitative in their understanding of the mechanisms of change.

The interaction of weighted parameters has been used to explore the mechanical relationship between rock mass strength and slope angle with the concept of slope strength equilibria (Abrahams and Parsons, 1987). The equilibrium slopes can be plotted within a 95% confidence envelope to define the limiting equilibrium conditions of the rock masses described in the field. In addition to assuming the ability to accurately characterise rock mass parameters (Jaeger, 1972), analyses based on rock mass rating schemes often rely on direct and simple responses to changes in certain predefined factors. The assumptions upon which many of the hypothesised responses are based however lack both an empirical basis and a detailed consideration of complex and interacting processes involved with cliff behaviour. Whether or not a slope will indeed reach an equilibrium condition with its environment over time is important to understanding the nature of mechanisms governing behaviour but has yet to be satisfactorily proven for rock cliffs; the usefulness of such analyses therefore remains questionable. Rather than assign static parameters to a landform, it

is perhaps better to form dynamic models capable of accounting for processes and mechanisms that change over time.

Table 2.1: Rock mass strength classification (Selby, 1980).

Parameter	*1 Very Strong*	*2 Strong*	*3 Moderate*	*4 Weak*	*5 Very Weak*
Intact rock strength (N-type Schmidt Hammer 'R')	100-60	60-50	50-40	40-35	35-10
Rating	20	18	14	10	5
Weathering	Unweathered	Slightly weathered	Moderately weathered	Highly weathered	Completely weathered
Rating	10	9	7	5	3
Spacing of joints	>3 m	3-1 m	1-0.3 m	0.3-0.05 m	<0.05 m
Rating	30	28	21	15	8
Joint orientations	Very favourable. Steep dips into slope, cross joints interlock	Favourable. Moderate dips into slope	Fair. Horizontal dips, or nearly vertical	Unfavourable. Moderate dips out of slope	Very unfavourable. Steep dips out of slope
Rating	20	18	14	9	5
Width of joints	<0.1 mm	0.1-1 mm	1-5 mm	5-20 mm	>20 mm
Rating	7	6	5	4	2
Continuity of joints	None continuous	Few continuous	Continuous, no infill	Continuous, thin infill	Continuous, thick infill
Rating	7	6	5	4	1
Outflow of groundwater	None	Trace	Slight <25l/min/10m²	Moderate 25-125l/min/10m²	Great >125l/min/10m²
Rating		6	5	4	1
TOTAL RATING	100-91	90-71	70-51	50-26	<26

2.9.2 Modelling the mechanisms driving rock cliff change

The ability to develop accurate models of material and process interrelations provides a key aspect to improving understanding of landforms (Richards *et al.*, 1995). Models are used to identify, interpret and define rock slope failure mechanisms through the simulation of specified interactions according to a prior level of knowledge of the system (Eberhardt *et al.*, 2004). Current understanding of the mechanisms through which rock cliffs evolve has been significantly advanced with the use of models (Davies *et al.*, 1998), although the varied and multifaceted controls on response over time has left many questions over the role of different mechanisms in governing change. Models are therefore limited by both the quality of existing input data and also the adequacy of the algorithms used in representing the rock slope mechanics.

Computer models have been used consistently for over 30 years to investigate the mechanisms of rock slope evolution, attempting to simulate the link between applied stresses and the responses in material strain. Strain is a measure of the deformation of material and, when stresses exceed the resisting strength of the rock

mass, failure occurs (Kalaugher *et al.*, 2000). The behaviour of most cliff material is non-linear, undergoing progressive weakening, permanent deformation and failure. Failure in rock masses is a complicated four-dimensional event, with responses that vary spatially and through time according to both inherited and current controls (Brunsden, 1999). Failure mechanisms have been investigated and defined by carefully controlled variations in model inputs, derived from measured field and laboratory data (Kimber, 1998). Simulating phenomena such as the thresholds of rock slope failure can provide powerful tools in understanding more about landform change, when viewed within the limitations of the model being applied (Henscher *et al.*, 1996). Dynamic numerical codes for instance, including limit equilibrium, finite and discrete element models, use Newton's laws of motion to determine the movement and interaction of material constituents over successive time steps. The modelled interactions offer more sophisticated and versatile forms of analysis than the static parameterisation of the influences on behaviour although once again caution must be exercised over the assumptions made in each model applied.

2.9.3 Limit equilibrium models

Failure is the primary component of how cliffs change. Thus, an essential problem to be addressed in rock cliff studies is whether or not a slope will fail (Cruden and Eaton, 1987). Limit equilibrium models of rock slope behaviour usually determine a factor of safety based on vector analysis of predefined discontinuity interactions (e.g. Hudson and Harrison, 1997), in order to establish whether it is kinematically possible for a specific rock block to move and become detached from the rest of the rock mass. Early deterministic equilibrium solutions that considered the factor of safety for a single block have been replaced by evaluations for several element masses within a slope. Based upon the solution of two criteria, block sliding and block toppling, the normal and parallel forces can be resolved to derive a factor of safety for the potential movement of a rock slope with many interacting elements (Goodman and Bray, 1976).

Although limit equilibrium models have offered a means by which more detailed considerations of the mechanisms of rock slope change can be investigated (Duncan, 1996), the rigid criteria and simple and predefined nature of possible responses limits their application to the reality of complex landform behaviour (Pritchard and Savigny, 1989). Useful limit equilibrium analysis is generally confined to small-scale engineered slopes (Wyllie, 1980; Zanbak, 1983), using only a static balance of forces to calculate the retaining force required for engineering structures (Piteau, *et al.*, 1985). Thus, limit equilibrium techniques are best suited to determining behaviour in rock masses with simple, regular and widely spaced discontinuity networks (West, 1996), and have been

verified with simple physical models (Nash, 1987; Aydan *et al.*, 1989). This generally restricts geomorphological understanding of failure mechanisms to user-defined and planar failure surfaces determined exclusively by joint shear and separation (Pritchard and Savigny, 1989). Limitations are also encountered in understanding the multiple, interacting aspects of material response, with no consideration of strains and the failure of intact material. A deeper understanding into the processes and interactions of cliff failure has been gained by the development of more powerful numerical element models (Coggan *et al.*, 1998), which can be divided into finite element, discrete element and, most recently, combined finite/discrete element approaches.

2.9.4 Finite element models

One of the most challenging issues in evaluating landform behaviour is to account for the deformation of a material under applied stresses. In order to model rock slope responses through time finite element models (FEMs) use continuum mechanics to simulate variability within different materials. The finite element model mesh is able to adjust as material progressively fails, accounting for the nonlinear behaviour typical of rock masses. Developments in FEMs have taken analyses of jointed masses beyond assumptions limited to a simple computational force and movement equilibria (Zienkiewicz, 1977), allowing the development of first time failures to be investigated without assuming a shear plane and failure mechanism (Duarte *et al.*, 2000). The model mesh allows more complex rock slope stability problems to be considered (Hicks and Samy, 2002), relating to detailed face geometry, material anisotropy and *in situ* stresses. In order to solve a continuous problem, the nodes are ascribed infinite degrees of freedom, mathematically confined within sub-domains that conform to the continuity condition (Jing, 2003). The continuity condition allows material deformation but prevents the development of tears or fractures dividing the material. The homogenization of the microscale discontinuities in the material allows generalised patterns of change to be simulated in rock masses with variable material and structural properties. Slope stability is subsequently modelled and analysed by inducing failure, either through the increase of gravitational loading, or the reduction of strength characteristics over time.

FEMs have improved understanding into a variety of failure mechanisms in rock slopes such as block toppling (Cruden, 1988; Cruden and Hu, 1996; Kakani and Piteau, 1976), flexural toppling (Adhikary *et al.*, 1996), wedge sliding (St John, 1971), and sliding and toppling movements (Bovis and Evans, 1995). The ability to simulate the initiation of failure has promoted FEMs as an effective tool for the assessment of slope stabilisation (Wyllie, 1980), and the deployment of remedial measures such as

the reduction of slope height and face angle and the constraint of the slope toe (Wyllie and Wood, 1983). Treatment of the problem slope as a continuum allows FEMs to analyse the effects of changes in material state (Hall, 1996).

Despite enabling complex and non-linear failure mechanisms to be studied, the use of continuous model meshes restricts FEMs to indications of movements provided by relatively small displacements in the simulated material. Furthermore finite element analyses cannot consider the interaction of multiple individual blocks. This has limited continuum applications in the consideration of situations where rock mass behaviour is governed by large movements and even detachments of rigid portions of rock. Although well-suited to analyses of homogeneous slopes, the focus on a single, coherent problem material causes continuum models to significantly overestimate the strength of rock formations that are weakened by discontinuities (Senseny and Simons, 1994). Appropriate models of hard rock slope geomorphology require the simulation of material behaviour beyond initiation to progressive degradation, failure and adjustment.

2.9.5 Discrete element models

The importance of structural weaknesses such as bedding planes, joints, faults and tension cracks mean that rock slope behaviour is not coherent but discontinuous, fragmented and therefore spatially and temporally complex. Discontinuous numerical methods such as the Distinct Element Method (DEM) developed by Cundall (1971) and Discontinuous Deformation Analysis (DDA) developed by Shi and Goodman (1984) consider the rock mass to be an assemblage of interacting blocks. Both approaches have been successfully applied to stability problems involving highly jointed rock masses (Shi, 1993; Kimber, 1998). These applications have enabled the investigation of discontinuity orientation effects of entire joint sequences (Brady *et al.*, 1990; Sitar and MacLaughlin, 1996). The models provide more useful interpretations of rock slope behaviour because the development and interactions within the rock mass can be simulated after the initiation of failure.

Discrete models represent the rock slope materials as an assemblage of blocks, considering joints to be interfaces between block boundaries rather than specific elements. This flexibility allows assemblages of blocks to accommodate both complex deformations such as slides and localised responses where joints, or block divisions, open and close (Hart, 1993). The individual blocks are considered to be discrete elements that are allowed to move in response to applied stresses within each time step of constant velocities and accelerations. The individual elements can be

attributed constant-strain properties enabling distinct element analyses to consider complex non-linear structural influences on slope development (Kimber, 1998), in addition to failure resulting from material deformation (Itasca, 2000). Discrete models have shown rock masses to be sensitive to both discontinuity spacing (Hencher *et al.*, 1996) and orientation (Stead and Eberhardt, 1997), highlighting the importance of obtaining accurate initial structural data for the model.

One of the main limitations of discrete analyses is the assumption that joint networks are continuous. The validity of assuming discontinuities visible in the rock face extend uniformly throughout the rock mass, and can be predefined through either regular or stochastic determination (Lee *et al.*, 1990), is questionable for many cliffs. Many rock joints do not form complete divisions between distinct blocks. The non-continuity of joints in rock slopes was first investigated with limit equilibrium analyses (Lajtai, 1969; Jennings, 1970). The interaction between shear and tension failure in the intact rock and the expansion of discontinuous joints was found to be a particularly important control on rock mass development (Einstein *et al.*, 1983). Subsequent attempts have been made to account for the progressive development of discontinuities under stress using FEMs, adapted to allow fracture through the material (Scavia, 1995).

2.9.6 Combined finite/discrete element models

For the majority of rock mass mechanisms to be modelled accurately, numerical models capable of simulating the degradation, yielding, fracture, failure and release of material are required (Singh and Goel, 1999). The implication is that models must be able to represent the interaction between both continuum and discontinuum element analyses in order to increase their relevance to the behaviour of natural rock masses. An early attempt to account for the progressive nature of failure in rock slopes used thin layers of finite elements to replicate joint properties that could then be simulated over time (Fishman *et al.*, 1991). Linear elastic fracture mechanics have since been applied to represent fracture propagation along non-continuous geological weaknesses (Scavia, 1995). The rock structure, its geometric configuration and the mechanical characteristics along its discontinuities have been used to define the behaviour of cracks; allowed to open, slip and tear. The ability to simulate fractures through rock material indicated that the incorporation of continuous joints extending through the rock mass may generate conservative estimates of stability, while the rock divisions between blocks resulting from fixed length discontinuities may equally overestimate slope stability (Scavia, 1995). Improved models of the mechanisms governing rock cliff behaviour therefore require the capacity to simulate the propagation of discontinuities,

dependent on both the stress concentration at crack tips and the cohesive material strength (Dershowitz and Einstein, 1988).

The problem of accounting for the mechanisms of failure, from the accumulation of stresses, to responding strains, deformation and material yielding has led to the use of hybrid approaches in rock slope analyses. New codes, typically based on a finite element fracturing mass which requires no assumption to be made in advance over the shape or location of the failure surface, have been developed which are capable of adaptive re-meshing (Rockfield, 1999). Adaptive re-meshing enables individual elements to fracture and subdivide when stressed beyond critical material thresholds, allowing both pre-existing discontinuities and material fracturing to be modelled within the same simulation (Eberhardt *et al.*, 2004). Although the potential now exists for the complex and progressive nature of failure in rock slopes to be studied, from initiation through to the release and deposition of material, such analysis remain unexplored with respect to coastal cliff development.

Stereographic projection methods enable the static characterisation of rock joint planes in three-dimensions (Lin and Fairhurst, 1988) and have been used to differentiate between the preconditions for plane sliding, wedge sliding and toppling failure mechanisms (Leung and Kheok, 1987). However, the complexity of three-dimensional change has limited most dynamic numerical rock slope simulations to two-dimensional representations. Questions remain over the assumption that the third dimension of cross-sectional failures can be uniformly extruded (Dershowitz and Einstein, 1988; Eberhardt *et al.*, 2004), particularly in the case of rock slopes, which are inhomogeneous both planimetrically and vertically (Agliardi and Crosta, 2003). Although the complex mechanisms of failure can potentially be more realistically simulated, the importance of accurate and representative rock property characterisations increases by an order of magnitude. Any three-dimensional variation in slope geometry, material and structural properties or loading conditions will alter the nature of slope response away from generalised model behaviour. In addition to the complexity of analysis and interpretation (Warburton, 1981), the excess processing required for three-dimensional models has meant that advances to understanding of rock cliff evolution provided by numerical simulations have been largely restricted to two dimensions.

The study of the material and structural rock mass properties with numerical models continues to significantly advance understanding of the mechanisms of landform evolution, although the performance of such models is constrained by the

quality and adequacy of the site information obtained from field measurements (Richards *et al.*, 1995). The complexity of rock slopes means that selection and weighting of appropriate model properties has proven problematic. The general geotechnical principles within numerical models must therefore be tempered to site specific conditions (Purrer, 1997), and used to provide insights into the phenomena of rock mass failure rather than to attempt to recreate reality (Lemos, 1990).

2.10 Discussion: cliff behaviour

Much analysis of slope behaviour is focussed upon failure, with the focus on whether an event will or will not occur (Figure 2.9). Through field tests and models based on limit equilibrium approaches for example, established practices are able to determine whether or not certain types of failure are feasible. Such static, failure/no failure analyses reveal little about the true nature of the driving processes and responding mechanisms that govern landform evolution. Brunsden (1999) argued that in order to improve understanding into the nature of rock slope behaviour the initiation of failure should not be considered as an end point, but merely a transition to a new mode of activity. Questions must therefore be raised as to the validity of viewing the failure as an event. It is perhaps more appropriate to consider the release of material from the slope as merely a phase in the continual development of the landform rather than an independent incident. The process of failure may reveal more about landform response than about the event itself. Furthermore, in the context of rock slope studies, an over-emphasis on failure events, or top/toe retreat rates in the case of coastal cliffs, has meant many aspects of rock slope behaviour such as the patterns, scale and time dependency and controls on change remain poorly understood. Neither aerial surveys nor manually collected slope toe measurements provide appropriate data on the actual changes occurring in the cliff face. The investigation and interpretation of aspects of rock slope behaviour should exercise caution over concepts, such as magnitude-frequency relationships, scale dependencies and episodicity, which have become entrenched in studies of landform response but for which only limited supporting data exist.

Rock slope studies to date have largely concentrated upon understanding the mechanics of slopes of uniform lithology and structure (Kimber *et al.*, 2002) or uniform lithology and variable structure (Einstein and and Dershowitz, 1988). However, many natural slopes comprise materially and structurally variable constituents that do not readily conform to idealised behaviour patterns. Geomorphologists, geologists and engineers alike have tried to account for some of the complexity with the use of a wide range of monitoring, parameter characterisation and modelling techniques. All

approaches have advantages and disadvantages. Every concept of slope development is limited in its representation of reality by the accuracy of data on the processes and responding mechanisms of change. All rock slopes are subject to a range of mechanisms of change at any one time, acting and interacting over different spatial scales. Hard rock coastal rock cliffs for example are often overlain by softer glacial or fluvial sediments, or inter-layered with softer strata such as weak shales, governed by mechanics more closely associated with soils. A materially complex slope may therefore fail through creep and mud sliding in addition to block falls.

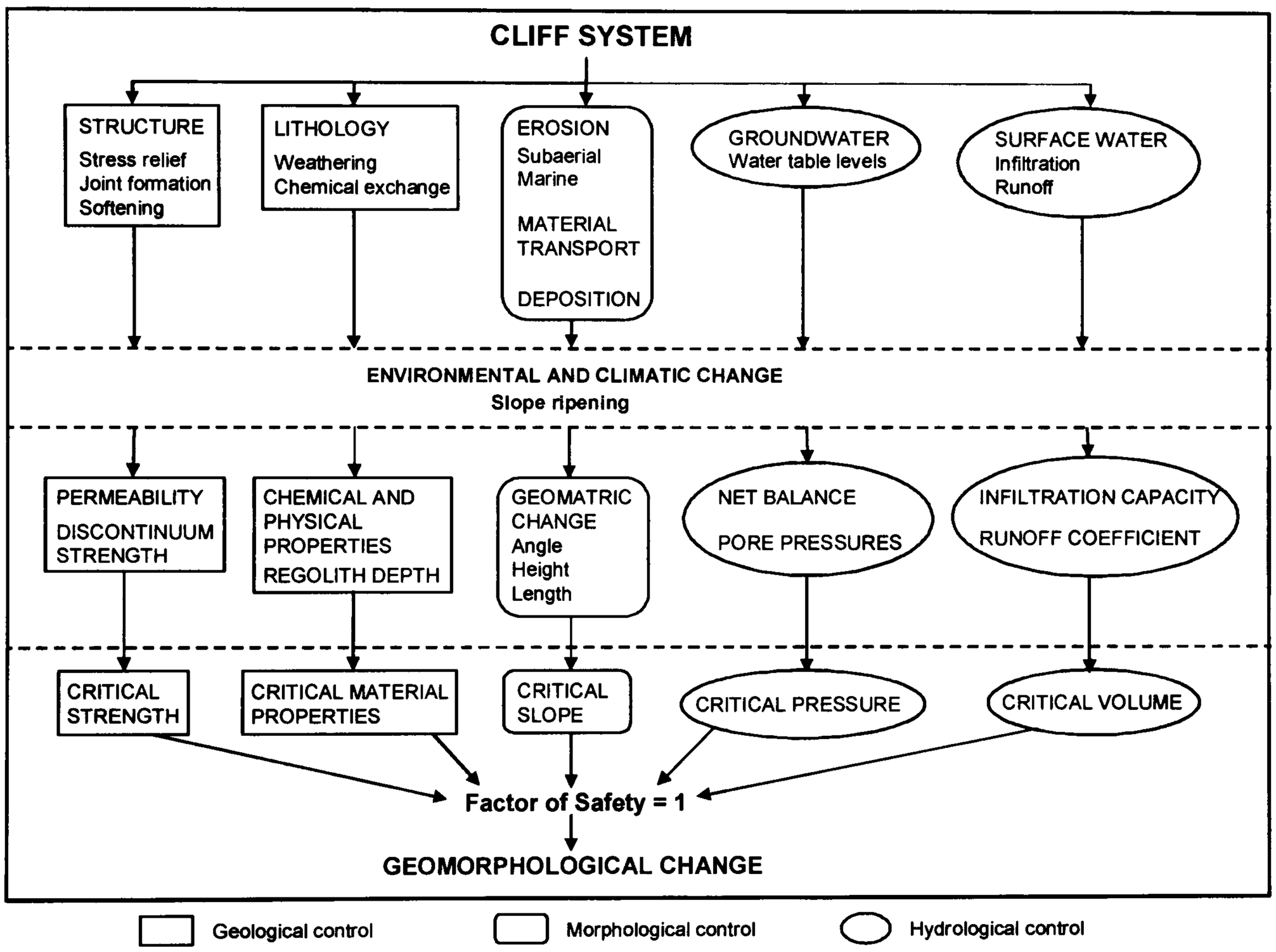

Figure 2.9: The development of coastal cliffs based on whether or not change will occur. The increased likelihood of change occurring is often over-emphasised at the expense of understanding the nature of the change and what it means for landform development. (After Brunsden and Lee, 2004).

Much of the weakness in our understanding of rock slope behaviour originates from the under–provision of high quality, long-term datasets. A benchmark paper in addressing this deficit was that of Rapp (1960) who measured creep, solifluction, debris flow, landslide, fluvial and chemical processes in Karkevagge, northern Scandinavia (Allison and Brunsden, in press). Detailed inventories were collected at least once a year between 1952 and 1960 gaining an appreciation of the processes influencing rockfalls, rock slides, snow avalanches and slush avalanches. Rapp (1960)

was able to identify the occurrence of pebble, small boulder and large boulder falls, and suggest possible controls on their development and resultant rates of slope retreat. This early analysis of the timing and triggers of different volumes of material failure underpins many of the current theories on rock slope evolution.

Studies into the frequency of events of different sizes have indicated that larger releases of material from slopes occur relatively less often than smaller events (Lee and Clark, 2002). Classic magnitude-frequency models have been proposed to explain this relationship for steep-sided rock slope behaviour (e.g. Luckman, 1976; Thornes, 1978; Agliardi and Crosta, 2003). Douglas (1980) used rock traps to estimate volume losses from cliffs in County Antrim, Northern Ireland. Quantification of the magnitude-frequency relations led to the distinction between losses of volumes below 0.2 kg, seen to be continuous throughout the year, and larger rockfalls, demonstrating seasonal frequencies. The data suggested that volumetric losses due to smaller but more frequent falls were greater over the two year monitoring period than those caused by larger events.

Despite significant advances into the occurrence of different magnitude events undertaken by the likes of Rapp (1960) and Douglas (1980), little is known about the processes which govern the spatial patterns of change over rock slopes. In order to infer process, detailed records of the mechanisms at each site are required. Whalley (1984) argued that it is rare to have any catalogue of magnitude, let alone frequency for large rockfall events, although perhaps the same could be said for medium and even small scale failures. Often, understanding of rock slope processes is theoretical, assumed from a specific set of characteristics, or laboratory based (Whalley, 1984).

Much of the current understanding of the spatial patterns of change in coastal rock slopes has been based on the analysis of rockfall inventories (e.g. Bray and Hooke, 1997; Hall *et al.* 2002; Lee *et al.*, 2002). The likelihood of similar scale events occurring are typically calculated from the cumulative probability distributions of historical records. The cumulative probability distribution refers to the time periods over which different magnitude failures are expected to occur. The increments of cumulative probability get progressively smaller with time to account for the increased chance that the event has occurred in previous years. Probabilities of failures of a certain size are often based on recurrence intervals, calculated by dividing the number of events of a certain magnitude by the number of years of continuous monitoring. Lee *et al.*, (2002) describe the temporal sequencing of a steady, relatively consistent basal retreat rate punctuated by brief episodes of larger scale fluctuations for example.

The dependence on historical distributions of rockfall events imposes significant limitations on the validity of model predictions. Return period statistics for example are highly sensitive to the reliability of the historical record. In order to achieve 95% confidence on the return period of a 50 year event, 110 years of continuous records are required (Benson, 1960). Contemporary monitoring records are also inadequate to quantify the potential for extreme events, such as the 1/1000 year recession, making analysis of such events particularly problematic (Hutchinson *et al.*, 2004).

In addition to the length of historical records, questions have also been raised as to how representative they can be considered to be. Every successive modification to the form of the cliff has the potential to alter the stress state away from conditions of the past. Slopes respond to environmental triggers such as rainfall over a range of time periods. Cliff movement may reflect an immediate response to a single, intense event that alters pore water pressures (Terlien *et al.*, 1995; Harp and Savage, 1997), or follow cumulative responses after successive sequences of wet years (Bromhead *et al.*, 2002). The use of historical records also assumes that the data provide consistent and reliable records of cliff failure, although the errors involved, as discussed above, are rarely considered and even large events often remain unrecorded if they do not directly affect human activity. Attempts have been made to address the problem of the commonly coarse spatial resolution of historical records with the use of site specific adjustment factors (Fell *et al.*, 1996), although probabilistic analyses will remain limited by the direct inference between past and future cliff behaviour and the lack of understanding of the nature of failure.

The reality of cliff retreat studies is that they are often based on rockfall inventories that are lacking, inaccurate and of insufficient temporal extent. The empirical relationships upon which probabilistic models are based, linking recession with triggering events, assume critical threshold levels can be determined and that these remain constant over time. Commonly used subjective estimates of modelled parameters, such as the semi-quantitative stability rating for San Diego cliffs (Benumof and Griggs, 1999), may be biased towards the personal experience of the investigator and often lead to varied estimates (Lee and Jones, 2004). Rock slope models often contain limited consideration of the wider range of influences on a rock mass, causing them to be highly sensitive to changes within a few parameters. Datasets of alterations in the line of coastal cliffs for example offer little specific information on the location, timing, rate and significance of the losses. Indeed coastal cliff retreat, involving the landward movement of the cliffline, has become synonymous with coastal cliff erosion,

which inherently involves three-dimensional changes over time, leading many studies to oversimplify the nature of cliff behaviour.

Material becomes detached from the cliff as either coherent blocks or interacting masses. With a few notable exceptions (Gardner, 1970; Douglas, 1980), intact block failure is rarely considered an important factor in the overall shaping of rock slopes (Carson and Kirkby, 1972). Surprisingly little is known about the impact of large magnitude events on rock cliff evolution, but such failures are often thought essential in determining the long-term form of the slope. Variations in the nature of failures and the multiple mechanisms that might potentially become involved at any stage mean it is difficult to combine the characteristics into a coherent model of rock slope behaviour (Gerrard, 1988). Brunsden (1999) warns against focusing on the rare but dramatic events in landform evolution at the expense of everyday processes. Questions remain over the nature of the interaction between small scale frequent changes and less common but more significant episodes of slope alteration and their relative influences in shaping the development of coastal cliffs. The volumetric contribution of small verses large events, the spatial and temporal patterns of change for different magnitudes, and whether the controls on different sized failures can be recognised have yet to be determined. If such patterns of spatial, volumetric and temporal change can be recorded, perhaps with the use of terrestrial remote sensing techniques, further conclusions might be drawn over the appropriate scales at which to analyse distinct processes and mechanisms.

The scale and nature of the elements involved requires careful consideration of the level of detail required to identify, characterise and interpret behavioural patterns in rock slopes (Cojean, 1995). Magnitude-frequency relationships imply a scale dependency to the data, making the scale at which geomorphological processes are analysed a key determinant of the outcome (Heuze, 1979; Brown, 1987; Allison, 1993; 1994; 1996). The scale of the landform itself is also thought to relate to the rate and magnitude at which failures occur (Richards and Lorriman, 1987). Scavia (1996) used fractals to determine a marked scale effect on fracture roughness, generating implications for understanding the propagation of discontinuities in rock masses.

The temporal scale at which processes are analysed may also influence the interaction between the determinants of slope form. Slope activity rates may respond to diurnal, seasonal and climatic fluctuations over time (Rapp, 1960). The limited temporal extent of records on slope behaviour mean that most theories on accelerated episodes of slope change are restricted to qualitative or semi-quantitative assessments

of relict landforms. For this reason, the appropriate temporal scale upon which to analyse slope behaviour remains problematic. Focussing on particular and specific scales of influences on rock slopes may prove inadequate. Rather it is hierarchical systems which constitute the true form and function of landscapes (Brunsden and Jones, 1980; Sunurmura, 1999). It is more appropriate to consider multiple mechanisms acting at different spatial and temporal scales, driven by equally diverse processes, rather than sets of clearly defined failure criteria.

The complex and spatially variable *in situ* properties of many rock slopes make the temporal evolution of the landform as a whole particularly difficult to determine. Block detachment may occur relatively frequently along a joint exposed in the cliff face, metres away from a stable section that changes little over the same timeframe. Questions over the temporal changes in the patterns in rock slopes echo back to earlier debates on slope evolution, most notably during the 1920s, between Davis (1922) and Penck (1924). Although there were many aspects to the debate on landscape evolution, one of the most stark divisions was between the temporal aspect to slope change: Davisian theory requiring short lived episodes of rapid change followed by long periods of stability while Penck's slope models retreat in a more continual sequence (Carson and Kirkby, 1972).

In the case of coastal cliffs many of the theories of change have been dominated by rare, large scale events (Brunsden, 1999). The influence of high magnitude changes on the long-term behaviour of slope form implies a natural episodicity to slope evolution. Episodic change refers to the release of material from the rock slope at usually irregular intervals. Others have described cycles of episodic behaviour, with failed material temporarily armouring the cliff (Hutchinson, 1973; Quigley *et al.*, 1977; Everts, 1991; van Rijn, 1998). Lee (1997) considered cliff erosion as part of a four step sequence, from the detachment of material, its transport down the inclined surface under gravity, deposition at the base of the cliff and ultimate removal from the system.

Perhaps the most widely used model for episodic evolution of cliffs is that of Sunamura (1992). Sunamura (1992) theorised that steep coastal cliffs develop through intermittent mass movements induced by basal undercutting. He suggested the same cliff profile will repeatedly be assumed through time as the cliff recedes, estimating a period of 10 years after failure for the parallel profile to be achieved in the mudstone cliffs of Taito-misaki, Japan (Sunamura, 1992). The failure surface passes through the deepest part of the undercut notch linking directly to the cliff top or to the base of a

tension crack (Figure 2.10). However, without the availability of readily obtainable accurate and representative data on slope changes through time, it seems questionable to assume either marine undercutting as the sole control on slope form or the reoccurrence of certain cliff profiles.

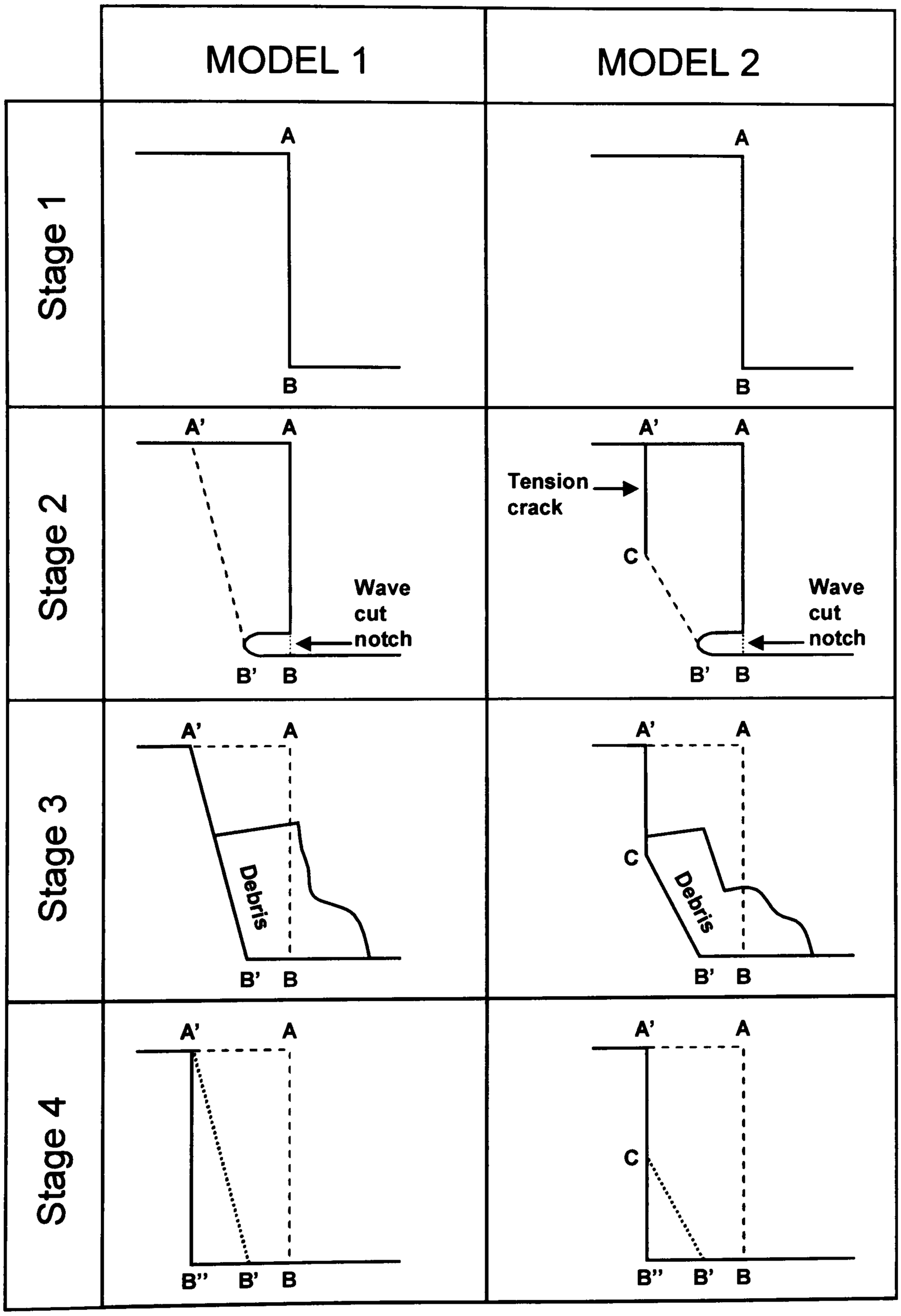

Figure 2.10: Two suggested models for cliff recession, both associated with wave cut notch development. A failure surface develops from the notch to the cliff top (Model 1) or tension crack (Model 2) when the sliding force exceeds the resisting force of the slope forming materials. The four stage development of the cliff is governed solely by the rate of marine activity, with both models returning to a vertical slope over time (Sunamura, 1992).

The assumption of episodic pulses of activity in rock slopes, and coastal cliffs in particular, has led many investigators to draw links between accelerated process rates and high magnitude triggering events in order to explain the episodicity. Along the Californian coastline specific events such as storms associated with El Niño (Griggs and Johnson, 1983, Griggs and Savoy, 1985, Storlazzi and Griggs, 1998) or earthquake-induced seismic shaking (Hapke and Richmond, 2002) have been directly linked to large scale failures in coastal cliffs. In order to investigate the interplay between rare and everyday processes some geomorphologists have subdivided change into ensystemic and eksystemic change (Ahnert, 1988). Ensystemic, or internal, change is driven by the geomorphic system within which the landform is contained. Ensystemic change in coastal cliffs refers to any landform response to the natural base of drivers within the coastal system. Eksystemic changes originate from outside the operating system and consequently have the potential to alter the nature, location and intensity of the processes governing landform development. They are sometimes referred to as formative events in reflection of their importance in controlling the long-term morphology of certain landforms (Brunsden and Thornes, 1979). Eksystemic change in coastal cliffs might include sea-level rise and increased storm incidence due to climate change, or subsidence of the cliff induced by mining activities (Humphries, 2001). Although this type of analysis may be valid for certain landforms such as unconsolidated slopes, the link between external, eksystemic change and large, formative events has yet to be convincingly proven for hard rock cliffs.

The temporal constraints on failure processes are a poorly understood aspect of slope studies (Nelis, 2005), and considerable further investigation is required in this area. Recent developments in landslide studies have indicated that once past a critical threshold, failure is ultimately controlled by the strain state within the shear plane (Petley, 2004). A body of material that has exceeded its critical strain level will inevitably continue to failure, although the precise timing of the failure may take years to reach completion, depending on the volume involved. This analysis of rock slope behaviour has been supported with the use of numerical models. Eberhardt *et al.* (2001) for example concluded that failure in the Randa rockslide, Switzerland, was only able to occur when the shear plane was nearly completely developed. In the light of these recent advances it is perhaps more appropriate to consider the behaviour of rock slopes as continuous rather than static 'event - no event' scenarios. Slopes can be seen as coherent bodies, responding dynamically to a set of processes with spatially and temporally different responses in strain rate, with the release of material viewed simply as a period of high strain rate in the landform (Petley, 2004). Emphasising the

importance of periods of critical strain, rather than the conventional focus on periods of critical stress, places greater significance on the patterns of failures that are no longer considered independent of each other. The whole cliff can therefore be seen as active but activity rates vary.

2.11 Key questions concerning rock slope evolution

The mechanisms of cliff retreat respond to system controls, preparatory processes, inherited conditions, precursory criteria and triggering factors determining the occurrence, frequency, magnitude and duration of the change events. The magnitude of failed material, the manner in which materials are released from the rock mass, coherently or intermittently, rapidly or slowly, and the location and timing of the event are all poorly understood aspects of rock slope change. Progress has been limited by inadequate monitoring techniques, and reliance on models and theories based on qualitative or semi-quantitative observations. Questions remain over current understanding into the material-process-form interactions that govern hard rock cliff evolution. Some of the key themes concern the spatial patterns, the nature and the temporal development of rock cliff changes and the environmental controls influencing the rate at which change occurs. Four key questions arise from gaps in current knowledge.

1. Is hard rock coastal cliff change characterised by frequent small scale failures and infrequent large scale failures?
2. Are the patterns of change within coastal rock cliffs scale dependent?
3. Is hard rock coastal cliff behaviour episodic?
4. To what extent is hard rock coastal cliff behaviour governed by environmental processes?

2.12 Summary

This chapter has discussed hard rock coastal cliff behaviour through the consideration of both the mechanisms and the process interactions that drive change. Coastal cliffs can be viewed as self-regulating cascading systems, dynamically adjusting between process and form controls over time. The processes and mechanisms associated with the rock slope environment interact to influence the rate and nature of change respectively. Much of the understanding into this interaction has been developed from datasets of insufficient spatial and temporal resolution to accurately record rock slope change. Many of the theories concerning rock slope behaviour are therefore based on poor quality data and hence are open to interpretation. As a consequence this study investigates the Liassic cliffs at Staithes, North Yorkshire, to evaluate the nature of

coastal cliff behaviour. The following chapter details the characteristics and controlling influences of the site and selects specific sections for the development of a new approach for the analysis of hard rock cliff behaviour.

Chapter 3
Study site: Staithes, North Yorkshire

3.1 Introduction

This chapter describes the research area and the specific sites used for the study. The lithological, structural, material and geomorphological characteristics of the cliffed coastline north of Staithes, North Yorkshire, are discussed. The climatic, marine and anthropogenic processes acting within the research area are considered. Finally, justification is given for the selection of six specific cliff sections used for detailed study.

3.2 Research area: lithology and structure

The English coast includes about 1100 km of sea cliffs, comprising a wide range of geology and morphology (Mitchley and Malloch, 1991). The variations lead to diverse cliff types along the coastline (Figure 3.1). Hence, selection of appropriate field locations for any study into the processes associated with coastal cliffs requires careful consideration (Lee and Clark, 2002). The cliffs of Staithes, North Yorkshire, have been selected for this investigation into hard rock cliff behaviour because of their complex material properties and scale, reaching over 80 m in height. The study area extends for about 2 km along the Cleveland coast, from Boulby (NZ 764190) to Staithes Harbour (NZ 782189), which forms Management Unit 3B of the Huntcliff (Saltburn) to Flamborough Head Shoreline Management Plan (1996) (Figure 3.2).

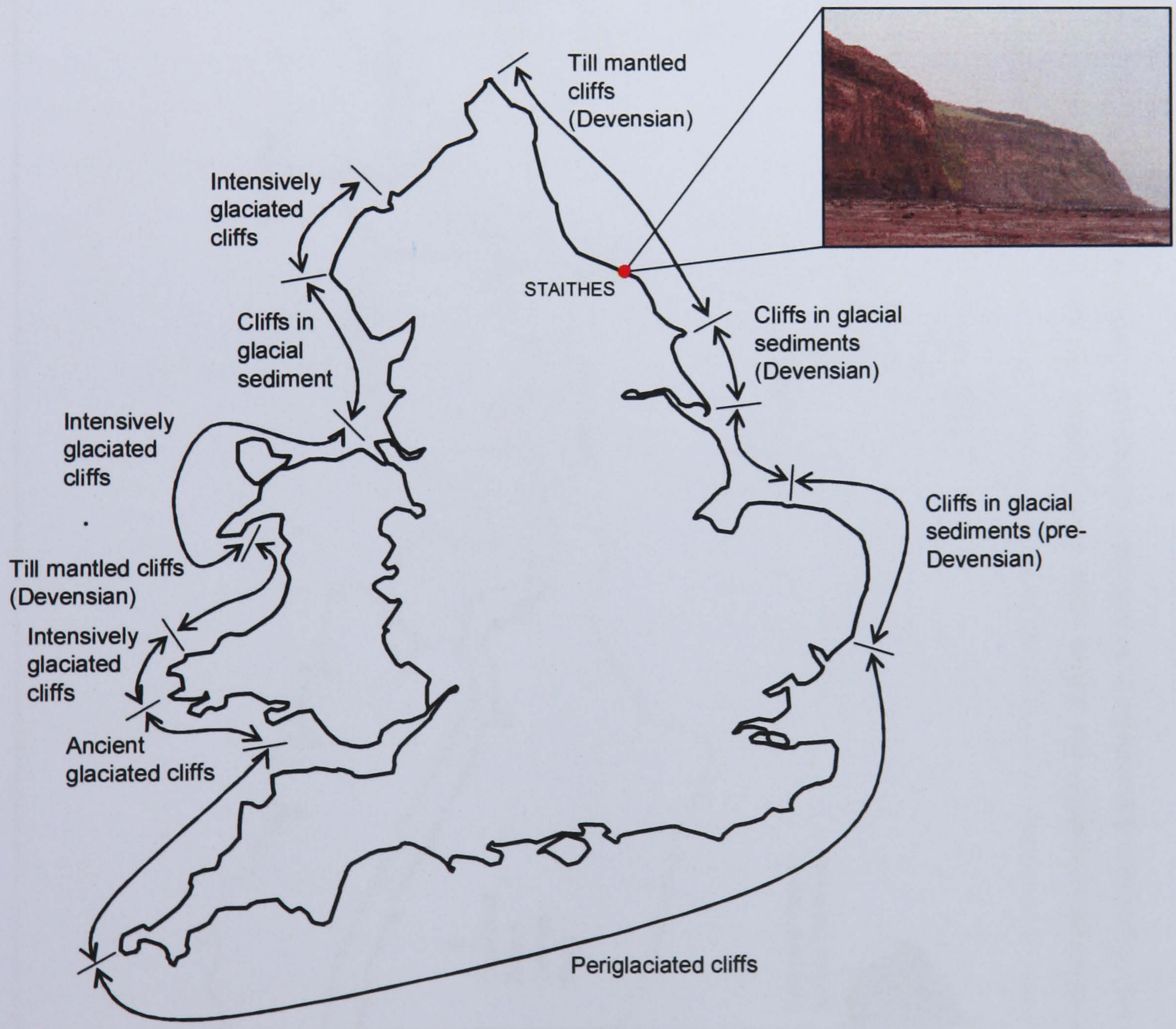

Figure 3.1: The study location set in the context of the variety of cliff types along the English and Welsh coastlines (Adapted from Brunsden and Lee, 2004). Although containing some of the highest cliffs along the east coast of England, the general morphology is typical of cliffs in the area.

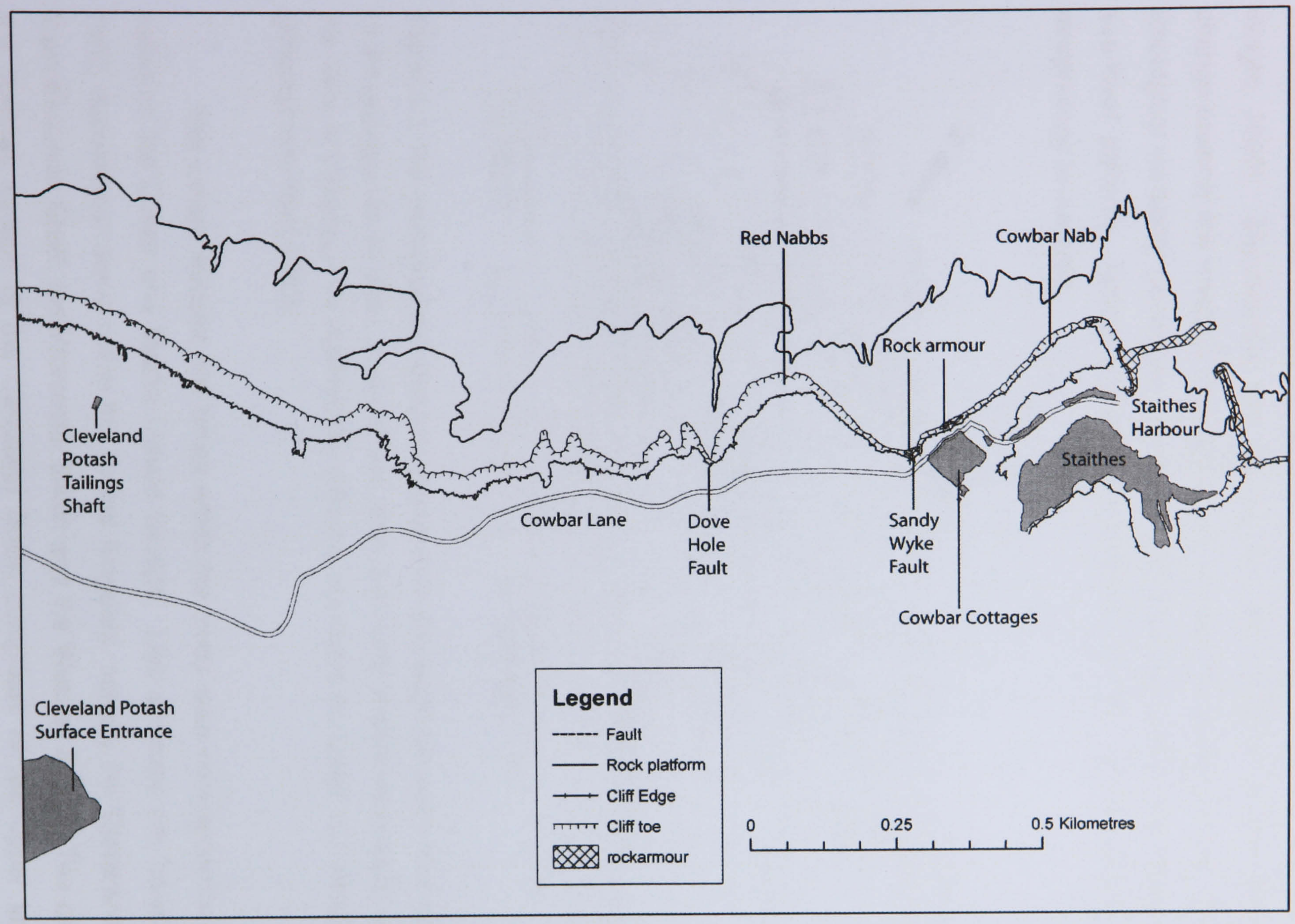

Figure 3.2: The research area encompasses the cliffed coast from Staithes Harbour to the land adjacent to the tailings shaft owned by Cleveland Potash Limited. The coastline includes many distinctive features such as the nabs of Red and Cowbar and the faults at Dove Hole and Sandy Wkye.

Structurally, the study area is situated within the Cleveland sub-basin (Figure 3.3), formed as the Mesozoic strata differentially subsided at the end of the Triassic (Kent, 1980). Uplift during the transition from the late Cretaceous to the Tertiary led to inversion of the Cleveland Basin. The resulting north-south trending dip provides a continuous sequence of Lower Jurassic lithologies exposed at the coast (Rawson and Wright, 2000). Significantly, this causes the base material of the cliff sections to change towards the west, as new layers are revealed in the rock mass. The resultant lithological variability generates diverse responses within basal rock layers to regional sea-level patterns, raising important implications for the understanding of coastal morphology in the area.

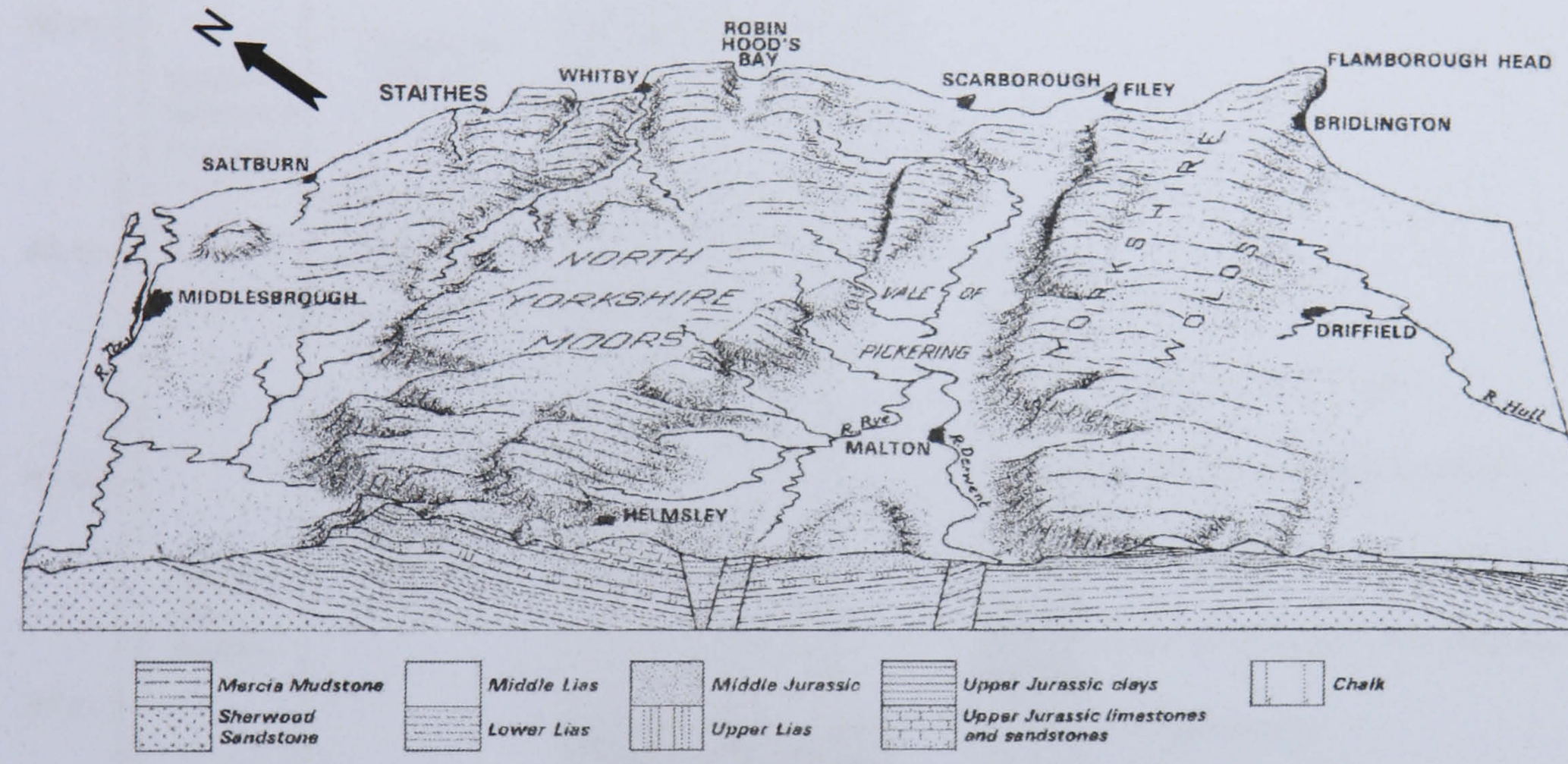

Figure 3.3: The geological and structural setting of the Cleveland sub-basin. The north south dip of the geology can be seen, which causes older sediments to become exposed northwards of the Vale of Pickering. At Staithes the cliffs are dominated by Lower and Middle Lias rocks (Adapted from Kent, 1980).

The Lower Jurassic cliff strata within the study area correspond to the division between the Lower and Middle Liassic Groups. Lias outcrops are found within four main depositional areas within the United Kingdom, namely the Cleveland Basin, the East Midlands Shelf, the Worcester Basin and the Wessex Basin. The cliffline within the Staithes section of the Cleveland Basin comprises of the upper layers of the Redcar Mudstone Formation overlain by the Staithes Sandstone Formation, which forms the base of the Middle Lias (Figure 3.4). The inter-layered mudstones, shales, siltstones, sandstones and occasional ironstones and impure limestones generate variable geotechnical properties (Staniforth, 1993), forming complex patterns of slope behaviour, spatially and temporally. Little is known about the manner in which such

cliffs fail, but it seems likely that the interaction between the different materials may provide a key control on the evolution of the landform. The Liassic shales and siltstones, which were deposited as fine silts and muds under a deep sea, are weak and thus erode easily in comparison with the more resistant sandstone and mudstone bands which commonly protrude from the rock mass (Staniforth, 1993). The entire heterogeneous succession is cross-cut by varied joint patterns, tension zones and occasional minor fault lines. The structural weaknesses are often concentrated, providing focal points and potential failure surfaces for cliff change.

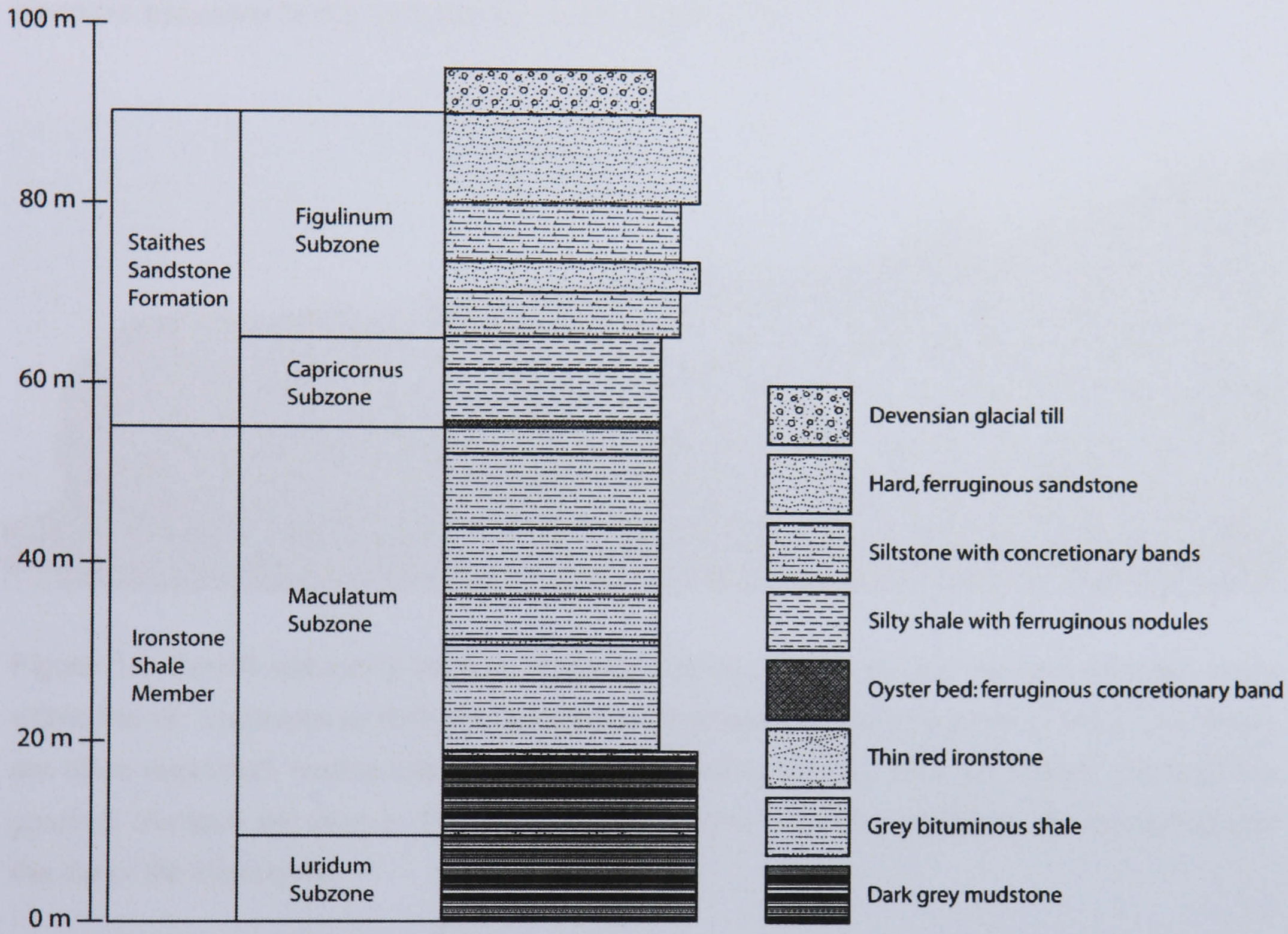

Figure 3.4: Schematic cross-section through the cliffs within the research area. The two main formations within the rock mass contain varied materials, causing a complex profile, and are separated by a distinctive ferruginous oyster bed (Howarth, 1992). The rock mass is capped by glacial till.

The topography of the North Yorkshire coastline is dominated by networks of basin-dome and bay-headland structures. The cliffs at Staithes form some of the highest cliffs on the eastern coast of the British Isles. The rock sections range in height to over 90 m and are mantled with up to 20 m of glacial till. Along this coast, cliff types can be broadly divided into four classes based upon morphological and compositional characteristics:

1. Soft Cretaceous clay or drift cliffs;

2. Jurassic cliffs with no glacially deposited layers;
3. Cretaceous Chalk cliffs;
4. Composite interbedded Jurassic cliffs overlain by glacial drift.

The glacial deposits overlying the composite interbedded Jurassic cliffs at Staithes generate conditions that separate them from other types of cliff behaviour. Cuspate failures in the capping till commonly stain the cliffs red-brown, leading to large differences in cliff appearance throughout the year (Figure 3.5), and a concentration of the flow of water over the rock face. Failures from the till may capture or dislodge rock material as it falls, particularly on protruding areas, causing rock mass responses to become sensitive to the processes influencing the till.

Figure 3.5: Runoff commonly leads to localised staining of the cliff face beneath exposed scars within the till. Variations in both the amounts of seepage and the exposure of the scars, which are often vegetated, means that slope face appearance may vary on a daily basis; although the greatest changes are seen in the wetter winter months. Note the localised rock armouring and the dip of the lithologies.

The cliffs are generally fronted by an extensive wave-cut platform, varying in width from 50 m to over 300 m. The gradients of the platform are low-angled and are punctuated by outcrops of more resistant strata that generate small-scale scarp and dip ridge outcrops, stepping the profile. The platform is divided by channels and inlets and its topography is complicated by temporary beaches, cliff material and mushroom block or sheep stone pedestals. In 1969 a geophysical survey was conducted in the near-shore off the Staithes coast. A combination of medium and high resolution seismic profiling indicated that seawards of Staithes the seabed is founded upon Lias rocks overlain by superficial accumulations of Pleistocene and Recent age material (Hunting Geology & Geophysics Ltd., 1969). A submarine rock slope beyond the shore platform was thought to be a fossil cliffline, formed during periods of lower sea-level.

3.3 The geomorphology of the coastal cliffs at Staithes

The diverse influences on the cliff behaviour along the North Yorkshire coastline render it difficult to uncouple interactions between materials, processes and landforms. These problems have meant cliff evolution in the research area is often viewed deterministically, forecasting future rates of retreat based on measurements of change in past years. An influential study by Agar (1960) compared Ordnance Survey maps between 1892 and 1960 to generate historic retreat rates which form the basis of many contemporary planning strategies (Table 3.1). The comparisons of the cliff top and toe position seem to suggest coastal features will become enhanced through time, with lower retreat rates of headlands contrasted against higher rates of change in embayments. Cliff face angles were suggested to become steeper through time as the toe was eroded faster than the top, with differences also detected between the average rate of retreat within the Jurassic rock mass (0.0725m a^{-1}) and capping glacial till (0.285m a^{-1}) (Table 3.2). Consideration of the potential error margins involved with the technique of historical map comparisons, discussed earlier, poses questions over the true nature of cliff recession in North Yorkshire. It does not seem logical that such trends could continue indefinitely, as is assumed by many management plans (Mouchel Associates Limited, 1996), with ever steeper and more pronounced clifflines. Rather it appears more likely that there are errors in the data or that there are patterns and processes governing cliff behaviour that have yet to be considered, or a combination of the two.

Table 3.1: Patterns in landform scale erosion subdivided by morphology, as determined by Agar (1960).

Recession by morphology	Average cliff erosion by morphology	
	Cliff top erosion (m a^{-1})	Cliff toe erosion (m a^{-1})
Headlands only	0.01	0.04
Bays only	0.04	0.07
Whole coast	0.02	0.05

Table 3.2: Variations in cliff erosion of the coast by geology for locations throughout the research area coastline as provided by Agar (1960) and summarised by Mouchel Associates Limited (1996).

	Shoreline erosion rates (m a^{-1})				
Cliff recession by location	Lower Lias	Middle Lias	Upper Lias	Deltaic Series	Glacial drift
Huntcliff Station	0.04				
Staithes, Cowbar Nab		0.05			
Staithes, Penny Nab		0.1			
Port Mulgrave, south pier			0.1		
Runswick Great Ship Rock			0.1		
Upgang, nr Whitby					0.26
Whitby West Cliff				0.03	
Whitby East Cliff			0.09		
Whitby East Cliff			0.19		
Saltwick Nab and Black Nab perimeters			0.04		
Near Black Nab			0.11		
Robin Hood's Bay	0.07				
Robin Hood's Bay					0.31
Robin Hood's Bay	0.16				
Low Peak	0.05				
AVERAGE	0.08	0.075	0.105	0.03	0.285

Key:

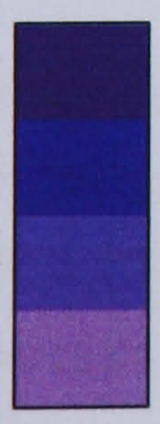

Glacial deposits

In order to investigate the application of cliffline surveys for the research area, cliff top and toe positions between 1928 and 2000 have been compared using County Series maps and Ordnance Survey Landline sheets respectively. Even ignoring errors associated with map production, interpreting the precise location of the cliff toe proved to be highly problematic, often indecipherable against debris at the cliff base. At one

point the cliff toe appears to advance through time as material was removed to reveal more of the underlying cliff face (Figure 3.6). Erroneous advances of the cliffline were also found in a previous study between 1998 OS maps and historic positions (Highpoint-Rendel, 1999). Such errors perhaps explain some of the differences between cliff top and cliff toe recession rates. Therefore the historical data, upon which much of the current understanding of cliff behaviour in the area is based, seem inadequate to describe either the temporal and spatial changes occurring over the cliff at Staithes or the processes and mechanisms that cause them.

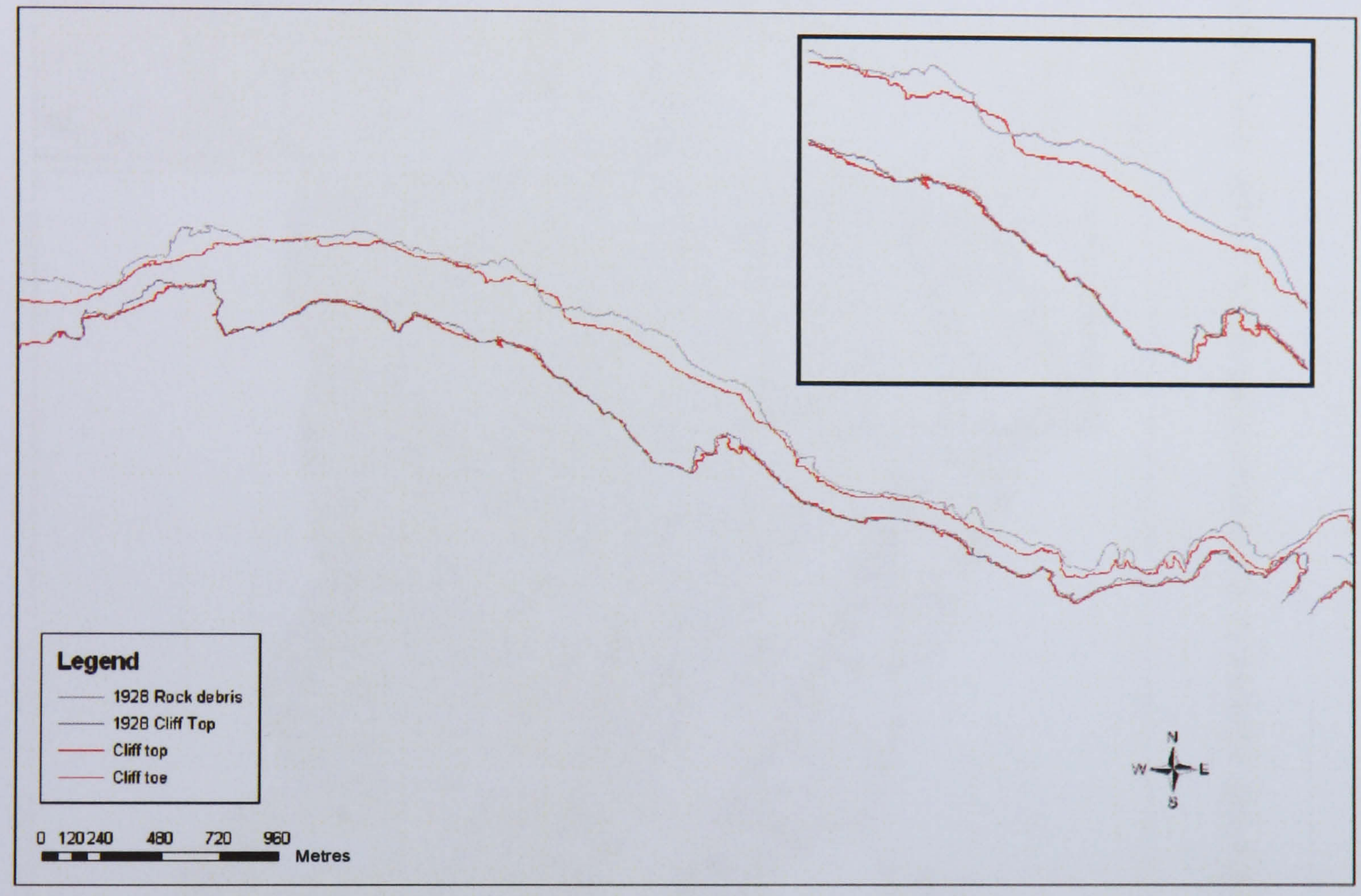

Figure 3.6: Historical desk study of cliff recession between 1928 and 2000 in the research area. The inset area demonstrates the problematic nature of locating the cliff toe which appears to have advanced from its 1928 position, although the difference actually corresponds to the removal of loose debris at the base of the slope.

A 0.25 m ground resolution aerial photograph was used to generate a geomorphological map of the research area (Figure 3.7), which was ground-truthed in the field. Mudstone at the base of the cliff provides significant resistance within the series, leading to profiles that generally regress landwards with height. The main failure mechanisms at Boulby are thought to include wave erosion of the mudstone cliff toe (Rawson and Wright, 2000), weathering of the shales in the middle cliff sections (High-Point Rendel, 2002) and landslips and flows in the capping glacial till (Howell and Barrow, 1888; CIRIA, 1999).

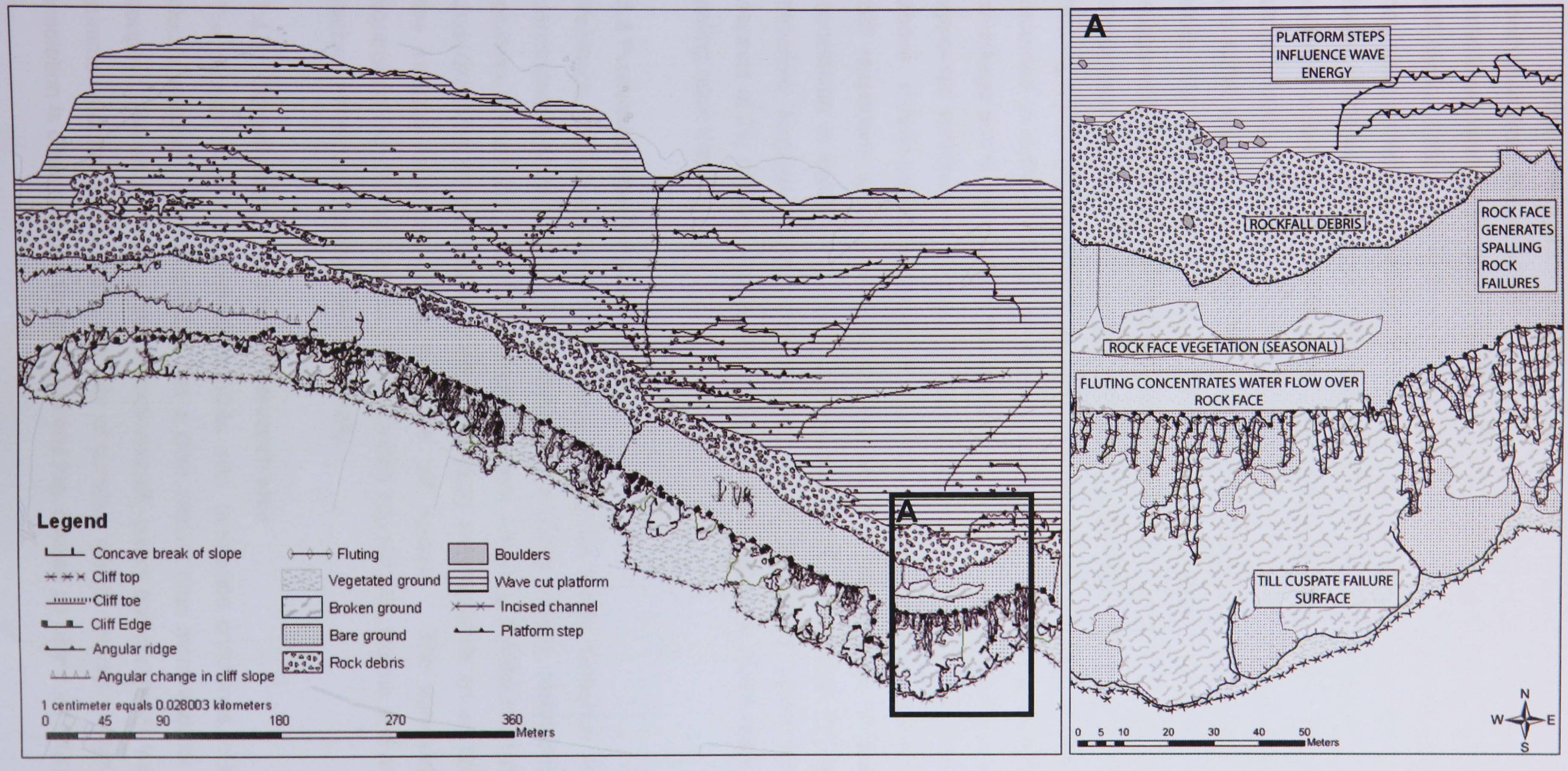

Figure 3.7: Section of the geomorphological map showing the cliff adjacent to the tailings shaft of the potash mine. Inset (A) demonstrates the detail required to accurately map the processes operating within the system.

In the current study analysis of the research area included site investigations conducted from the foreshore. Undercutting and limited basal debris were found to provide evidence of the power of marine activity, also demonstrated in the near-vertical cliff faces. Little detail is known about cliff evolution in the area although much work has been carried out elsewhere on the influence of material properties on coastal rock faces, which generate a wide variety of geomorphic features. Hampton *et al.* (2004) for example noted the differential erosion between alternating beds of sandstone and shale, produced an irregular cliff face with ledges of more resistant sandstone between the softer shales. Elements of the differences in material response are seen at the study site with the persistent protrusion of several layers within the cliff section, suggesting that the rate of change and potentially the nature of change differ spatially throughout the cliff. The complex processes associated with material and structural heterogeneity are important to the understanding of cliff evolution but have yet to be recorded in sufficient detail by existing techniques. Davies *et al.* (1998) noted that shrinkage and swelling within the interbedded shales of the Lias cliffs in South Wales appeared sufficient to contribute to the disintegration of more brittle sandstone layers above. If such mechanisms operate within the study area they may fundamentally alter cliff responses away from idealised behaviour of the material components when considered in isolation. A true understanding of cliff behaviour in the research area therefore requires a cliff geomorphology to be considered where the embedded aspects of the cliff are viewed with respect to their responses to the system influences acting upon them.

3.4 Processes operating at Staithes

Robinson (1974) examined cliff retreat throughout North Yorkshire in detail and concluded that the coast is a dynamic and evolving system, responding to current process interactions, rather than a relic landform reflecting Pleistocene influences. An understanding of cliff behaviour within the study area depends on an appreciation of the external influences acting upon the cliff system. The dominant processes controlling the cliffs at Staithes can be divided into climatic, marine and anthropogenic factors, which vary spatially and temporally.

3.4.1 Climatic influences on the research area

The climate of Britain generally exhibits mild, temperate conditions, often with wet, cloudy weather. North Yorkshire has a drier climate than more western parts of the country. The winter months are characteristically colder and marginally wetter than the summer months although the intensity of summer rain is commonly high (Table 3.3). Insolation is often reduced by low cloud and fog, caused by humid air brought on to the

coast from the Atlantic. Snowfall may occur in winter months, but rarely settles in coastal locations. Future climatic predictions suggest increased storm incidence in terms of recurrence intervals and magnitudes (Houghton *et al.*, 2001). If circulatory systems and storm tracks in the region were to alter, the energy exerted by climatic forces on cliff systems in the area may increase. The climatic processes influencing the cliffs at Staithes are therefore far from constant and should be viewed within the wider patterns occurring over the history of the study area.

Table 3.3: Climatic conditions for Yorkshire in 2003 (Research Machines plc, 2003).

Month	*Average Sunlight (hours)*	*Temperature*				*Relative humidity*	*Average Precipitation (mm)*	*Wet Days (+0.25 mm)*
		Average		*Record*				
		Min	*Max*	*Min*	*Max*			
January	1	1	6	-14	15	89	59	17
February	2	1	7	-10	17	87	46	15
March	3	2	10	-13	21	81	37	13
April	5	4	13	-3	24	73	41	13
May	6	7	16	-1	29	71	50	13
June	6	10	19	2	32	71	50	14
July	6	12	21	5	31	74	62	15
August	5	12	21	4	33	77	68	14
September	4	10	18	-1	29	80	55	14
October	3	7	14	-4	26	85	56	15
November	2	4	10	-7	19	88	65	17
December	1	2	7	-8	16	88	50	17

3.4.2 Marine influences on the research area

The region has not experienced significant isostatic adjustment in the last 5000 years (Shennan, 1989; Shennan and Horton, 2002), suggesting the marine impact on the coastline is largely determined by eustatic changes in sea-level. IPCC predictions estimate that future sea-level will rise between 0.3 m and 1.1 m by 2100, with their best estimate of 0.66 m if current trends were to continue unchanged (Houghton *et al.*, 2001). This equates to water-level rises of between 4.5 mm a^{-1} to 6 mm a^{-1} (Shennan and Horton, 2002), double the rates thought to have occurred globally over the past 100 years (Jelgersma and Tooley, 1992). The cliffs of North Yorkshire may therefore currently be responding to levels of marine processes greater than those of the recent past. Zenkovich (1967) related lowering of the foreshore and sea-level rise to the rate of horizontal cliff retreat. Considering bedrock erosion in the area to be 0.001 m yr^{-1} (Robinson, 1977) and the 1:40 gradient of the foreshore, Highpoint-Rendel (1999) rearranged Zenkovich's (1967) formula to calculate a cliff recession rate of 0.24 m yr^{-1} for Staithes, forecasting a 240 % increase in recession rates over the next 50 years.

The validity of such forecasts and whether direct links between sea level and cliff recession can be reliably assumed has yet to be determined.

3.4.3 Anthropogenic influences on the research area

Human activity has become an increasingly important factor in studies of coastal landscapes. The human agency within the study area includes both historic and contemporary activities. The historical influences of human activity on the coastline were dominated by mining and quarrying. The nearshore exposures of North Yorkshire have been much modified by the commercial extraction of materials such as jet, ironstone and alum shales. The first known activity within the cliffs occurred with jet harvesting during the Bronze Age (*c.* 4000 years BP). Mining was often opportunistic, with shallow excavations into the cliff face or in close proximity to Alum mines, taking advantage of the jet outcrops immediately below the Alum Shale (Staniforth, 1993). The comparatively thin but easily accessible sideritic seams of the Cleveland Ironstone Formation were worked sporadically during the 19th and 20th centuries. Staithes in particular saw significant foreshore quarrying (Howard, 1985), resulting in a lowered shore platform and networks of rutways and channels used for transporting material (Rawson and Wright, 2000). The effect of human activity on the foreshore process dynamics is likely to have led to an overall increase in wave impact at the cliff base and the focus of marine energy on cliff sections adjacent to the cut channels. Quantification of the effects of historic activity on cliff behaviour remains problematic. Since the early 17th century millions of tonnes of alum have been mined from the Alum Shale Member of the Upper Lias shales (Figure 3.8), exerting a major influence on the contemporary form of the coastline throughout North Yorkshire (Staniforth, 1993). Despite its rural setting, North Yorkshire was once a world centre in mineral extraction, particularly alum production for which 100 tonnes of alum shales had to be extracted for every tonne of alum.

To date there is no quantitative analysis of the effect that historic mining has had on cliff systems in the area although the extensive nature of the activity is clear from mine records (Figure 3.9). The coastline, and the landscape as a whole, cannot therefore be considered "natural". Rather it reflects intensive and diverse activities on an industrial scale. No specific records of historic activities were found for the cliff sections monitored in this study, although records of several large ironstone and alum mines immediately to the west, and of significant foreshore ironstone works at Old Nab to the east, suggest it is unlikely the study area has remained completely unaffected by similar influences. Evidence to support this can be seen in the presence of rutways and pillar post holes in the foreshore. The possibility that the present day study sites

are still responding to historic anthropogenic changes must therefore be considered. The degree to which changes such as the removal of up to 3 m of rock platform in a single year can be deciphered from natural or base rates of change has yet to be determined.

Figure 3.8: Entrances to Boulby Alum mine, an example of human modification of the cliff. The full extent of the mines is not known, although many of the conduits are unstable, causing the loss of support to rock layers above when they collapse.

A less easily identified influence on the study area is that of contemporary mineral extraction. Since 1973, Cleveland Potash Limited has mined over 3 million tonnes of potash and about 650,000 tonnes of saline evaporates per annum from Permian lake deposits at depths between 900 and 1300 m below Ordnance Datum. The mining induces subsidence of the ground which, at the coast, creates an effective rise in the influence of the sea. Quantification of the localised effect of mining-induced subsidence in the study area has been achieved by annual levelling surveys of the area since mining started. Mineral extraction has caused subsidence of the coast by up to 0.55 m since the onset of mining, with a maximum rate of 0.05 m a^{-1}. The pattern of subsidence shows a peak at the cliff section adjacent to the tailings shaft of the Potash mine, declining towards Staithes Harbour where the effect has been negligible (Figure 3.10). The result is a continuum of artificially lowered cliff sections throughout the study area, with the maximum effect equivalent to conservative estimates for sea-level rise over the next 100 years.

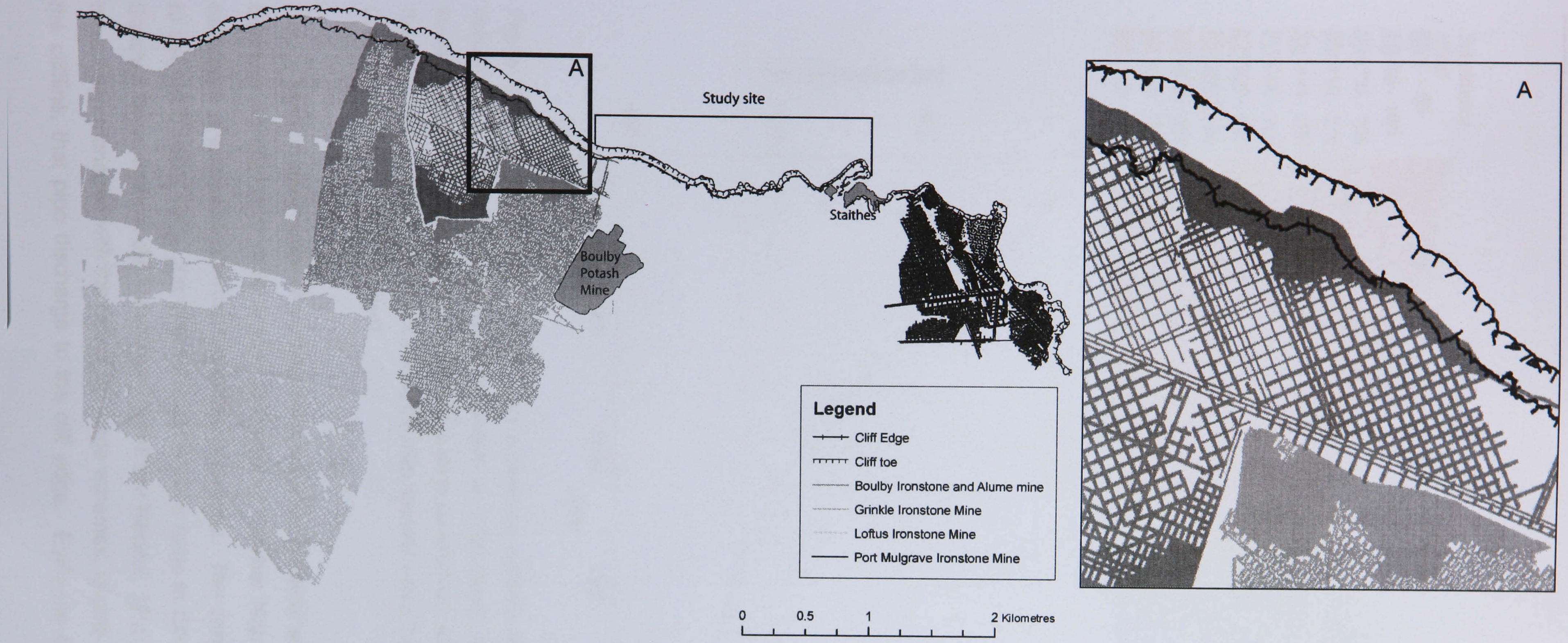

Figure 3.9: Location of historic mining galleries in the area. The extensive networks of mines often relied on exposures in valley sides or cliffs to gain easy access to valued seams. Due to the dip of the strata the study area appears largely unaffected by historic mining activity. The current state of the mines cannot easily be determined due to the risk of collapse.

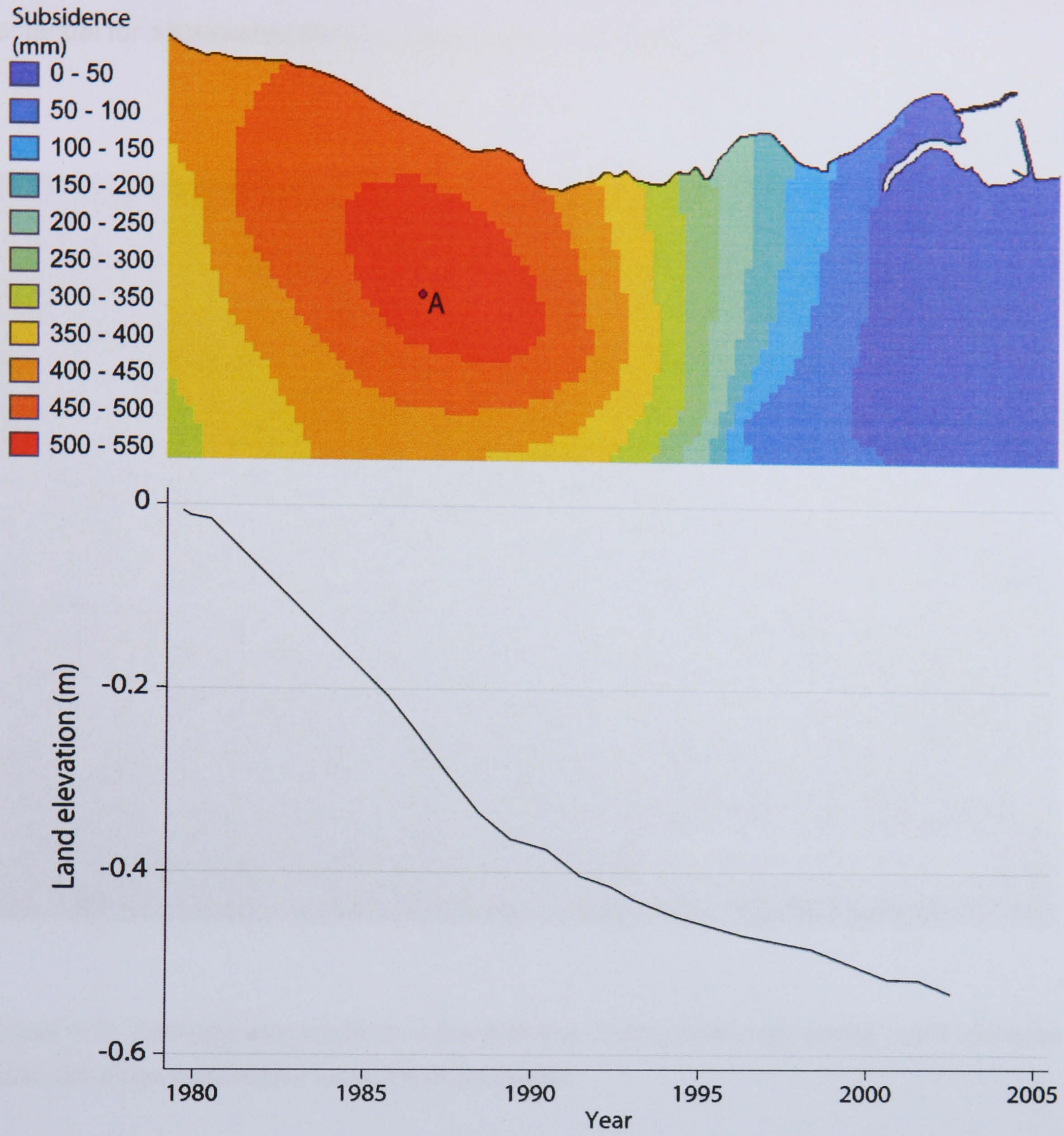

Figure 3.10: Interpolated total contemporary subsidence patterns within the study area. The nature of the subsidence curve typically involves an initial steady acceleration followed by a sustained period of reducing rates before tailing off to comparative stability. This is illustrated by the graph which corresponds to point A on the map, located within the peak area of subsidence (Source: Cleveland Potash Limited).

Many modern coastlines have been modified to better suit the needs of society. Staithes Harbour and rock armour defences at Cowbar Nab and Sandy Wyke are examples of engineering structures in the study area. The defences were constructed to defend Cowbar Lane, the only vehicular access route to Cowbar Cottages, north of Staithes beck, against cliff recession (High-Point Rendel, 1999). Subaerial processes have been managed with the use of drainage schemes, largely in the fields adjacent to the cliffline, that pipe discharge to the cliff edge. Evidence of poor management is

seen in several instances where drains stop short of the cliff edge, concentrating water flows into the front few metres of cliff face material (Figure 3.11), generating the potential for accelerated erosion rates (Emery and Kuhn, 1982).

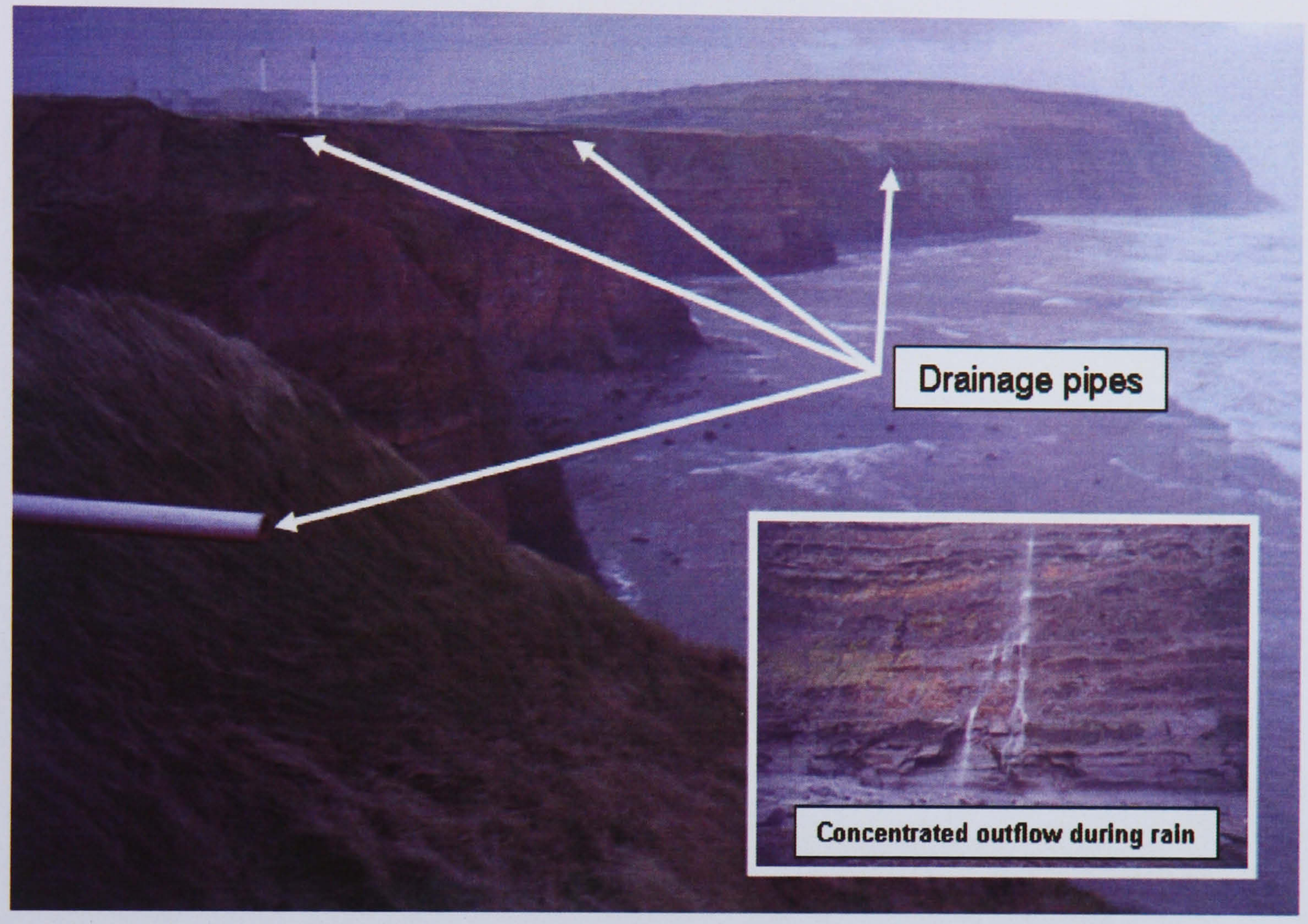

Figure 3.11: Drainage pipe locations in the field area. During heavy rain events runoff cascades down the slope immediately below the pipes (inset).

3.5 Study site selection

The heterogeneity of the rock masses mean it is unlikely that a single cliff section could be considered representative of the diverse processes acting in the research area. Investigation of the area identified three main slope types, found along the Staithes coastline (Table 3.4). From the characteristic slope profiles six key sites were targeted for the specific investigation of lithological, morphological, structural, subaerial and marine controls as well as anthropogenic effects on cliff behaviour (Figure 3.12). The choice of each site was justified in terms of primary and secondary characteristics which may influence the changes at each site (Table 3.5). The selected sites allow the hypotheses outlined in Chapter 2 to be tested with respect to specific controls on the behaviour of rock slopes.

Table 3.4: Characteristic slope profiles identified in the study area. Although simplistic, the generalised slopes were used to select an appropriate range of sites for the investigation.

Type	Generalised profile	Characteristics	Type code
Protruding toe		Base of the rock mass is its most seaward part. The profile recedes back from the base, often containing a smooth shallow angled step in the mid portion of the cliff, separating steeper sections towards the cliff top and cliff toe.	A
Overhanging top		Rock slope ranges from near vertical to overhanging. Cliff base is typically vertical with mid and upper portions causing the overhang.	B
Undercut toe		Base layer is undercut which often causes layers immediately above to overhang. Mid portions of the cliff typically recede back from the protruding layers above the overhang although layers at the cliff top may also form a second overhang.	C

An initial characterisation of the rock mass was conducted using the Rock Mass Strength Classification (Selby, 1980) to assess the relative stability of each site (Table 3.6). The scheme classed all sites as moderate to strong, with the weakest site at Site 3 due to dense jointing. There were few significant differences between the sites although jointing appeared to be more continuous within the embayments at Sites 2 and 3. Geologically, the bases of all of the sites and their rock platforms consisted of the Ironstone Shale Member of the Redcar Mudstone formation, overlain by the Staithes Sandstone Formation (refer back to figure 3.4). The east-west dip of the strata meant the geological boundary between the two formations began from 45 m above the cliff base at Site 1 slanting downward to eventually become exposed at the cliff toe at Site 6, Staithes Harbour.

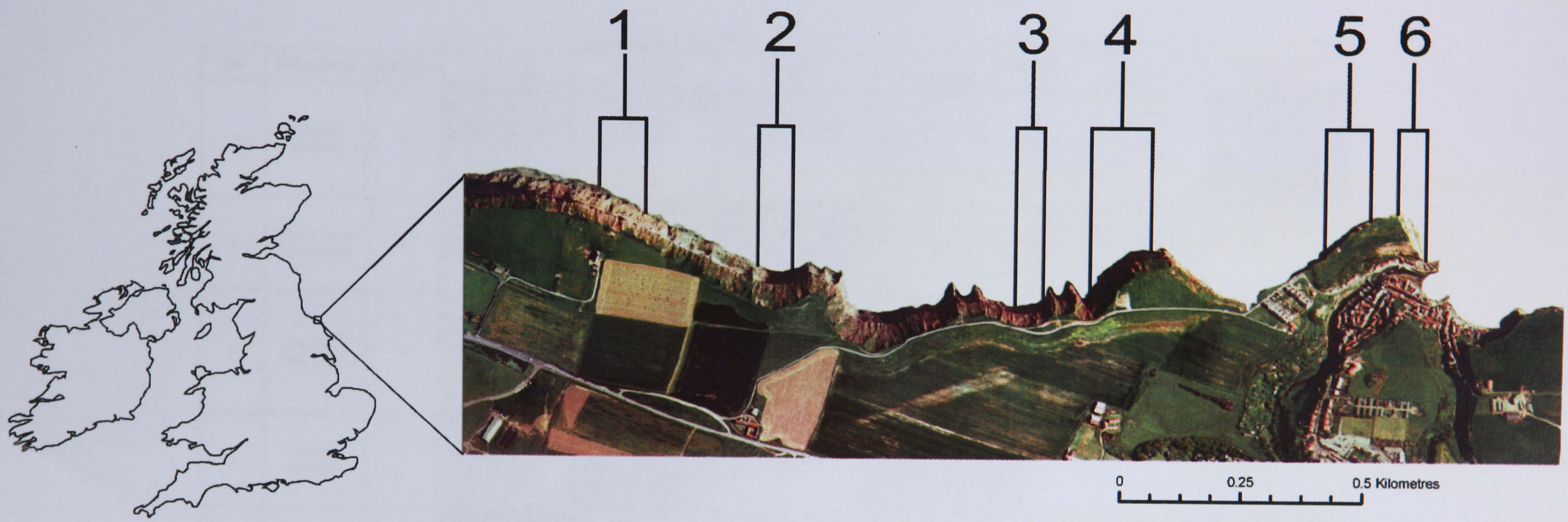

Figure 3.12: Sites selected for investigation into the controls on the behaviour of hard rock coastal cliffs at Staithes, North Yorkshire.

Table 3.5: *In situ* characteristics and influencing processes at each site. Although the behaviour at all sites is subject to a wide variety controls that vary over time, the selection of these sites allows attributes specific to each monitored section to be examined in the context of wider scale change. NB: The site number and site identifier will be used synonymously throughout the remainder of this study.

			***In situ* characteristics**			**Processes**		
						Climate		**Anthropogenic influences**
Site	**Site Identifier**	**Slope type**	**Lithology**	**Morphology**	**Structure**	**Subaerial**	**Marine**	
1	Subsided headland	A	The only site that displays all of the lithological layers in the monitored area	Headland with extensive rock platform, over 200 m. It is the tallest monitored slope.	Least well jointed of all the sites, although it does contain a tension zone to the east which is highly jointed	Regularly stained red/brown by overflow from till above. Shale layers in the mid portion of the cliff often show areas of seepage, concentrated upon the tension zone.	Hard mudstone toe and extensive wave-cut platform provide strong defences against wave pounding causing the toe to protrude from the rock mass.	Area of peak subsidence induced by contemporary mining activity
2	Arched-failures embayment	C	Contains all monitored layers except for the basal mustone found at Site 1	Embayment, reduced wave-cut platform,as low as 89m in places. Stepped slope profile	Well jointed in the lower portion of the cliff in which two arch formations appear to be undergoing active failure.	Overflow from till above leads to stark contrasts in colour between the middle and upper sections and the fresher, exposed rock at the cliff base.	Marine energies are concentrated at the cliff by a channel cut into the rock platform.	Site has subsided approximately 0.2 m since 1973
3	Well-jointed embayment	B	As bands thin eastwards the dip of the strata, more steep than at other sites, the basal two mudstone layers and top sandstone layer are missing	The face of this embayment is oversteepened with upper portions vertical or overhanging lower sections. Extensive shore platform reaches 260 m.	The most heavily jointed site, bounded by two tension cracks. The dense, sub-vertical joints in lower section commonly cause the loss of angular blocks.	Seepage from shale bands and overflow from till scars above combine to create localised patches of moisture over the cliff face	Despite the extent of the rock platform, its shallow gradient means it affords little protection against marine energy. The over-steepened face is testement to marine activity at the site.	Minimal
4	Seepage headland	C	The strata are the most consistent here displaying little variation in width across the 100 m section.	The face of this prominent headland ranges from near-vertical to overhanging in parts, fronted by a stepped rock platform.	The headland forms the eastern side of the Dove Hole Fault. Jointing is relatively sparse.	The shale bands immediately above the less permeable mudstone commonly display patches of seepage throughout the year.	The base of the cliff shows minimal undercutting.	Site is below a drainage outflow pipe which stops several metres short of the cliff edge.
5	Geology headland	C	Displays the most clearly identifiable and representative sequence of the Staithes Sandstone Formation	The longest stretch of continuously monitired rock face, and also the lowest. Fronted by a stepped rock platform up to 180m wide	The headland forms the eastern side of the Sandy Wyke Fault. Jointing is sparse and relatively regular although certain bands are more densely jointed	Sporadic scars in the till cause the rock face to have a patchy appearance as runoff stains the cliff below	The effectiveness of the rock platform is reduced by a channel to the west, although the stepped profile means the cliff bases here are some of the last to become inundated by the encroaching tide.	The western part of the monitored section has been armoured and drained by a conduit passing from the cliff top to emerge just above the rock armour. The till has also been regraded.
6	Protected headland	B	Comprises the same bands as Site 5 although the divisions are less evident.	This slope face forms the eastern side of the Cowbar headland. Much of the slope face is overhanging.	Most joints are perpendicular to the slope face causing detachments to typically be angular and blocky.	The rock slope is east-facing potentially exposing it to climatic influences not experienced at the other, more notherly orientated sites.	The harbour defences mean waves seldom reach most of the cliff base, even at high tide. The northern edge however is not defended allowing marine activity to influence behaviour.	The cliff base has been protected with substantial volumes of rock armour and the harbour walls severely limit wave attack.

Primary motivation

Secondary motivation

Table 3.6: Table of rock-mass strength classification for each site. All sites were classed as strong or moderate (Selby, 1980). The most noticeable differences resulted from variations in joint properties between sites.

	Rating					
Parameter	*Site 1*	*Site 2*	*Site 3*	*Site 4*	*Site 5*	*Site 6*
Intact rock strength	5	5	5	5	5	5
Weathering	7	7	7	7	7	7
Spacing of joints	30	28	21	28	28	28
Joint orientations	14	18	18	18	14	18
Width of joints	7	6	6	7	6	6
Continuity of joints	7	5	5	6	6	6
Outflow of groundwater	5	4	4	3	4	4
Total rating	75	73	66	74	70	74
Classification	Strong	Strong	Moderate	Strong	Moderate	Strong

3.5.1 Site 1

Site 1 (NZ 765190) is located at the cliff section immediately adjacent to the tailings shaft used by Cleveland Potash. The site contains the highest exposed rock slope along the research coastline and was chosen to test the performance of the monitoring technique against the most challenging landforms in the area. The cliff section is the furthest north of the monitoring sites and had the highest rock mass strength rating. The scarp reaches up to 60 m above Ordnance Datum and is capped by 15 m of till with an angle of 35° (Figure 3.13). The foot of the cliff comprises of resistant mudstone layers 11 m thick that protrude from the cliff face, standing at 75°. The middle portion of the cliff is dominated by extensive sections of shales and the upper rock layers consist of hard sandstones and siltstones, creating an overhang. The rock face contains a tension zone that defines the eastern edge of the site. It comprises of a band of vertically jointed and shattered rock extending 45 m from the base that has been eroded to leave a sharp cleavage in the cliff face. The rocks contain relatively few joints, which dip slightly into the rock mass and strike roughly perpendicular to the rock face. Its location at the centre of contemporary mining activities has meant the cliffs here have seen the greatest amount of subsidence, over 0.35 m since 1973. At their peak, the cliffs were subsiding at 0.05 m per annum, the equivalent to over 8 years of current rates of sea-level rise in a single year. A piped outlet to the east and channelled flow to the west lead to concentrated cascades of water flow either side of the monitored section during rain events. During drier conditions, water can occasionally be seen seeping out from the tension zone. This headland feature is orientated north-northeast (032° from north) and is fronted by over 200 m of rock platform. The platform itself contains numerous large boulders to the east that reduce in size but increase in number westwards, and a network of small dendritic channels.

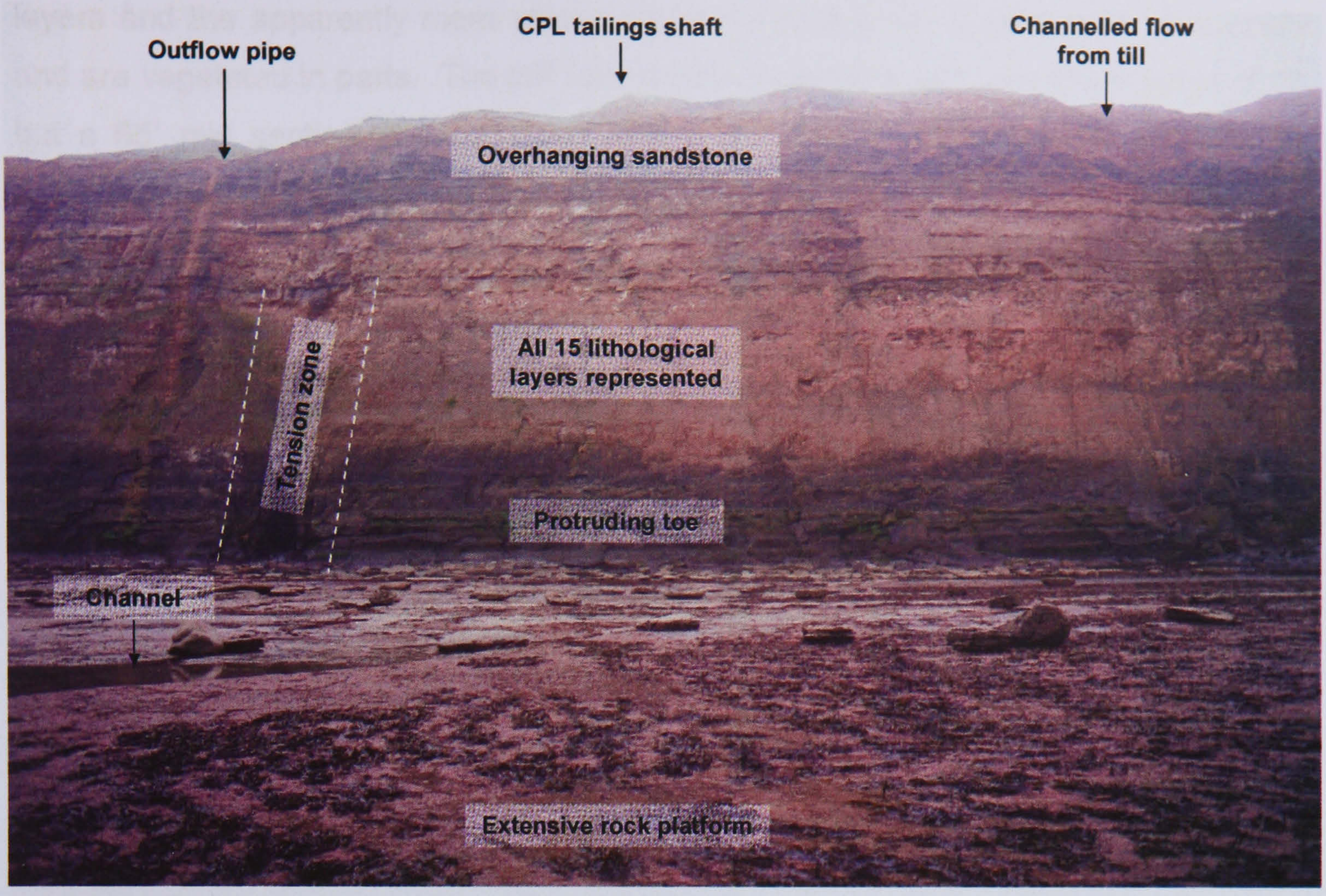

Figure 3.13: Annotated picture of Site 1, which was selected on the basis of the scale of the landform and its recent history of subsidence.

3.5.2 Site 2

Site 2 (NZ 768189) is located 300 m east of the subsided headland, and forms the backwall of a shallow embayment. The site was chosen as an area of interest due to the presence of two distinct arch formations within the lower eroding rock layers (Figure 3.14). Terzaghi's (1946) rock load concept suggests rock masses undermined from below will naturally stabilise in arched structures. Arched configurations are common throughout the coastal stretch at Staithes, raising questions of whether they reflect an important mechanical response of the rock mass or are merely superficial characteristics of the jointing. It was hoped that monitoring this site would reveal the role of arches in cliff behaviour, if their form is stable within the cliff through time or if they propagate to other areas.

Due to the dip of the strata the basal mudstone band at Site 1 is not visible at this site, reducing the mudstone toe and so the overall height of the cliff. The rock mass at Site 2 reaches over 47 m high and is capped by 15 m of till, which is inclined at 35°. The mudstone base is 7.5 m thick and dips from west to east, forming a 3 m deep step in which lower mudstone layers become exposed immediately west of the site. The shales above are well jointed, forming a marked contrast between the clean lower

layers and the apparently more stable upper layers that are stained with till seepage and are vegetated in parts. The cliff face profile is stepped, with an overall angle of 75° but a 65° mid section of weathered shales, and once again orientated towards the north-northeast (020° from north). The rock platform is relatively free of boulders and pedestals and limited to a minimum of 89 m at the eastern edge of the cliff section by a channel running perpendicular to the cliff face. The platform immediately in front of the cliff is covered by a temporary sand beach that fluctuates in width between 10 m and 40 m throughout the year. Historical analysis of the site seems to indicate that in 1977 the beach extended significantly further than at present (Figure 3.15). It is unclear whether the apparent reduction of the beach extent is a response to sea-level rise, altered sediment cascades, seasonal patterns or reflects historic and contemporary mining activity or a combination of factors.

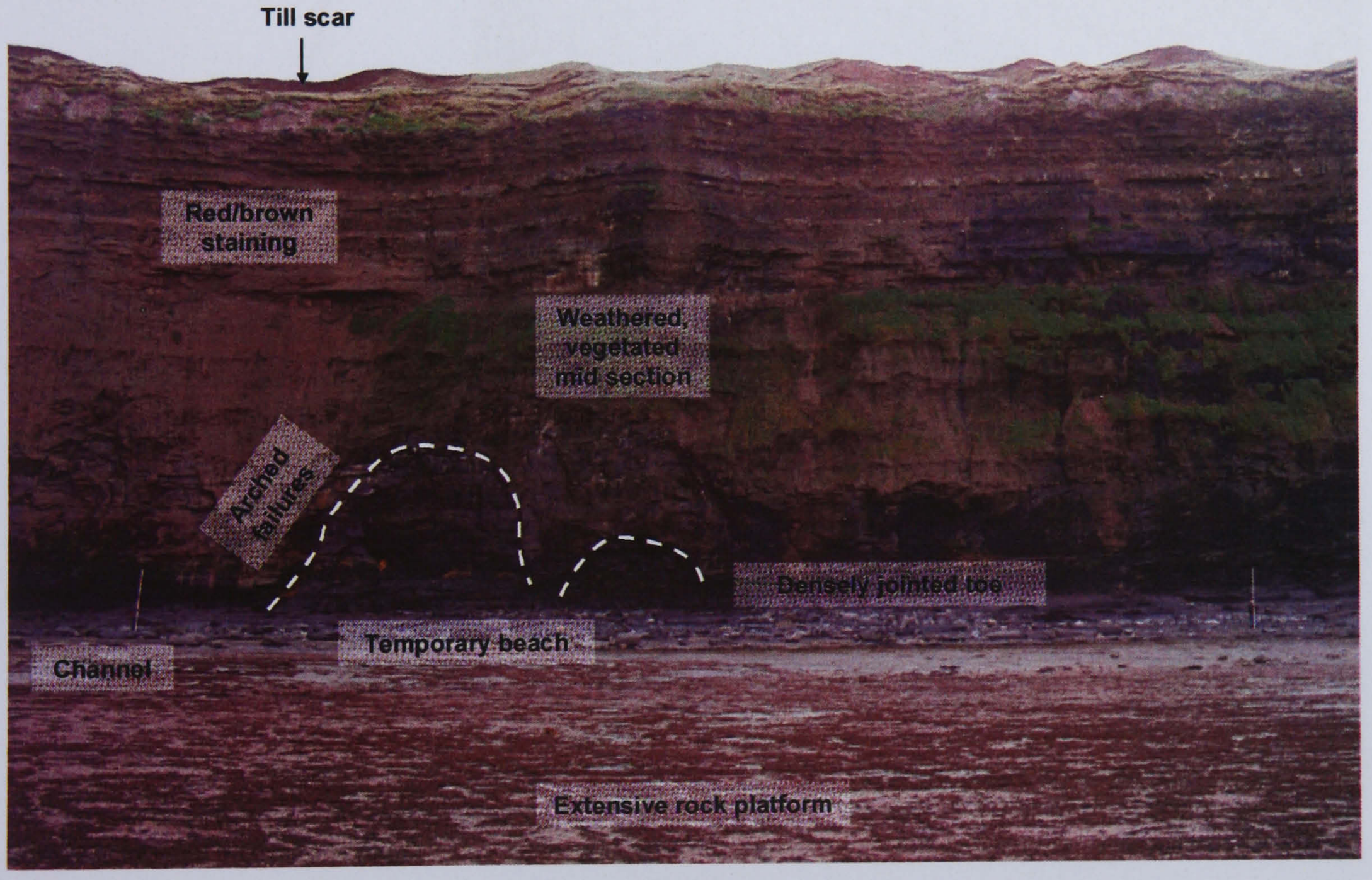

Figure 3.14: Annotated picture of Site 2, selected to investigate the response over time of arched failures within the cliff.

The site was formerly referred to by locals as 'Egg Point' because, within living memory, landslide debris accumulated at the cliff toe formed a debris fan that allowed access to central cliff sections where seagull eggs could be collected in summer. The debris slope has now been eroded although evidence of its existence can still be seen in relic deposits left suspended on the cliff face as the majority of debris was removed

(Figure 3.16). The historic evidence of activity at this site is supported in the currently active failures occurring within the exposed cliff face.

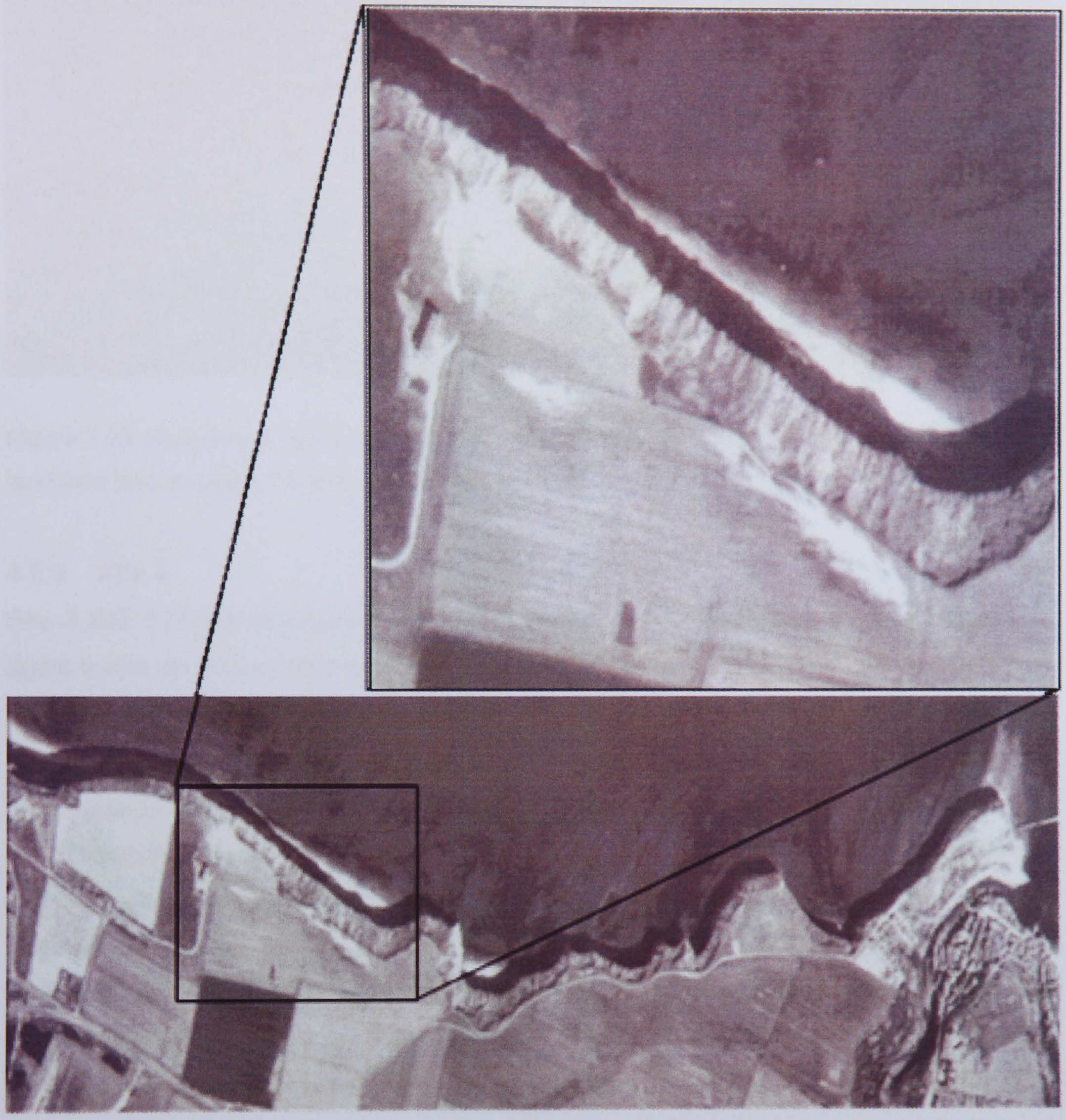

Figure 3.15: 1977 Aerial photo (1977) revealing a more extensive beach (inset) than is currently present at Site 2. The photographic evidence has been corroborated by locals who describe a continuous sand bar fronting the headland. The changes in dynamic coastal features such as beaches are easily identified, but the significance on cliff systems of the changes, and the processes which caused them, are less clear.

Figure 3.16: Suspended debris cemented to cliff face (inset) demarcates the location of a relic landslide that occupied the site in the recent past.

3.5.3 Site 3

Site 3 (NZ 774188) is located 580 m due east of the arched-failures embayment, and again forms an embayment backwall (refer back to Figure 3.12). The site was selected for monitoring to investigate the nature of the effect of dense joint patterns and whether the greater density of joints leads to accelerated rates of recession. The monitored rock mass is near-vertical and consists of a section of heavily jointed strata 38 m high in between two continuous tension cracks, 35 m apart. The tension zones form narrow swathes of shattered, blocky rock that extend vertically 25 m from the toe and give this cliff section strength values significantly lower than the other sites (Figure 3.17). The mudstone base is 5.3 m thick and contains numerous horizontal weaknesses crosscut by the sub-vertical fractures causing many small angular failure scars. Sandstone bands in the upper part of the cliff form distinct overhanging ledges that protrude from the rock mass and are used as nesting sites by seagulls. The average inclination of the till was recorded at 36°, although the oversteepened front portion of till at the junction with the rock mass reaches 51°. As with all sites, seepage from the till stains the rock face reddy-brown, which causes the areas of recent change to be highlighted by fresh, clean rock exposures. The cliff face is orientated north-south and fronted by up to 260 m of rock platform. The platform dips 5° from west to east and contains scattered large pedestals and a small shingle beach at the cliff toe, the level of which varies significantly through the year. The access road behind this site has been rerouted inland from its original position, indicating that the cliff has been active in recent times. The contemporary subsidence effect here is markedly less than at the previous sites, with foreshore lowering of some 0.2 m.

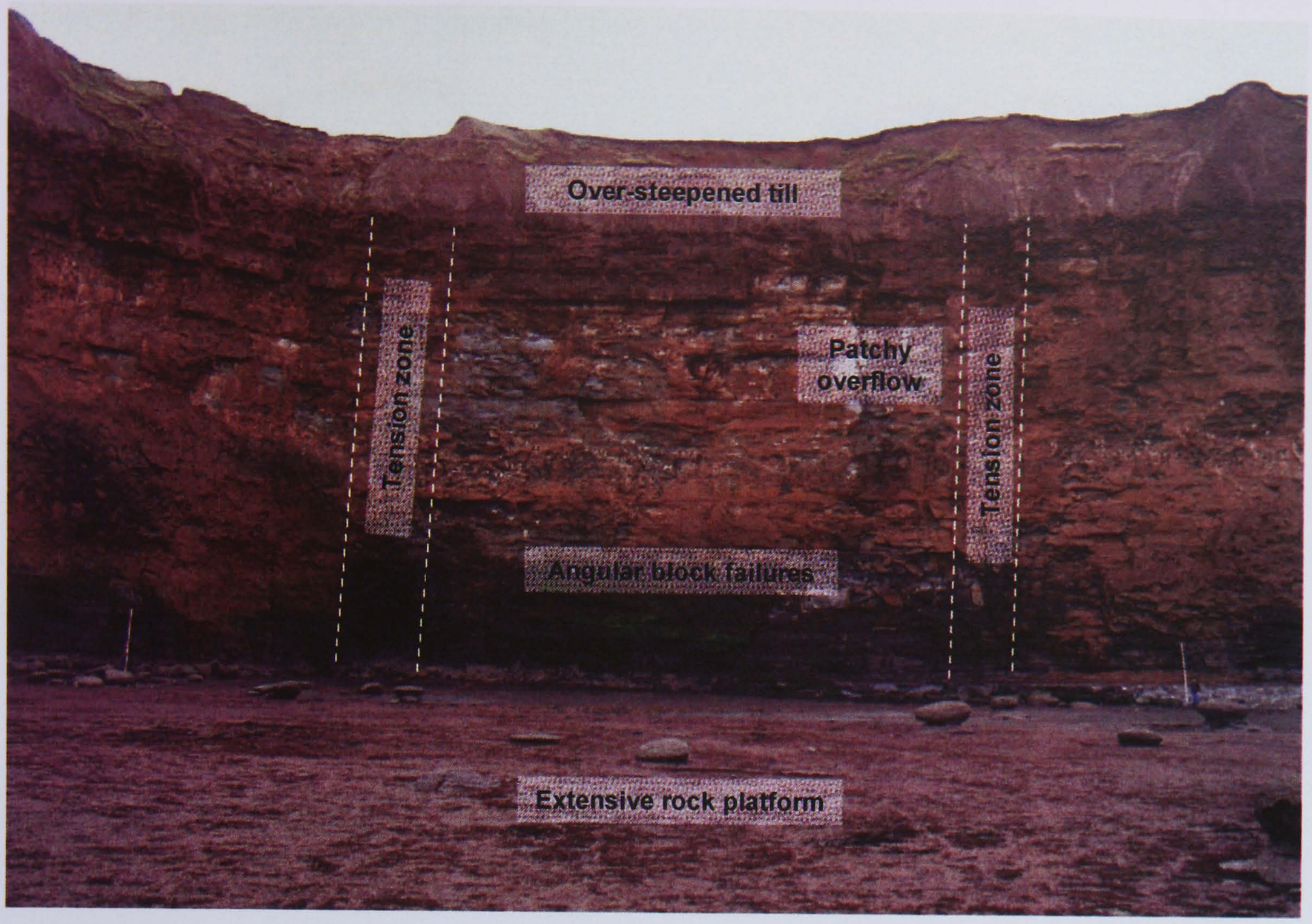

Figure 3.17: Annotated photo of Site 3, selected to investigate the effect of dense jointing on the nature and rate of failures in the rock mass.

3.5.4 Site 4

Over 270 m northeast from the well-jointed embayment lies Site 4 (NZ 776188), the Red Nabbs headland. The site was selected to investigate whether differential patterns of change exist across a headland feature and whether seepage flowing through a rock mass can have a detectable influence on its behaviour. The headland reaches a position 150 m seawards from the base level of the coastline. The headland begins at Dove Hole Fault which has caused the headland material to be displaced 0.2 m below the mass to the west. The monitored section extends over 100 m across the western side of the headland and round onto its northwards face. The rock mass is consistently around 33 m high, with a 3.7 m thick mudstone toe. The shale layers above show marked patches of seepage through the rock face, concentrated in a shale layer 10.5 m from the toe (Figure 3.18). The rock mass is sparsely jointed and capped by 20 m of till that reaches angles of over 50° in places. The till is drained by an outlet pipe that stops short of the cliff edge, leading to a flow of water over the leading edge of the headland. The rock platform in front of the headland ranges from 70 to 100 m at the front of headland and contains a 0.5 m step, delineated by a thin ironstone band, 17 m from the cliff toe. The foreshore is littered with weathered boulders that increase in size from the back to the front of the landform and appear to be mostly failed rockfall debris.

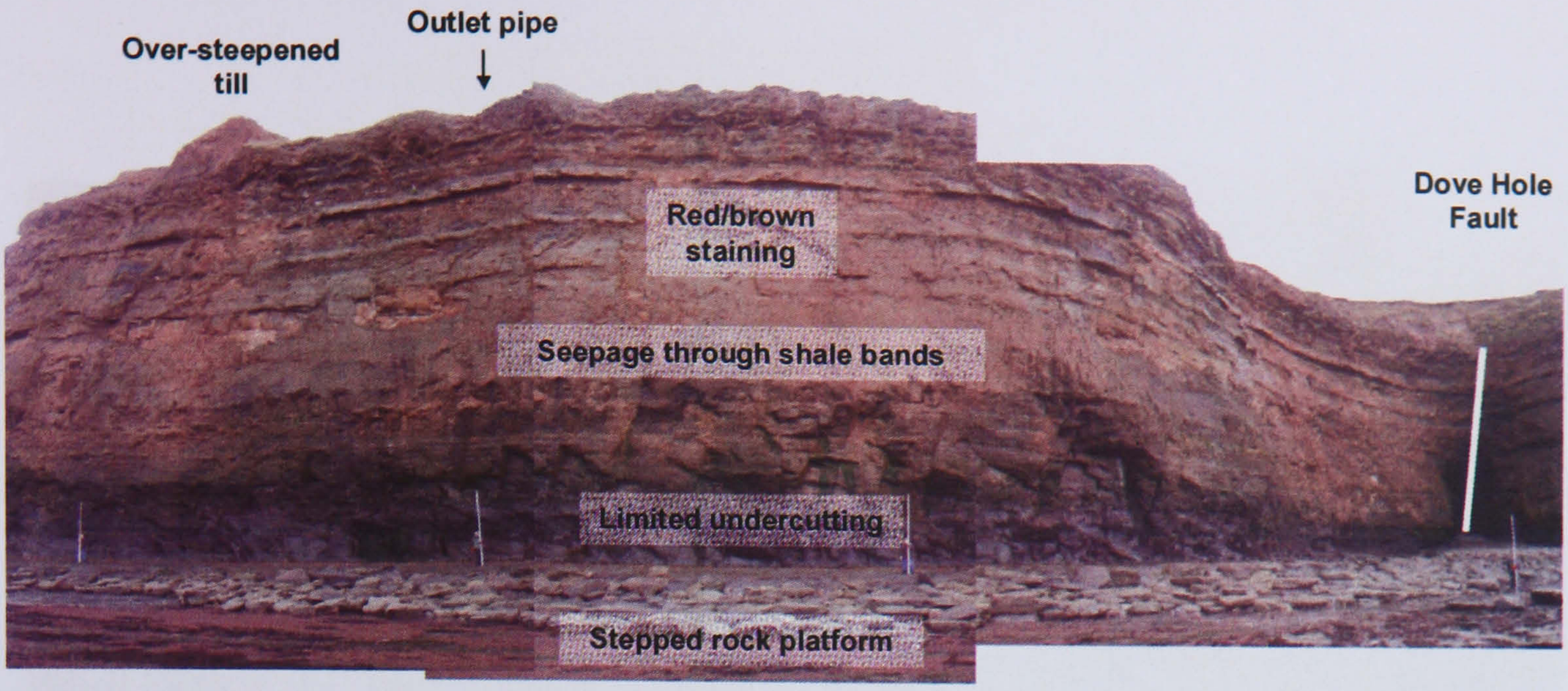

Figure 3.18: Annotated photo of Site 4. The headland was selected because of its structural and material properties which result in examples of potentially important processes such as undercutting, ledge overhangs and groundwater seepage.

3.5.5 Site 5

Site 5 (NZ 780189) is located on the north western face of Cowbar Nab, 470 m due east from the seepage headland and orientated 330° from north. Cowbar headland was selected for the consistency and clarity of its lithological exposures of the Staithes Sandstone Formation (Rawson and Wright, 2000). The headland begins at Sandy Wyke Fault, which has been protected against wave attack with rock armour. Rock armour has also been laid down to limit the erosion of the cliff adjacent to the pinchpoint where Cowbar Lane passes through a narrow gap between Cowbar Cottages and the cliff edge (Figure 3.19). Here the till has been regraded and a drainage conduit passes through the rock mass, exiting just above the 9 m high rock armour. The dip of the strata increases east of Sandy Wyke causing the rock mass height to decrease from 37 m in the west to 23 m at the eastern edge of the monitored area. The uppermost sandstone layers are thicker here than in any of the other sites but the vertical displacement means the cliff is based in shale rather than mudstone. The rock platform contains a 0.9 m step 12 m from the cliff toe and ranges from 140 to 180 m in width. It is covered by numerous pedestals that break up the foreshore topography, although its effectiveness as a wave energy sink is reduced to the west by a channel following the fault line at Sandy Wyke. The site was chosen to analyse both the effect of artificially armouring the cliff base against marine influences and the importance of interactions between different geological bands in constituting cliff form over time, a consideration often overlooked in rock mass studies (Eberhardt *et al.*, 2001).

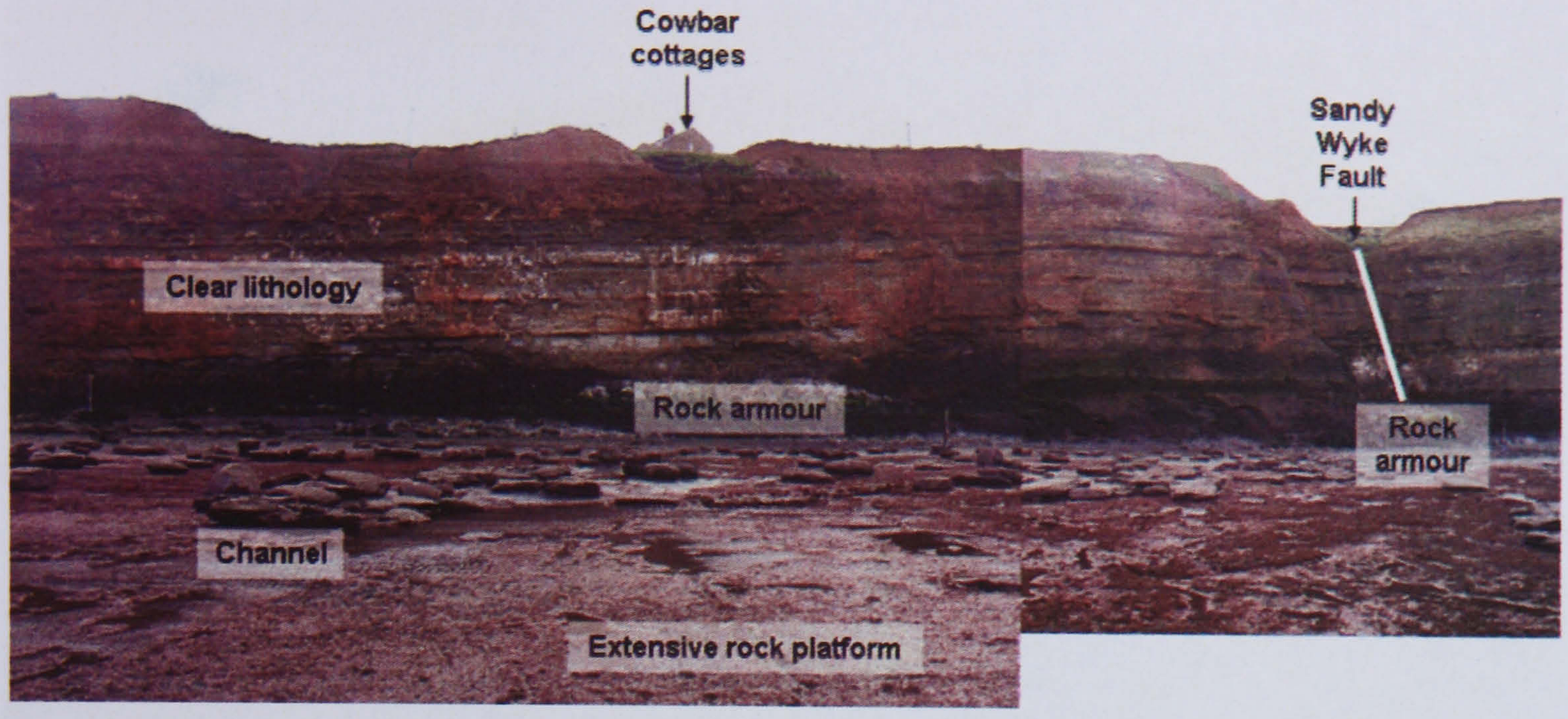

Figure 3.19: Annotated photo of Site 5, selected to investigate the interaction between different lithologies and the effects of armouring the cliff toe on slope behaviour.

3.5.6 Site 6

Site 6 (NZ 782190) is the eastern face of Cowbar Nab and forms the western side of Staithes Harbour. The site was chosen to investigate the influence of marine activity on rock slope behaviour through the comparison of sections of the same mass exposed to and removed from marine influence. The base of the cliff comprises of the thin oyster bed that divides the Staithes Sandstone Formation from the underlying Redcar Mudstone Formation. The sandstone layers protrude from the cliff face, causing the upper profile to overhang the toe significantly in parts. The rock mass is cross-cut by numerous perpendicular joints that form angular block failures in overhanging material. The harbour defences, completed May 2001, raise the exposed cliff face to above highest astronomical tide, effectively removing the rock mass from all but exceptional tidal inundations (Figure 3.20). The line of the eastern harbour defence strikes perpendicular to the cliff, causing an enforced division between the protected rock slope landwards of the revetment and the seawards area exposed to marine influence. The site is also beyond the effect of contemporary mining induced subsidence. The protected headland is comprised of the same geological and structural properties and is subject to the same climatic forces as the other monitored sites. It is however not considered to have been directly effected by subsidence and part of the cliff section has been protected from wave influence for the entire period of this research.

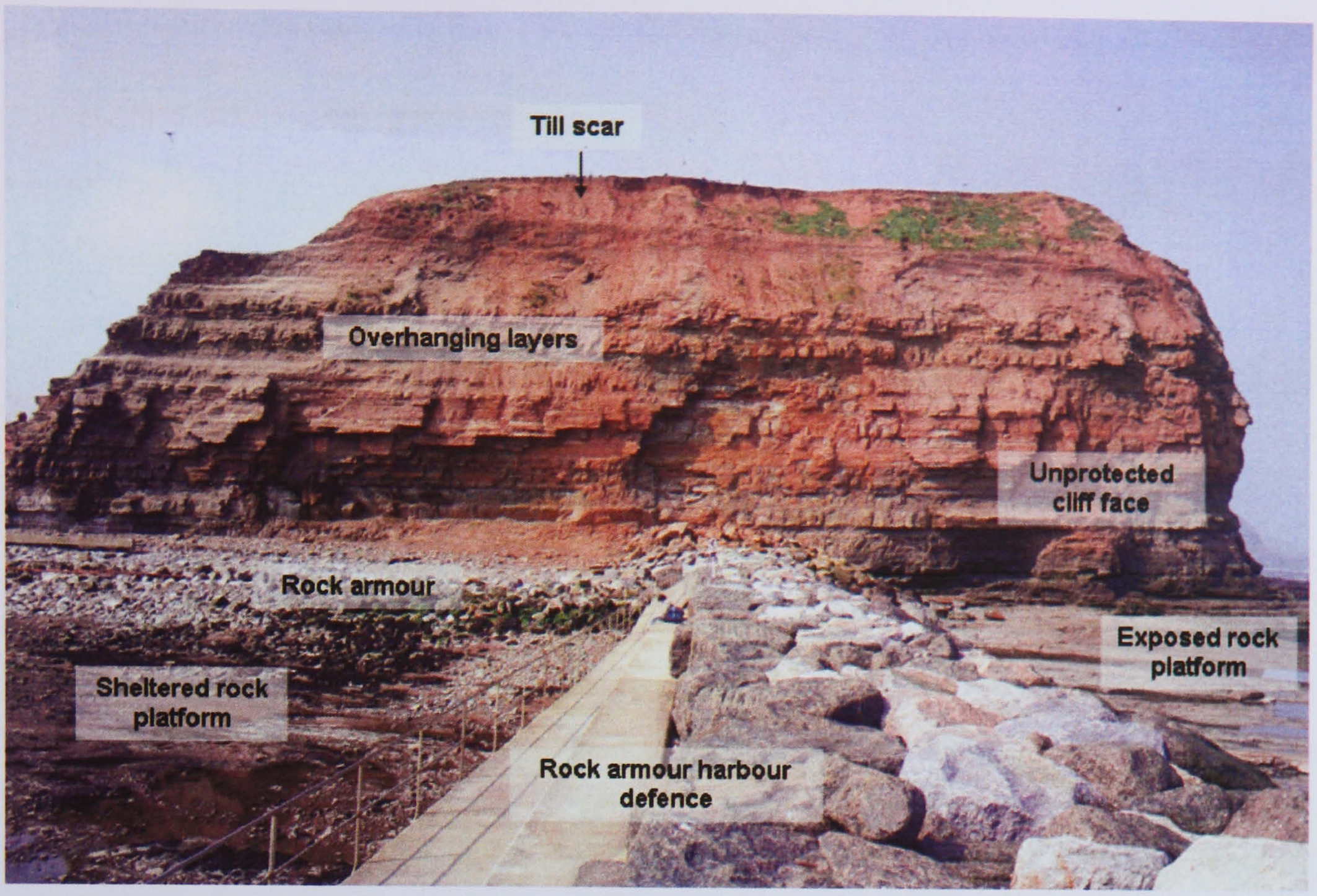

Figure 3.20: Annotated photo of Site 6, selected to gain an insight into cliff behaviour without the control of marine activity.

3.6 Summary

This chapter has introduced the research area of Staithes, North Yorkshire. The sequences of Lower Jurassic strata form interlayered bands, complicated by a structural history of uplift and subsidence, and glacial and interglacial episodes. Both climatic and anthropogenic processes operating at the coast have been considered and the current geomorphological understanding of the cliff behaviour in the area reviewed. The selection of six key sites has been made for the consideration of specific influences on rock slope behaviour. The following chapters investigate these site specific controls in the context of the wider geomorphological issues on the spatial and temporal patterns of change outlined earlier.

Chapter 4

Recording cliff change

4.1 Introduction

Problems hindering the accurate quantification of rock slope changes through time have meant that many questions on the nature of cliff behaviour have remained unanswered despite the advances made in monitoring and modelling techniques. This is because of the challenges posed by the collection and interpretation of quantitative data from large, inaccessible, sheer-sided coastal rock faces. Without an effective method to understand cliff change, many aspects of rock cliff evolution remain unclear. The new approaches used in this study require grounding in an established methodological framework. The overall approach adapts Carson and Kirkby's (1972) methodology for hillslope studies to collect data appropriate to better understanding rock slope behaviour (Figure 4.1).

A key requirement of this research has been to devise a technique capable of identifying and quantifying the patterns of change characteristic of rock slope behaviour. This chapter describes the development of a remote sensing approach which has overcome the barriers to monitoring cliff change in high-resolution. The relative advantages of terrestrial digital photogrammetry and terrestrial laser scanning have been investigated in order to assess their potential for recording accurate rates and patterns of cliff recession.

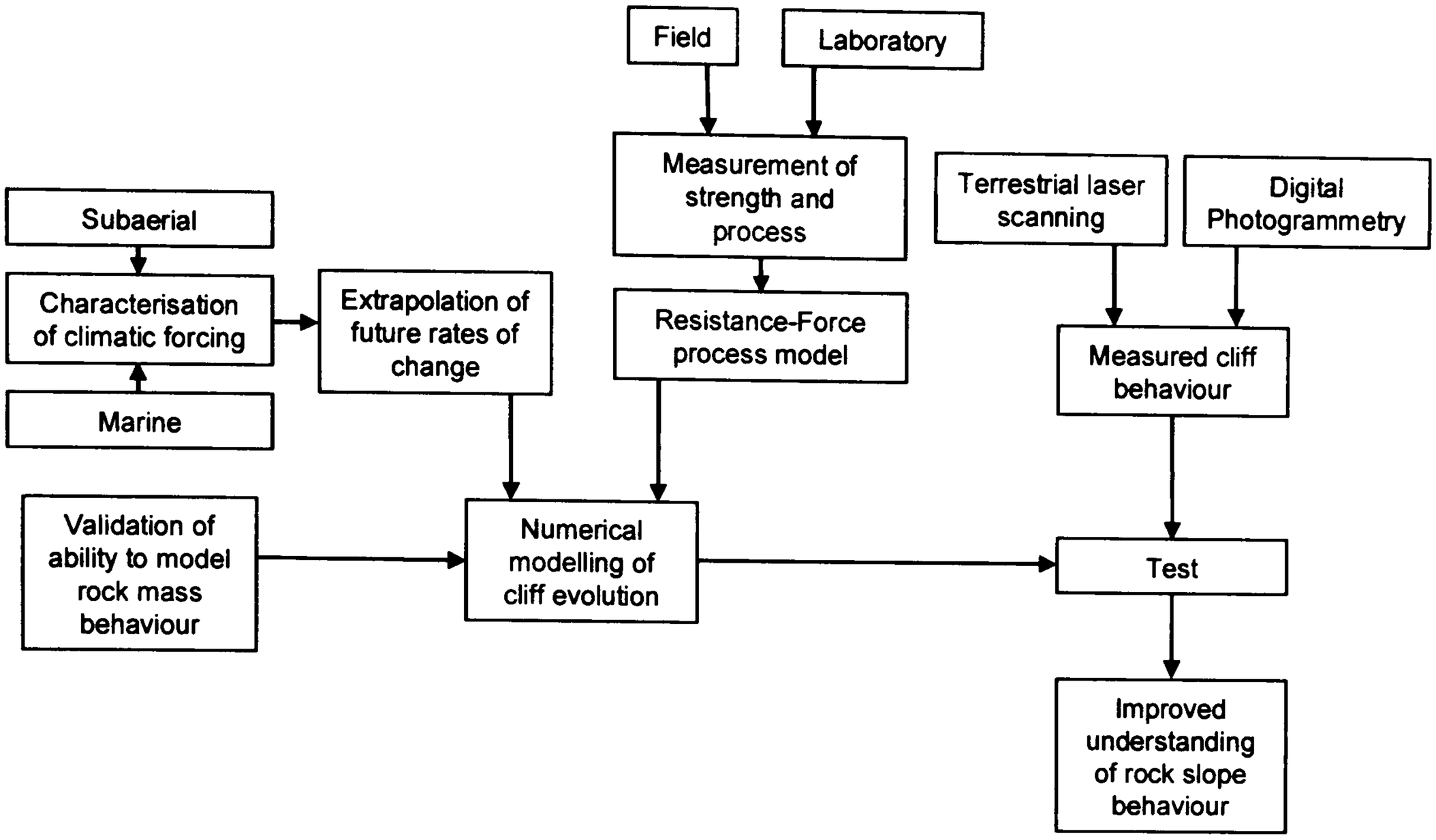

Figure 4.1: Approach adopted by this study, adapted from Carson and Kirkby's (1972) approach to hillslope studies. The aim is to address the inability to accurately measure and analyse three-dimensional cliff forms over time with the right-hand section of the workflow, before examining the findings with numerical modelling of the mechanisms recorded.

4.2 Barriers to recording change in hard rock coastal cliffs

Understanding of rock cliff behaviour requires quantitative measures of how they change. Such has been the inability of existing approaches to quantify the full range of cliff changes, that little is known about where on a cliff face change occurs and how much material is lost at what times of the year. As discussed in chapter 2, many of the barriers to recording cliff change arise from practical problems concerning the nature of the cliff environment. The scarcity of data on cliff face change has led to gaps in understanding of how cliffs evolve, which have caused further uncertainty over issues such as the relevant spatial and temporal coverage and resolution required to adequately monitor cliff forms. Terrestrial remote sensing techniques now offer the possibility of addressing the practical issues associated with intertidal bases, sheer-sided slope faces and often overhanging tops. This potential, however, has not been realised because the application of remote data capture to coastal cliff monitoring comes with its own set of problems concerning data collection, processing and analysis (Table 4.1). The technical issues specific to the application of digital photogrammetry and terrestrial laser scanning to cliff monitoring are referred to by number throughout this chapter, with particular emphasis on the areas of concern for which no protocols have been established by previous studies.

Table 4.1: Issues which require consideration in the application of digital photogrammetry and terrestrial laser scanning to coastal cliff monitoring; many of which remain unanswered.

	No.	ISSUE	SOLUTION
PRIMARY QUESTION		Within what error margins can change be reliably detected?	Unknown for this application
DATA COLLECTION	1	How can data be collected in sufficient resolution to monitor the changes in coastal cliffs?	Unknown for this application
	2	How to collect optimum data for digital photogrammetry?	The established laws of photogrammetric survey can be used
	3	How to collect appropriate data for photogrammetric processing?	OrthoBase terrain extraction requires images to be aerially orientated, but Chandler (1999) discussed the transformation of terrestrial to aerial orientations
	4	How to collect control points from inaccessible cliffs?	Methods for accurately recording points remotely such as with reflectorless total stations exist but have not currently been used for such an application
	5	How to collect laser scans of comparable resolution to the photogrammetric output?	The increments of the passes and density of points collected can be used to specify the resolution of the outputs
	6	How to orientate the laser scans consistently?	The scanner is equipt with an optical plummet and an internal compass which can zeroed on triangulation points to reorientate successive scans
	7	What it the effect of reflectance on accuracy?	Unknown for this application
	8	How does the scanner perform in the variety of coastal conditions?	Unknown for this application
DATA PROCESSING	9	How should data be processed?	OrthoBase has capability for DEM extraction, but only for aerial projects
	10	How to correct for internal and external orientation of the camera?	Established calibration practices exist
	11	What is the effect of increasing the number of tie points on block performance?	Unknown for this application
	12	How can elevations be extracted from topographically complex surfaces	OrthoBase can use tailored extraction schemes for subsections within each stereopair
	13	How should multiple images be triangulated effectively?	Studies suggest separate triangulations should be made for each stereo pair
	14	What is the appropriate strategy parameters to use for DEM extraction?	Several studies on the effect of varying stategy parameters but none on those appropriate for cliff faces
	15	How should data be processed?	Demon software has been developed to process scanned data
	16	How can each scan be related to the next in the sequence?	Demon possesses an iterative convergence procedure which can be used to relate different scans
	17	How can point errors such as fowl activity on the cliffs be removed?	Demon enables point removal
	18	What errors are incurred within individual scans?	Unknown for this application
	19	What are the errors between scans taken over successive epochs?	Unknown for this application
DATA ANALYSIS	20	Can change be reliably detected?	Unknown for this application
	21	How accurate are the outputs?	Unknown for this application
	22	How do software based error detections perform?	Unknown for this application
	23	What are the effects of the physical characteristics of the rock slope on error?	Unknown for this application
	24	What are the effects of pixel content on error?	Unknown for this application
	25	Can change be reliably detected?	Unknown for this application
	26	How accurate are the surface constructions?	Unknown for this application
	27	What are the effects of the physical characteristics of the rock slope on error?	Unknown for this application

Refers to photogrammetric monitoring
Refers to laser scanned monitoring

4.3 Field set up

It is evident from the questions raised that there are significant technical barriers to the application of remote sensing to cliff monitoring, which require data validity to be established within known error margins before it can be used. The accuracy of information collected from a remote point must deal with contrast, perspective variations and the lack of artificial control markers in addition to the height, angle and topographic complexity of the slope. Due to the lack of data on the changes occurring over cliff faces, the appropriate scale(s) at which to monitor such landforms remain undetermined. This is a critical component of cliff studies which has meant little is known about whether or not current datasets are monitoring at the scales of change

that actually influence cliff geomorphology. A key concern in the application of remote sensing to cliff faces is therefore the effective resolution required from the reconstructed surfaces. Resolution refers to the ability to differentiate between visual information (Lillesand and Kiefer, 2000), and is the main influence on the size of block losses that can be reliably detected from the cliff. Prior to the development of a monitoring methodology, the requirements for data capture at specific spatial resolutions were planned in order to investigate whether the form of cliff faces could be recorded in sufficient resolution for monitoring purposes (refer back to Issue 1: Table 4.1). The varying height of the cliff across the research area required each site to be considered separately to balance spatial coverage with the highest possible resolution.

4.4 Preparation for photogrammetric data collection

The aim of the preparation stage for cliff monitoring was to calculate the optimal position of the data capture stations in order to record cliff change at the highest resolution possible. The minimum required image pixel spacing was set so that each pixel represented no more than 0.02 m on the cliff face. This produced a DEM of 0.1 m grid resolution in the photogrammetric processing software, given the five by five pixel search area used to derive each elevation. The relationship between the focal length and effective pixel content of the camera was used to determine the coverage and flying height or range required from the monitoring stations. Given the 28 mm focal length of the lens and the 4536 x 3024 size of the imaging array, the maximum required distance to the cliff face was determined to be 70 m (Figure 4.2). This distance was reduced when the cliff height permitted, further improving the resolution of the monitoring.

Cliff change occurs at a range of scales, from small detachments through to large and dramatic cliff failures. The success of the photogrammetric application to cliff monitoring therefore depends on the ability to accurately record the widest possible range of cliff changes. Critical to the photogrammetric accuracy of any project is the quality of the stereo overlap of photographs used. The "height to base ratio" is the ratio between the distance separating the capture stations and the average range of the camera to the subject (Williams *et al.*, 2002). Variations in this ratio influence the stereo coverage between overlapping images and consequently can be related to the errors associated with the elevations determined (Equation 4.1).

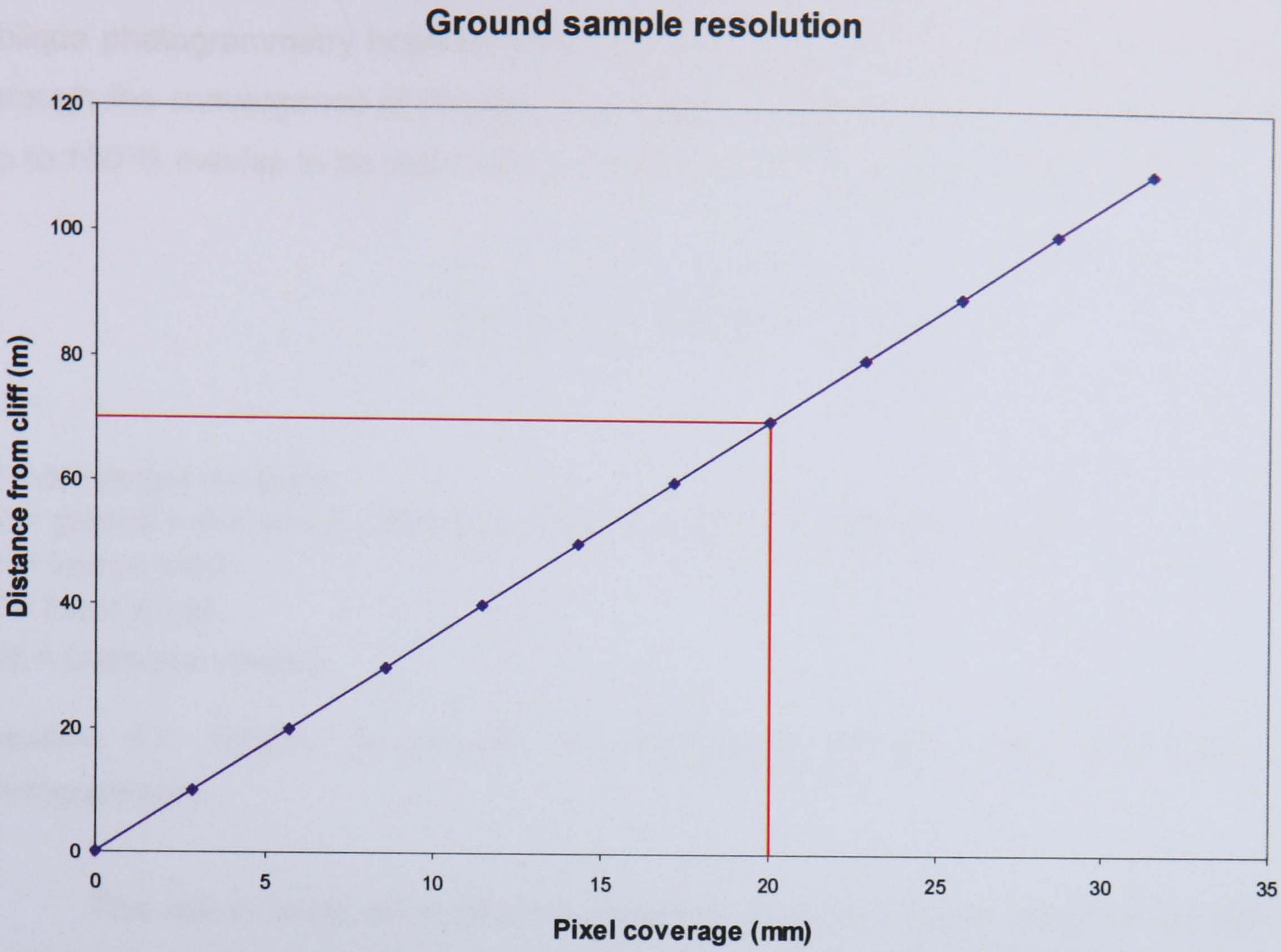

Figure 4.2: Calculation of ground sample resolution based on a 28 mm lens and 4536 x 3024 imaging array.

$$\Delta H = \left(\frac{H}{f}\right)\left(\frac{H}{B}\right)\Delta P_x$$

ΔH = elevation error
H = range to cliff face
f = focal length
B = separation of exposure stations
ΔP_x = measurement error

Equation 4.1: Equation of terrain error in photogrammetric models as a function of the station locations and camera properties.

The relationship between terrain error and image capture location suggests that the smaller the distance to the cliff with respect to the baseline, the more accurate the elevation calculations, thus enabling finer scale changes to be reliably detected. At 70 m and a height to base ratio of 0.4, an error of 0.001 m in images taken with a 28 mm lens would produce uncorrected elevation errors of 6.25 m. The same positional error in images related by a height to base geometry of 1, would incur 2.5 m of height determination error. The established convention for aerial photogrammetry is an overlap between images of 60 %. Given the 4536 pixel width of the images used, at 70

m the maximum distance between the image collections was 54.43 m. The use of oblique photogrammetry however enables reduced baselines to gain greater accuracy through the convergence of images. The ability to alter the stereoscopic angle allows up to 100 % overlap to be calculated using the following equation (Slama, 1980);

$$\frac{\theta}{2} = \frac{1}{2}\sin^{-1}\left[\frac{NW_f(1-OL)}{f}\right]$$

θ = convergence angle
N = ground point on the cliff face directly in line with perspective centre
W = image width
f = focal length
OL = fractional overlap

Equation 4.2: Equation to calculate the convergence between image pairs used for photogrammetry.

The use of large stereographic angles to generate greater areas of overlap is limited with respect to cliff faces by rapid changes in perspective. Digital stereo matching requires sufficient correlations between the image contents of convergent images to be found within the predefined search area. If the changes in perspective are too great, the relative distortions in the shape and content of the correlation area will result in failure of the stereo model. In order to collect optimum photogrammetric data (in relation to Issue 2: Table 4.1), a balance must therefore be set between the spatial extent of the overlap and the minimisation of perspective differences. The degree of acceptable convergence between images varied from site to site, depending on the specific geometry of the monitored cliff face. Where the cliff geometry caused large overlaps or included significant changes in perspective it was found to be beneficial to increase the intersection angles and segment the area mapped by increasing the number of images. The specifications of the camera, the lens and the geometry of the cliff face were used to generate bounding conditions for the positioning of the camera stations at each site. Survey nails were installed into the shore platform to create semi-permanent markers, which could be used to relocate the camera during repeated visits. The established boundary conditions for the location of the studs were used to define the correct area for each station, but the precise positioning was largely determined by the topography of the rock platform. In addition to the image collection points, triangulation markers were installed roughly equidistant to adjacent stations at the cliff base. These were used to confirm the orientation of the camera, and also as control points to aid the matching between datasets.

4.5 Photogrammetric field data collection

The camera system used to collect the photographic images was a fully calibrated Kodak DCS Pro 14n, fitted with an F mount Nikon Nikkor 28 mm 2.8d lens to minimise radial distortion. This professional medium format camera uses CMOS technology to produce a 13.5 mega pixel imaging array. The robust, light weight magnesium alloy body and fully integrated nature of this model make it well suited to the practicalities of fieldwork in a coastal environment.

The increases in image resolution mean the collection, processing and storage of data must be carefully considered. As with many modern digital cameras, the Pro 14n is capable of saving the images to multiple file types. Raw image file types preserve all image information collected by the sensor at the time of capture. These digital equivalents to the photographic negatives of film cameras can be enhanced and balanced after capture. The size of the file however, averaging at 15 MB imposes practical restrictions on the number of images that can be collected before downloading is required. Due to the number of images required to monitor six or more sites in a single field session, the smaller Joint Photographic Experts Group (JPEG) file type was used. This reduced the size of each image to 5 MB, tripling the effective storage capacity of the 1 Gb IBM microdrive compact flash card. The JPEG file structure employs a lossy image compression algorithm which classifies and removes both redundant and irrelevant information from the file. Robinson *et al.*, (1995) investigated the effect of the resultant loss of image content on automated DTM extraction performance for a feature-based matching software system, MATCH-T. The magnitude of the effect on software performance was found to be dependant on the image resolution and compression ratio used. JPEG images were captured at the highest resolution possible and converted to an uncompressed Tagged Image File Format (TIFF) to maintain the maximum amount of image information.

The use of JPEG images placed a larger emphasis on the use of appropriate camera settings during image capture as they cannot be reset like the raw files, although Kodak's JPEG imaging file format does allow certain post-capture image enhancements to be made. A particular problem with obliquely photographing cliff faces became evident when sections of sky were included in the frame. This caused the automatic photobalance to overexpose the cliff face, degrading the image content. The background contamination was compensated for by weighting the exposure metering, emphasising the brightness within a 12 mm diameter circle in the centre of the viewfinder. In extreme cases of contrast caused by bright ambient conditions,

image quality was improved by initially centring the viewfinder entirely on the cliff face and noting the correct auto shutter speed and aperture levels before re-orientating the camera and manually resetting the exposure settings. This sensitivity to contrast and exposure differences demonstrates a major limitation of photographic collection from a dynamic intertidal environment where the temporal window for data collection is limited.

The camera body was fitted with a dual spirit level enabling gross tilt errors to be minimised. The camera was mounted on a heavy weight Manfrotto frame to reduce vibrations during image capture. A survey plummet was used to centre the tripod over the locator nail and the height from the ground surface to the perspective centre, marked on the camera frame, recorded. A geared tripod head allowed the camera orientation to be precisely controlled (Figure 4.3). Camera elevation was recorded with a clinometer positioned on the camera mount. This field set up quantified rotations of the camera about the X, Y and Z axes to within one degree accuracies. Initial results from test images indicated that large overlaps were necessary even in relatively smooth cliff faces to reduce occlusion and maximise image correlation. The optimum angle of inclination was found to be close to 10˚ with matching impractical beyond 15˚ due to perspective distortions, shadowing and lack of image content. These angles are typical of those found in architectural photogrammetry (Clowes, 1999), an indication perhaps that common laws govern different terrestrial photogrammetric applications.

An essential element to photogrammetric applications is a good coverage of clearly identifiable control points within the stereoimage. When accurately known with respect to a particular coordinate system, control can be used to calculate the exact spatial position and orientation of the sensor at the point of capture (Lillesand and Kiefer, 2000). The conventional method employed in aerial photogrammetry involves the location of high-visibility phototargets with a global positioning system (Stone and Clowes, 2004). Some terrestrial applications also use retro-reflective markers which can be surveyed with a calibrated total station to gain ground control (Desmond and Bryan, 2003). The use of artificial reference markers and ground-survey techniques to collect ground control is extremely problematic in near-vertical rock slopes which cannot readily be accessed above the cliff toe (Issue 4: Table 4.1). To overcome inaccessibility, a Leica TPS1200 reflectorless total station was used to collect the precise coordinates of distinguishable natural features on the cliff, forming the basis of a control point network. An evenly distributed grid of points was supplemented with targeted collection from more problematic areas of significant topographic complexity (Figure 4.4). The ease with which data can be collected enabled a significant redundancy of points to be achieved. This surplus control proved essential in

mitigating the problems of using natural features, such as the loss of rock material over time and variable errors between the unmarked points.

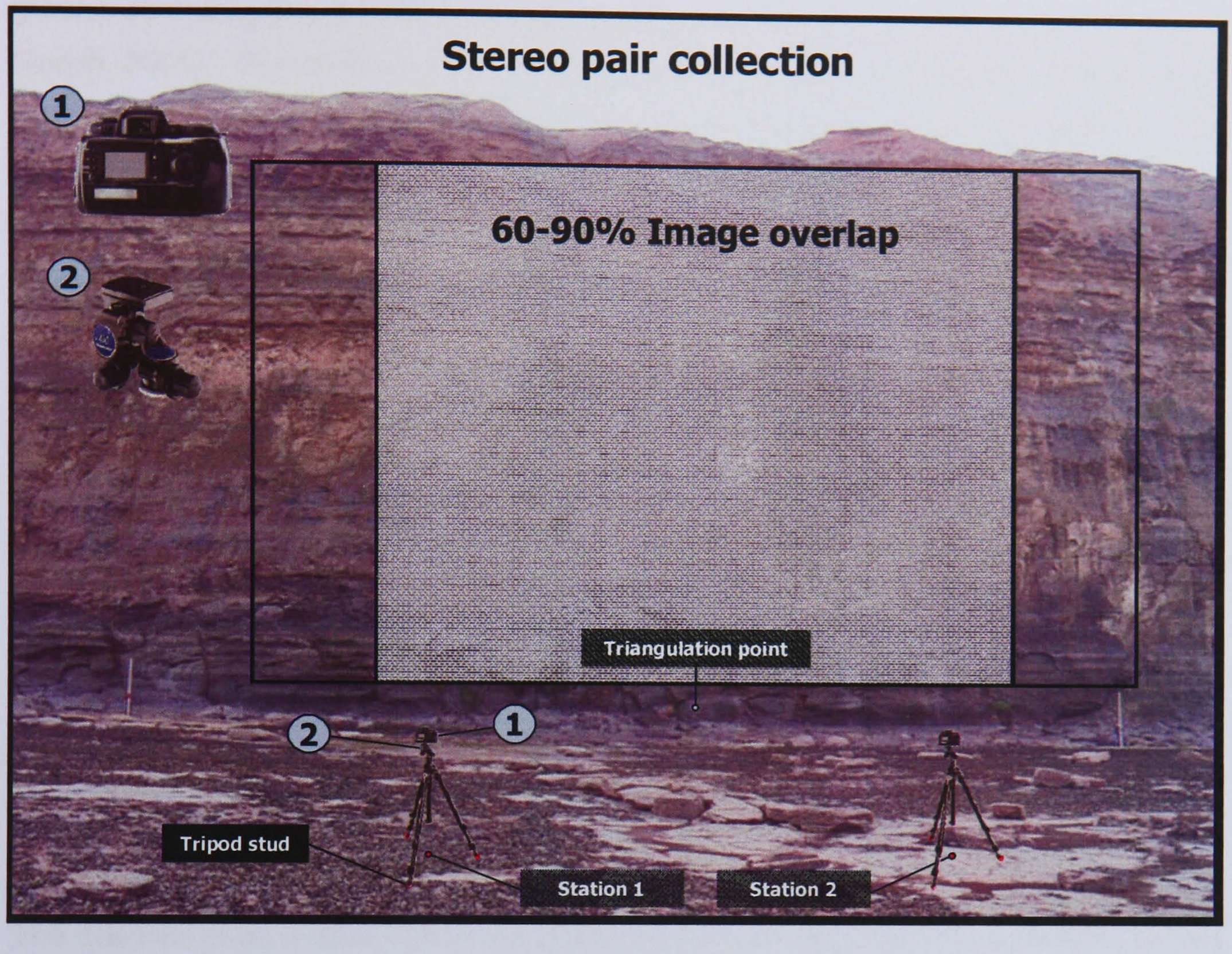

Figure 4.3: Field set up for collection of stereopairs, using semi-permanent studs and a geared tripod head to locate and orientate the camera for convergent images.

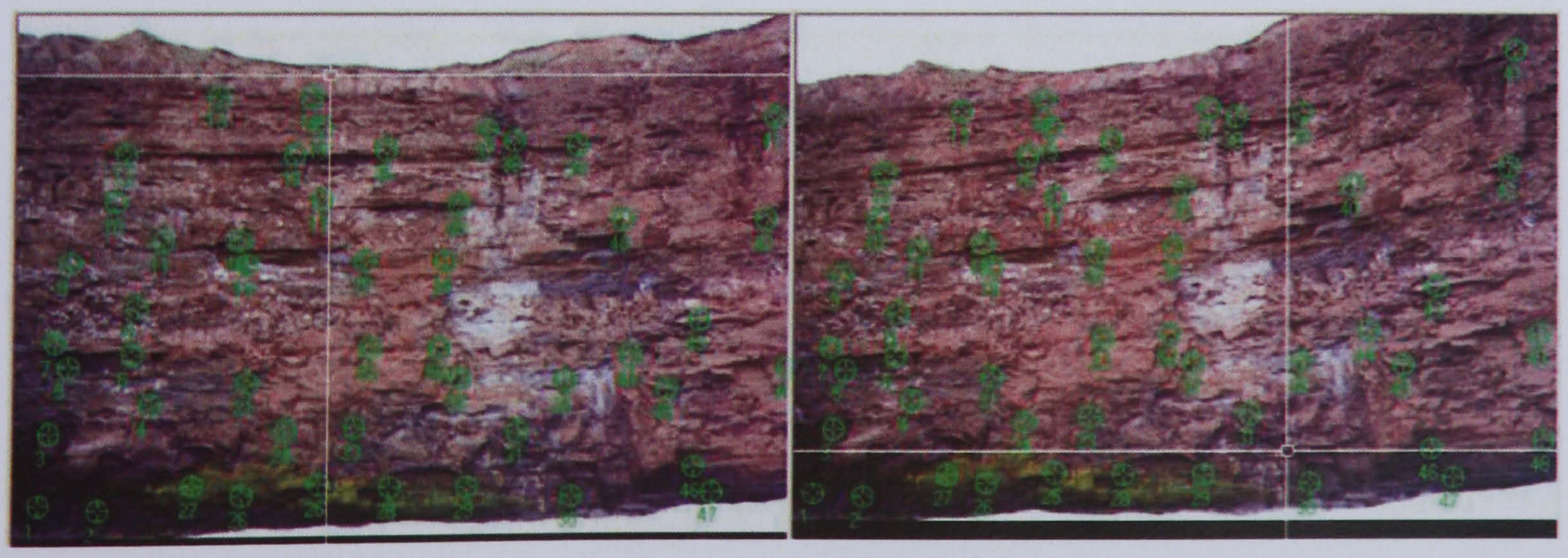

Figure 4.4: Natural control point collection, using a reflectorless total station to select extensive control point coverage, representative of the general topography of the cliff face.

Despite overcoming the long-standing barrier to obtaining accurate control from inaccessible surfaces, a concern with the reflectorless survey technique is the use of clearly identifiable natural features across the cliff face. An important element of ground control is that it should be representative of the surrounding terrain (Fox and Gooch, 2001). The location of clearly identifiable features on a rock slope is likely to be biased towards the collection of points that stand out from the overall topography. The restriction of control to areas of difference such as recognisable joints or the corners of overhangs may reduce the suitability of selected points in controlling photogrammetric procedure. Optimisation of ground control quality therefore required cliff features to be carefully chosen, where a precise point target could be identified, away from rocks of different reflectance and generally representative of the wider rock face in that area.

4.6 Laser point cloud field data collection

The laser scanning point clouds were collected with an MDL LaserAce 600, which uses time-of-flight data capture. The time taken for the 905 nm laser pulse to strike and return from surfaces up to 700 m away is used to generate accurate point coordinates. The optics of the scanner have been calibrated to an accuracy of 0.05 m at a distance of 200 m. The laser module is constructed from machined aluminium and is water and dust resistant to IP66 specifications. This robust design performed well under the range of conditions within the coastal environment (in answer to Issue 8: Table 4.1). The scanner head is attached to a levelling tribrach and mounted on a wooden survey tripod to minimise wind vibrations during scanning sessions. Motorised wheel drives turn the laser vertically through -45˚ to 90˚ and horizontally through 0˚ to 360˚, to a calibrated accuracy of 0.01˚. The motors are powered by a 12 volt 85 AH marine battery to avoid data loss under conditions of intensive data capture and sub-optimum operating temperatures. The actual accuracy derived from rock face targets may be subject to certain variables. The resolution of the location for each scanned point is the size of the width of the laser lens, 0.046 m, plus the 0.003 milliradians divergence of the beam by the time it reaches the rock face and returns to the scanner. The derived point will be significantly more precise than this because the scanner will record only the strongest part of the signal. The highest intensity is subject to certain variations caused by the reflectance levels within the cliff face causing the precise reading to belie possible inaccuracies in measurement.

The scanner was located over the most central photogrammetric station at each site with an optical plummet built into the frame of the scanning module. The MDL scanner uses the measured height of the optics to reference the scan to ground level. The scan resolution is a function of the desired density of points, the size of the area

surveyed and the estimated average distance to the face. The LaserAce has an internal compass which zeros itself when the device is activated. To relate successive scans to each other and ultimately to the photogrammetric data, a common coordinate system was devised at each site (Issue 6: Table 4.1). The baseline between the capture stations was defined as the X-axis, the Y-axis defining the vertical cliff height and the Z-axis the distance to the rock face. This was achieved by sighting on to the adjacent right-hand station, turning the scanner's internal compass through 270° and then resetting the compass. In addition, the 700 m range of the scanning system allowed permanent artificial control points such as radio masts on peripheral cliff sections to be repeatedly targeted to aid matching between scans. All point clouds were collected at 0.05 m increments to achieve a level of precision comparable with the photogrammetry (Issue 5: Table 4.1). The specified resolution required the collection of over one million points at some sites. Recording a maximum of 250 points per second, single scans regularly took over an hour to complete, limiting the number of sites that could be monitored in a single tidal cycle. The three-dimensional coordinates and an intensity reading for each point were written to 32 MB memory cards, capable of holding two or three scans.

4.7 Photogrammetric processing

Photogrammetry was once a highly skilled and time-consuming process; the same operations can now be performed within automated digital work flows (Saleh, 1996; Heipke, 1999a). This has led to the rise of increasingly diverse photogrammetric applications and a large degree of specialisation within the discipline. Selection of appropriate software should reflect the intended purpose of the outputs (Heipke, 1999b; Mills *et al.*, 2000). The key criterion in the development of photogrammetric models of cliff faces is the ability to accurately record detail across complex surfaces. Thus, photogrammetric processing was conducted using OrthoBase Pro, an add-on module to Erdas Imagine 8.6. OrthoBase was chosen because of the degree of control it gives the operator (Gooch and Chandler, 2000; Issue 9: Table 4.1). The flexibility to select any localised coordinate system, sensor type, image size and resolution makes OrthoBase ideally suited to the development of a new application such as cliff face monitoring. It also allows for obliquely orientated images to be processed, an important capability in the modelling of landform structures where standard vertical imagery performs poorly.

OrthoBase, like the Erdas Imagine geographic imaging suite, is modular. Each module refers to a stage of processing during the generation of three-dimensional surfaces. OrthoBase uses known control points and the internal sensor geometry,

location and orientation at the point of capture to establish a geometric relationship between the images (Wang, 1998). The sequential workflow corrects the error distortions leaving only the differences between the stereo images caused by surface elevation. The corrected image block is then adjusted and a further module, OrthoBase Pro, allows for the extraction of calculated elevations and generation of orthoimages. Like most photographic processing suites, OrthoBase has been designed for aerial applications. Consequently, the coordinate systems within which the software algorithms work differ from the terrestrially orientated data collected in the field. Terrestrial systems use the X-axis as the horizontal, Z as the vertical and Y as the depth field or range to the subject. Although the software does provide for terrestrially collected images, the extraction of digitally constructed elevations is not possible. This is because the algorithms used to calculate the elevations rely on having an absolute base level from which to build the DEM. In aerial applications, the base is sea-level, but in terrestrially orientated coordinate systems the origin is the instrument position. Therefore to process the stereo pairs the local Cartesian system had to be re-orientated and translated to simulate aerial data capture of the ground surface or cliff face in this instance (Chandler, 1999). Affine rotation and translation matrices were used to re-orientate the coordinate systems for each site (Figure 4.5), enabling OrthoBase to process elevations from the images. Image processing can be divided into four distinct stages; internal calibration, external calibration, tie point collection and aerial triangulation.

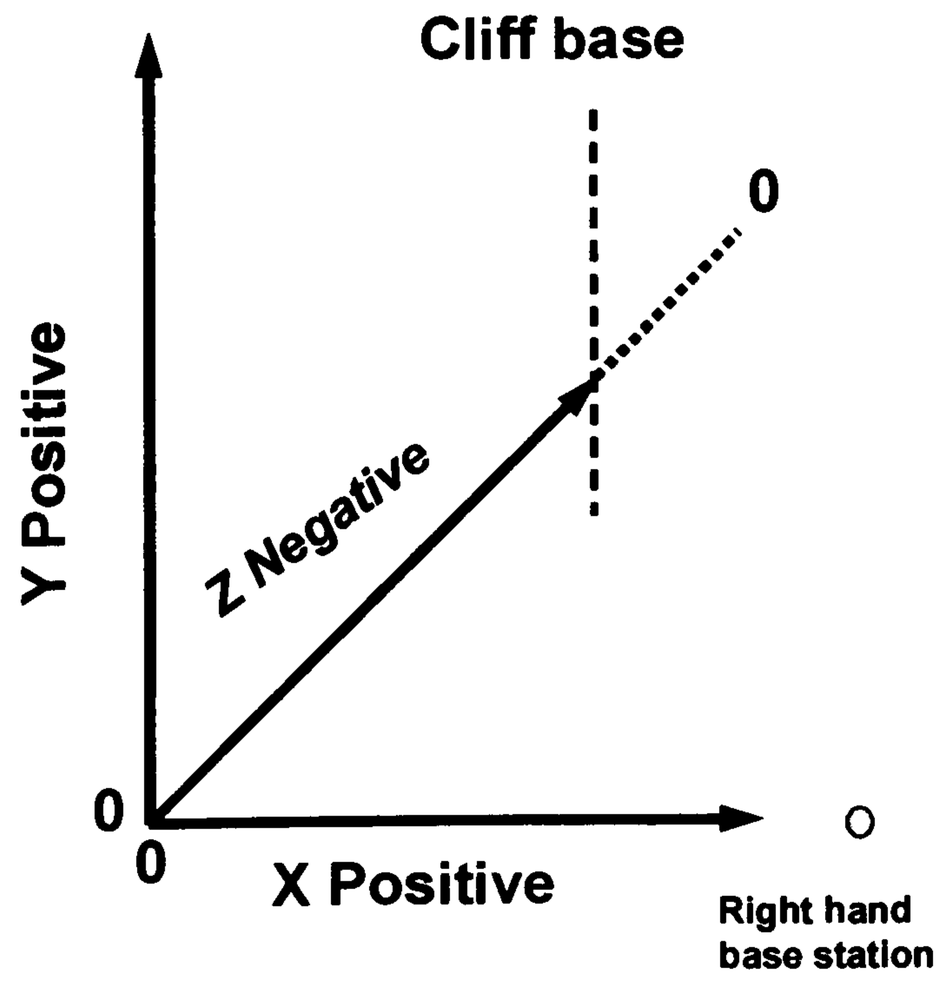

Figure 4.5: Coordinate system used after rotation and translation matrices have been applied. By rotating the coordinates through 90° about the X-axis and translating them so that the Z-axis values are above a 0 m base plane, aerial data collection is simulated (relates to Issue 3: Table 4.1).

A fundamental concept within the triangulation procedure used to extract elevation data from stereo images is that of colinearity. This assumes that for any point in real world coordinates, the so-called object space (A), the lens focal point (S) and its corresponding projected point in image space (a) can be joined by a straight line relative to the optical axis (Figure 4.6). The unique idiosyncrasies within each individual camera however mean that this is not the case and elevation is not the only influence on parallax within raw images (Fraser, 1997). The implication for cliff monitoring is that differences in successive elevation models may actually be caused by errors such as lens imperfections rather than by actual surface changes. The reconstruction of geometrically correct elevations requires the removal of both systematic and non-systematic errors.

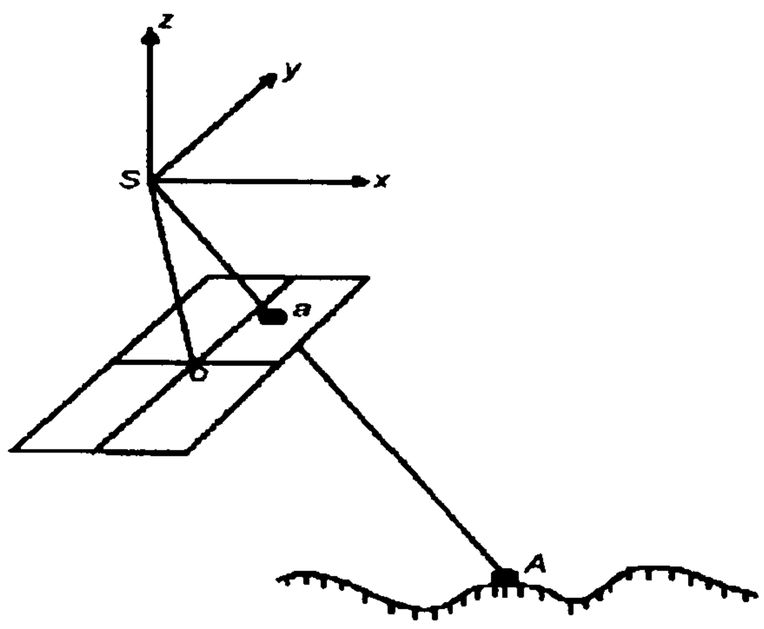

Figure 4.6: Collinearity condition for photogrammetric calculations (Erdas, 2001).

Internal calibration involves the removal of errors to image location and image quality caused by the camera system and lens specifications (Fryer, 1995). The two main concerns in generating accurate photogrammetric cliff reconstructions are the correction of radial and tangential distortions on image location and the precise definition of the camera's focal length and principal point. Determining the effect of offsets caused by the camera system itself is an essential component in the quality of the cliff monitoring data because very small perturbations can lead to significant errors in the final surface. The calibration procedure for the camera system involved the collection of two sets of images of a test field containing 111 targets from convergent stations. The image sets were converged at a range of angles from 0° to 60°, ensuring that a minimum of 66% of the control targets were covered by each image. The camera was rolled though 90° clockwise and anticlockwise and focused at infinity throughout. The targets were surveyed to millimetre accuracy in three dimensions and used to analyse the interior orientation parameters of focal length, principle point offset, radial lens distortion (k_1, k_2, k_3) and tangential distortion. The camera lens was locked at infinity focus in order to maintain the geometric stability of the setup, enabling focal length and principal distance to be used synonymously. The focal length is the

perpendicular distance from the perspective centre to the image plane. Although it is defined generally by the lens specifications, minor aberrations occur in the focal length of each lens, influencing the precision of the error removal. The specified 28 mm focal length for the camera used was actually determined to be 28.7190 mm during calibration testing under laboratory conditions. The principal point of autocollimation is the point in the image plane onto which the perspective center is projected. It is often considered to be the intersection between the fiducial and optical axes of the image (Wolf and Dewitt, 2000). In reality imperfections in the lens fractionally offset the ideal principal point, requiring the X_p and Y_p distances from the reference centre to be considered (Figure 4.7). The principal point was found to deviate from the geometric centre by 0.0362 mm in the X direction and 1.2924 mm in the Y direction.

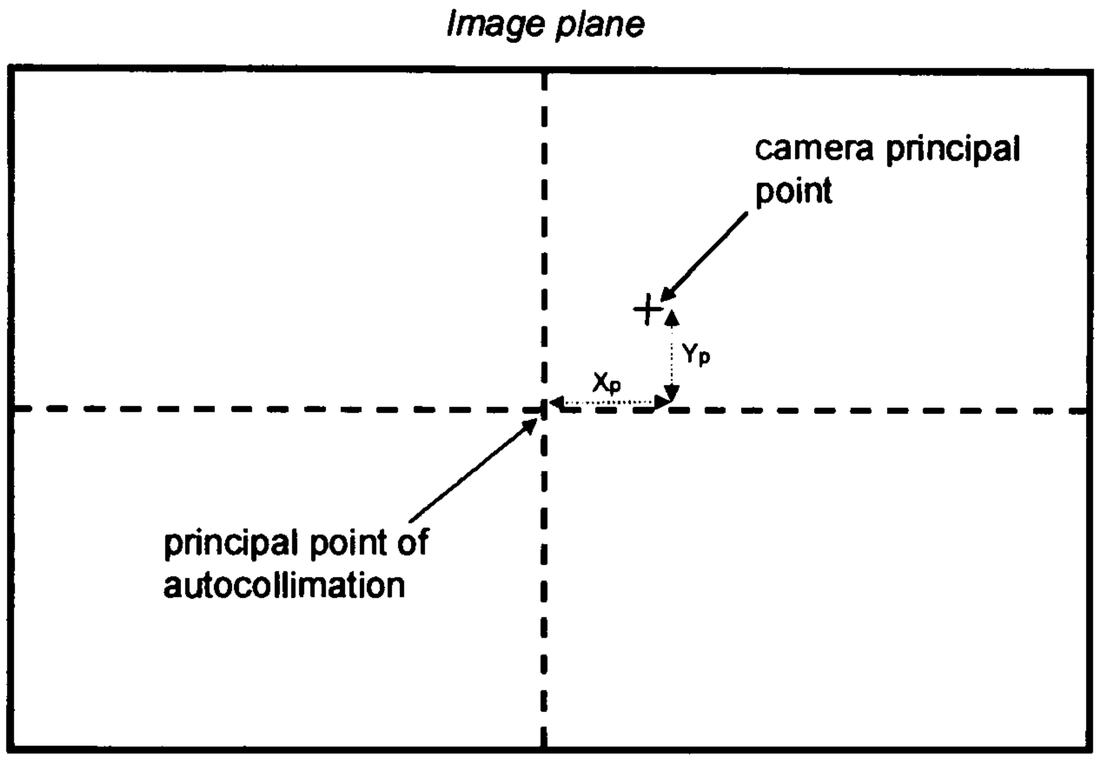

Figure 4.7: Principle point offsets caused by geometric distortions, with scale exaggerated to demonstrate the nature of the error.

Radial or symmetric displacement refers to the distortion of an off-axis target along the radial lines from the principle point. At infinity focus, radial distortion for the Kodak Pro 14n can be expressed in terms of three Konrady coefficients (Wolf, 1983),

$$\delta_r = k_0 r + k_1 r^3 + k_2 r^5$$

δ_r = radial distortion

$k_0 r = K_0$

$k_1 r^3 = K_1$

$k_2 r^5 = K_2$

Equation 4.3: Equation for radial distortion as a function of the Konrady coefficients.

The Konrady coefficients K_0, K_1 and K_2 enable the instability of the lens at the point of capture to define radial lens distortion to a sub-micrometre level. The distortion

increases away from the lens centre, generating a concentric pattern of radial error. This is particularly important in the consideration of steep-sided cliffs photographed from the base which means the subject surface is likely to extend to the edges of the image where distortions are greatest. The radial distortion for the 22.5 mm radius of the Kodak's 28 mm Nikon lens was calculated during calibration. OrthoBase statistically related the lens curve to derive coefficients of K_0 =1.8516400e^{-04}, K_1 = 4.9001600e^{-07} and K_2 = -4.1196300e^{-09}. The difference between radial and tangential effects is illustrated in Figure 4.8. Tangential or decentring distortion occurs when the elements in the lens system are not collinear with the optical axis (Fryer, 1995). Decentring of an object in the image plane increases with radial distance, but remains an order of magnitude smaller than radial distortion. It is only considered important as the camera ages or if it becomes subjected to excessive vibrations. The calibration statistics used in correcting the internal geometry of the camera have been summarized (Table 4.2).

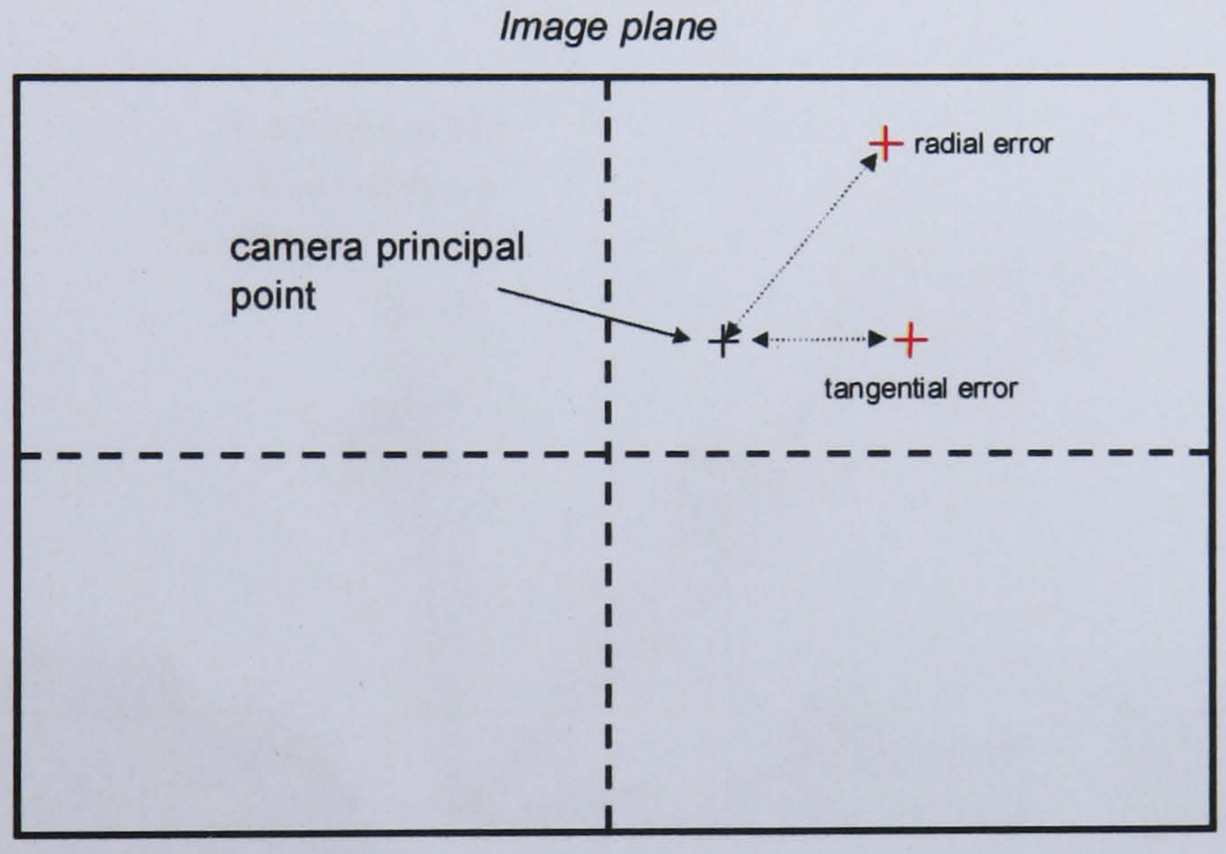

Figure 4.8: Radial and tangential lens distortions, with scale exaggerated to demonstrate the nature of the error.

Table 4.2: Summary of calibration statistics used for the correction of errors associated with the camera system (in relation to Issue 10: Table 4.1). For further details refer to Appendix 1.

Camera calibration statistics summary		
Camera	Kodak Pro 14n	
Lens	Nikkor468225	
Focal length (mm)	28.719	
Imaging array (pixels)	4536 x 3024	
Pixel size (mm)	0.008467	
Principal point offsets (mm)	X_p	0.0362
	Y_p	1.2924
Radial distortion (mm)	K_0	1.85E-04
	K_1	4.90E-07
	K_2	-4.12E-09

Having corrected for internal errors within the camera system, OrthoBase requires the exterior orientation of the camera as it existed when the imagery was collected. The quality of the final data on cliff change is dependent on being able to accurately and precisely establish the location and orientation of the camera as it captured each image. In modern aerial approaches this information is automatically registered with the use of an inertial navigation system. Terrestrial data collection must rely on manually recorded position measurements calculated in a local Cartesian reference system. The orientation was defined by omega, phi and kappa rotations about the X, Y and Z axes respectively. When related to the physical frame of the camera these rotations are influenced by the angle of inclination, the aspect and the horizontal tilt of the camera (Figure 4.9). The external measurements taken in the field are used by OrthoBase to set the initial orientation before a space resection technique is used to refine the precise exterior parameters using the collinearity condition.

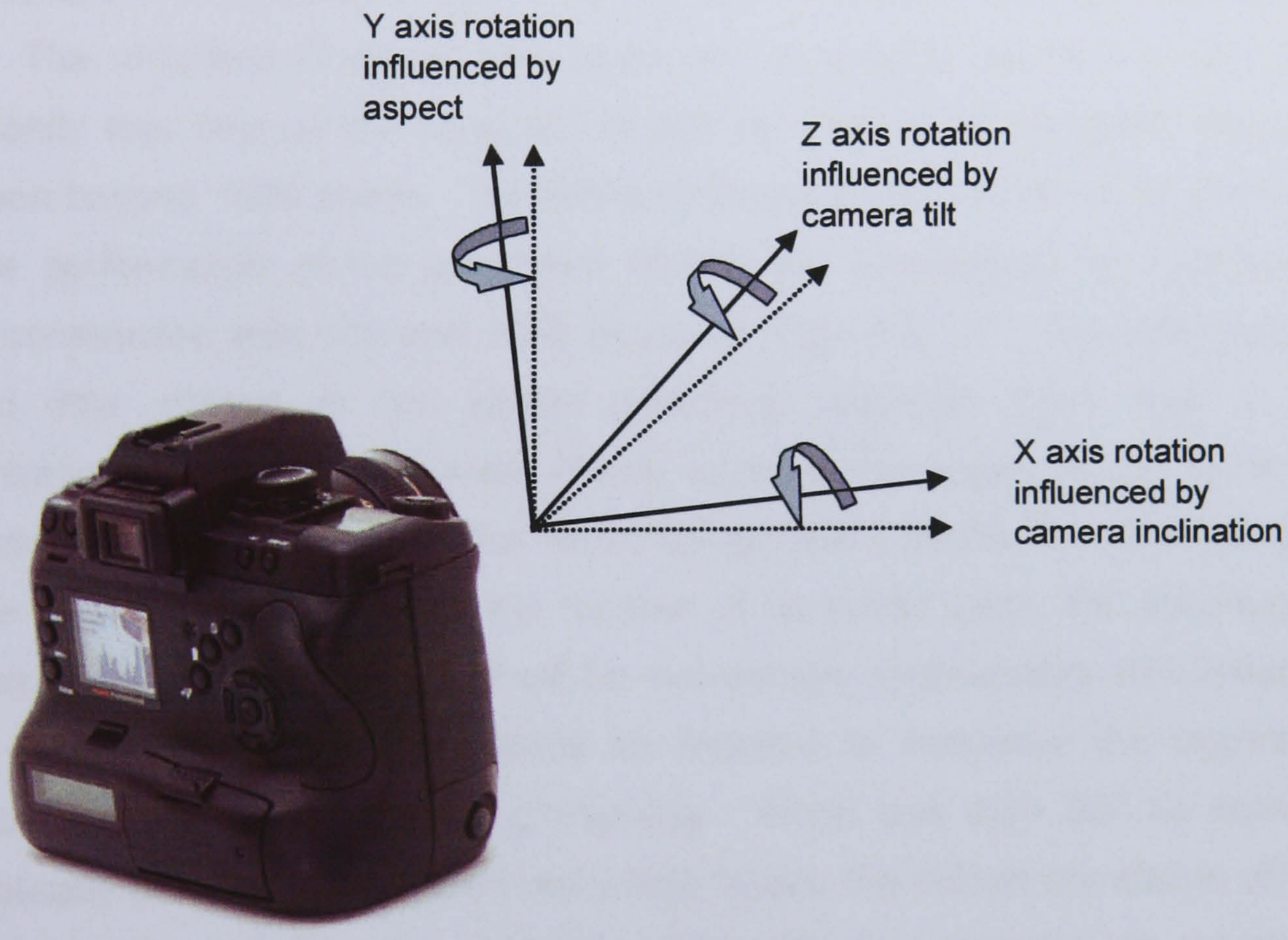

Figure 4.9: Camera exterior orientation: Z axis rotation was always minimized and X and Y axis rotations carefully recorded for every image.

Once the physical aspects of image capture have been geometrically related, the images are searched for corresponding features and matched together. The highly automated procedure involves the collection of up to 500 distinct tie points, within overlapping areas of stereo pairs. Identified tie points are visually recognisable features common to two or more overlapping images. OrthoBASE uses the Förstner

interest operator to conduct feature based matching, with additional area correlation and geometrical and topological constraints to define point collection (Wang *et al.*, 2002). A hierarchical system of searching is employed and least squares matching performed on the last iteration of the correlation to calculate the errors of the collection (Chandler *et al.*, 2003). The approach performs well when features appear different across images due to steep terrain or viewing angles, demonstrating the value of processing the photogrammetric reconstruction of cliff surfaces in OrthoBase.

The topographic complexity of rock slopes adds emphasis to the importance of tie point numbers, concentrations and matching strength which can be user defined in OrthoBase to suit the specific characteristics of the overlapped area. Increased numbers of tie points are thought to be important in ensuring block stability, because they reduce the relative percentage of erroneous points (Wang, 1996; Käser *et al.*, 1999), although little is known about their effect on the reconstruction of complex rock surfaces (Issue 11: Table 4.1). The effect of increasing the number of tie points on root mean square error (RMSE) of control points within the block was investigated (Figure 4.10). The reduction in errors associated with increasing numbers of ties became significantly less beyond the collection of 500 tie points and negligible improvement was seen beyond 1000 points. The effect of reducing the number of tie points on the ultimate performance of the generated DEMs was investigated by subtracting the DEMs constructed with 600 and 1000 tie points (Figure 4.11). The difference model showed little change in the spatial patterning, although there was a marked concentration of deviation between blocks towards the edges of the DEMs. The implication for cliff monitoring is that whilst the general patterns of rock slope changes may be detected irrespective of the number of tie points used, the accuracy of the changes at the edges of the DEM will be increasingly questionable with fewer points. Up to 1000 tie points may therefore be required to maximise the accuracy and precision of the photogrammetric processing. When less than 300 tie points were automatically detected across the three image layers, the default correlation of 0.8 was lowered to 0.7, reducing the inclusion thresholds for accepted tie points. The manipulation of assement criteria produced larger numbers of tie points although the less rigorous selection required the adequacy of each point to be manually assessed. It was found that reducing the correlation below this to the minimum of 0.6 produced relatively small increases in the number of detections and higher tendencies for gross errors.

The most important aspect of the digital rectification of cliff images involves automatic aerial triangulation or aerotriangulation of the image block (Jacobsen and

Wegmann, 1998). It merges the processes of measuring the image coordinates of generated tie points and refining and accepting the orientation parameters of the camera. The procedure relates each image through a similarity transformation to the camera, the object or ground space and the images around it (Shenk, 1997). The autonomous nature of image triangulation raises its own set of problems and uncertainties (Gooch and Chandler, 2000). Heipke (1999a) raised theoretical concerns over whether images should be matched as pairs or multi-image blocks and the most appropriate types of correlation that have yet to be adequately addressed by automated triangulation procedures (see Issue 12: Table 4.1). In the new application to cliff surfaces variables such as the initial accuracies of the estimated exterior orientations, the pixel sizes used and the degree of image compression will all influence the final relationship between images (Heipke and Eder, 1999). There is a pressing need to consider the nature of automation itself in order to understand the digitally generated outputs (Heipke, 1999a). In this study, processing errors have been minimised with the use of carefully constrained exterior orientation calculations, large numbers of well-spaced control points, uncompressed images and a minimum of 1000 tie points within each stereo pair.

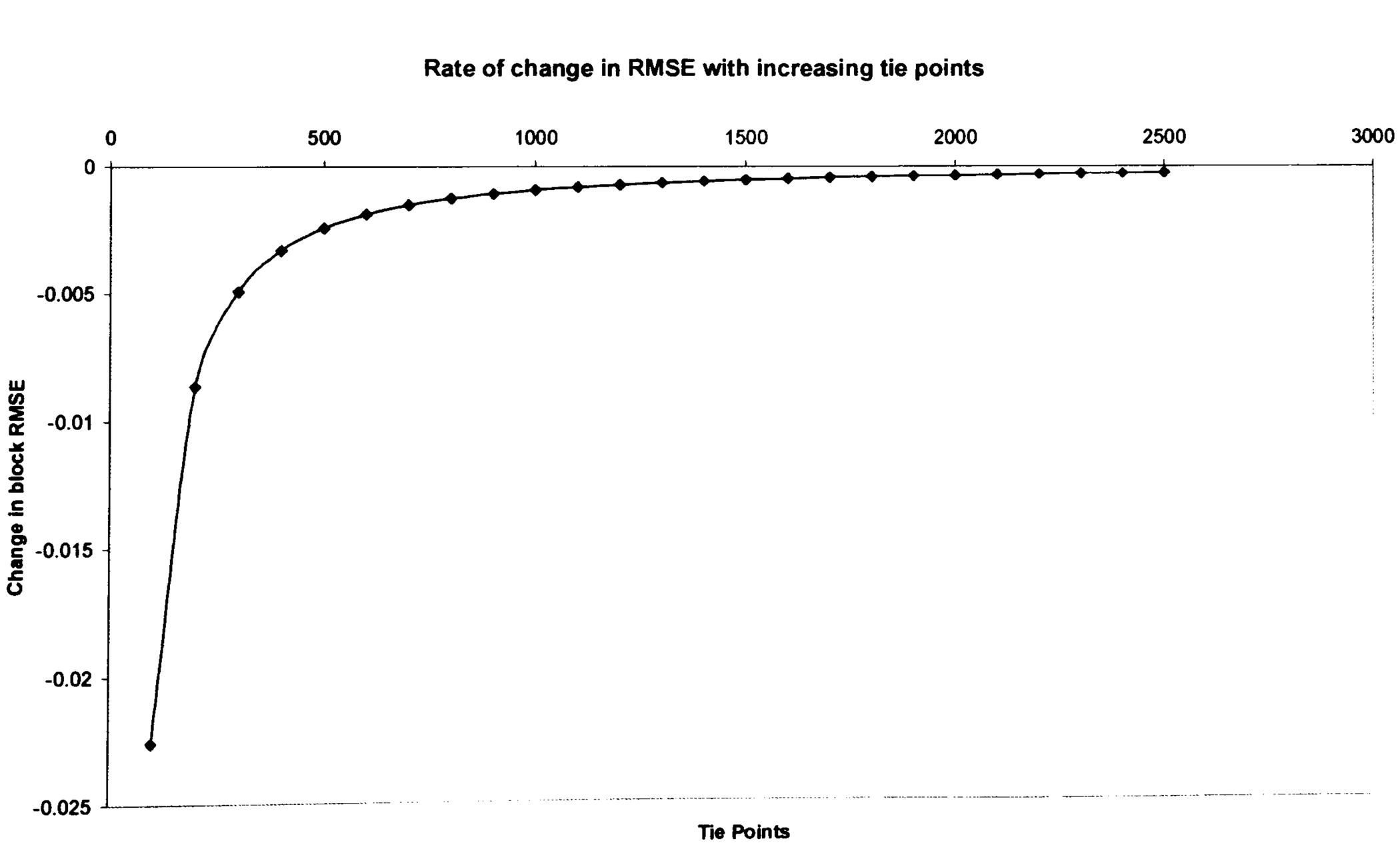

Figure 4.10: The proportional effect of increasing the number of tie points on block RMSE. Increasing tie point numbers beyond 1000 had little effect on RMSE.

Number of ties	600	800	1000
Block X RMSE	0.2092	0.2112	0.2100
Block Y RMSE	0.3246	0.3287	0.3317
Block Z RMSE	0.4267	0.4231	0.4231
Spatial distribution of extracted elevations	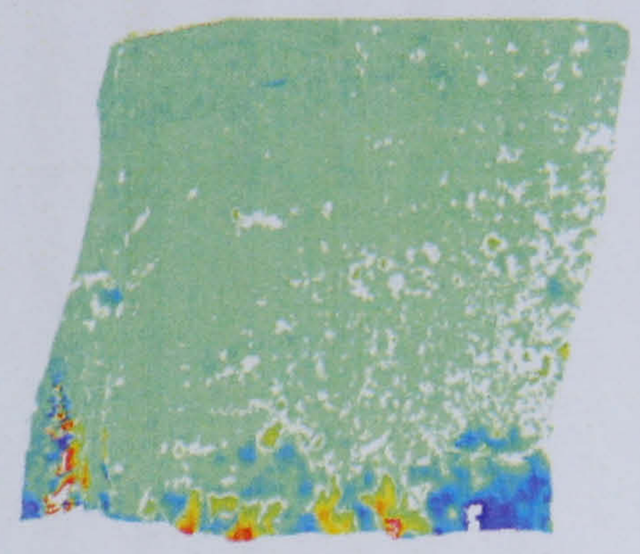	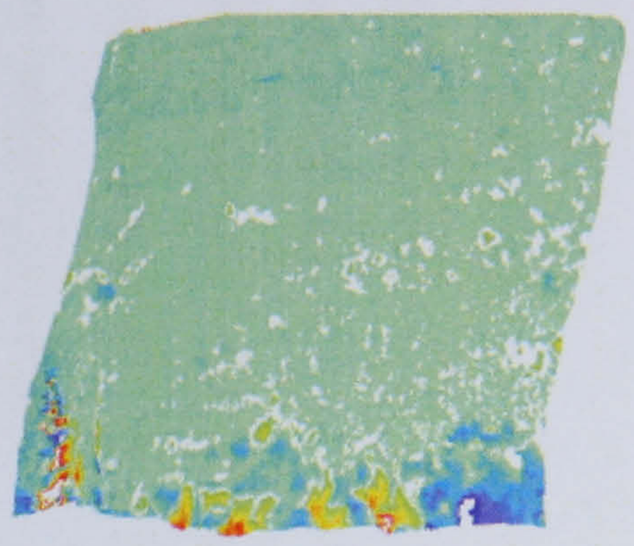	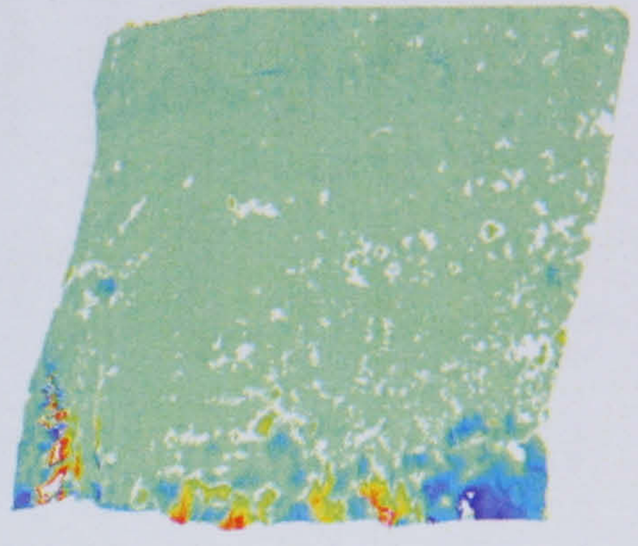
Difference between models using 600 and 1000 ties	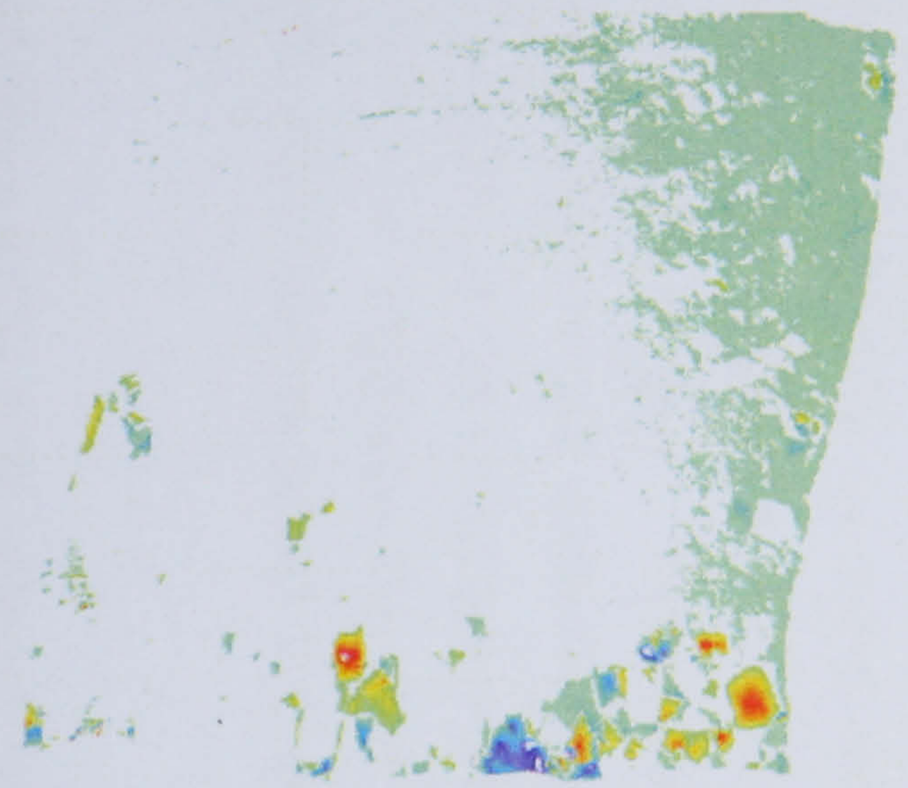		

Figure 4.11: The effect of increasing tie point numbers on block performance, distribution and accuracy of elevations derived. Although the patterns of elevations and RMSE calculations do not change significantly with increasing ties, edge differences are noticeable between models, implying tie points are important in complex topography.

The ability to match images depends on how the triangulation uses the correction information to generate coplanarity. The iterative least squares adjustment used by OrthoBase is considered the most accurate matching algorithm (Heipke, 1999b), relating the search window to a reference window by both radiometric and geometric pixel characteristics. The performance of the triangulation is detailed in a report of the overall solution quality which can be used to identify and remove the control points with the greatest error residuals (Wang, 1996). Control points can also be weighted as full, horizontal or vertical to emphasise their performance in all directions, the X and Y values or in the height or Z value (Lillesand and Kiefer, 2000). The weighting facility is particularly important in rock slope monitoring because the use of natural cliff features means that the precise quality of control points inevitably varies across the surface. The ground control residuals for the triangulated blocks were edited to ±0.1 m accuracy. To achieve the desired accuracy, control towards the upper sections of the cliff face consistently required removal. The increasing distortions caused by the perspective effects of a receding rock face could not be accounted for in the adjustment, highlighting a major limitation of the photogrammetric approach to monitoring cliff faces (see Issue 20: Table 4.1). Removing the upper control allowed high quality triangulations to be achieved but raised questions over the accuracies of the DEMs they would generate.

The problematic nature of DEM edge areas is of concern because they are likely to correspond with the cliff top and toe, often considered the most important indicators of cliff behaviour (Moore, 2000). Furthermore, in order to monitor cliffs over time, DEMs generated by successive image pairs must be closely related so that the only differences between them are the genuine alterations to cliff morphology. It is likely that photogrammetric models, under the sub-optimal conditions found at the coast, will incur errors. The decision over whether to triangulate successive image pairs separately, or to process the whole monitoring sequence together, influences how the errors are propagated through the surfaces (see Issue 13: Table 4.1). Correcting all of the successive monitoring images within the same triangulation resulted in consistent quality although the incorporation of the total errors across all stereo pairs reduced the precision of the procedure and led to a higher tendency for gross errors. Triangulation was therefore performed on each image pair separately. Separate triangulations enabled the largest GCP residuals to be targeted specifically, improving the precision of the procedure, although occasionally the individual corrections led to small systematic errors between models. Once the required degree of accuracy was achieved the triangulation solution was accepted, defining the relative orientation between the images. Bundle adjustment procedures were then conducted and gross

error detection applied to identify correlations with an increased likelihood of error. RMSE is also provided as a method of assessing the overall triangulation performances in terms of generating orientations, ground coordinates and minimising blunders.

The remaining parallax differences in the correlated images were used to extract elevation information on the cliff surfaces. The variation in terrain on cliff faces means the adequacy of the fit between two or more images will vary, often closer over smoother than rougher areas. OrthoBase Pro offers a number of default terrain settings which can be manually specified to differing topographic situations within the same overlapping area (Table 4.3; see also Issue 12: Table 4.1). Selection of the appropriate strategy parameters, varying in search area, correlation size, coefficient limit, topographic relief type and land cover object type, optimised the likelihood of obtaining reliable image matching results. When the criteria are not met a point will be interpolated from the standard deviation from the surrounding postings. DEM generation has been shown to be sensitive to even small parameter perturbations (Smith and Smith, 1996; Zhang and Miller, 1997). Once a surface specific strategy had been devised, generating spatially distinct extraction properties sensitive to the variable roughness of each cliff section, it was kept constant throughout the monitoring period.

Table 4.3: Terrain parameter settings used for OrthoBASE (Erdas, 2001).

	Search Size		*Correlation Size*		*Coefficient Limit*	*Topographic Type*	*Object type*	*DTM Filtering*
	X	Y	X	Y				
Custom Strategy	5	5	3	3	0.8	Rolling Hills	Low Urban	Low
Default	21	3	3	3	0.8	Rolling Hills	Open Area	Low
High Mountains	27	3	3	3	0.8	Mountainous	Open Area	Moderate
Middle Mountains	21	3	3	3	0.8	Mountainous	Open Area	Moderate
Rolling Hills	15	3	3	3	0.8	Rolling Hills	Open Area	Moderate
Flat Areas	7	3	3	3	0.8	Flat	Open Area	High
High Urban	19	3	3	3	0.8	Rolling Hills	High Urban	Low
Low Urban	11	3	3	3	0.8	Rolling Hills	Low Urban	Moderate
Forest	17	3	3	3	0.8	Mountainous	Low Urban	High

Terrain matching is a critical component in generating accurate cliff surfaces. OrthoBase, like many photogammetric packages uses reduced resolution datasets to aid matching (Shenk and Toth, 1991), initially searching a wider area for a correlation before steadily refining the window used to pinpoint the match. Additionally it uses an adaptive change function to mitigate the effects of rapid topographic differences. The dual matching capabilities allowed a customised strategy to be generated, with a reduced correlation area used initially, before a wider than specified area searched and refined if a match within more constrained boundaries was not found. The approach

reflects the suggestion by Lane *et al.*, (2000) that template size should be minimised over complex topography to reduce erroneous matches, despite the propensity for increased interpolation.

The way in which pixels are matched is important to the suitability of the procedure to the specific terrain being constructed. Images of rock cliffs are characterised by angular geometries and are often distorted by variable illumination and reflectance. The incorporation of feature-based matching allows OrthoBase to outperform area-based correlations in areas of large perspective difference (Gooch and Chandler, 2000), making it ideal for processing terrestrial information on rock cliff surfaces, although the repeatability of individual points may be limited (Erdas, 2001). Overall the automatic correlation of homologous pixel pairs enables successive DEMs to be directly comparable (Bailey *et al.*, 2003), free from the issues of reproducibility in manually collected DEMs (Krupnik, 2003). The file size of digital models requires careful consideration of the trade-off between finer, more representative grids and processing time and storage capacity (Zhang and Montgomery, 1994). This study sought to optimise the technique and consequently the customised algorithms were used to extract DEMs at the minimum five by five pixel spacing (Pauska *et al.*, 1991; McCullagh, 1998).

The elevations derived from the matching were interpolated to create a DEM associated with the image overlap (Hsia and Newton, 1999). The extracted DEMs were used to remove the distortions within the cliff imagery caused by variations in terrain elevation to form a planimetrically true representation of the cliff face. The resultant orthoimages were re-sampled with output cell sizes of three by three pixels and mosaicked to adjoining stereo pairs. Accurately orthorectified images have a consistent photoscale allowing real world, three-dimensional measurements to be taken of the monitored cliff faces viewed in stereo. The accuracies of the measurements are consequently highly dependent on the accuracy of the elevation model used. The resulting rasters were then available for difference modelling and quality analysis.

4.8 Laser scanned data processing

The raw point clouds were read into the Demon software package produced by Archaeoptics, maintaining the resolution of the scans to maximise the quality of the final outputs (in relation to Issue 15: Table 4.1). The scan data was initially rotated and translated through the same matrices as the photogrammetry to allow the two datasets to be directly comparable. A view-dependent triangulation was used to generate a

surface between the scanned points. The position of the triangulation origin was optimised when the distribution of points across the scene was even, minimising the occurrence of occluded points. A comparison between the optimal 'face-on' triangulation view point and a triangulation from an aerial perspective demonstrates the information loss in poorly triangulated surfaces and highlights the limitations of aerial data capture in cliff face monitoring (Figure 4.12). The triangulation procedure produced a mesh of individual triangles directly connecting all points within the scans, maintaining the precision of the raw data in the final surfaces rather than interpolating generalised topographic patterns. The ratio of triangle edges was used to identify and eliminate areas where inadequate point coverage caused triangles to become stretched.

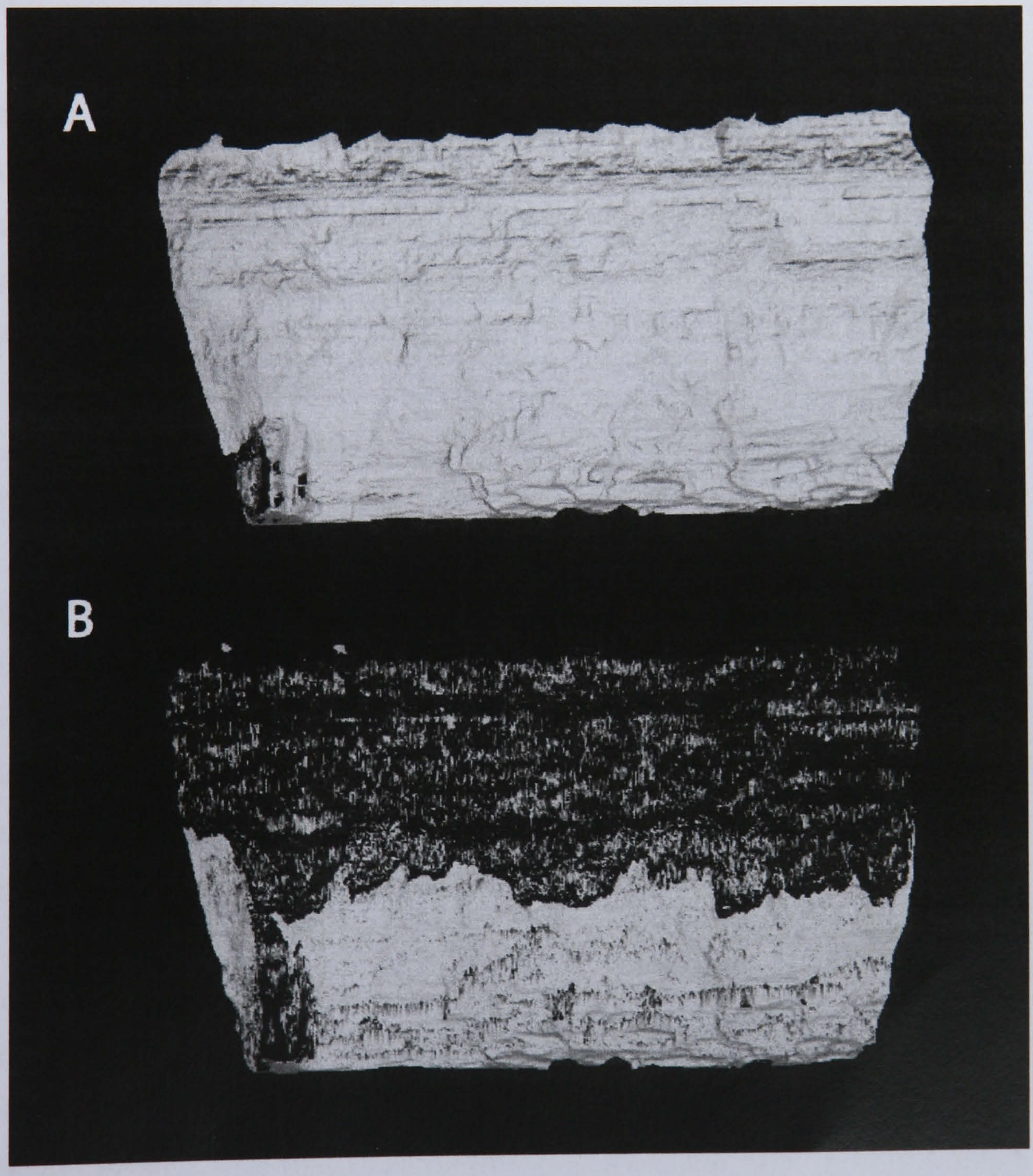

Figure 4.12: Triangulation of laser scanned point clouds. The view dependent procedure shows the importance of locating the origin in the optimal location (A), with significant information loss when constructed from an aerial perspective (B).

Demon was used to converge each scan to the next in the monitoring sequence (refer back to Issue 16: Table 4.1). The convergence operation processes the point clouds in two stages to find a least-squares best fit between the three-dimensional coordinate sets. Every point in the first scan is searched for the point of closest Euclidean distance within the second scan. The best-fit between the paired datasets is then calculated within Demon using a three-dimensional transformation algorithm to determine the vector translation and quaternion required for an optimal transformation (Horn, 1987). The root mean square deviation between the two scans is then computed and if greater than the desired deviation, the algorithm reiterates. The weighting in Horn's (1987) solution also limits the contribution of poor quality points, containing weaker matches than surrounding pairs, to the overall transformation. By specifying each mesh as non-deformable the surface is not altered, maintaining the accuracy of the original data throughout the processing. The sequential scans, representing different temporal epochs in the cliff monitoring, are drawn together based on reducing the distance separating the majority of points, ignoring the localised areas of genuine change. By monitoring a section of cliff face of sufficient size to avoid the influences of actual change to the cliff face, the errors associated with the positional accuracy of the scanner can be significantly reduced.

One additional error source, specific to the application of cliff face monitoring, arose from the presence of seabirds on and around ledges protruding from the rock mass. The birds are present all year round although populations increase significantly in summer months, causing significant degradation of the point data. Roosting birds often move and enter and leave the scan area. The LaserAce plots at sufficient resolution to be influenced by this motion. When the scanner strikes a bird flying in front of the cliff face the error is easily detectable, causing a large spike in the DEM (Figure 4.13). Identification of birds on the cliff face within the scan however is more problematic. Despite being aided by images captured at the time of the scan, errors due to cliff fauna are compounded by the time taken for data collection, imposing a limitation on the precision that can be reached with the scanning approach. The limitation is minimised in photogrammetry because any movement by the bird will cause differences between the images and the matched point will be rejected and an interpolation used.

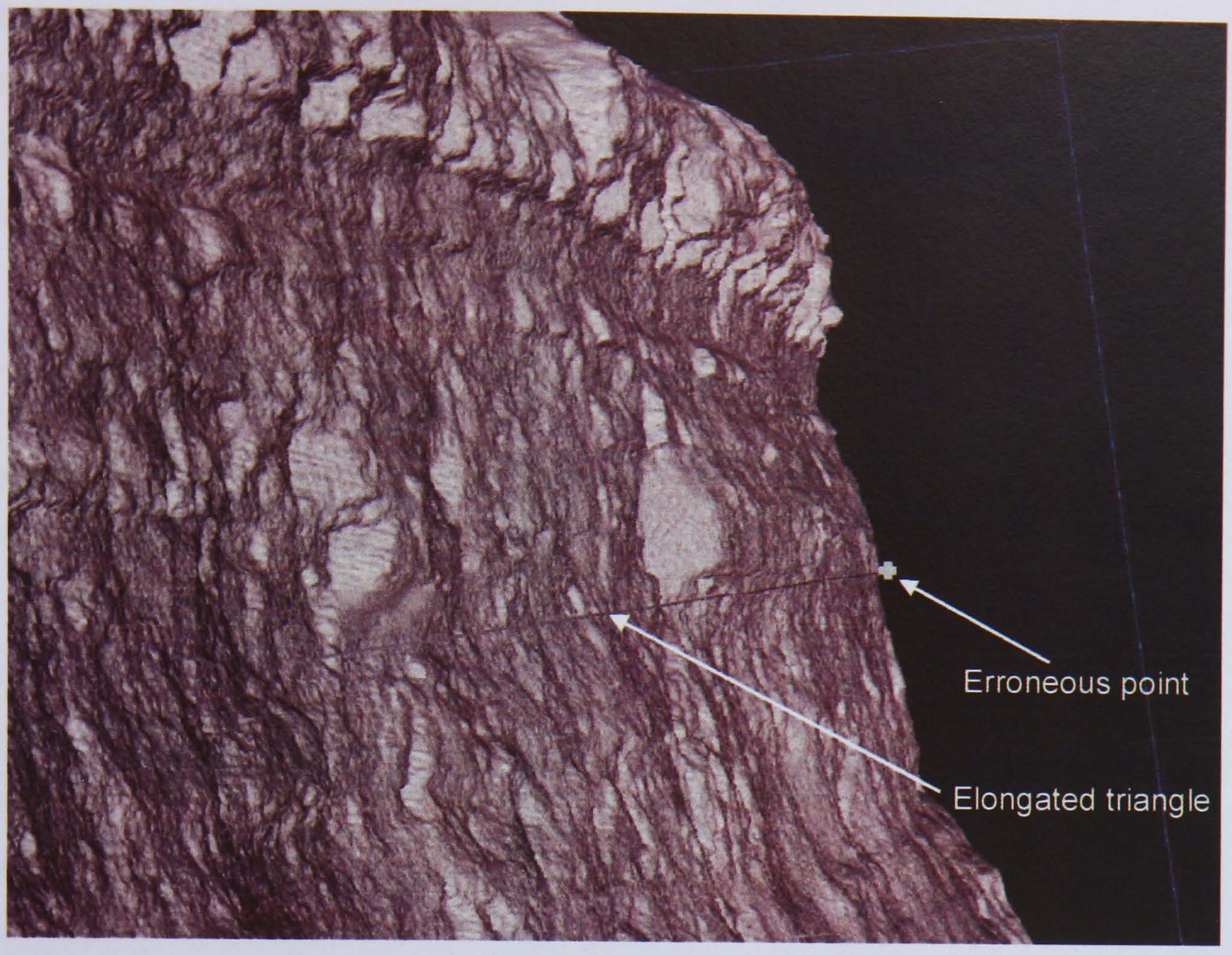

Figure 4.13: Laser scanning error caused by bird flight (refer back to Issue 17: Table 4.1).

4.9 Error assessment of remote sensing approaches

Increasing automation has made remote sensing approaches such as digital photogrammetry and laser scanning available to a wide range of non specialists, pushing both the techniques and their application further (Saleh, 1996). The technological advances that have facilitated this growth have introduced certain unknowns in terms of the accuracies of the outputs derived (Chandler and Padfield, 1996; Gooch and Chandler, 1999). The relative ease of DEM generation provided by autonomous digital processors has emphasised data analysis over data quality in many projects (Cooper, 1998). The automatic collection and extraction of elevation models generates vast datasets, with each posting referring to a single point on the true surface with more or less accuracy. The potential for variability within points, sections or even the DEM as a whole has caused DEM quality assessment to remain problematic. The limitations are particularly evident in the reconstruction of complex geomorphological surfaces such as cliff faces (Huang, 2000). Accuracy is ultimately dependent upon a range of factors such as the data source, the spatial resolution of the matrix, the collection method used and the processing applied. It is therefore essential that the errors associated with any new technique are established before it is applied.

4.9.1 Photogrammetric DEMs

The photogrammetrically-derived DEMs achieved high levels of precision, exceeding the resolution of even the finest laser scanned DEMs. The triangulation algorithms, tailored to each individual DEM, generated responsive surfaces and presented detailed records of individual block changes. The related orthoimages also revealed much about the circumstances causing the differences such as presence of boundaries between geological sequences or failure planes. In Figure 4.14 surface moisture is clearly seen above the highlighted area (A) but not below it. The sharp divide between the wet and dry zones marks the position of a joint in the strata which ultimately became a failure surface when the block was detached. Colour maps of the change were used to successfully identify small scale block losses. The photogrammetric DEMs however displayed noticeable inconsistency between samples, despite the high-resolution of the models. Small systematic differences were commonly detected between models, becoming increasingly evident towards the sections of the DEM that represented the cliff top. The inability to accurately relate successive models within the same degree of accuracy cast doubt of the quantification of change identified by the photogrammetric approach.

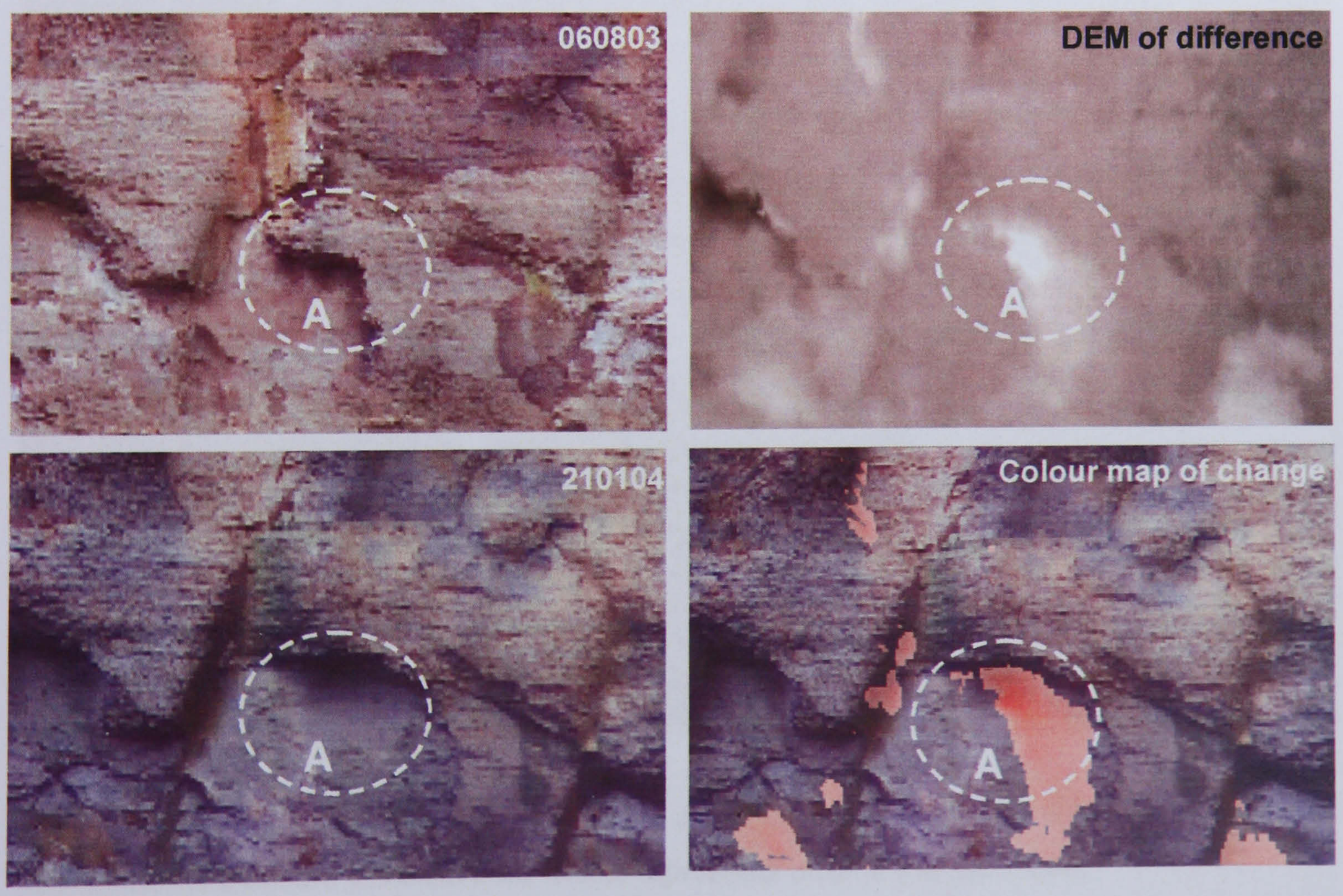

Figure 4.14: Orthophoto and difference model of small block loss, demonstrating the potential of photogrammetry for the application of slope monitoring. This change was located in the basal 10 m of the rock slope where photogrammetric performance was optimal.

The application of digital photogrammetry to coastal rock faces is complicated by a range of factors. The narrow time window of foreshore exposure provided by the tidal cycle restricts the collection of images. Many sets were collected in sub-optimal lighting conditions. Despite compensations offered by modern camera systems such as centre weighted metering, the images were often degraded by the effects of contrast and exposure. Particularly changeable conditions associated with cloudy skies led to differences between the images, a limitation of using one camera to obtain the stereo pairs. The establishment of model validity is therefore an essential concern of the photogrammetric study of coastal cliff slopes.

Many authors have expressed concern at the inadequacies of photogrammetric DEM assessment methods (Cooper, 1998; Gooch and Chandler, 2000; Bailey *et al.*, 2003). The so-called 'black box' approaches that use automated processing techniques provide for little understanding into the quality of the output produced (Loodts, 1996). The data validation approaches developed for photogrammetric DEM assessment were explored for cliff face monitoring with reference to Site 1, the tallest cliff section studied. During ideal light conditions created by overcast skies two sets of stereo pairs were collected in immediate succession, with no rockfall activity noted between images. A specific parameter strategy was designed and used to extract elevation models from the two datasets, which were then re-sampled to produce two orthoimages. Although theoretically identical, when one DEM was differenced from the other, significant changes were noted (Figure 4.15). The changes detected were concluded to be errors and required investigation. The errors are likely to have resulted from two sources: data collection and data processing.

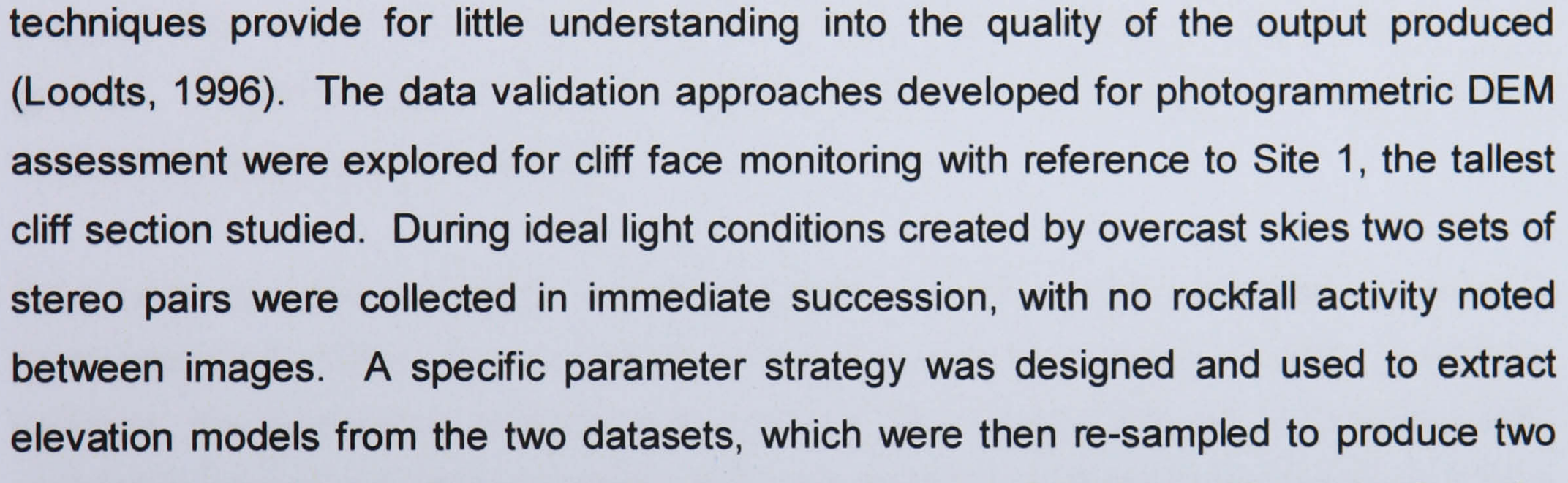

Figure 4.15: Comparison orthoimages of Site 1 and difference model. The images were taken in immediate succession, the difference model represents error in the technique.

The monitoring methodology was designed to minimise the errors associated with image capture in the field, although data quality is also dependent on the characteristics of the surface being recorded. The height, depth, aspect and angle of

the surface, and its associated colour properties may all control the accuracies obtained from the raw images. The variables were correlated and their level of significance in terms of the patterns of error established before a partial correlation was used to isolate the effect of each pair independently within the regression (Table 4.4). The covariance between each of the variables and change suggested the main influences on DEM difference came from height, depth, hue and intensity variations. The significance test however revealed that only depth and the pixel quality variables were significant (<0.5) The partial correlation illustrates how much variability within the response variable, error, can be explained through the variation of each variable in turn, while all others were held constant. The results indicated that hue and negative intensity explained the greatest amount of variation in error between the two image sets. Although this is not surprising given the direct relation between photogrammetric performance and pixel quality, the poor performance of the correlations in general suggest that many more subtle patterns within and between the data have been ignored. Therefore box plots were used to classify and investigate the trends within each of the explanatory variables.

Table 4.4: Summary statistics for the influence of cliff terrain variables on error in photogrammetric DEMs. The correlation shows how well the patterns of error fit with the variables, the significance indicates how much of the change explained is beyond a 95% confidence interval and partial correlation is a measure of the contribution or relative importance of the variable in explaining error when all other variables are held constant.

Variable	Correlation	Significance	Partial correlation
Height	-0.2690	0.941	0.0013
Depth	0.2599	0.000	0.0676
Slope	0.0914	0.512	0.0116
Aspect	-0.0451	0.552	-0.0105
Hue	0.2417	0.000	0.1336
Saturation	0.1109	0.000	0.0732
Intensity	-0.2096	0.000	-0.1060

The cliff section at Site 1 was chosen because it contains the largest landwards withdrawal from the base of the rock mass, over 10 m from the toe to the top. The trend of change against height appears to reflect the effects of radial distortion with a negative relationship to 25 m, before increasing with distance away from the image centre (Figure 4.16). The outliers from the bins are significantly smaller and more concentrated than for any other variable, suggesting radial distortion may be the most dominant factor in errors derived from terrain changes. The majority of the change was heavily weighted towards the base of the cliff, identifying the hard mudstone toe as a

problematic area for accurate DEM extraction. An attempt was made to investigate the effects of the toe and more subtle protrusions by plotting change against depth or distance from a zero base plane set behind the cliff face. The box plot of change with depth shows very little influence until the 20 m is reached. The 20 m threshold represents a protrusion of 7.4 m from the average depth for the cliff face. Such depths are again restricted to the lowest 10 m of the cliff, perhaps suggesting the geometrical differences of the toe should be treated as a separate mapping project if reliable information is to be obtained. A weaker relationship was seen with changes in slope angle. Slope angle was calculated with 0° aligned to the vertical plane of the cliff face. As slopes exceed 54° the line of sight of the camera stations to the face become increasingly acute, causing occlusion and differences between the images. Aspect or orientation towards the image centre showed no significant relation to error.

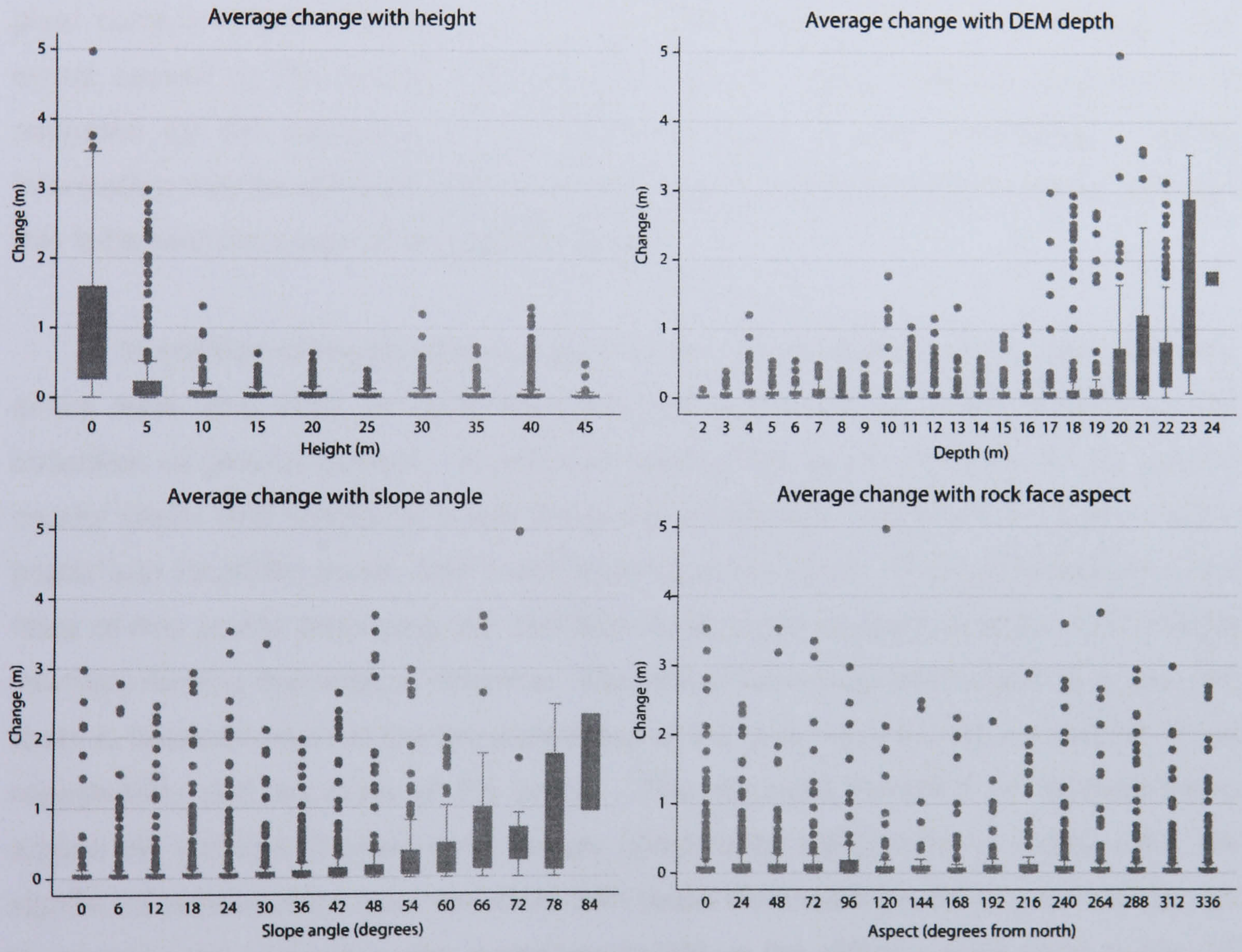

Figure 4.16: The effect of the physical characteristics of the slope on change between DEMs generated of the same surface (addressing Issue 23: Table 4.1).

By comparison to the physical characteristics of the cliff slope, the influences associated with differences in image content were minimal (Figure 4.17). The change with the hue of pixel colour banding showed significant scatter, even within classes. Increasing hue refers to the movement through the lighter to the darker (blue) part of the colour spectrum. The trend shows lighter colours perform slightly better than

darker pixel values, which typically relate to areas of shadowing. Pixel saturation is a measure of the trueness of the colour recorded. As saturation approaches unity the true colour portion of the pixel is at its highest and the grey value at its lowest. The positive relationship demonstrates the matching difficulty over terrain of pure colour values, with successful matches relying on the contrast generated by impure pixel contents. The errors show a weak negative relation with pixel intensity. Matching performance improves with increasing brightness until a threshold is reached at the last bin as pixels become too bright, reducing image texture. The implication is that despite favourable conditions, a small section of the pixels were overexposed during image capture. Ultimately the physical characteristics of the height and depth of the rock slope exert the most significant influences on the errors incurred during cliff face monitoring. The errors relate directly to radial distortion, which is enhanced due to the oblique angle of image capture. The more subtle changes of slope characteristics and pixel content reflect influences on the availability of information for matching. The errors caused by the nature of the physical cliff environment will be compounded or mitigated by the adequacy of the algorithms used in data processing. Further information may be obtained with radiometric analysis of the erroneous areas, although this is beyond the scope of the present study.

In addition to the problems caused by the nature of the reconstructed surfaces, errors were also likely to have been incurred in the set up of the instrument and collection of ground control. In order to assess the actual accuracy of the ground control under field conditions a test study was conducted. A grid of 25 natural control points was identified across Site 1 and resurveyed ten times. The grid consisted of five rows of five points dissecting the cliff face horizontally at approximately 10 m height intervals forming five vertical columns. The reflectorless total station was removed and reset in between each of the ten collections of the grid, establishing a measure of the repeatability and accuracy of the points. The standard deviation of measurements across the network showed error ranges consistently within 0.03 m (Table 4.5). No significant relationships were identified with radial distance from the survey station, nor by control point row either with increasing height up the cliff or position across the cliff face. The reflectorless total station therefore provides highly accurate ground control relative to the magnitude of changes under examination on the cliff face.

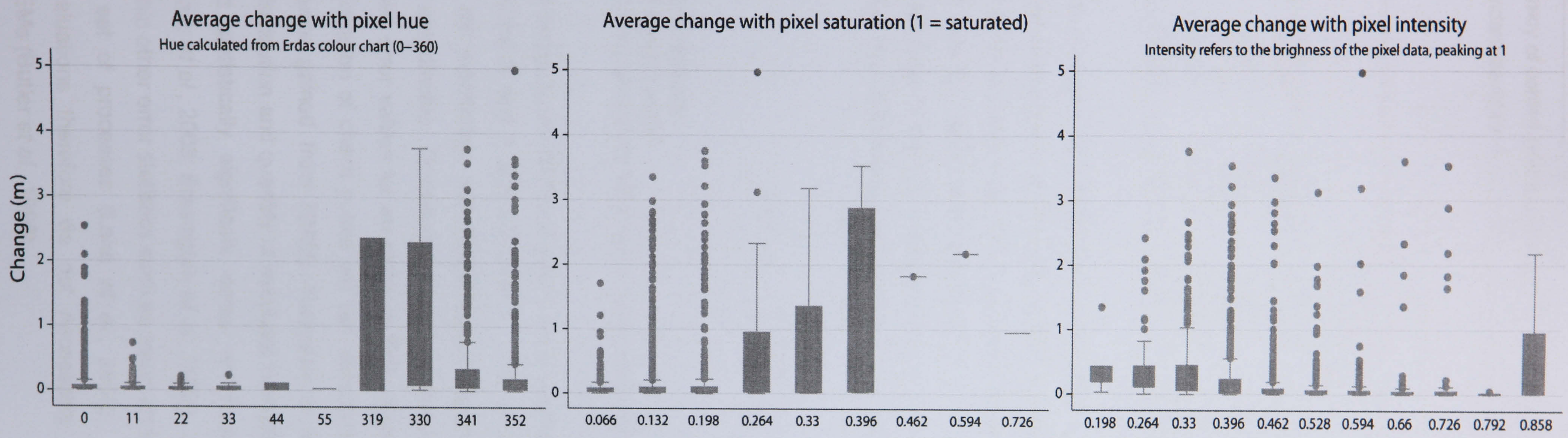

Figure 4.17: The effect of the pixel quality on change between identical DEMs (addressing Issue 24: Table 4.1).

Table 4.5: Accuracy of control points obtained with the reflectorless total station, expressed as the average standard deviation in x, y and z axis for each point aggregated across the survey network.

GCP Row	*Standard Deviation (m) GCP column*					
	1	*2*	*3*	*4*	*5*	*Average*
5	0.025	0.025	0.021	0.022	0.021	0.023
4	0.023	0.021	0.019	0.023	0.021	0.021
3	0.022	0.020	0.022	0.022	0.025	0.022
2	0.021	0.022	0.021	0.022	0.022	0.022
1	0.022	0.021	0.023	0.022	0.024	0.022

The true accuracy of a DEM can be defined as the root mean square error (RMSE) of every interpolated point in the model (Huang, 2000). In practice, such a complete evaluation is impractical and therefore the function is commonly performed on check point data (Li, 1988; 1993; Brasington *et al.*, 2003). The procedure provides a quantitative estimate of bilinear interpolations using localised errors associated with data independent from the DEM construction process, represented in Equation 4.4.

$$R.M.S.E = \sqrt{\left(\frac{\sum dh^2}{n}\right)}$$

dh = check point residual
n = number of check points
Equation 4.4: Equation evaluating DEM performance using check points.

The RMSE achieved for the DEMs of Site 1 were refined to check point accuracies of within 0.1 m in the X and Y and 0.3 m in Z. The values were typical of the DEMs generated for cliff monitoring, with height values repeatedly incurring greater errors than positional coordinates. Questions have been raised as to the validity of deriving a finite set of point error values for an entire surface (Lane *et al.*, 2003). The variable accuracy and location of check points are key determinants in the impression of the DEM performance gained from RMSE observations (Gooch and Chandler 2000). Tests on the distribution and quantity of residuals from discarded ground control points have identified statistically significant errors which are not conveyed in RMSE calculations (Baily *et al.*, 2003; Brasington *et al.*, 2003). Significant variability has also been noted within other error statistics such as mean error and standard deviation error for the same set of processes (Lane *et al.*, 2000). Statistical improvements in processing evaluations therefore do not necessarily equate to more accurately represented DEMs (Butler *et al.*, 1998).

Many softcopy digital photogrammetric suites can produce spatial classifications of the degree of interpolation and therefore matching performance associated with each DEM extracted. Interpolation of elevations may result if the parameters defining the matching algorithms are not met, relocating a point to its most probable value (Wolf and Dewitt, 2000). Surface regularity and texture are important controls on the amount of interpolation required. In particularly rough areas, as is common to many geomorphological features, a greater degree of interpolation is likely due to the complexity of the surface. In OrthoBase Pro for example, points are considered 'suspicious' if they are three times larger than the standard deviation of the surrounding points (Erdas, 2001). The threshold for interpolation and therefore the degree of smoothing applied may prove a critical factor in the ultimate performance of the model (Lane *et al.*, 2003). Higher correlation minimums equate to greater confidence in the matching success of the model, but are also likely to generate increased interpolation as fewer points meet the acceptance criteria.

The interpolation maps generated for the DEMs from Site 1 highlighted isolated geometric irregularities (Figure 4.18). Despite the presence of scattered 'suspicious' areas, the quality assessment fails to conclusively detect significant degradation of results in the most problematic areas of the orthoimage. The majority of points within the rapid elevation changes across the cliff toe and crevice were classed as 'good' to 'excellent'. Where one point is of particular interest it may ultimately prove preferable to accept a point with a poorer correlation (Baily *et al.*, 2003). The validation approach provided by OrthoBase is consequently limited to indicating an increased probability of erroneous matches (Erdas, 2001). False elevations may exist within 'excellent' matches while 'suspicious' performances may contain accurate fixes (Butler *et al.*, 1998). The reliance on neighbouring values may also cause problems in projects where fewer images are used in DEM construction, because edge effects lead to interpolations based on other interpolations rather than successful matches. The construction of complex surfaces increases the likelihood of data redundancy (Moore *et al.*, 1991). The problem is particularly evident in the case in the lithologically complex cliff faces where transitions from highly textured and defined areas to smooth featureless terrain are common. A key question remains as to the extent to which an increase in confidence of matching success equates to an improvement in surface representation and therefore accuracy (Lane *et al.*, 2000).

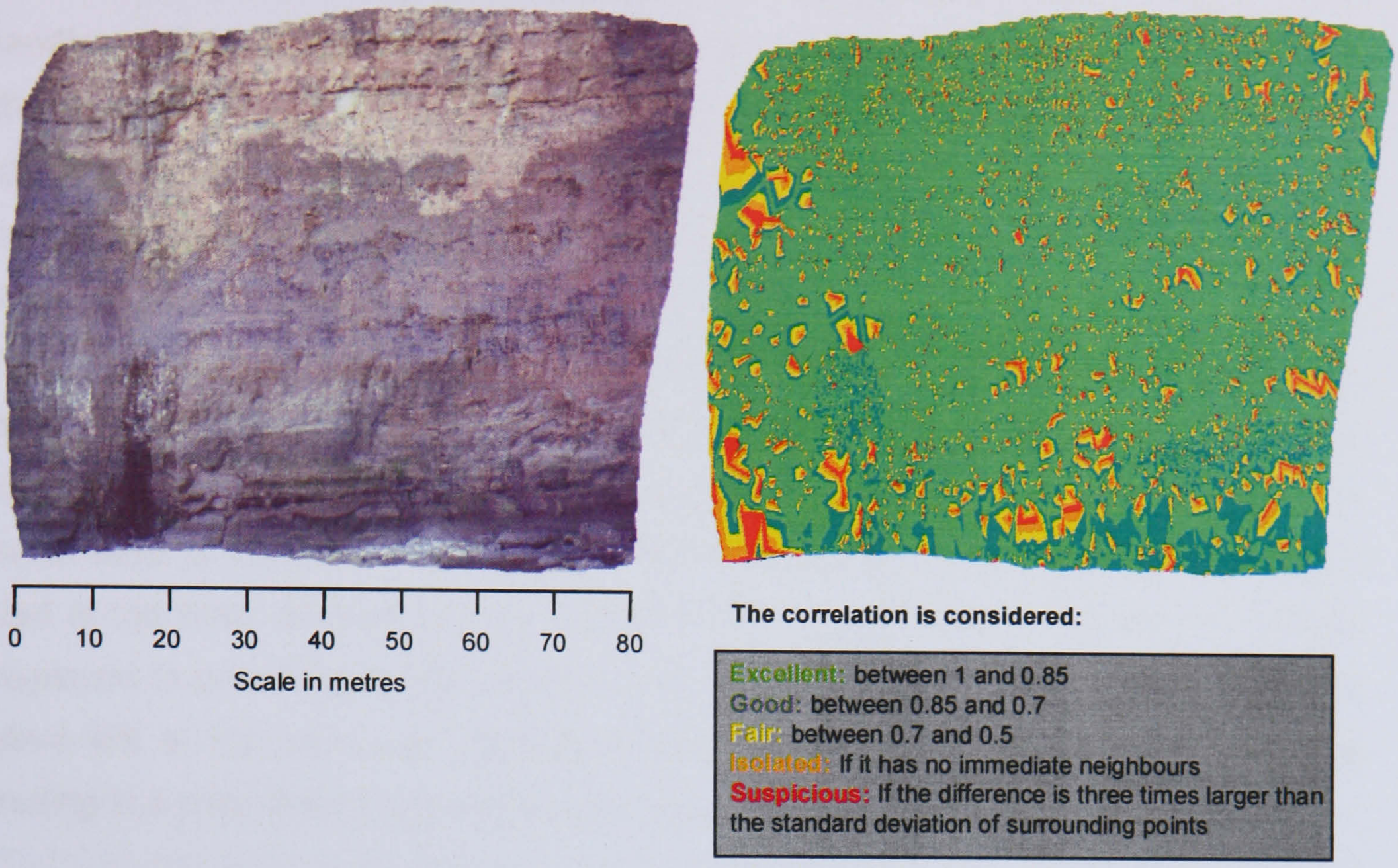

Figure 4.18: Erdas OrthoBase quality assessment: orthoimage and interpolation map for Site 1 (refer back to Issue 22: Table 4.1).

The limitations of software supported DEM assessments have led to the development of new independent methods for checking data fidelity (Gooch *et al.*, 1999). DEM success and quality are heavily reliant on the adequacy of the algorithms used to reconstruct the terrain. Any single set of extraction properties for rugged cliff face terrain will involve compromise over the most suitable algorithm (Liang and Heipke, 1996). The increasing range of choices and varied combinations of factors that influence DEM production raise questions over the most appropriate strategies for obtaining required accuracies (Cheeseman and Cutler, 1999). An idealised set of search parameters would generate an accurate DEM where only successfully correlated points were used (Gooch and Chandler, 2000). In reality, DEMs may often include unsuccessfully correlated areas and consequently distort or even reject some correctly matched points (Loodts, 1996; Butler *et al.*, 1998). The influence of the false fixes is hard to quantify and even an extensive and highly accurate network of check points may fail to adequately gauge such error (Fox and Gooch, 2001).

Gooch and Chandler (1999) developed a strategy-based error detection scheme to analyse the spatial distribution of suspect correlations within a DEM. The technique involves subtracting two identical DEMs, varying only in the parameter settings used, to generate a difference DEM. The greatest change on the difference DEM will be principally determined by the heightened response of erroneous or 'failed'

areas that are commonly mismatched under different parameters (Gooch and Chandler, 1999). A second DEM was generated for the first set of images of Site 1 with opposing parameter strategies defined. Where the topographic relief was originally defined as 'High Mountains', around deeply jointed or creviced areas for example, the terrain was redefined as 'Flat Areas'. The DEM of varied parameters was subtracted from the optimised DEM and the resultant failure indication model overlain on the original map of change (Figure 4.19). The failure warning model identifies the majority of the areas of error, particularly the isolated points across the cliff face. It appears to be biased towards areas of gross error, with the toe of the cliff covered in a blanket area of suspicion. Similar topographic effects on stereomatching have been noted at the base of smaller slope surfaces such as river banks, resulting in chaotic foreground in orthoimages (Pyle and Richards, 1997). The large crevice towards the bottom left of the monitored area also caused problematic extremes of shadowing resulting in a poor matching performance across different strategies.

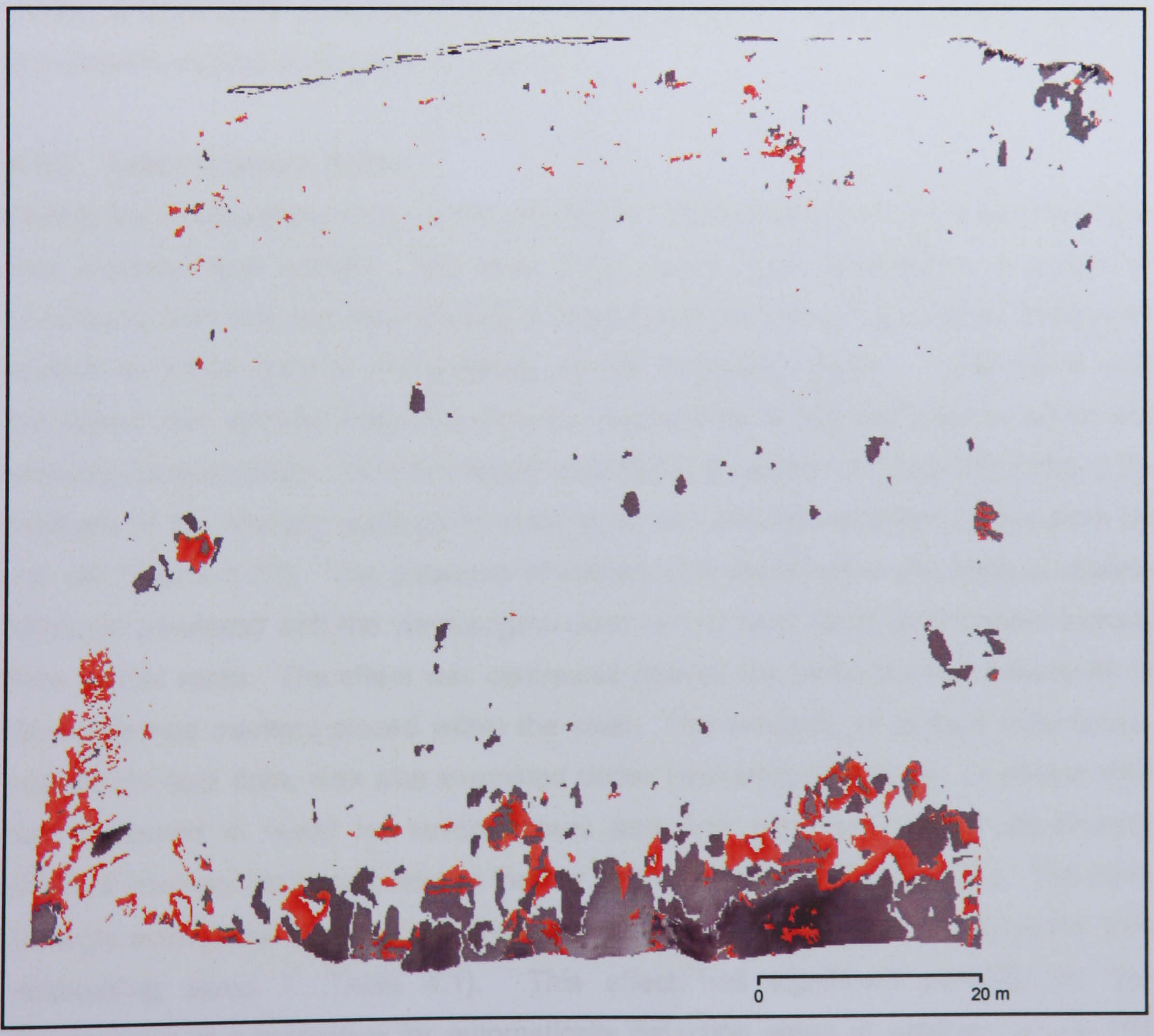

Figure 4.19: Failure warning model used to identify error within DEMs, after Gooch and Chandler (1999).

The selection of different strategy parameters is often complicated by the technical language used and software dependent nomenclature (Smith *et al.*, 1996). Certain parameters may also cause conflicting alterations to the algorithm used. In general a larger pixel area is searched when the relief is more changeable to increase matching success, although this consequently increases the likelihood of obtaining a false match (Gooch and Chandler, 2000). Establishing the precise effect of multiple interacting parameters and quantifying their contribution to DEM extraction is difficult to achieve. The procedure also casts doubt on the areas that receive most benefit from the optimisation of parameter strategies. When the correct match is achieved as a direct result of appropriately selecting the correlation criteria, the points are most likely to be rejected by the failure warning model. Nevertheless, when considered within its limitations, the failure warning model has proven to be a robust answer to the identification of poor performance within DEMs from a range of image scales. Ultimately however, in order to accurately identify and quantify the errors within a model, a truer DEM constructed without the constraints of photogrammetry and to a comparable degree of accuracy is required.

4.9.2 Laser scanned DEMs

During the development stage of the monitoring, DEM production from laser scan data was explored and refined. The laser point clouds were collected in a variety of conditions, from rain and sleet through to bright sunshine but all scans were statistically related to within 0.04 m convergence of the previous sample. The result was consistent and detailed three-dimensional impressions of the cliff face in which the physical characteristics could be clearly quantified (in relation to Issue 25: Table 4.1). Analysis of the intensity readings for each point also showed sensitivity to moisture on the cliff (Figure 4.20). The presence of wetted rock strata within the zone of marine influence interfered with the wavelengths used by the laser, producing weaker signals from wetted rocks. The effect was contrasted against the artificially high reflectivity of retro-reflective markers placed within the scan. The influence of surface reflectance, noted from field data, was also examined under laboratory conditions. A paving slab half immersed in water for several hours and then scanned showed significantly different intensity readings between the dry and wet surfaces (Figure 4.21). The point distance accuracies appeared unaffected by the moisture differences across the slab (addressing Issue 7: Table 4.1). This effect has significant potential for the development of a technique for automatically detecting areas of seepage on the cliff face, which could then be verified with the use of orthoimages.

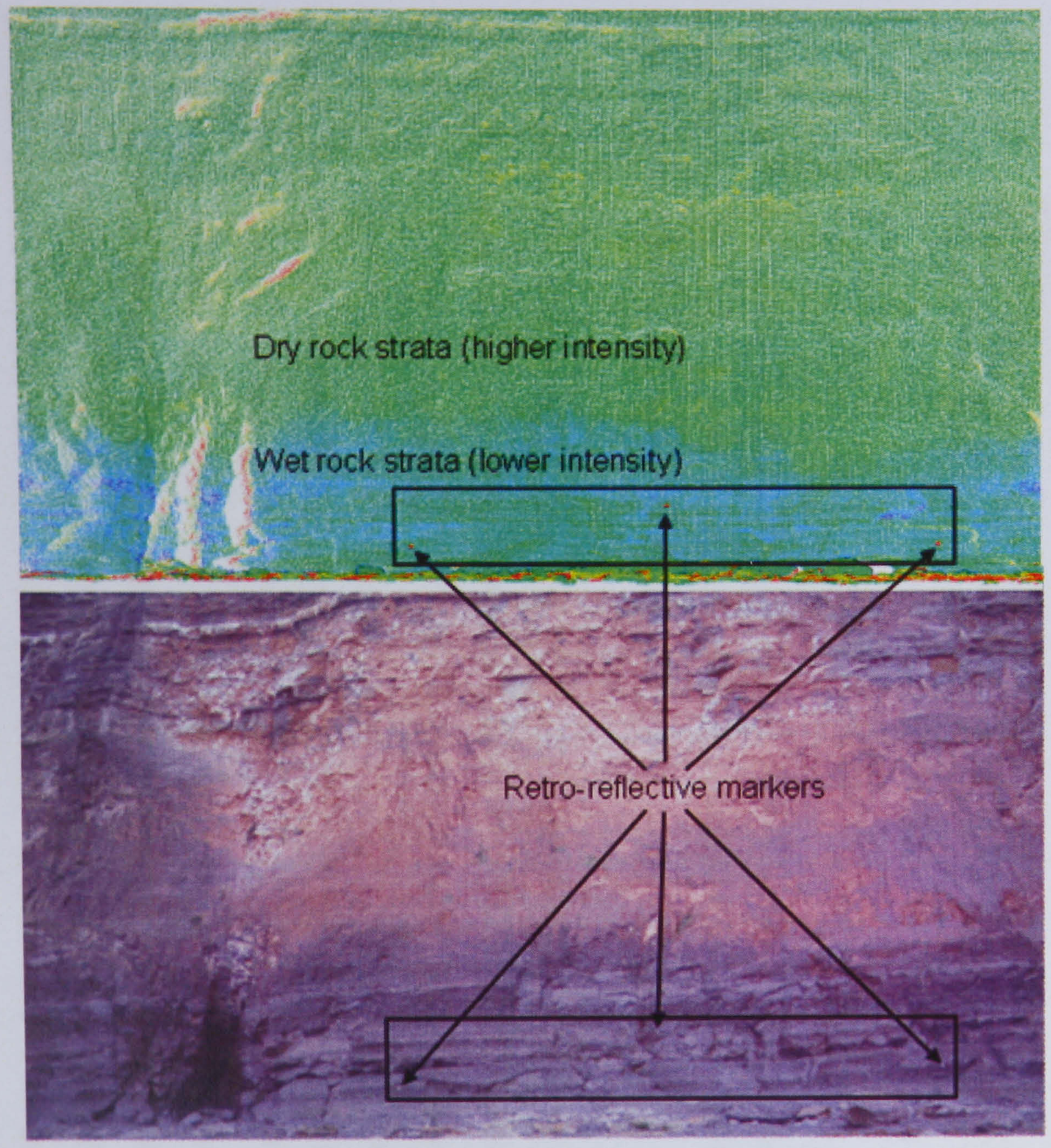

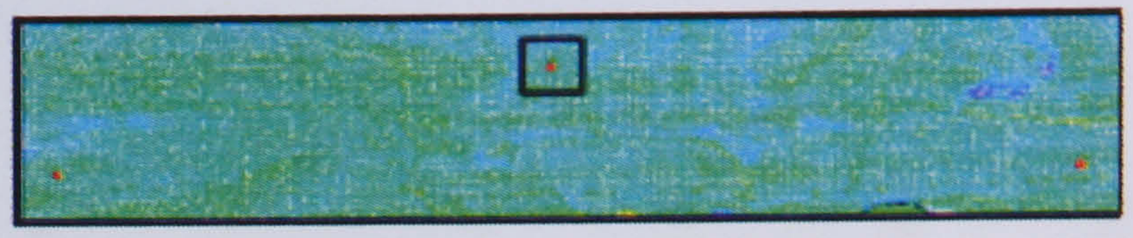

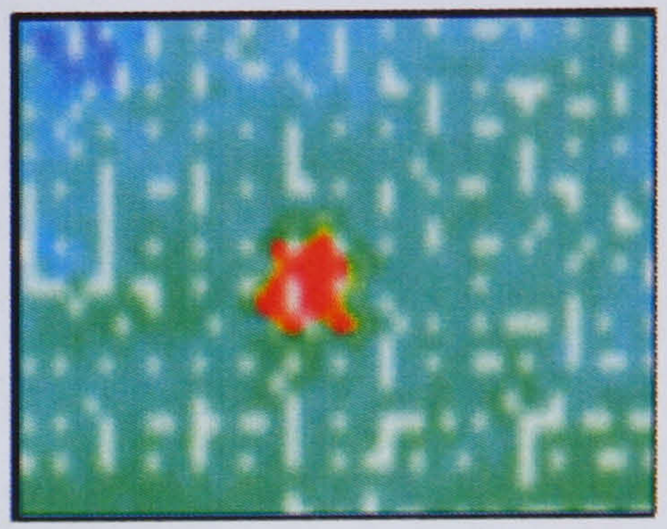

High intensity readings

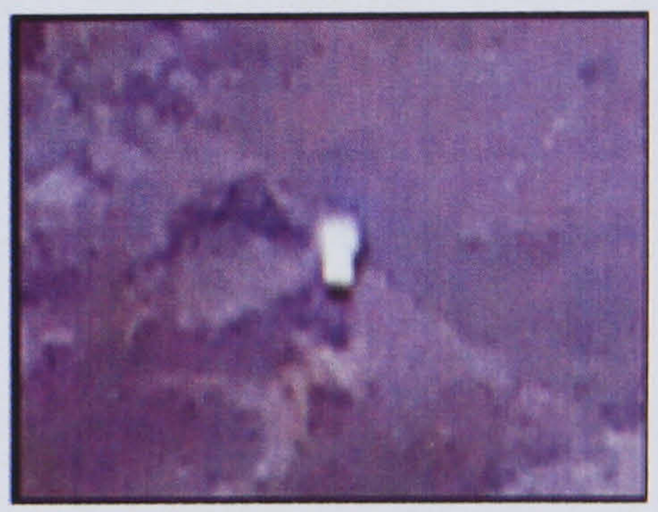

Retro-reflective marker

Figure 4.20: Intensity variations across Site 1, contrasting the wetter, darker basal mudstone with the drier shales above and artificial reflective markers placed in the scan.

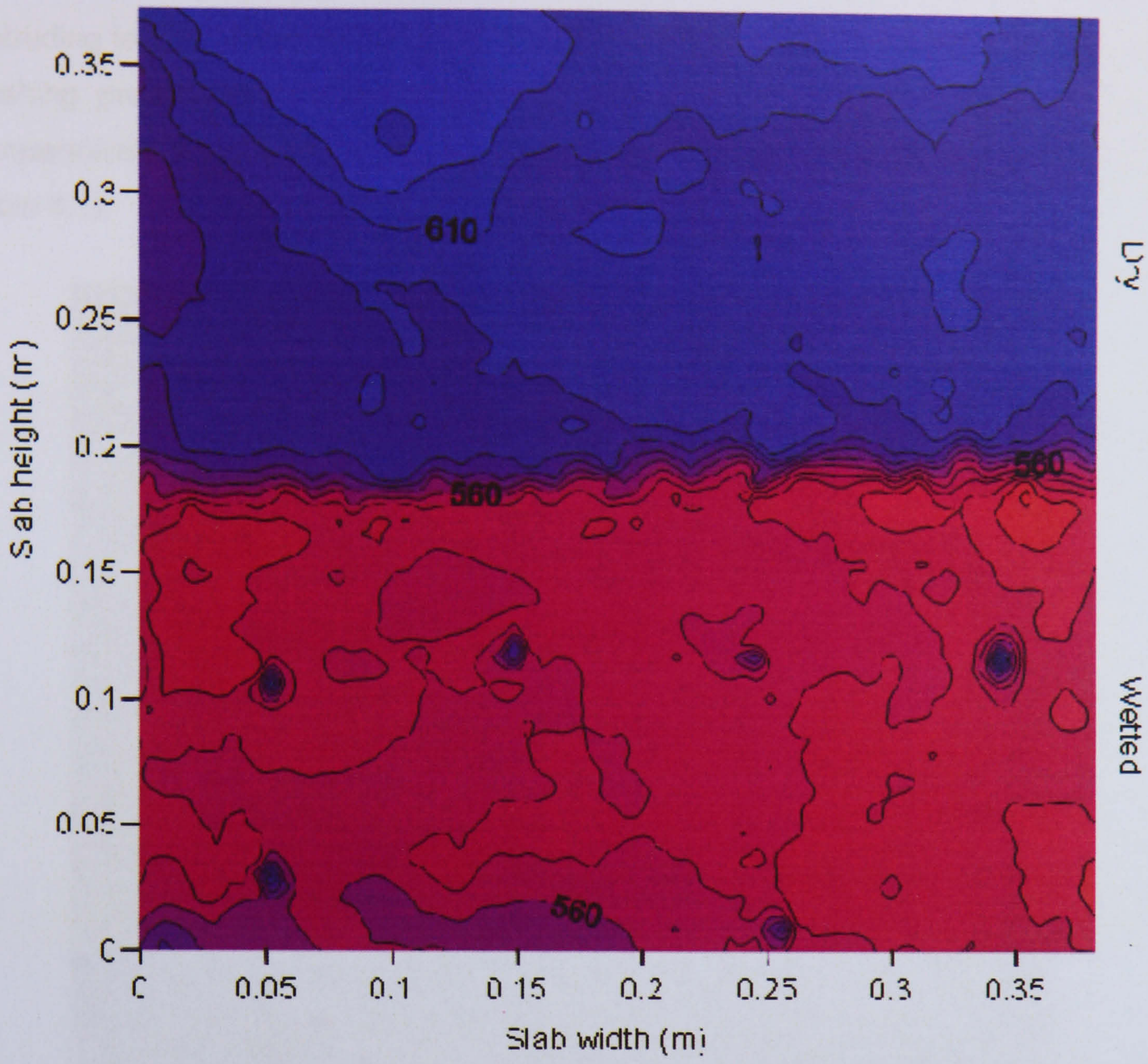

Figure 4.21: Laboratory test on the effect of wetness on laser scanned intensity readings. The sensitivity of the intensity readings were evident with isolated patches of higher readings occurring in the bottom half of the slab as it began to dry out.

Despite the consistency of the laser scanned models, the high degree of automation requires the accuracy of the outputs to be more carefully assessed. The positional accuracy and precision of the scanning system were assessed during calibration (Section 4.2.3). The limited number of scans permitted by the intertidal exposure of the monitoring stations raised concerns over the adequacy of the field of view of the cliff faces obtained by the scanner (related to Issue 18). The overall performance of the derived elevation models were tested by generating two 0.05 m resolution point clouds of the same cliff section in immediate succession, resetting the instrument in between. No changes were recorded during the scans, meaning that two identical surface representations should theoretically be produced if no errors were involved. The difference model of the scans however revealed small errors between the meshed surfaces, which typically appear as triangular irregularities caused by subtle differences in mesh generation (Figure 4.22). More substantial geometric differences were also detected, highlighted in the subsection, resulting from occlusion.

Such line of sight errors are concentrated towards the edges of scans and on protruding ledges where occlusion is more likely to increase the variability between the meshing procedures of different models. The resultant errors, within 0.03 m, are comparatively small when compared with photogrammetric accuracies (see Issue 26: Table 4.1).

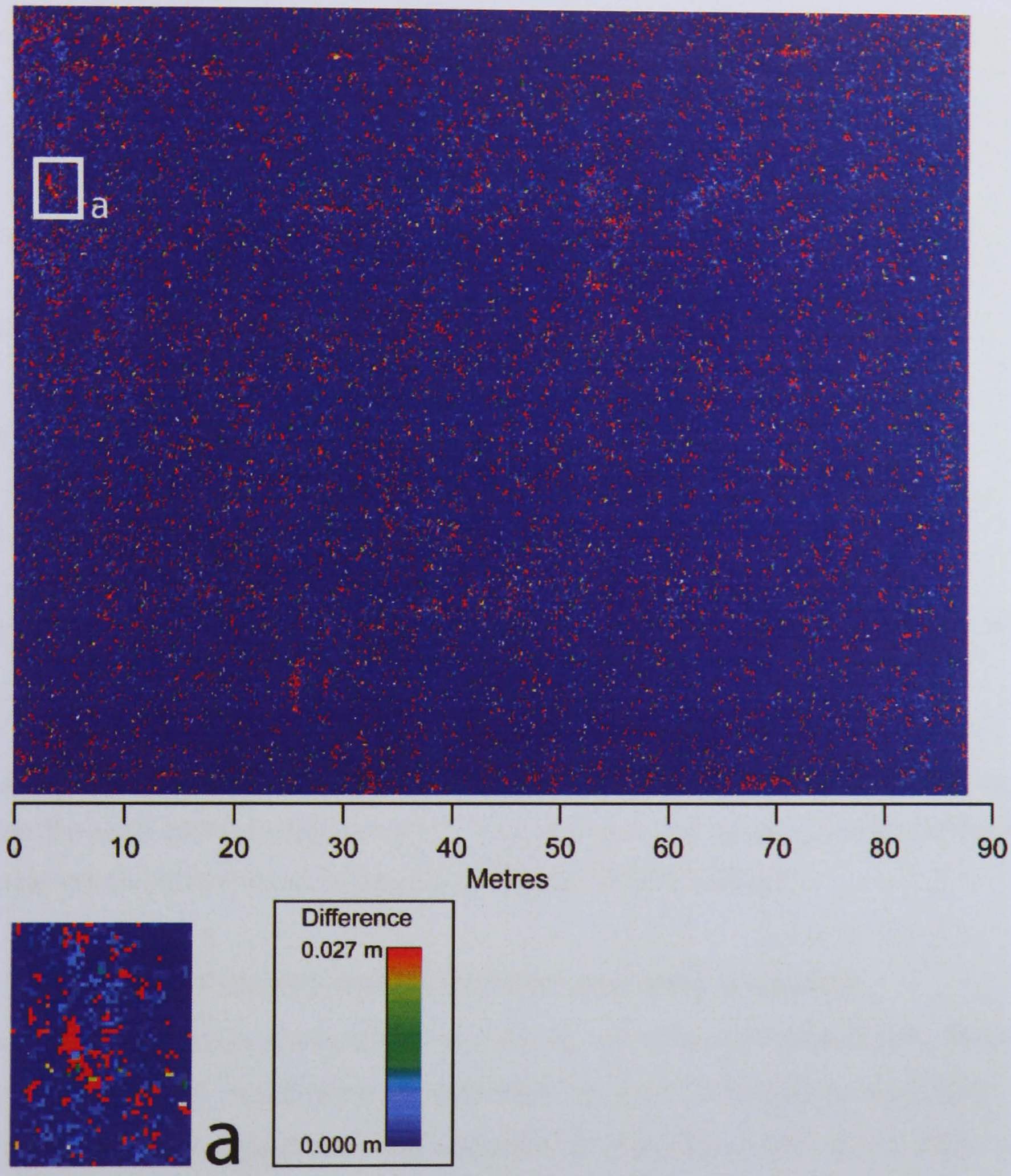

Figure 4.22: Difference between two scans taken of the same rock face (Site 1) in immediate succession. The difference was deemed to be error, primarily caused by occlusion.

When change through a temporal sequence is analysed, the differences can either be established between independently classified images or as a single consideration of the series as a whole (Eastman and McKendry, 1994). To differentiate true change from noise due to errors between collections, thresholding may be applied (related to Issue 19: Table 4.1). Rosin (2001) proposed a simple algorithm designed specifically for use with unimodal difference histograms. The thresholding procedure was performed on a histogram of the absolute surface differences from a year of

monitoring at each site, and the maximum threshold determined to be 0.03 m at Site 5 (Figure 4.23). The thresholds for noise were added to the maximum occlusion errors and subsequently all change within 0.06 m was discarded from further analysis (in answer to Issue 27: Table 4.1).

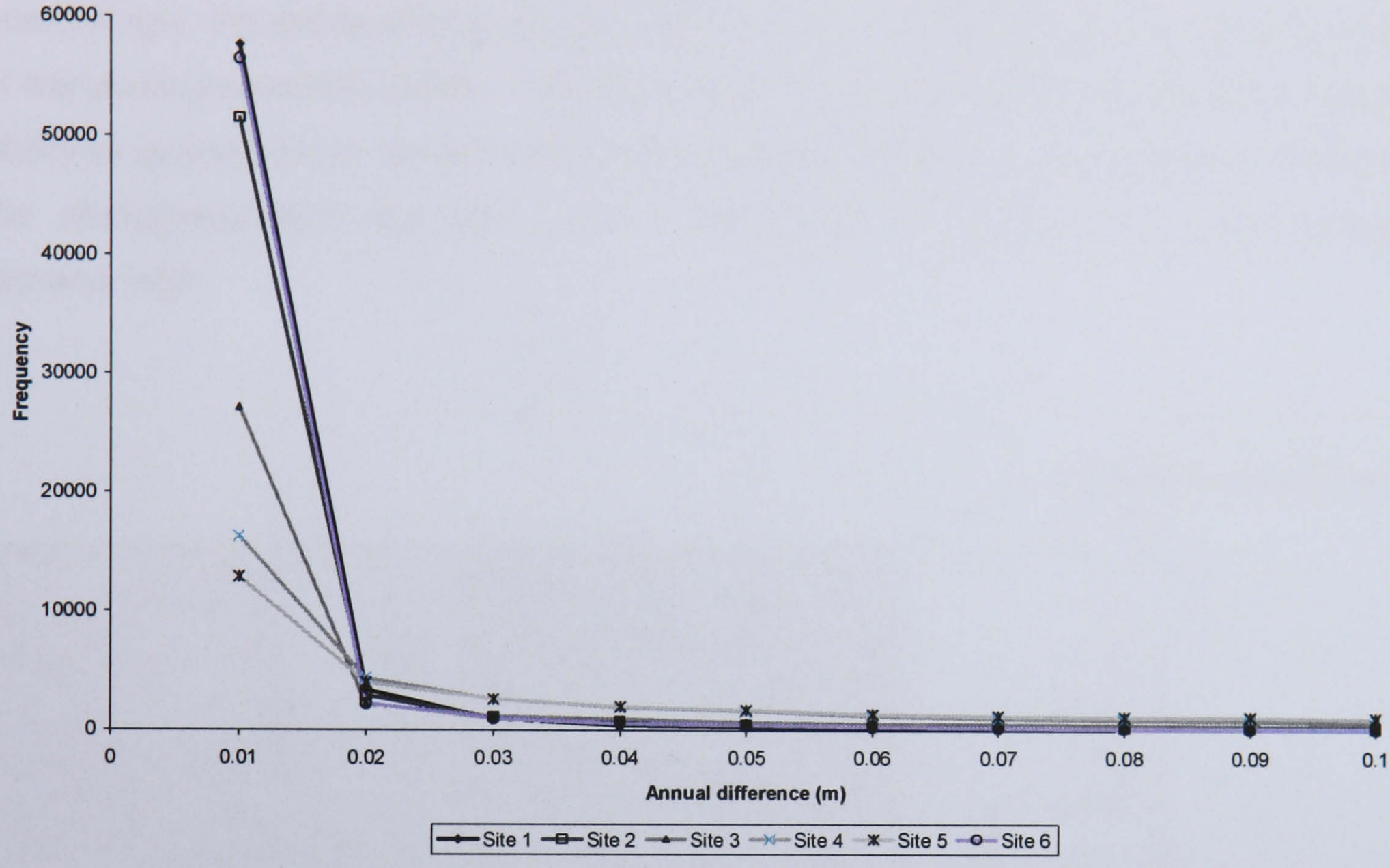

Figure 4.23: Histograms of difference over a year for every site. The thresholding procedure calculates the apex of the histogram which corresponds to the greatest perpendicular distance reached by the curve from a line joining the peak and minimum values.

4.10 Integration of digital photogrammetry and laser scanning

The results of the photogrammetric monitoring demonstrate significant sensitivity to changes in cliff face morphology, confirmed by the orthoimages produced. Many questions have been raised over the accuracy of the application, which often required the removal of independently located control points to achieve satisfactory bundle adjustment. The benefit of control surfaces has been realised in small scale investigations, restricted to sample sizes of a few metres, spatially identifying and quantifying the errors with constructed (Chandler *et al.*, 2003) or measured (Mills *et al.*, 2001) surfaces. The consistent accuracy of a laser scanned point cloud was differenced from a photogrammetric surface reconstruction in order to compare the performance of the DEMs. Profiles taken though both surfaces demonstrated a broad agreement in the overall representation of cliff geometry, with the photogrammetry marginally more sensitive to the small-scale undulations across the face (Figure 4.24). The most noticeable difference was the increasing disparities in depth above 10 m from

the cliff toe. The increasing distortions caused by the perspective effects of a receding rock face could not be accounted for in the bundle adjustment, highlighting a major limitation of the photogrammetric approach to monitoring cliff faces. Software-based quality assessments failed to detect this systematic error within the triangulation. The direct effect of perspective errors on elevation has limited the use of photogrammetry in the study of sheer-sided rock slopes which commonly withdraw from the base. Interestingly, the subtle changes in the cliff face were still detected in the upper portion of the photogrammetric DEMs. The implication is that despite losing accuracy and the ability to quantify block detachments with increasing height up the cliff, the precision of the photogrammetric technique, and consequently its capacity to detect change, remains high.

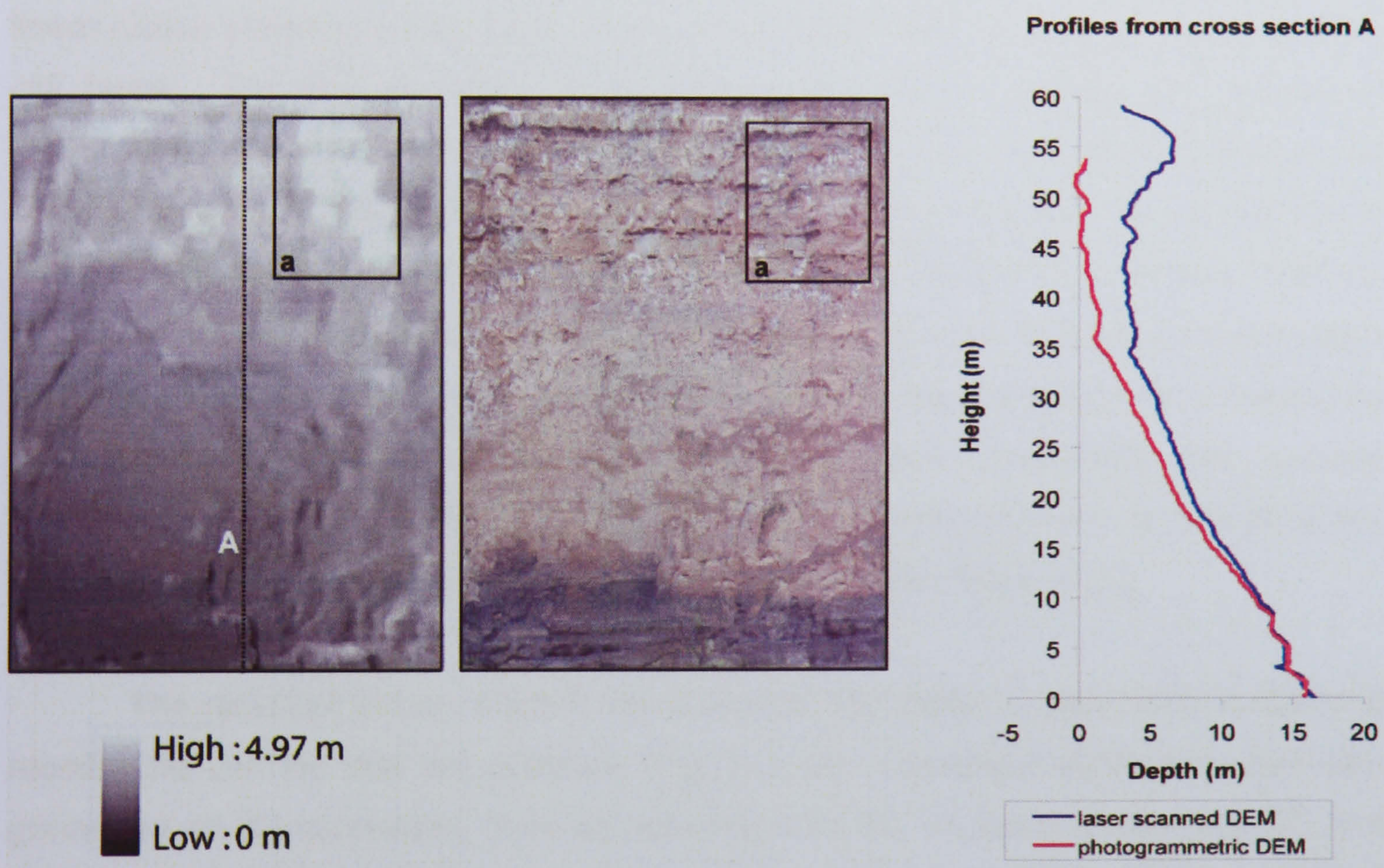

Figure 4.24: Comparison between photogrammetric and laser scanned monitoring of steep-sided hard rock cliffs. The difference model between the approaches increases with surface complexity, highlighted in the sharp protrusion in subsection 'a', and with height, seen in the cross sections through profile 'A'.

The monitoring study has highlighted the advantages and disadvantages of the two techniques. Photogrammetric techniques proved sensitive to changes in cliff face topography despite the challenges posed by scale and the nature of the environment (answering Issue 21: Table 4.1). The result suggests that significant potential exists for the application of digital photogrammetry to less extreme cliff heights. Qualitative

information provided by the orthoimages was found to be invaluable in validating change and in deriving information such as the location and conditions of the material before and after failure. The accuracies recorded were inversely related to cliff height, causing a key problem with the quantification of change. The consistent laser scans solved issues concerning the accuracy of data over the higher portions of the cliff face but provided little understanding of the situations under which changes occurred. It was therefore resolved to combine the relative advantages of each technique to provide a new approach to monitoring coastal cliffs (Lim *et al.*, 2005).

The successful combination of different remote sensing techniques requires the careful consideration of the format, orientation and resolution of the outputs. In order to generate accurate orthoimages, ASCII data files of the edited laser scanned point data were read into Erdas 3D surfacing tool. Cell resolution was set to 0.01 m and a non-linear rubber sheeting interpolation was used to better reflect the actual contours of the cliff faces. The high-resolution of the DEM was used to minimise the amount of information lost between the reconstructed surface, of finite interval, and the ground surface (Huang, 2000). The output surface was then imported into OrthoBASE Pro in order to re-correct for the distortions within the imagery caused by variations in terrain elevation. The images were re-sampled with output cell sizes of three by three pixels and adjoining orthophotos mosaicked. The final workflow combined the consistency and accuracy of laser scanned models with the colourised and precise photogrammetric data, enabling rock faces to be both quantitatively and qualitatively monitored within the diverse conditions found at the coast (Figure 4.25).

The resultant terrain models demonstrated the ability to accurately locate and monitor the cliff top and toe positions (Figure 4.26). Important information was also generated on the processes, such as seepage from the till above (subsection C), and on the mechanisms of failure, seen in the fresh rock face exposed following a recent fall (subsection D). By re-sampling the rectified imagery with the laser scanned point clouds, substantially larger portions of cliff face can be accurately monitored without multiplying errors of contrast, shadowing, perspective and geometry. Photomosaics of complex cliff sections such as protruding headlands and arcuate bays were constructed across monitored sites that spanned in excess of 100 m at certain sites.

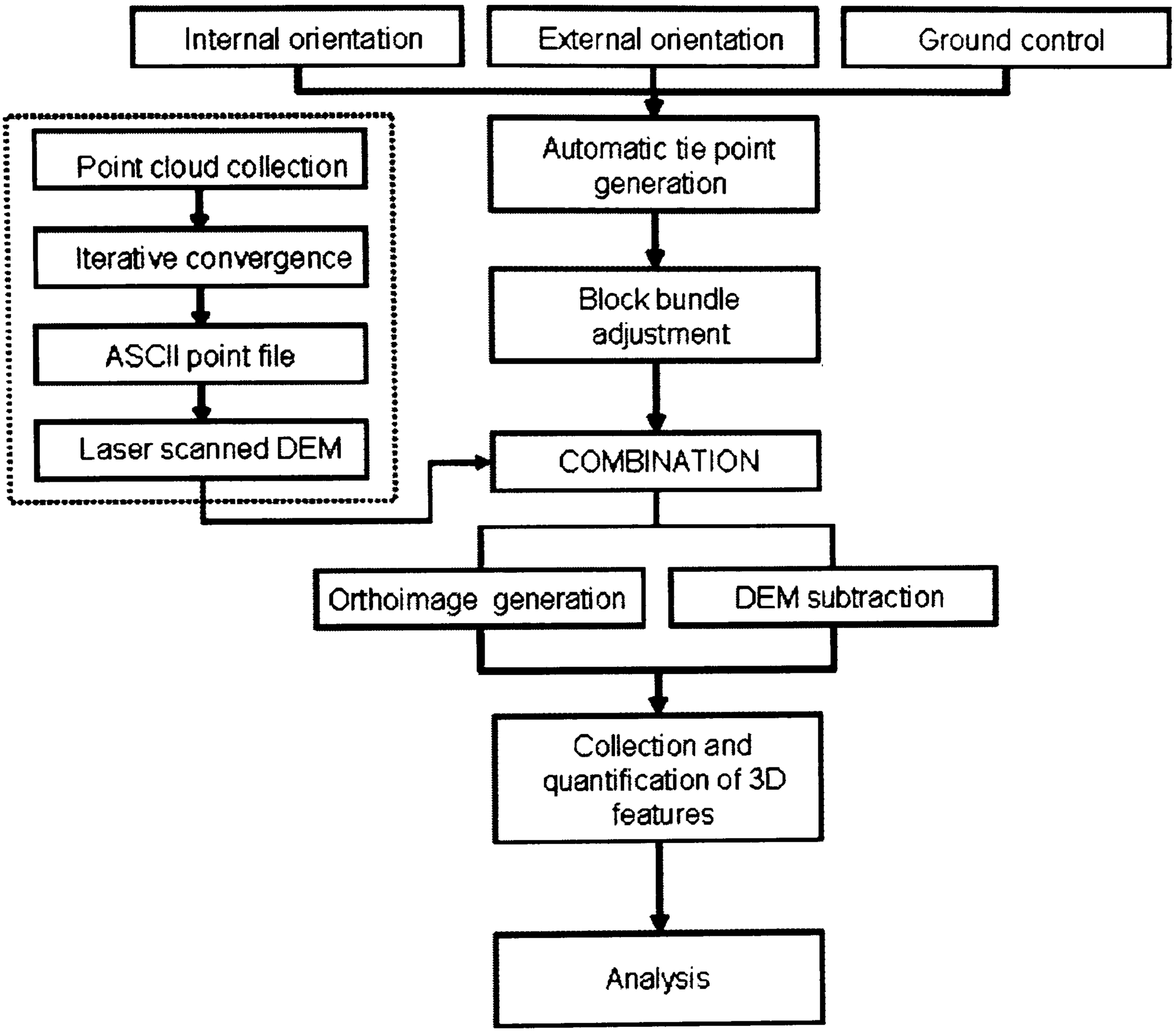

Figure 4.25: Combined workflow using digital photogrammetry and terrestrial laser scanning for monitoring of rock slope change. The synthesis of the relative advantages of both techniques is offered as an effective answer to the challenges of recording in detail the behaviour of sheer-sided hard rock coastal cliffs.

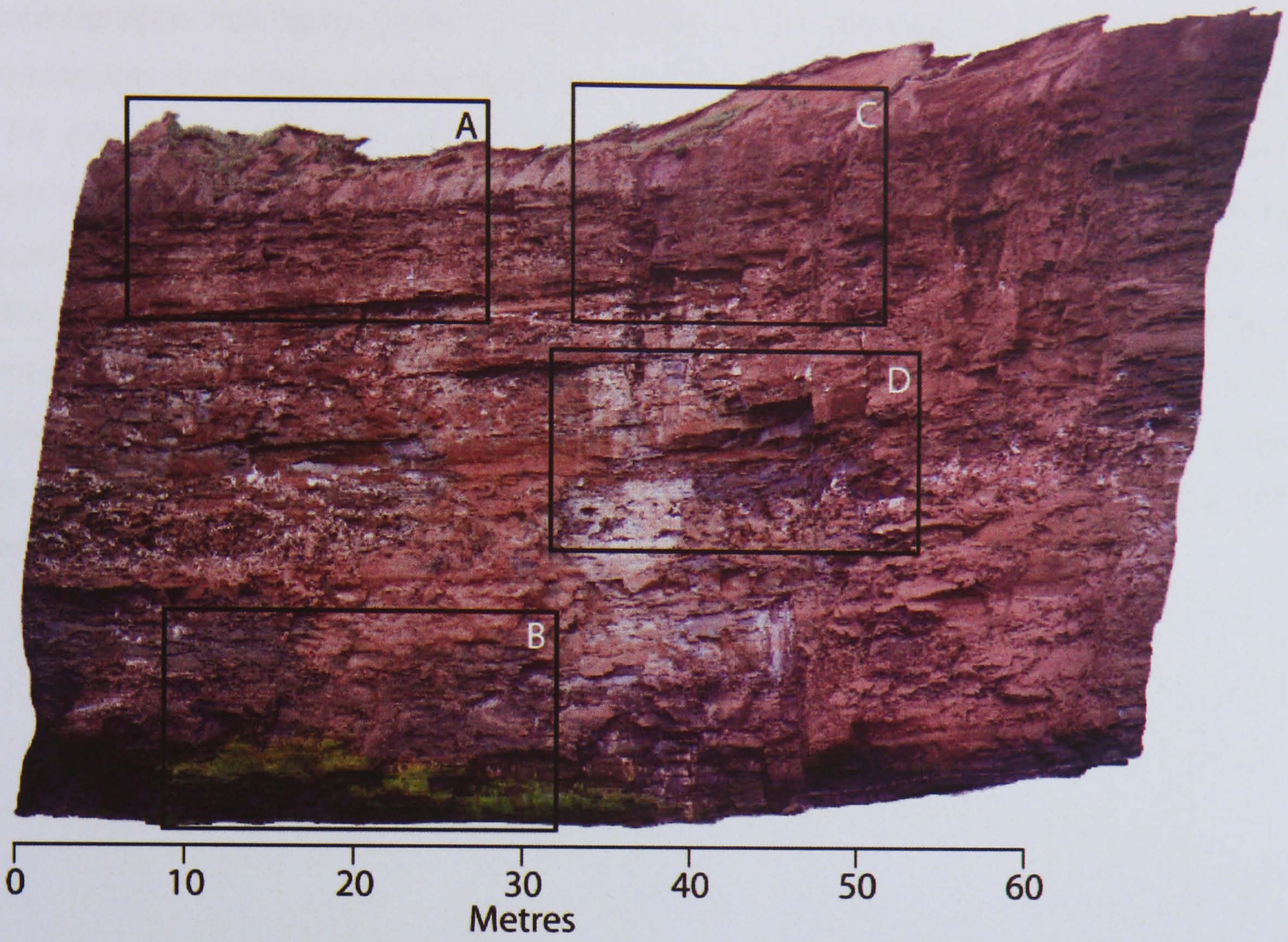

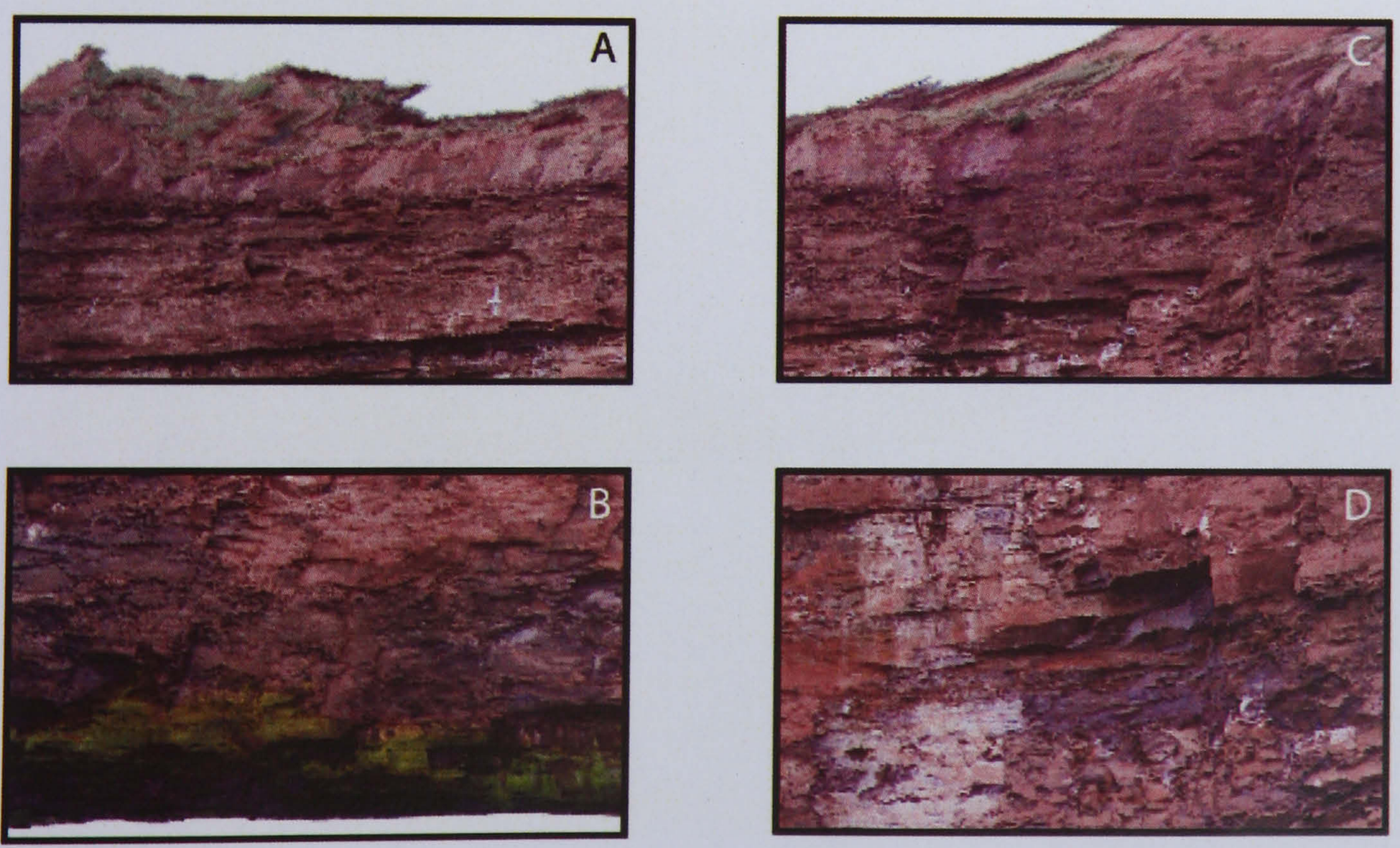

Figure 4.26: Combined terrestrial photogrammetric and laser scanned monitoring of sheer-sided coastal cliffs. The cliff top (A) and cliff toe (B) are clearly identifiable in the orthoimage resampled with a laser scanned DEM. Additionally, qualitative assessment can be made of aspects of cliff behaviour such as areas of seepage (C) or fresh failure surfaces (D).

4.11 Summary

This chapter has detailed the development of a combined terrestrial laser scanning and digital photogrammetry approach for quantifying rock slope surfaces. Careful consideration has been given to the potential errors involved in the collection and processing of remotely sensed data from dynamic natural features such as cliff faces. The differences detected can be reliably resolved to a resolution of 0.06 m. The synthesis of the precise and colourised photogrammetric information with the extensive coverage and consistently high accuracies of time-of-flight laser scanning provides an effective answer to the critical barriers which have prevented change being quantified from large scale landforms in dynamic coastal environments. It is now possible to describe both quantitative and qualitative changes from monitored cliff sections in order to analyse the contemporary spatial and temporal patterns of hard rock coastal cliff behaviour.

Chapter 5
Results: contemporary cliff behaviour

5.1 Introduction

The lack of high quality monitoring data on steep-sided coastal cliffs has limited understanding into the detailed nature of their behaviour. This chapter presents the data generated from the application of the methodology developed in Chapter 4 in order to characterise cliff behaviour at each of the selected study sites. The results are compared with the rates of change previously established for the coastline by aerial surveys and historic map studies.

5.2 Site-specific changes

Data were collected at monthly intervals between September 2003 and April 2005, providing 20 months of monitoring that encompasses two winter periods. Over the 20 month monitoring period, 19 difference models were produced for each site, revealing over 100 000 changes ranging in volume from $1x10^{-6}$ m^3 to over $2.5x10^3$ m^3, with a mean of $6x10^{-2}$ m^3. In addition to the quantitative results, qualitative aspects of the monitoring also proved invaluable in characterising each site. For example, orthoimages were used to delineate the precise location of individual bands within the rock (Figure 5.1), revealing transitions between band thickness, position and dip that enabled each site to be analysed in the context of its location within the wider geological sequence in the area. The characterisation of each site in this way allowed every individual change to be analysed with respect to the rock type or band with which it was associated.

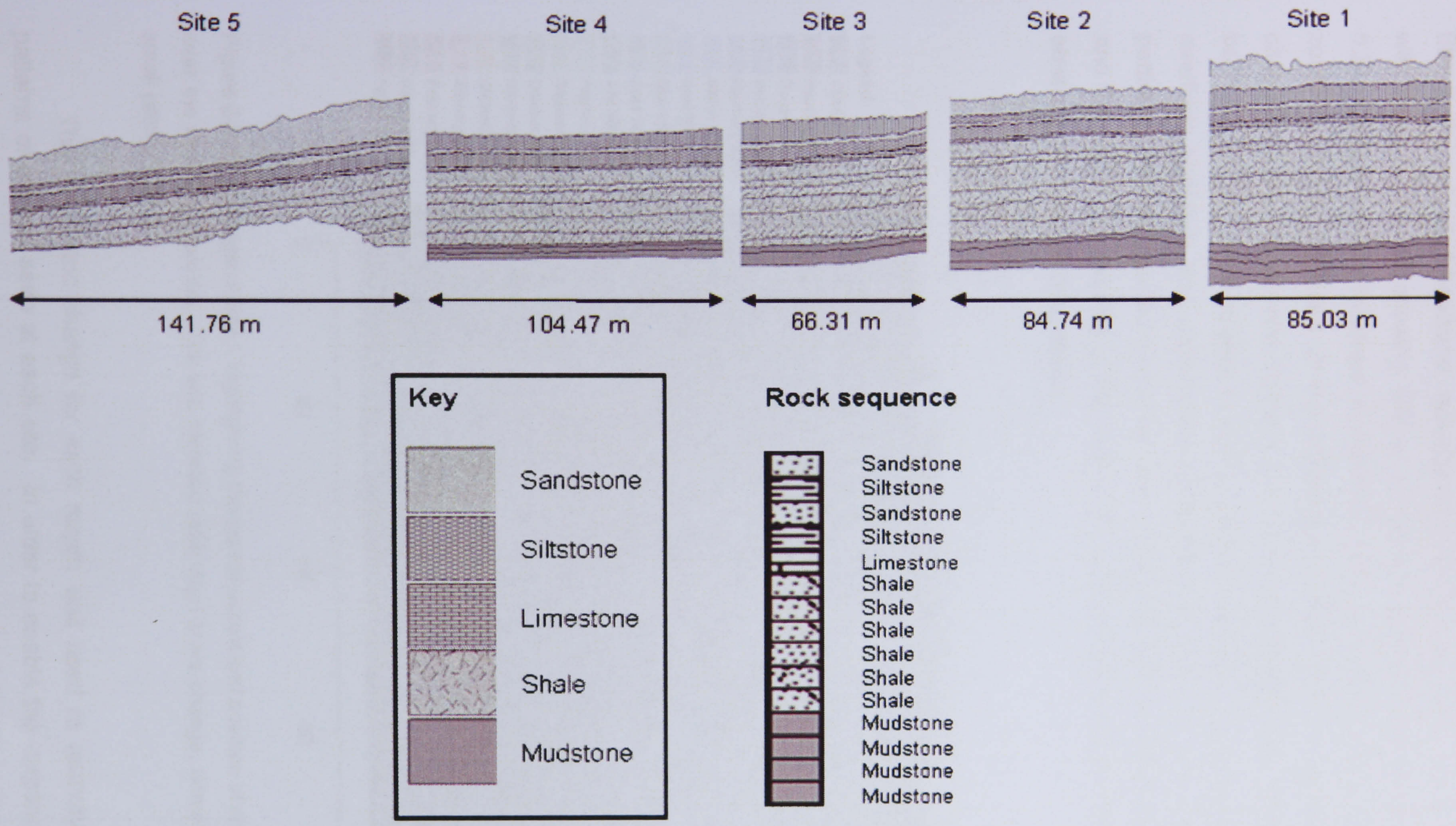

Figure 5.1: Scale representation of the lithological sequence through monitored sites. The variations in the thickness and position of different rock types were used to analyse the controls on recorded failures.

5.2.1 Site 1

Site 1, the subsided headland, was the only site not to show a large volume failure, with much of the cliff showing little or no change over the monitoring period (Figure 5.2). Certain areas of localised change were detected, particularly around the tension zone at the left hand side of the orthoimage (subsection A in Figure 5.2). Larger changes, up to 5.48 m^3, were found to be concentrated towards the basal layers with a band of smaller block changes at the junction between the upper shale and the overlying siltstones and sandstones (subsections B and C). The shale in the mid portion of the cliff was dominated by very small scale patchy change (subsection D), and the red/brown staining of the rock slope from till layers above demonstrates the absence of fresh failure surfaces.

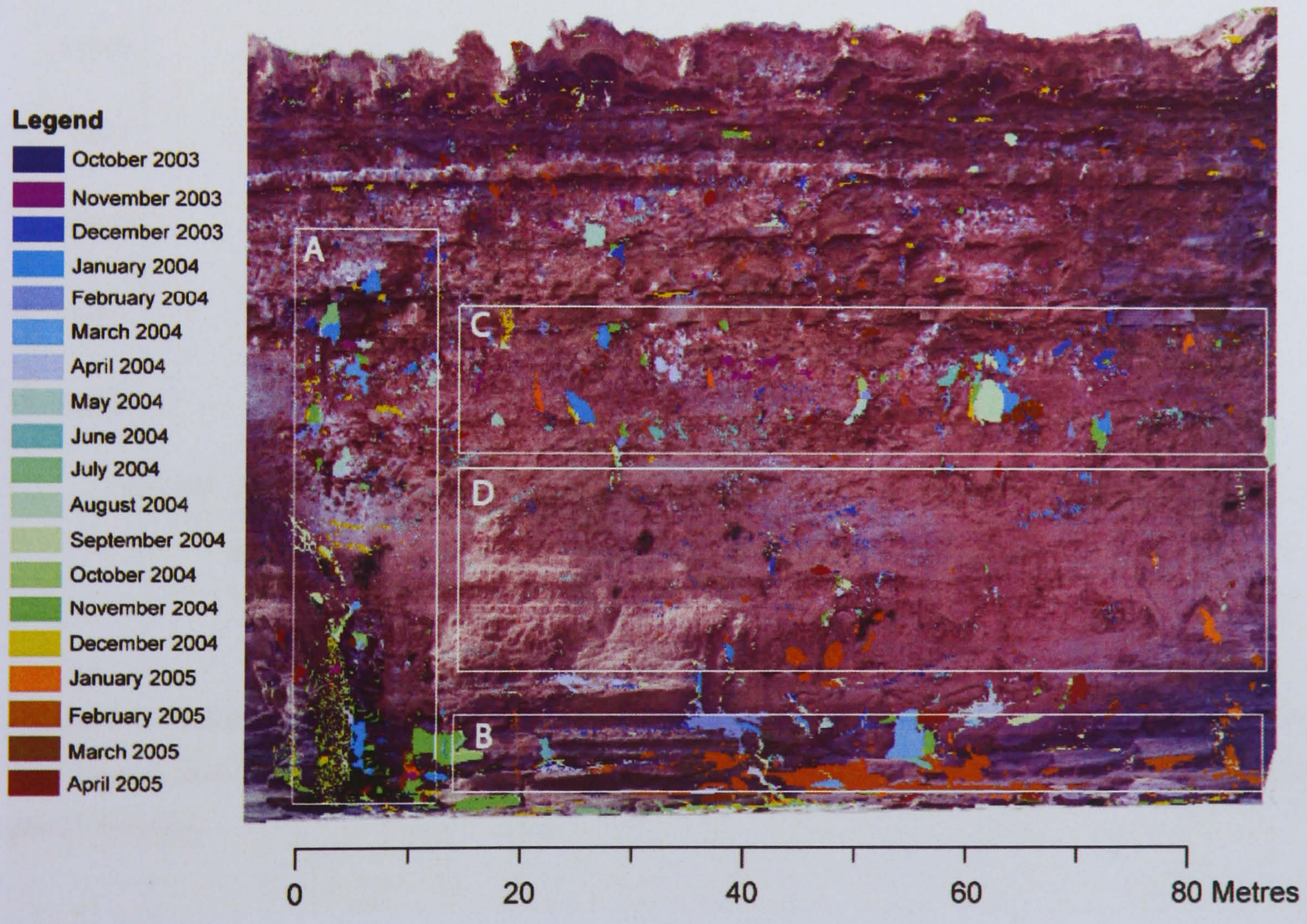

Figure 5.2: Orthoimage of Site 1 highlighting the spatial extent and position of changes recorded over the monitoring period. The site recorded little large scale change, dominated instead by small patchy losses.

The volumetric change for each month was used to quantify the temporal patterns of change seen at each site. In order to enable the responses of different sites to be compared, the volumes recorded were calculated as volumes lost per m^2 during each month. The volumes lost from the subsided headland were relatively small

(Figure 5.3), possibly reflecting its rock mass strength classification, the highest of all the monitored sites (refer back to Table 3.6). The monthly volumetric losses demonstrate significant variability, fluctuating around 0.0005 m but punctuated by months of larger change, peaking at over 0.0025 m. The length of the monitoring period, although limited, does highlight some of the issues concerning the assumption of uniform rates of cliff retreat. In January 2004 the rock face lost the equivalent to almost 0.001 m of material, double the total losses recorded the following month. In contrast the 2005 total for January was insignificant when compared to the 0.0025 m lost in February. Similar reversals in volumetric patterns of losses were seen between the final months of 2003 and 2004 illustrating the spatial and temporal complexity of rock slope response.

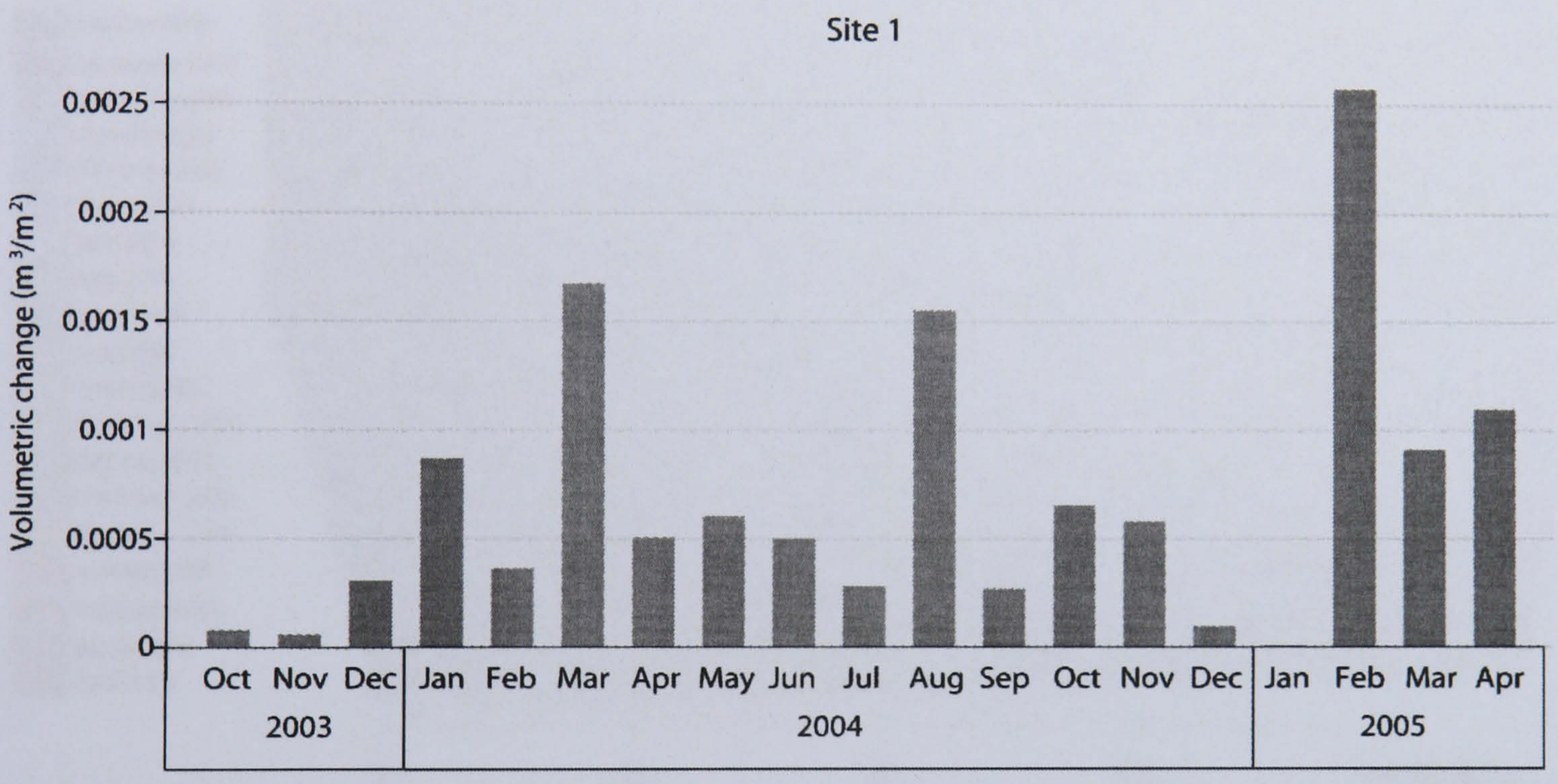

Figure 5.3: Volumetric losses recorded from the subsided headland over the monitored period. The losses detected were relatively small, significantly below those predicted for headlands by aerial surveys.

5.2.2 Site 2

The changes recorded at the arched-failures embayment were dominated by several months in which large amounts of rock were lost from the slope face, most notably two large failures in November 2004, one of which involved over 70 m^2 of rock face (Figure 5.4). The scales of the change recorded were up to an order of magnitude larger than those recorded at Site 1. The potential for larger failures may be attributed to the wider spaced but more continuous joint sets at the site, forming a weaker rock mass subdivided into large segments (refer back to Table 3.6). The principal reason for the selection of Site 2 was the arched formations in the cliff face (denoted by the dashed

lines, Figure 5.5). Over the course of the monitoring period failures were seen to be concentrated towards the base of the cliff and particularly at the edges of the arches. The central division between the two failure zones was eventually removed, forming one continuous arch. Little change was recorded from the rock within the backwalls or tops of the arches, giving the appearance that the failures were propagating horizontally but not vertically. Many of the basal failures were elongated, forming beam-like detachments, coinciding with the shallow mudstone at the toe of the cliff. The mid and upper portions of the cliff were, by contrast, seen to be relatively stable, with a few large failures within the siltstones and sandstones.

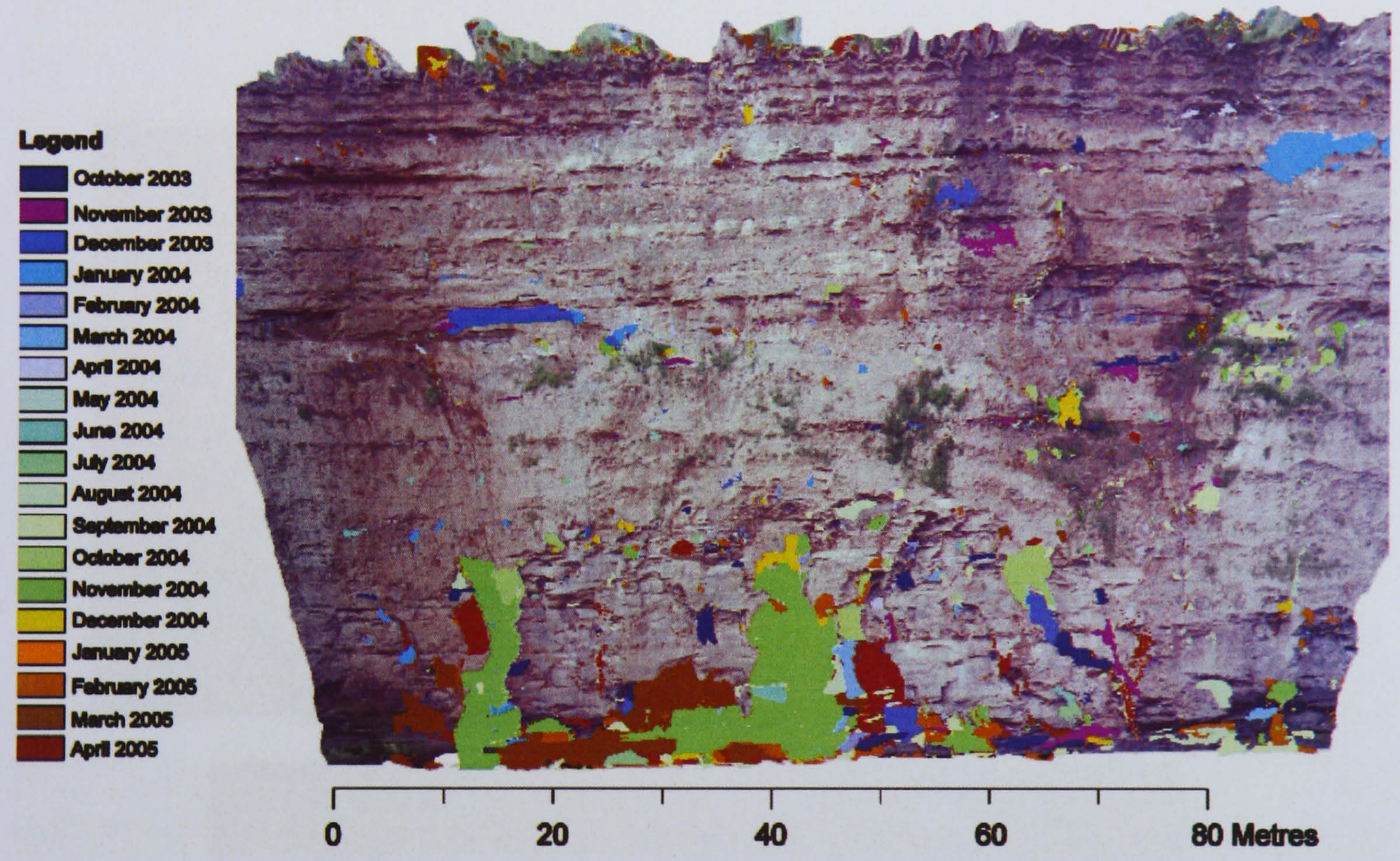

Figure 5.4: Orthoimage of Site 2 overlaid with a shapefile locating the spatial extent and position of changes recorded over the monitoring period. The changes were concentrated towards the edges and intersection of the two arches, causing the failure to develop into one continuous, lateral spreading arch.

The volumetric patterns of change per m^2 recorded at the site reflect the dominance of a few months in which the large scale losses occurred (Figure 5.6). Whilst the general levels of per m^2 volumetric losses were roughly comparable with those from the subsided headland, large changes in November 2004 and February 2005 caused monthly peak losses to be over 17 times larger. The data show a progressive increase in the level of rock slope activity throughout 2004 with larger volume losses continuing into 2005. The changes detected in August 2004 and January 2005 were insignificant compared to those incurred during other months, with

a maximum recorded individual block loss of 0.063 m^3. Often periods of higher amounts of volumetric losses per m^2 were separated by months of less active landform behaviour. Above average monthly losses recorded in February and April 2005 were separated by a more stable response in March 2005, demonstrating the patterns associated with more active episodes of change are not uniform through time. The arched-failures embayment was characterised by a few months of large change, although the temporal extent of the data is not sufficient to determine whether this is true for the longer term evolution of the cliff at the site. The concentration of activity on the arches within the rock layers suggests that the monitored response of the cliff through time may largely reflect the influence of mechanisms associated with development of such forms.

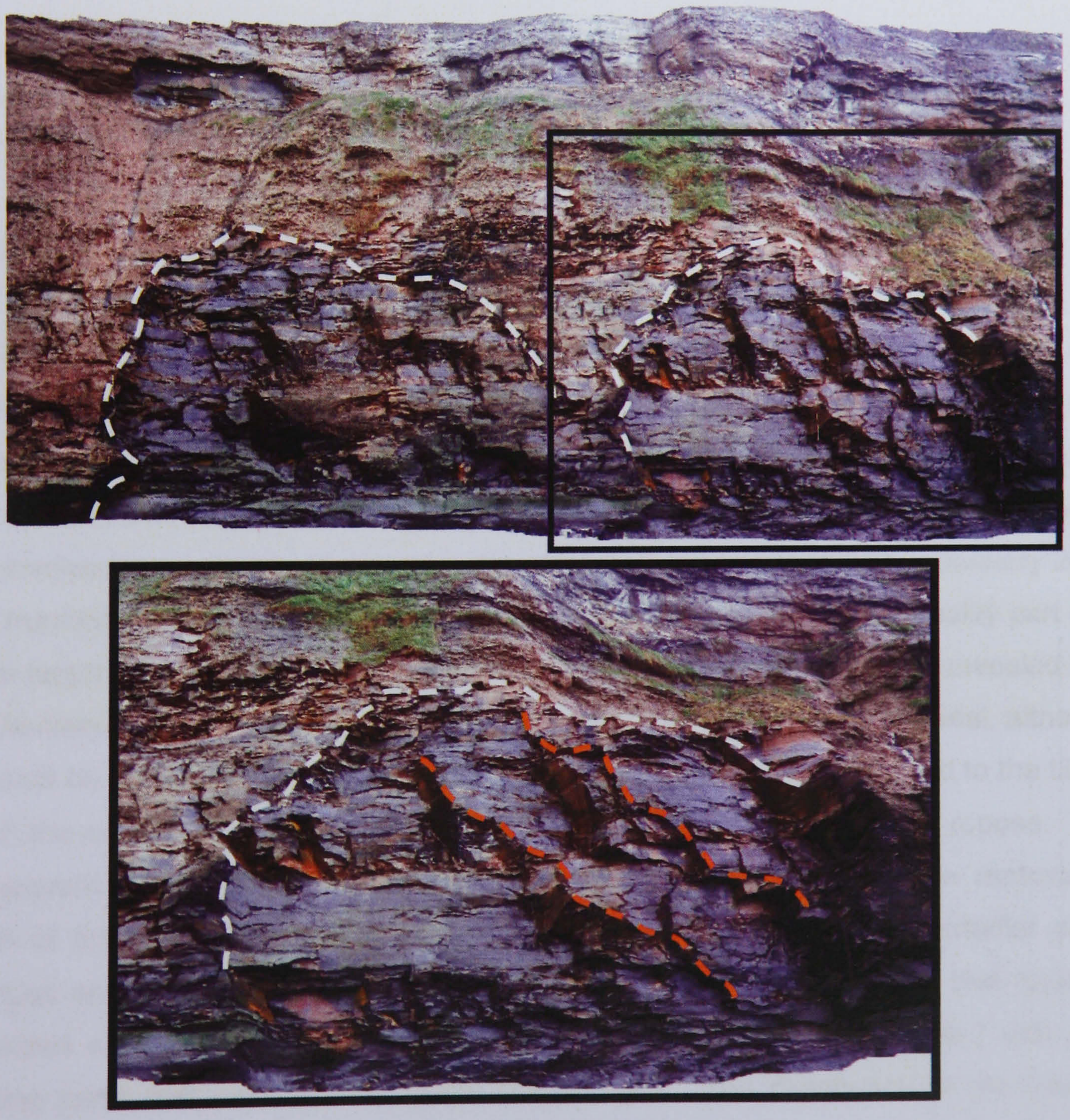

Figure 5.5: Angled views of orthoimages of Site 2 taken at the start of the monitoring. The lines of current (white dashed lines) and past (orange dashed lines inset) edges of the arches demonstrate that the failures represent a highly active part of the cliff face, which may be important in understanding how face-parallel jointed rock sections fail.

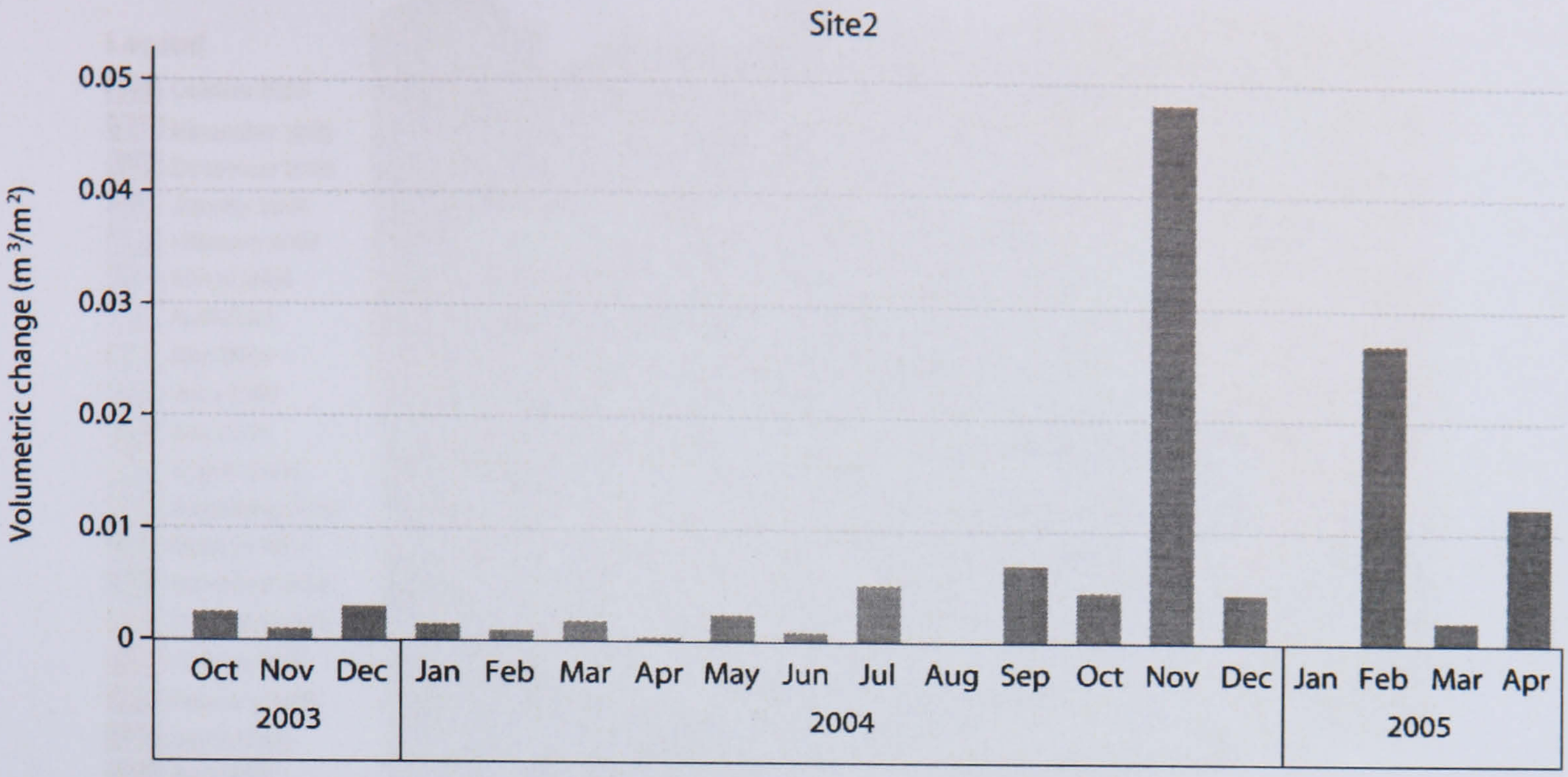

Figure 5.6: Volumetric losses recorded from the arched-failures embayment over the monitored period. The site shows a period of apparent stability followed by a more active phase during the 2004/2005 winter months.

5.2.3 Site 3

The well-jointed embayment at Site 3 recorded extensive change throughout the monitoring period, with several large failures concentrated on a tension crack towards the right of the site (Figure 5.7). Successive patterns of losses in October 2003 (A in Figure 5.7, recorded in the November 2003 change), July and August 2004 (B and C) and January 2005 (D) seem to match up, forming a semi-continuous area of change that involved every lithological band in the cliff. The change recorded in January 2005 was truncated by the limit of the monitoring area for the site, but was in reality part of a much larger loss that formed an extensive debris apron. The orthoimage revealed that the January losses involved substantial amounts of both rock and till material, although it should be noted that the validity of the change detection does not extend to the till for which the angles of incidence were exaggerated by the shallow angles of repose. The subsequent large change detected in February was associated with the removal of much of the failed material from the foot of the cliff. Elsewhere the smaller scale changes appear angular in nature, with a few noticeable larger failures that typically coincided with protruding ledges. The failure surfaces typically coincided with pre-existing joints that were evident in the orthoimages. The distribution of the failures appears to be concentrated towards the tension cracks at the margins of the monitored area, with lower frequencies at the centre of the site. Many of the largest changes and most active cliff responses appear associated with the presence of the dense and continuous jointing at the site.

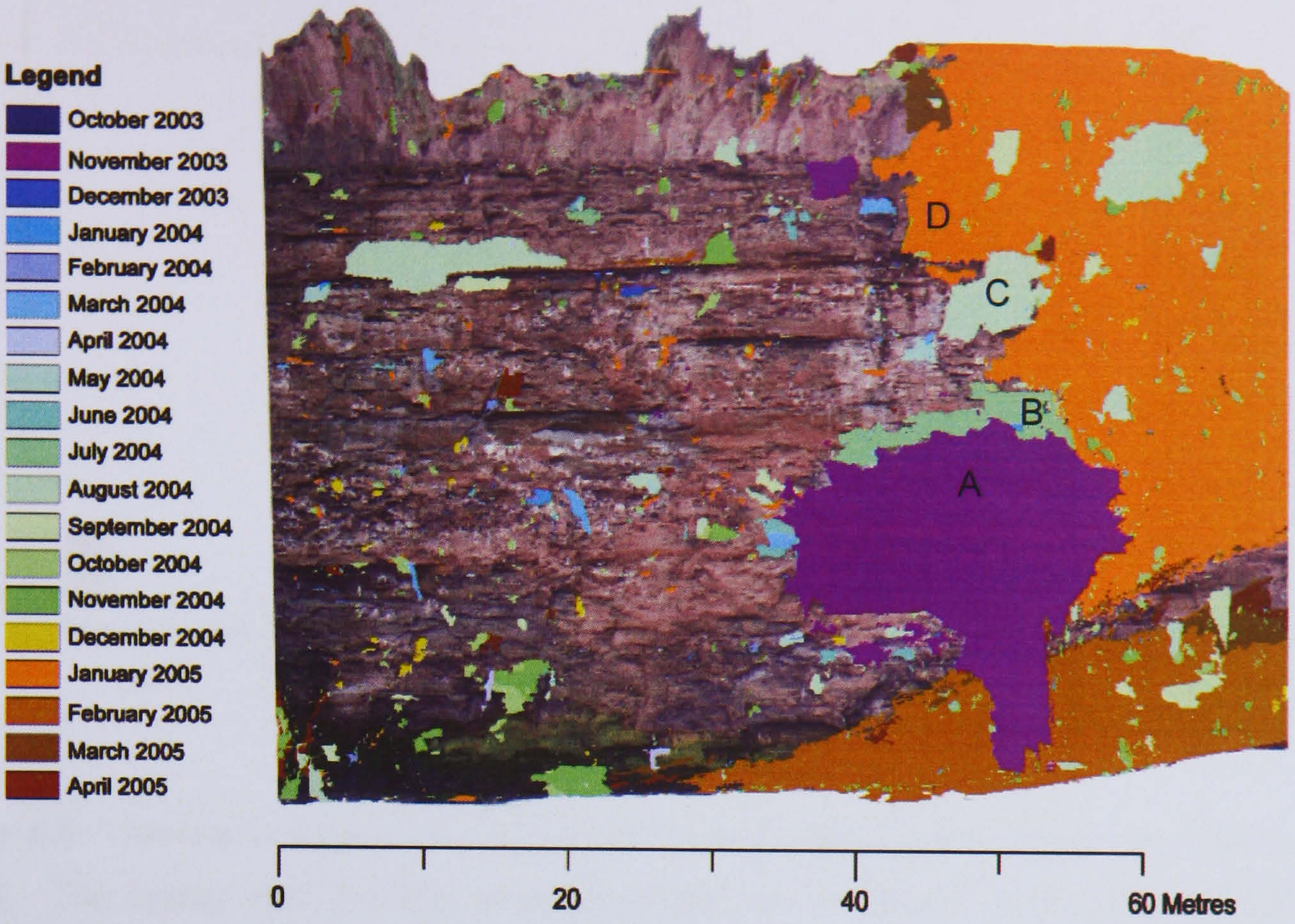

Figure 5.7: Orthoimage of Site 3 overlaid with a shapefile locating the spatial extent and position of changes recorded over the monitoring period. Despite being separated by several months, the outlines of many of the larger failures connect (areas A, B, C and D).

As with the arched-failures embayment, the monthly volumetric losses per m^2 recorded at the site were dominated by a few months of very large change (Figure 5.8). Although the site included the smallest monitored area of rock face, the maximum volumes of change were significantly greater than at any other site. To put the magnitudes of the changes into context, the losses recorded in October 2003 were minor in comparison with the volumes lost in 2004, although only one other monitored site recorded a larger change during monitoring. The volumetric losses per m^2 throughout 2004 appear small but in actual fact yielded higher values than many other sites, particularly during the winter months. The change for 2004 was greatest in July, largely due to a single area that overlapped with the upper limit of the large failure recorded in October 2003. The following months recorded significant but lower volumes of change throughout 2004 until the high magnitude losses in 2005, up to five times greater than those during October 2003. Orthoimage analysis revealed that the sequential pattern of reducing but still large scale changes recorded after the rockfall in January 2005 related to the removal of the debris deposited at the cliff base. The first month following the failure was associated with the greatest loss of the deposit, truncating the talus cone as marine activity eroded much of the most seaward material. Progressively less material was removed over the following months, leaving a compact, steep-angled core of material which remained beyond the end of the monitoring period.

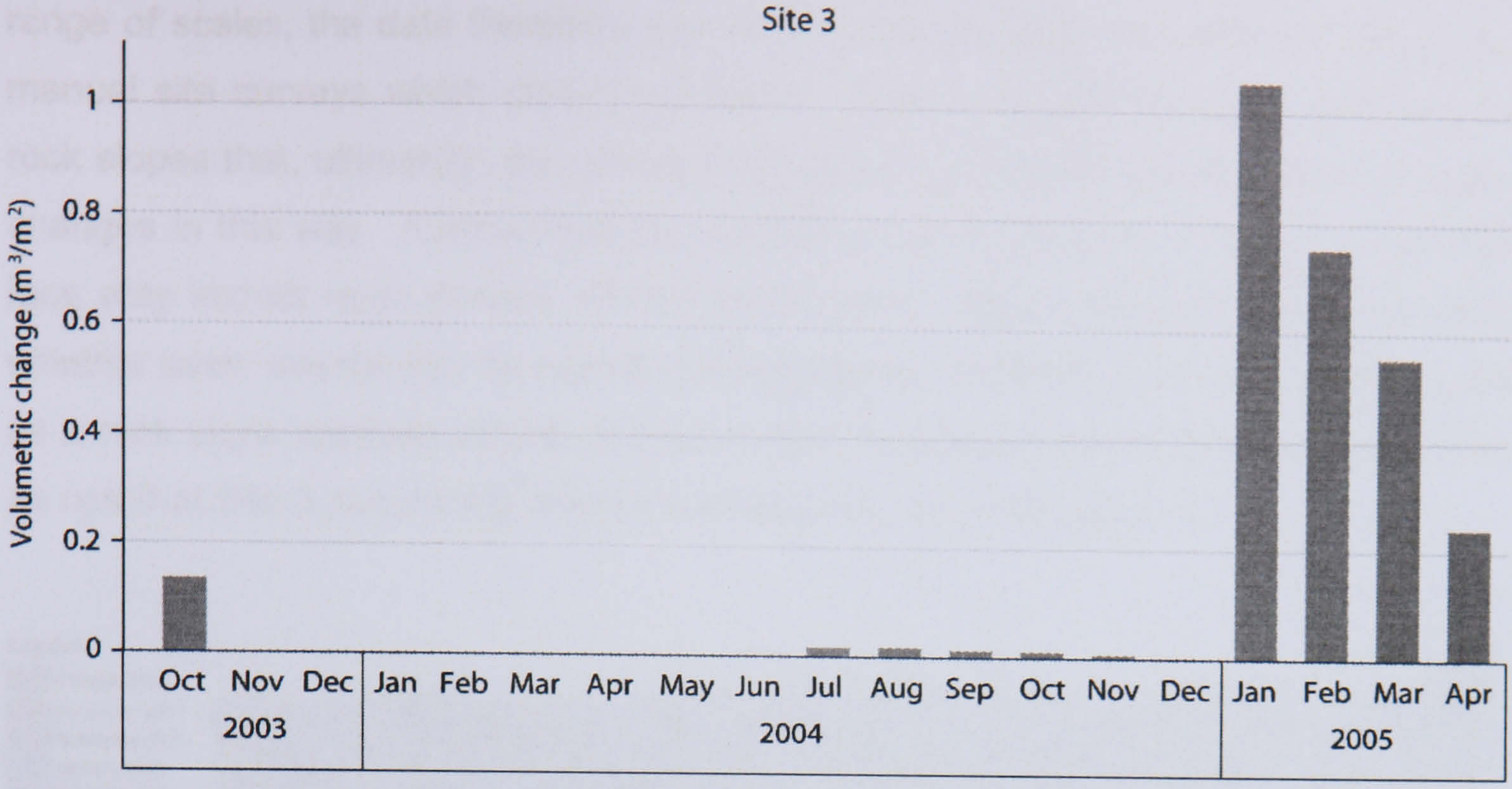

Figure 5.8: Volumetric losses recorded from the well-jointed embayment over the monitored period. The losses from the site were dominated by the largest failure recorded which was followed by several months of adjustment, removal of failed material and further losses.

5.2.4 Site 4

Site 4, the seepage headland, displayed relatively small areas of change in comparison to the adjacent well-jointed embayment (Figure 5.9). Much of the change was focussed on the left hand side of the monitored area, which represents the most seaward extent of the site. A few patches of localised change were found at the base of the cliff, although much of the cliff toe remained unchanged throughout the monitoring period. A band of very small change was located on a vertical step in the rock face, suggesting exposed edges may be worn down iteratively over time wherever they are on the cliff face (A in Figure 5.9), although it must also be considered that the changes could represent errors associated with the problematic nature of sharp, angular changes in geometry. A particularly large change was detected towards the front of the headland in February 2004 (B in Figure 5.9). The failure consisted of a protruding lobe, partially separated from the rest of the rock mass by a tension crack running parallel to main cliff face. Difference modelling also revealed a small loss in the cliff toe during the same month, confirmed by the orthoimages (Figure 5.10). The smooth, sheared surface and location of the truncated toe indicated the mechanism of the larger block failure above was likely to have been sliding, rather than toppling or falling movements for which the trajectory of the failed mass would not have passed through the toe. The smaller loss at the toe was not recorded in the field survey conducted at the time, due to the larger failure which drew attention away from the rest of the rock mass and the debris from which obscured the material lost from below. In addition to illustrating the effectiveness of the technique in recording changes on a

range of scales, the data therefore also raise questions over the validity of relying on manual site surveys which cannot confidently detect or quantify smaller changes on rock slopes that, ultimately, may prove important in understanding the nature of larger changes in this way. Furthermore the indication that a failure from higher on the cliff face may impact upon entirely distinct areas below raises important questions as to whether such 'events' can be considered separately. Within a connected system such as a rock slope spatially distinct changes may therefore be connected temporally and, as noted at Site 3, temporally distinct changes may be linked spatially.

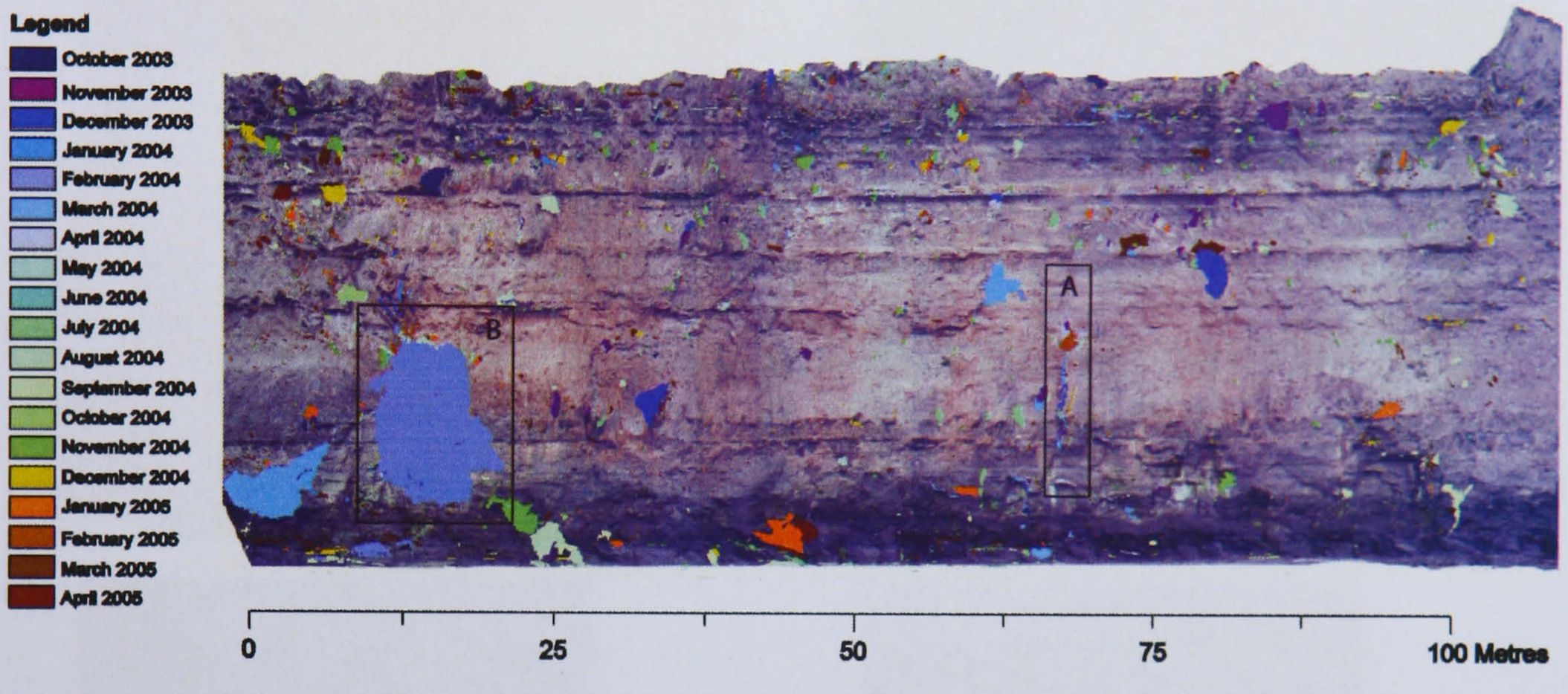

Figure 5.9: Orthoimage of Site 4 overlaid with a shapefile locating the spatial extent and position of changes recorded over the monitoring period. The headland was relatively stable throughout the monitored period with concentrations of change on vertical steps in the cliff face (A) and towards the seaward edge of the site where the largest failure occurred (B).

In agreement with the material changes from the previous two sites, the volumetric losses per m^2 for most months at Site 4 were made insignificant by the presence of a month which included a relatively large failure (Figure 5.11). The single protruding lobe failure in February 2004 was the greatest volumetric loss recorded at the site, involving 137 m^3 of material. The change is two orders of magnitude larger than the maximum single block loss from the previous headland at Site 1. The volumetric patterns of total change detected were similar to those found at the adjacent Site 3, where July 2004 showed a significant increase before steadily declining for the rest of the year. The correspondence raises important questions over the influences governing cliff development and whether the same drivers can be detected in different landforms, such as embayments and headlands for example. The correlation between the patterns at the neighbouring sites is interesting because the changes recorded from Site 3 are up to 20 times greater, implying that while there may be associations between the responses of different cliff sections to the same drivers of change, the

nature of the behaviour may be site specific. Unlike the well-jointed embayment, the volumetric losses per m^2 for the headland continued to remain relatively low through the start of 2005, although there was a small but detectable increase in February.

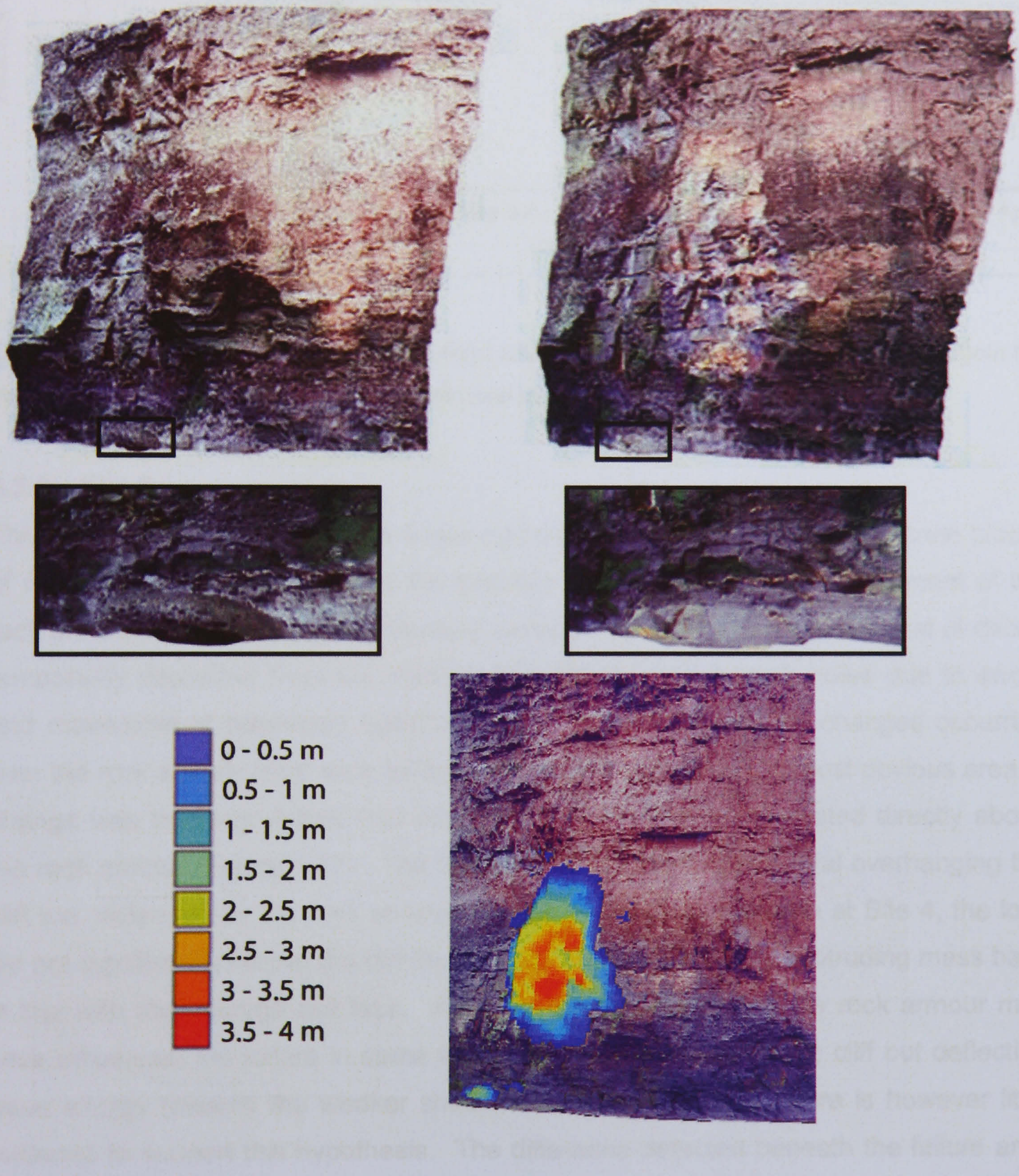

Figure 5.10: Subsections of the orthoimages for January and February 2004 and resultant difference model. A large protruding lobe of material failed from the cliff to reveal a fresh exposed scar although this soon became indistinguishable from the rest of the cliff by red/brown staining from the till above.

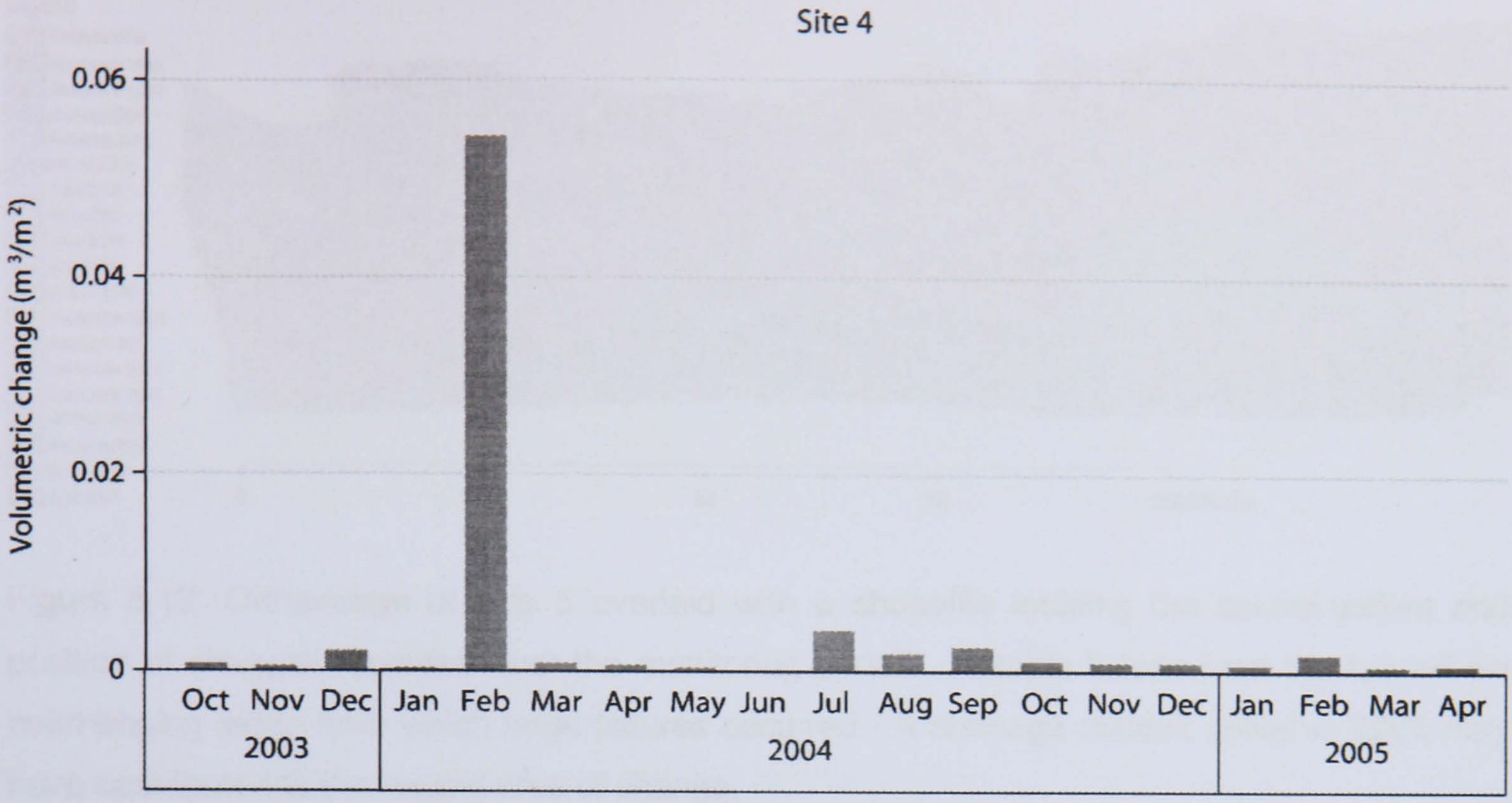

Figure 5.11: Volumetric losses recorded from Site 4 over the monitored period. Once again the material losses appear concentrated within one month of change in February 2004.

5.2.5 Site 5

The change detected across Site 5 was complicated by the presence of discrete blocks of rock armour placed to defend the westerly extreme of the Nab. Movement of the rock armour, the large, angular divisions between the blocks and the removal of debris temporarily deposited from the overhanging cliff generated much noise due to errors and movement of previously failed material. For this reason the changes occurring over the rock armour itself were excluded from the analyses. The most obvious area of change was the large failure that occurred in November 2004, located directly above the rock armour (Figure 5.12). The failure involved undercut material overhanging the cliff toe, defended by the rock armour. Much like the largest failure at Site 4, the loss did not significantly retreat the cliff face, rather it simply brought a protruding mass back in line with the average cliff face. A logical assumption is that the rock armour may have influenced the failure in some way, protecting the base of the cliff but deflecting wave energy towards the weaker shales immediately above. There is however little evidence to support this hypothesis. The difference detected beneath the failure area before November 2004 was insignificant, indeed the very reason for the rock armour was the identification of the site as particularly prone to recession. It should also be noted that the failed area is centred on a drainage conduit drilled through the rock, which may have weakened the overhanging mass through fracturing or surcharging caused by pipe leakage.

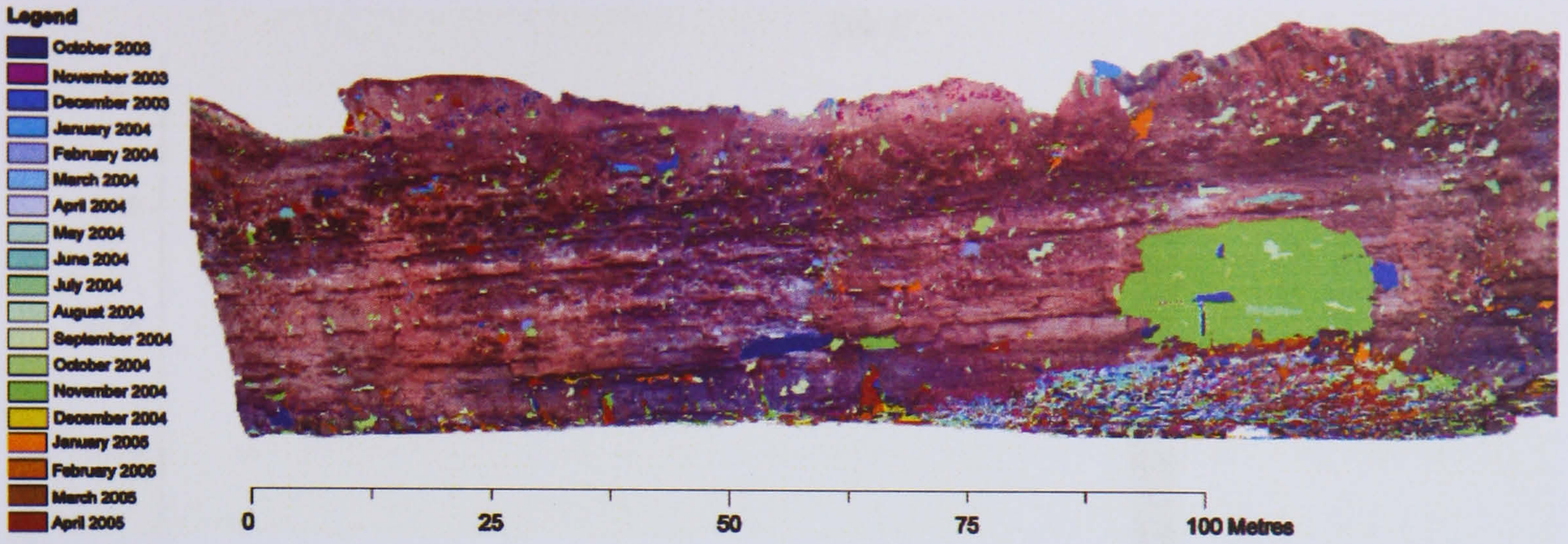

Figure 5.12: Orthoimage of Site 5 overlaid with a shapefile locating the spatial extent and position of changes recorded over the monitoring period. Notable losses from the toe left an overhanging ledge from which large failures occurred. A drainage conduit drilled in 2002 may have contributed to the largest area of change.

Elsewhere along the cliff section much of the erosion is concentrated towards the base of the cliff, characterised by the removal of vertically elongated blocks which typically coincided with cross-cutting joints. The resultant undercutting has left a protruding ledge above from which larger magnitude failures were recorded, often delimited vertically by lithological boundaries. Change across the rest of the rock mass is relatively evenly spread, with little evidence of concentrations upon specific bands or within rock stained by till overflow.

The volumetric change recorded at the site demonstrated a more progressive continuum of material losses than at any other site (Figure 5.13). After a larger monthly total than the previously monitored months in February 2004, volumetric change rose steadily from a minimum of less than 6 m^3 in March 2004, equating to a retreat rate of 0.001 m a^{-1}, to over 25 m^3, approaching 0.01 m a^{-1}, in October 2004. The dramatic change in material losses in November, involving over 350 m^3 of rock, was followed by significantly smaller losses in December 2005, which then increased again throughout the early part of 2005. Elements of this cyclic temporal pattern, involving progressive increases in volumetric losses before a significantly larger event was recorded, were seen at other sites but none so marked as at Site 5. The volumetric losses peaked at almost 0.1 m in a single month, with only Site 3 recording more significant levels of monthly change. The amount of change occurring to the cliff face may correspond to the length of cliff section monitored. Although the cliffs at Cowbar are some of the lowest in the study area, the site was over 140 m long, exposing relatively more material to marine influence than at any other monitored site.

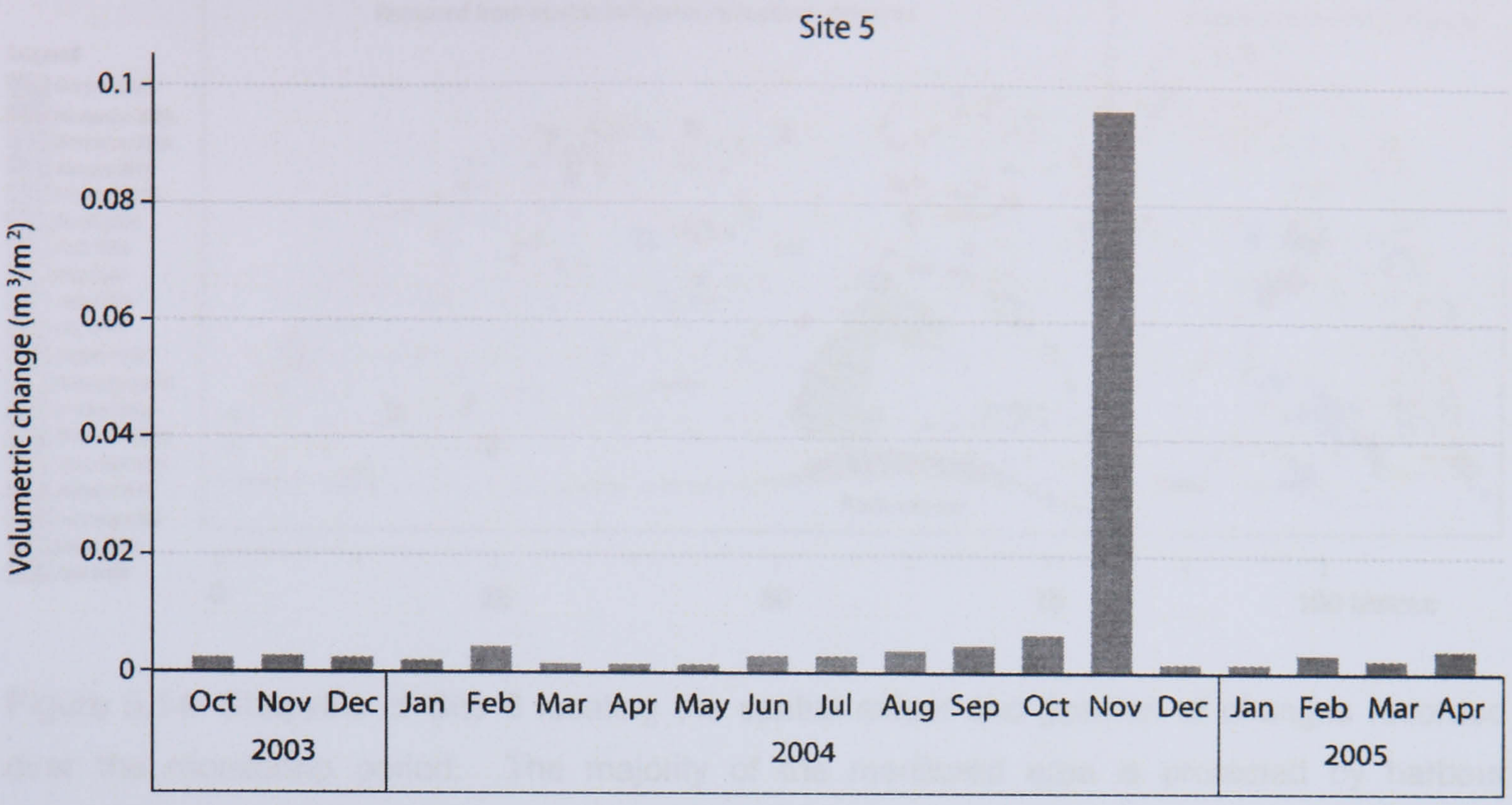

Figure 5.13: Volumetric losses recorded from the geology headland over the monitored period. The material losses increase progressively throughout the year, terminating in an above average month of change.

5.2.6 Site 6

The limited extent and two tiered nature of the foreshore in front of the protected headland prevented the collection of appropriately located stereo pairs. The omission of orthoimages of the site restricted the ability to associate changes with specific lithological bands, demonstrating the value of using both techniques to monitor change. As with the previous site, the changes recorded on the rock armour itself were ignored. Spatially the changes were concentrated to areas above the base of the harbour defence and to the seaward side of the headland (Figure 5.14). The mid section of the rock mass was found to overhang lower sections. While much of the protruding rock remained unchanged during the monitoring period, two arched failures were identified and seen to concentrate change towards the edges of the arches in a similar manner to that noted at Site 2. The largest recorded single change involved over 65 m^3 of rock and comprised the landward half of an arched failure. The loss incurred in October 2004 was added to in March 2005, again expanding the arched failure horizontally. Much of the larger change on the seaward side of the harbour defence was noted as marine quarrying in field surveys. Incised notches were seen, up to a metre deep, restricted to certain basal rock layers. As with many sites the failure processes often involved sheeting effects with layers of rock removed to form a flat failure surface, generally closer to the average position of the cliff face (Figure 5.15).

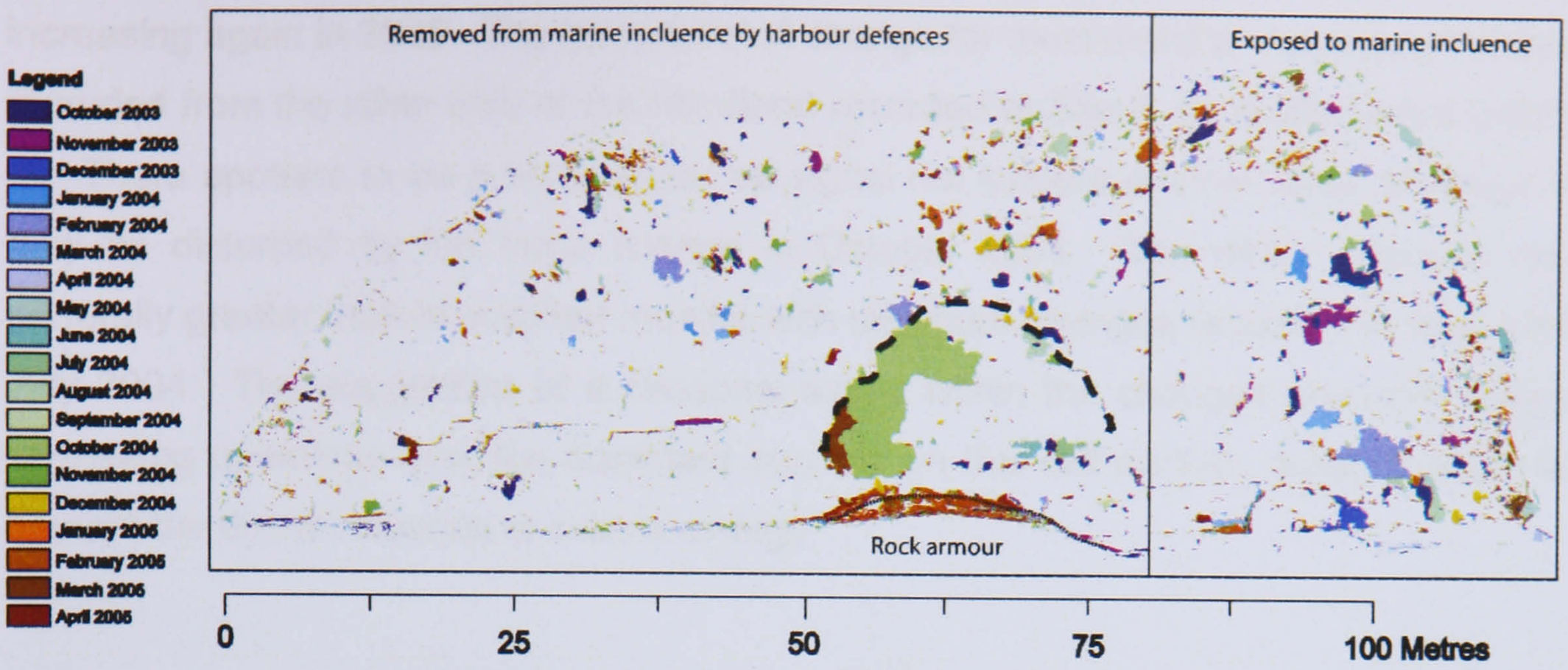

Figure 5.14: Shapefile of Site 6 locating the spatial extent and position of changes recorded over the monitoring period. The majority of the monitored area is protected by harbour defences, although the seaward extreme is exposed to marine influence. An arched failure above the rock armour (dotted line) is denoted by the dashed line.

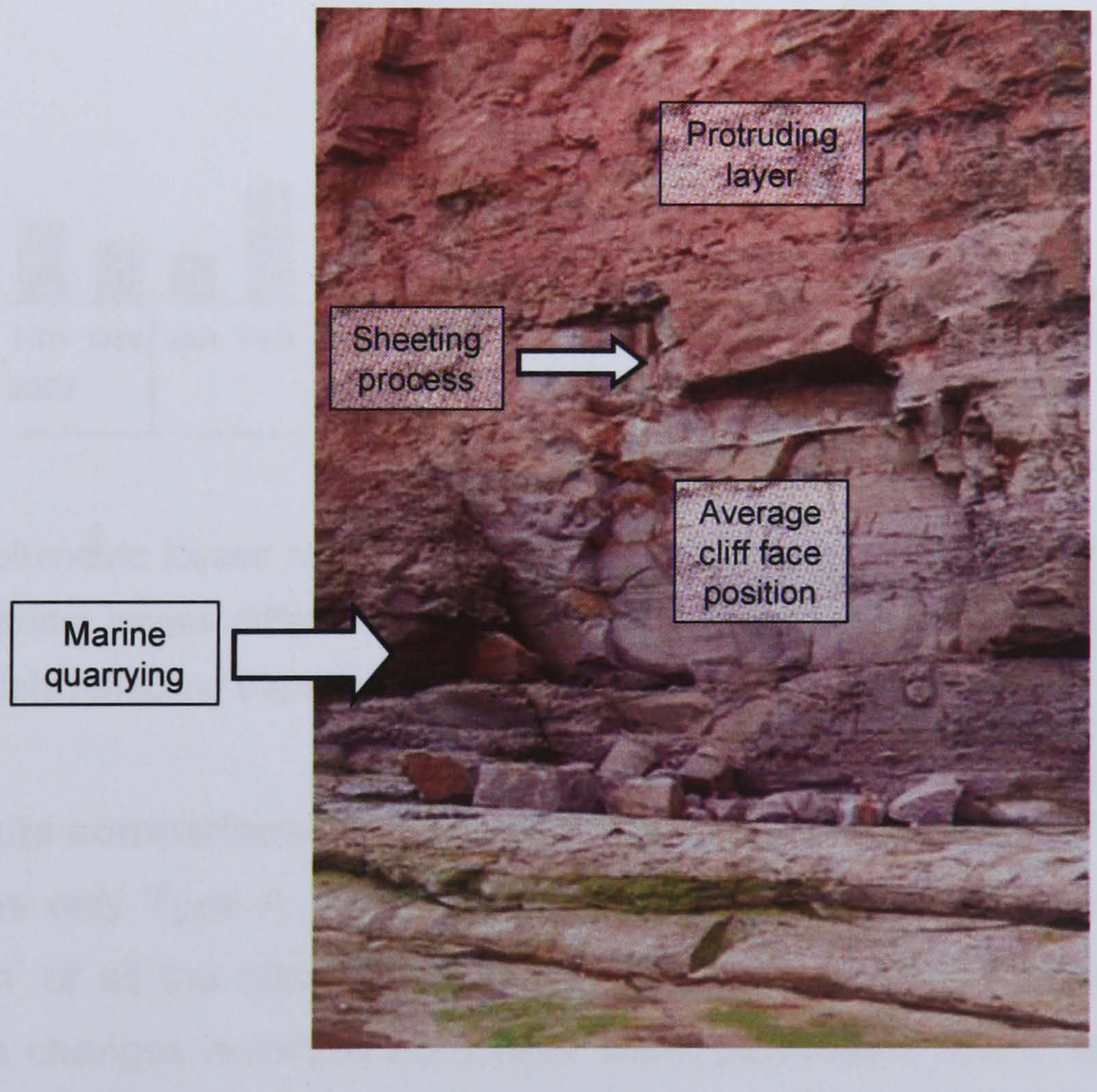

Figure 5.15: Marine quarrying and resultant sheeting of material at the seaward extremity of the headland. During monitoring many failures were seen to bring localised areas into line with the wider rock slope.

Once again the total monthly volumetric losses per m^2 were significantly greater in one particular month (Figure 5.16). The loss of material to a single coherent area of change was over three times greater than the next largest volumetric loss. Although the progressive monthly losses were not as consistent as those found at Site 5, the

October 2004 failure was followed by comparatively small losses late in 2004, increasing again in 2005. The base-level of change for most months was similar to that recorded from the other side of the headland recorded at Site 5, generally below 0.005 m. There appears to be a weak seasonal signal not evident in other sites, although it may be disturbed by the large change in October 2004. The winter changes are generally greater than in summer months with minimum changes recorded in June and July 2004. The suggestion of a seasonal signal within the changes recorded raises interesting questions over the dominant controls on this cliff section, most of which is beyond the direct influence of marine energy.

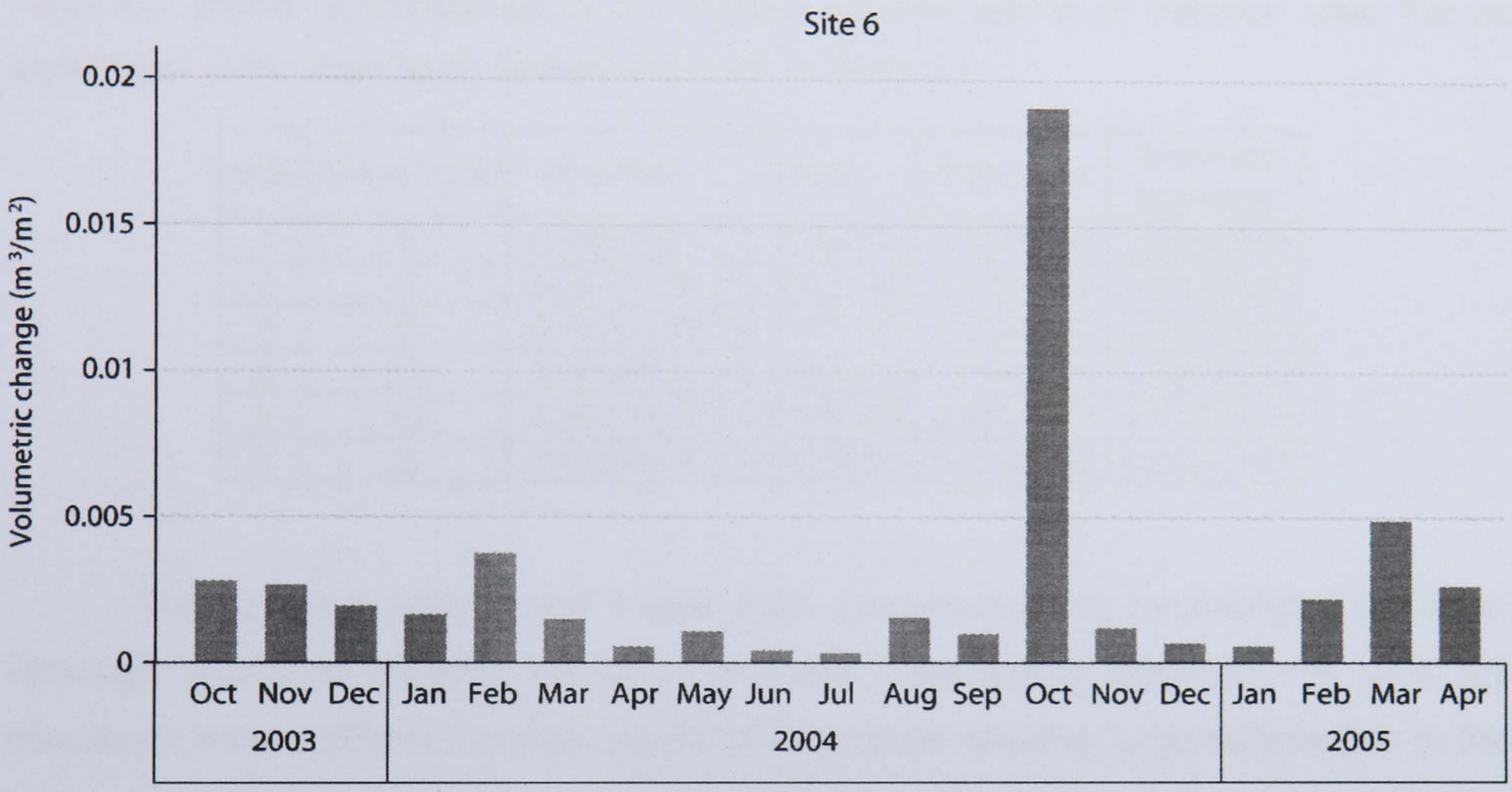

Figure 5.16: Volumetric losses recorded from Site 6 over the monitored period. The patterns detected in material losses differ considerably from those of Site 5 on the other side of the headland, possibly reflecting the effect of harbour defences.

5.2.7 Inter-site comparisons

Site 1 was the only Type A slope monitored, and it recorded the lowest volumetric change per m^2 of all the sites (Table 5.1). In general the volumes of retreat were comparable to changes recorded from other sites, particularly Site 6, an overhanging slope with a well defended toe. The comparison is interesting because Site 1 was chosen because it has subsided more than any other site as a result of contemporary mining activity. Logically it might be expected that this site would have experienced greater volumes of change, if marine undercutting was the sole cause of cliff slope change. Throughout the monitoring period however the site appeared more stable than even the protected headland in terms of minimum, maximum and mean m lost, which was largely removed from much of the effective influence of marine activity. The

comparison between the behaviour of the Site 1 and the other sites demonstrates the importance of the material and structural properties and the position of the rock within the cliff, in this case the thick, competent mudstone base. It is therefore unlikely that the drivers of change in hard rock coastal cliffs, such as relative sea-level rise will ever be linked directly to landform response unless the site-specific influences of *in situ* conditions are considered. The analysis of just a single Type A slope means questions remain as to whether lower response rates are characteristic of slopes with protruding toes; therefore further analysis has been conducted into the patterns of change recorded.

Table 5.1: Statistical comparison of the monthly volumes lost in m^3 between sites. For an explanation of the slope types defined refer back to Table 3.4.

Site	Slope Type	Minimum	Mean	Maximum	Standard Deviation
1	A	0.0000273	0.0006303	0.0025795	0.0004946
2	C	0.0000355	0.0093190	0.0484834	0.0119899
3	B	0.0000758	0.1151730	1.0549780	0.2402533
4	C	0.0000820	0.0162183	0.0542886	0.0238020
5	C	0.0013358	0.0150525	0.0958893	0.0307810
6	B	0.0000914	0.0026900	0.0190762	0.0035183

The slopes at sites 3 and 6 were both characterised by overhanging cliff tops. Although minimum monthly losses in m^3 were very similar between the sites the maximum losses differed by two orders of magnitude causing large differences in the mean per m^2 recession. Both of the Type B slopes were dominated by occasional, comparatively large events. Despite monitoring an overall area of over 20 000 m^2, five out of six of the largest changes were concentrated on the smallest monitored area, Site 3. The propensity for so many of the largest changes across the study area to be detected within the same site suggests localised conditions may be crucial to the occurrence of larger events. The rock mass strength classification of the well-jointed embayment was significantly lower than that of Site 6, although the general strength properties remain identical save the spacing and continuity of the joints (refer back to Table 3.6).

The patterns of declining change per m^2 before the largest monthly losses at Site 3, and to a lesser extent Site 6, contrast with those of the Type C slopes at Sites 2 and 5 which increase steadily before a dramatic larger failure. The segregation of responses into Type B and Type C slopes is made more pertinent given the incorporation of both headland and embayment morphologies in the two groups. The embayment at Site 2 and the headlands at Site 4 and Site 5 for example generated

similar maximum and mean volumetric changes per m^2, although Site 5 demonstrated relatively higher minimum levels of activity during the monitoring period. The general agreement within the temporal differences between the responses of slopes of different types may hold important implications for the way in which the coastline is understood to evolve. The division of results by slope type has been complicated by localised sea defences that mean parts of Site 5 and Site 6 are protected from the majority of marine influence. Both of the rock slopes immediately above the rock armour incurred significant failures which were followed by a month of minimal change which steadily increased over time, perhaps indicating that the rock armour may also influence post-failure change. Although the evidence suggests that slope form and the processes of change may be integrally linked, a wider, more extended time series is required to confirm and explore these patterns.

The failures recorded were a complex combination of scattered, apparently random losses and concentrated, localised zones. The concentrations were typically focused towards the base of the cliff although they were also found specific to certain lithological bands or structural weaknesses. In addition to the *in situ* conditions influencing change spatially at the monitored sites, consistencies were also noted over time during the monitoring period. Headland sites 4, 5 and 6 for example all recorded an increased monthly volumetric loss per m^2 in February 2004. Sites 2 and 5 both recorded volumetric changes far in excess of other months in November 2004, suggesting that general, cross-site patterns of change may be identified in addition to site specific influences. The monthly patterns imply that the resolution of the technique used may be sufficient to attribute changes in cliff form to numerous factors including both *in situ* conditions and external influences.

5.3 The rate of retreat at Staithes

The application of the combined photogrammetric and laser scanning technique for cliff monitoring has yielded new data on the location, size, timing and nature of change in monitored sections of hard rock coastal cliffs. A key consideration of this study is the comparison between these data and the rates of retreat currently established for the area by conventional techniques. The overall rate of retreat at Staithes, as indicated by the conventional approach, is 0.05 m a^{-1}, subdivided into 0.04 m a^{-1} and 0.07 m a^{-1} for embayments and headlands respectively. Implicit in these averaged rates is that the processes and mechanisms governing rock slope development are dependent on morphology, although no indication is given as to the nature of the change. It is evident that the conventional rates established for the Staithes coastline are of insufficient temporal resolution to account for the significant variability in monthly rock slope

changes, whilst the new dataset presented covers an inadequate time period from which to draw conclusions on longer term aspects of cliff change. A key issue then is how appropriate the conventional use of annual rates of change is for analysing cliff response.

In order to assess the reliability and effectiveness of the existing measurements of annual retreat rates the volumetric changes recorded in 2004 were compared to those established for the area by aerial surveys (Table 5.2). There was significant correspondence between the two approaches in the overall retreat calculated for the area, within 0.02 m a^{-1}. The slight difference could be attributed to the proportions of headlands and embayments that constitute the two datasets; the ratio between the morphologies monitored may differ from that across the whole area. However greater variability was noted between the two approaches when more specific aspects of change were considered. Sites 2 and 3 recorded similar losses to those established by aerial survey for embayments, with measured annual recession rates within 0.01 m of those predicted. The rates used for headlands performed poorly, ranging from being four times too large at Site 1 to constituting only one third of the actual rate at Site 5. Interestingly the rates obtained from the protected headland at Site 6, where marine influence has little effect on much of the monitored area, were the closest to rates established by aerial surveys. The data may therefore reflect the inability of aerial surveys to adequately record the behaviour of coastal cliffs where marine activity means the changes to the base of the rock slope are not necessarily the same as those occurring at the cliff top. Furthermore it must be remembered that the comparison is complicated by the fact that aerial surveys rely on cliffline retreat whilst the terrestrial remote sensing approach includes the whole cliff face, and so the similarities could represent false accuracies.

Table 5.2: Comparison between rates of recession and total volumetric losses established by aerial survey and terrestrial remote sensing for the year 2004.

Site	Monitored area (m^2)	Rate of recession measured by aerial survey		Rate of recession measured by terrestrial monitoring		Total volumetric losses	
		For the area (m/yr)	For the site morphology (m/yr)	For the area (m/yr)	For the site (m/yr)	Measured by aerial survey (m^3/yr)	Measured by terrestrial monitoring (m^3/yr)
1	4100.27	0.05	0.04	0.065	0.009	164.01	34.89
2	3090.49	0.05	0.07	0.065	0.079	216.33	243.36
3	2484.92	0.05	0.07	0.065	0.073	173.94	180.48
4	3080.70	0.05	0.04	0.065	0.068	123.23	210.93
5	3922.35	0.05	0.04	0.065	0.128	156.89	503.79
6	3638.95	0.05	0.04	0.065	0.033	145.56	119.76

The practicalities of deriving cliffline changes for extensive stretches of coastline restrict the resolution at which data can be recorded. A simple comparison between the most detailed Ordnance Survey Landline data derived from aerial photographs and the terrestrial technique highlights the difference in resolution achieved by the two approaches (Figure 5.17). The precision of the laser scanned positions of the cliff top and toe is such that the removal of a single block of debris at the cliff base can be detected (subsection A). The limited temporal extent of the new data raises questions however over the longer term aspects of cliff change.

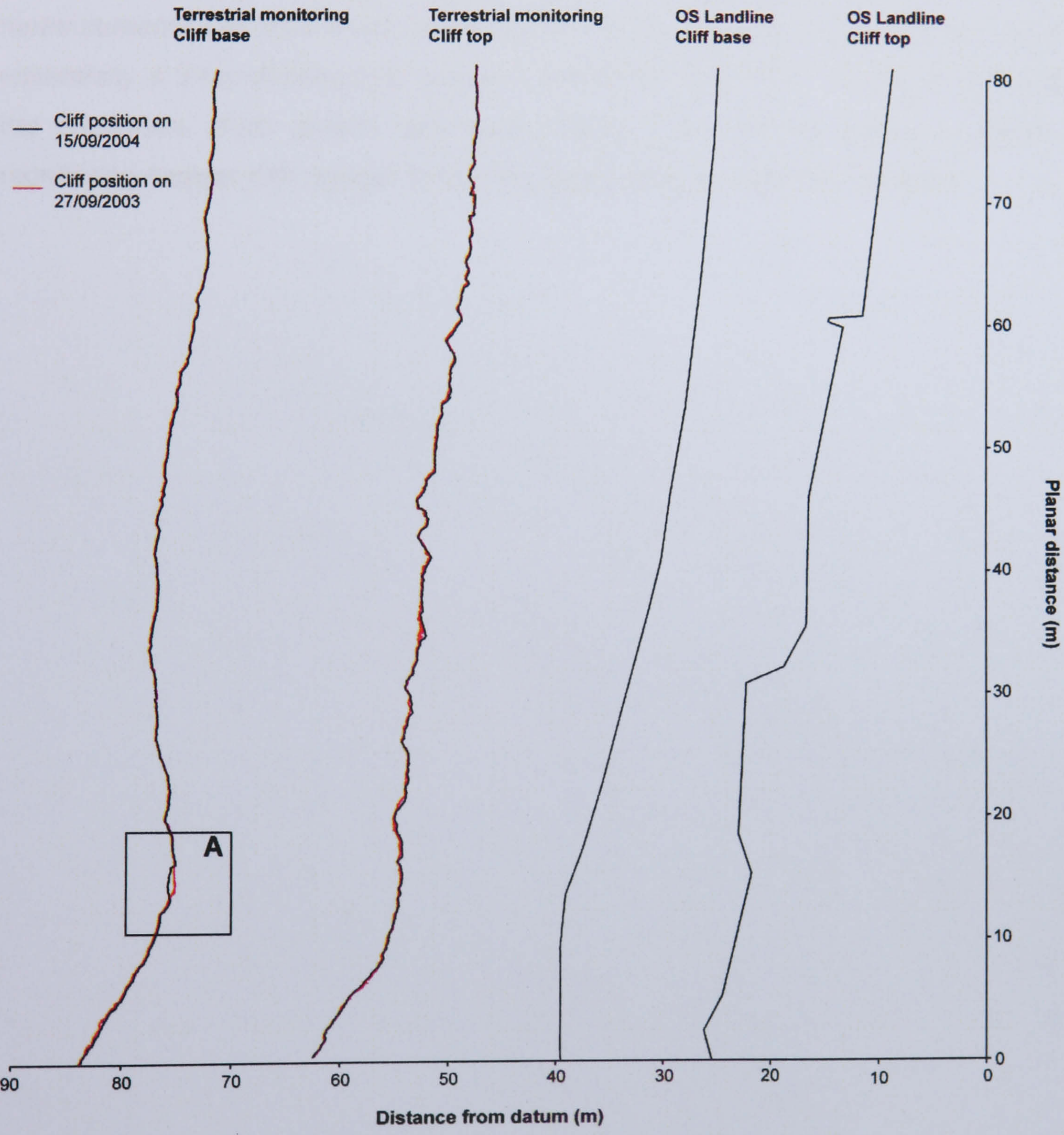

Figure 5.17: Comparison of the cliff top and toe positions recorded in September 2003 and 2004 by combined terrestrial photogrammetry and laser scanning and Landline data provided by the Ordnance Survey in 2001. The top and toe, and the two datasets, have been separated by an arbitrary distance for clarity. Noticeable differences in resolution were evident both between the two approaches, and within the Landline data between the cliff top and the less easily located cliff toe.

5.4 Summary

The data demonstrate both the importance of distinguishing between one-dimensional cliff retreat and three-dimensional cliff recession and the inadequacies of average annual retreat rates when specific cliff sections are considered. Even when subdivided by morphology or lithology, annual cliff change may be site-specific and deviate significantly from the long-term average, implying important patterns relating to the detailed nature of coastal rock cliff behaviour may be overlooked with conventional datasets. Monthly volumes of change at monitored sites were typically below average with a few months of very large change. This pattern suggests that cliffline measurements are insufficient to represent the true nature of cliff change, which is essentially a three-dimensional process, non-linear over time. To better understand the processes which govern rock slope change the following chapter analyses the monitoring dataset with respect to the four key questions raised in Chapter 2.

Chapter 6
Analysis: contemporary cliff behaviour

6.1 Introduction

The monitoring data have been used to analyse fundamental concepts in geomorphology such as how landforms change, whether the patterns are determined by the scales at which they are analysed, whether they alter over time and the extent to which they are controlled by variations in environmental processes. The chapter concludes by summarising the extent to which the approach has addressed these issues, and identifies some of the remaining gaps in understanding of hard rock cliff evolution.

6.2 Magnitude-frequency relationships

A key question in the consideration of the relationships between the size of rock losses and the frequency with which they occur is as follows:

Is hard rock coastal cliff change characterised by frequent small scale failures and infrequent large scale failures?

Many measures of magnitude have been employed to establish patterns of rockfalls, for example using analyses of cliffline retreat (Agar, 1960; Pinckney and Lee, 1973), retreat area (Stafford, 1971; Dias and Neal, 1992; Neves and Pereira, 1999) or volumetric data (Moore and Griggs, 2002). In this study a magnitude-cumulative frequency graph has been constructed for one-dimensional (failure depth), two-dimensional (area of change) and three-dimensional (volume of change) datasets (Figure 6.1). Logically, the volumes, which included the greatest degree of measured data, provide the truest representation of actual change. Although the two-dimensional monitoring is limited in the quantification of the smallest changes, under-predicting the frequency of change and offset towards larger rockfalls, the distribution mirrors the volumetric alterations and converge, becoming indecipherable when changes reach 0.01 m. This may provide a lower threshold for the effective use of area datasets for applications where volumetric data are unavailable. The one-dimensional retreat of the cliff provides a poor representation of reality, sensitive only to changes several orders of magnitude larger than those registered with multi-dimensional monitoring, raising questions over the use of retreat distances to gain a quantitative understanding of cliff processes.

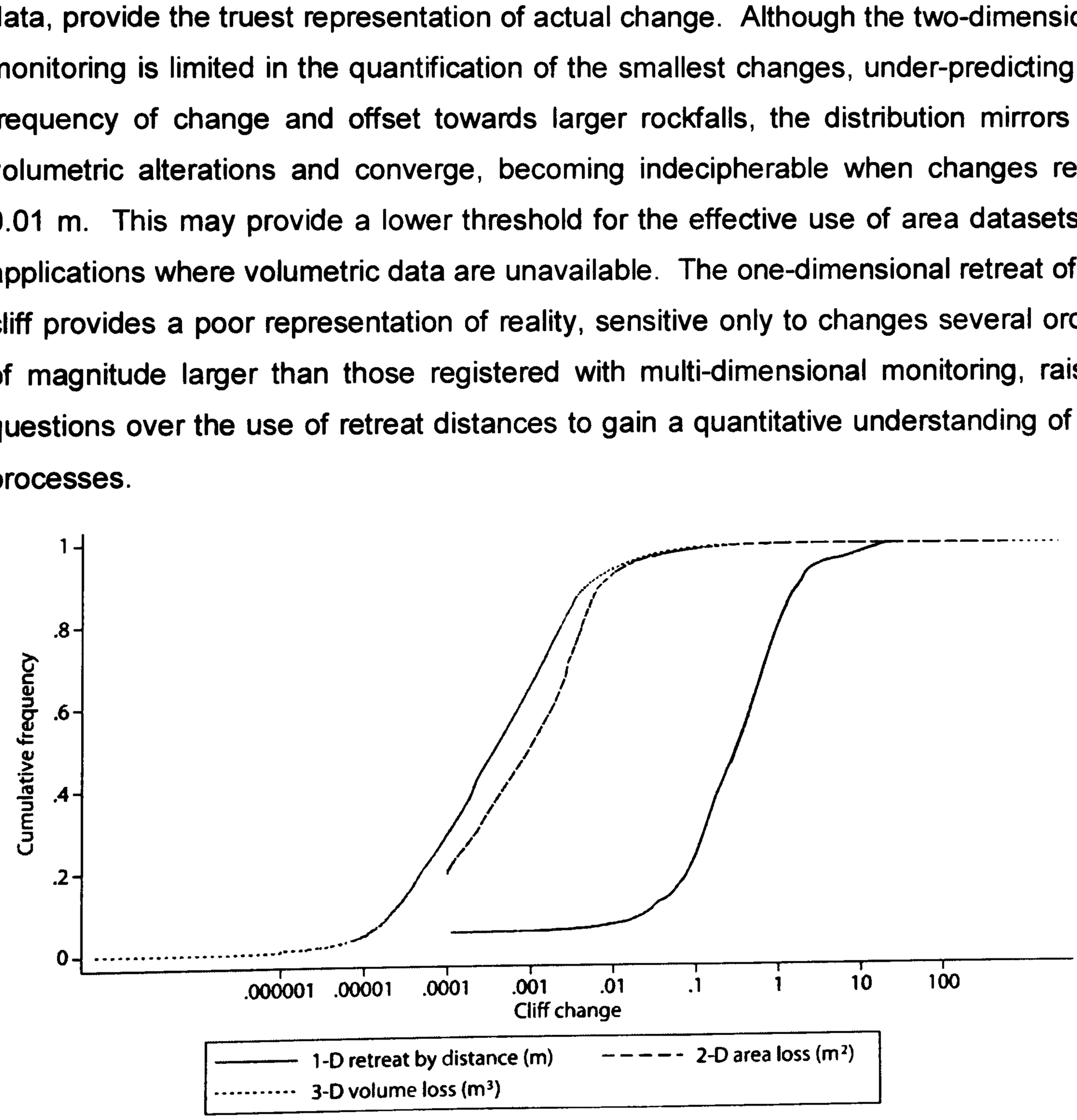

Figure 6.1: Cumulative frequency analysis of one-, two- and three-dimensional data on the magnitude of losses from monitored sites.

The magnitude-cumulative frequency graph for all of the monitored data displays a classic 'S' curve, with the vast majority of changes detected below 0.1 m^3 (Figure 6.2). The smooth curve demonstrates that a continuum of scales was detected with the monitoring technique. For simplicity of analysis the magnitudes were divided into arbitrary classes: 'Class 1' (0 to <0.1 m^3), 'Class 2' (0.1 to <1 m^3), 'Class 3' (1 to <10 m^3), 'Class 4' (10 to <100 m^3) and 'Class 5' (100 m^3 and over). The magnitude class labels are used throughout the analysis although it must be noted that the terms are purely descriptive. The recurrence intervals of one month, three months, six months and 1 year for each of the magnitude classes were calculated and used to annotate the cumulative frequency graph. The results suggest that although the cliffline at Staithes is considered to be moderately stable (Mouchel Associates Limited, 1996), the monitored area is almost certain to contain Class 5 events over the course of a year.

One of the most widely used analyses of rockfall patterns is to establish the probability of different sized events, which can then be used to forecast future occurrence. The consistency of activity rates of different magnitudes was investigated by comparing the probabilistic predictions based on a year of monitoring data for the next one, three and six months against the changes that were actually observed (Figure 6.3). The predictions proved relatively responsive to the trends of actually monitored data, with the smallest losses most accurately represented. The other magnitude classes consistently under-predicted the monitored data for the next 6 months, reflecting the enhanced rates of activity associated with the winter of 2004/2005. The limitations of the dataset can be seen in the large magnitude events which are predicted for one month (although none were recorded) and then underestimated over longer time periods. The usefulness of annual rates of change predicted for cliffline retreat, particularly with regard to the larger changes, is once again drawn into question.

The analysis of magnitude-frequency patterns is often biased towards changes at the large magnitude end of the scale due to both their more easily recorded occurrence and the problems of reliably measuring smaller slope alterations. It is evident that there is an overall relation between high numbers of the smallest events and progressively fewer numbers of larger losses. The continuous transition between rockfall size and frequency however raises questions over both the validity of focusing on the large magnitude events, and the concept of change as being either very small and iterative or very large and infrequent. An investigation has been conducted into the nature of magnitude and frequency patterns, with specific consideration of both the

spatial controls such as locality or material properties of the rock slope and the temporal aspects of the relationship. Having broken down some of the key aspects of the controls on the patterns of rock losses, the actual and relative contributions of the different magnitude classes were then analysed.

Recurrence interval within the whole monitored area	Class 1	Class 2	Class 3	Class 4	Class 5
1 month	100%	100%	99%	66%	27%
3 months	100%	100%	100%	96%	61%
6 months	100%	100%	100%	99%	85%
1 year	100%	100%	100%	99%	97%

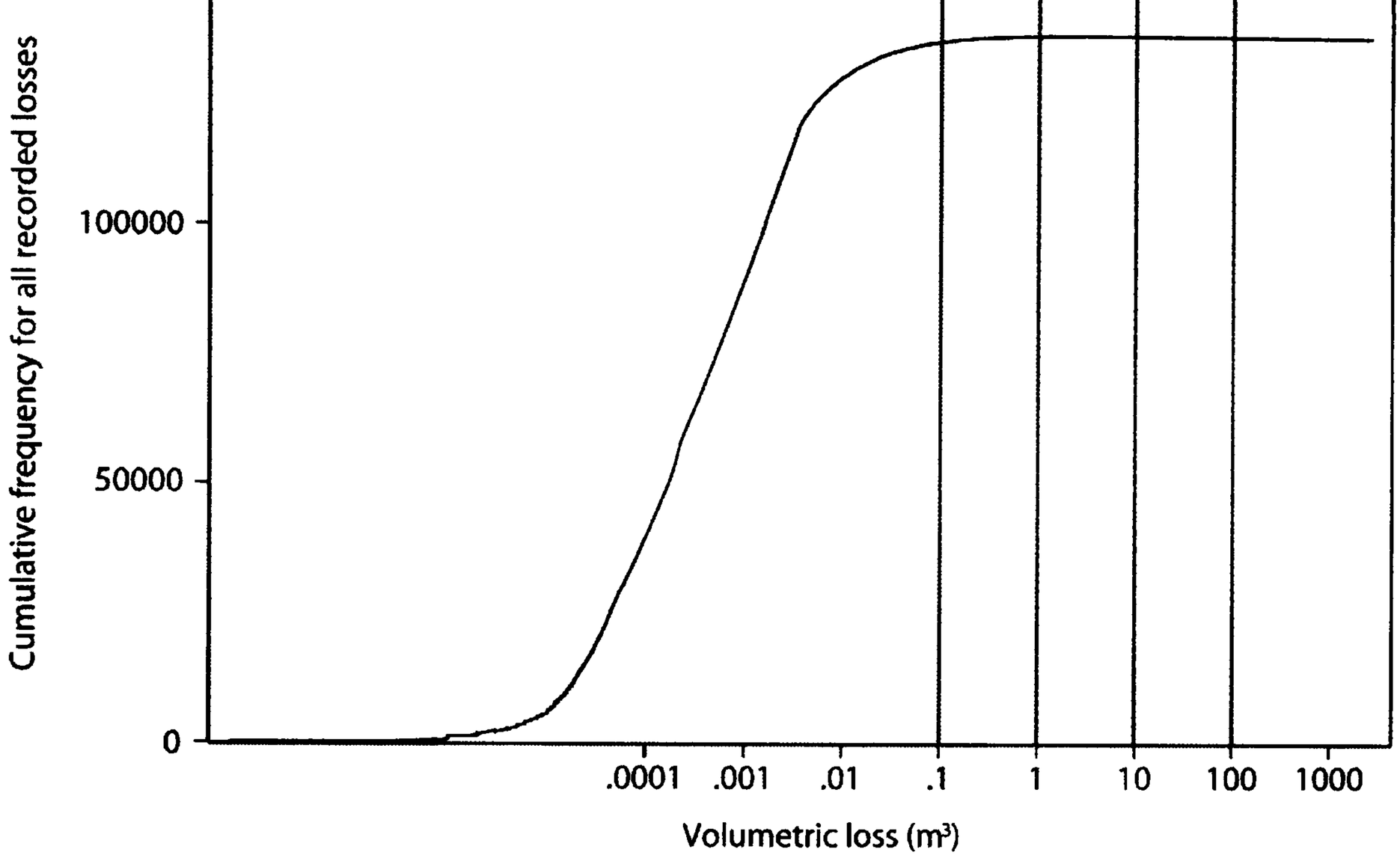

Figure 6.2: Magnitude-cumulative frequency graph for the entire dataset annotated with recurrence intervals of the different magnitude classes arbitrarily selected for analysis purposes.

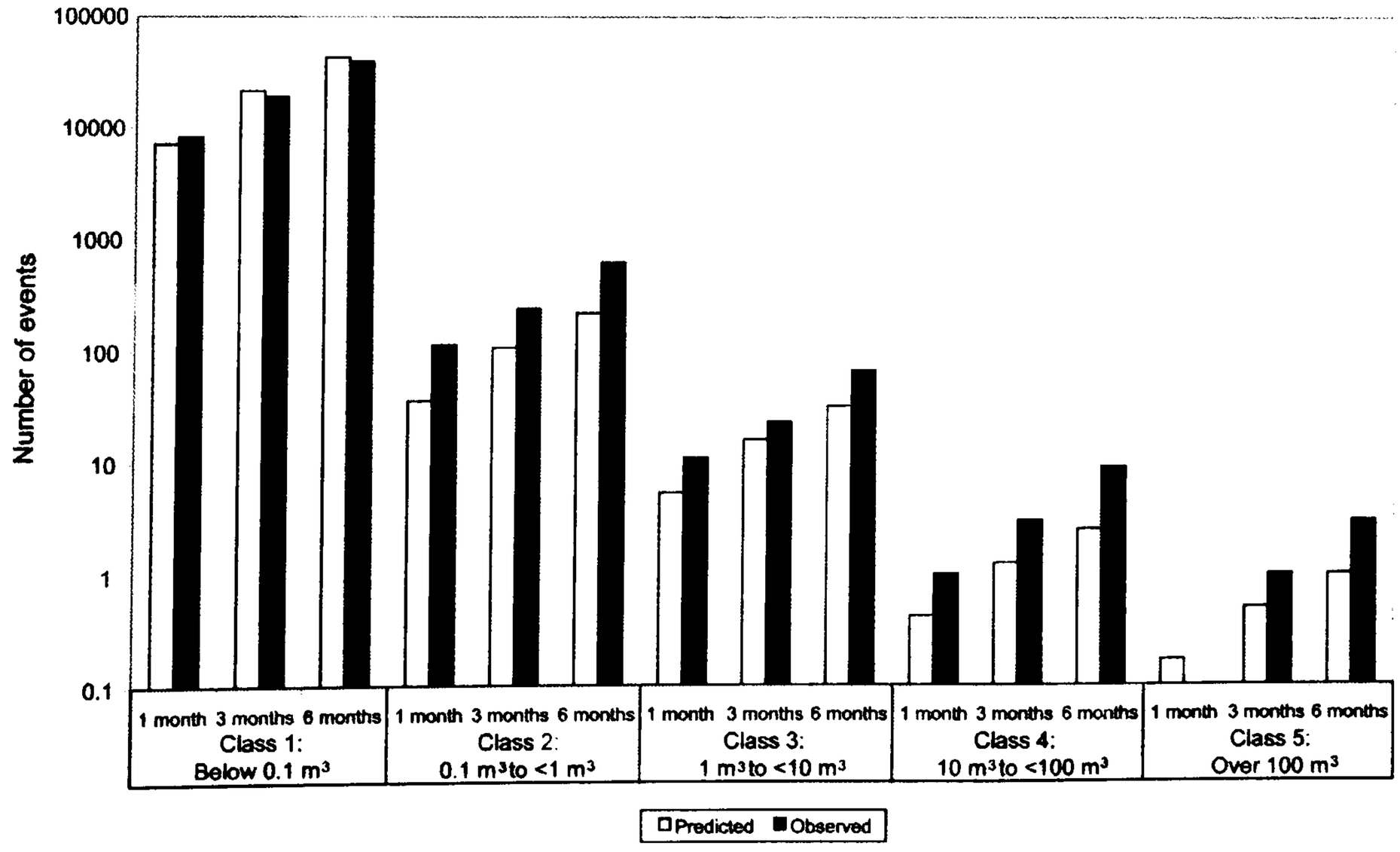

Figure 6.3: A year of monitoring was used to generate probabilistic predictions for the occurrence of different sized failures over the next 6 months, which were compared with observed frequencies.

6.2.1 Location controls

In order to investigate whether the magnitude-cumulative frequency relationships within the dataset were location dependent, cumulative frequencies of rockfalls were subdivided by each site. The data on volume losses at individual sites were normalised by frequency to compare the distribution of losses of different sizes (Figure 6.4). Site 1 recorded one of the highest relative frequencies of Class 1 change, with most losses less than 0.01 m^3, and the lowest mean rockfall size of 0.003 m^3 (Table 6.1). This suggests that the activity rate at the subsided headland was largely controlled by processes and mechanisms that influence the smallest scale losses from the cliff. Whilst the minimum rockfall size was comparable to the other sites, the maximum loss and the standard deviation of the rockfalls were significantly lower. The data indicate that variability of rockfall patterns is directly related to the magnitude of losses recorded.

Site 6 demonstrated an almost identical distribution of change to Site 1, but the events were displaced towards magnitudes up to three times higher, converging with the subsided headland at 0.1 m^3. Although the frequency of events and mean rockfall size were comparable, the maximum loss recorded was almost 13 times greater, and the standard deviation was larger. The reason for the bias towards larger rockfalls at Site 6 may be the weaker structural properties than those at Site 1 where wider, less continuous and more closed joints cause the slope to be more stable with respect to joint-determined failures (refer back to Table 3.6). The similarities in the distribution and the differences in the magnitude of the changes between the protected and subsided headlands raise interesting questions over the controls on the magnitude-frequency relationship. The thick, competent mudstone base at Site 1 provides an effective natural barrier to marine erosion in a similar manner to the artificial defences laid down at Site 6. If both cliff sections are responding more to subaerial rather than marine drivers of change, although the failures at Site 6 appear larger and more joint-controlled in general, then the similar patterns suggest that some consistency may exist in rock slope response to the same environmental drivers.

Site 2 demonstrated a similar smooth continuum of magnitudes to that seen at Site 6, with a marginally shallower gradient of tiny scale change. The lines converge briefly at Class 2 magnitudes before diverging slightly for larger losses. The small divergence demonstrates the greater number of larger changes seen at the arched-failures embayment, although the close overall position of the curves may reflect similar processes, with arched-failures recorded at both sites. The number of rockfalls

recorded at Site 2 was lower than at any other site and the mean rockfall size, an order of magnitude greater than at Sites 1 and 6, reflects the dominance of significantly larger failures. The presence of larger rockfalls, involving almost 99 m^3, generated variability over one standard deviation from the mean.

The magnitude-cumulative frequency distribution at Site 5 closely resembled that of the Site 6, but was distributed towards change two to three times larger. Despite similar frequencies of events, the largest change at Site 5 increased both the average size and variability of rockfalls about the mean in comparison to the protected headland which acted as a control for marine influence. The similar patterns and frequencies of change provide further evidence that rock cliff response may demonstrate some consistency, even when the magnitudes caused by controlling factors differ. This is particularly the case when *in situ* conditions are analogous. Sites 5 and 6 for example are positioned on two sides of the same headland feature. The comparison between sites 5 and 6 suggests marine activity may have caused a shift towards larger scale change.

Site 4 revealed a curve that differed significantly to the previous sites, particularly Site 1 which involved changes an order of magnitude smaller. The range of the data at Site 4 was the most concentrated of any site with the majority of rock losses involving magnitudes around 0.001 m^3, although the mean was raised to 0.007 m^3 by failures involving up to 137 m^3. This site recorded the largest number of failures during the monitoring period and many of the changes were observed to occur along pre-existing joints in the basal mudstone and overlying shale, causing material losses to involve more coherent masses than the less jointed mudstone at Site 1 for example. When magnitudes of 1 m^3 are reached all sites become indistinguishable except Site 3. The well-jointed embayment was the only site to show a marked step in the relationship, with steep increases in magnitudes up to 0.001 m^3 and then a much shallower gradient for larger magnitudes. The top part of the curve confirms field observations that Site 3 contained the greatest number of larger magnitude events. The maximum loss was an order of magnitude greater than at any other site causing a dramatic increase in both the mean and standard deviation of rockfalls at the site. The large proportion and stepped patterning of the changes around 0.003 m^3 may reflect a limitation of the technique, noted during processing, where the edges of particularly large areas of change were typically surrounded by high numbers of very small change. Although it is possible that the differences reflect edge effects as small volumes of peripheral rock are dislodged or shattered, they may also be a product of the thresholding procedure and should be regarded with caution.

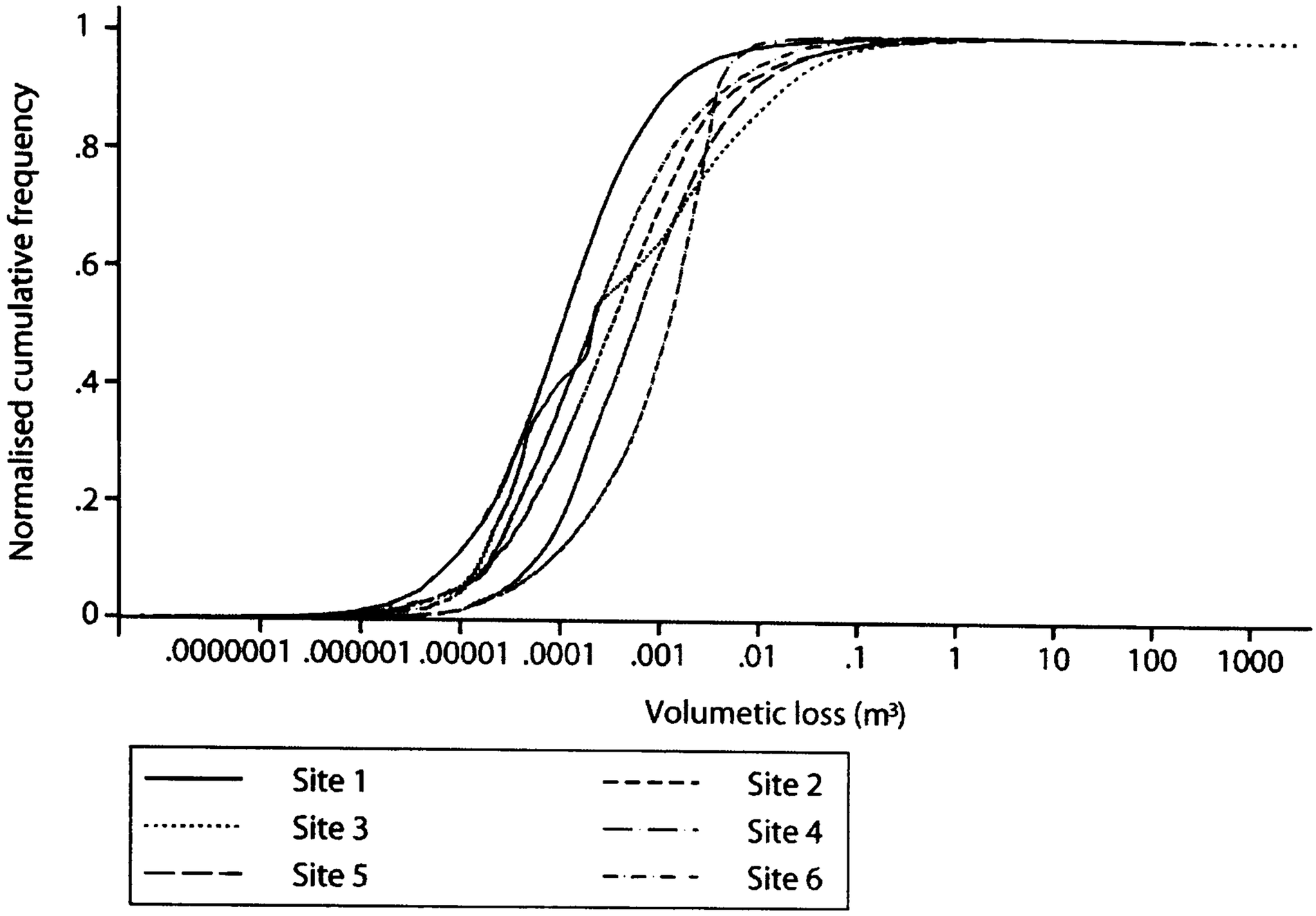

Figure 6.4: Magnitude-cumulative frequency relationships subdivided by site. Idiosyncrasies between sites reveal variations in the distribution of different sizes of failure although similarities in the overall shape confirm the consistency of the interplay between many of the smallest losses and fewer of the largest losses.

Table 6.1: Statistical summary of rockfall patterns by location.

	Number of rockfalls	Mean (m^3)	Standard Deviation	Minimum (m^3)	Maximum (m^3)
Site 1	17584	0.003168	0.060482	0.000000015	5.476
Site 2	9825	0.040053	1.265803	0.000000008	98.883
Site 3	28440	0.245863	20.279400	0.000000006	2614.880
Site 4	33415	0.006984	0.751136	0.000000014	136.843
Site 5	25241	0.022819	2.238869	0.000000021	355.548
Site 6	22989	0.008028	0.445911	0.000000057	65.879

The effect of location produces subtle differences in magnitude-cumulative frequency patterns, with significant overall similarity between all curves. Whilst location cannot be said to be the sole control on the nature of slope change, important site-specific responses have been noted, some involving an order of magnitude difference. Site 1 for example has subsided by up to 0.35 m more than Site 6 at Staithes harbour since 1972. It might have been expected that the higher energy environment inferred at Site 1 would have resulted in larger losses but instead the distribution was influenced by smaller scale losses distributed throughout the shale layers above the wave impact zone. Despite the subsidence at Site 1 the direct contact area with

incoming waves remained in mudstone layers. This effect was contrasted with that of Site 5, based in shale layers providing a more effective comparison with Site 6 in terms of *in situ* conditions, which demonstrated greater proportions of larger events. The differences suggest that rock type may provide an important consideration in the nature of such relationships.

6.2.2 Material controls

To further analyse the patterns of change spatially across all sites, magnitude-cumulative frequency graphs were divided by rock type and again normalised by frequency (Figure 6.5). Of the four main rock types found in the study area the mudstone displayed the greatest range of failures overall, reflected in the large standard deviation about the mean (Table 6.2). The curve of the mudstone layers, located at the cliff base, shows that magnitudes between 1 m^3 to 10 m^3 still make significant contributions to the patterns of change. The largest change however reflects a limitation of the data, relating to the removal of failed material from the base of the cliff rather than the erosion of the actual mudstone layers and thus should be discounted. Despite this influence on the maximum change, the greater magnitude of failures from the mudstone in general is a reflection of its competence, revealing a more even distribution between smaller failures, most likely caused by the abrasive effects of marine erosion, and the larger, more coherent losses along joint planes.

The magnitude-frequency relationship for sandstone layers was very similar to that of the mudstone for the smallest changes although the two curves diverge with increasing magnitude; the sandstone contained comparatively more change below 0.01 m^3. The sandstone layers contained the most limited range of failures of all the rock types monitored, reflected in the steep gradient of the curve and the lowest standard deviation. The consistency of the sandstone losses reflects the characteristics of the rock layers, typically involving protruding ledges with cross-cutting joints which resulted in the loss of regular shaped bocks.

The distribution of the siltstone losses were closely associated with the sandstone, both of which were confined to the upper section of the cliff, although the weaker siltstone recorded significantly smaller changes. The high mean and standard deviation were distorted by the maximum change recorded in the siltstone, which is misleading because it involved the whole rock face, although its centre point fell within a siltstone layer. In reality the finer scale at which changes occurred from the siltstone is reflective of the stable joint configurations and thin nature of the bands.

The shale layers initially showed a very similar relationship to that of mudstone, although they diverge as magnitudes increase, with relatively fewer large magnitude losses recorded from the shale. This pattern suggests the shale layers are dominated by small scale change, further supported by the minimum sized change recorded in the shale, which was the smallest of all the rock types. The dominance of smaller losses may be due to subaerial weathering or abrasion where the bands are located within the zone of marine influence. The close association with small scale patterns recorded from the mudstone, almost entirely within the zone of marine influence, shows that despite being more competent, the position of the mudstone within a higher energy environment may cause it to respond more like a weaker material such as the shale.

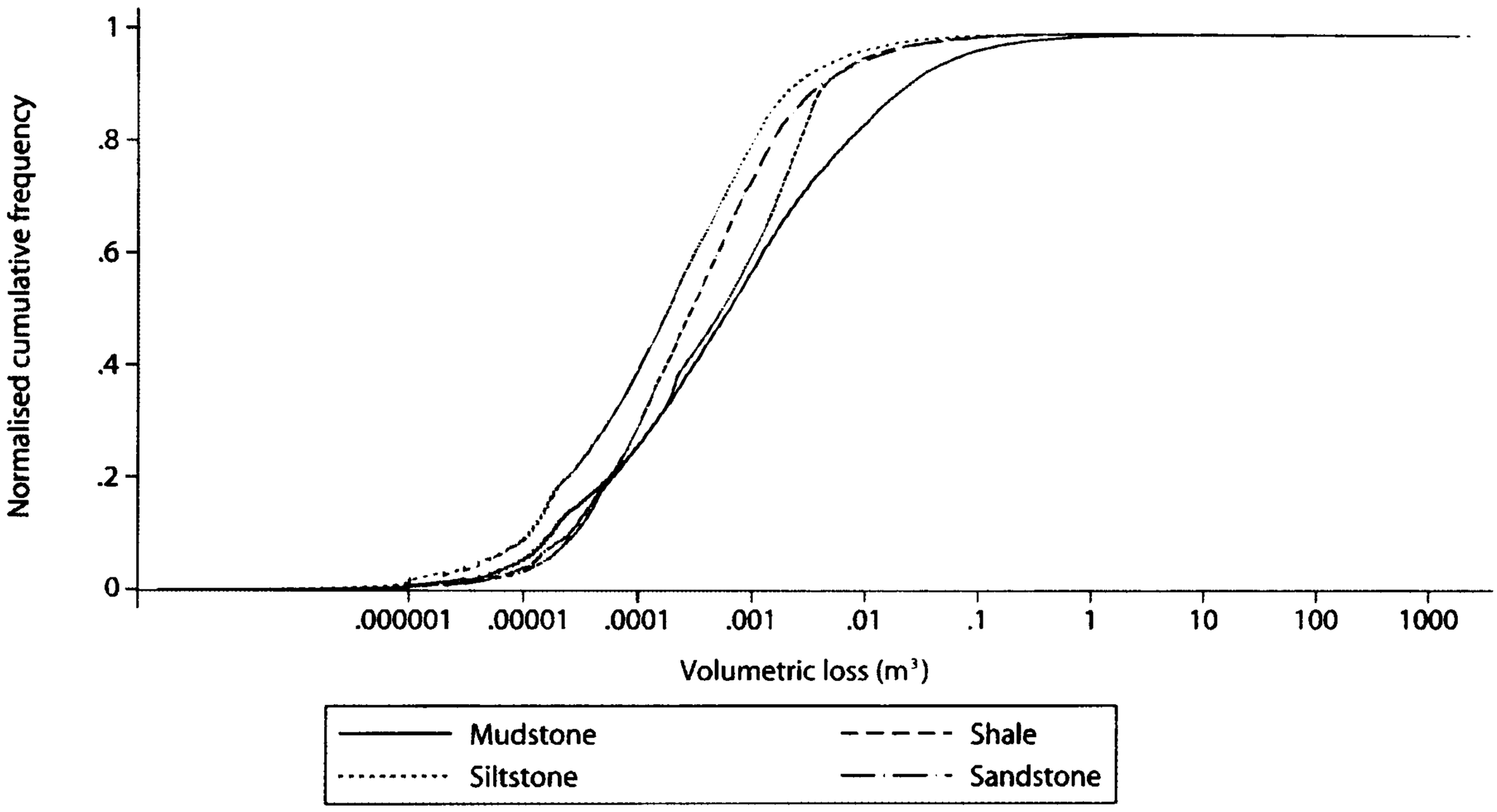

Figure 6.5: Magnitude-cumulative frequency relationships subdivided by rock type. All rock types displayed similar distributions although shale and siltstone had greater numbers of the smallest scale changes.

Table 6.2: Statistical summary of rockfall patterns by material.

	Number of rockfalls	Mean (m³)	Standard Deviation	Minimum (m³)	Maximum (m³)
Mudstone	18306	0.226246	16.12681	0.000000008	1776.600
Shale	74660	0.018375	1.86185	0.000000006	355.548
Siltstone	11222	0.239023	24.68489	0.000000014	2614.880
Sandstone	10317	0.005334	0.0806199	0.000000016	6.515

6.2.3 Temporal controls

The dataset allows the analysis of the occurrence of rockfalls through time. Magnitude-cumulative frequency graphs have been generated for each month of 2004 (Figure 6.6). The actual frequencies were used instead of normalising the data in order to

assess the changes in the total amount of activity within each month as well as the monthly patterns of difference. Throughout the year significant variation was recorded between the numbers of rockfalls per month, although the general pattern of the magnitude-cumulative frequency relationship was similar for most of 2004. The position of the graphs demonstrate that for all months except July the distribution of volumes were generally concentrated within the 0.0001 m^3 to 0.1 m^3, Class 1 range. Furthermore the gradients of the curves show consistent ranges of magnitudes were recorded, with the exception of July. The rockfalls recorded during July were dominated by events smaller than 0.0001m^3, and was the only month to record a step in the magnitude-cumulative frequency relationship. It has already been noted above that such steps, particularly involving very small changes such as in this case where a large number of failures of 0.00025 m^3 is suggested, may be associated with thresholding error around large change. A failure of over 40 m^3 was recorded at Site 3 in July 2004, significantly greater than in any of the changes during the other summer months (Table 6.3), which may have been the source of the error. Even ignoring the stepped values, July recorded notably smaller changes but in comparable numbers to other months. Whether the smaller changes are reflective of higher temperatures causing the rock to dry out and release flakes of material or some other process requires further investigation.

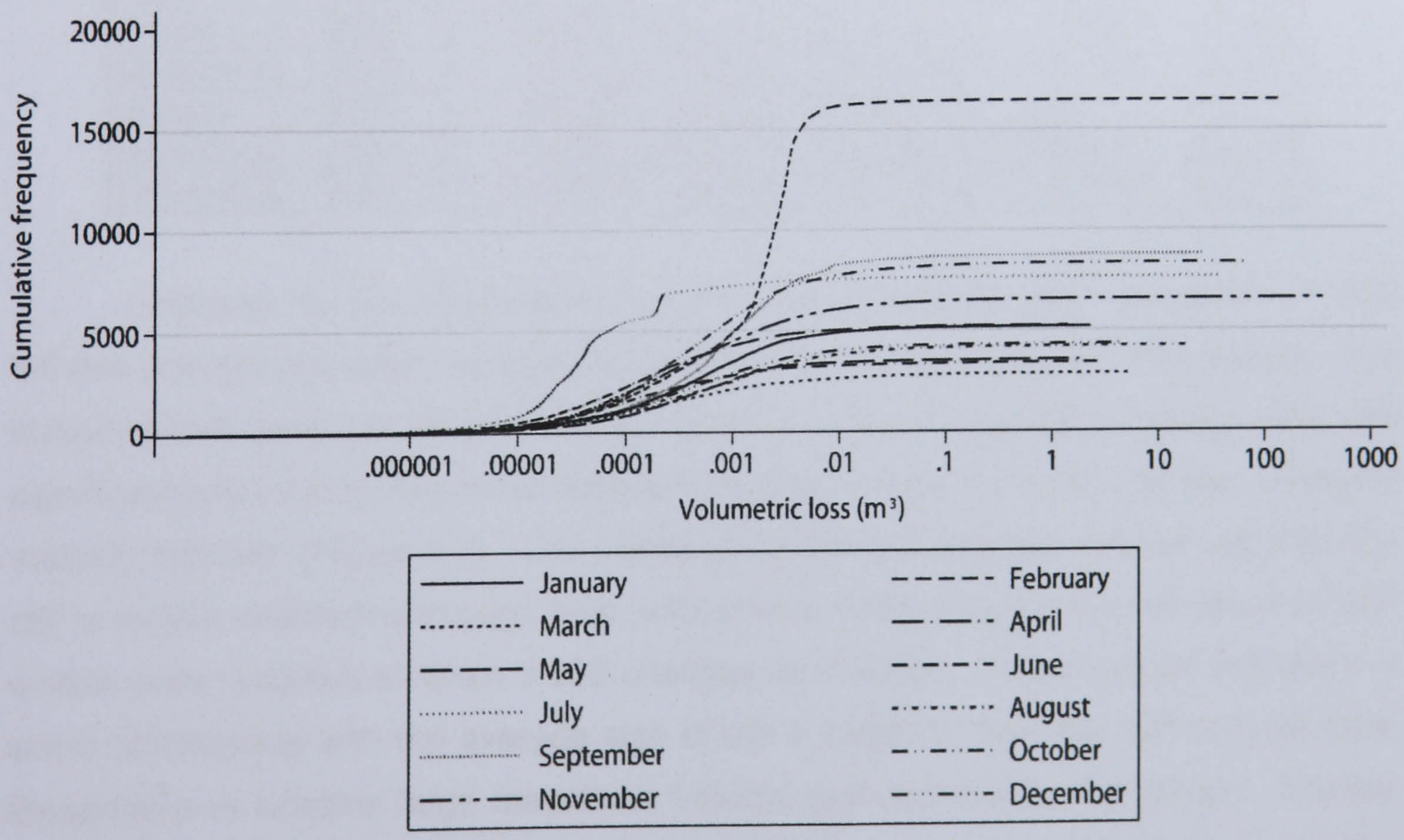

Figure 6.6: Magnitude-cumulative frequency distributions by month for the year 2004. The patterns indicate that dominant controlling mechanisms for various sizes of failure may differ over a monthly timescale. The temporal aspects to the cliff behaviour evidently require further consideration.

February 2004 recorded the highest number of rockfalls, over three times the amount recorded during less active months. Much of the lowest magnitude changes were indecipherable from the patterns in other winter months such as October, but the February pattern is made distinct by large amounts of change between 0.002 m^3 to 0.005 m^3. This significant increase in larger changes may indicate the effects of higher energy conditions. It can also be seen that the heightened activity in February was not confined to Class 1 changes, with a maximum recorded loss of over 130 m^3. Cliff response to environmental processes such as the characteristically stormy conditions during January and February or peak temperatures during summer months will be investigated later in the chapter (Section 6.5).

Table 6.3 Statistical summary of rockfall patterns over time during 2004.

	Number of rockfalls	Mean (m^3)	Standard Deviation	Minimum (m^3)	Maximum (m^3)	Total volume lost (m^3)
January	5162	0.005	0.046948	0.000000127	2.279	25.008
February	16472	0.012	1.068171	0.000000035	136.843	202.358
March	2819	0.010	0.130634	0.000000228	5.476	29.430
April	5205	0.003	0.024901	0.000000011	1.403	13.638
May	3512	0.006	0.063107	0.000000020	1.802	22.107
June	3363	0.006	0.066556	0.000000045	2.660	18.743
July	7635	0.006	0.355107	0.000000006	40.571	85.773
August	4180	0.019	0.361688	0.000000043	18.937	77.491
Septembe	8736	0.010	0.287361	0.000000087	25.886	87.431
October	8321	0.018	0.731585	0.000000008	65.879	146.116
November	6534	0.085	4.594079	0.000000018	355.548	554.101
December	4288	0.007	0.087294	0.000000016	4.716	31.006

Changes to the relationship between the magnitude and frequency of rock failures through time hold important implications for the way in which cliffs evolve. The statistical indicators can be graphed to further analyse cliff response through time. No significant relationship was found between the mean rockfall volume and the number of monthly rockfalls (Figure 6.7). The values show that the average volume lost from the cliff is largely unaffected through time, with similar mean magnitudes lost when 16 000 events were recorded to when 3 000 changes were noted. This suggests that there is some consistency with the average size of event released from the cliff through time, irrespective of whether large magnitude failures occurred during that month. Another important consideration concerns the suggestion from the magnitude-cumulative frequency curves that the spread of the data may be related to the volumes lost from the cliff face. A strong positive relationship was found between the monthly volumetric losses and the standard deviation of the distribution (Figure 6.8). The direct tendency

for a greater proportion of the data to be more closely clustered about the mean with smaller losses of material highlights the complexity of cliff responses, becoming more variable with greater periods of activity. The two graphs may also be linked, with the relative constancy of the mean weakening the normal distribution of the data as larger failures are included in the monthly totals.

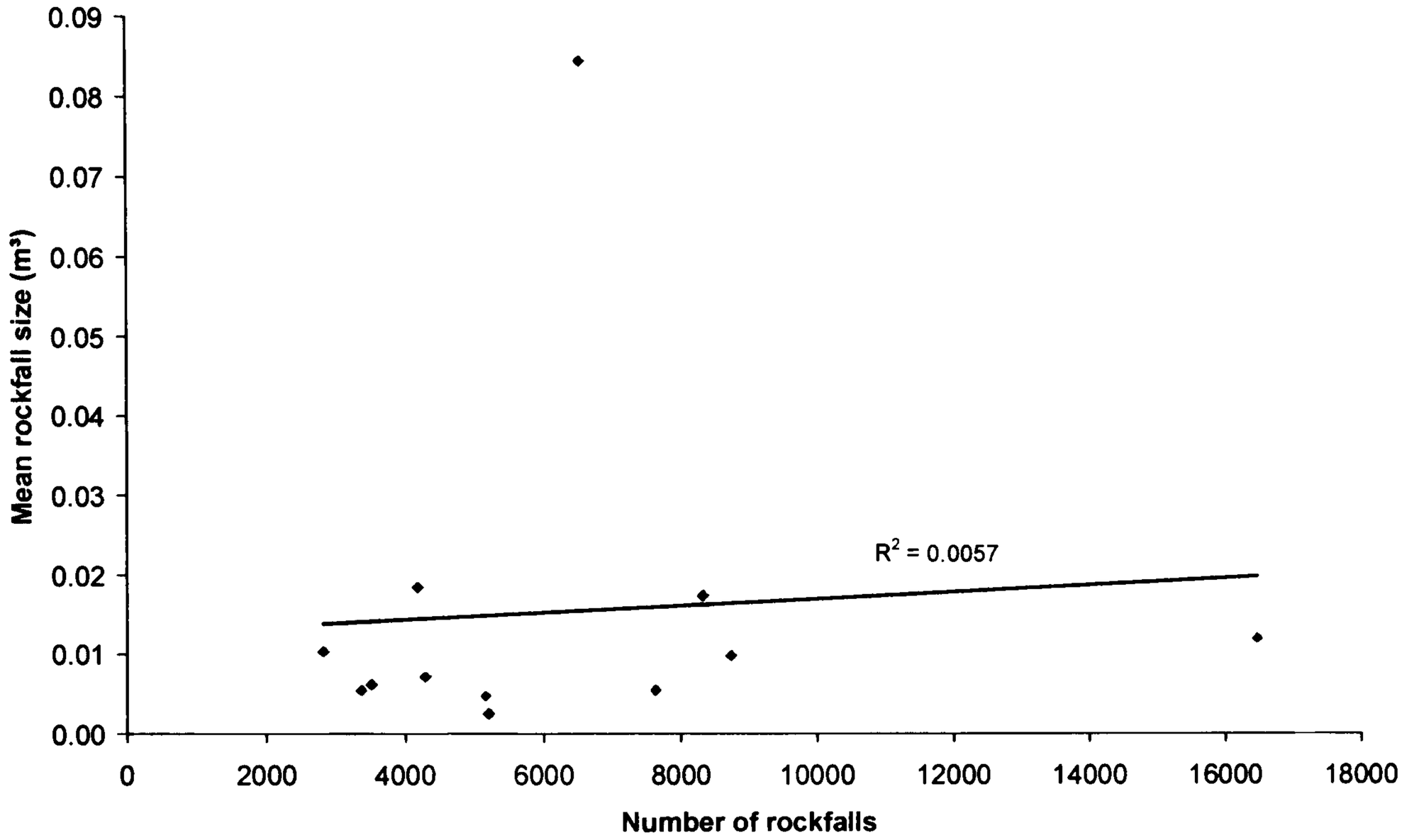

Figure 6.7: Mean monthly volumetric losses against the total number of rockfalls during 2004. The flat relationship illustrates that mean block size varied little through time in contrast with the frequency of events.

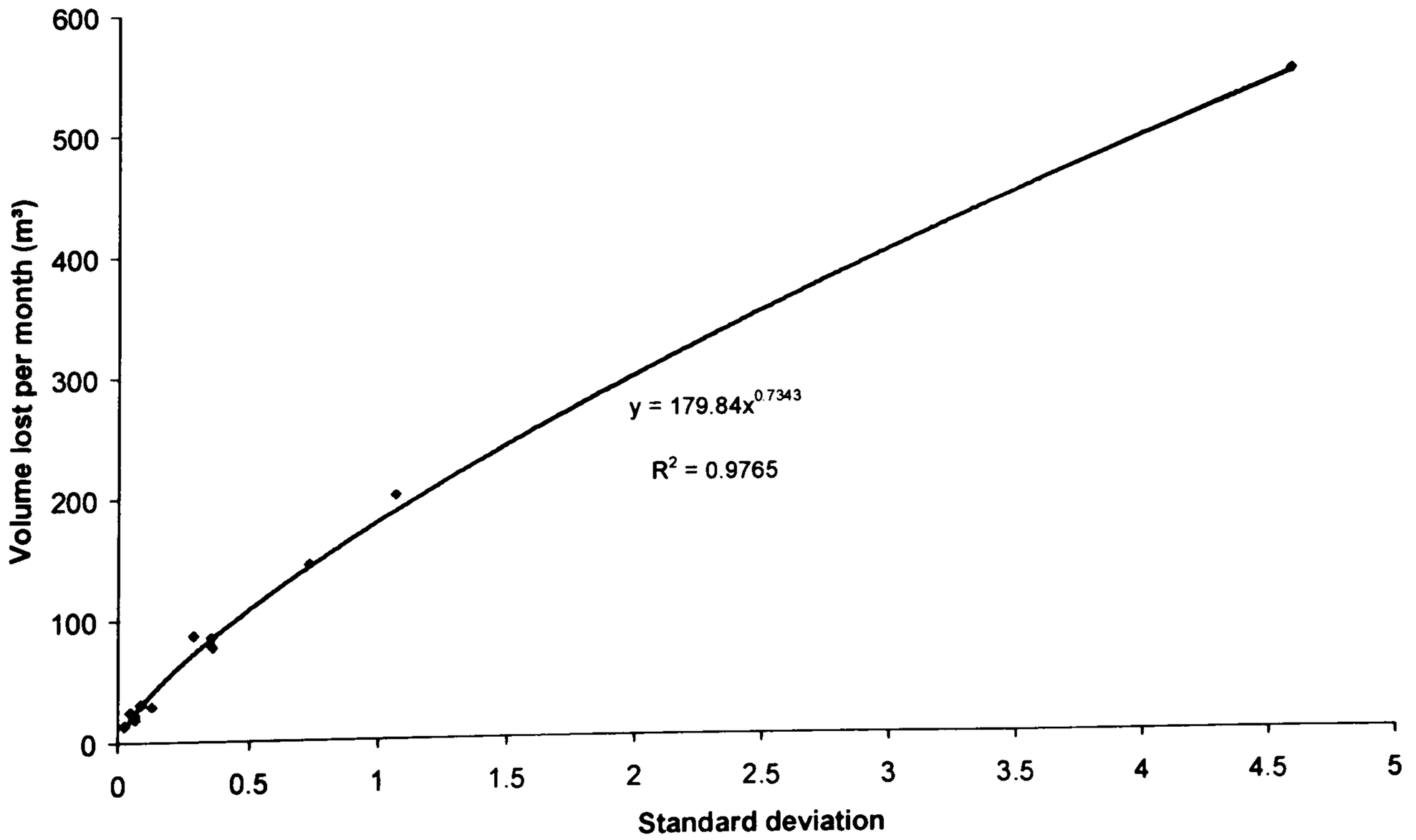

Figure 6.8: Total volumes lost against the standard deviation of the data for each month of 2004. A power law was fitted to the data to reveal a strong positive relationship between the amount of change and the spread of the values about the mean.

The ability to quantify volumetric changes across sheer-sided cliff faces has enabled the relative influence of losses of different scales to be directly compared. A key question in rock slope geomorphology has been the interplay of frequent small scale change and infrequent but large magnitude failures, and the physical contribution they make in determining slope form. The actual volumetric contributions of different magnitude failures on the total change monitored at each site have been analysed (Figure 6.9). The large failures at Site 3 dominate the changes that have occurred across all sites during the monitoring period, accounting for a total of over 6000 m^3 of material, although much of the change involved the reworking of fallen debris. The well-jointed embayment also shows the highest amounts of changes of all the magnitude classes. This suggests the rock mass is genuinely more active at this locality rather than succumbing to a single large event.

To investigate further the relative contribution of different magnitude losses to the change at each site the total volumetric differences were converted to percentages (Figure 6.10). The total change at Site 3, as might be expected, was dominated by Class 5 scale losses although the seemingly insignificant contributions of changes of all other scales were the higher than those recorded at any other site (refer back to Figure 5.8). It is evident that where losses over 100 m^3 do occur within a rock slope they constitute a disproportionately high percentage of the overall change, accounting for over half of the total changes whenever they occur. The same can be said although to a lesser degree of Class 4 scale events, between 10 m^3 and 100 m^3, which still exert a significant influence on total change. Perhaps most interesting however is the impact of smaller scale failures which, despite containing only changes between 0 and 10 m^3 and therefore falling within a range at least nine times smaller than the larger classes, still account for considerable proportions of material lost from the cliff. At Site 1, the subsided headland, where no medium or large losses were recorded, the change was entirely composed of these failures. This suggests that for certain localities studies which concentrate purely on the larger, more visible events may ignore important processes controlling the short- to medium-term development of the landform. The smaller class divisions are each separated by an order of magnitude although the balance between them at Site 1 is relatively even. In general the percentage contribution of Class 1 changes from the monitored sites is greater than either Class 2 or Class 3 losses, implying that the overall magnitude-frequency relationship causes a concentration of influence towards failures of particularly large or particularly small magnitude. The contribution of events of different magnitudes to shaping cliff form can therefore be represented schematically (Figure 6.11).

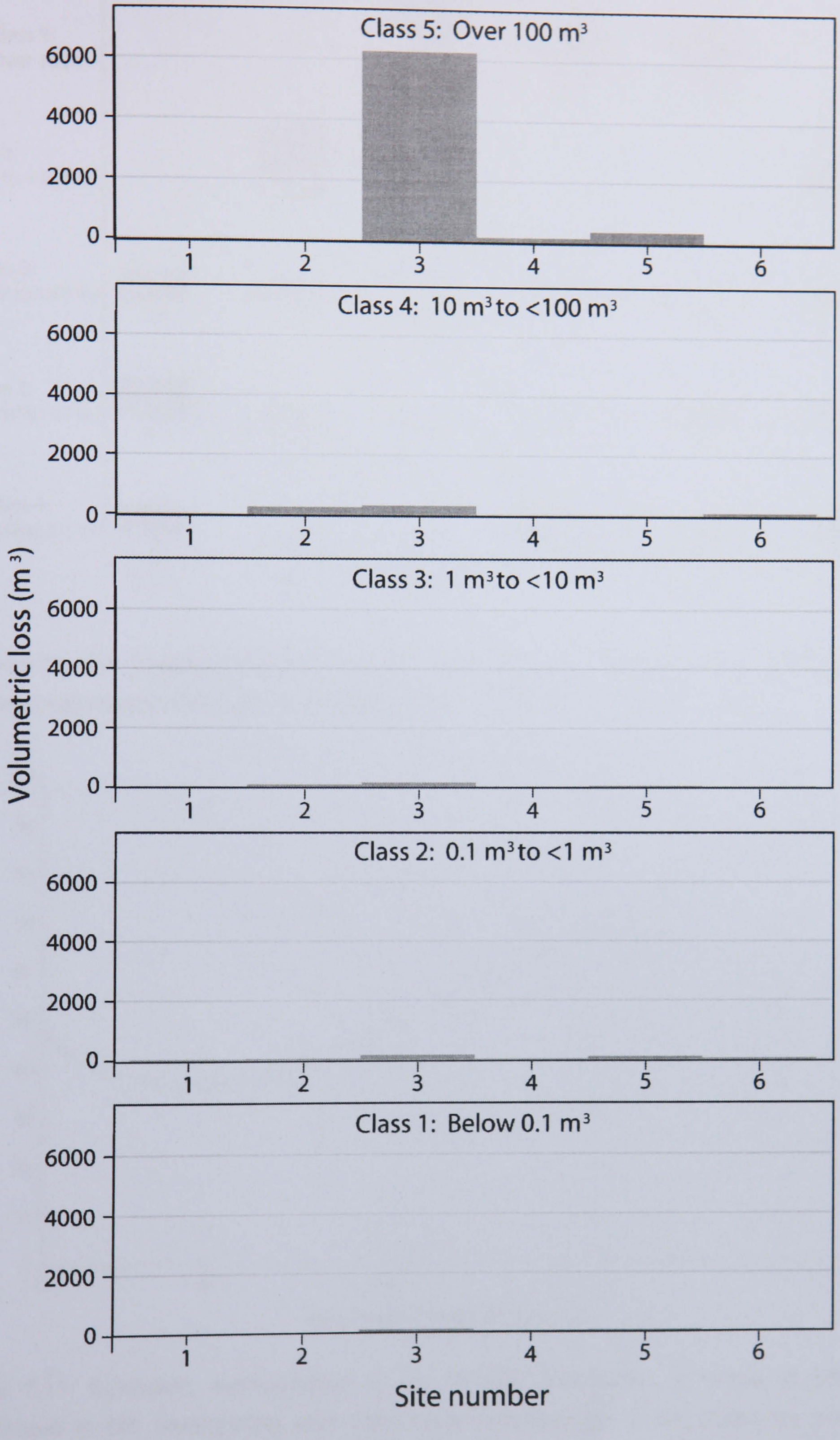

Figure 6.9: The total volumetric contribution of different magnitude classes by site for the whole monitoring period. The magnitude divisions are purely descriptive but there appears to be a clear bias of material losses towards larger failures.

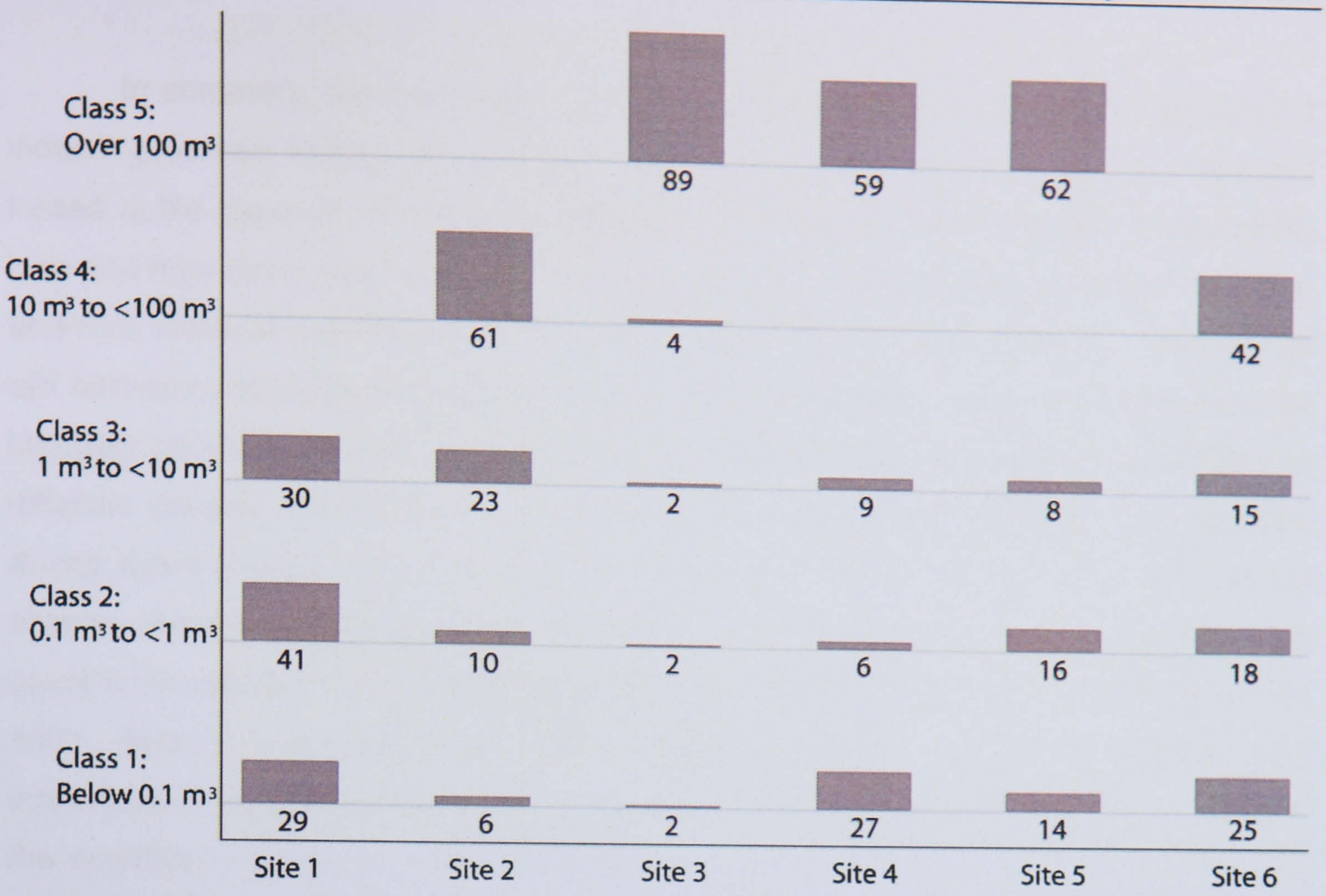

Figure 6.10: The proportion of total volumetric change for each site accounted for by failures of different magnitudes during the monitoring period.

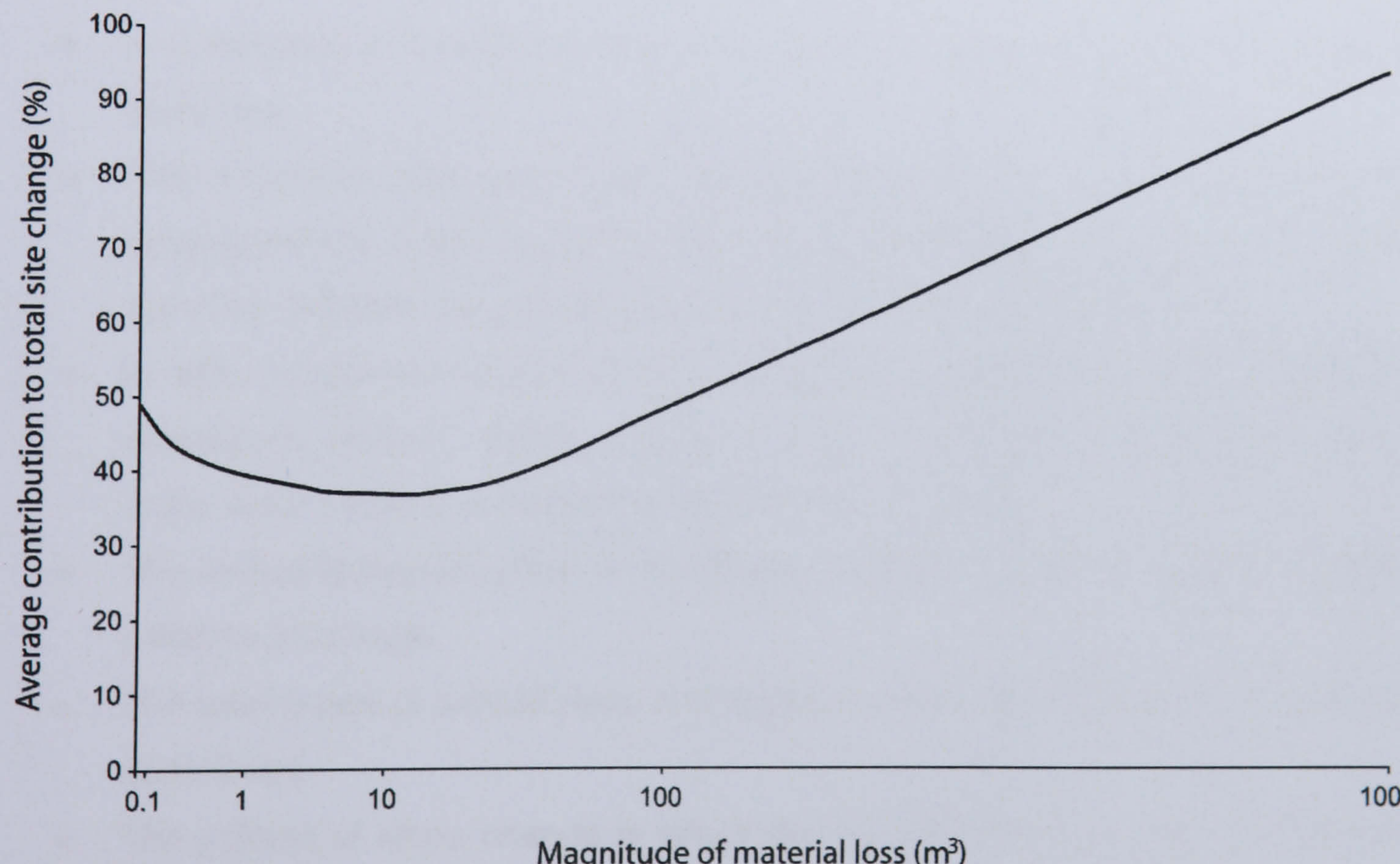

Figure 6.11: Schematic representation of the average contribution of losses of different magnitudes to cliff development when they occur. For example 10 m³ losses on average constitute 37% of the monthly volume lost from a site when they occur. The overall magnitude-frequency relationship is such that the total change is weighted more towards large, and to a lesser extent very small scale losses than intermediate changes, although the curve position suggests the significance of all magnitudes of failure.

In summary, the results above have provided evidence that rock slope form is indeed governed largely by both rare, high magnitude and very small but frequent losses at the expense of more intermediate scale change. The patterns of volumetric loss and frequency were seen to be sensitive to both spatial aspects such as location and rock material and temporal elements such as monthly environments. The bias of cliff behaviour towards changes driven by extremes of scale raises questions over the interplay between different magnitude losses. Although the analysis was subdivided by different classes of magnitude, a continuum of changes was recorded from all sites during every month. The ability to record the finer end of the spectrum of landform change therefore casts doubt on the validity of such arbitrary divisions, which have become embedded in many rock slope analyses (Phillips, 1988; Selby, 1980; Schumm, 1991; Blöschl and Sivapalan, 1995; Palmström, 1995). In reality process-form interrelations may be fundamentally misrepresented by imposed boundaries. Many of the questions raised over the influence of spatial processes, *in situ* conditions and external controls on the patterns of rock slope change over time therefore require further investigation. Insights into the nature of cliff behaviour provided by the analysis of magnitude-frequency relationships can be summarised as follows:

- A continuum of volumetric slope changes can be detected with the monitoring technique.
- The monitored cliffs were most significantly influenced by low frequency, high magnitude and high frequency, low magnitude losses although a continuous transition between magnitude and frequency was seen overall.
- In cliffs considered to be moderately stable, such as those at Staithes (Mouchel Associates Limited, 1996), events of over 100 m^3 were statistically likely to occur over a year in a monitored area of over 20 000 m^2.
- The limited temporal extent of the dataset restricted the ability to estimate future patterns of change.
- The usefulness of annual rates of change predicted for cliffline retreat has been questioned.
- The pattern of slope change is influenced by both the type and the location of the constituent rock.
- Whilst exposure to and protection from marine processes may determine the overall magnitude of losses, the relationship between magnitude and frequency often remained unaffected.

- The significance of the smallest rockfall magnitudes suggests that for certain localities studies which concentrate purely on the larger, more visible events may ignore important processes-form relations.
- The specific nature of magnitude-frequency relationships is spatially and temporally complex.

6.3 Scale dependency

The establishment of complex magnitude-frequency relations governing change in the monitored coastal cliffs raises many questions over landform development. One of the most important aspects to the patterns of geomorphological change has been whether they are scale dependent or scale independent. A key question in the consideration of scale in coastal cliffs is as follows:

Are the patterns of change within coastal rock cliffs scale dependent?

Scale variability in geomorphology must consider both the scale of the process-form relations and the scale of the investigation. A major concern in rock slope analyses has therefore been whether the scale of the investigation influences the particular processes recorded. In order to assess the extent the scale at which monitoring is conducted influences the patterns and processes recorded, a series of windows were used to subset the data. At each site a 900 m^2 area (30 m X 30 m) was randomly located on the cliff face, although care was taken to ensure that as much of the window was located on the actual rock face as possible. The 900 m^2 area was deemed to be the largest area that would not cause significant data loss at the sites with lower cliff heights. The 900 m^2 areas were then reduced to 400 m^2 (20 m X 20 m), 100 m^2 (10 m X 10 m) and 25 m^2 (5 m X 5 m) areas to create a series of scaled windows within which only the change entirely encompassed by the window was considered. The subset windows were initially concentrically ordered, focussing on the centre of the 900 m^2 window before two additional datasets were collected, situated within the bottom left and top right corners of the largest window at each site (Figure 6.12). The size of the 900 m^2 window relative to the entire cliff face was such that the base of the subset area invariably comprised the basal layers of the cliff. It should be noted that the largest window exceeded the height of the cliff at Site 5 causing small areas of no data at its top left and bottom right extremities.

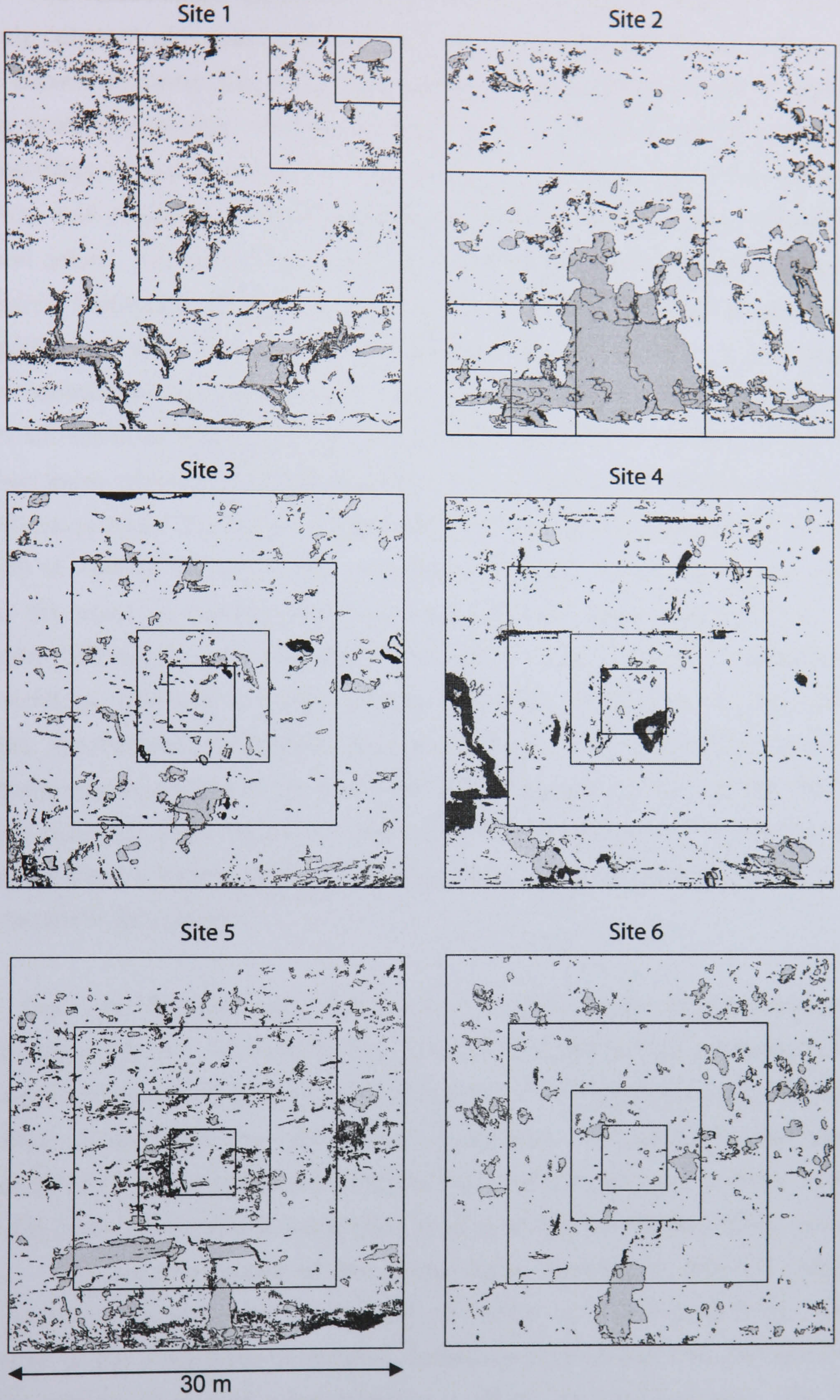

Figure 6.12: Monitoring windows used for the investigation of the effects of scale on the patterns of rockfall recorded. Note: Sites 1 and 2 show examples of the datasets positioned at the top right and bottom left respectively; all other sites show the concentrically ordered windows.

To compare the patterns detected within the scaled windows, magnitude-cumulative frequency graphs were constructed from each of the three datasets (Figure

6.13). The relationships agree with the patterns previously identified and appear relatively constant with scale with the vast majority of change detected within 0.01 m^3 for all curves, implying that the overall magnitude-cumulative frequency relationship may be scale independent. The curves were separated from the patterns, distributions and quantities of losses noted from the landform as a whole by subtle variations in curvature and placement, which indicate that different controls may influence more localised areas. The 900 m^2 windows were inseparable from the general magnitude-cumulative frequency relationship for the whole dataset. Many of the windows, averaged for all sites, showed close association with the patterns. For example the 400 m^2 central and top right windows, and those from the 100 m^2 top right and 25 m^2 bottom left areas all showed marginally greater proportions of change up to 0.005 m^3 and then lower amounts of larger change than recorded in the landforms as a whole. This inflection about the dataset wide pattern of change was reversed in the 400 m^2 and 100 m^2 bottom left monitoring subsections perhaps demonstrating that variability due to the scale of analysis increases with changes away from 0.005 m^3. More significant differences were recorded in the 100 m^2 central and 25 m^2 central and top right windows which all showed steeper gradients reflecting a reduced range of changes, concentrated on smaller classes of failures. The tendency for areas in the middle and upper localities of the rock face to be influenced by less diverse and smaller changes than the lower sections emphasises the importance of monitoring a large enough area to be representative of the patterns of change governing the development of the landform as a whole.

The three datasets were averaged to compare scale effects irrespective of location (Figure 6.14). The monitoring windows revealed strong agreement between the magnitude-frequency patterns, with all but the 25 m^2 windows indecipherable from the pattern found within the total monitoring dataset. This suggests that the scale independency of the magnitude-frequency relationship may have a lower constraint where the scale of analysis is insufficient to encompass the representative patterns of change. The responsiveness of the relationships detected at different scales was finally examined by analysing the patterns of change by site (Figure 6.15). Although the shape of the magnitude-cumulative frequency relationship was site specific, the general patterns of change were reflected in all of the data subsets. The 900 m^2 monitoring areas, which often encompassed almost the entire rock slope, were found to be inseparable from the complete data sets. At every site, progressive reductions in the scale of analysis distorted the magnitude-cumulative frequency relationship towards distributions towards more concentrated and smaller volumetric losses. The curves derived from the 25 m^2 monitoring windows typically produced the most erratic

and outlying curves, reflecting the smaller size of the dataset and the reduced propensity to include larger losses. The variance altered from site to site, minimal at the most stable sites such as 1, 5 and 6 and peaking in the more active sites. It can thus be concluded that the existence of magnitude-frequency relationships is scale independent, at least above a 100 m^2 threshold, but the nature of the relationship is location dependent, varying substantially between sites.

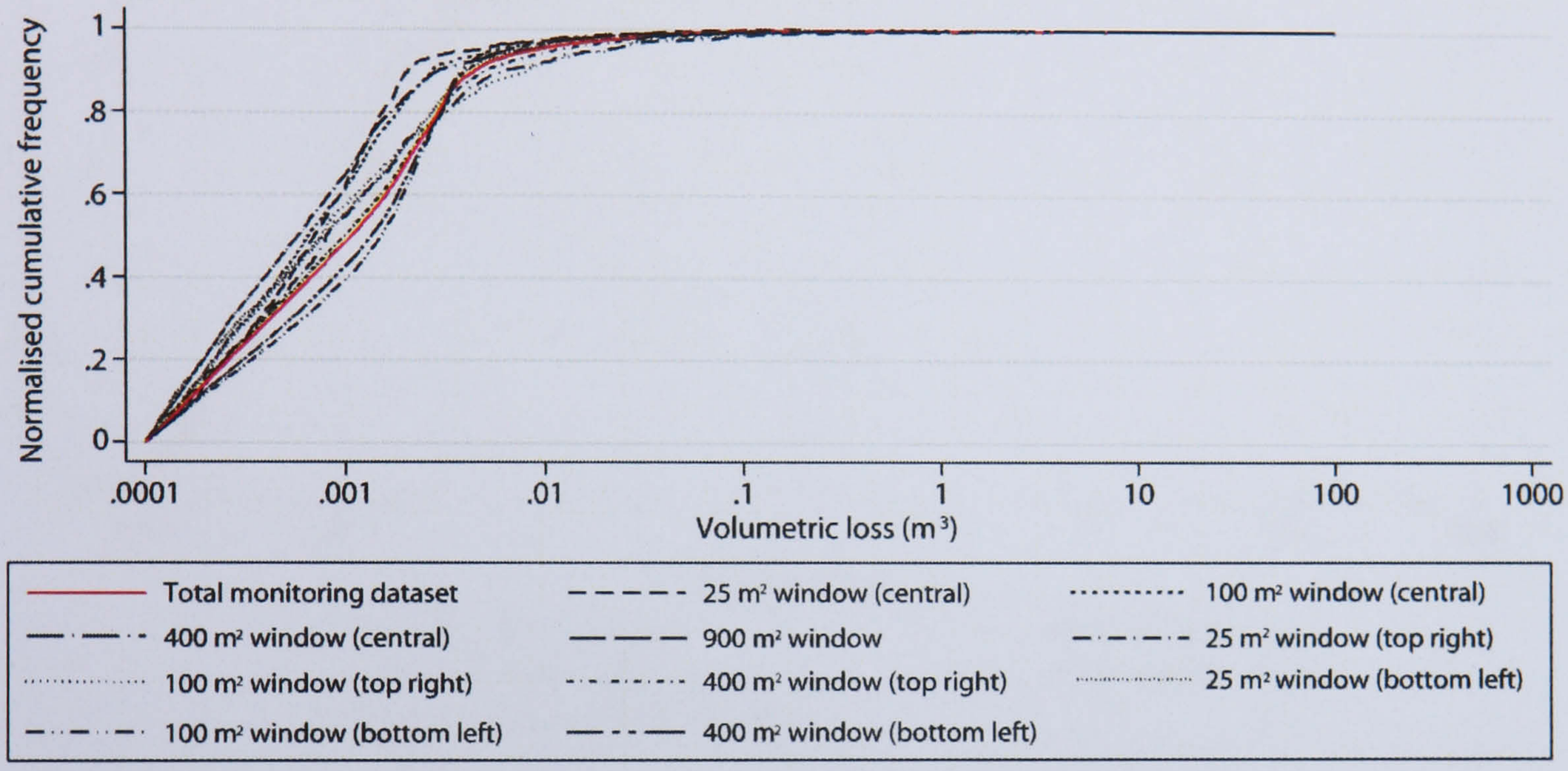

Figure 6.13: Magnitude-cumulative frequency graphs produced from each of the different subset monitoring windows for all three dataset locations, averaged across all sites. Note: Site 4 contained particularly high numbers of change below 0.0001 m^3 associated with the peripheral effects around a much larger change, which are viewed with caution. Therefore changes below 0.0001 m^3 (approximately 0.05 m X 0.05 m X 0.05 m) have been excluded from the analysis of scale effects on the patterns of change for ease of comparison.

Although the presence of magnitude-frequency relationships associated with rockfalls may be considered scale independent, scale influences on the distribution and range of losses from cliff faces raise questions as to the importance of scale on the relative quantities of material lost over time and the processes and mechanisms that drive change. To investigate the sensitivities of quantitative material losses to changes in scale the relative monthly changes per m^2 were plotted for every window in the three datasets and for the whole monitored area at each site. Site 1 revealed similar trends to those noted above with the 25 m^2 window behaving more erratically than the larger windows (Figure 6.16). When a significant change was registered within the smaller windows from the central and top right positions there was a tendency to generate disproportionately large values per m^2 causing an overestimation of the actual rate. This overestimation, relative to the other locations, was less evident in the 25 m^2

window positioned at the bottom left of the 900 m^2 area. One reason for this is the location of the window within the zone of marine influence and the insufficient size of the window to encompass the larger areas of change. As the windows increase in size the larger magnitude changes are incorporated, increasing with monitoring scale until the whole site is considered and the changes are reduced to a representative proportion of total change.

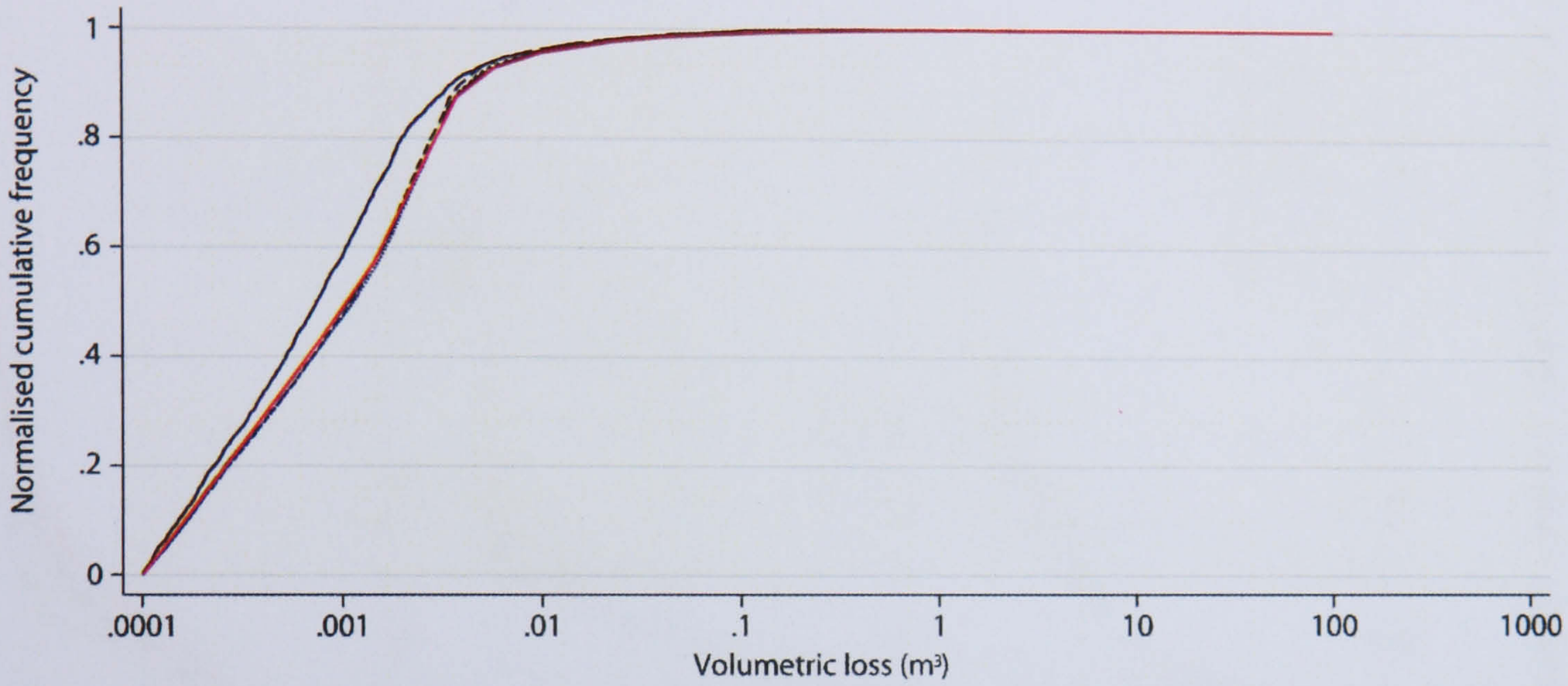

Figure 6.14: Scale effects on the patterns of magnitude-cumulative frequency relationships, irrespective of location. The similarities between the averaged curves suggests that the differences within the previous graph were caused by location rather than scale which, when averaged, produces very similar trends.

The subset monitoring areas at Site 2, the arched-failures embayment, revealed numerous fluctuations that were not evident when the entire cliff slope was considered. The 100 m^2, 400 m^2 and 900 m^2 areas in particular recorded graded patterns increasing or decreasing with scale (Figure 6.17). In December 2004 the 900 m^2 area over-predicted actual rates of recession per m^2, exaggerating a much smaller but significant increase in the rates of change for the site as a whole. The over-estimation in monthly rates was only evident in one other scaled window, the 400 m^2 located at the bottom left hand corner of the 900 m^2 area. Once again the location of the monitoring window within the marine influenced base of the cliff proved to be important. The fact that the 25 m^2 and 100 m^2 areas were not influenced by the change demonstrates the importance of scale in determining the ability to accurately quantify changes in the rock slope. The graded patterns between different scales, which often appear in all three datasets, also suggest that scale dependent processes insignificant to the overall response of the cliff may dominate localised subsections of the cliff face.

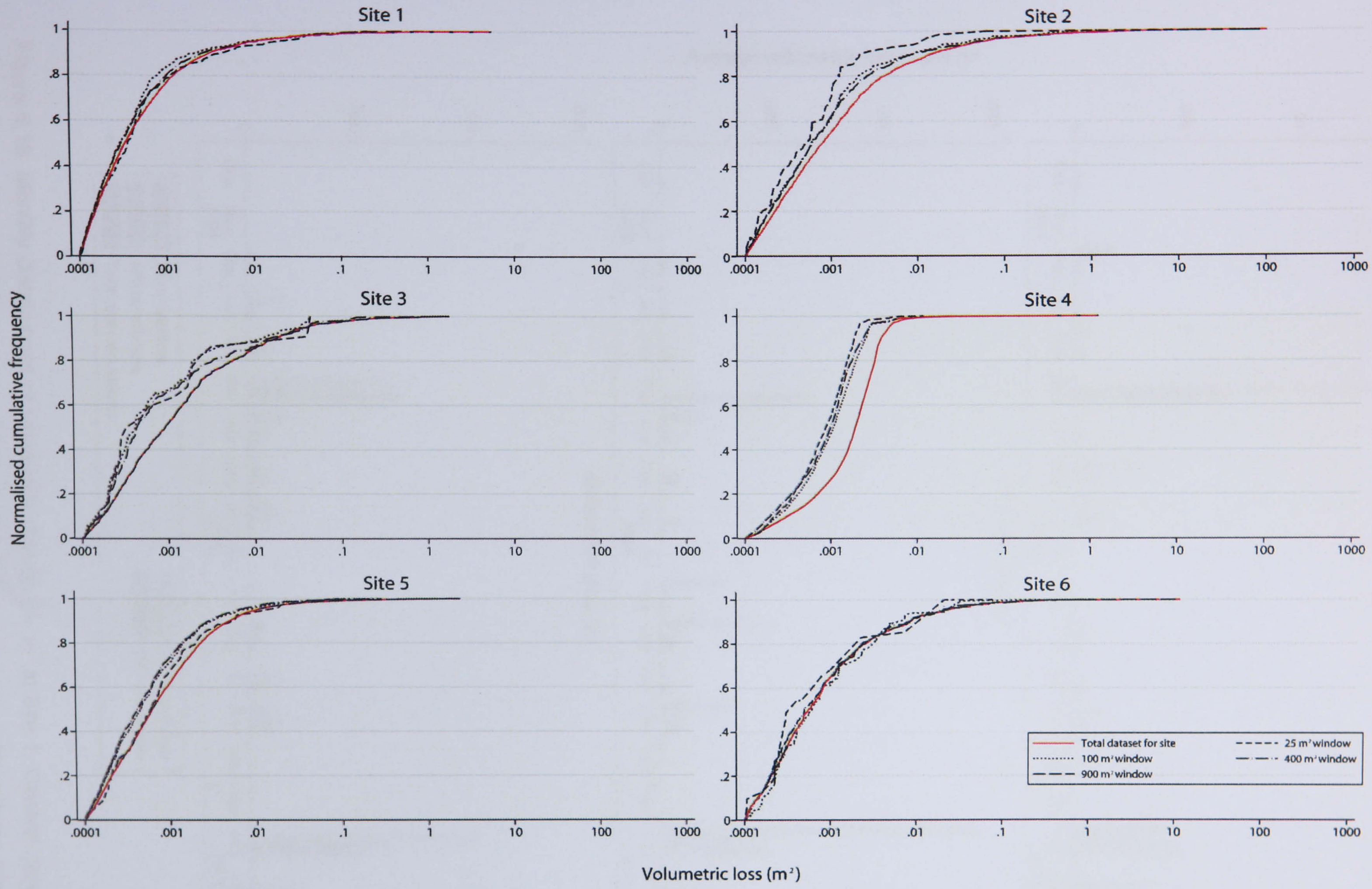

Figure 6.15: Normalised magnitude-cumulative frequency relationships by site. Differences in specific patterns detected by monitoring at different scales at each site reveal the precise nature of the patterns are location dependent.

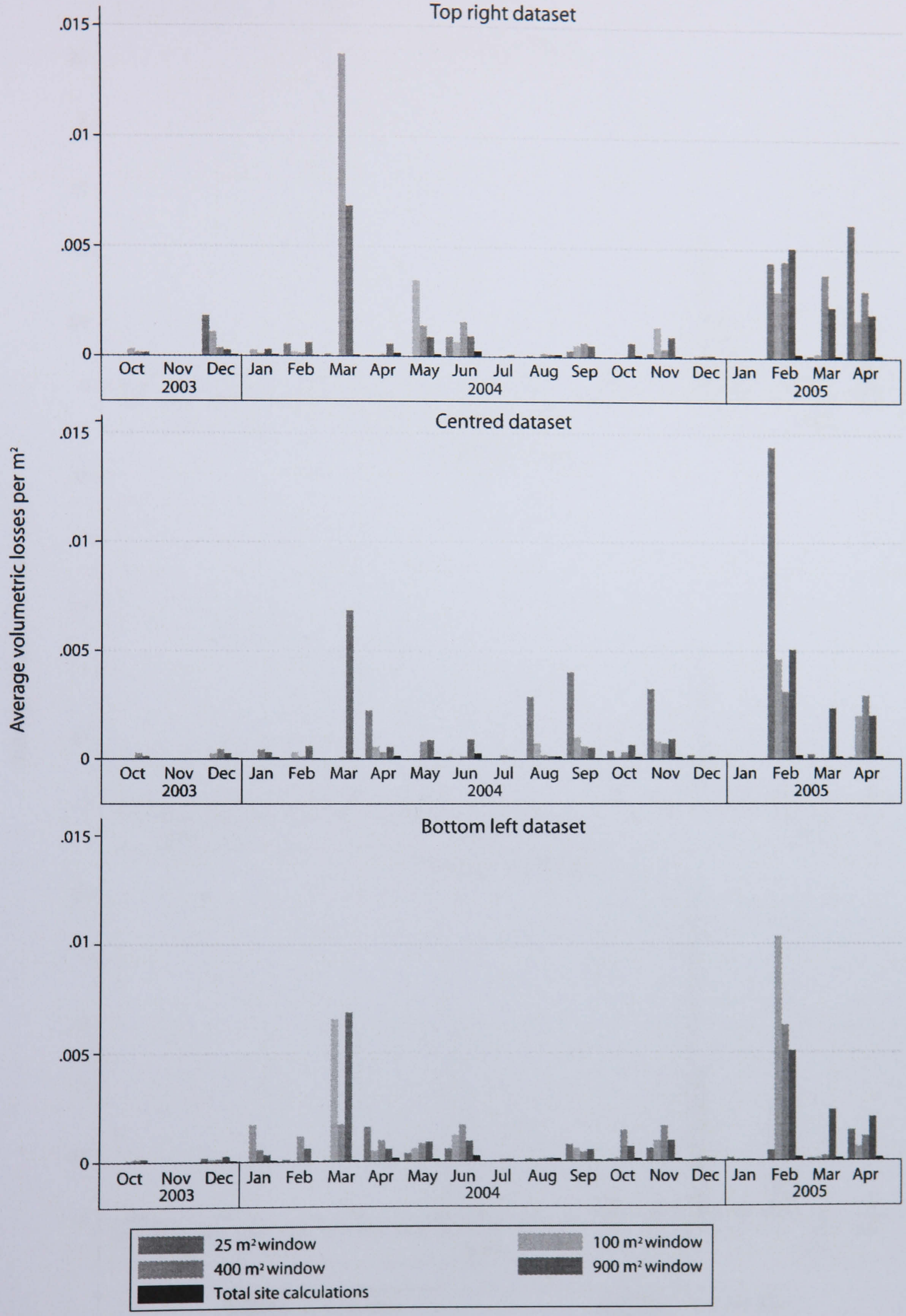

Figure 6.16: Monthly distributions of volumetric change per m^2 at Site 1. General consistency was seen between the patterns recorded from the different locations although the bottom left dataset demonstrated less variability between scales.

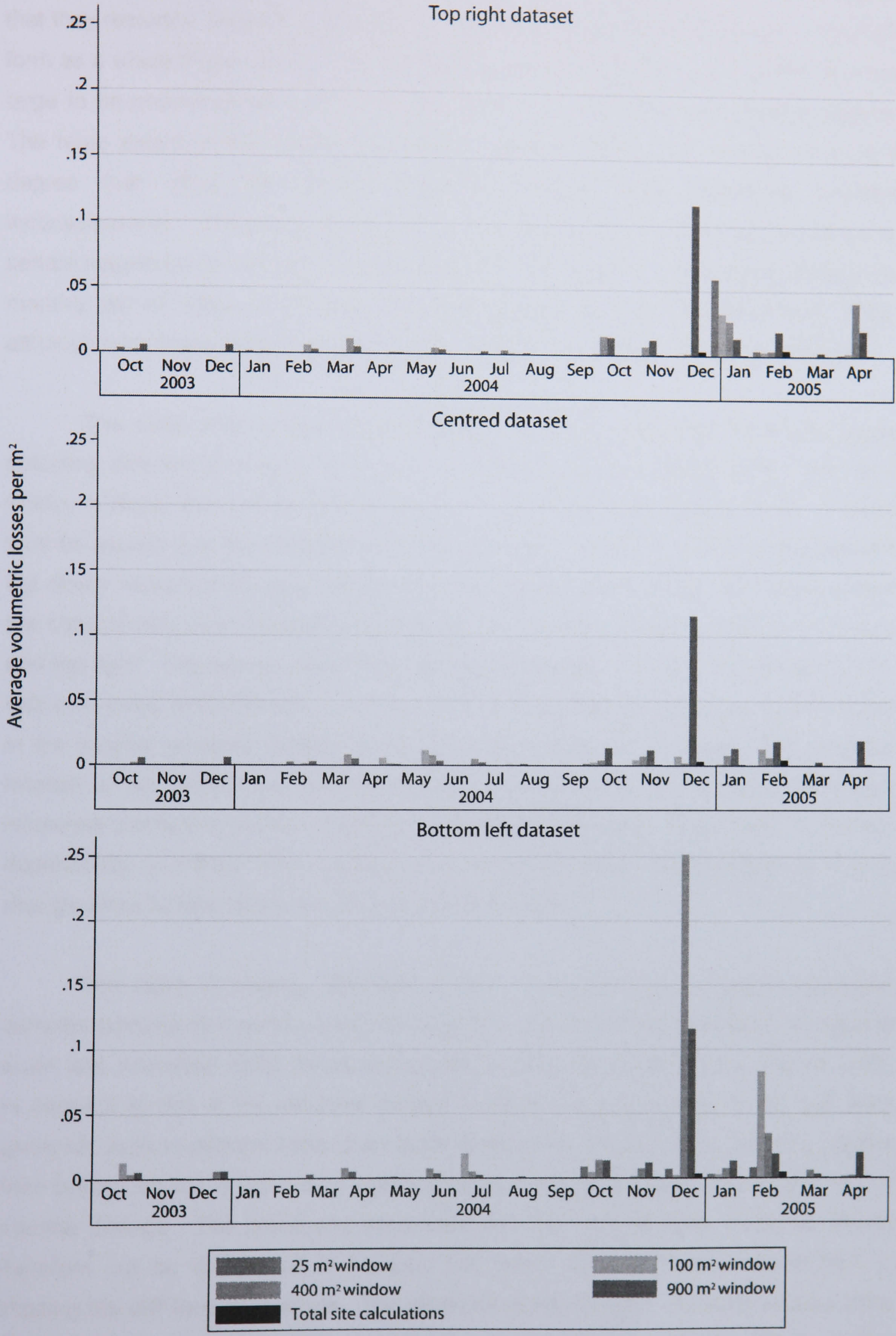

Figure 6.17: Monthly distributions of volumetric change per m^2 at Site 2. The scale considerations reveal patterns not evident when the landform is viewed as a whole.

The patterns of change at Site 3, the well-jointed embayment, were unusual in that they recorded areas of large-scale change that had a significant impact on the cliff form as a whole (Figure 6.18). The size of the changes that occurred in 2005 were too large to be encompassed by the windows and do not feature to any notable degree. The large extent of the failures governs the patterns of landform change to such a degree that other inter-relations between smaller scale processes become inconsequential. There appears to be a scale threshold in which events above a certain magnitude do not register within smaller scale windows. The largest changes in monthly per m^2 rates of material loss were found in October and November 2004, although even these were only consistently evident in the larger monitoring windows.

The scale effects were more consistent in Site 4 with most monitoring areas detecting differences during the months of greatest actual change to the site as a whole, in November and December 2003 and February 2004 (Figure 6.19). It could thus be argued that the changes within the seepage headland are scale independent but closer inspection reveals that the windows located at the bottom left of the subset are considerably more responsive to the key changes than those located at the centre and top right. The largest actual site change for example, recorded in February 2004, was only found within the 400 m^2 window of the central dataset, and poorly represented in the smaller windows located at the top right of the 900 m^2 area. The windows located at the bottom left towards the cliff base however all displayed significant increases during this month; including the smallest 25 m^2 area. Once again, a location dependency is implied with monitoring at all scales more representative of overall change when located within the area of greatest activity.

The rates of change detected at Site 5, the geology headland, displayed complex patterns with some months increasingly over-estimating change as monitoring scale was increased while others converged towards the actual values (Figure 6.20). In contrast to Site 4 the windows located towards the upper parts of the cliff were generally seen to perform better than those lower down the rock face, with the dataset from bottom left of the focus area significantly over-estimating all but the largest rate of monthly change. The processes associated with the zone of wave influence should therefore not be considered in isolation but rather viewed on their contribution to shaping the cliff face as a whole. The windows at the top right of the focus area were most representative of the actual rates of retreat for the whole site and invariably improved with scale.

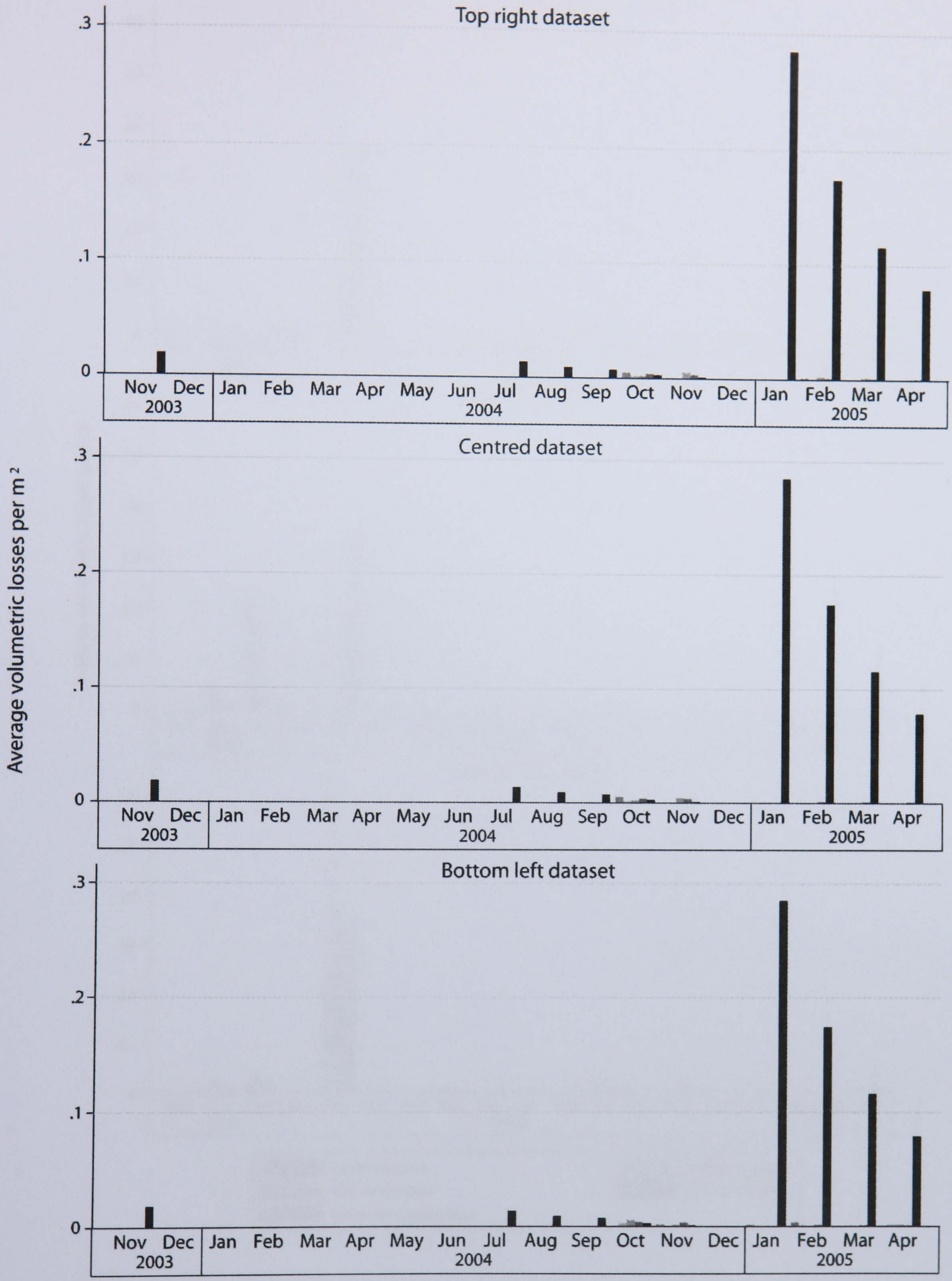

Figure 6.18: Monthly distributions of volumetric change per m^2 at Site 3. A particularly large failure generates actual rates of change in excess of those recorded from the subsets which were not large enough to encompass the area of change.

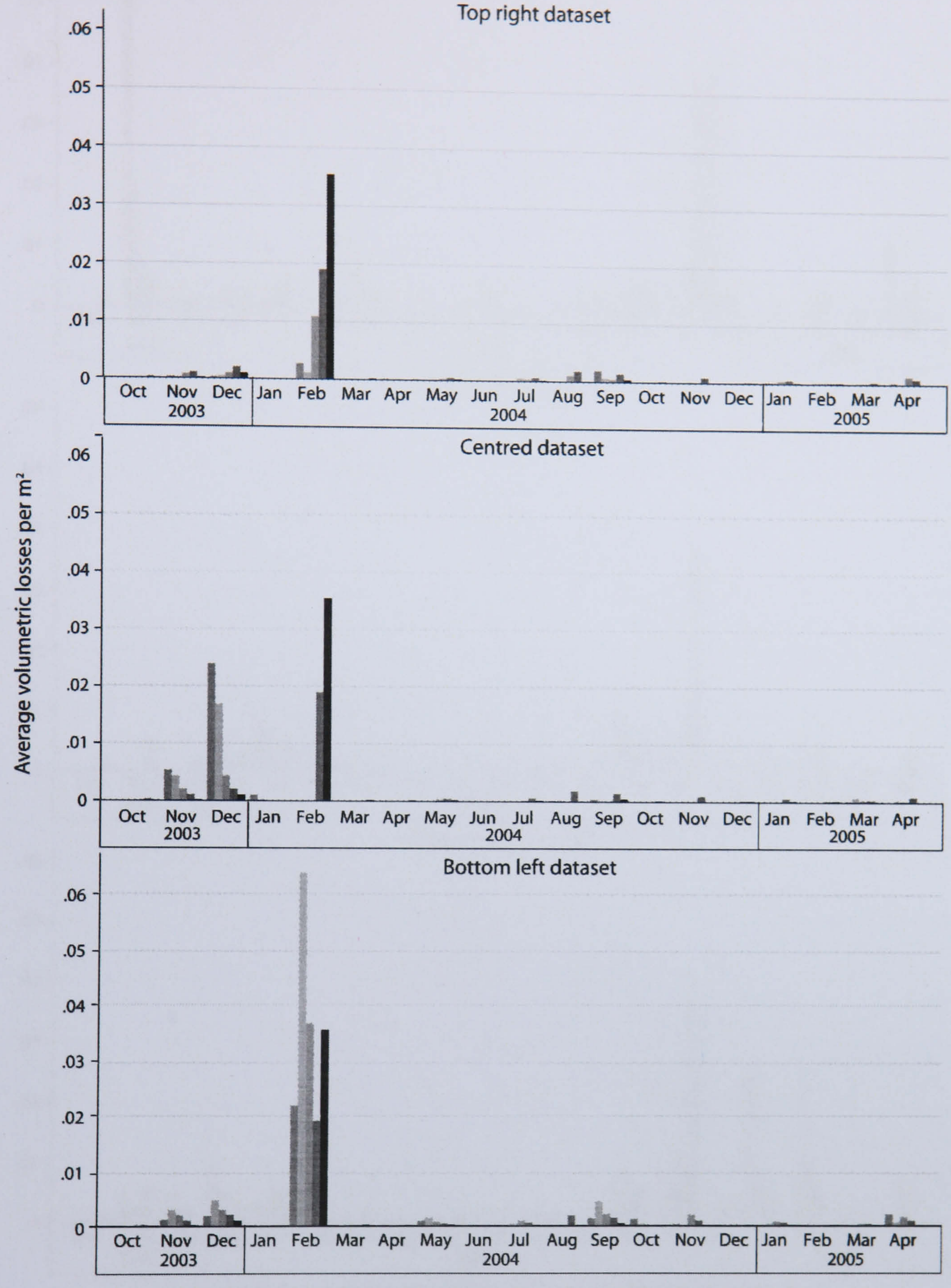

Figure 6.19: Monthly distributions of volumetric change per m^2 at Site 4. The scale windows located towards the base of the cliff were more responsive to the changes experienced by the rock slope as a whole.

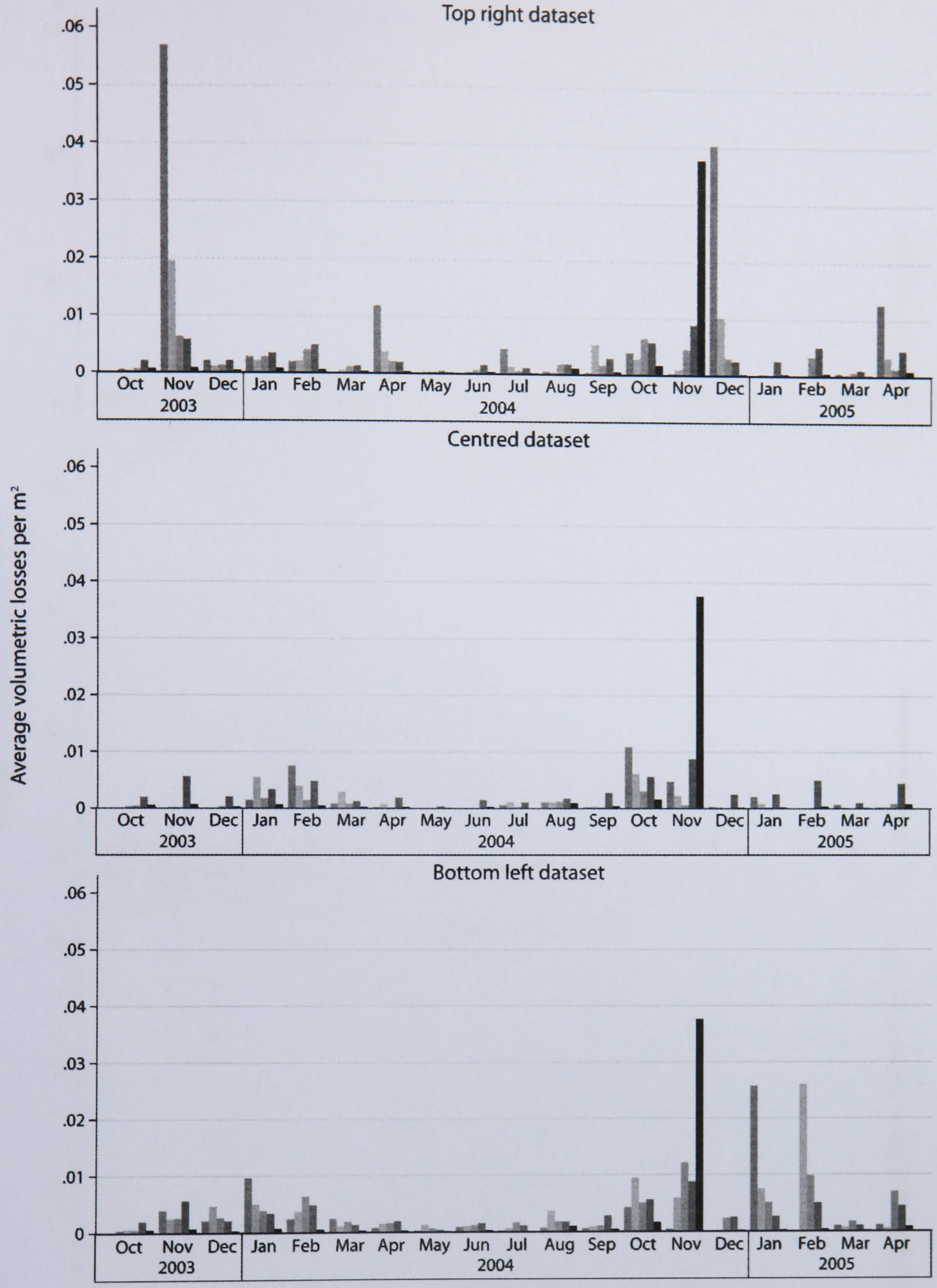

Figure 6.20: Monthly distributions of volumetric change per m^2 at Site 5. Marked scale effects were noted, particularly in the dataset from the top right, with greater accuracies associated with increased scale of the analysis.

The monthly rates at Site 6 recorded from the subset windows within all three datasets provided more accurate representations of material losses than at any other site (Figure 6.21).

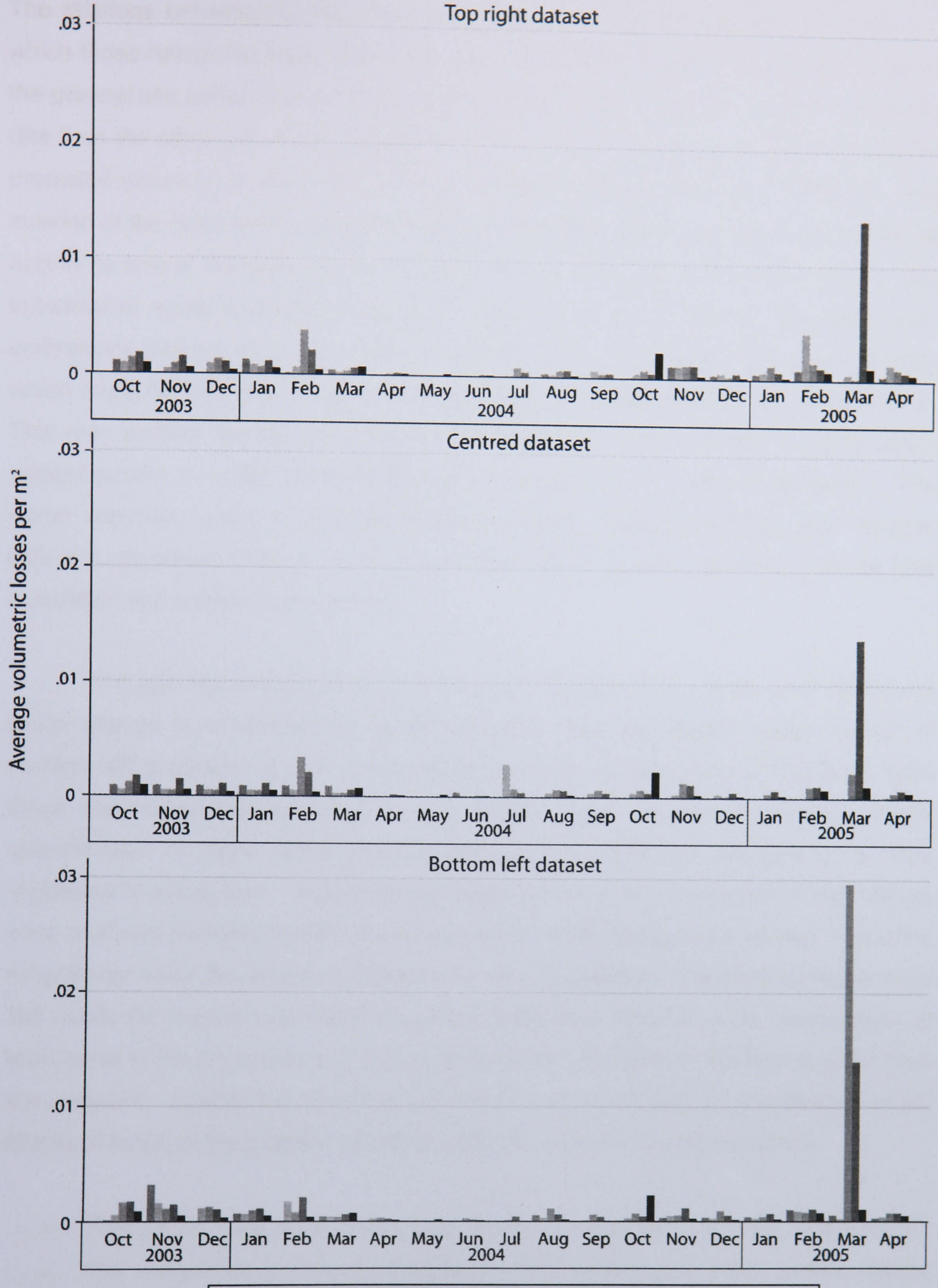

Figure 6.21: Monthly distributions of volumetric change per m^2 at Site 6. The scale patterns at the protected headland represent a reversal from those recorded from the other side of the headland at Site 5 indicating that the scale differences may reflect localised processes.

The relations between the three sets of windows contrast with several other sites in which those nearer the base of the cliff over-estimate actual site rates of loss. Instead the general site patterns were best predicted by the lower windows, in stark contrast to Site 5 on the other side of the headland. The reason for this reversal is likely to be the protected nature of much of the cliff base, largely removed from tidal influence. The location of the lower strata has therefore been artificially altered from an area of intense activity to one of inactivity as the controls on slope form are shifted from marine and subaerial to solely subaerial processes. This shift is also evident in the slight over-estimations derived from the windows located at the top right of the selected area which might be expected to be the most exposed to influences such as rain and wind. This may explain the apparent seasonality within the rates of monthly losses which appear greater in winter months, although such links require further investigation. The upper windows reveal a stronger seasonal signal, raising questions over whether different responses may be seen across the cliff to specific controls such as tidal inundation and subaerial processes.

Through the investigation of the effects of altering the scale and location at which change is monitored it is evident that the most appropriate scale at which to monitor cliff processes is that of the entire landform. Subsections of rock face, even those that encompassed much of the overall slope, proved inadequate in the quantification of wider scale patterns although the significant changes were often registered in some form. Reducing the scale at which the processes of cliff change were analysed revealed additional patterns which were clearly scale related, becoming insignificant when the whole monitored area was considered. The data therefore imply that, while the overall magnitude-frequency relationship may be scale independent, at least some of the processes governing cliff form are sensitive to the scale at which they are analysed. Insights into the nature of cliff behaviour provided by the analysis of the effects of scale on the patterns of cliff change can be summarised as follows:

- The overall magnitude- cumulative frequency relationship is scale independent.
- The magnitude-cumulative frequency distributions are often similar across different scales of analysis but the changes per m^2 were overly sensitive to larger failures when less than the whole rock slope is considered.
- The scale independency of the magnitude-frequency relationships detected is constrained to areas above 100 m^2, below which the scale of analysis is insufficient to encompass the representative patterns of change.

- Magnitude-cumulative frequency patterns are location and time dependent although the site specific relationships have been recorded within all of the monitored scales.
- A transition is typically found with increasingly erratic and outlying magnitude-frequency curves produced by reducing the scale of the analysis.
- In many cases the variability in the distribution and range of the changes recorded produced by reductions in scale increases with change away from 0.005 m^3.
- The position of the monitored area on the cliff face governs both the accuracy and the responsiveness of the analysis at different scales.
- Scale dependent processes insignificant to the overall response of the cliff dominate localised subsections of the cliff face.
- Monitoring at all scales becomes increasingly representative of overall cliff form change when located within the area of greatest activity.

6.4 Episodicity

Spatial aspects to the quantities, frequencies, scales and relationships that influence the nature of slope change are fundamentally linked to the temporal development of the landform. A key question in the consideration of how coastal cliff behaviour changes over time is as follows:

Is hard rock coastal cliff behaviour episodic?

It is commonly assumed that cliffs behave episodically rather than continually (Neves and Pereira, 1999; Hampton *et al.*, 2004; Hapke, 2005), although very little consistent quantitative evidence has been provided to confirm this. In order to investigate the temporal nature of cliff behaviour, both episodic and continuous aspects of change have been considered.

6.4.1 Rock cliff change as an episodic process

Episodic change refers to irregularity in the temporal divisions between the occurrences of different events. Recurrence intervals are generally thought to vary between events of different magnitudes, with longer intervals for larger material losses. The magnitude-frequency patterns previously established for the dataset provide a strong indication that change at certain sites was indeed dominated by large events. Quantitatively the material changes caused by the largest class of losses made the contribution of smaller failures inconsequential (refer back to Figure 6.10). Although the importance of larger events was clearly evident, the infrequency of their occurrence

meant that the proportion of smaller failures became significant to the behaviour of the cliff where large losses were limited within the monitoring period. Therefore, to investigate the nature of episodicity within the record the percentages of the monthly totals constituted by different magnitude failures were examined (Figure 6.22). In accordance with the spatial patterns noted earlier, it can be seen that whenever the largest, Class 5 magnitude changes did occur they dominated the material losses for that month. The complex nature of cliff responses over time is also evident in the large failures that occurred. Despite constituting 90% of the total changes the Class 5 October 2003 failures were not followed by any such failures during the following months, in contrast to January 2005 in which large losses were followed by a succession of months containing Class 5 failures. Inspection of the data revealed that all of these particular large scale losses occurred from Site 3, the well-jointed embayment, suggesting that large scale instability had propagated across the rock face. As has been already noted, the top of the scar of the first large failure at the site in October 2003 formed part of the bottom line of the latter failures in 2005 (refer back to Figure 5.7). This raises important questions over whether the two failures can be considered separately. Although separated temporally by 14 months of apparent quiescence, spatially the failures form part of the same failure surface. The inadequacy of using historical records to improve understanding of the nature of cliff change is evident. They are likely to assume that a complete rockfall scar would be caused by a single episode of change. It also seems questionable to refer to such failures as individual 'events'; rather they should be seen as part of the same process of change. Therefore, in addition to viewing the landform as a whole spatially, it is perhaps also preferable to view the rock cliffs holistically over time, as a continuum in which all alterations are connected.

In order to further investigate the temporal patterns within the data the relative contribution of losses of different magnitude classes to the monthly totals were considered for each site. The contribution of Class 1 losses through time appears to be distinguishable by morphology with the patterns of headlands generally declining from an initial peak but embayments experiencing more even distributions and increasing over the monitoring period (Figure 6.23). The smallest class of losses appear more significant in shaping the form of the headland cliffs (Sites 1, 4, 5 and 6), contributing in excess of 20% of the total change in some months, than in determining cliff form in embayments where they constituted less than 10% of the monthly totals at Sites 2 and 3. Strong similarities were seen between the patterns of Class 1 change over time at Site 5 and Site 6. The relative monthly contributions followed identical sequences, although the effects at Site 5 were more exaggerated than at Site 6. The

correlations between the sites imply that despite differences due to the presence and absence of marine influence at sites 5 and 6 respectively, the smallest changes recorded appear to have responded to the same controls. Evidence of a morphological susceptibility to the contribution of Class 1 change is also supported by Site 1 which demonstrates a similar pattern to the headlands at sites 4, 5 and 6 during many months but was less sensitive to changes, particularly during the 2003-2004 winter. Site 1, the subsided headland, is the least pronounced of the headlands and therefore the effect of Class 1 change is closer to that of the embayments. In general it appears the trends of the smallest losses were relatively more important factors in headland behaviour during the winter of 2003-2004 than in embayments, before becoming more uniform across all sites in the 2004-2005 winter. The high frequency of failures required for Class 1 losses to become consistently significant in the overall behaviour of a rock slope implies that the change is driven by processes with wide ranging influence. Whether such patterns can be attributed to specific or combinations of environmental influences requires further investigation.

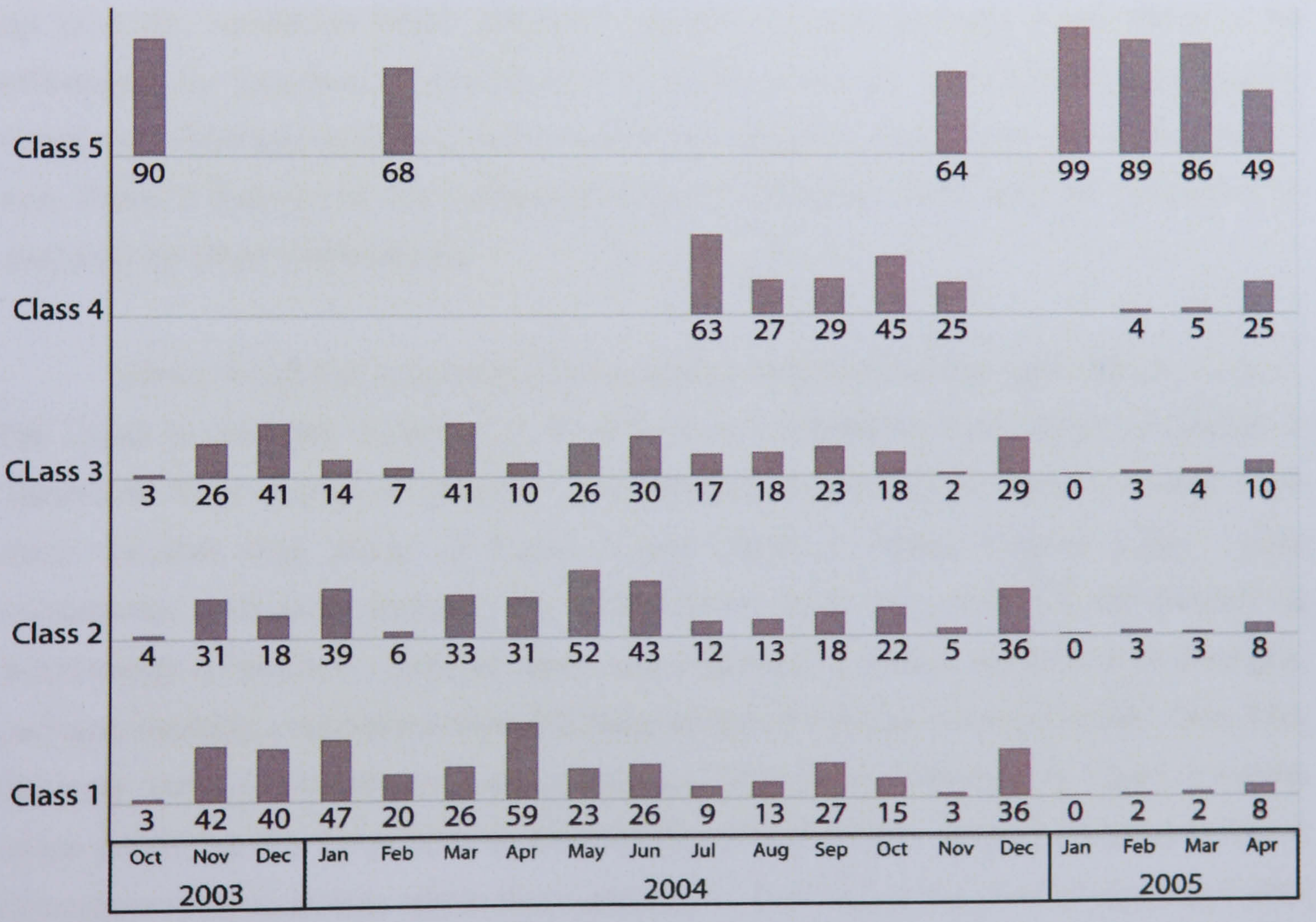

Figure 6.22: Percentage contribution of magnitude classes for the monitoring period. Apparently isolated failures were seen to become connected to subsequent losses spatially despite gaps of several months or more.

The Class 2 scale losses recorded over time displayed marked differences with the patterns of Class 1 change, most notably at the headland sites (Figure 6.24). The contribution of the changes to the total monthly losses appear relatively less important in shaping headlands than the smallest failures, with contributions rarely exceeding 15%. Although the patterns were again very similar between Site 5 and Site 6 there were notable differences in the quantitative contribution of Class 2 losses, which appear less significant at Site 6, the protected headland. The largest divergence from the patterns of Class 1 change, however was seen at Site 4, with dramatically lower percentage contributions to total monthly site change. The embayments recorded almost identical patterns and very little quantitative difference between the importance of Class 1 and Class 2 scale events. Although the magnitudes of Class 1 and Class 2 failures were separated by less than 1 m^3, the increase in size may represent a fundamental alteration in the processes of failure. Loss of the smallest blocks, less than 0.1 m^3, is likely to result from the processes of continual downwearing caused by abrasive weathering or flaking due to wetting and drying cycles within the weaker rock. Such processes might explain the heightened significance of Class 1 failures to the more protruding and therefore exposed headland sites. The Class 2 changes however, up to 1 m^3, constitute more coherent masses of rock and are more likely to be influenced by localised destabilising influences such as undercutting and marine quarrying. Perhaps most interesting then is the apparent consistency between Class 1 and Class 2 failures at the embayment sites, indicating they may be controlled or captured by other mechanisms.

Whilst remaining relatively minimal when compared to the rock cliff as a whole, the Class 3 changes, between 1 m^3 and 10 m^3, represent a significant increase in magnitude from very small change. The temporal responses of Class 3 failures were more variable than those of Class 1 and Class 2 losses (Figure 6.25). Less consistency was seen between the sites which could not obviously be divided by morphology or location. Instead, each site displayed a distinct sequence of changes, perhaps marking a departure from the base levels of change across all sites. Site 2 for example, the arched-failures embayment, was repeatedly affected by Class 3 events which accounted for up to 25% of the total monthly changes, in stark contrast to Site 3 which recorded no events within this class for the first half of the monitoring period after October 2003. The temporal sequence of Class 3 failures exhibits signs of episodic behaviour with periods of normally distributed influence followed by periods in which no such losses were recorded. This pattern was seen throughout the sites, with periods of activity lasting several months, reinforcing the suggestion that rock cliff failures should not be viewed in isolation as 'events' but as part of a continuum of change. The

mechanisms associated with Class 3 losses are therefore less responsive to every day processes than the smallest changes recorded. The progressive contribution of these failures over successive months implies that they may be internally driven once initiated, propagating instability over time.

The Class 4 scale failures, between 10 m^3 and 100 m^3, were only recorded at three sites and even then only within eight of the total 20 months (Figure 6.26). Although the occurrences of these losses were much lower than smaller scale losses, the proportion of total monthly change accounted for was much higher, reaching over 45% at sites 3 and 6. The pattern of failures over time appears to be episodic, with periods of stability followed by significant change, although the periods of activity were much shorter than for the Class 3 changes, often involving a single month of change. The limited number of Class 4 scale losses makes it hard to establish definitive patterns of change, but for several of the periods of activity it appears medium scale failures decline in significance after an initial peak monthly contribution. The only contradiction to this trend occurred in the last months of monitoring at Site 3 in which a particularly large scale event had been recorded. The orthoimages revealed that many of the subsequent records of medium scale losses were associated with the removal of material from the accumulated debris at the cliff toe.

The largest losses were again restricted to just three sites, although Site 3 was the only site to record both medium and large scale failures during the monitoring period. The latter months of monitoring saw several large changes at Site 3 which produced substantial amounts of debris that was later removed by the sea. This may account for the slight increases in failures of all other scales at the site during the following months. Like the Class 4 scale changes, Class 5 failures occurred in isolation and all but the largest were contained within a single month (Figure 6.27). None of the Class 5 magnitude failures from different sites occurred within the same month indicating they may be governed more by site specific controls rather than regional environmental processes or triggers. The rarity of large scale events in rock slopes may be due to the time taken for preparatory factors to create the conditions for such large quantities to fail (Guzzetti *et al.*, 2002; Brunsden and Lee, 2004). The percentage contributions however reveal that when such failures do occur, their effect on the monthly total, and indeed the annual total, is greater than any other scale change, peaking at over 99% of monthly contributions.

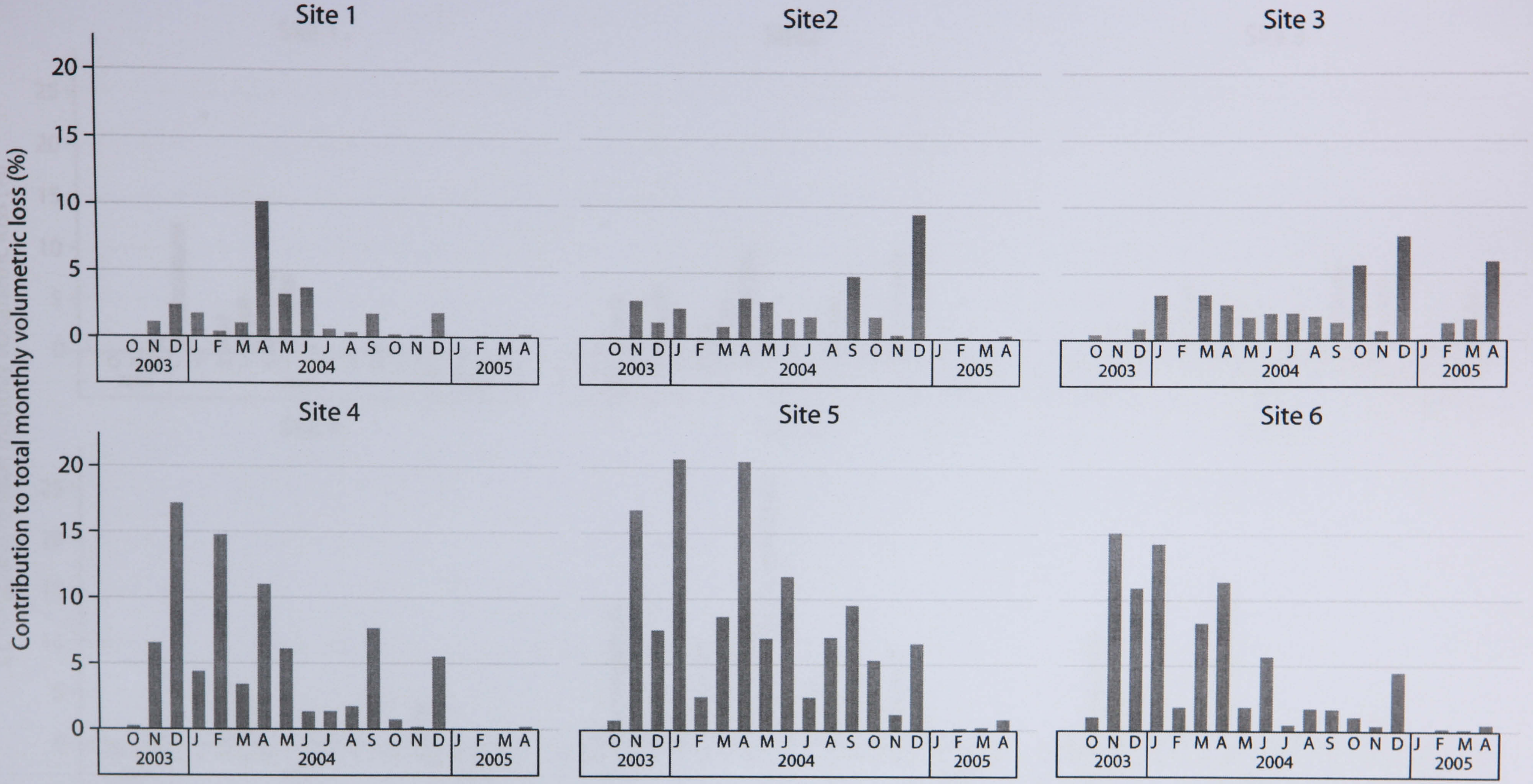

Figure 6.23: Percentage contribution of Class 1 scale losses (<0.1 m^3) to the monthly totals of each site. Correlations were apparent between the headland sites 4, 5 and 6 and between embayments at sites 2 and 3.

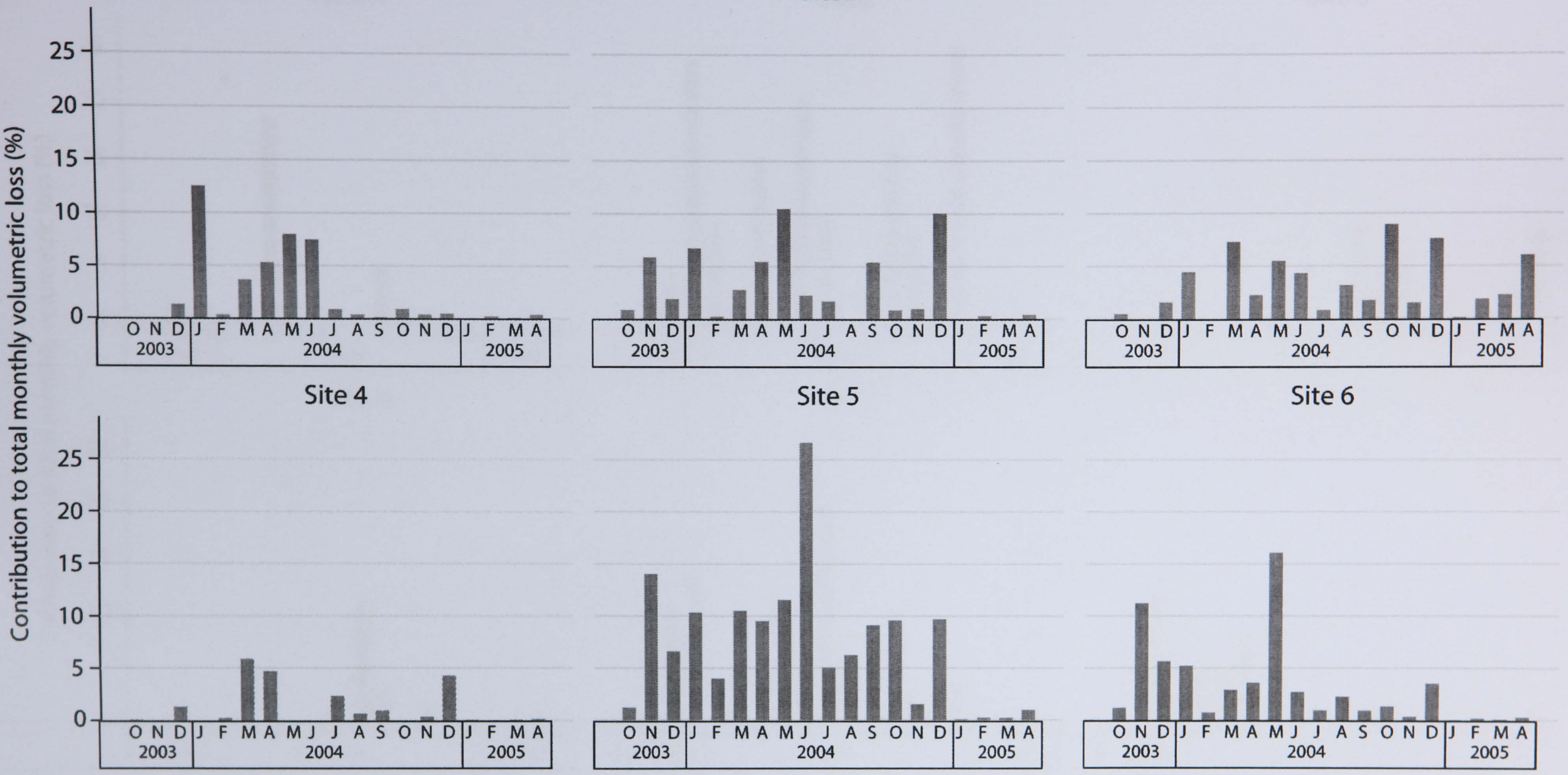

Figure 6.24: Percentage contribution of Class 2 scale losses (0.1 m^3 – 1 m^3) to the monthly totals of each site. Significant differences with the patterns detected in Class 1 scale changes suggest very small failures may be determined by different controls.

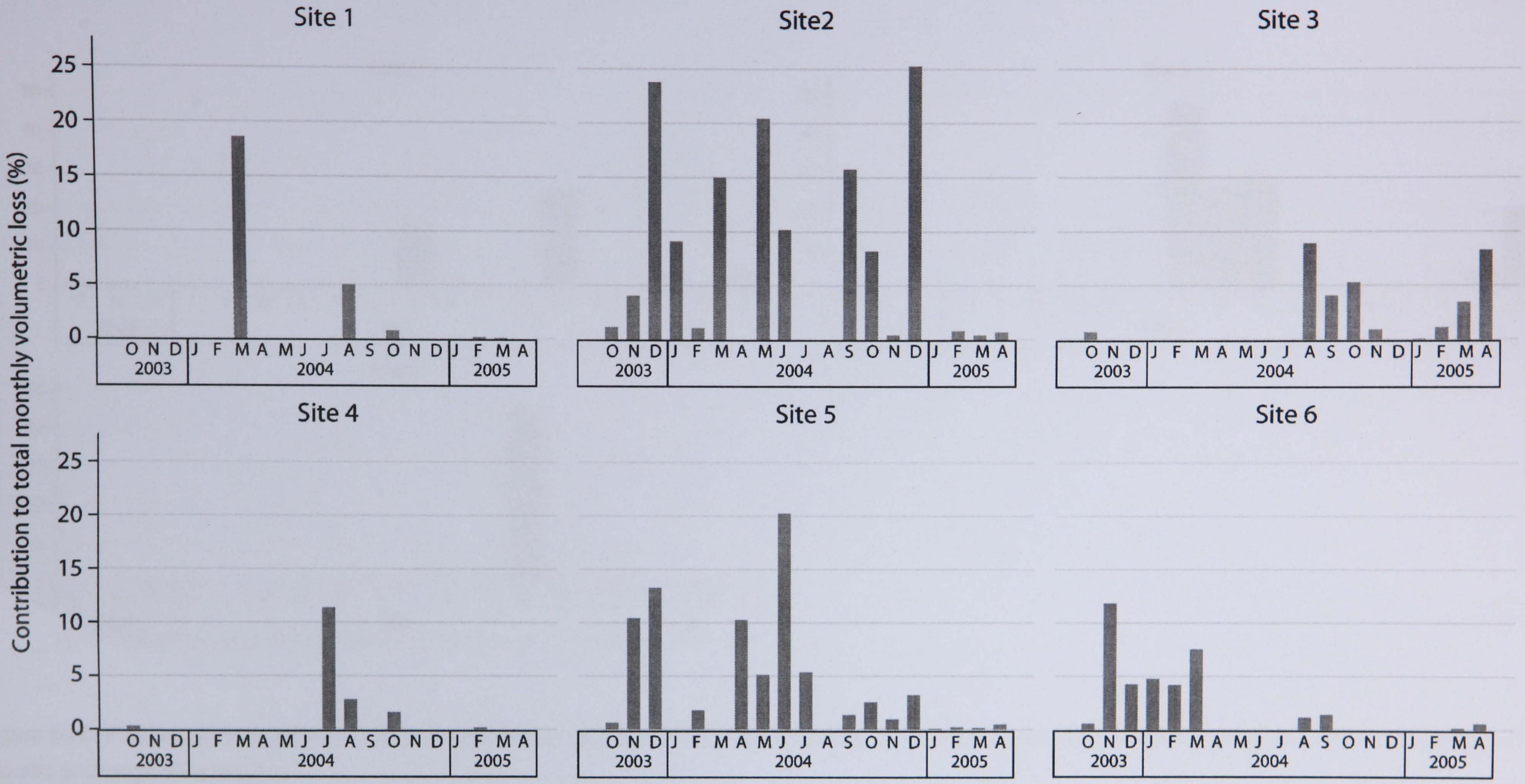

Figure 6.25: Percentage contribution of Class 3 losses (1 m^3 – 10 m^3) to the monthly totals of each site. Many sites demonstrated periods of instability followed by several months of no activity.

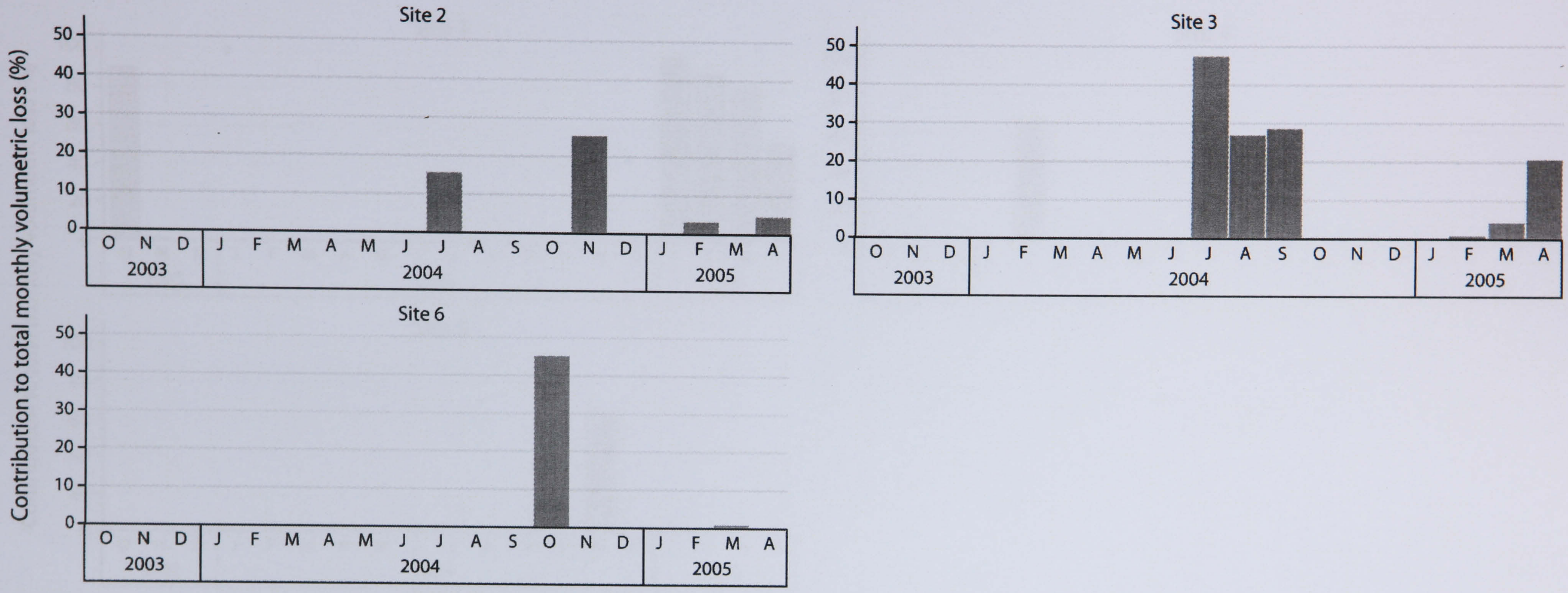

Figure 6.26: Percentage contribution of Class 4 scale losses (10 m^3 – 100 m^3) to the monthly totals of each site. The occurrence of failures was more sporadic with months of change often isolated.

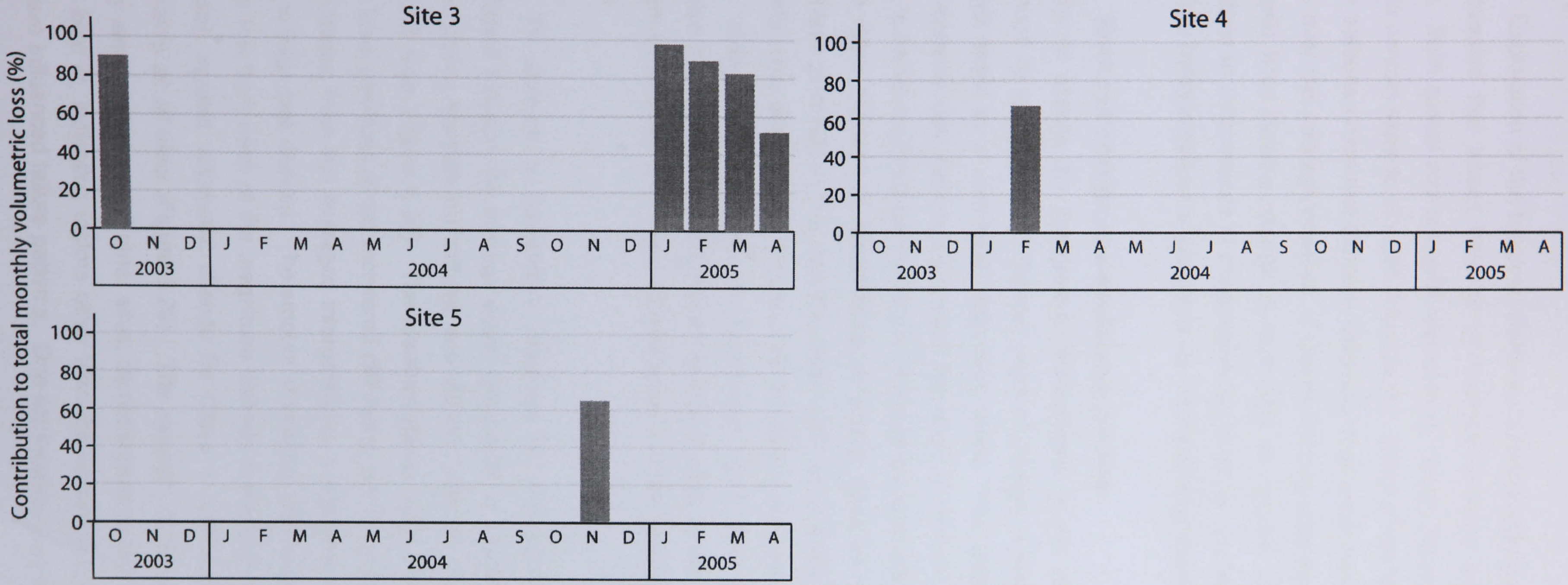

Figure 6.27: Percentage contribution of Class 5 scale losses (>100 m^3) to the monthly totals of each site. Site 3 was the only site to contain both Class 4 and Class 5 failures and these were within the same month. This suggests that for many of the monitored sites larger volumes of material may be lost through either medium or large scale change rather than a combination of the two.

Exploration of the temporal patterns of rockfalls throughout the monitored sites has revealed that losses become increasingly episodic with the magnitude of the failure. Both spatial and temporal elements of rockfall behaviour have therefore been seen to contain aspects of scale dependency. Many of the failures appear to generate similar patterns within and between sites over time which have caused questions to be raised over the conceptualisation of losses forming discrete 'events'. The switch of emphasis from viewing change in rock cliffs as random collections of independent alterations to a continuum of progressive but spatially and temporally variable change over time holds important implications for understanding slope behaviour.

6.4.2 Rock cliff change as a continuous process

In order to assess the progressive development of the cliffs, which are inevitably influenced by sporadic and localised areas of change, it has been useful to consider the rock slope as a continually deforming mesh. The failures within coherent rock slope systems may therefore represent variations in the rate at which deformation, or strain, is transferred through the mesh. Areas of the rock cliff that protrude significantly will be more exposed to destabilising influences, such as environmental processes, than those generally in line with the mesh (cliff) as a whole and hence may become relatively more likely to fail. Furthermore the loss of material from one part of the rock slope, undergoing high strain or deformation rates, may consequently result in a response in the mesh, causing the strain rate in other areas to alter. It was therefore decided to examine the effect of protrusion on the spatial and temporal nature of failure.

To achieve a quantitative measure of protrusion a planar surface was constructed through the average slope, generated by creating a DEM from just two lines of points, towards the cliff top and cliff toe, with the resolution set to that of the entire cliff face (Figure 6.28). The resultant planes were considered to represent the datum level positions of the monitored cliff faces and by subtracting the DEMs of true rock surfaces from the averaged interpolations, a distance of protrusion or inversion from the base was derived. The amount of material protrusion was compared with the volume lost from each of the magnitude classes at every site. The logarithmic plot of protrusion against volumetric change for Class 1 scale losses revealed a positive relationship at all sites (Figure 6.29). The strength of the correlation at Site 2 was notably weaker than at the other sites, demonstrated in the shallower gradient of the line of best fit, indicating factors other than the accumulated strain in the rock mass may have influenced failure patterns. One explanation may be the heightened activity

from the arched failures within base of the cliff which was associated with larger, more coherent losses of material, limiting the exposure time of rock to weathering processes.

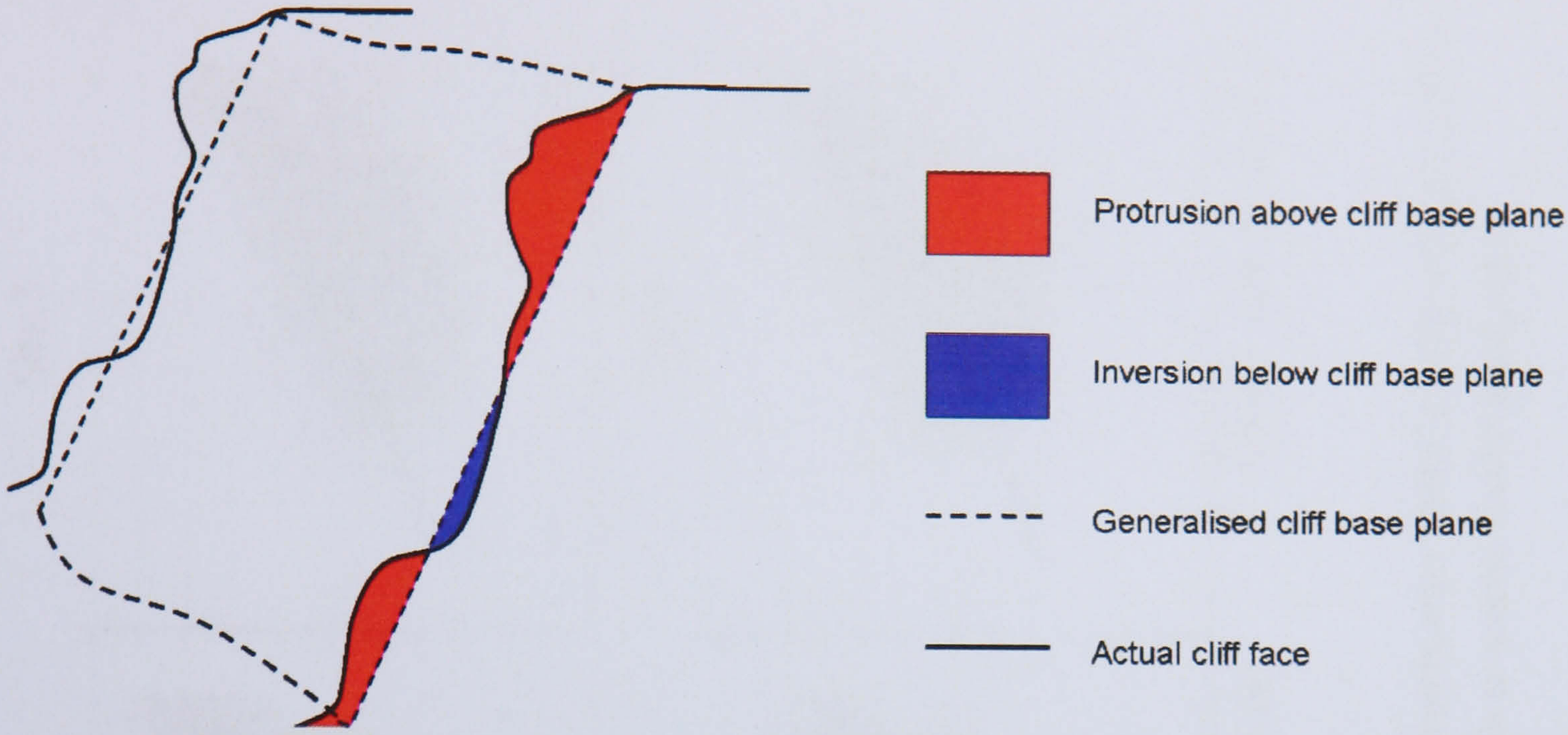

Figure 6.28: Approach to gain a measure of protrusion and inversion within the rock face.

The positive trends suggest that, in general, as protrusion from the cliff face increases the volume of Class 1 failures increases. Although the monitored areas contained rock which protruded over 5 m from the base level, almost all of the Class 1 scale change was linked to rock face protrusions of less than 0.1 m, with the only the largest changes linked to protrusions over 1 m. The positive trends at all sites appear weakened by significant numbers of failures occurring within areas of very minor protrusion. The limited number of Class 1 losses from material that protrudes beyond 1 m suggests that such failures may have already failed from the rock mass by the time the protrusion becomes more pronounced. The patterns of tiny scale change may also reflect specific processes operating on the rock slope. Sheet flow over the cliff face is likely to have become concentrated on the lowest terrain, which was often located at or around the base plane, causing any minor protrusions within these areas to become detached or worn down during rain events. As areas of rock become increasingly pronounced from the overall rock face however, perhaps beyond 0.1 m, the likelihood of sheet flow passing over is reduced as less resistant flow paths are taken. The correlation of failures with environmental factors such as storm events is investigated in more detail in the following section.

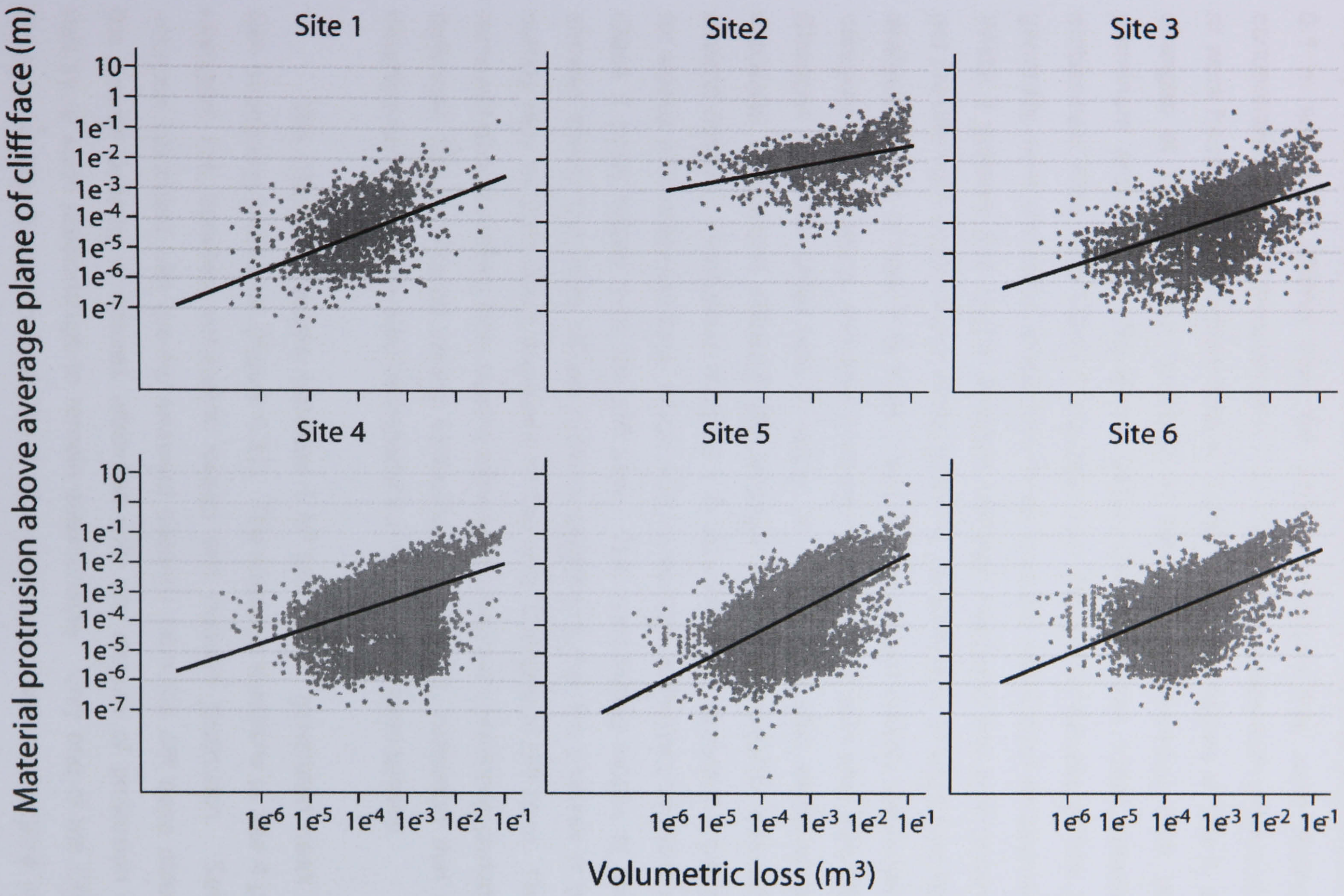

Figure 6.29: The relation between protrusion and volumetric loss for Class 1 scale change. Positive trends were noted at every site although the spread of values was often more scattered below the line of best fit indicating many of the smallest losses were located in or around the cliff base plane.

The statistical relations of protrusion with Class 2 scale change were seen to be less significant than with Class 1 losses, exerting little or no control over change at several sites (Figure 6.30). Many of the sites did however show that the majority of change between 0.1 m^3 and 1 m^3 was associated with material protrusions of between 0.1 m and 1 m, distinct from the smallest changes that were disproportionately concentrated within protrusions of 0.1 m. Clusters of losses from protrusions of up to 1 m were found at the headland sites 4, 5 and to a lesser degree at Site 6, although the changes at the subsided headland at Site 1 were recorded from smaller, less prominent protrusions. Significant differences were also noted between the two embayment sites, with Class 2 changes from the arched-failures at Site 2 plotting in generally more protruded areas than those from the well-jointed embayment at Site 3. Whilst it appears that simple divisions between headland and embayment sites may not provide valid explanations of the patterns, consideration of slope type has aided the analysis. Lines of best fit at sites 2 and 4 were almost entirely within the 0.1 to 1 m category of protrusions, and type C slopes were found at both sites (refer back to 3.5). Changes from the other type C slope, at Site 5, was also clustered within these moderate protrusions although the strength of the relationship was weakened by several outliers. Protrusions of up to 1 m may therefore represent a critical threshold for slopes with under-cut toes, which may be strongly influenced by the detachment of Class 2 scale losses from the cliff face. The overhanging slopes at sites 3 and 6 showed similar but more diffuse patterns suggesting that the process of basal under-cutting may be particularly important for low level changes to cliff form. Despite being removed almost entirely from marine influence throughout monitoring period by harbour defences Site 6 showed strong similarities with Site 5, indicating that *in situ* and inherited conditions may also be important in determining such failures.

The Class 3 changes, between 1 m^3 and 10 m^3, generated weak correlations with increasing protrusion (Figure 6.31). The seepage headland at Site 4 provided the strongest link between volumetric losses and material protrusion. Several larger volumes coincided with greater seaward distance from the cliff base plane, although the overall scarcity of failures attributed with any degree of protrusion causes the validity of such relationships to remain questionable. Only one of the Class 3 scale changes at Site 3 and none at Site 1 were associated with any degree of protrusion above the base level of the cliff face. While the amount of protrusion may therefore increase the likelihood of failure, significant material losses may also occur from other parts of the rock slope which are in line with or even behind the cliff face.

Material protrusion beyond the average cliff face datum appeared to be a more significant factor in Class 4 (Figure 6.32) and Class 5 changes (Figure 6.33), although only eight and five such failures respectively were recorded from protruded areas, which meant statistical trends could not reliably be established. Most of the losses involving between 10 m^3 and 100 m^3 were linked to protrusions of 2 m or more, in contrast with the smaller scale changes, the vast majority of which were from protrusions of within 2 m. Furthermore all but one of the largest, Class 5 failures, which was associated with the erosion of debris at the base of the cliff rather than intact rock, came from rock material which exceeded the base level of the cliff by 3 m. Although there is insufficient data to establish relationships between volumetric losses over 10 m^3 and greater degrees of protrusion, the general level of protrusion may be a fundamental precondition to failure. It may also be the case that only the largest coherent volumes of material are sufficient to provide the strength required to support a protrusion of 3 m or more from the cliff face. The association of large scale rock slope failures with areas of significant protrusion may hold important implications for the way in which the coastline is managed if potentially hazardous sites with particular characteristics such as protrusions beyond 3 m can be identified.

In order to ascertain the extent to which the amount of protrusion could be explained by different geologies the failures across all sites were divided by rock type (Figure 6.34). All of the four main rock types displayed positive relationships with protrusion, largely reflecting the dominant frequencies of Class 1 scale change in all bands. Siltstone and sandstone layers revealed similar relationships with protrusion, both dominated by a weak but direct correlation with increasing protrusion and relatively small amounts of scatter in which protrusion made no effect on the magnitude of the failure. The mudstone and shale layers by contrast exhibited greater levels of scatter, particularly within the smallest changes. The shale was the weakest rock to be found within the rock mass and constant spalling of material was often observed during data collection, caused by its flaking composition. The weathering and erosion of such bands is therefore likely to continue irrespective of whether they protrude or not. The monitored mudstone bands were significantly more competent than the shale but invariably found at the base of the cliffs and almost all were located within the zone of marine influence. The more diffuse scatter of the points below the positive trend may therefore indicate marine control, with increased levels of activity causing larger volumetric losses in less prominent areas of the cliff toe, in addition to the heightened erosion of protruding areas.

The amount of protrusion from the cliff face has been shown to be an important but complex consideration in rock cliff failures. The data support the concept of an ever changing and deforming rock mass, responding dynamically to imbalances with variable rates of strain. Logically protruding areas may have resulted from a lower susceptibility than the surrounding rock or simply have been less exposed to process rates. Although the areas of greater protrusion can be considered more likely to experience larger material losses, the processes and patterns associated with the areas withdrawn from the cliff base remain poorly understood. The graph of volumetric change with protrusion was therefore re-plotted against distance behind the cliff base plane, with increasing inversion made positive for ease of comparison (Figure 6.35). The inverted areas of the monitored rock slopes reached considerably greater distances than the protruded areas. The relationship of volumetric change with inversion was weaker than that of protrusion for all rock types, and the scatter larger, but positive relationships indicate that volume losses increase with greater distance behind the average cliff face. The volumes involved were considerably smaller with inverted areas rarely yielding failures above 1 m^3. The scatter is noticeably lower in the mudstone than any other rock type. The stronger relationship may reflect the processes of marine undercutting and to a lesser extent subaerial scour in other rock types mostly above the cliff base.

The data imply that the geological properties of a slope and more specifically their influence on cliff face smoothness may be an important control in nature of retreat. The precise nature of the responses of different rock materials, and the interaction between them, is often ignored in rock slope analyses, but the tendencies towards a planar or undulating surface may influence the overall stability of the landform. Ultimately, the mechanisms of failure can only be tentatively deduced by monitoring change at monthly intervals, and further modelling investigations are required to understand the true mechanics driving such failures.

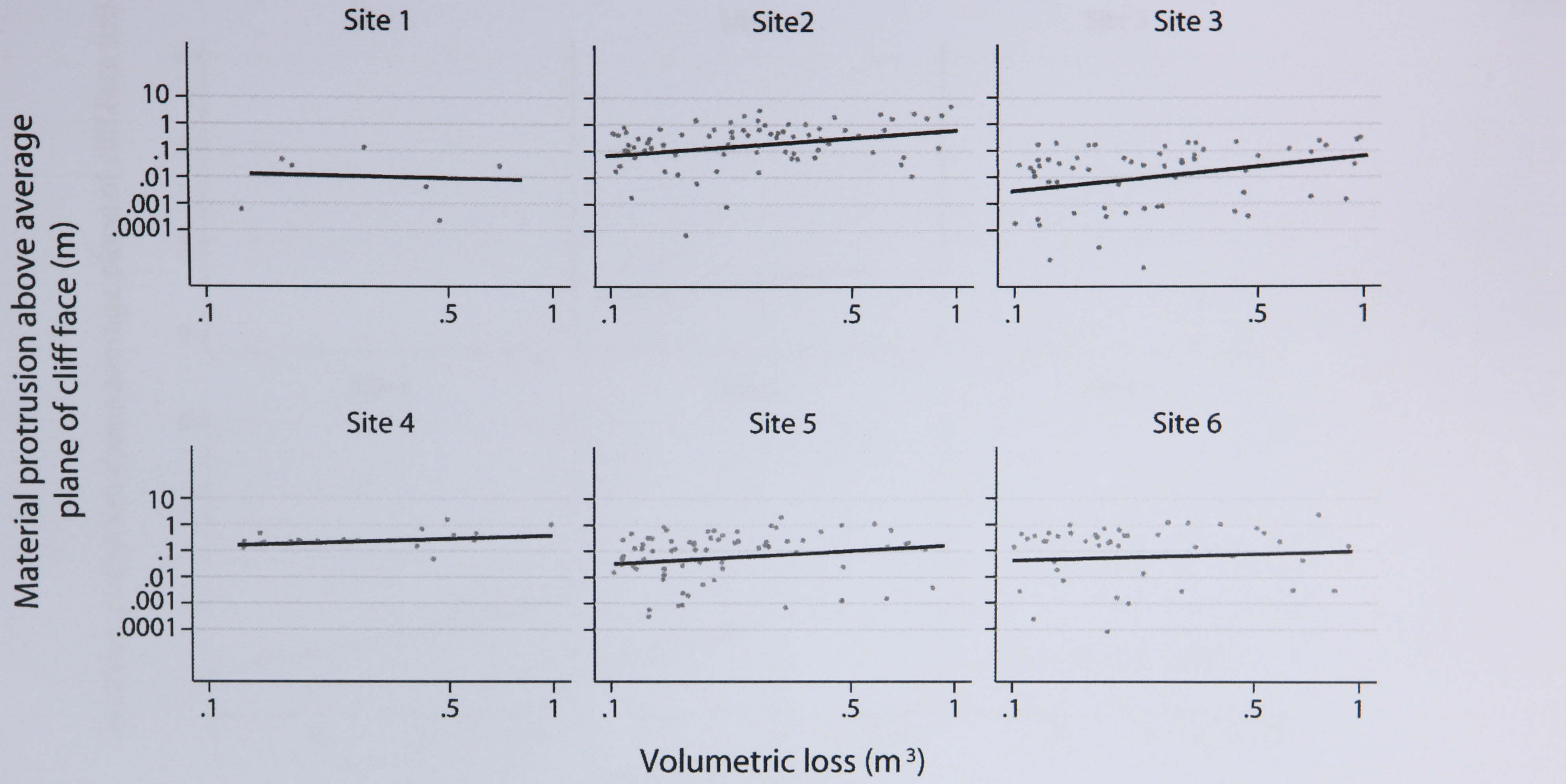

Figure 6.30: The relation between protrusion and volumetric loss for Class 2 scale change. The correlations were significantly weaker than with the smallest changes monitored although the Class 2 scale failures were related to more protruded areas.

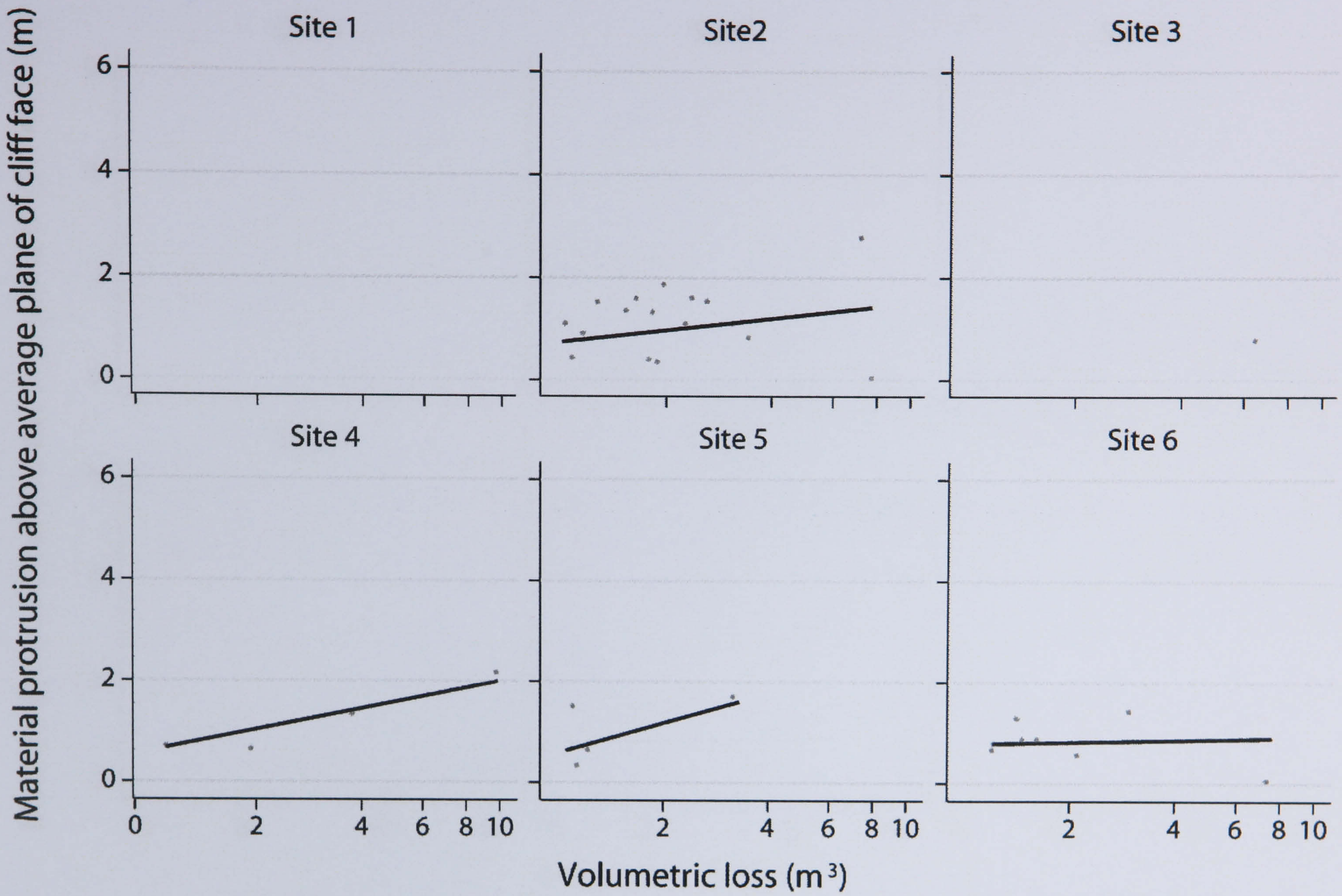

Figure 6.31: The relation between protrusion and volumetric loss for Class 3 change. The scarcity of Class 3 scale failures from protruded areas casts doubt on the weak positive relationships recorded.

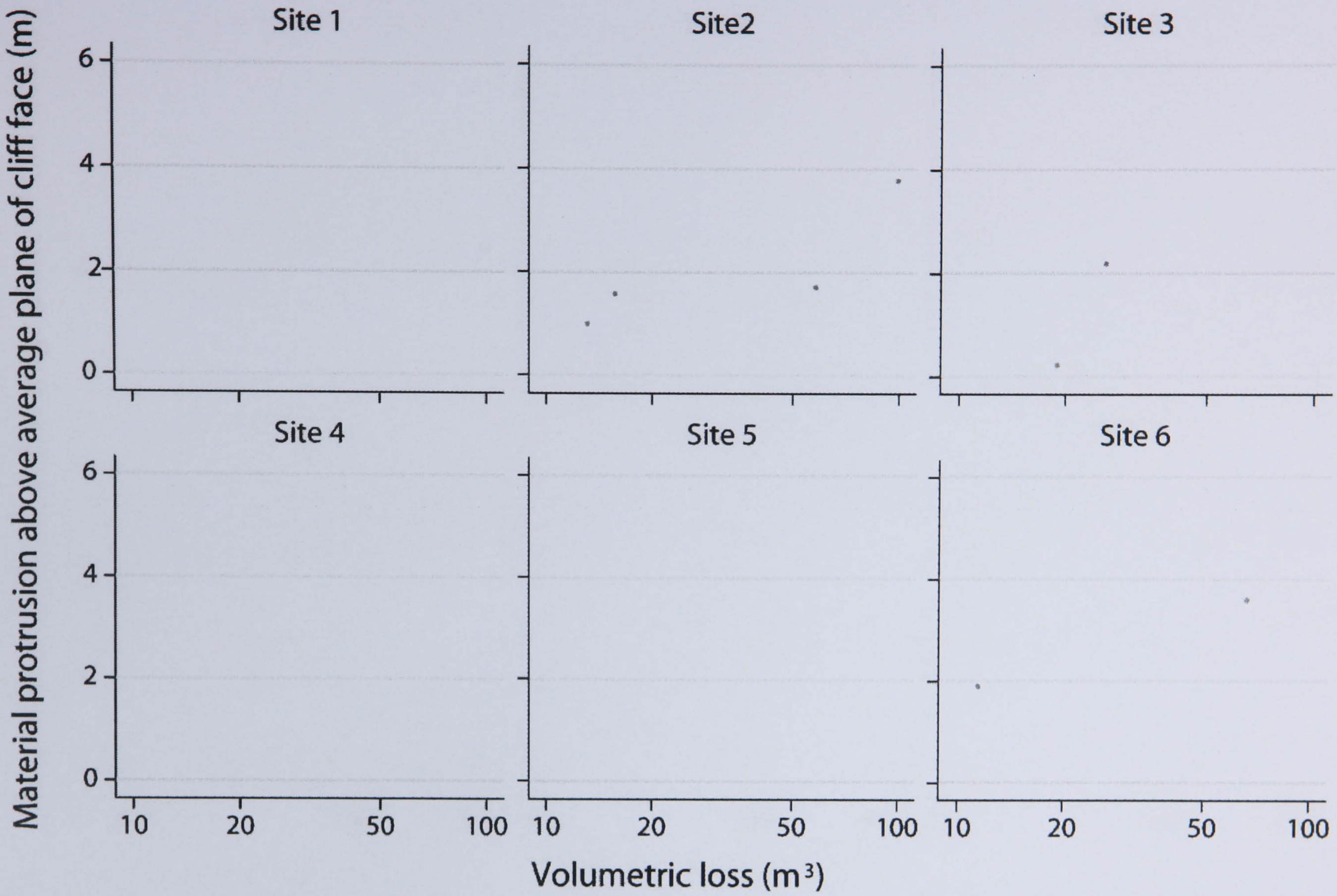

Figure 6.32: The relation between protrusion and volumetric loss for Class 4 change. Strong correlations were seen between protrusion and volumetric losses although limited data points restrict the establishment of such relationships.

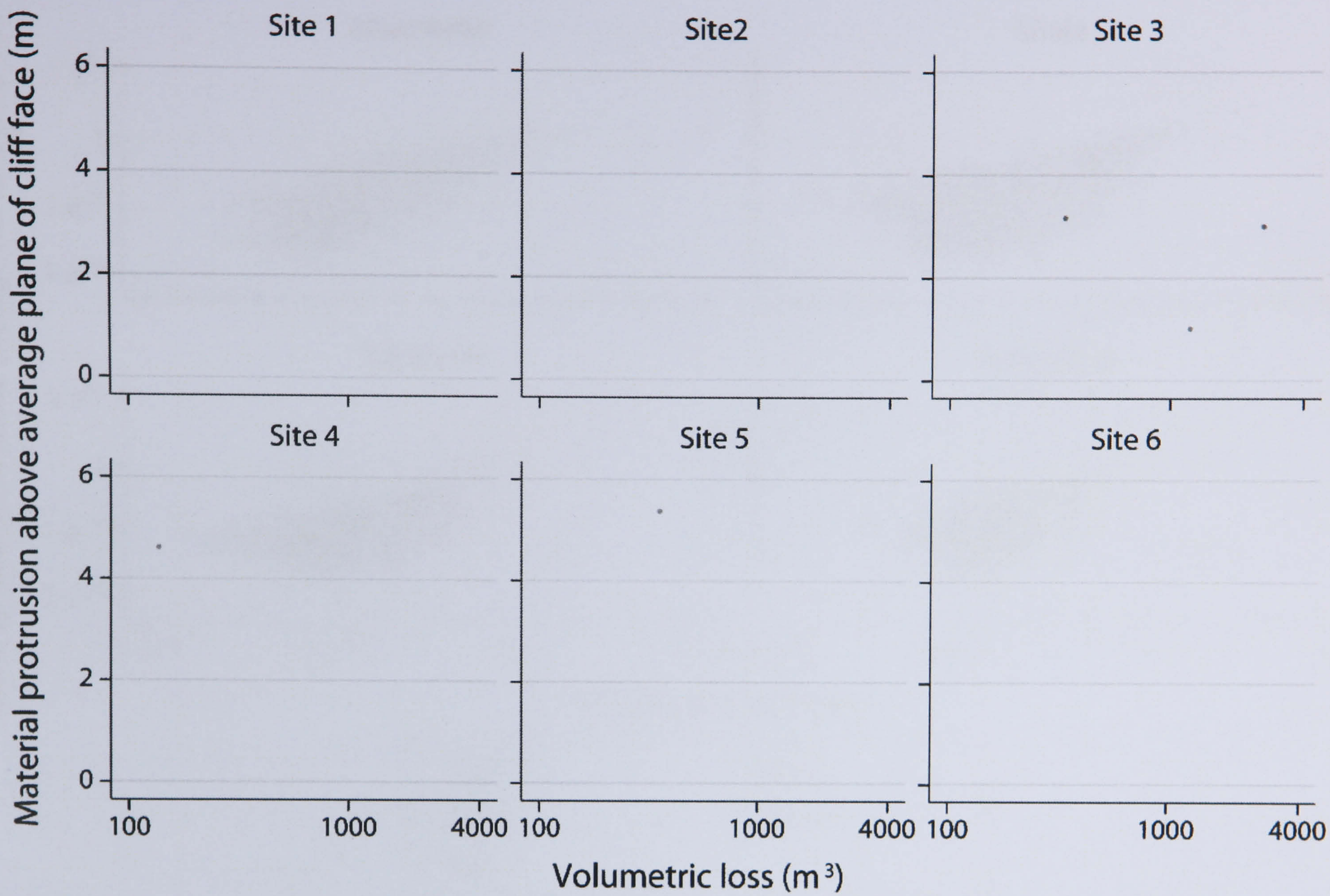

Figure 6.33: The relation between protrusion and volumetric loss for Class 5 change. All of the largest failures recorded were associated with the greatest degrees of protrusion.

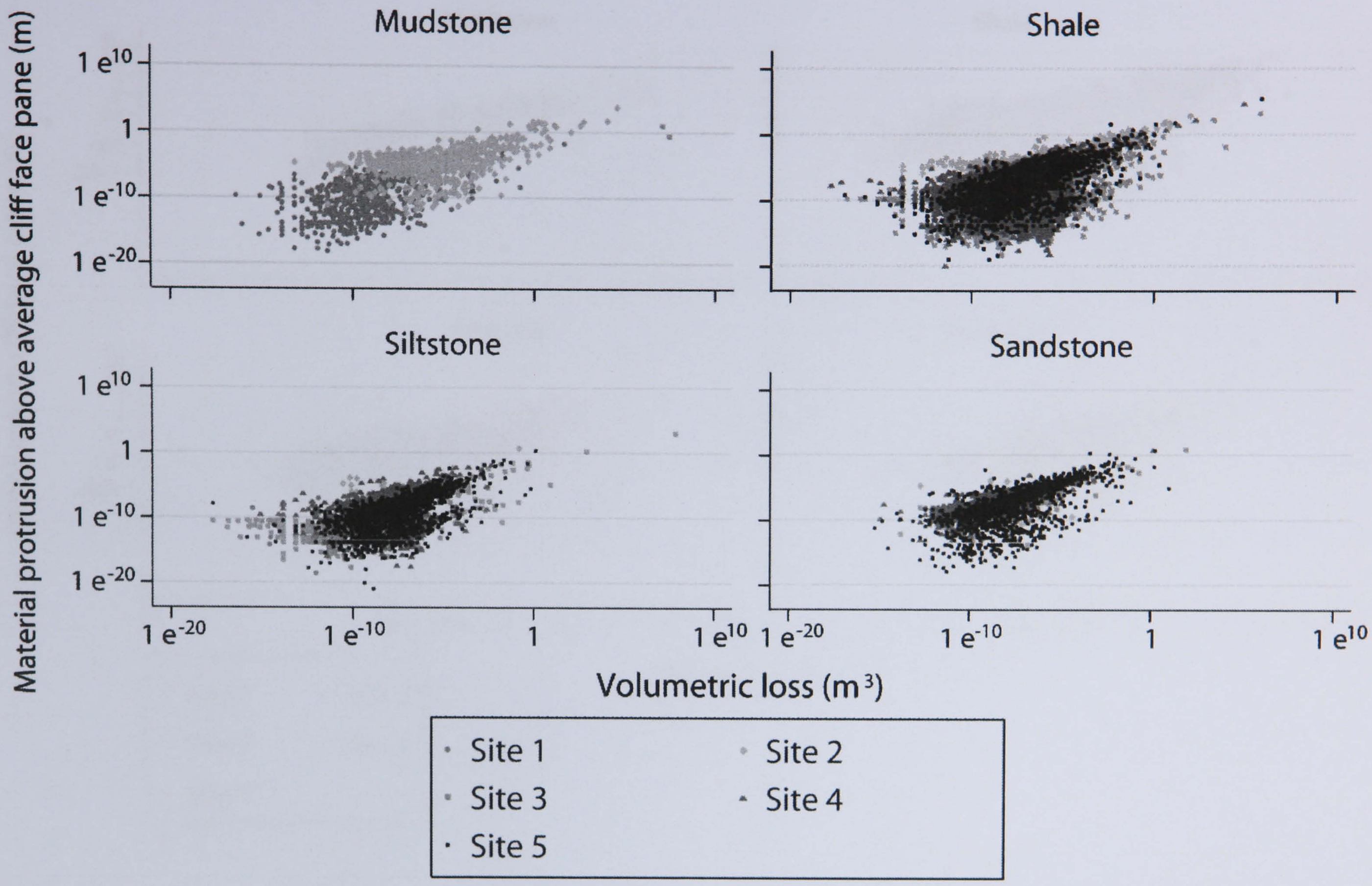

Figure 6.34: The relation between protrusion and volumetric loss for each of the four rock types found within the rock mass. The more diffuse scatter within the mudstone and shale, may reflect the different influences of marine processes and geotechnical characteristics respectively.

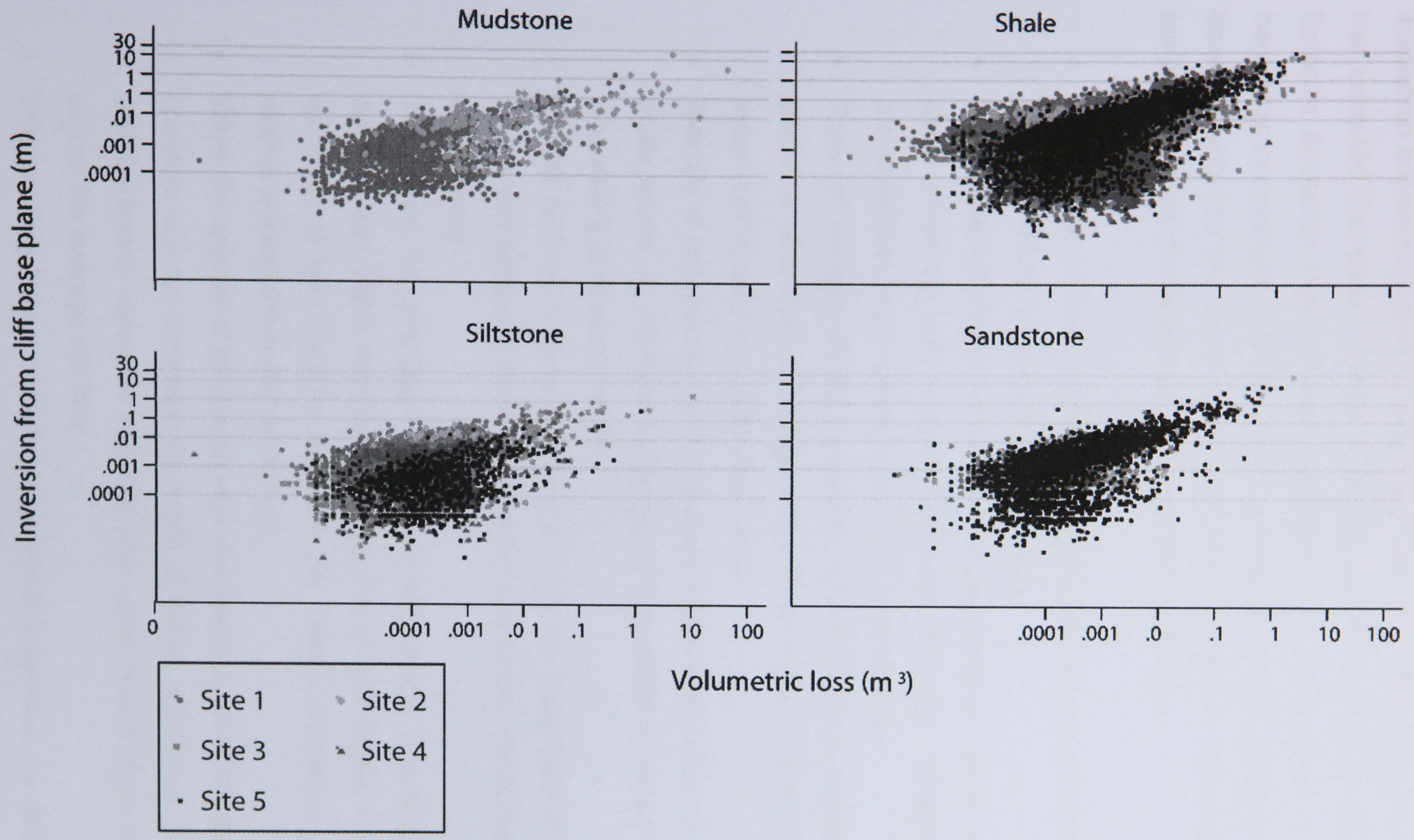

Figure 6.35 Volumetric change against inversion from the cliff base plane. The increasing amounts of inversion or withdrawal from the base plane have been made increasingly positive to aid comparison with the effects of protrusion.

Despite the dominance of large scale failures in terms quantitative cliff changes established in the previous analyses, consideration of the relative contribution of failures over time has revealed important relationships governing cliff evolution. The interaction between aspects of both magnitude and frequency and scale dependency has indicated that some aspects of episodicity do exist within the rock cliff system. Episodic behaviour may be scale sensitive, with the occurrence of larger failures becoming increasingly variable and clustered to periods of heightened activity over time. Insights into the nature of cliff behaviour provided by the analysis of spatial and temporal patterns of change can be summarised as follows:

- Cliff change involves elements of both continual and episodic behaviour which alter with failure magnitude and over time.
- The smallest (Class 1) losses reflect a base level of change and appear to have been driven by wide ranging influences that may represent a fundamental alteration from the processes governing larger failures.
- Rock cliff changes should be viewed not in isolation as separate 'events' but as part of a continuum of change culminating in the release of material from the slope during periods of peak strain rates.
- Aspects of episodicity may be internally rather than externally driven, with small scale losses for example exhibiting cyclical patterns through time rather than responding to seasonal shifts.
- Losses become increasingly episodic with the magnitude of the failure. Both spatial and temporal elements of rockfall behaviour contained aspects of scale dependency.
- The extent of protrusion may represent critical thresholds for phases of development within both overhanging slopes and slopes with under-cut toes; reflective of the interplay between the distinct processes of subaerial and marine activity and *in situ* conditions.
- While the amount of protrusion may represent accumulated strain and therefore correlate with an increased likelihood of failure, significant numbers of smaller material losses were also detected from areas of rock slope in line with or even behind the average cliff face.
- Whether they induce episodic or continual behaviour, the circumstances under which mechanisms can operate in cliffs are location specific.

Any explanation as to the precise timing of rock failures is complicated by the effect of multiple and interacting processes acting upon coastal landforms. The

questions considered so far have been concerned with the identification and investigation of the spatial and temporal patterns of change that determine cliff behaviour. Inevitably in the analysis of such landforms, questions over how cliffs change across space and through time are followed by why they change in this way.

6.5 Environmental drivers of change in coastal cliffs

One of the most widely studied aspects of rock slope geomorphology is the environmental processes that cause them to change. Although many responses can be associated with specific preconditions to failure, several of the patterns detected have suggested the potential influence of environmental processes acting on the cliff. Different environmental processes interact to varying degrees over time, reducing or enhancing their impact on the cliff, which makes them particularly difficult to attribute to periods of rockfall activity. A key question in the consideration of the drivers of change in coastal cliffs is as follows:

To what extent is hard rock coastal cliff behaviour governed by environmental processes?

The processes driving cliff behaviour are often based on theoretical assumptions and qualitative observations. A deeper understanding of coastal cliff change requires the controls and triggers associated with rock failures to be quantitatively investigated. Whether seasonal elements can be attributed to the rockfall patterns and the extent to which different environmental conditions can be directly linked to the nature of failure provides the basis for the following analysis.

6.5.1 Rockfall correlations with environmental conditions

To investigate the effect of climatic triggers on landform change a dataset on the weather conditions throughout the monitoring period was established for the area. The main data source consisted of records acquired from Loftus and Middlesbrough Meteorological Stations, extending back to January 2003. The data included measures of hourly temperature, wind and rainfall patterns which were then converted to monthly values. The average temperatures in the area recorded seasonal patterns throughout the monitoring period, peaking in August 2005 before declining to February 2005, the coldest month within the record (Figure 6.36). The monthly temperature ranges show that although August 2004 was the warmest month, the highest recorded temperature occurred earlier in June of the same year. The minimum temperatures suggest that the 2004/5 winter began slightly earlier than that of 2003/4, in which November temperatures did not fall below freezing. The summer months generally displayed

larger temperature variations than the winter months with ranges consistently around 14°C. The summer months therefore demonstrated the greatest potential for heating and cooling the rock mass, although perhaps more critically, the winter months regularly fluctuated around 0°C.

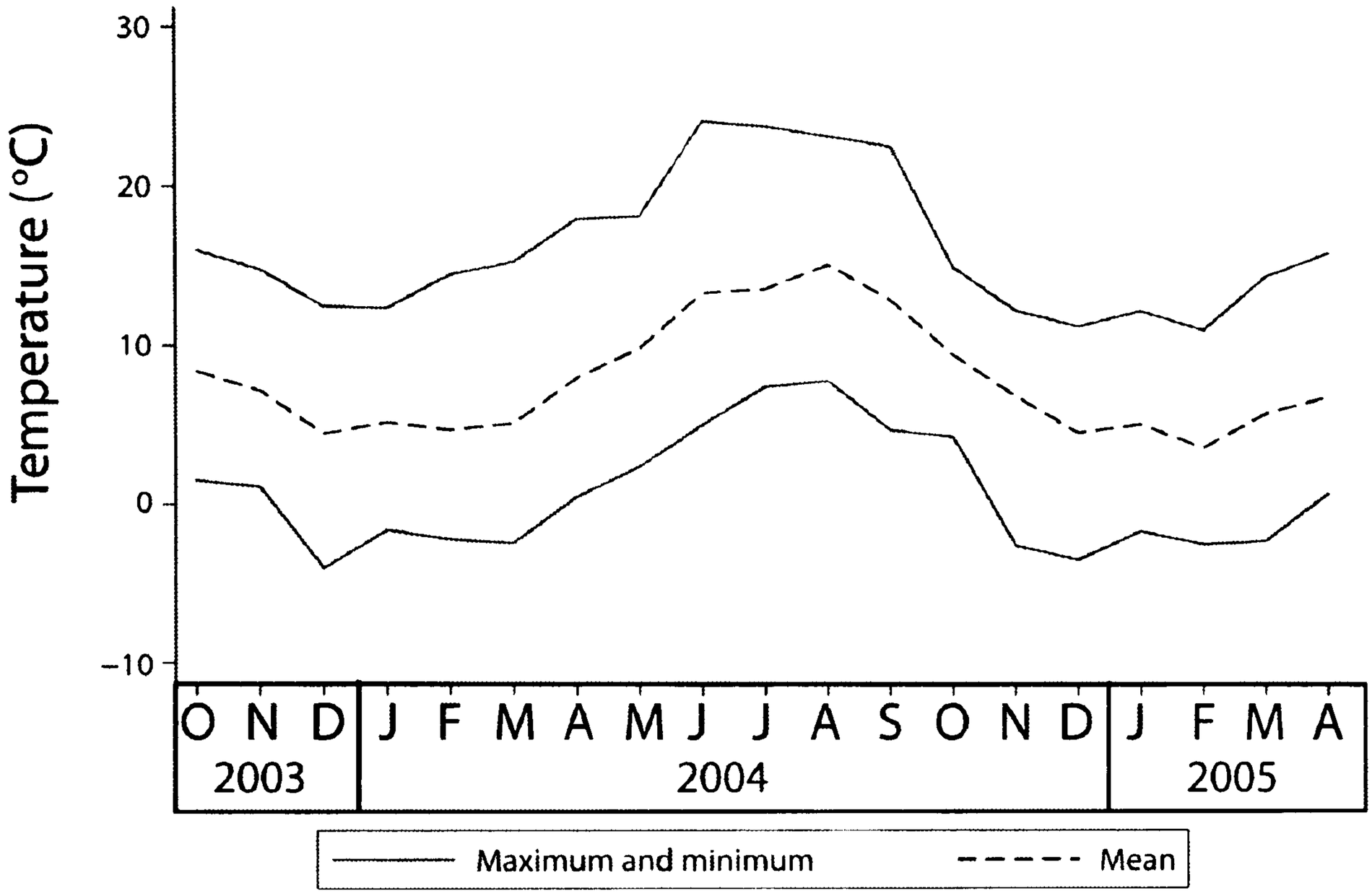

Figure 6.36: Fluctuations in temperature over the monitoring period (Source: Loftus Meteorological Station). A clear seasonal pattern was recorded although highest and lowest mean temperatures did not always correspond with peak and minimum values.

The wind patterns in the area during the data collection period again showed strong seasonal fluctuations but were inverted from the temperature changes, peaking in winter months when storms were more prevalent (Figure 6.37). The prevailing wind direction was from the north east, generating onshore winds throughout most of the year, although winter months were occasionally dominated by calmer regimes from the south west. The strongest winds were recorded in January 2003 and January 2004 following similar sequences of increasingly high energy conditions. The repetition of wind patterns, and the implications for heightened storm activity, suggests January may be a particularly important time for both the evolution of coastal cliffs. Equally the summer months can also be seen to have experienced significantly calmer conditions, with the cliffs subject to weaker winds, which might be expected to correspond with less dramatic periods of change.

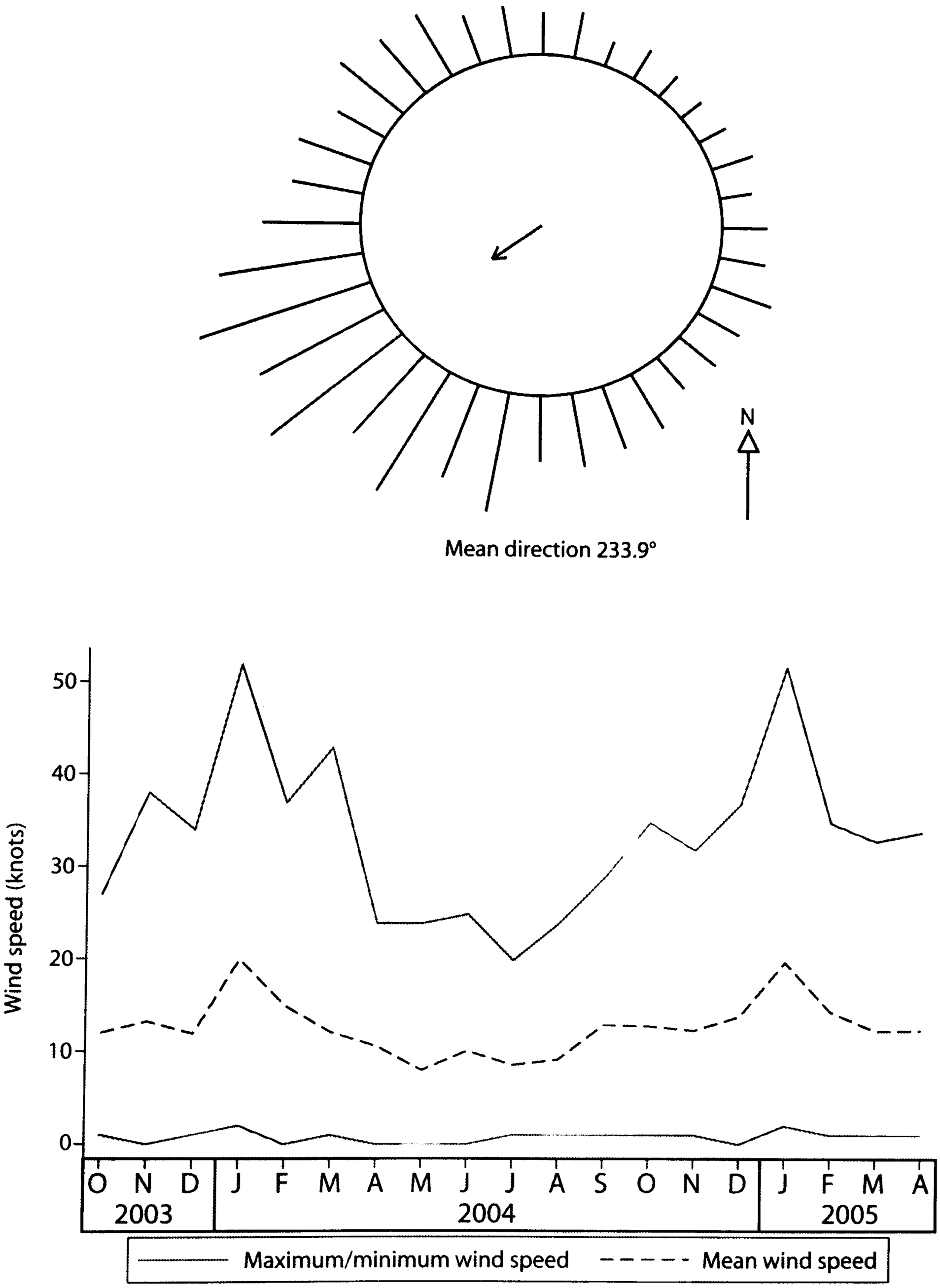

Figure 6.37: Wind characteristics during the monitoring period highlighting the importance of both wind direction (top vector plot) and speed (bottom line graph) in influencing the energy available to processes of cliff erosion (Source: Loftus Meteorological Station).

The total monthly rainfall amounts showed the greatest variability of any of the climatic influences recorded (Figure 6.38). There was no clear seasonality to the patterns of rainfall which fluctuated between wetter and drier months. This sporadic input of water into the cliff system may generate significant differences in hydrostatic pressure within the rock mass on a monthly timescale. Two of the four largest rainfall totals were associated with higher intensities, while the other two had a more even distribution throughout the month. Whether the manner in which water is delivered into hard rock cliff systems has a discernable effect on hard rock cliff response has yet to be determined, but many high intensity events have been attributed to accelerated periods of slope change elsewhere (Hapke and Griggs, 2002; Hapke, 2005; Hampton *et al.*, 2004). Whilst the intensity readings are an indication of the temporal distribution of the rain within the month it should be remembered that such summarised data give little indication about the precise nature of each storm event. Therefore peak hourly rainfall has been used in the analysis as a more appropriate measure of intensity.

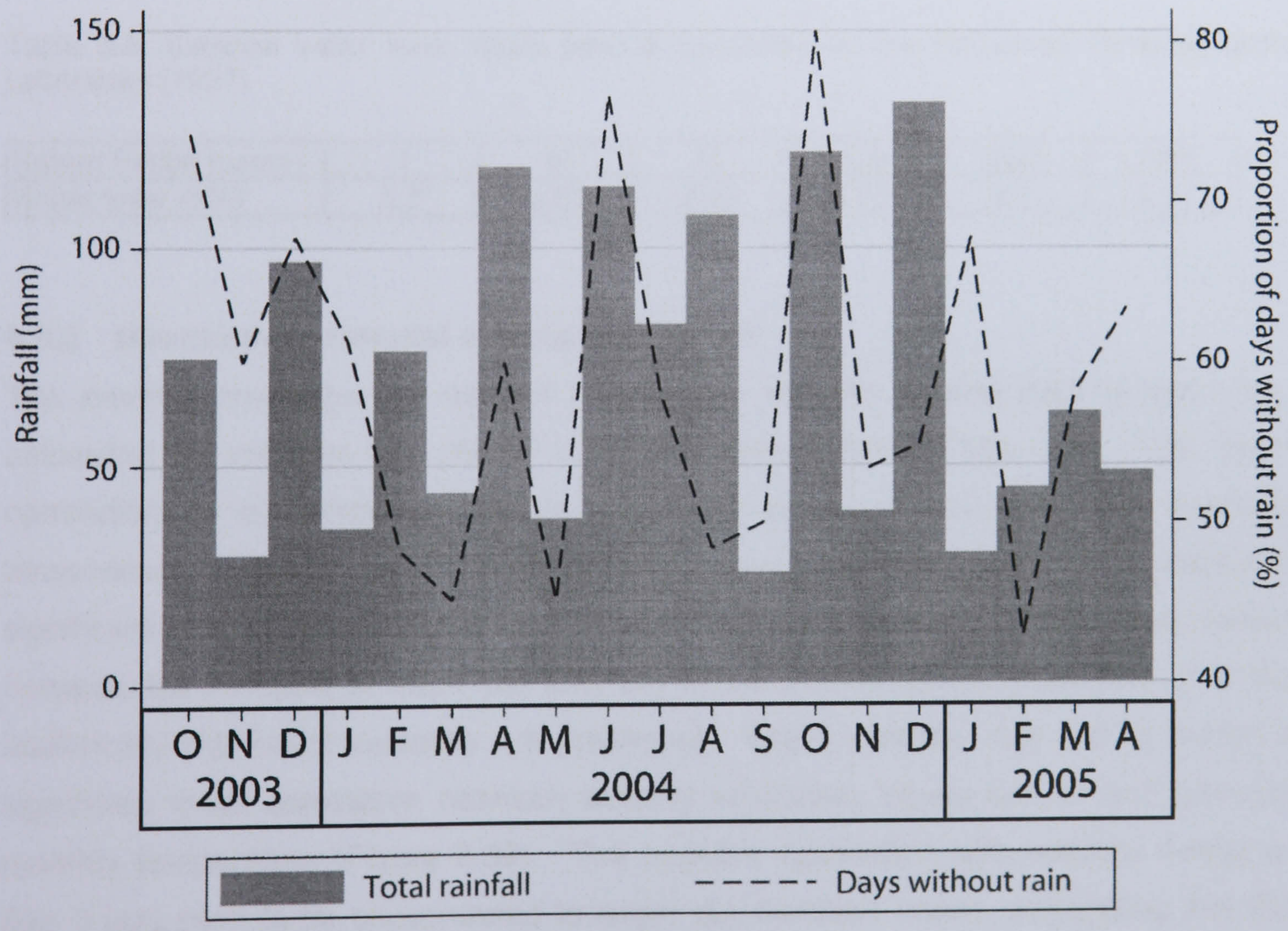

Figure 6.38: Monthly rainfall at the study area during the monitoring period (Source: Loftus Meteorological Station). Monthly totals demonstrate flashy inputs into the cliff system. The number of days without rain was used to calculate a measure of rainfall intensity; increasing dry days indicate the rainfall occurred within a smaller timeframe.

The influence of marine processes has become widely viewed as the defining control on coastal rock slope form (Sunamura, 1992). The Staithes coastline has a 6 m tidal range with mean tide level just above Ordnance Datum (Table 6.4). A measure of the variability in marine conditions can be seen in the extreme water levels calculated for the area for different return intervals by the Proudman Oceanographic Laboratory (Table 6.5). Data on mean, maximum and minimum tidal levels was obtained from tide gauge measurements in Whitby, collected by the British Oceanographic Data Centre.

Table 6.4: Tidal characteristics at Staithes.

Highest Astronomical Tide	+ 3.00 m OD
Mean High Water Springs	+ 2.40 m OD
Mean High Water Neaps	+ 1.30 m OD
Mean Tide Level	+ 0.13 m OD
Mean Low Water Neaps	- 1.00 m OD
Mean Low Water Springs	- 2.20 m OD
Lowest Astronomical Tide	- 3.10 m OD
Chart Datum	- 3.00 m OD

Table 6.5: Extreme water level return periods calculated by the Proudman Oceanographic Laboratory (1997).

Return Period (years)	1	10	50	100	200	1000
Water level mOD	3.3	3.61	3.85	3.99	4.1	4.31

6.5.2 Direct environmental correlations by site

The monthly environmental dataset was related with the rockfall data at each site, calculated as volumes lost per m^2 to enable comparability (Table 6.6). The direct correlation of environmental factors performed poorly overall, with only average temperature, average and maximum wind and minimum sea-level considered significant at any of the selected sites. Due to the lack of statistically valid relationships between the rockfalls at each site and any of the environmental influences, just the statistically significant variables are presented. Site 3 was the only site to record a significant linear correlation between monthly volumetric losses per m^2 and average monthly temperature (Figure 6.39). The negative correlation with material losses at Site 3 was seen to be concentrated to larger standardised losses, suggesting that the most significant periods of cliff change at the site were associated with colder temperatures. Furthermore the lowest temperatures appear to generate greater variability in slope response, with the scatter narrowing towards warmer average temperatures. However, weaker correlations with monthly minimum temperatures, the diffuse nature of the scatter throughout Site 3 and the non-relationships at the other

sites, cast considerable doubt on whether any discernible link with temperature truly exists.

Table 6.6: Least squares correlation coefficients between environmental variables and rockfalls at monitored sites. The red numbers denote negative relationships while black relate to positive correlations. The correlations above 0.5, highlighted in yellow, are considered significant.

	Site 1	Site 2	Site 3	Site 4	Site 5	Site 6
Total monthly rainfall	-0.012	-0.138	-0.049	0.058	-0.082	0.080
Peak hourly rainfall	-0.023	0.000	-0.446	-0.106	0.087	-0.019
Average monthly temperature	-0.001	-0.069	0.521	-0.195	-0.016	0.003
Monthly minimum temperature	0.000	-0.076	-0.434	-0.132	-0.106	0.036
Monthly maximum temperature	-0.006	-0.135	-0.444	-0.050	-0.125	-0.007
Hours below freezing	-0.007	0.078	0.192	0.317	0.048	-0.018
Monthly average wind velocity	0.001	0.664	0.074	0.081	0.911	-0.009
Monthly maximum wind velocity	-0.007	-0.162	0.431	0.124	-0.554	0.011
Monthly maximum sea-level	0.279	0.069	0.140	0.141	0.000	0.033
Monthly mean sea-level	-0.033	0.006	-0.217	0.048	0.132	0.036
Monthly minimum sea-level	-0.001	-0.124	-0.014	0.020	-0.651	0.062

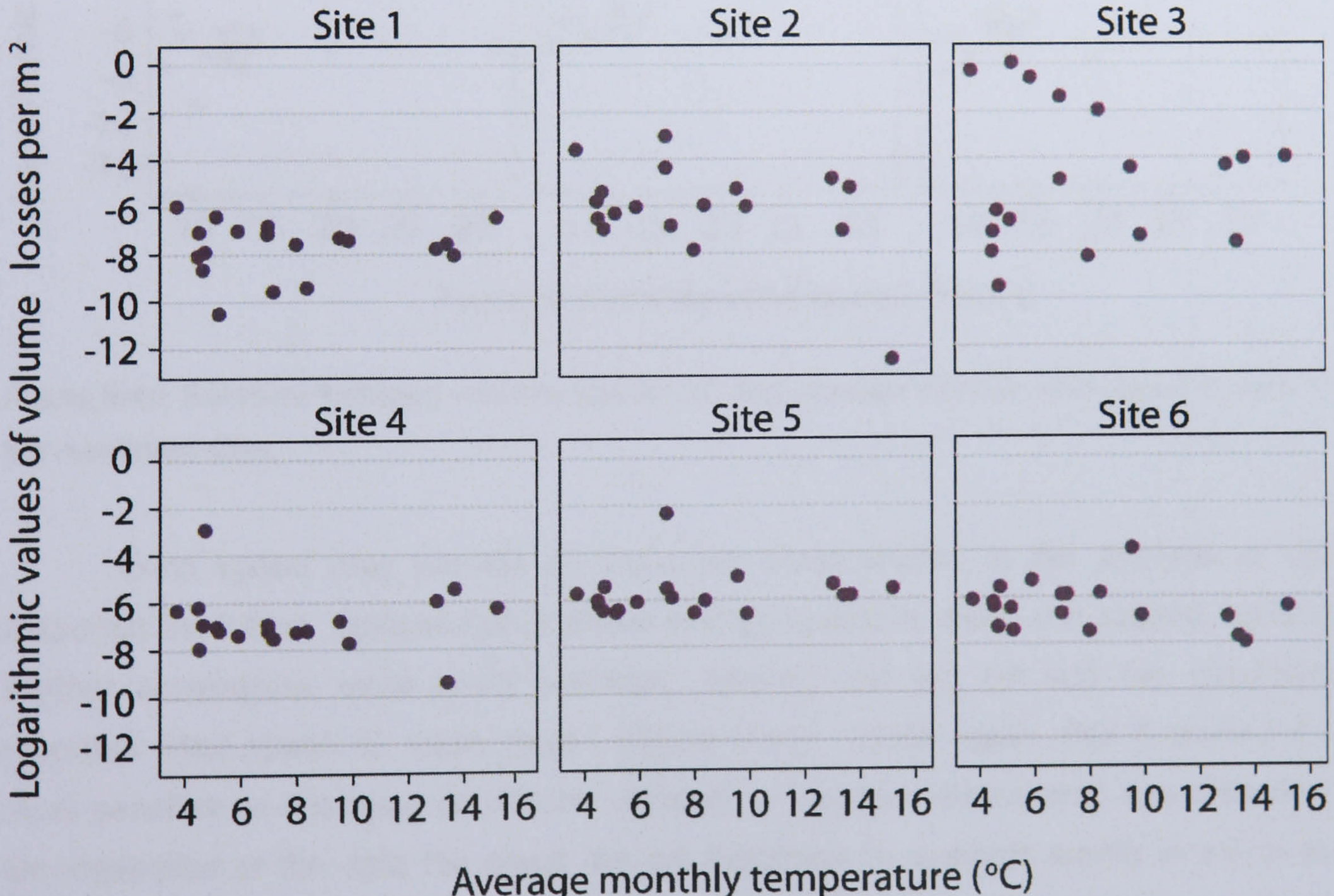

Figure 6.39: Relations between volumes lost per m² and average monthly temperature at each of the monitored sites.

Monthly average wind velocity produced significant positive correlations at Site 2 and Site 5, in which the strength of the relationship was particularly strong, suggesting that cliff change at these localities was sensitive to increasing wind speed

(Figure 6.40). However, when related graphically the strength of the correlations can be largely attributed to isolated outliers. Although positive tendencies can be seen at most sites, the scatter is once again too large to confirm any direct relationship with wind conditions. The scatter may reflect the complexities provided by the direction of individual gusts of wind with respect to the aspect and morphology of the cliff sections, or the tidal conditions if the positive correlations are an indirect measure of wave energy.

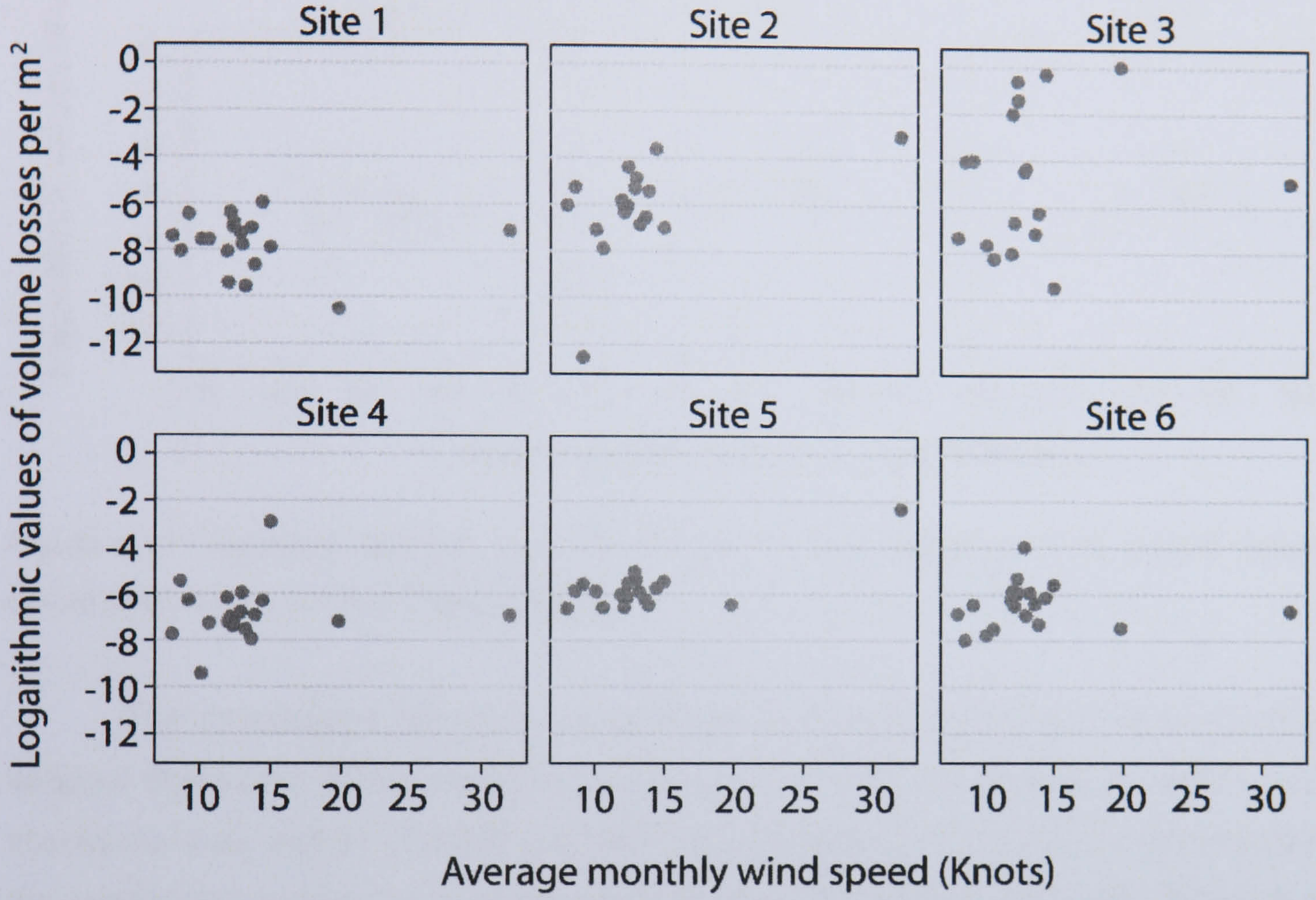

Figure 6.40: Relations between volumes lost per m² and average monthly wind speed at each of the monitored sites.

Wind speed may provide an important consideration in the analysis of cliff response over time, representative of the energy available within the coastal system. Further correlations were noted between volumes lost per m² and the maximum recorded wind speed for each month (Figure 6.41). Once again, Site 5 proved the most sensitive to changing conditions, although a negative relationship was recorded. On inspection of the data the result can be explained by a single month in which an unusually low maximum wind speed was recorded despite relatively high volume losses per m² (approximately 0.01 m³, or -2 on a logarithmic scale). It could be concluded that the average wind conditions, rather than maximum gust speed is a better indication of aeolian influences on rock slope. The correlation may reflect an interdependency with sea-level conditions, although the lack of consistency between sites means such findings require further investigation.

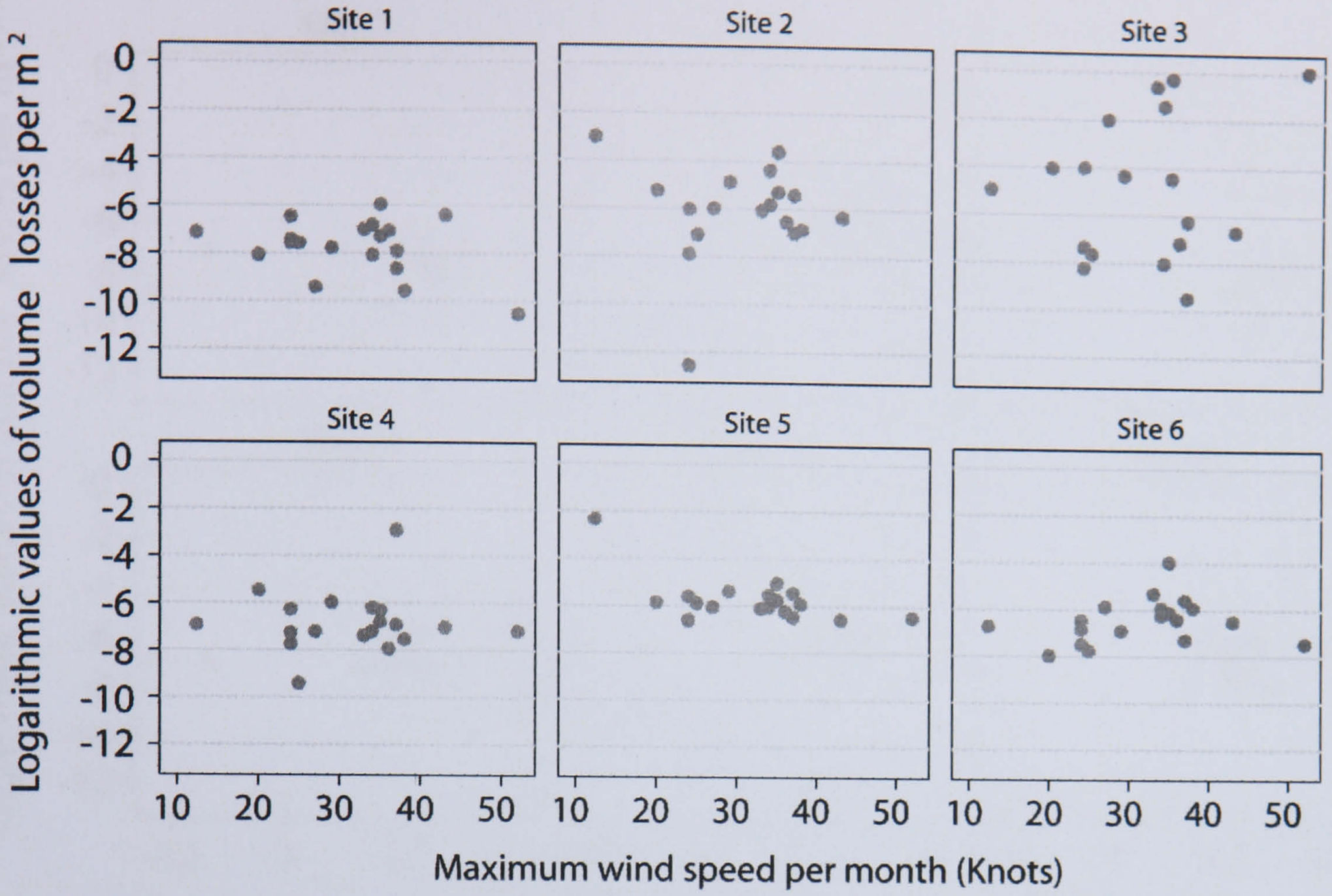

Figure 6.41: Relations between volumes lost per m² and maximum wind speeds recorded during each month at the monitored sites.

The correlations between standardised volumetric losses and wind conditions suggest that some of the monitored sites may be more susceptible to environmental processes than others. Further evidence for site-specific sensitivities was recorded in the relationship between volume losses and minimum monthly sea-levels (Figure 6.42). In accordance with the correlations with wind conditions, Site 5 was again the most responsive to the minimum sea-level recorded during each month. The negative relationship implies that volume losses increase with lower sea-levels but again the graphical representation shows the correlation is influenced by a single outlier. Indeed at all other sites the scatter appears to increase with higher sea-level minimums. The effect of higher sea-levels may therefore generate greater potential for landform change, although such conditions do not necessarily lead to direct responses. The results should be viewed in the context of site specifics. For example, the patterns show that the majority of monthly sea-level minimums occur at or near -2.5 m OD. At Site 5 the cliff responses are relatively stable to these conditions, in contrast to Site 3 in which large variability was recorded. Questions remain over whether the potential impacts of sea-level change, due either to eustatic rises or human-induced subsidence, would cause a threshold to be passed at Site 5 causing a more variable response as was seen at Site 3.

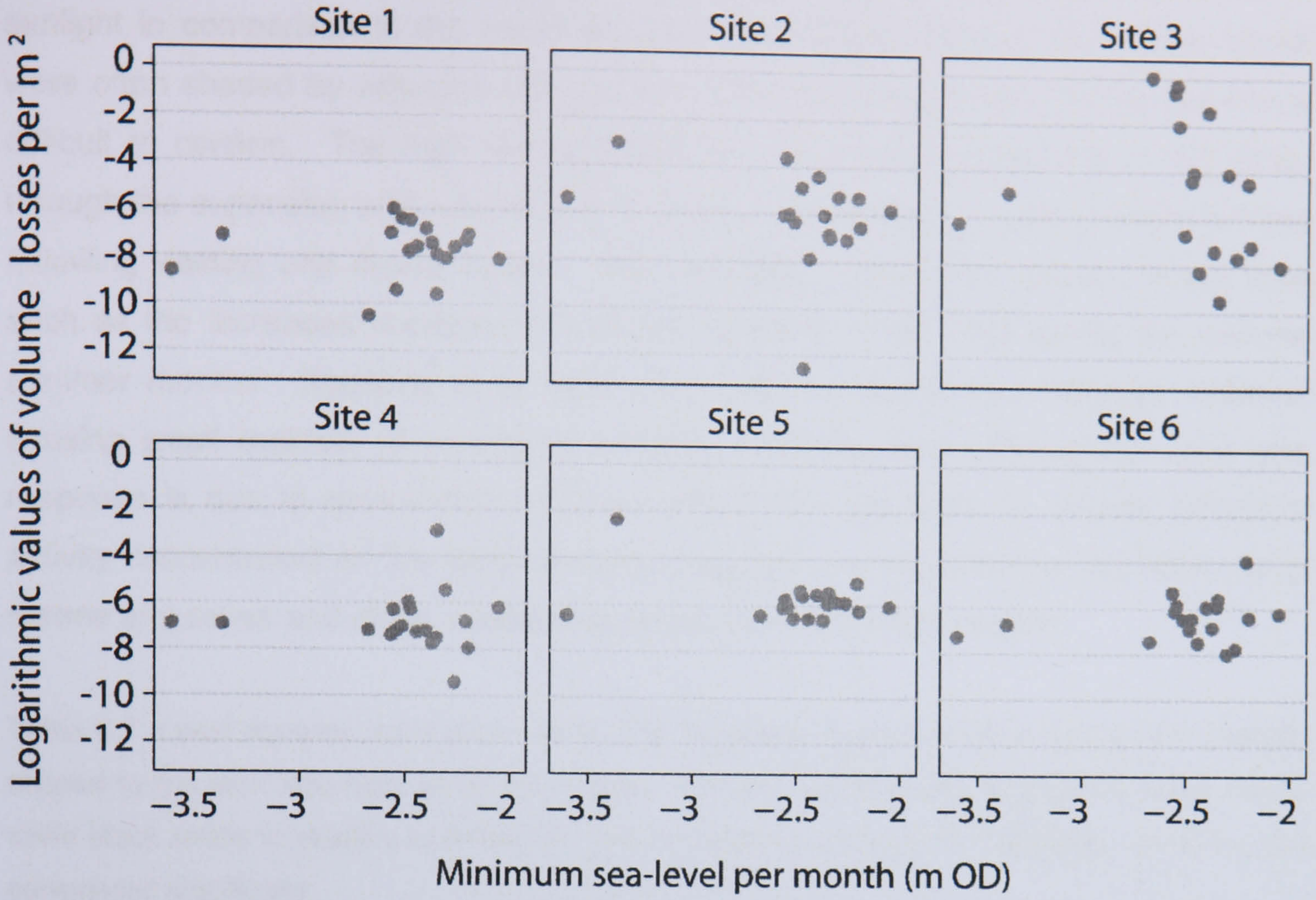

Figure 6.42: Relations between volumes lost per m² and minimum sea-levels recorded during each month at monitored sites.

6.5.3 Direct environmental correlations by rock type

Although the correlations between cliff responses and environmental variables revealed very weak relationships, the difference in the behaviour of individual sites has highlighted the importance of the sensitivity of the monitored locations. In order to investigate the nature of variations in spatial responses, the environmental dataset was correlated with volumetric losses per m² for each of the four main rock types found within the rock mass. The volumes lost for specific rock types were again poorly correlated with environmental drivers of change (Table 6.7). Only the mudstone and sandstone layers were significantly affected by any of the processes recorded, and even then were weakly related to sea-level and temperature respectively. All the interrelations were analysed graphically, but again only the significant correlations are presented.

Average monthly temperatures were found to be significantly correlated with the sandstone bands within the cliff sections (Figure 6.43). The scatter plot shows a very weak increase in volume losses as average monthly temperature increases, a pattern which can also be seen in the siltstone, although the correlation is distorted by a single outlier. The cause of the consistency between these rock layers may lie in their

positioning towards the cliff top at all sites. This leads to greater exposure to direct sunlight in comparison to the mudstone and shale layers lower in the slopes which were often shaded by adjacent cliff sections. The physical process behind the link is difficult to confirm. The high temperatures may cause the weakening of the strata through the expansion and subsequent contraction of material, or lead to brittle failures following wetting and drying cycles. The correlation could also reflect indirect links such as the increased numbers of seabirds attracted to the cliffs during the warmer summer months. Roosting birds were often seen to disturb and dislodge material, causing small rockfalls of weathered material. Whether the difference in rock type response is due to composition, location within the rock slope or reflects biological activity concentrated on the ledge-forming materials, the weakness of the relationship means any cause and effect relationships must be viewed with caution.

Table 6.7: Least squares correlation coefficients between environmental variables and rockfalls divided by the rock type from which they came. The red numbers denote negative relationships while black relate to positive correlations. The correlations above 0.5, highlighted in yellow, are considered significant.

	Mudstone	Shale	Siltstone	Sandstone
Total monthly rainfall	0.046	0.009	0.006	0.225
Peak hourly rainfall	0.451	0.004	0.010	0.116
Average monthly temperature	0.352	0.047	0.020	0.508
Monthly minimum temperature	0.287	0.054	0.014	0.563
Monthly maximum temperature	0.274	0.050	0.023	0.296
Hours below freezing	0.106	0.064	0.000	0.203
Monthly average wind velocity	0.000	0.414	0.016	0.049
Monhtly maximum wind velocity	0.066	0.039	0.118	0.058
Monthly maximum sea-level	0.540	0.056	0.020	0.003
Monthly mean sea-level	0.178	0.115	0.017	0.084
Monthly minimum sea-level	0.000	0.100	0.003	0.081

Similar patterns were noted in the correlations between volume losses per m^2 and minimum monthly temperatures (Figure 6.44). Once again weak positive trends were recorded in the sandstone and siltstone layers whilst the mudstone and shale were more negatively correlated. Below 0 ˚C however, all sites showed increasing scatter towards both greater and lower volumetric changes with reducing minimum temperatures. As with the site specific relations to average monthly wind speed presented earlier (Figure 6.40), the scatter reflects a more complex, variable response to environmental changes, with some decreases leading to detectable changes to slope activity, and other similar conditions having little effect on cliff morphology. The divergent response at 0 ˚C suggests that the mechanical influence of freezing water may be an important factor in causing material to become detached although colder

temperatures are also associated with the more stormy winter months, making it difficult to decipher the exact cause of the correlations.

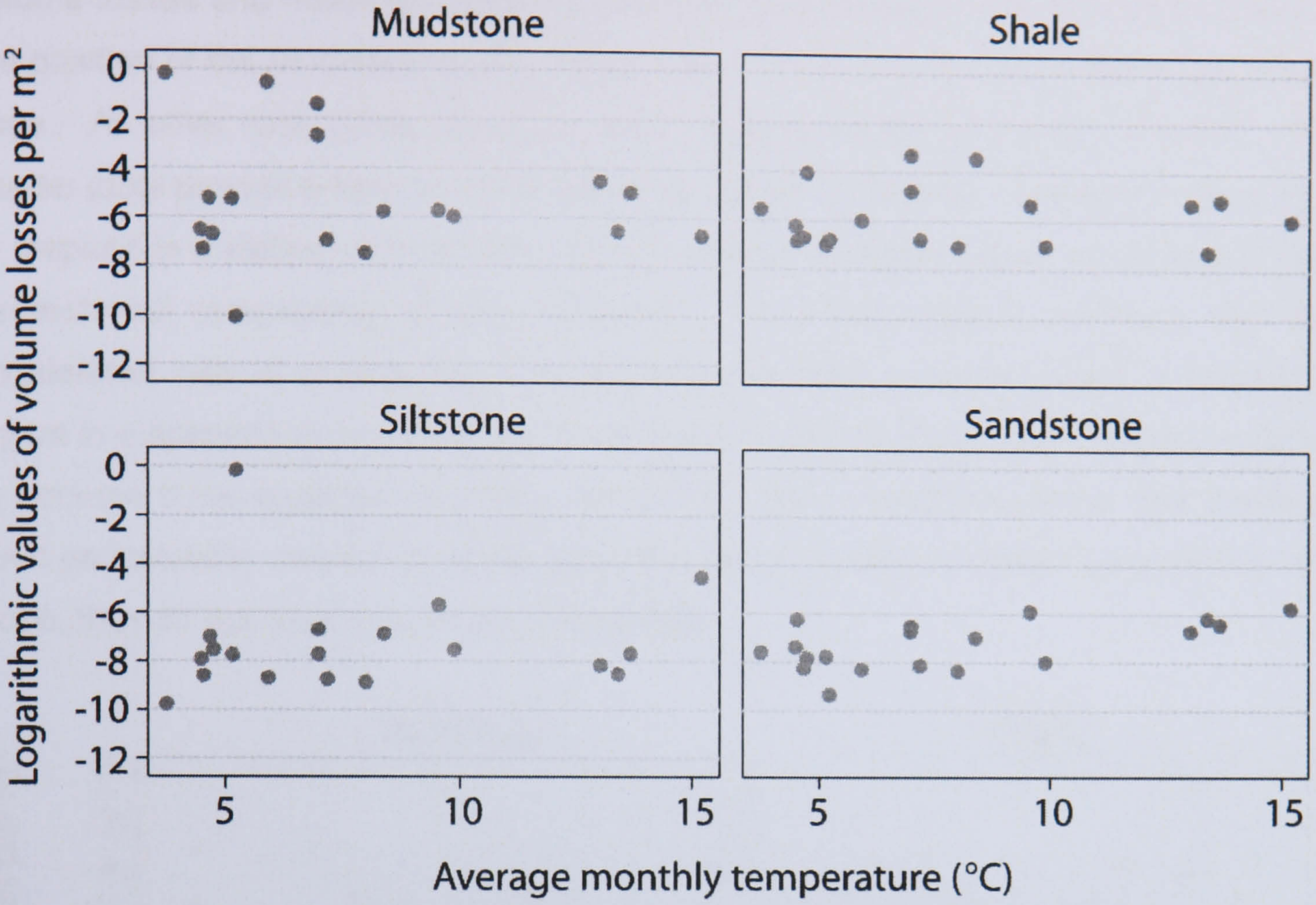

Figure 6.43: Monthly rockfall correlations with average monthly temperatures for each of the four main rock types.

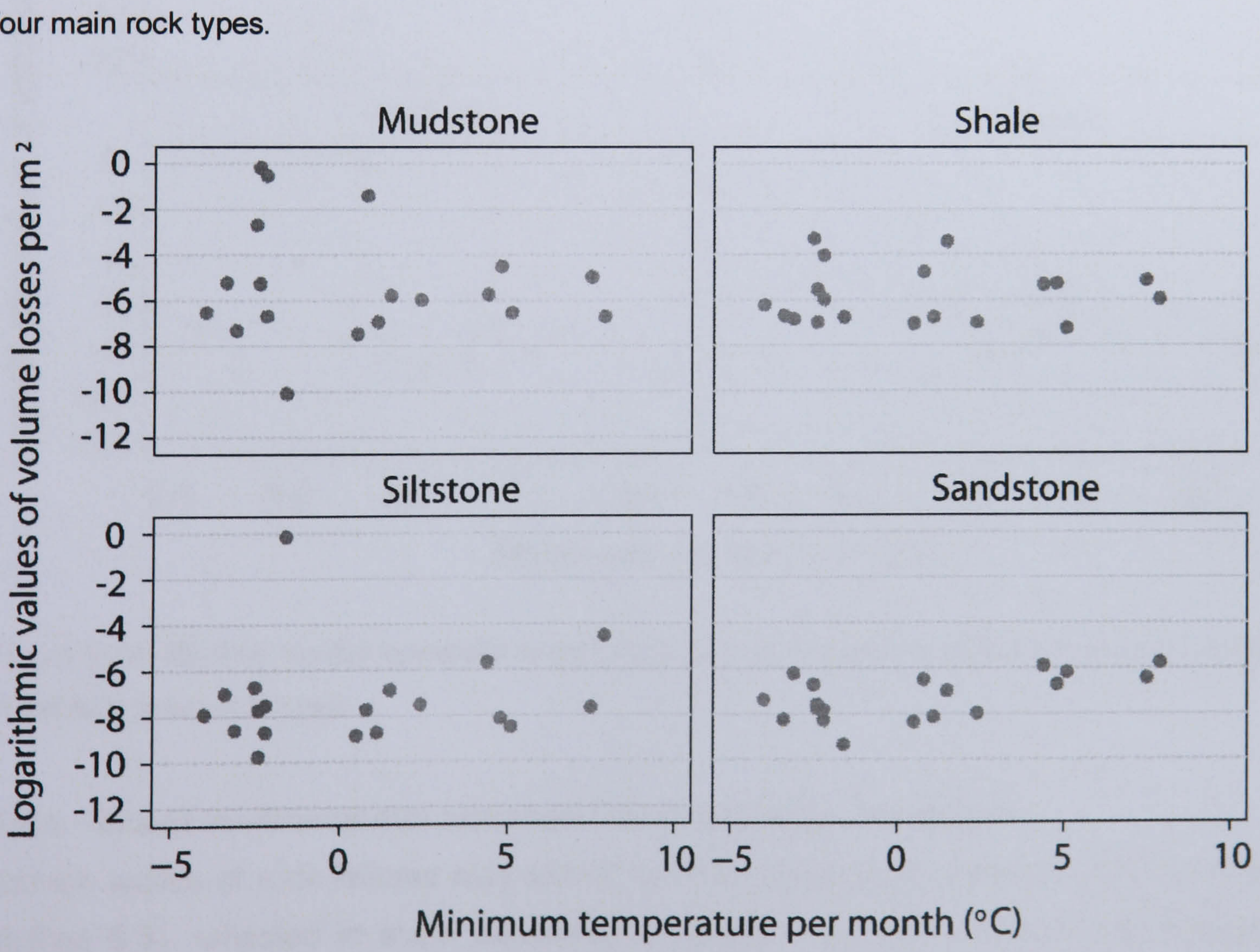

Figure 6.44: Monthly rockfall correlations with minimum temperatures recorded during each month in the four main rock types.

Mudstone was the only rock type that showed a significant relationship between volume losses and maximum monthly sea-level (Figure 6.45). The correlation reflects the position of the mudstone layers, which were almost entirely within the wave impact zone. All other rock types recorded weak negative tendencies with sea-level. The scatter plots provide evidence of the influence of marine activity, causing the basal rock to respond in a distinct manner from the rest of the cliff face despite the relatively high geotechnical competence of the mudstone. The finding raises questions over the accelerated rate of change likely to occur at the sites currently based in mudstone layers in a scenario of sea-level rise or subsidence which would cause weaker material to become more exposed to marine influence. The correlations show that if effects such as instability caused by wave pounding do propagate to higher parts of the rock slope, they do not appear to do so immediately.

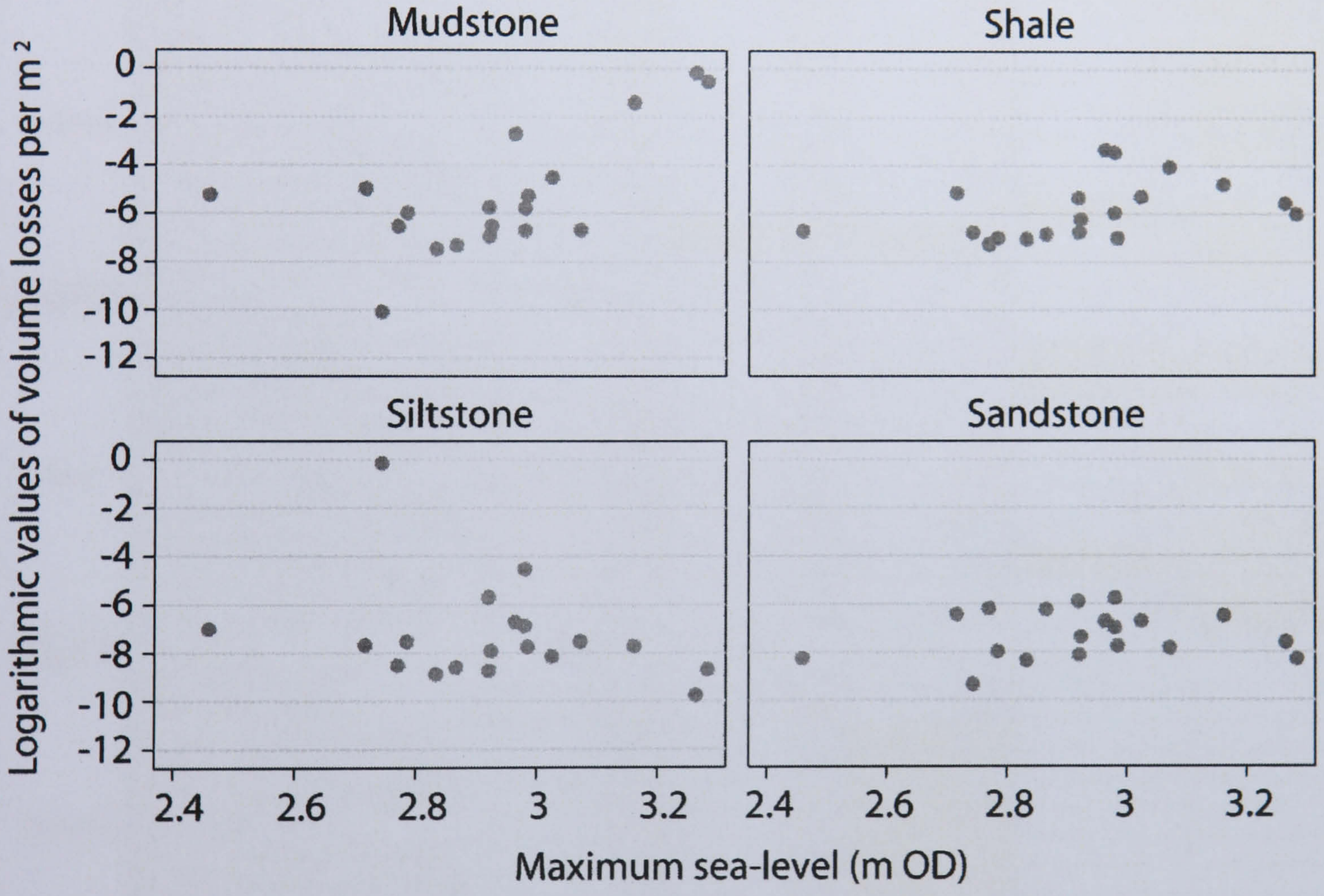

Figure 6.45: Monthly rockfall correlations with maximum sea-levels recorded during each month in the four main rock types.

6.5.4 Direct environmental correlations by rock type and volume

Certain scales of rock failures may exhibit specific behavioural patterns (refer back to section 6.3), reflected in scale dependencies noted both across space and through time. It was therefore decided to subdivide the responses of each of the four main rock types by the volume classes used previously in the analysis (Table 6.8). On initial inspection the number of significant correlations appears to have increased

substantially, but the reduced numbers of failures in the larger class categories are insufficient to draw any conclusions on the influence of environmental processes. Only the classes with significant correlations and which include 10 or more rockfalls are presented, this corresponds to one event every two months of monitoring. This meant that both the shale and the siltstone had insufficient failures within the scale classes for the relationships to be considered valid, highlighting the limitations of the dataset.

Table 6.8: Least squares correlation coefficients between environmental variables and rockfalls for each of the main rock types, subdivided by the size of the material loss. The red numbers denote negative relationships while black relate to positive correlations. The correlations above 0.5, highlighted in yellow, are considered significant.

		Class 1: Below 0.1 m³	Class 2: 0.1 m³ to <1 m³	Class 3: 1 m³ to <10 m³	Class 4: 10 m³ to <100 m³	Class 5: Over 100 m³
Number of observations		17736	481	72	14	3
Mudstone	Total monthly rainfall	0.151	0.206	0.033	0.715	0.006
	Peak hourly rainfall	0.201	0.270	0.302	0.137	0.892
	Average monthly temperature	0.218	0.330	0.186	0.057	0.899
	Monthly minimum temperature	0.103	0.118	0.113	0.079	0.889
	Monthly maximum temperature	0.103	0.149	0.084	0.140	0.883
	Hours below freezing	0.011	0.000	0.018	0.005	0.983
	Monthly average wind velocity	0.004	0.041	0.049	0.326	0.614
	Monhtly maximum wind velocity	0.173	0.297	0.131	0.042	0.148
	Monthly mean sea-level	0.052	0.219	0.152	0.593	0.971
	Monthly maximum sea-level	0.485	0.534	0.665	0.000	0.736
	Monthly minimum sea-level	0.024	0.108	0.055	0.190	0.807
Number of observations		74071	523	60	3	3
Shale	Total monthly rainfall	0.001	0.000	0.118	0.289	0.389
	Peak hourly rainfall	0.093	0.001	0.050	0.918	0.913
	Average monthly temperature	0.194	0.006	0.011	0.523	0.769
	Monthly minimum temperature	0.154	0.000	0.101	0.216	0.115
	Monthly maximum temperature	0.088	0.120	0.002	0.466	0.042
	Hours below freezing	0.317	0.000	0.085	0.000	0.597
	Monthly average wind velocity	0.084	0.277	0.024	0.075	0.226
	Monhtly maximum wind velocity	0.192	0.064	0.020	0.043	0.751
	Monthly mean sea-level	0.098	0.135	0.014	0.589	0.976
	Monthly maximum sea-level	0.293	0.136	0.071	0.023	0.999
	Monthly minimum sea-level	0.011	0.042	0.135	0.347	0.532
Number of observations		11162	53	4	0	0
Siltstone	Total monthly rainfall	0.148	0.400	0.493	.	.
	Peak hourly rainfall	0.004	0.069	0.281	.	.
	Average monthly temperature	0.001	0.011	0.737	.	.
	Monthly minimum temperature	0.011	0.108	0.523	.	.
	Monthly maximum temperature	0.072	0.070	1.000	.	.
	Hours below freezing	0.009	0.147	0.932	.	.
	Monthly average wind velocity	0.105	0.000	0.976	.	.
	Monhtly maximum wind velocity	0.000	0.058	0.990	.	.
	Monthly mean sea-level	0.236	0.174	0.992	.	.
	Monthly maximum sea-level	0.002	0.005	1.000	.	.
	Monthly minimum sea-level	0.023	0.087	0.298	.	.
Number of observations		10241	69	7	0	0
Sandstone	Total monthly rainfall	0.002	0.514	0.151	.	.
	Peak hourly rainfall	0.070	0.121	0.037	.	.
	Average monthly temperature	0.053	0.000	0.358	.	.
	Monthly minimum temperature	0.086	0.084	0.297	.	.
	Monthly maximum temperature	0.002	0.097	0.247	.	.
	Hours below freezing	0.135	0.131	0.122	.	.
	Monthly average wind velocity	0.112	0.011	0.197	.	.
	Monhtly maximum wind velocity	0.041	0.193	0.086	.	.
	Monthly mean sea-level	0.146	0.243	0.043	.	.
	Monthly maximum sea-level	0.027	0.018	0.048	.	.
	Monthly minimum sea-level	0.004	0.232	0.130	.	.

The Class 4 failures from the mudstone layers correlated significantly with total rainfall, although the data were restricted to 14 events which meant the relationship must be viewed with caution (Figure 6.46). The negative trend suggests that higher volume losses were associated with lower amounts of rain. The response of the mudstone may again be explained by its location at the base of the cliff sections. The other rock types all generated null or weak positive correlations with monthly rainfall totals suggesting that the negative trends in mudstone failures of every size class may reflect a distinct set of processes. The summer months with larger than average rainfall totals also coincided with calmer wind and therefore wave conditions. The distinct behaviour of the mudstone may therefore reflect the presence or absence of marine influences rather than the direct effect of rainfall amounts.

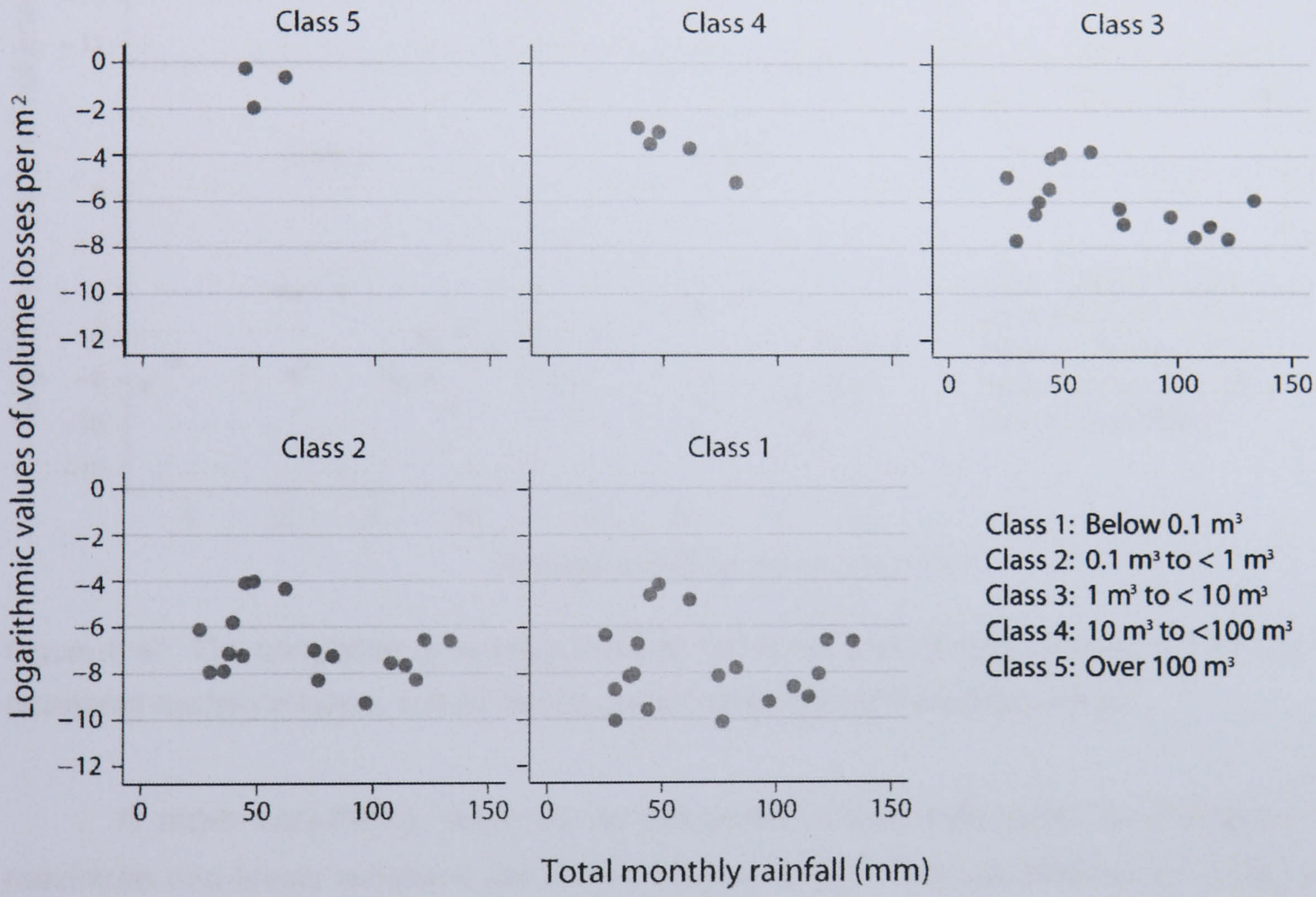

Figure 6.46: The correlation of total monthly rainfall with rockfall volumes per m² from monitored mudstone layers, subdivided by classes of the size of individual failures.

In accordance with the suggestion that marine influence may cause the mudstone strata to behave distinctly from the other rock layers, it was found to be the only rock type, with sufficient failures, which correlated significantly with sea-level characteristics. A positive correlation was recorded between Class 4 sized failures and mean monthly sea-levels setting them apart from smaller scale events which did not appear to be related (Figure 6.47). The sensitivity of failures involving between 10 m^3 and 100 m^3 may relate to the potential for higher sea-levels to lead failures which have become increasingly unstable over time. For example, several such failures were

recorded from the arched formations at Site 2 at which the discontinuity characteristics caused large bodies of material to be particularly susceptible to undercutting. It is possible that the occurrence of failures corresponded with a month of higher sea-levels in which the rate of undercutting would have been high. Ultimately, the lack of correlations in different scale failures raises doubt over the importance of average monthly sea-levels as a trigger for rockfall activity.

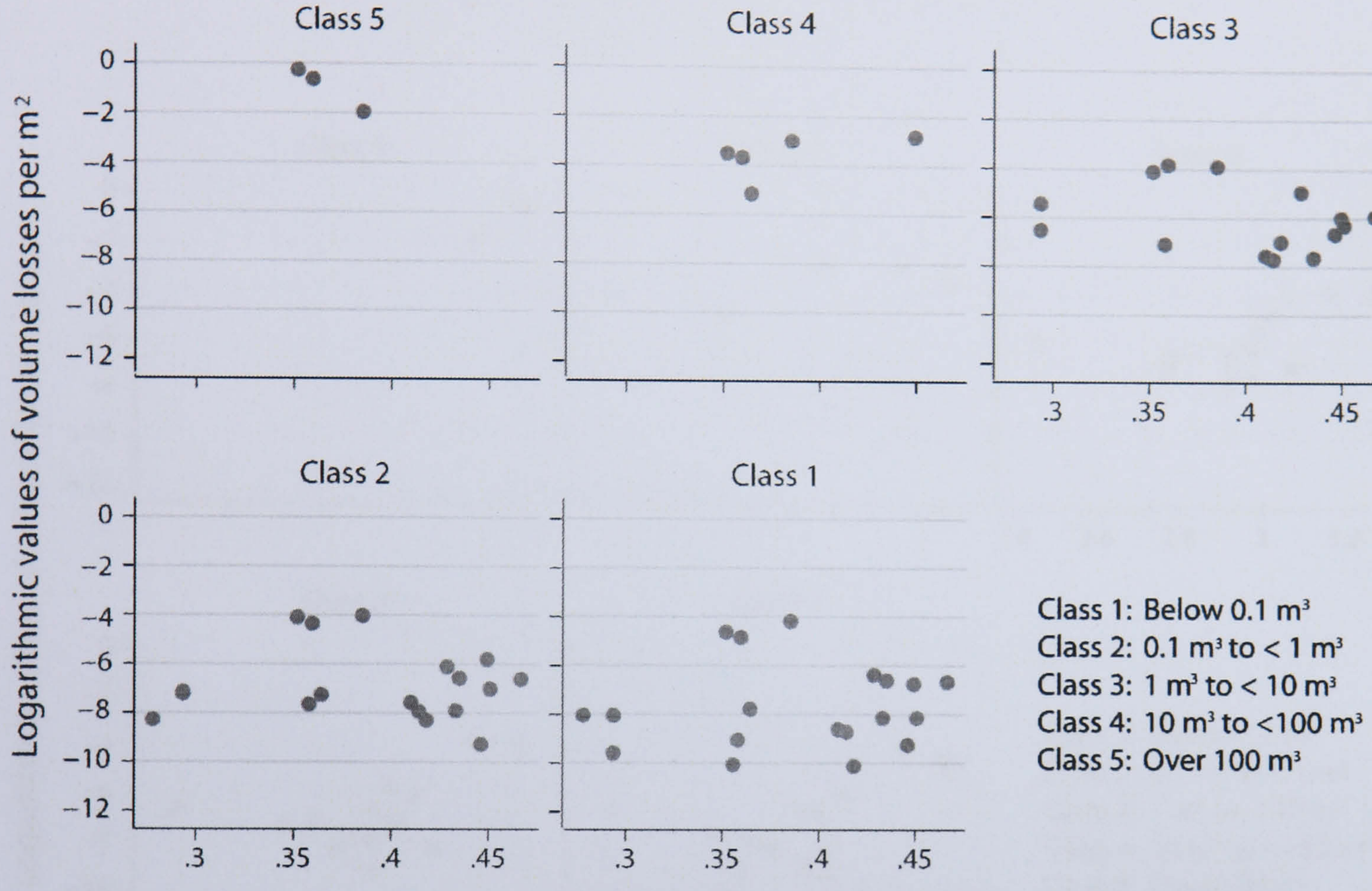

Figure 6.47: The correlation of average monthly sea-levels with rockfall volumes per m² from monitored mudstone layers, subdivided by classes of the size of individual failures.

A more convincing response in volumetric losses was seen to changes in maximum sea-levels recorded per month (Figure 6.48). The correlations for Class 2 and Class 3 were based on 481 and 72 observations respectively, adding validity to the positive relations recorded. An increased number of occurrences in the full range of size classes were associated with more extreme sea-level maximums. This suggests that maximum sea-levels may be a more important characteristic than monthly average levels, and that rock slope activity may be more closely associated with extreme marine conditions rather than general changes in base levels. Interestingly, the only scale range not to show a relatively strong positive relationship with sea-level maximums was Class 4. It may therefore be that this specific scale of event is more susceptible to extended periods of marine activity rather than the triggering influence of a few particularly high tides. Furthermore the interplay between cliff response to extreme and average conditions is evident in the distribution of the relationships with

the sea-level record. Average monthly sea-levels generally produced an even spread in the data, and weaker correlations. However the response of volume losses to maximum sea-levels appears to demonstrate a threshold at about 2.8 m OD, beyond which higher maximum sea-levels cause significant changes in the mudstone at all failure scales. If such sensitivity does exist it holds implications for the potential of future sea-level change, switching the emphasis from the average height of the sea to variability in extreme tides and the propensity for critical heights to be reached.

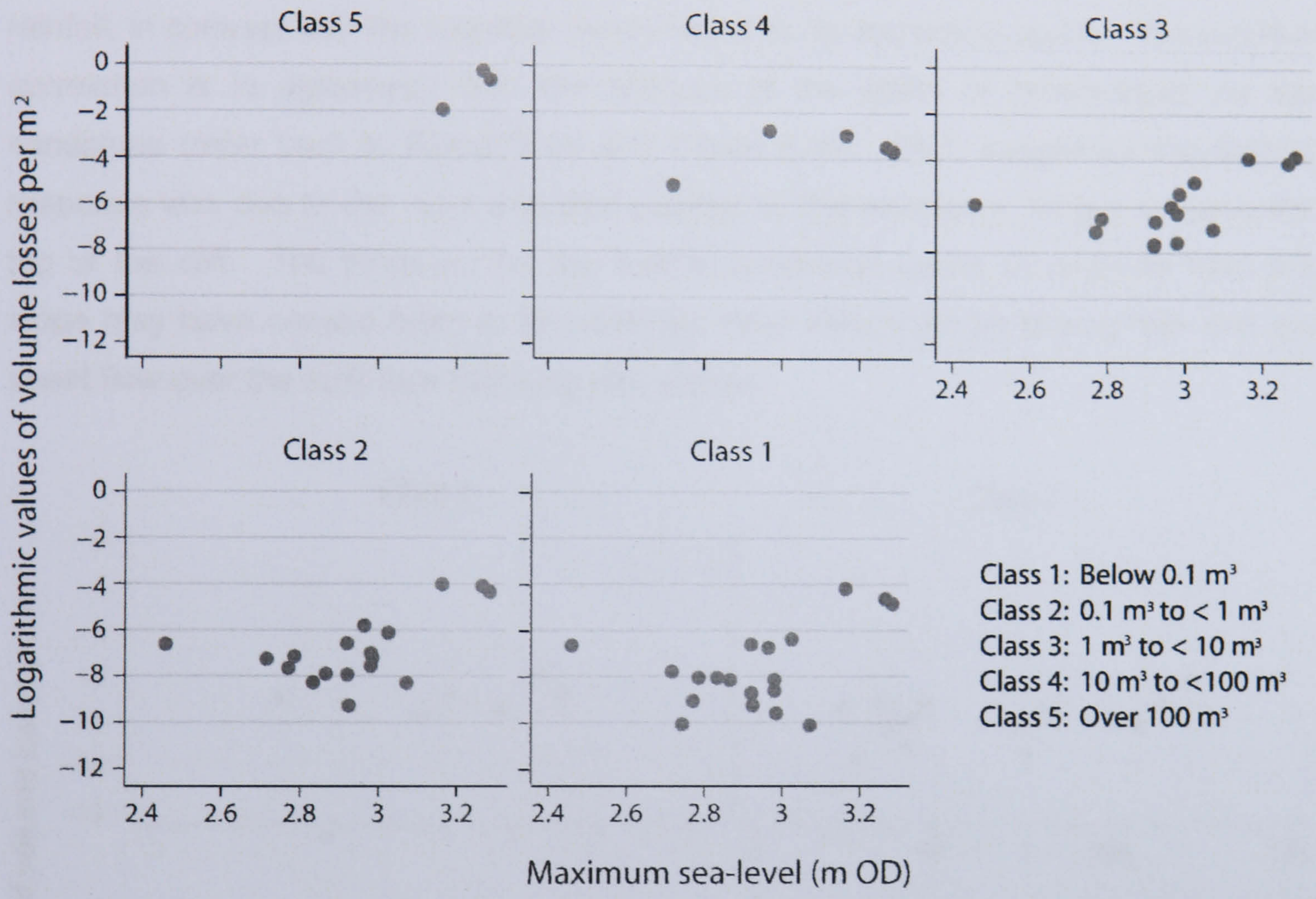

Figure 6.48: The correlation between maximum sea-levels recorded per month and rockfall volumes per m² from monitored mudstone layers, subdivided by classes of the size of individual failures.

The shale and siltstone layers recorded no significant direct correlations with any of the variables in the environmental dataset when 10 or more failures were considered. In the case of the siltstone this was largely due to the small proportions of the rock slopes accounted for by the rock type. This was not the case for the shale layers which constituted more of the monitored slopes than any other rock type. One possible reason for the poor correlations with environmental processes in the shale bands may be that the failures were dominated by the smallest scale classes of failures. It was noted earlier that the temporal patterns in the Class 1 and Class 2 exhibit less seasonal, more cyclical changes (refer back to Figure 6.23). The smallest

volumetric losses, which dominate change in the shale strata, may therefore occur more consistently, irrespective of prevailing weather conditions. The data reinforce the suggestion that there may be a base level of cliff change, perhaps internally rather than externally driven.

Although the sandstone accounted for a similar proportion of the monitored rock slopes as the siltstone a significant correlation involving sufficient numbers of losses was detected with changes in total monthly rainfall (Figure 6.49). The Class 2 failures, involving material between 0.1 m^3 and 1 m^3, revealed a weak positive relationship with rainfall, in contrast with the negative trends noted in the mudstone layers. The positive correlation is in agreement with the analysis of the effect of temperature on the sandstone (refer back to Figure 6.43 and Figure 6.44), which suggested the distinct response was due to the more exposed position of the sandstone ledges towards the top of the cliff. The tendency for the harder sandstone layers to protrude from the slope may have caused them to be relatively more influenced by driving rain and the sheet flow over the rock face following rain storms.

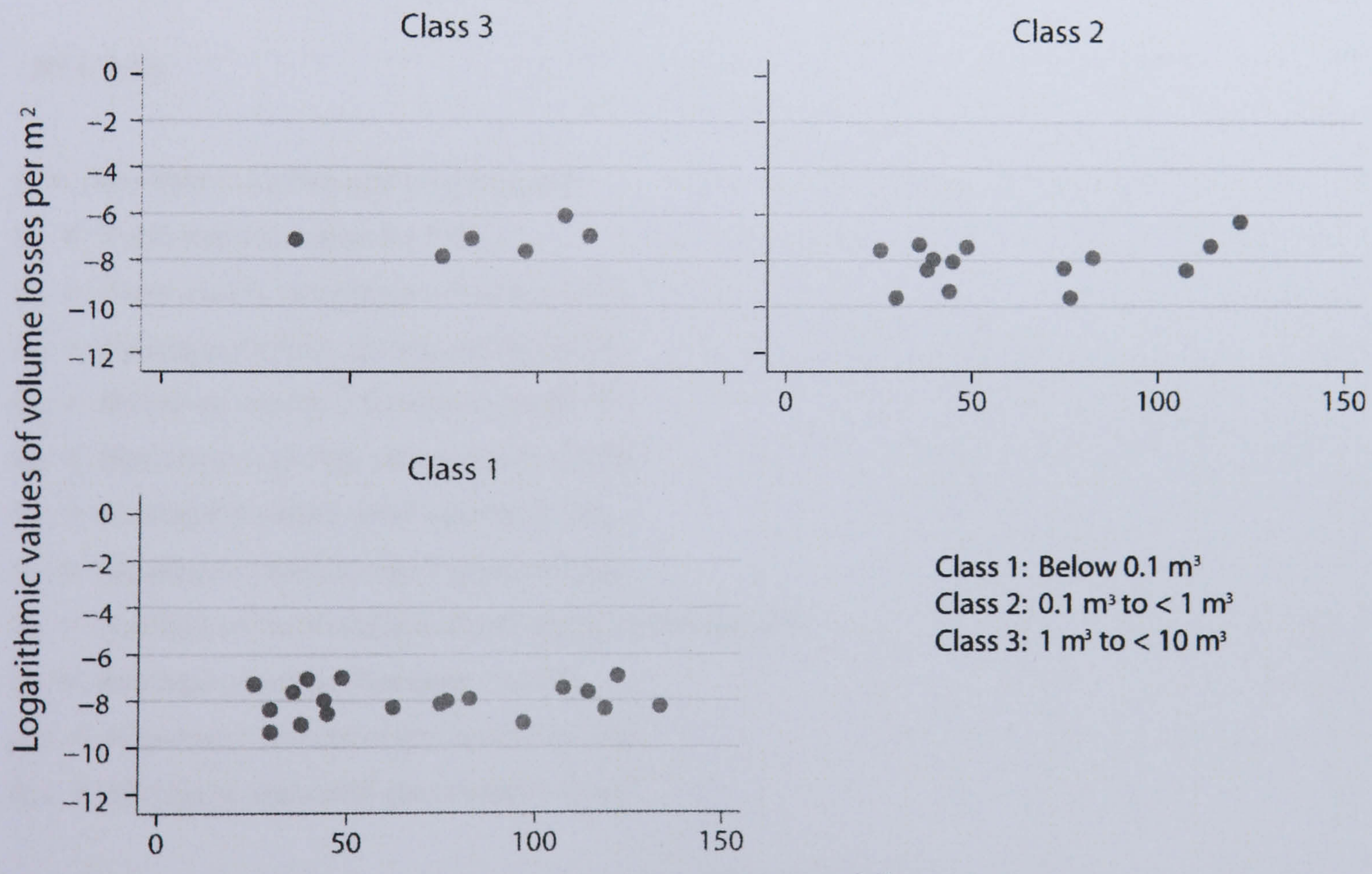

Figure 6.49: The correlation of total monthly rainfall with rockfall volumes per m^2 from monitored sandstone layers, subdivided by classes of the size of individual failures.

Many of the environmental processes recorded have failed to show any direct links to changes in standardised volumetric losses. One explanation for the poor correlations may be an inability to separate out distinct environmental elements. For

example, a weak correlation between rock slope response and average monthly temperatures may reflect the cooling influence of higher average monthly wind speeds. An attempt was made to account for the numerous environmental influences on volumetric losses with the use of multiple regression. Initially, all of the available variables were regressed and their standardised beta coefficients calculated (Equation 6.1). The beta coefficients represent a measure of the relative importance of the regression coefficients in the model, when standardised to a mean of 0 and a standard deviation of 1. When the weaker coefficients were removed, the regression performed poorly suggesting that all of the environmental variables need to be considered in the analysis of hard rock cliff change. Although use of all of the environmental measurements achieved an R^2 value of 0.66, the validity of the regression is drawn into question by sensitivity of the model and the assumption that the predictors are uncorrelated. Evidently there exists intercorrelation between average variables and extremes of the same process such as maximum and minimum values.

$$y = -824.7374 - 6.916\,(ß_1) - 95.143\,(ß_2) + 116.310\,(ß_3) + 115.755\,(ß_4) - 135.743\,(ß_5) + 23.444\,(ß_6) + 26.320\,(ß_7) + 7.019\,(ß_8) - 6380.505\,(ß_9) + 1032.952\,(ß_{10}) - 640.606\,(ß_{11})$$

$R^2 = 0.66$

y = Monthly volumes lost from the cliff

$ß_1$ = Total monthly rainfall (-0.37)

$ß_2$ = Peak hourly rainfall per month (-0.43)

$ß_3$ = Average monthly temperature (0.69)

$ß_4$ = Minimum monthly temperature (0.71)

$ß_5$ = Maximum monthly temperature (-0.95)

$ß_6$ = Average monthly wind speed (0.18)

$ß_7$ = Maximum monthly wind speed (0.33)

$ß_8$ = Number of hours below freezing per month (0.24)

$ß_9$ = Average monthly sea-level (-0.47)

$ß_{10}$ = Maximum sea-level per month (0.30)

$ß_{11}$ = Minimum sea-level per month (-0.34)

Equation 6.1: Performance of monthly volumetric losses regressed against all monitored environmental variables. The numbers in brackets relate to the standardised beta coefficients which provide a measure of the significance of each variable in the regression. When the weaker predictors were removed the regression performed poorly suggesting the high R^2 may reflect the intercorrelation of the variables rather than a high model performance.

A more appropriate regression was performed on the measures representing average environmental conditions (Equation 6.2). The performance of the model using just average variables was notably weaker than the model including the whole dataset, with an R^2 of 0.37. Average monthly sea-level was the more significant than the climatic variables but the weak overall performance meant that the regression could not be improved by the further removal of predictor variables. The regression suggests that in general, average monthly environmental conditions provide little benefit in explaining the patterns of behaviour in hard rock coastal cliffs. The data hold important implications for the way in which we view environmental influences on rock slope development.

$$y = 2661.157 - 3.567\ (ß_1) - 55.989\ (ß_3) + 30.026\ (ß_6) - 4864.809\ (ß_9)$$

$R^2 = 0.37$

y = Monthly volumes lost from the cliff

$ß_1$ = Total monthly rainfall (-0.19)

$ß_3$ = Average monthly temperature (-0.33)

$ß_6$ = Average monthly wind speed (0.23)

$ß_9$ = Average monthly sea-level (-0.36)

Equation 6.2: Performance of monthly volumetric losses regressed against the environmental variables considered representative of average monthly conditions. The numbers in brackets relate to the standardised beta coefficients which provide a measure of the significance of each variable in the regression.

An important distinction can be made between the environmental effects of average and extreme events. A regression of volumetric losses against the extreme environmental measures in the dataset performed relatively poorly, but provided a marked improvement from the use of average conditions (Equation 6.3). When maximum wind speed was removed, the regression performed equally well suggesting it could be dropped from the regression; the other regression coefficients were important to the model performance. The tendency for more extreme environmental factors to be more closely associated with rock slope change further suggests that understanding into contemporary and future cliff behaviour requires a consideration beyond general base levels to the magnitude and variability of weather conditions.

$$y = -1573.647 - 41.591\ (ß_2) - 67.557\ (ß_4) + 7.858\ (ß_7) - 11.494\ (ß_8) + 1112.151\ (ß_{10})$$

$R^2 = 0.44$

y = Monthly volumes lost from the cliff

$ß_2$ = Peak hourly rainfall per month (-0.19)

$ß_4$ = Maximum monthly temperature (-0.47)

$ß_7$ = Maximum monthly wind speed (0.10)

$ß_8$ = Number of hours below freezing per month (-0.40)

$ß_{10}$ = Maximum sea-level per month (0.32)

Equation 6.3: Performance of monthly volumetric losses regressed against environmental variables considered to represent the most extreme weather conditions. The numbers in brackets relate to the standardised beta coefficients which provide a measure of the significance of each variable in the regression.

6.5.5 Least squares correlation coefficients

Attempts to identify direct links between environmental variables and rockfalls have proven problematic. Although discernible patterns were detected, they were often weak and inconsistent, even when subdivided by site, rock type and/or volume size of failures. One possible cause for the scatter recorded in the data may be the way in which the relationship is analysed. Some of the complexity involved with cliff response to environmental conditions was attributed to distinct behaviour associated with different magnitude failures. It is possible that the sensitivity of the cliff to environmental variables varies according to the size of losses considered. Therefore it may be more appropriate to investigate the strength of the correlation between rockfalls and environmental variables, rather than the quantitative changes between datasets. Least squares correlation coefficients were used to analyse how the strength of the relationship between rockfalls and environmental processes changes when just losses below certain magnitude cut-offs were considered. Failures above 10 m^3 were excluded from the analysis because, as demonstrated above, when subdivided by rock type the scarcity of data points leads to artificially high correlations. It should be noted that the emphasis of the analysis is on how the strength of the relationships change rather than the actual quantitative correlations which are likely to be as low as those previously established fro the data.

The strength of the relationship between the four main rock types and total monthly rainfall was compared for different maximum sizes of failure volumes (Figure

6.50). The relationship between mudstone and rainfall was strongest for changes below 0.001 m^3, once again showing a negative correlation which demonstrates wetter months do not necessarily increase the occurrence of changes. The correlation remains relatively unchanged until losses of 0.05 m^3 are included, above which the strength of the relationship with rainfall steadily decreases. A similar trend is seen in the shale material with the inclusion of increasing material size associated with decreasing correlations. Both the mudstone and shale behave in a logical manner because as increasing magnitudes are included, greater numbers of failures increase the potential for variability to be included in the response which reduces the correlation. However, the behaviour of siltstone differed significantly, recording a dramatic fall in its relationship with monthly rainfall totals when material losses above 0.001 m^3 were considered; causing both a drop in the correlation and an inversion of the relationship. The implication is that the smallest changes in the siltstone occurred during drier months, whilst changes above 0.001 m^3 were weakly associated with increases in rainfall which had similar effects despite increasing failure size. Sandstone was the only rock type to show positive correlations for every size of failure up to 10 m^3. Monthly rainfall has minimal impact on the smallest losses but has greatest influence when changes below 0.004 m^3 are considered. The larger losses can be less well associated with monthly rainfall. These results reinforce the decision made earlier to exercise caution over the environmental correlations with the largest magnitude class of failures which appeared to be biased by the low numbers of such losses recorded. With the use of least squares correlation coefficients the trend of reducing susceptibility to environmental factors with increasing size of failure can clearly be seen in many instances.

The correlations of peak hourly rainfall with losses from mudstone strata suggested that failures were increasingly affected by rain intensity up to 0.05 m^3 before the significance decreased with larger volumes (Figure 6.51). The negative correlations, peaking between 0.01 m^3 and 0.1 m^3, add a scale definition to the observations noted earlier that the rainfall characteristics were inversely correlated with mudstone losses (refer back to Figure 6.46). It was suggested that the response of the mudstone may reflect calmer sea conditions during summer months rather than directly relating to rainfall. The highest correlations in the shale were found at a maximum cut-off an order of magnitude smaller than the mudstone, once again declining with the incorporation of larger failures. The initial increase in the strength of the relationship suggests the smallest failures recorded may be responding to a different set of processes. This trait was common to many of the relationships analysed, causing the least squares correlations to behave distinctly in the smallest failures, typically below

0.005 m^3. The pattern was also seen in the sandstone layers, decreasing after 0.005 m^3 with larger changes. The positive correlations indicate that the sandstone was the only rock type to experience greater activity with higher amounts and intensities of rainfall, possibly caused by its exposed and protruding position within the cliff. Siltstone revealed a direct relation with peak rainfall exerting significantly more influence on the smallest losses becoming negligible with failures over 0.05 m^3.

The correlations with average monthly temperature were very similar to those found with peak hourly rainfall for the mudstone, shale and siltstone layers (Figure 6.52). The strongest correlations with average temperature were marginally more significant than with peak hourly rainfall but the overall patterns were much the same for the two environmental variables. The consistencies suggest there may be intercorrelation between higher monthly temperatures and rainfall intensity, both of which are concentrated in summer months. The connection between the two variables may be further supported in the behaviour of the losses from the sandstone. The correlations with average temperature performed less well for the majority of failure sizes, particularly when larger failures were included, but the highest correlations were greater than those calculated for peak hourly rainfall. The data indicate that whilst rainfall may be more important to the failure of the sandstone, it is only when combined with higher temperatures that the most significant changes occur. The correlations with minimum (Figure 6.53) and maximum (Figure 6.54) monthly temperatures support this analysis with very similar patterns of sensitivity. However, the correlations were slightly weaker suggesting that the activity in this instance was more closely associated with a rise in monthly base conditions rather than the occurrence of isolated extreme events.

The effect of the number of hours below freezing was minimal on the mudstone, which showed a relatively weak and incoherent pattern of correlations (Figure 6.55). The smallest losses in the siltstone and sandstone were more significantly related to monthly hours below freezing but the greatest influence was recorded on the shale layers. Failures involving up to 0.005 m^3 from the shale were at least four times more strongly correlated than losses from other rock types, the responsiveness tailed off when larger values were used. The data therefore suggest that the shale within the cliff was more sensitive to the freezing temperatures and that the processes associated had greatest effect on specific sizes of material.

Average monthly wind speed had significantly greater effects on the mudstone, shale and siltstone than on the sandstone failures (Figure 6.56). The mudstone and siltstone displayed progressively less sensitivity to monthly wind speed with the

inclusion of larger volumes of material, with influence becoming insignificant on change above 0.1 m^3. The response of the mudstone may reflect the propensity for higher winds to be associated with marine erosion during more stormy winter months. The patterns within the siltstone correlations were weaker and less consistent without the direct contact from pounding waves, but nevertheless appear influenced by higher energy conditions. Failures from the shale involving up to 0.005 m^3 proved most strongly correlated with average wind speed, illustrating the susceptibility of the weaker material to high energy conditions. Only the sandstone layers beyond 0.01 m^3 appear affected by monthly wind conditions and even then the correlation is so weak it would be hard to conclude they had any detectable influence on the rock behaviour.

It was noted previously in the analysis that the effect of wind may have been more site specific than correlated to rock type or volume size (refer back to Table 6.6, Table 6.7 and Table 6.8). The correlations with maximum wind speed demonstrate notable differences from the responses to average monthly wind speeds (Figure 6.57). In contrast with the direct quantitative analysis (refer back to Figure 6.41), the smaller scale changes from the mudstone, shale and siltstone correlated more strongly with maximum gust than average monthly wind speed. The pattern of the mudstone response also demonstrated a larger range of losses, volumes up to 0.1 m^3 were affected by maximum wind speeds. The change in sandstone correlations with maximum wind speed generated the greatest difference with average wind speeds. Maximum wind speeds were most strongly related to the smallest changes, dropping sharply with changes above 0.001 m^3. When combined the patterns indicate the smallest changes in the sandstone are more closely related to maximum monthly wind speeds, but the larger changes respond more with average monthly wind conditions; although once again the weak correlations mean the effects are likely to be minimal.

The correlations between mudstone and average monthly sea-levels were stronger than with any other variable (Figure 6.58), with the exception of wind speed, suggesting that the combination of the two influences may be important in understanding its behaviour. The findings are unsurprising given the location of the mudstone, almost entirely within the wave impact zone. The smallest shale failures, below 0.005 m^3, were also relatively strongly related to monthly sea-levels, possibly indicative of the positioning of several layers at the cliff base. The shift in sensitivity towards larger failures than in the mudstone correlations, which peaked at 0.001 m^3, is likely to be an artefact of the jointing in the shale which would have enabled slightly larger blocks to be more easily detached by the sea. The sandstone displayed a weak and erratic pattern of correlations, as might be expected for a rock type beyond marine

influence. However the siltstone, also located in the upper sections of the cliffs, did demonstrate a statistically valid relationship with monthly sea-levels. Whether this is a response to instability propagating upwards or some other factor has yet to be determined.

Maximum sea-level had the greatest influence on the monitored mudstone and shale layers (Figure 6.59), again suggesting that extreme rather than base-level conditions provided the greatest control on rockfall activity. The peak in the mudstone, between 0.01 m^3 and 0.1 m^3, also corresponds exactly with the minimum correlations with peak hourly rainfall (refer to Figure 6.50), supporting the conclusion drawn earlier that the inverse relationship with wetter months may actually be a positive relationship with sea-levels during summer months with intense rainfall but calm sea conditions. Furthermore the siltstone generated a stronger and more consistent relationship with maximum rather than average sea-levels, perhaps supporting the theory that wave energy delivered to the base of the cliff may influence material beyond the direct contact zone between the rock slope and incoming waves. The behaviour of the sandstone was inverted from its response to average sea-level; the inconsistency again raised serious doubts over whether any meaningful relationship could be identified.

The correlations with minimum sea-levels displayed significant differences to those detected with maximum water heights (Figure 5.60). The smallest failures in the mudstone were inversely correlated to sea-level minimums, suggesting that losses were actually higher when the sea-levels were lower. This may however reflect the influence of tidal range, with lower diurnal low water levels also corresponding to higher high waters. The peak correlations with minimum sea-level were over five times weaker than with maximum sea-levels in the shale layers. One reason for this may be the location of the shale in the cliff, often immediately above the mudstone base. Its higher elevation meant it was beyond the influence of low water but particularly sensitive to high water effects. The impacts on sandstone were again highly varied and negligible. The siltstone layers showed a large reduction in responsiveness in comparison to maximum sea-levels, perhaps indicating that higher sea-levels may hold greater potential to impact the cliff in such a way that the higher layers of rock become affected.

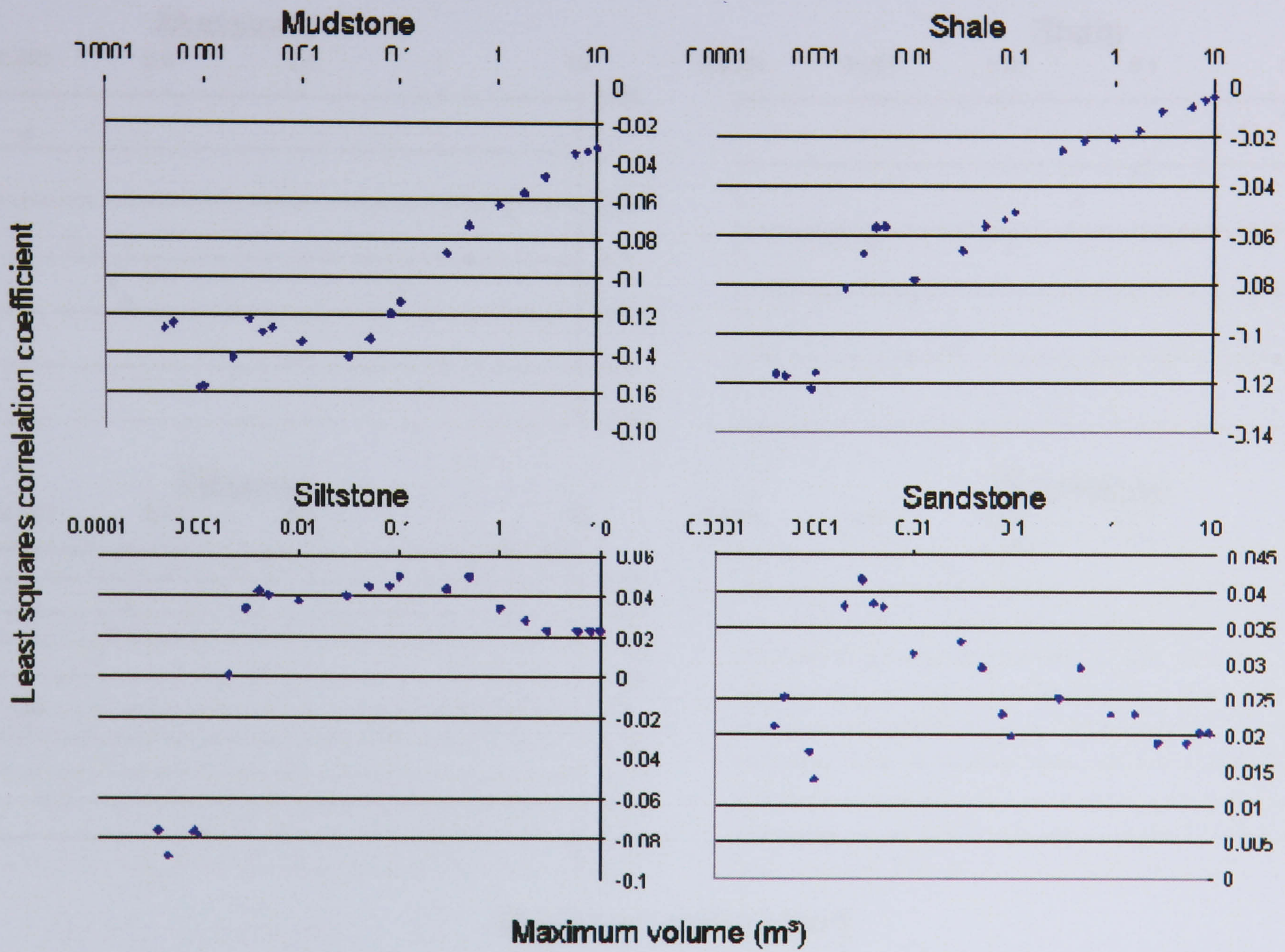

Figure 6.50: Correlation strengths between monthly rockfalls below certain volumes and total monthly rainfall (mm). For example a maximum volume of 0.1 means that the correlation has been calculated between rainfall and only the volumes recorded below 0.1 m³.

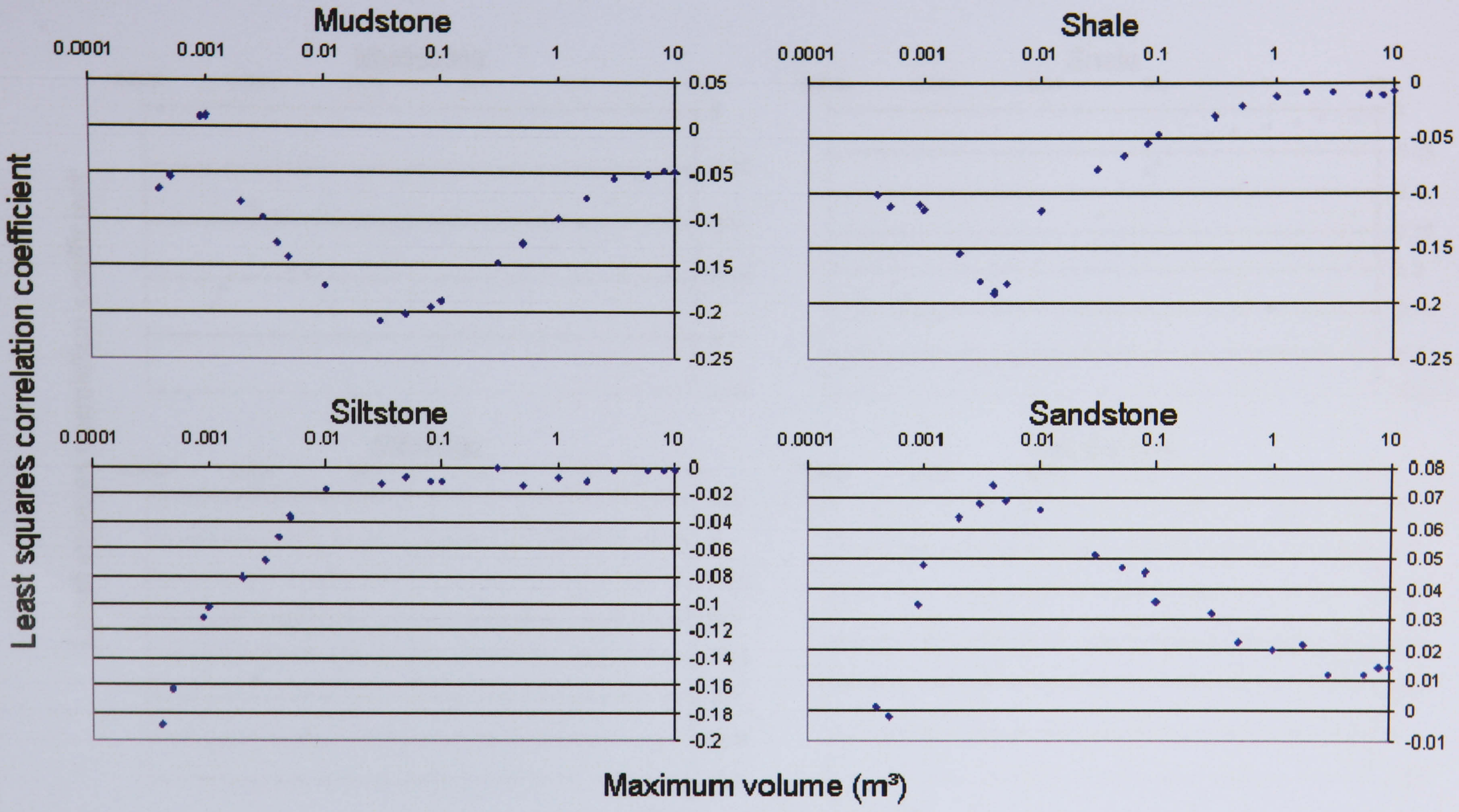

Figure 6.51: Correlation strengths between monthly rockfalls below certain volumes and peak hourly rainfall (mm).

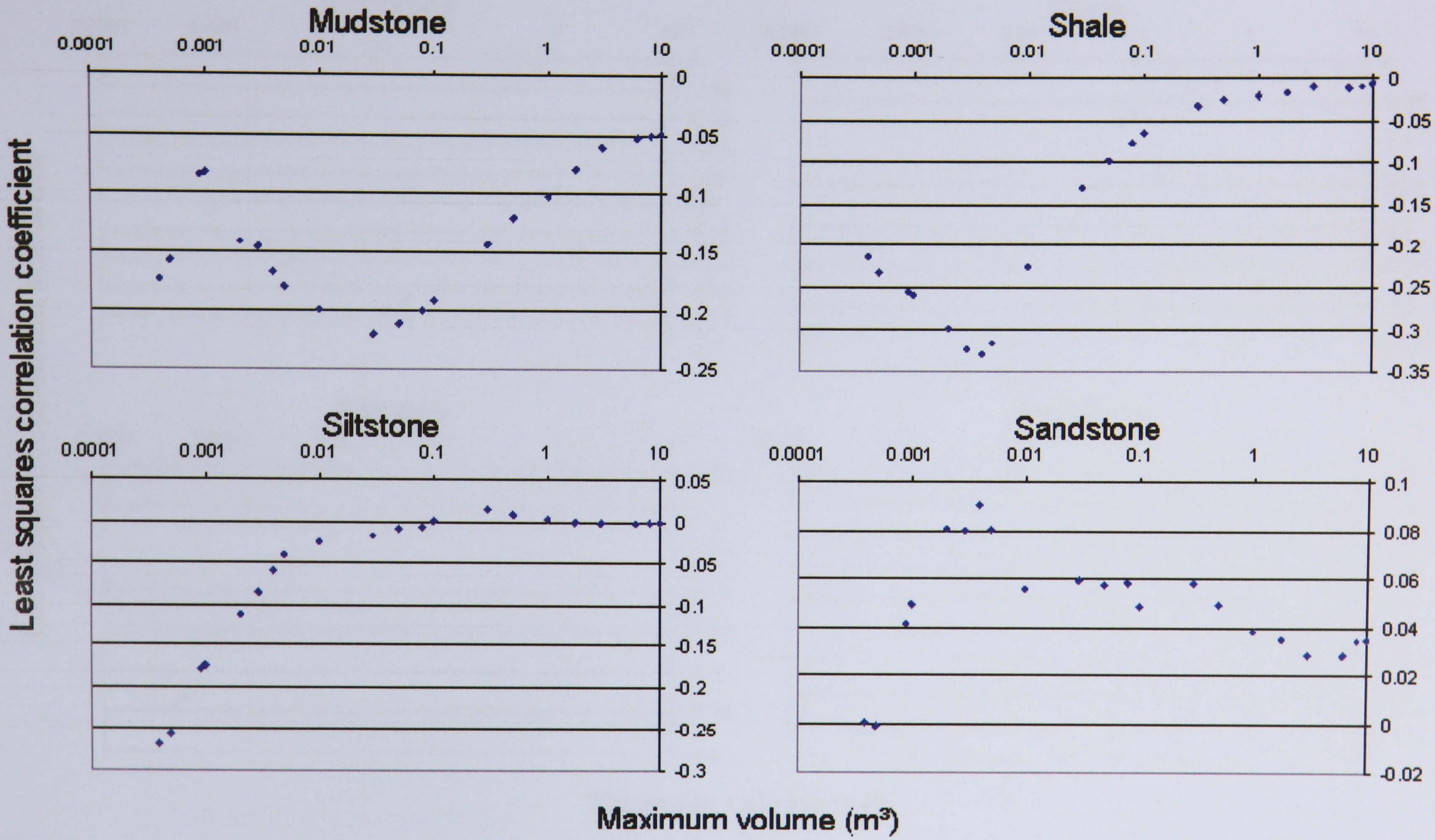

Figure 6.52: Correlation strengths between monthly rockfalls below certain volumes and average monthly temperature (˚C).

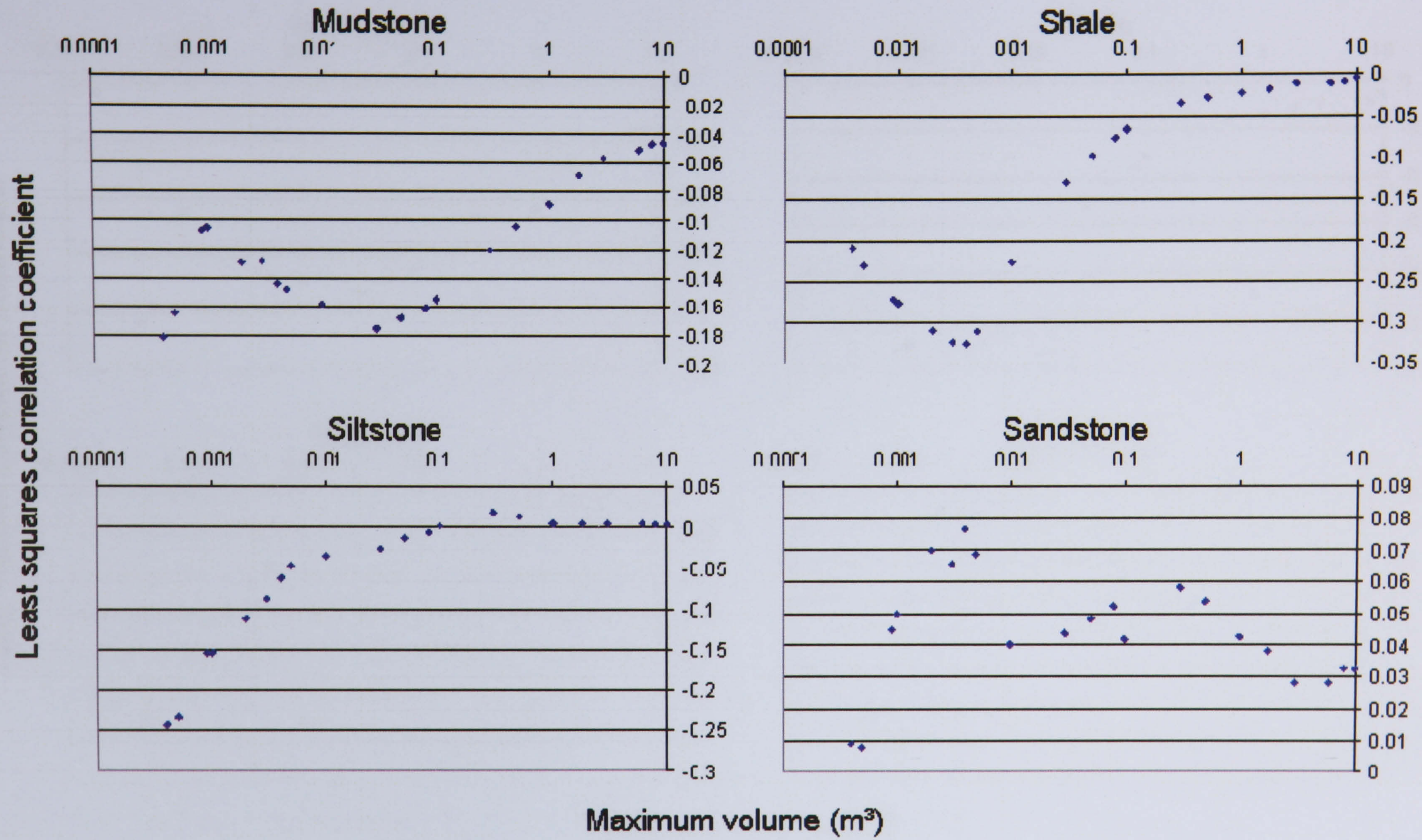

Figure 6.53: Correlation strengths between monthly rockfalls below certain volumes and minimum temperatures in each month (°C).

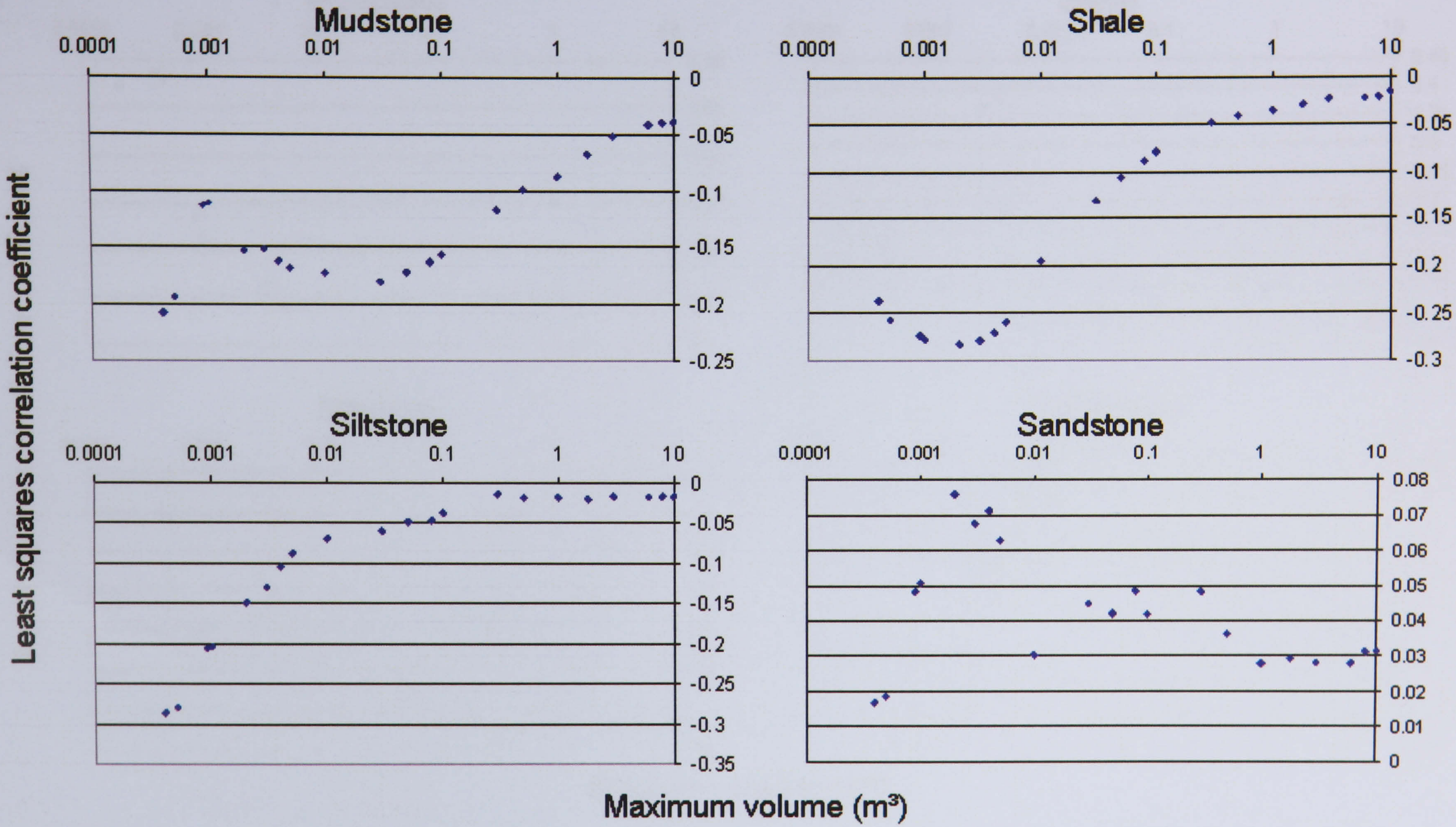

Figure 6.54: Correlation strengths between monthly rockfalls below certain volumes and maximum temperatures in each month (°C).

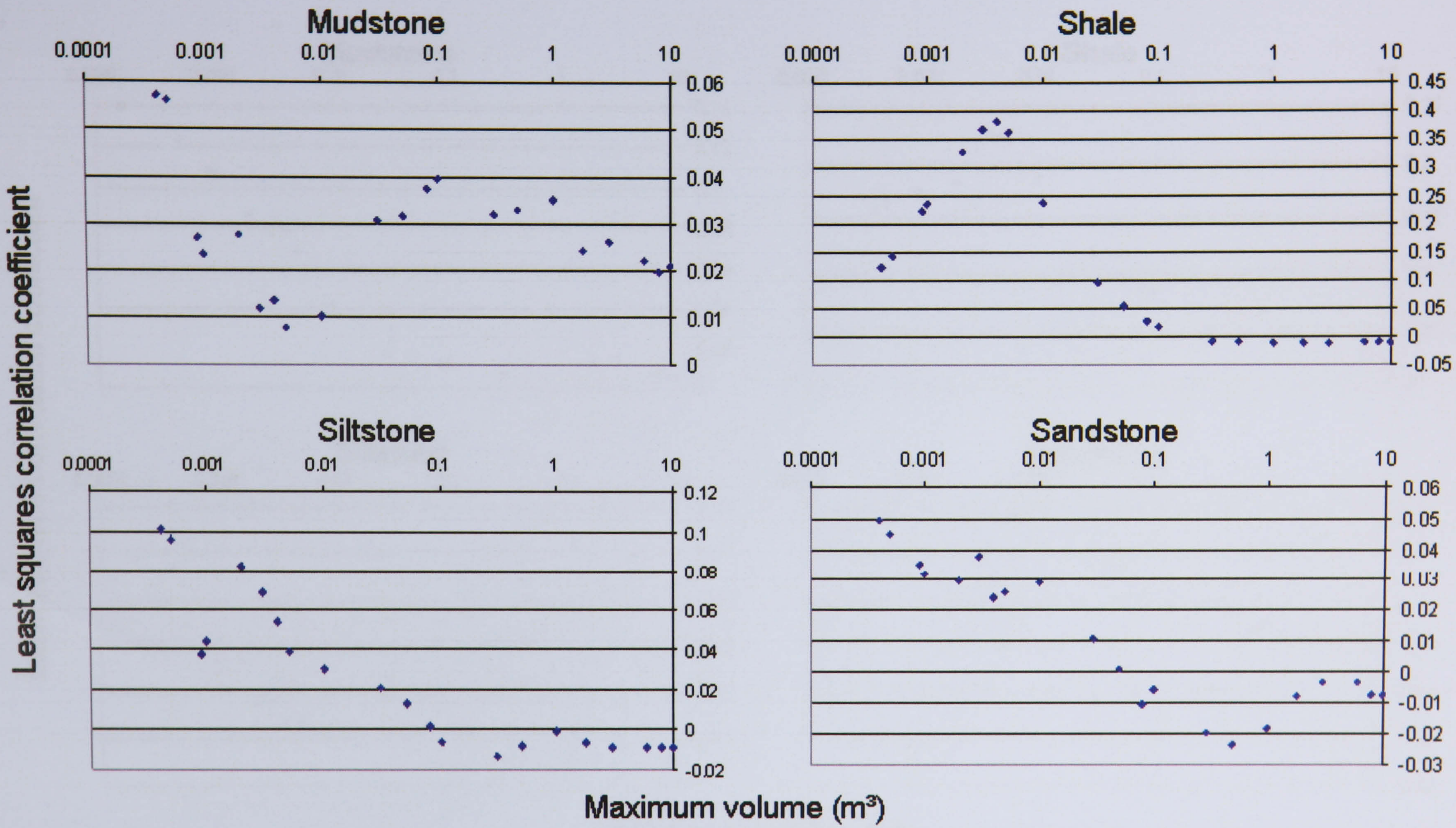

Figure 6.55: Correlation strengths between monthly rockfalls below certain volumes and the numbers of hours below freezing within each month.

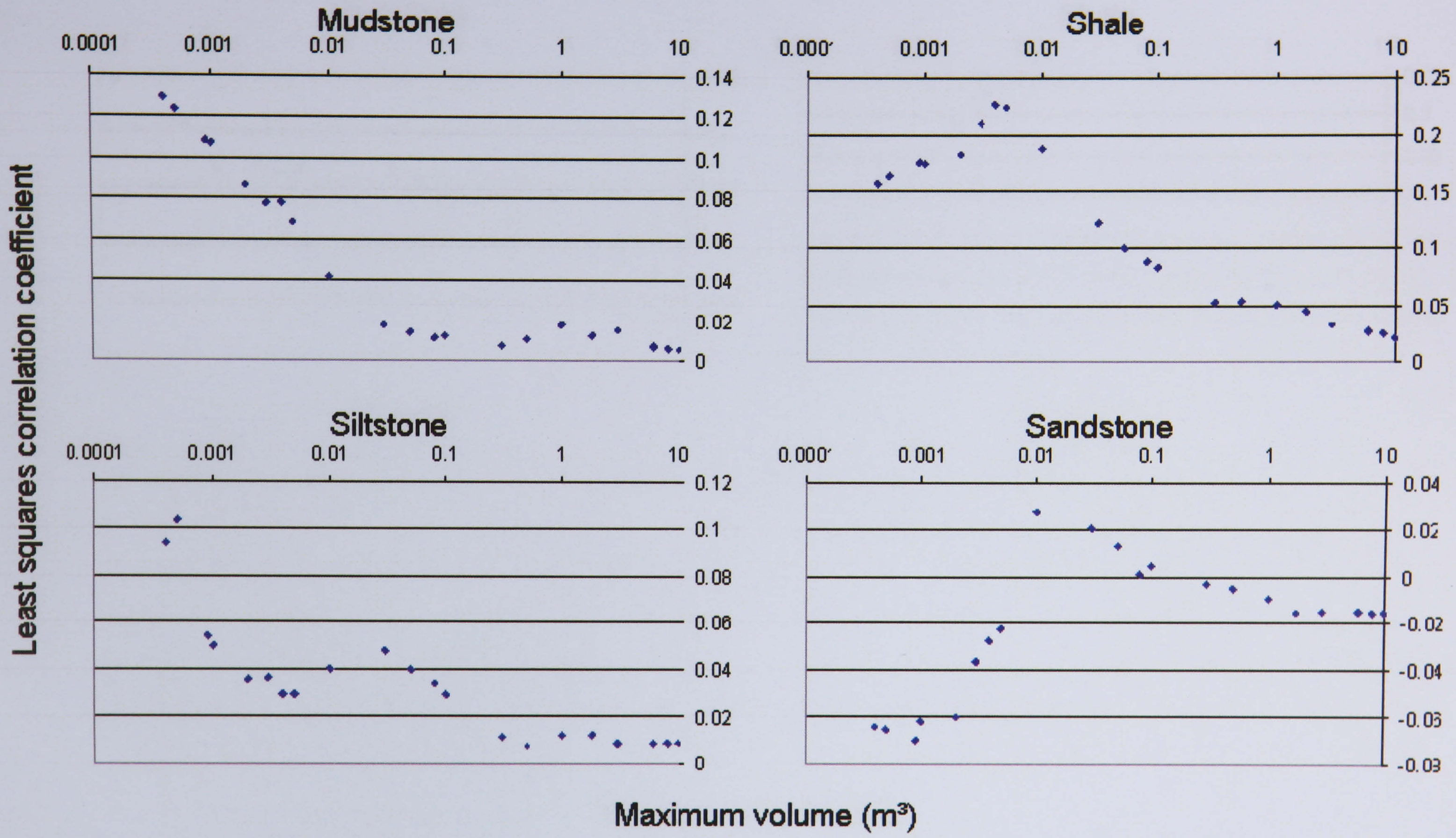

Figure 6.56: Correlation strengths between monthly rockfalls below certain volumes and average monthly wind speed (Knots).

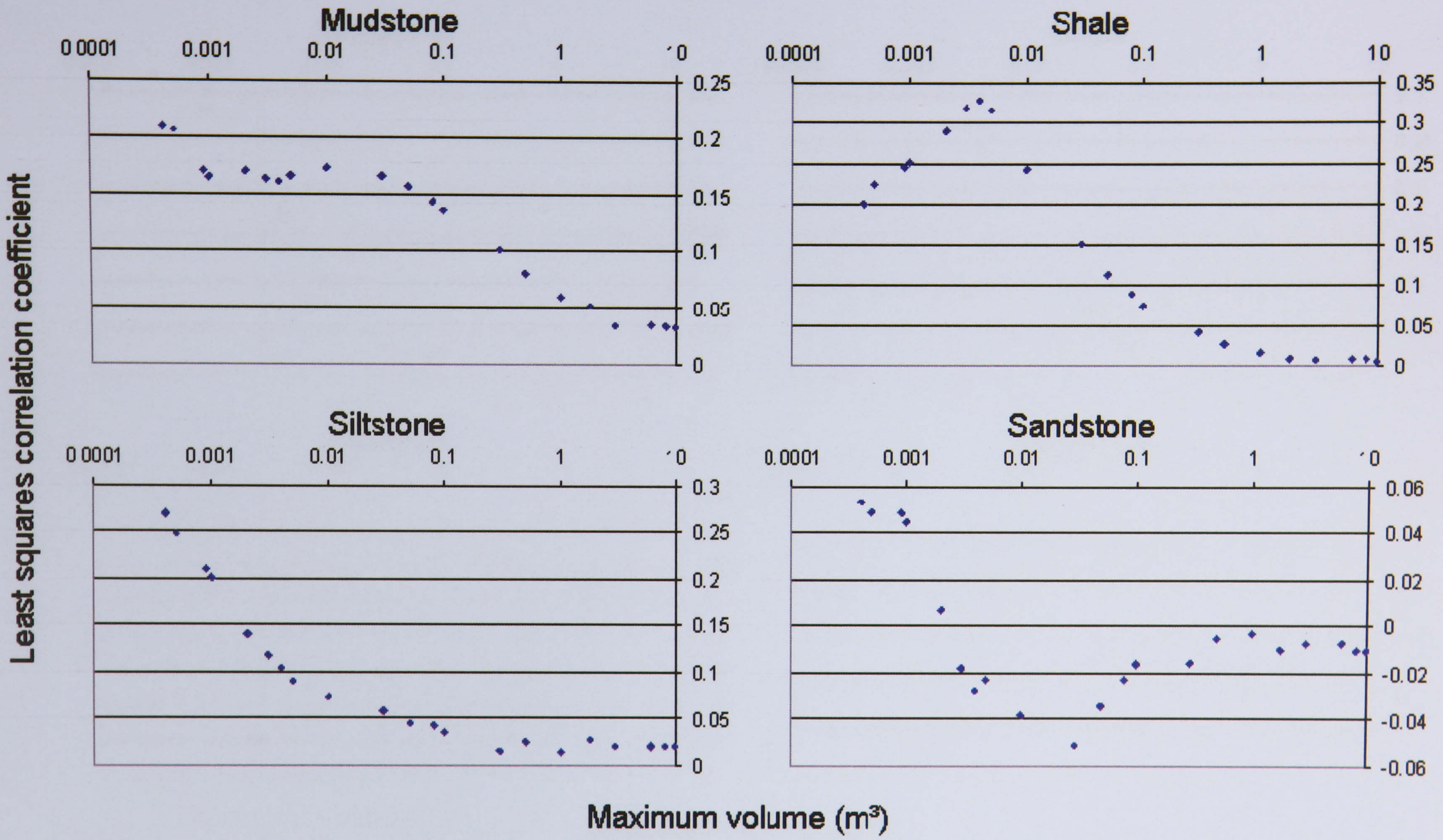

Figure 6.57: Correlation strengths between monthly rockfalls below certain volumes and maximum wind speeds recorded per month (Knots).

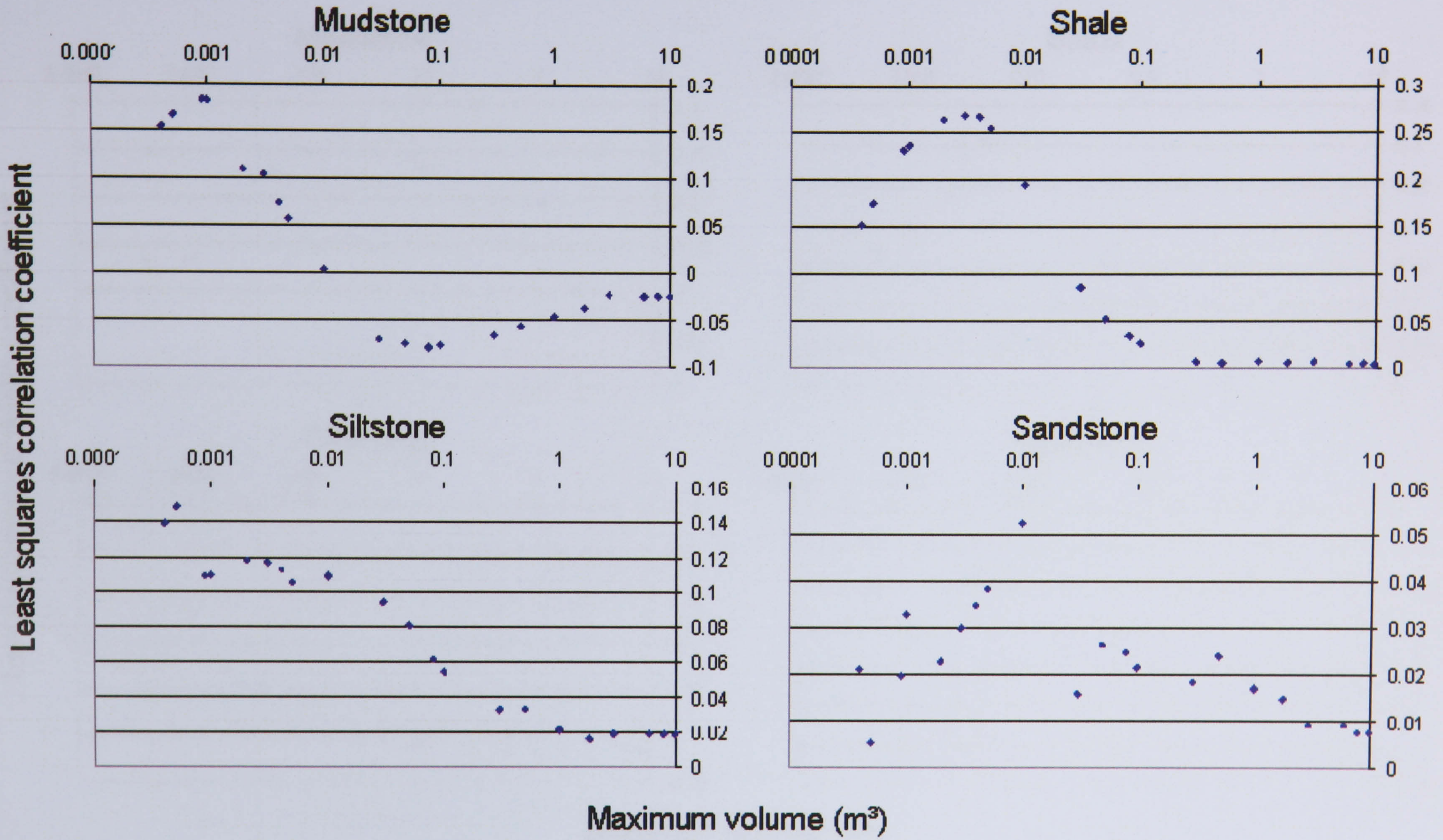

Figure 6.58: Correlation strengths between monthly rockfalls below certain volumes and average monthly sea-level (m OD).

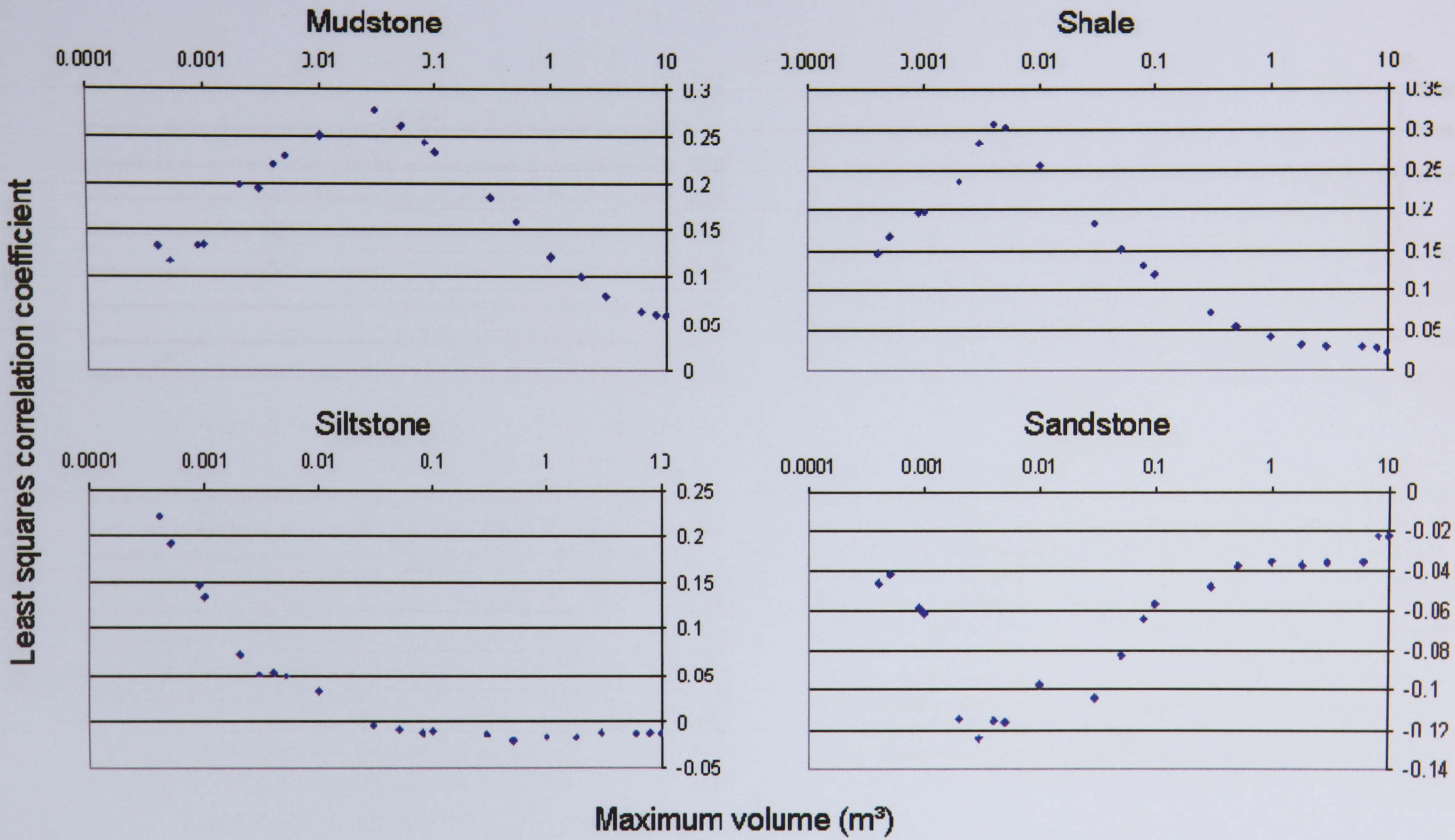

Figure 6.59: Correlation strengths between monthly rockfalls below certain volumes and maximum sea-levels recorded per month (m OD).

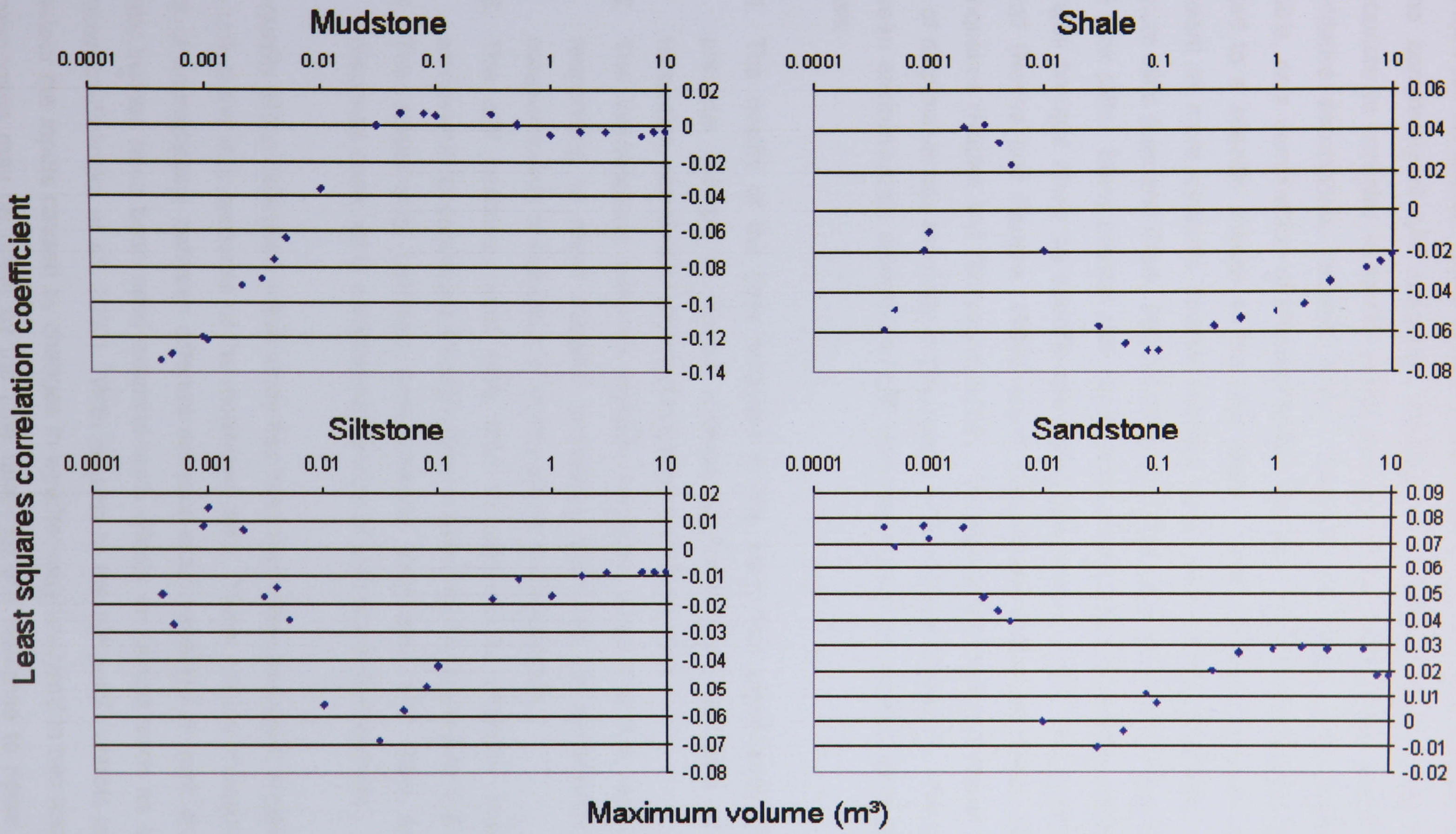

Figure 6.60: Correlation strengths between monthly rockfalls below certain volumes and minimum sea-levels recorded per month (m OD).

6.6 Rockfall response to environmental variables: a re-evaluation

The analysis above has raised questions over the effect of environmental variables on hard rock cliff behaviour. Scale sensitivity has been shown to be an important element in the complexity of cliff response, leading to indications that it may be more appropriate to consider variability in the strength of the relationship, rather than the quantitative associations between them. Evidently, a change in an environmental variable, or a combination of environmental variables, cannot necessarily be directly related to a specific change in the rock slope. Such simplistic analysis are often sufficient in more dynamic coastal features such as beaches (Hansom, 2001) or alluvium cliffs (Lee and Clark, 2002) but fail to explain the behaviour of the monitored hard rock cliffs. Many coastal cliffs have been documented as directly responding to changes brought about by specific sea-levels (Sunamura, 1977; Hutchinson, 1987), rainfall (Neves and Pereira, 1999), storm frequencies (Dias and Neal, 1992) and earthquakes (Hapke and Richmond, 2002). Questions are therefore raised over the lack of responsiveness recorded in the Liassic cliffs of North Yorkshire. The mismatch between environmental drivers and cliff responses could be caused by a number of factors:

1. The quality of the data achieved in this study has significantly surpassed previous records of rockfall change, typically based on data of courser resolution, specifically collected following extreme events.
2. The interrelations between climatic variables mean that the rock slope is responding to more complex processes than can be understood through measurements of individual or combinations of components
3. The cliff sections could take time to respond to changes imposed by environmental conditions through either a direct lag or accumulation of effects.
4. The relationship between environmental processes and hard rock cliffs response does not fit established theories of rock slope development.

The quality of the data used in this study has been rigorously assessed, suggesting the data reflect the true response of the monitored cliffs. There are few measures of the effect of interrelations between different environmental variables on rock slopes, but climatic indices have been used examine such effects on factors such as crop yield (Dabrowska-Zielinska *et al.*, 2002). With regards to the temporal controls on rockfall behaviour the inputs caused by changes in weather may analysed in two ways. Rock cliff responses may be offset by the time taken for the response to occur, or for a sufficient level in environmental conditions to be reached. The remaining analysis

considers a climatic index and lag and cumulative effects to further investigate the influence of the environment on hard rock coastal cliffs.

6.6.1 Climatic indices: soil moisture deficit

Moisture has the potential to alter the mechanical strength of rock material. Rock hardness has been used as a measure of resistance to erosion and shown to be inversely correlated with moisture content (Sumner and Nel, 2002). The combination of rainfall with groundwater circulation and geological permeability has been identified as an important control in certain coastal cliffs, such as the chalk and marl cliffs at Puys, France (Duperret *et al.*, 2002). Gaining a quantitative measure of the flow and volume of water reaching the cliff face could not easily be achieved. In order to gain an approximation of the availability of moisture to the cliffs, a record of soil moisture deficit for the area was obtained from the Meteorological Office Rainfall and Evaporation Calculation System (MORECS). MORECS uses an adaptation of the Penman-Monteith Equation, combining solar radiation, air temperature, vapour pressure and wind speed to estimate potential evaporation which is then combined with precipitation to derive measures of soil moisture deficit. In this instance, soil moisture deficit refers to the quantity of water required to saturate a free-draining grass covered soil.

The MORECS data demonstrated that the soil moisture deficits were high at the start of 2003 and continued to rise, peaking in November, significantly later than in other years of the record. The record reflects a combination of low rainfall and high evaporation which means the rock slopes are likely to have been unseasonably dry and desiccated at the start of the cliff monitoring. However the end of 2003 saw a rapid decline in soil moisture deficit, leaving almost saturated soils in January 2004 (Figure 6.61). The effect of this exceptionally dry year, followed by a sudden influx of soil moisture, is likely to have produced patterns of cliff behaviour distinct from years in which less extreme cycles occur. Temperatures in 2004 were again above the 30 year average although a relatively wet summer increased the availability of moisture to the area, producing a marked contrast with the more arid conditions during 2003. The substantial decline in soil moisture deficit during August 2004 was noted throughout the country causing an erratic pattern during late summer, with material becoming almost saturated from November 2004 onwards.

Figure 6.61: The soil moisture climatic index for North Yorkshire, data from Meteorological Office Rainfall and Evaporation Calculation System.

The correlations of rockfalls with soil moisture deficits were relatively weak, with none of the relationships considered significant at any of the monitored sites (Table 6.9). All of the relationships with moisture were negative, implying that there was a tendency for higher monthly rockfall volumes to be associated with lower deficits. The correlations perform significantly better than the correlations of rockfalls with the amount of rainfall per month at most sites. The data suggest that the numerous influences on the water content within cliff material may provide a more meaningful control on cliff behaviour than the raw input of moisture into the cliff system.

Table 6.9: Correlations of the soil moisture deficit climatic index and total monthly rainfall with rockfalls for each site. The correlations in red are negative. The measurement of moisture deficit means that greater amounts of rockfalls at Site 4 respond weakly to increases in rainfall but more significantly to decreases in soil moisture deficit.

Site	Soil moisture deficit	Rainfall
1	0.181	0.012
2	0.091	0.138
3	0.268	0.049
4	0.216	0.058
5	0.068	0.082
6	0.000	0.080

The rockfall correlations with soil moisture were recalculated for each of the four main rock types and once again compared to the response to total monthly rainfall (Table 6.10). The two datasets appear inversely correlated, with mudstone being significantly more affected by moisture deficit than rainfall but sandstone responding more to rainfall rather than soil moisture. The response of the mudstone to more arid conditions may suggest it is more susceptible to erosion when void of moisture. Sandstone is the only instance in which direct rainfall measurements generate stronger correlations with rockfalls than soil moisture deficit. One explanation, already implied from the previous analysis, is that failures in the sandstone correspond to its exposed position within the cliff face, making it more susceptible to driving rain rather than weakening caused by the moisture content of the rock. Overall, monthly volumetric losses appear to correspond more closely with negative soil moisture deficit than rainfall. If moisture content rather than moisture input does provide a critical influence on cliff behaviour then cliff responses to environmental change may be greatly more complex than has previously been assumed.

Caution must be exercised over the validity of the data. The soil moisture records have indicated that the cliff monitoring coincided with index values notably distinct from the average decadal patterns. The beginning of monitoring recorded cliff behaviour during the end of one of the most deficient periods of soil moisture within the 30 year MORECS record. Moisture deficits during 2004 did not show the typical patterns seen in other years, with particularly variable autumn conditions. Therefore limitations imposed by the relatively short temporal extent of the data are enhanced by the unusual conditions experienced by the cliff during this time. Furthermore questions must be raised over the assumption that soil moisture can be used as a proxy for the delivery of moisture to the rock face. It is possible that the weakness of the correlations reflects the inadequacy of soil moisture content as an indicator of rock mass moisture. Also a more complete analysis would require controls such as permeability to be considered. Ultimately the soil moisture deficit has enabled more complex interactions between environmental processes to explain a greater degree of variance than the raw data. Other such climatic indices may be developed to provide powerful tools for the analysis of rock cliff behaviour, provided more appropriate measures of rock moisture fluctuations can be found.

Table 6.10: Correlations of the soil moisture deficit climatic index and total monthly rainfall with rockfalls for each main rock type. The correlations in red are negative. Soil moisture deficit again appears to be a stronger influence on monthly rockfalls and the inverse patterns imply that the mudstone is more active when rainfall is low and soil moisture is high.

Rock type	Soil moisture deficit	Rainfall
Mudstone	0.198	0.046
Shale	0.018	0.009
Siltstone	0.018	0.006
Sandstone	0.000	0.225

6.6.2 Direct and cumulative effects of environmental processes on rockfalls

A delay or lag in the response of landforms to environmental stimuli is a well established concept in coastal geomorphology (Hosking and McInnes, 2002). Much of the previous analysis has been based on the assumption that any response in the cliff face would be immediate, or within one unit of the temporal monitoring framework: one month in this case. However, if the cliffs take longer to adjust to the changes or require further changes before a response is initiated then direct correlations may perform poorly. Two forms of analysis have been generated to investigate whether cliffs respond better to previous rather than current conditions. Firstly the rockfalls in each month were correlated with the environmental data from previous months, to identify direct lags of one through to six month intervals. Secondly the cumulative effects over time were investigated by comparing the rockfalls in each month with data from the previous months, again analysing the effects of up to six months of accumulation. Cumulative averages were used for the environmental variables which represented the general conditions of total rainfall, average temperature, average wind speed and average sea-level. Cumulative maximum or minimum values were used for the variables representing environmental extremes such as peak rainfall, minimum temperatures, maximum temperatures, hours below freezing, maximum sea-levels and minimum sea-levels. For example month 3 on the direct lag graphs means the rockfalls in each month have been correlated with the environmental data from the month 3 months before, but on the cumulative effects graph month 3 refers to the average or maximum or minimum conditions experienced over the previous three months.

The direct lag effects of total monthly rainfall were investigated for each of the four main rock types in the monitored cliffs (Figure 6.62). No discernible lag was detected in any of the rock materials with poor correlations irrespective of the delay used. The data support the suggestion that direct rainfall may not be the most appropriate measure for the effect of available moisture on cliff behaviour. When the

cumulative influence of successive months were analysed however, the correlations were consistently stronger. The data show a marked increase in the strength of the relationships with all rock types when the average of the month of rockfalls and the previous month were calculated (Figure 6.63). The cumulative effects then level off with the inclusion of more past months. The data imply that whilst there is little evidence for a one month lag, the cumulative conditions from the previous month may provide an important short-term control on cliff response to rainfall. The incorporation of data from the previous month may provide a temporal threshold for the maximum time required for the input of water to the cliff system to reach and influence material at the rock face.

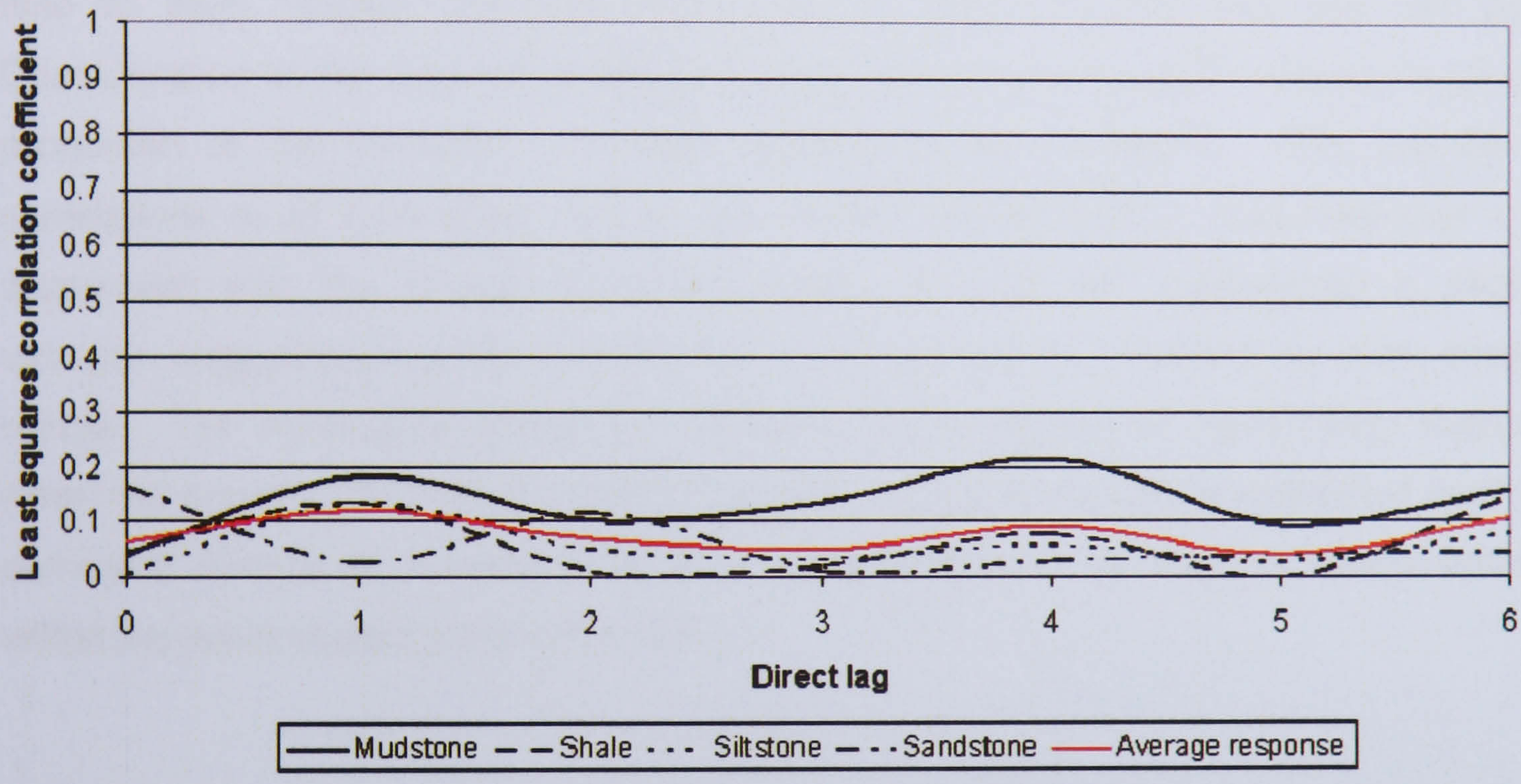

Figure 6.62: Direct lag effects of total monthly rainfall on monthly volumetric losses from each of the four main rock types monitored.

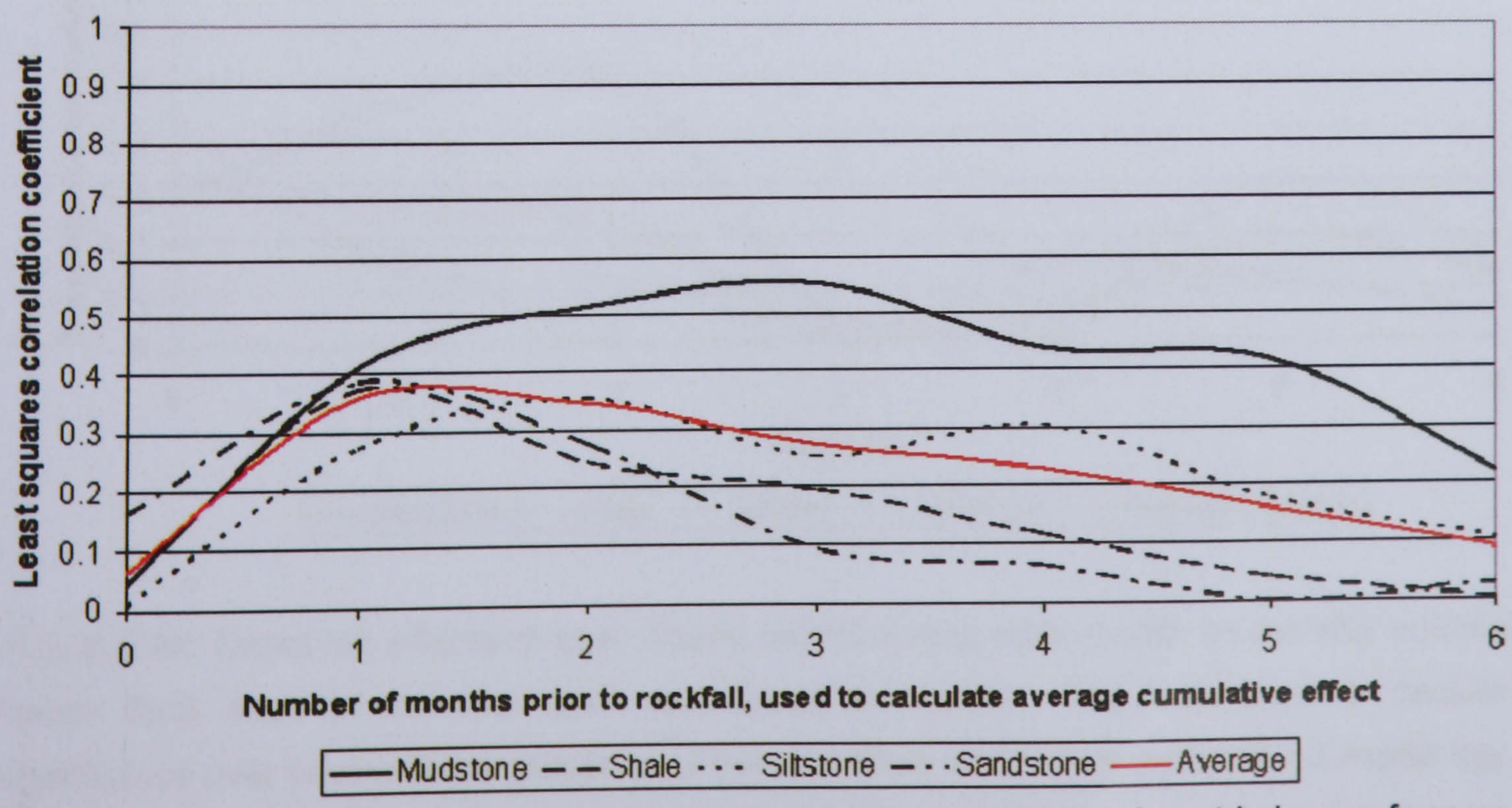

Figure 6.63: Cumulative effects of total monthly rainfall on monthly volumetric losses from each of the four main rock types monitored.

Peak hourly rainfall has been used as an indication of the rate at which water is delivered to the cliff system. The strength of the rockfall correlations showed greater variability than with total monthly rainfall but in general none of the different lags used produced a greater effect than the direct correlation with conditions in the month of the rockfall (Figure 6.64). The lack of a direct lag suggests, as might be expected, the effects of rainfall intensity are more likely to be immediate than delayed. The only exception to this relationship is found in the mudstone in which a two month lag may be evident. This response may be due to the position of the rock layers at the base of the cliff, where less exposure means responses are more sensitive to water that has taken time to seep through the rock mass than to water running over the cliff face. Consideration of the cumulative effects from previous months again enables a greater proportion of the variance in rockfall volumes to be explained. The strength of correlations in all rock types rise to one month (Figure 6.65). This response is in agreement with the effects of rainfall totals, although the relationship is slightly stronger, suggesting that the overall effect of rainfall may be enhanced by more intense rainfall. The cumulative effects on mudstone again appear to significantly increase when the previous two months are considered, but caution must be exercised over the dominant controls on a material which is made distinct by its location, almost entirely within the wave impact zone of the cliff.

Figure 6.64: Direct lag effects of peak hourly rainfall during each month on monthly volumetric losses from each of the four main rock types monitored. The data show a decline in significance over time with the exception of the mudstone which demonstrated a 2 month lag.

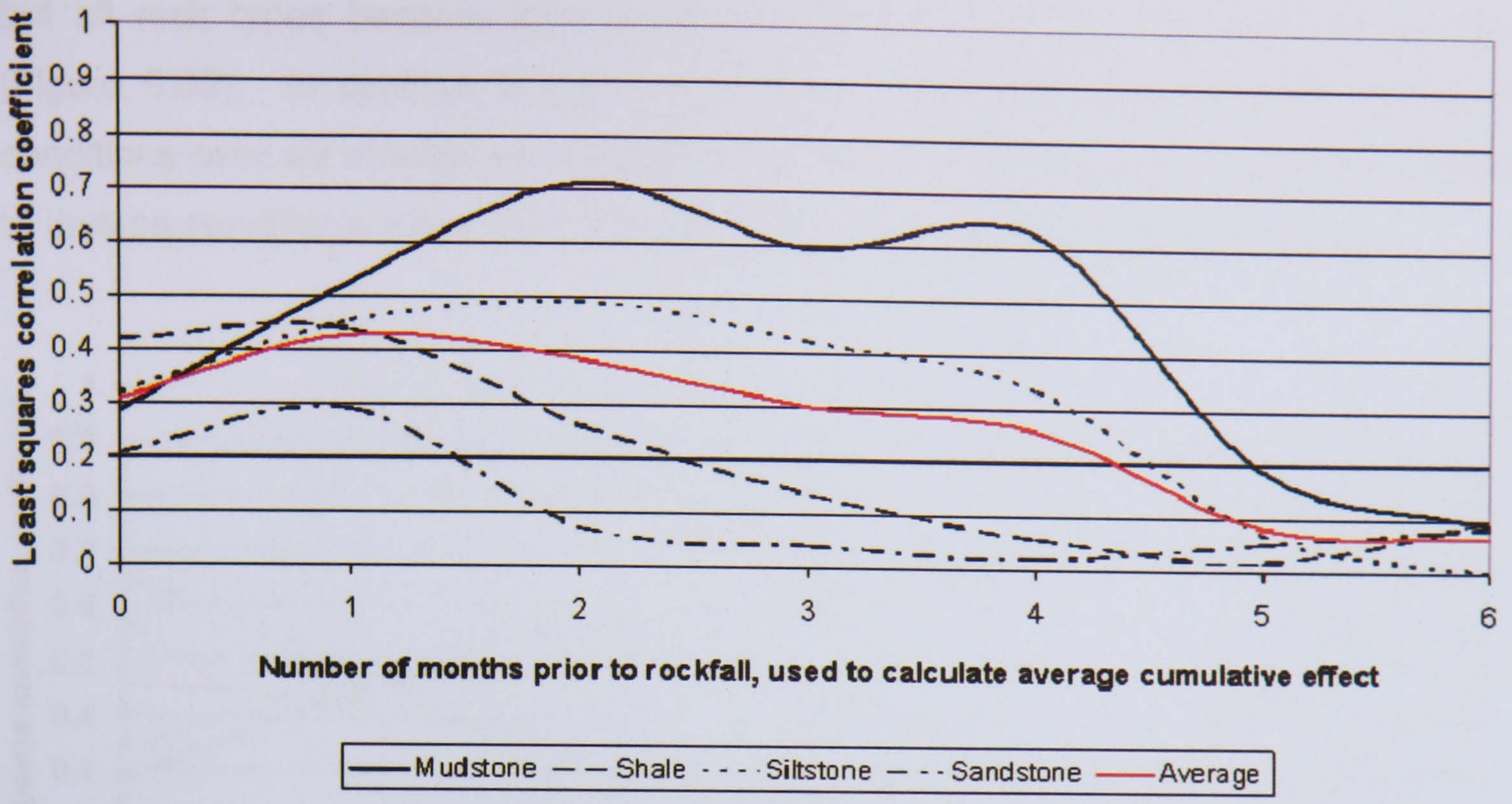

Figure 6.65: Cumulative effects of peak hourly rainfall during each month on monthly volumetric losses from each of the four main rock types monitored. The correlations showed improvements on direct lag effects.

The average correlation of rockfalls with average monthly temperatures fails to improve with any of the lags used (Figure 6.66). However, the specific responses of mudstone and siltstone do appear to be more sensitive to average temperatures between one and two months before. This lagged effect may reflect the time taken for the rock material to be suitably altered by temperatures to become susceptible to failures, although precise causal mechanisms are difficult to identify from average conditions alone. Similar but more consistent and significant patterns were detected when cumulative effects were considered. The steady decay of correlation strength indicates that average temperatures exert little effect on cliff susceptibility to rockfalls beyond the previous month (Figure 6.67).

Minimum temperatures recorded during each month were correlated with rockfalls to investigate whether colder extremes influenced the susceptibility of the monitored cliffs to failure. On average, volumetric losses coincided slightly better with minimum temperatures recorded during the previous month, but then all rock types show a decline in significance before a brief upturn in correlations with a six month lag (Figure 6.68). The six month delay may represent correlations with the inverse conditions during the opposite seasonal conditions. Once again the mudstone and siltstone layers appear more sensitive to temperature variations, but were less strongly influenced by minimum than by average temperatures. The trends are further supported in the graph of the cumulative effects caused by minimum temperatures, with mudstone and siltstone again peaking when the previous month was considered,

but all rock types became less responsive with the inclusion of additional months (Figure 6.69). In contrast to the direct lag of six months, the cumulative effect of conditions over six months was negligible, as would be expected if the lag was related to inverse conditions rather than a genuine influence transferred through the cliff.

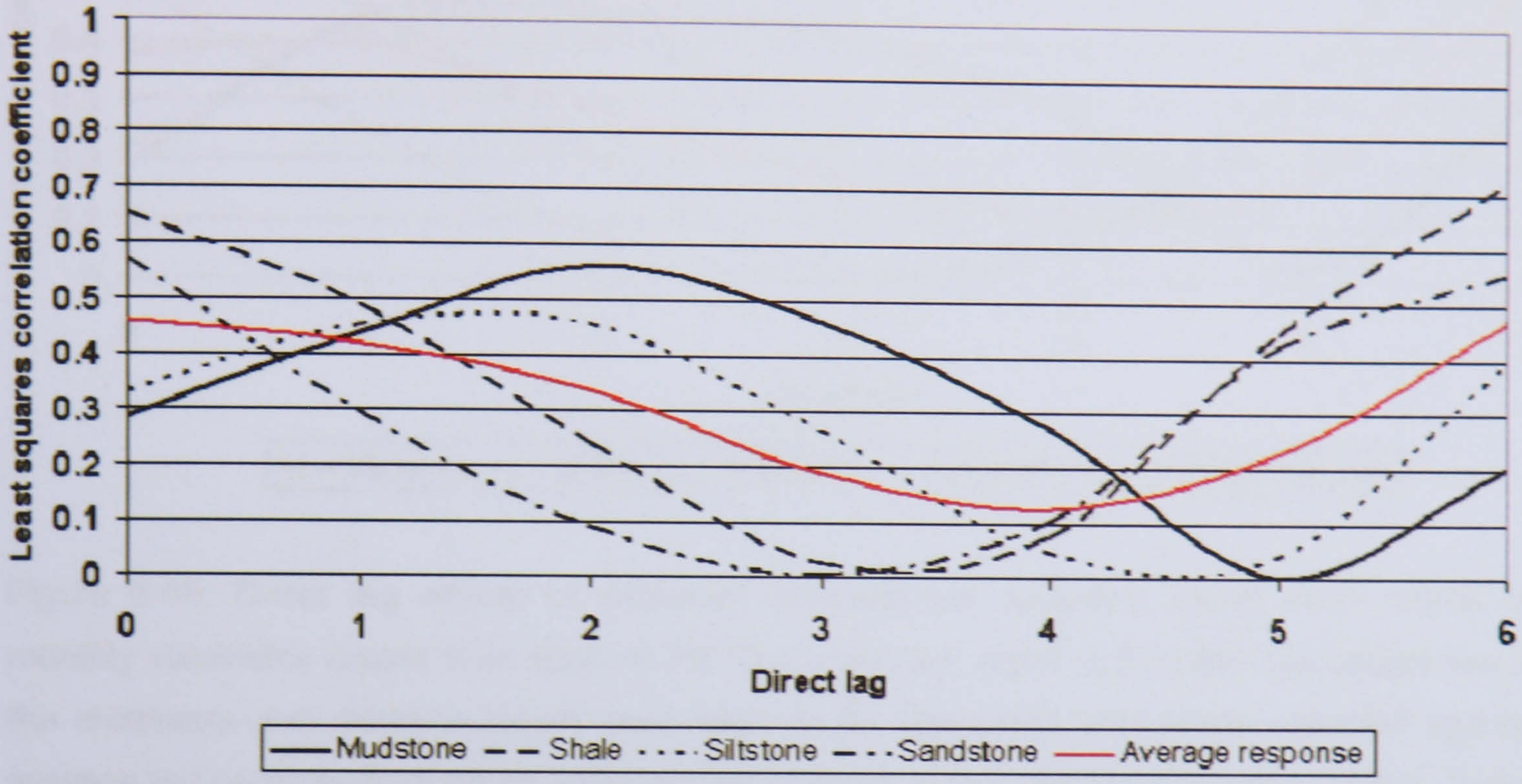

Figure 6.66: Direct lag effects of average monthly temperature on monthly volumetric losses from each of the four main rock types monitored. Mudstone and siltstone layers generated weak lag effects after 1-2 months.

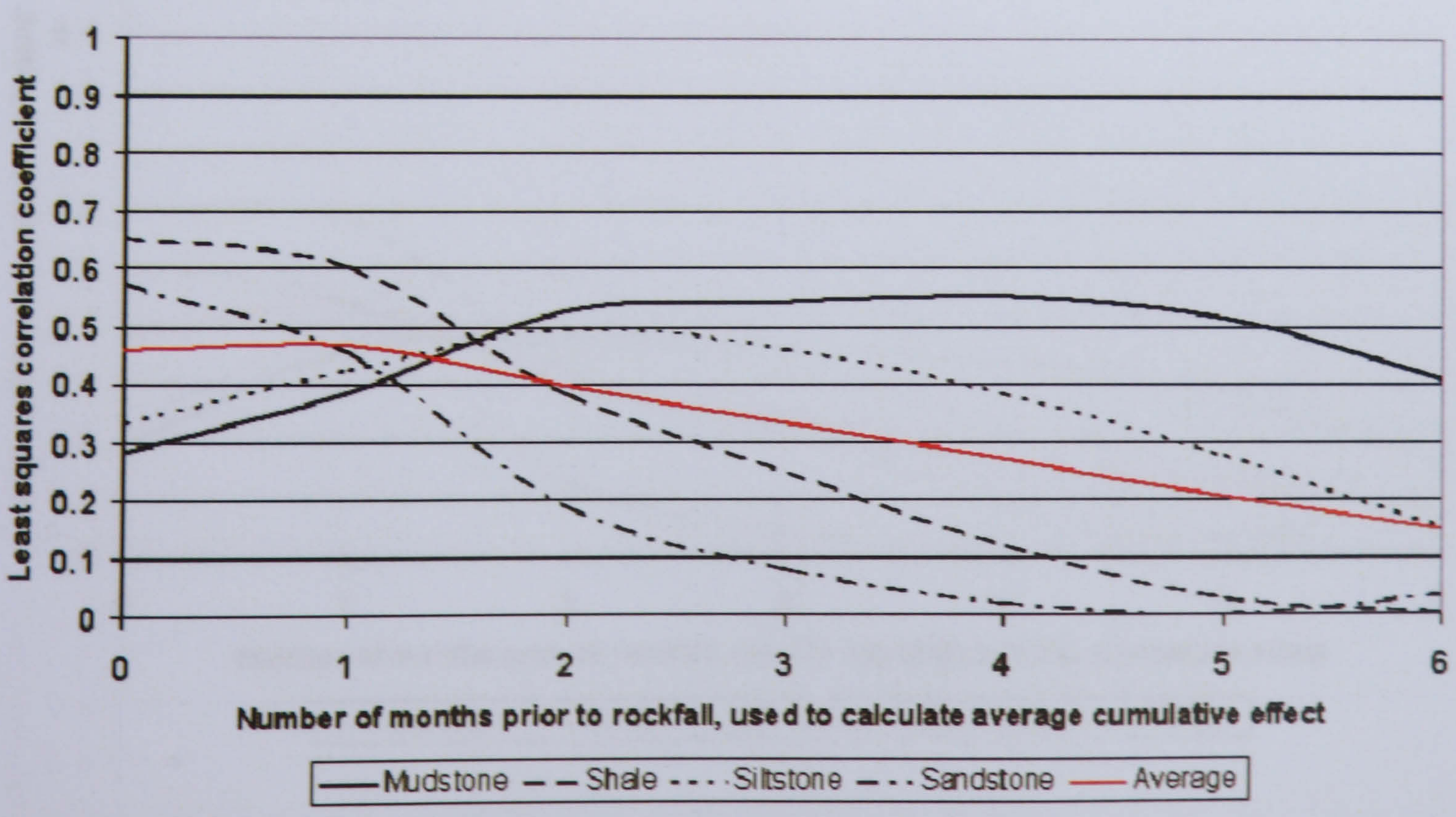

Figure 6.67: Cumulative effects of average monthly temperature on monthly volumetric losses from each of the four main rock types monitored. A consistent reduction in correlation strength was seen over time, although slight increases were seen in the mudstone and siltstone layers over the previous 2 months.

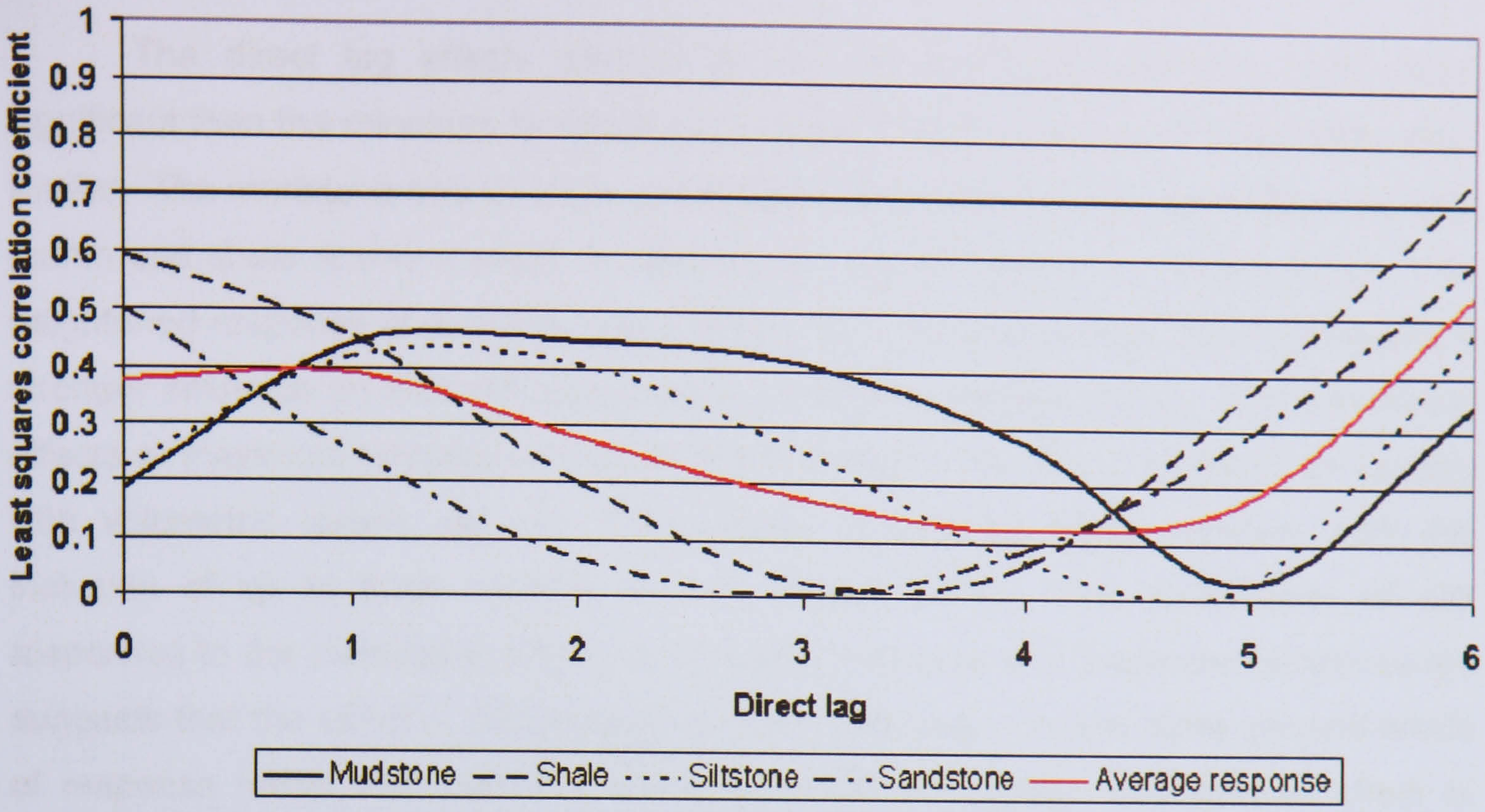

Figure 6.68: Direct lag effects of minimum temperatures recorded during each month on monthly volumetric losses from each of the four main rock types monitored. The responses of the mudstone and siltstone layers were seen to be consistent with those recorded against average temperature fluctuations although the strength of the relationships were weaker, failing to become statistically significant. Again an upturn in correlation strength was recorded with a direct lag of 6 months.

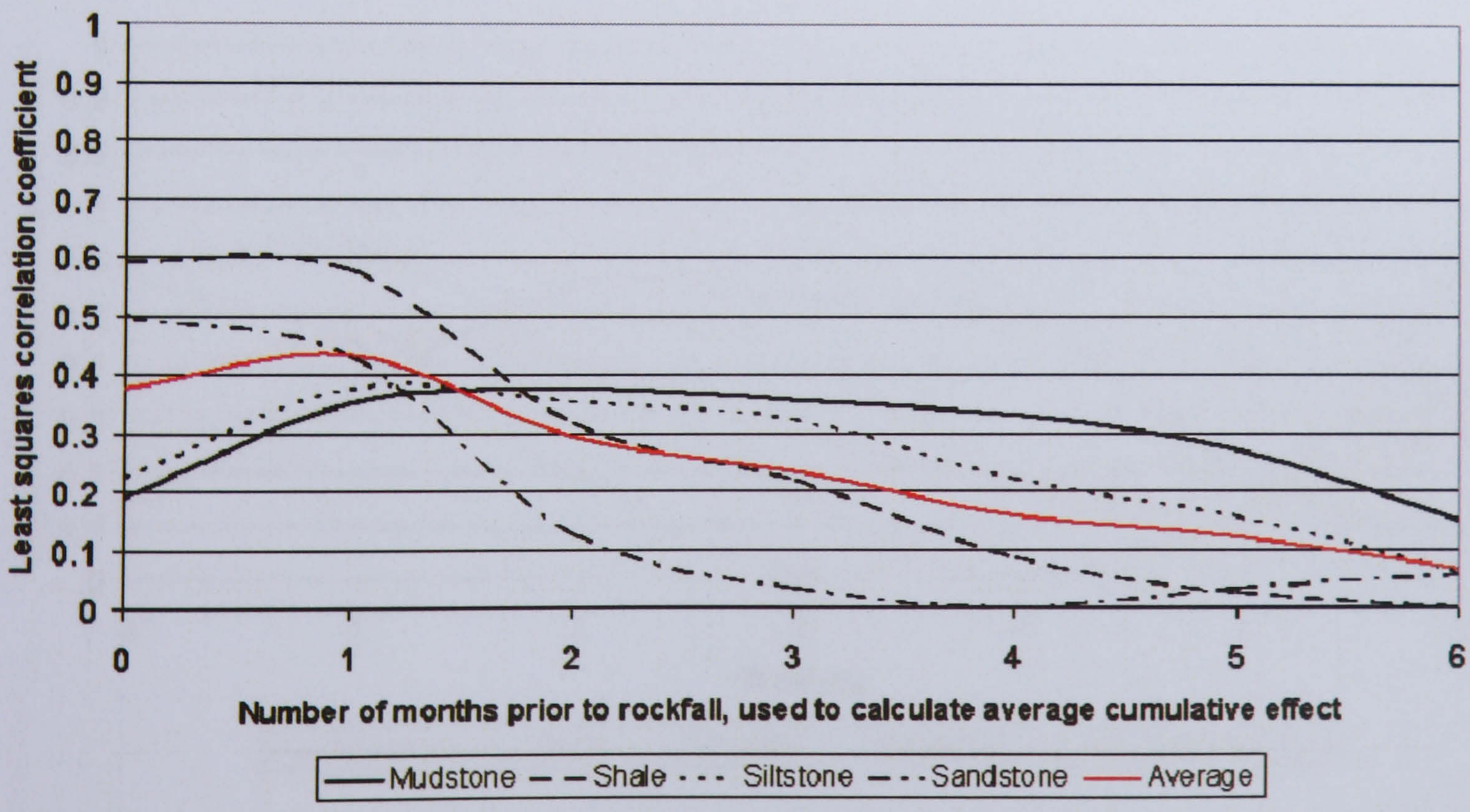

Figure 6.69: Cumulative effects of minimum temperatures recorded during each month on monthly volumetric losses from each of the four main rock types monitored. Shale was the only significantly affected rock type, with all other materials displaying a similar response to cumulative average temperatures despite the use of the most extreme minimum temperatures.

The direct lag effects caused by the maximum temperatures were more significant than the minimum temperatures, although the nature of cliff responses were similar. The mudstone and siltstone correlations peak after two months rather than one month and shale shows a slight increase with a lag of one month (Figure 6.70). The heightened response of rockfalls may indicate that maximum temperatures generate a stronger influence on rock cliff behaviour than minimum temperatures. The cumulative effects of maximum temperatures recorded in each month also correlate more closely with volumetric losses per m^2; the average relationship stays constant with the inclusion of up to three months of data (Figure 6.71). The consistency of cliff responses to the cumulative effects of average, minimum and maximum temperatures suggests that the effect of temperature on rock cliffs may produce more general levels of response rather than dramatic changes in cliff behaviour. The precise effect of temperature is particularly hard to analyse because physical processes by which the cliff may respond to temperature fluctuations are indirect. For example, it may be the associated reduction in rock moisture content rather than the increase in temperatures that causes more failures to occur. It is evident that the interpretation of the cause of many of the failures recorded has been limited by an inability to segregate individual environmental factors.

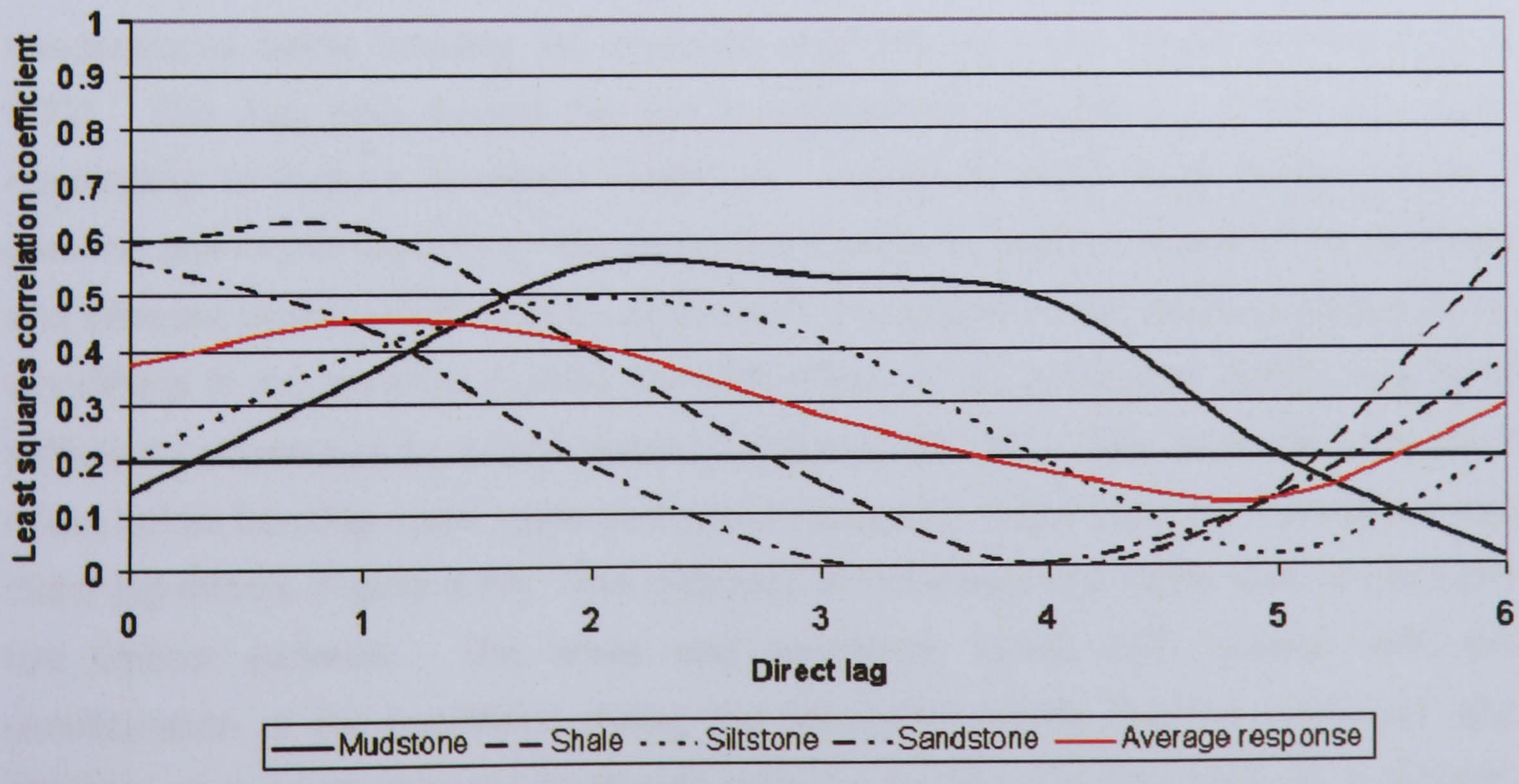

Figure 6.70: Direct lag effects of maximum temperatures recorded during each month on monthly volumetric losses from each of the four main rock types monitored. Similar patterns were detected across all measures of temperature suggesting a wider, more general cliff response.

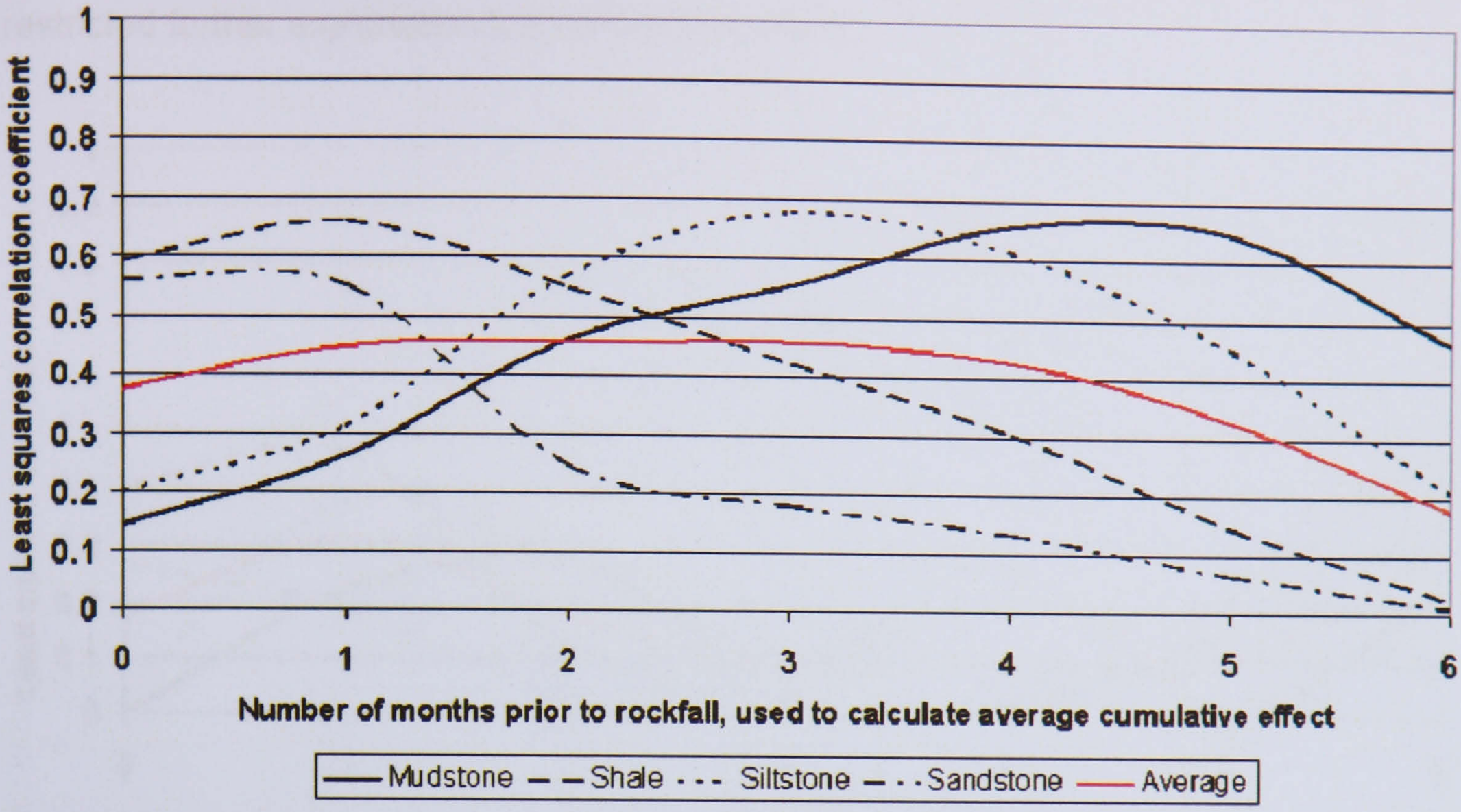

Figure 6.71: Cumulative effects of maximum temperatures recorded during each month on monthly volumetric losses from each of the four main rock types monitored. There was no clear peak in the accumulation of maximum temperatures required to increase rockfalls.

The number of hours below freezing within each month was used to investigate the specific response of cliff material to freeze-thaw cycles. The correlations show the effects are relatively weak, as might be expected for the North Yorkshire where temperatures below freezing are generally restricted to a few winter months (Figure 6.72). This may also explain the rise in correlations with the six month lag, again responding to inverse seasonal conditions. However, there does appear to be a genuine one month lag effect. The lag in the average is largely influenced by the shale and siltstone layers, which may be particularly susceptible to freeze-thaw mechanisms. Conditions in the previous months had little effect on the sandstone which may be of sufficient competence to remain stable during such periods. The cumulative effects of hours below freezing once again performed marginally better than the correlation with direct lag effects (Figure 6.73). The response of individual rock types were divided into two distinct patterns. The shale and sandstone layers both peaked with the consideration of the conditions during the preceding month, but the mudstone and siltstone were more strongly correlated with the trends over the previous 2 months. Perhaps a more useful distinction can be made between the more competent rock types and the shale, which was the only material to demonstrate a statistically significant relationship with hours below freezing. This may reflect the porous nature of the shale, which makes it more vulnerable to the effects of subzero temperatures.

Once again the inability to gain a measure of the moisture content within the rock has restricted further explanation the variance recorded.

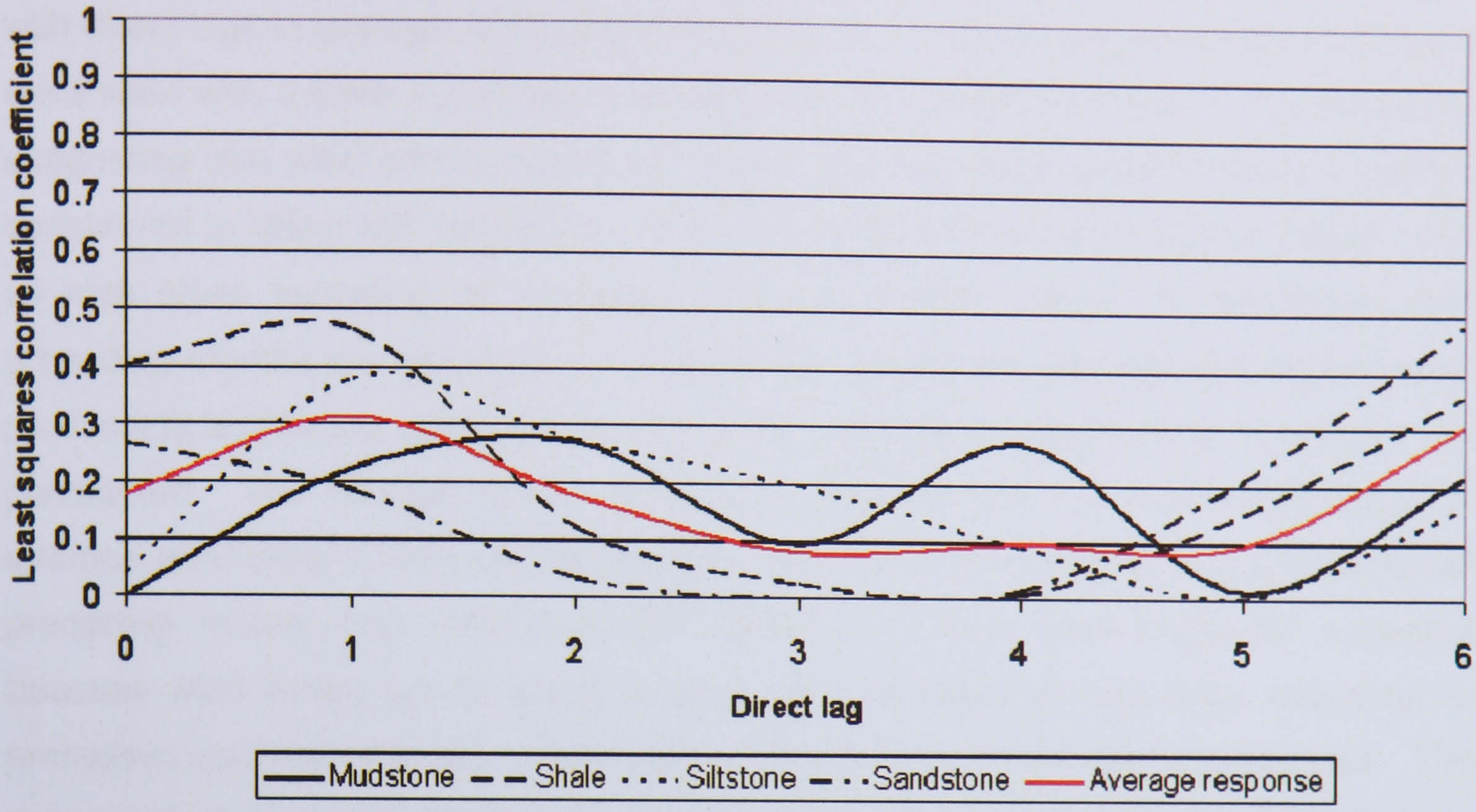

Figure 6.72: Direct lag effects of the number of hours below freezing recorded during each month on monthly volumetric losses from each of the four main rock types monitored. The data indicate that there may be a 1 month lag to the rock slope response to freezing conditions but overall the cliff remains relatively unaffected by sub-zero temperatures.

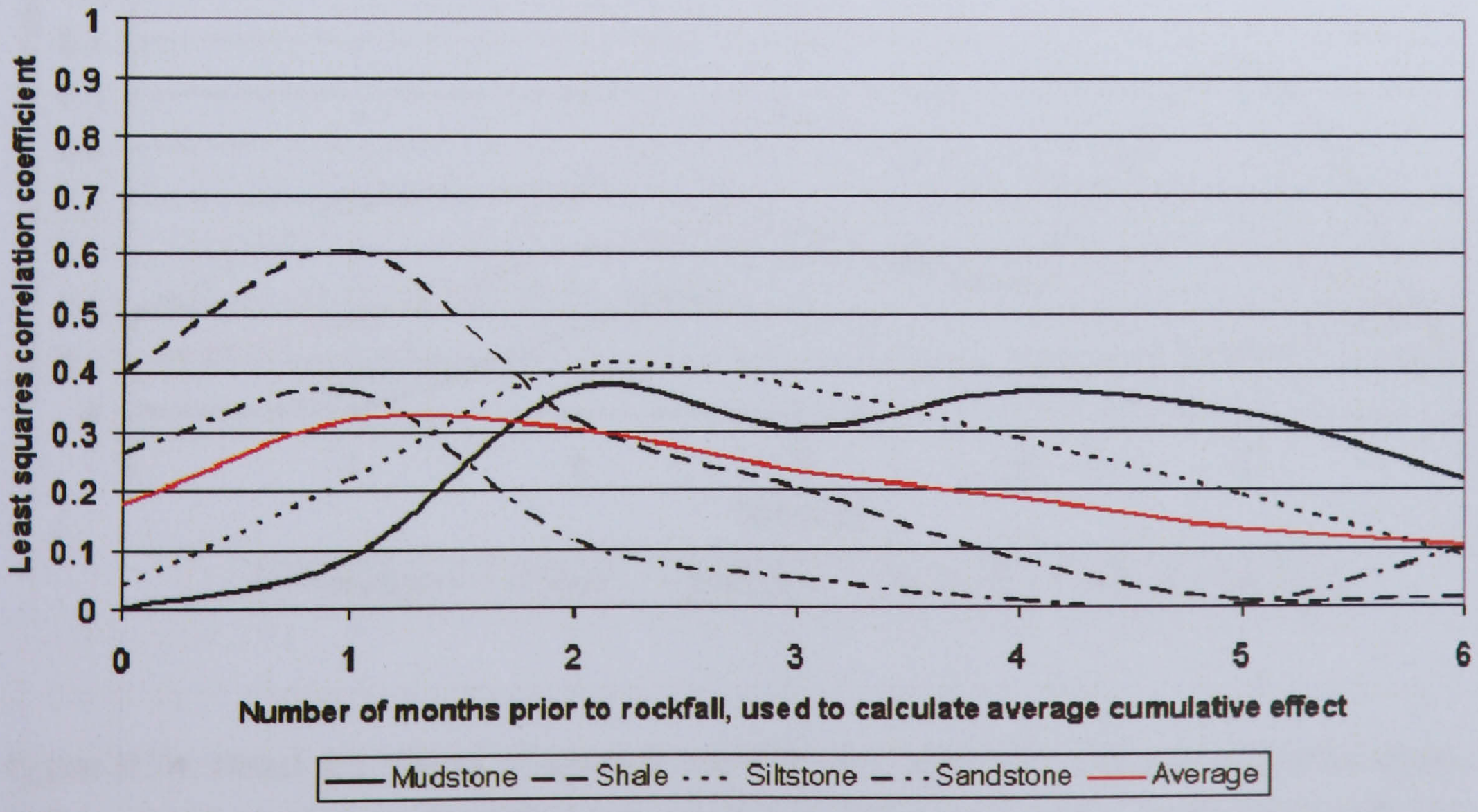

Figure 6.73: Cumulative effects of the number of hours below freezing recorded during each month on monthly volumetric losses from each of the four main rock types monitored. The response of the cliff can be differentiated by the less responsive harder rock material and the dynamic and significant relationship in the weaker shale layers.

The effects of average wind speed on monthly rockfall volumes were more difficult to identify. There was no clear pattern to the correlations of material losses with direct lags in average wind speed (Figure 6.74). Improvements in the relationship were seen with a three month lag in the siltstone and a five month lag in the mudstone suggesting that wind effects may take longer than the other environmental variables considered to affect cliff behaviour. The cumulative effects reinforce this pattern with all rock types recording an increase in the correlations when the conditions over preceding months are aggregated (Figure 6.75). Mudstone and siltstone layers reach particularly significant relationships when the cumulative effects over 5 months are considered. The strength of the correlations indicate that it is the accumulation of average wind speeds over several months, rather than the conditions in any particular preceding month, that influenced cliff behaviour. The result might be expected because wind forces are in direct contact with the exposed rock face, requiring no processes such as seepage in the case of rainfall before the rock is influenced. The data suggest it is more likely to be the cumulative stresses caused by wind regimes that have an effect on cliff behaviour, weakening material over time.

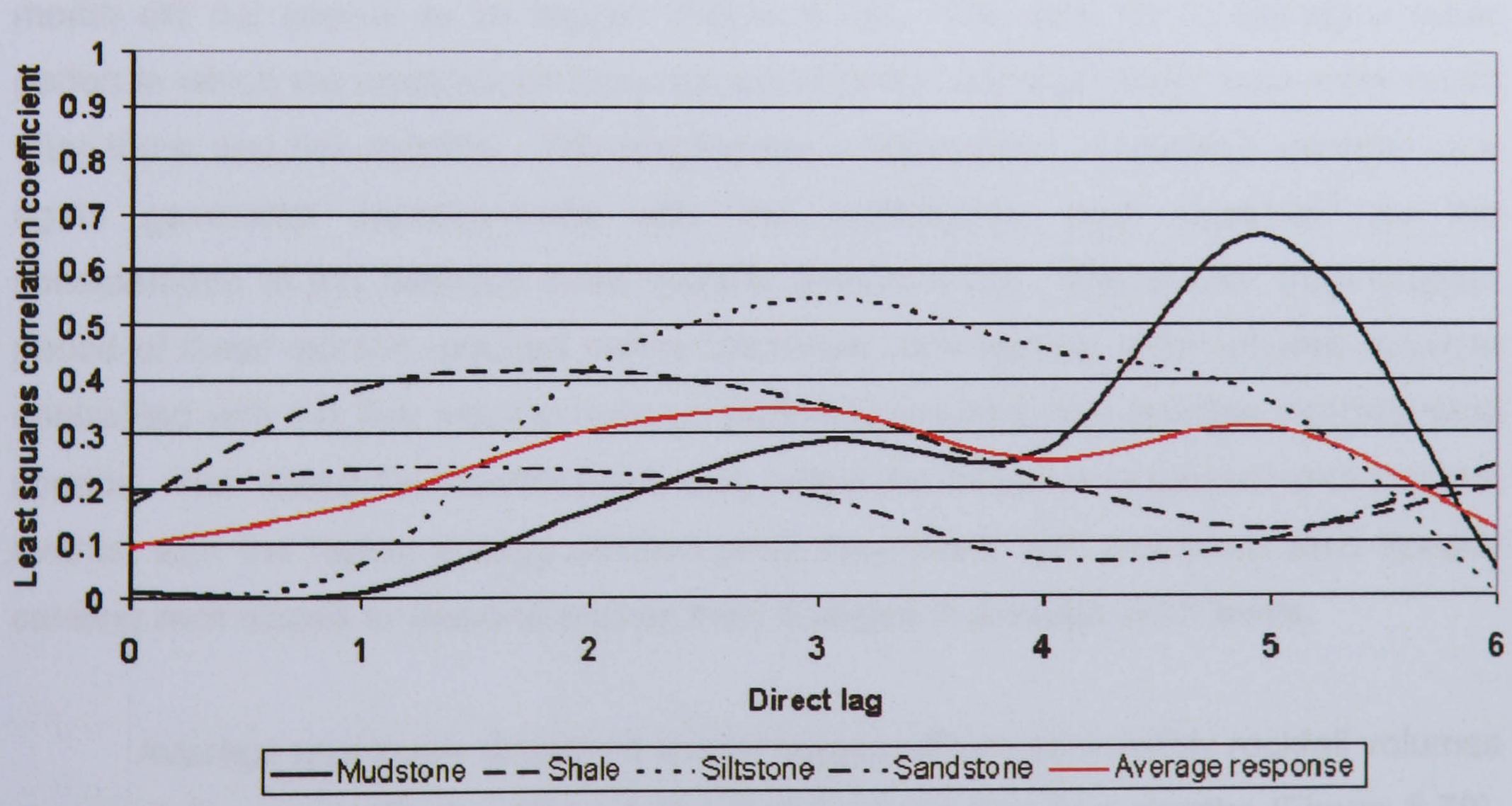

Figure 6.74: Direct lag effects of average monthly wind speed on monthly volumetric losses from each of the four main rock types monitored. Little clear effects were seen, with the possibility of a five and three month lag in the mudstone and siltstone respectively.

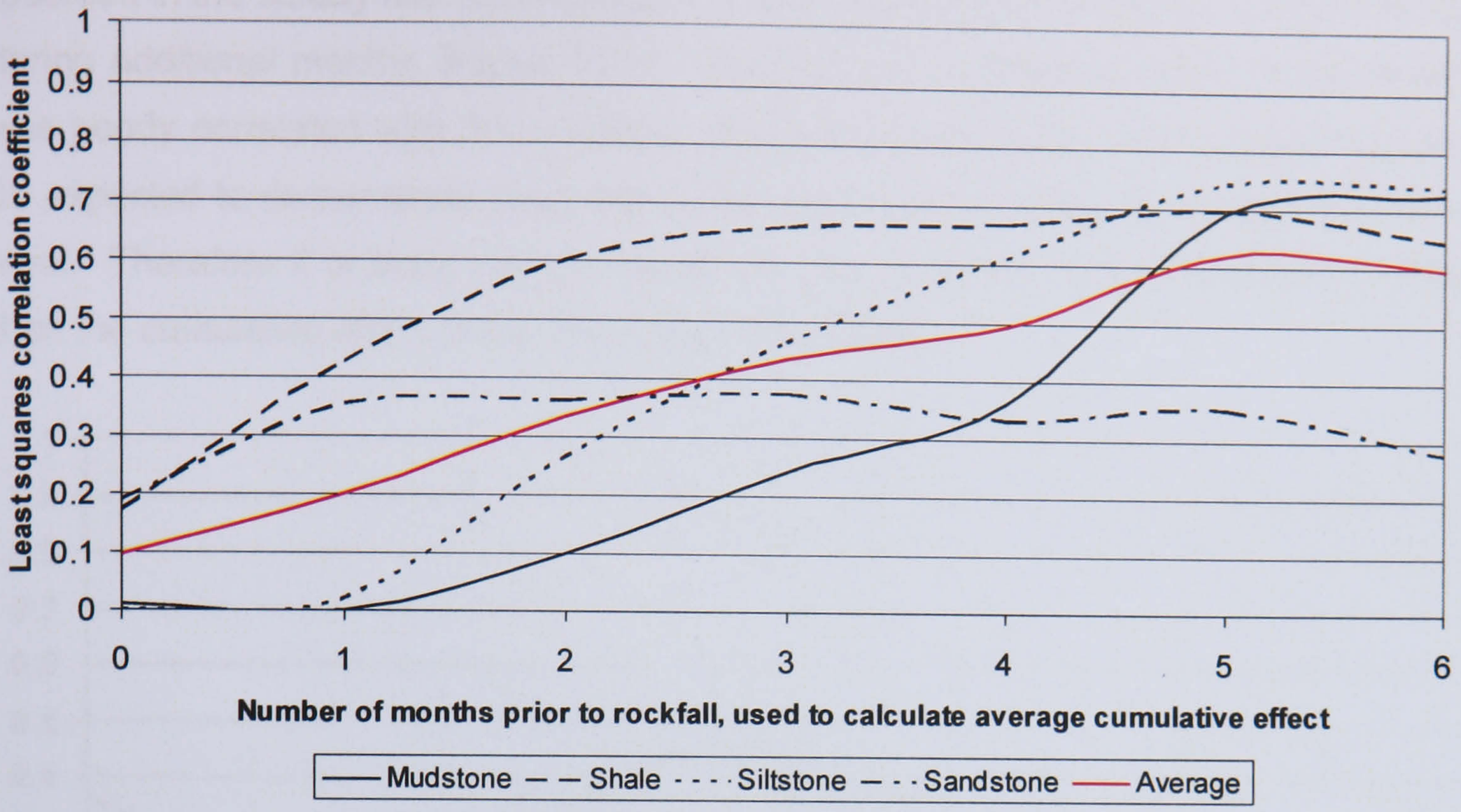

Figure 6.75: Cumulative effects of average monthly wind speed recorded during each month on monthly volumetric losses from each of the four main rock types monitored. Cliff response was seen to be more sensitive to aggregated effects than to direct lag effects.

The effects on rockfalls caused by maximum wind speeds recorded during each month did not appear to be lagged (Figure 6.76). The data fail to identify a delay period in which the correlations increase significantly, although small rises were noted after three and five months. The progressive incorporation of previous months once again generated improvements with the relationship, best explained by the consideration of the previous three months (Figure 6.77). The shorter accumulation period of three months required before maximum wind speeds affect rockfall volumes contrasted with the five months build up period associated with average monthly wind speeds. The reason for the difference may reflect the influence of general and extreme events, with the higher energy environments associated with maximum wind speeds causing rock slopes to respond sooner than changes in average wind levels.

Average sea-levels displayed similar lagged effects on monthly rockfall volumes as cumulative wind effects, although the dominant lag was four months (Figure 6.78). Similarities in the correlation patterns might be expected because both sea-levels and wind have progressive weakening effects on cliff material over time. Furthermore the two variables may be interrelated with higher and more destructive sea-levels occurring during storms in which wind speeds are also greater. The lag is most clear in the mudstone layers which are also in direct contact with breaking waves, becoming less influential with height up the cliff face, having a minimal effect on the sandstone at the cliff top. The progressive effect of average sea-level effects over time was also

recorded in the steady rise of correlations to five months with the inclusion of conditions during additional months (Figure 6.79). However, the cumulative effect of sea-levels was poorly correlated with the mudstone layers at the cliff base, which might logically be expected to demonstrate most clearly the effect of processes associated with sea-level. Therefore it is likely the four month lag has a greater direct effect on the cliffs than the cumulative effect of the preceding five months.

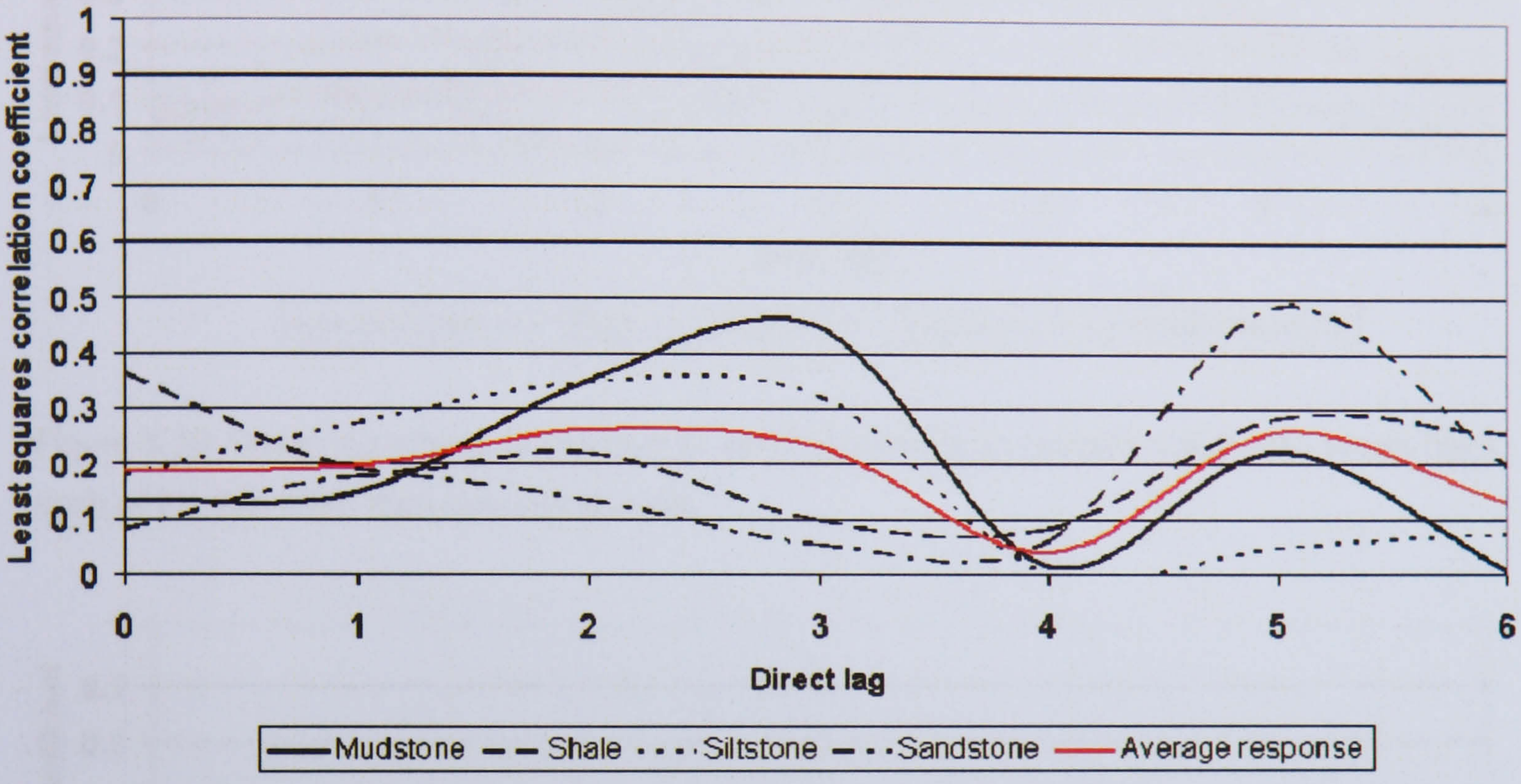

Figure 6.76: Direct lag effects of maximum wind speed recorded during each month on monthly volumetric losses from each of the four main rock types monitored.

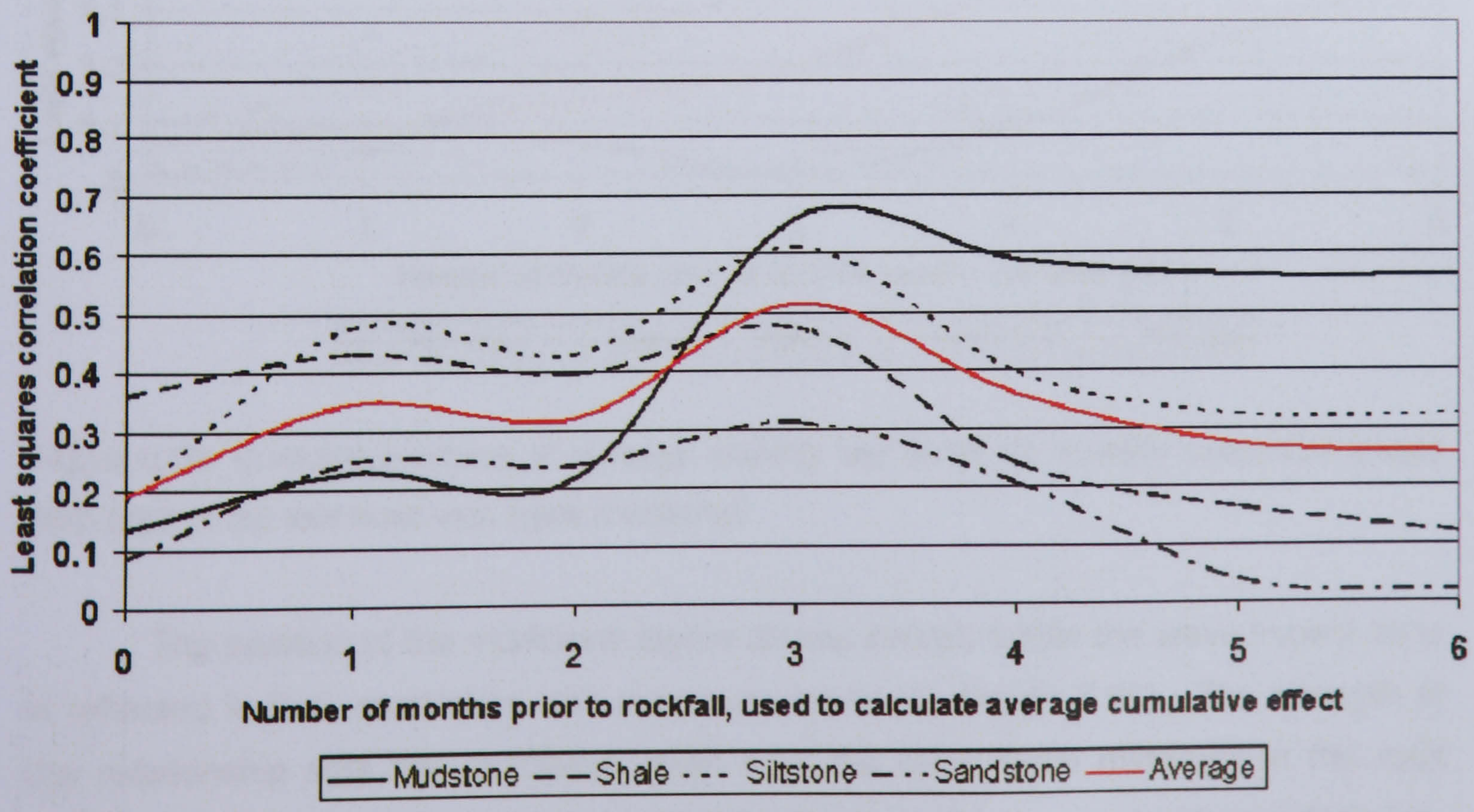

Figure 6.77: Cumulative effects of the maximum wind speed recorded during each month on monthly volumetric losses from each of the four main rock types monitored.

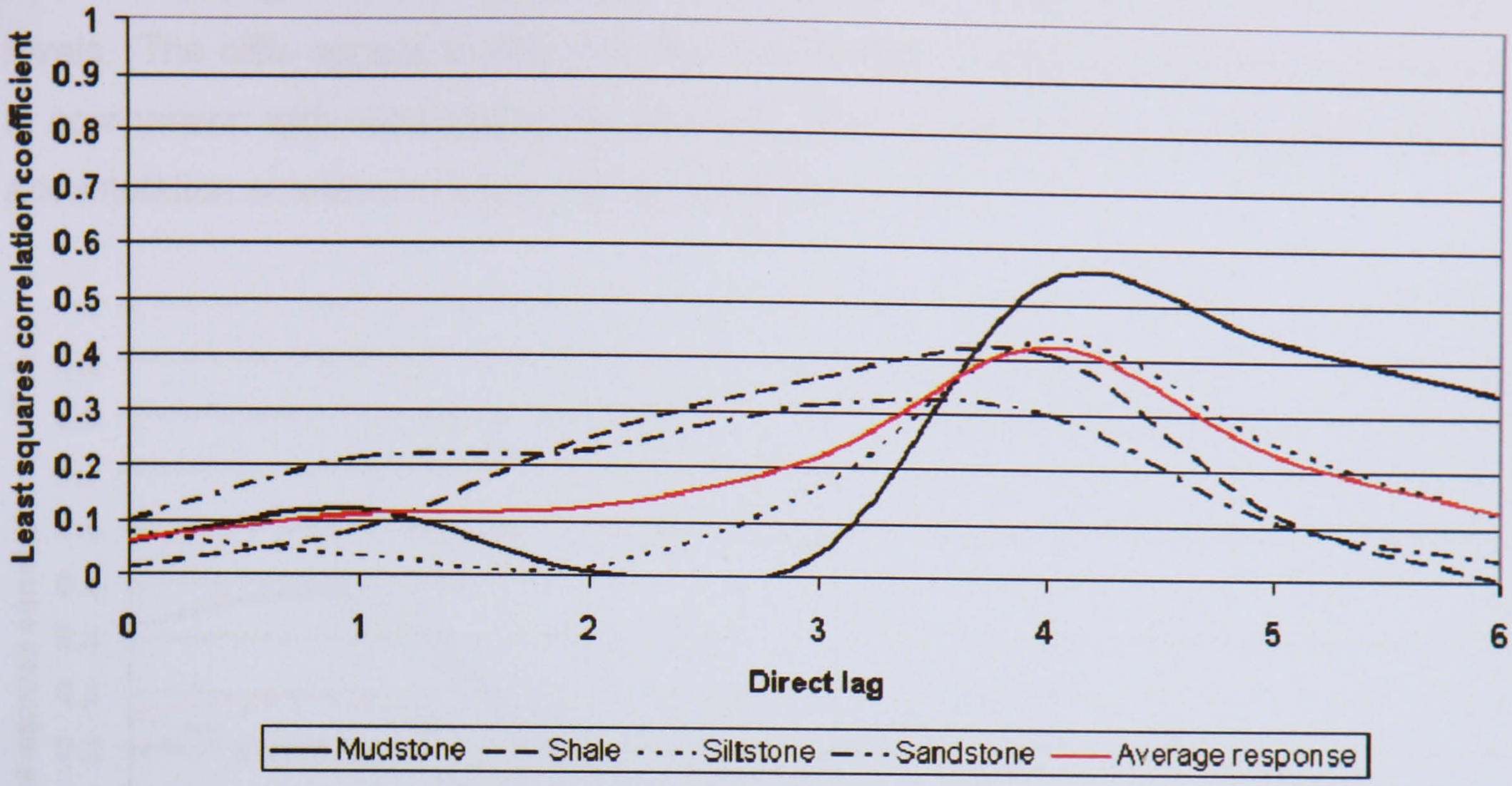

Figure 6.78: Direct lag effects of average monthly sea-levels on monthly volumetric losses from each of the four main rock types monitored.

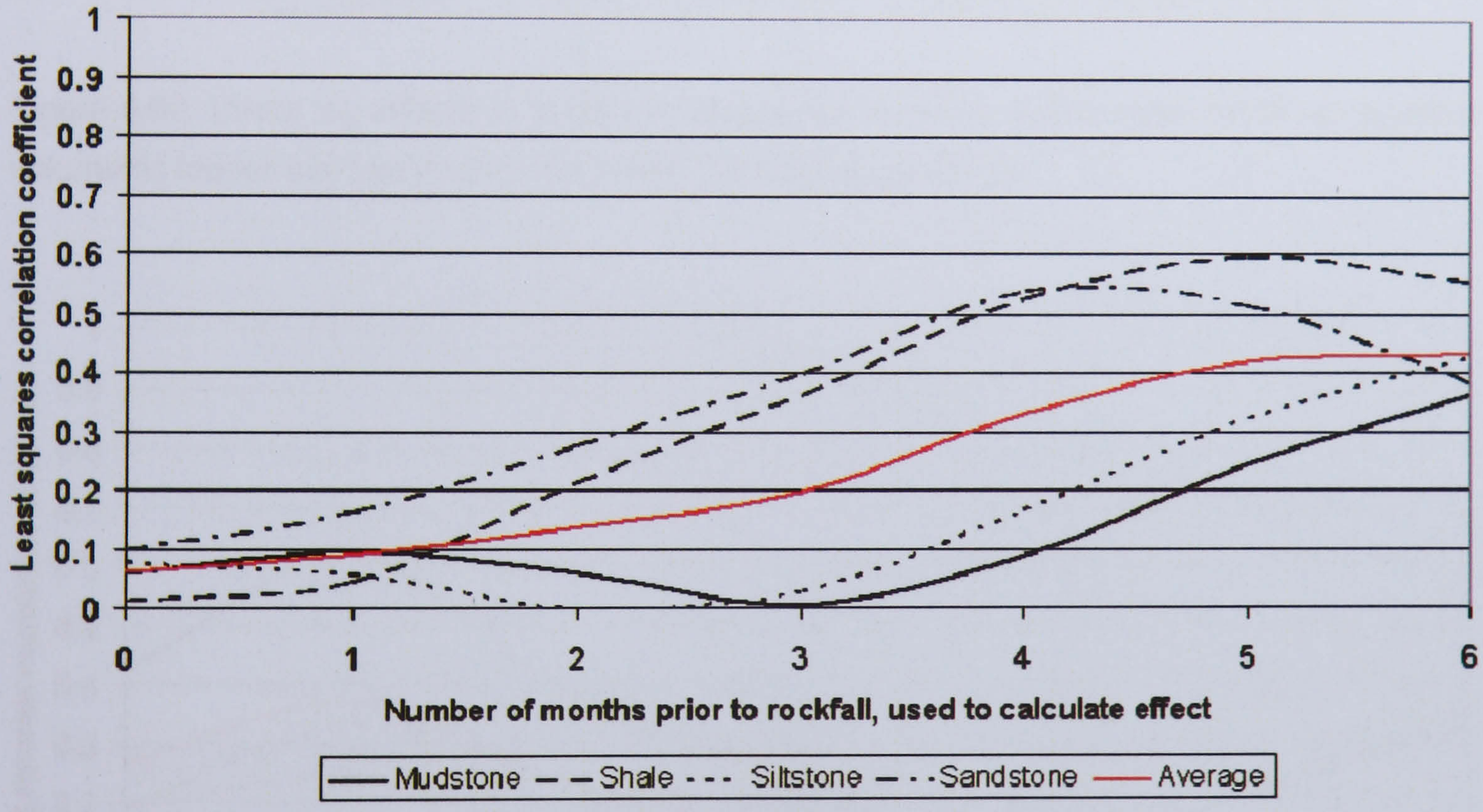

Figure 6.79: Cumulative effects of average monthly sea-levels on monthly volumetric losses from each of the four main rock types monitored.

The position of the mudstone layers almost entirely within the wave impact zone is reflected in their correlation with maximum sea-level (Figure 6.80). The strength of the relationship sets the mudstone apart from the other main materials in the rock mass, although they too show the general influence of a one and a four month lag. The sensitivity of the mudstone to the cumulative effects of maximum sea-levels differs to that of average sea-levels in that there is a temporal decay in the significance of the

relationship (Figure 6.81). Mudstone is again distinct in its sensitivity to maximum sea-levels. The cliffs appear to respond relatively quickly to maximum sea-level conditions, in comparison with wind effects for example, and the relationship is strongest with the accumulation sea-levels during just the previous month.

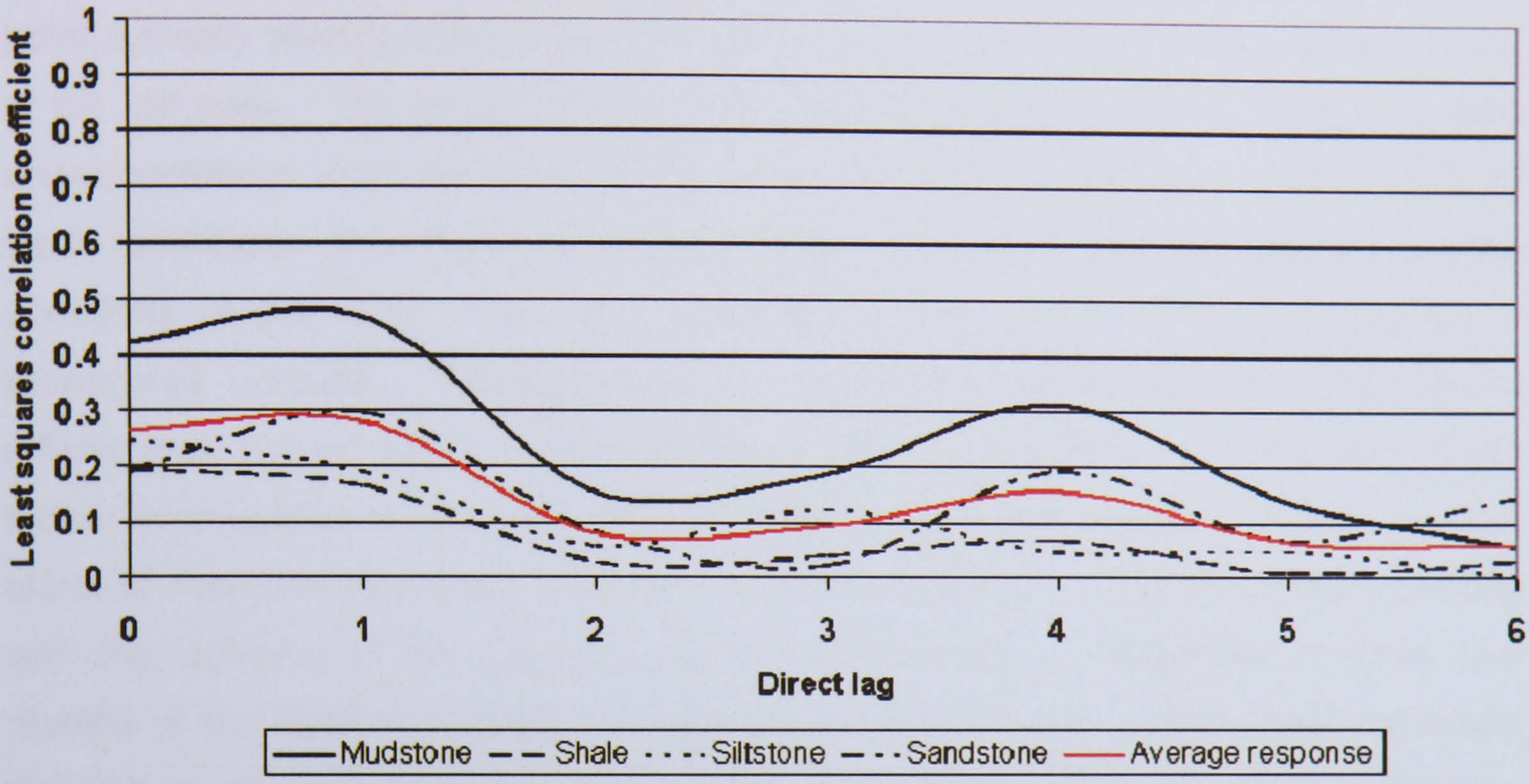

Figure 6.80: Direct lag effects of maximum sea-levels recorded during each month on monthly volumetric losses from each of the four main rock types monitored.

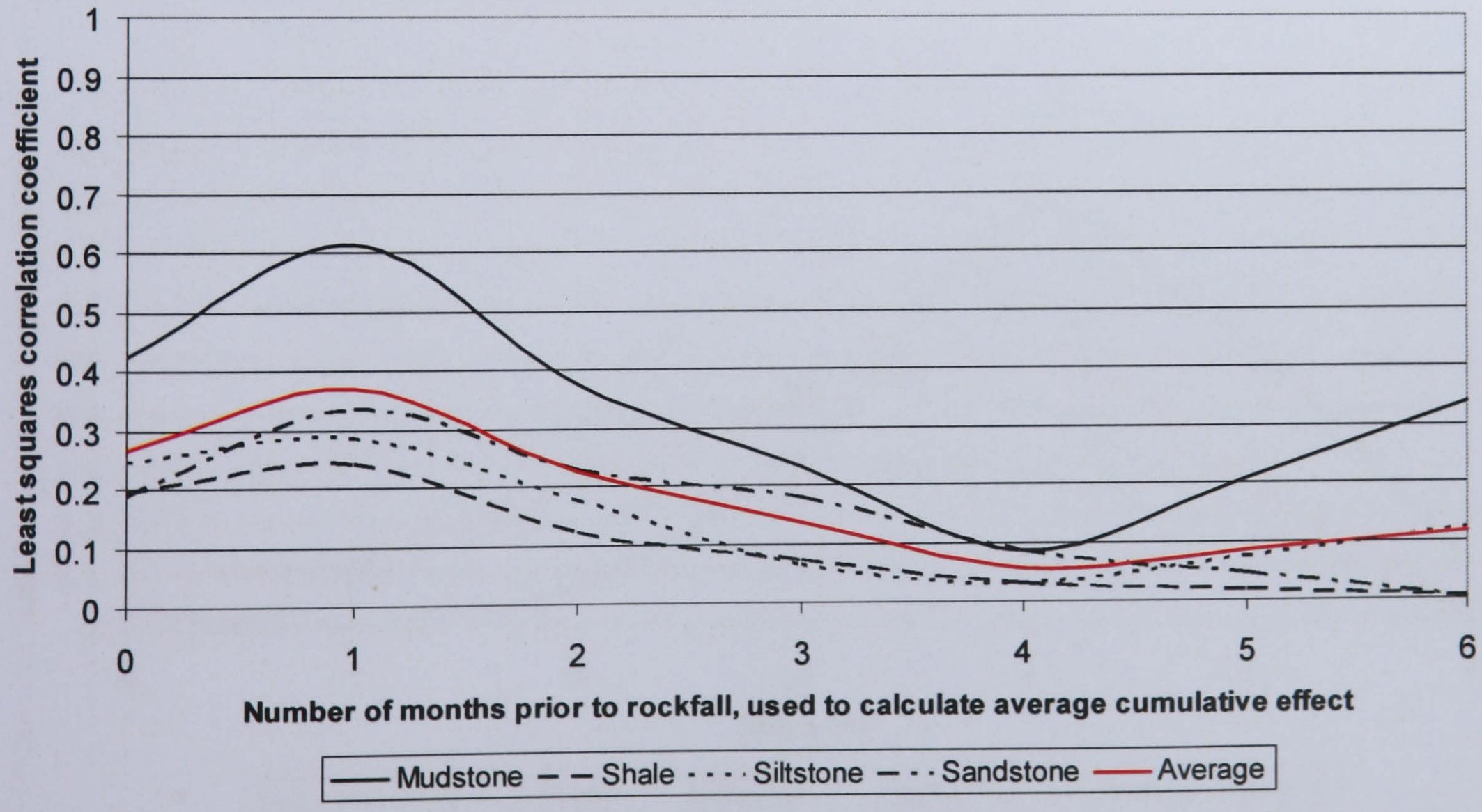

Figure 6.81: Cumulative effects of maximum sea-levels recorded during each month on monthly volumetric losses from each of the four main rock types monitored.

Minimum sea-level had a significantly stronger direct lag effect on the mudstone then either average or maximum sea-levels. The four month lag was again most strongly evident in the mudstone material (Figure 6.82). The strength of the relationship with minimum sea-levels may reflect their closer association with the junction between the cliff and the rock platform. Sea-levels that correspond to this point, typically around ordnance datum for most sites monitored, cause waves to break at the cliff base. The impact of such sea-levels is therefore likely to be greater than under conditions when the waves break on the foreshore or fail to break under deeper water conditions. The impact of waves breaking at the cliff base may also explain the sensitivity of the other main rock materials, as the shock of breaking waves is propagated upwards. Although the data provided tentative evidence that marine effects may extend beyond the material in immediate contact with the sea, much further investigation is required into the nature of such mechanisms. The cumulative effect of minimum sea-levels displayed an inverse pattern to the direct lags, peaking with the inclusion of the previous month and declining to insignificance when four months of sea-level minimums are considered (Figure 6.83). Once again mudstone was the most responsive material but the consistency within the other rock types suggests sea-levels may have had wider ranging influence than isolated quarrying at the cliff base. Unusually, the correlations are weaker for the cumulative effects than the direct lags which provided particularly strong influence on cliff behaviour. The significance of a four monthly lag requires further investigation.

Figure 6.82: Direct lag effects of minimum sea-levels recorded during each month on monthly volumetric losses from each of the four main rock types monitored. The 4 month lag in the mudstone has yet to be explained but may be associated with combinations of processes such as summer rains following on from winter storms.

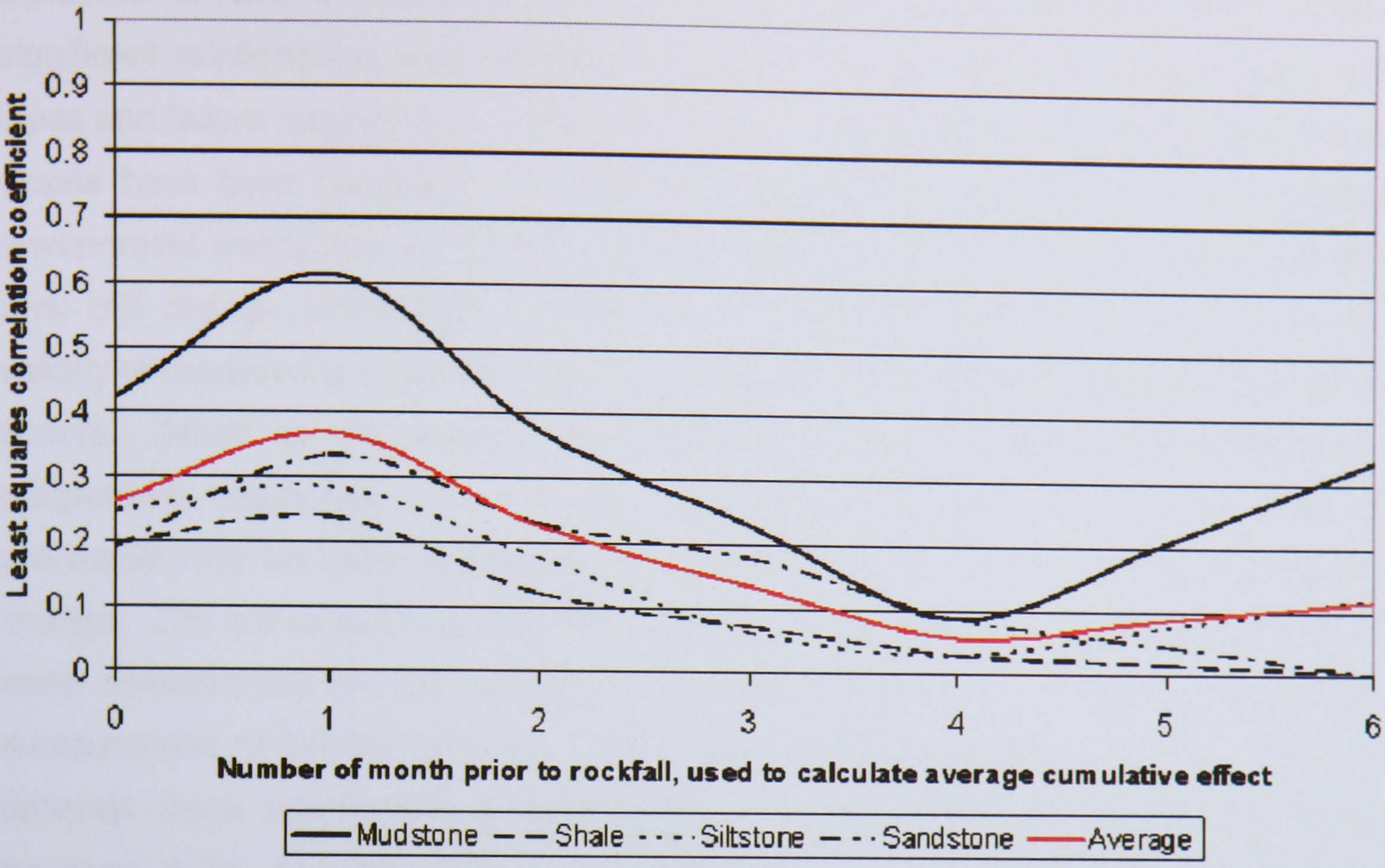

Figure 6.83: Cumulative effects of minimum sea-levels recorded during each month on monthly volumetric losses from each of the four main rock types monitored. Cumulative influences were less useful in the explanation of the effect of minimum sea-levels on rock cliff behaviour, producing weaker correlations than direct lag effects.

Direct lags and cumulative effects have proved valuable tools in the analysis of the effect of environmental influences on monthly rockfall volumes. Many correlations were improved with the consideration of the conditions leading up to the cliff response. The dual analysis of lag and cumulative correlations raises doubts over the validity of studies that make direct and immediate connections between forcing factors and landform behaviour. Direct responses or triggering events may be applicable to responsive materials such as soft rocks and clays but the processes governing hard rock coastal cliffs, in particular those that are lithologically varied, have proven to be more complex. The analysis conducted has been restricted to identifying relationships of sufficient strength to be recorded in spite of the noise produced by other influences. In reality, hard rock cliff responses are site and time specific; even the sub-division of the constituent cliff materials assumes that the properties of each rock type remain relatively consistent across all sites. This is evidently not the case with some sites significantly weakened by jointing patterns. A more complete consideration of the precise circumstances under which failures occur may explain some of the variance recorded.

Having analysed the influence of numerous environmental variables on the behaviour of hard rock cliffs, few direct links can be convincingly established. When significant relationships were identified they were often specific to certain sites, rock types and failure magnitudes. Instead new levels of complexity in the response of rock slopes have been revealed. The interaction between processes within the coastal environment makes the identification of connections between particular elements and rock cliff change problematic. Furthermore questions have been raised over the validity of considering rockfalls in relation to specific environmental factors or groups of factors. Much as the patterns of rockfalls have demonstrated more continuous, progressive responses, the data have suggested that the net effect of suites of processes may be more appropriate to understanding the factors driving rock slope change. The soil moisture deficit climatic index was tentatively used as an indicator of water availability to the cliff, explaining more of the variance in rockfalls than the raw measurement of rainfall amounts. With the continued production of high-resolution datasets more appropriate climatic indices may be developed providing a better measure of the complex interaction between the cliff and the environment. Perhaps the most important result from the use of the climatic index was the identification of extreme conditions produced by a combination of low rainfall and high temperatures at the start of the monitoring period. Although the raw inputs into the cliff system during the monitoring period were not exceptional, the interaction between them produced some of the largest moisture deficits within the 30 year MORECS record. It must therefore be recognised that the monitoring data may reflect cliff changes unrepresentative of the effect of longer term environmental processes.

The distinction between average or base-level conditions and extreme weather conditions has highlighted some interesting trends relating to the continual degradation of material strength and the triggers of more active phases of development respectively. However it should be noted that the effect of peak and average weather conditions are only general approximations, due to the monthly sample interval used to collect the rockfall data. The correlations with extreme conditions such as minimum temperature or maximum wind speed therefore have a temporal error margin of ±1 month because it cannot be determined whether the changes followed immediately after the process change. An attempt has been made to investigate the temporal elements to rock cliff responses with the use of direct lags and cumulative effects. Correlations were invariably improved to some degree with the consideration of past conditions. Insights into the nature of cliff behaviour provided by the analysis of the extent to which environmental processes can be attributed to change can be summarised as follows:

- Average monthly environmental conditions provide little benefit in explaining the patterns of behaviour in hard rock coastal cliffs.
- The tendency for more extreme environmental factors to be more closely associated with rock slope change further suggests that understanding into contemporary and future cliff behaviour requires a consideration beyond general base levels to the magnitude and variability of weather conditions.
- A change in an environmental variable, or a combination of environmental variables, cannot necessarily be directly related to a specific change in the rock slope.
- There may be a base level of cliff change that is more constant and perhaps internally driven rather than determined by external environmental processes.
- Higher monthly rockfall volumes are associated with higher moisture contents within the cliff material.
- The numerous influences on the water content within cliff material may provide a more meaningful control on cliff behaviour than the raw input of moisture into the cliff system.
- The effects of intense rainfall are more immediate than delayed.
- The cumulative conditions from the previous month may provide short-term control on cliff response to rainfall.
- The most significant periods of cliff change at the site were associated with colder temperatures.
- The lowest temperatures appear to generate greater variability in slope response, with the scatter narrowing towards warmer average temperatures.
- High temperatures produced responses specific to different rock types.
- The mechanical influence of freezing water may be an important factor in causing material to become detached.
- Weaker rock material such as shale is the most sensitive to freezing temperatures and the associated processes have greatest effect on specific sizes of material.
- Lagged response to temperature may reflect the time taken for the rock material to be suitably altered and weakened by temperature cycles to become susceptible to failure.
- The effect of temperature on rock cliffs may produce more general levels of response rather than dramatic changes in cliff behaviour.
- Average wind conditions, rather than maximum gust speed, provide a better indication of aeolian direct influences on larger losses from the rock slope,

although the smallest changes typically correlated more strongly with maximum gust than average monthly wind speed.

- Wind effects may take longer than the other environmental variables considered to affect cliff behaviour.
- It is the accumulation of average wind speeds over several months, rather than the conditions in any particular preceding month, which influenced cliff behaviour.
- Higher sea-levels generate greater potential for landform change, although such conditions do not necessarily lead to direct responses.
- The basal rock was more sensitive to marine activity than the rest of the cliff face despite its relatively high geotechnical competence.
- Maximum sea-levels may be a more important influence on rock slope change than average monthly levels.
- Maximum sea-levels suggest that extreme rather than base-level conditions provide the greatest control on rockfall activity.
- The combination of average monthly sea-levels and wind speed is important in understanding the behaviour of the basal layers.
- Interrelations were noted between processes, for example inverse relationships with wetter months may actually be a positive relationship with sea-levels during summer months with intense rainfall but calm sea conditions.
- Wave energy delivered to the base of the cliff may influence material beyond the direct contact zone between the rock slope and incoming waves.

6.7 Summary

The patterns of change across the monitored rock cliffs have shown complex responses to a variety of inherited and external controls. Cliff responses have been shown to vary spatially and over time to influences such as rock type, protrusion and environmental processes. Important contributions have been made to some of the persistent questions over the nature of rock cliff geomorphology. Magnitude-cumulative frequency patterns have been shown to be dominated by large failures of material although the volumetric contribution of tiny scale losses was also deemed to be more significant than intermediate scales of change. This magnitude-frequency association was found to be scale independent although the precise nature of the relationship was strongly influenced by location and therefore the scale of analysis.

The temporal patterns within the data have shown that failures become increasingly episodic with size although the spatial connectivity of many periods of

rockfalls separated by several months or more raise questions about viewing failures as discrete 'events'. Linkages between the degree of protrusion and the magnitude of the failure have promoted the idea of the rock mass as a continually deforming mesh. Explanations for the cause of rock cliff change have been investigated with respect to individual, multiple and combined processes, in terms of direct quantitative links, relationship strengths and past influences. Several different sizes of failure displayed particular sensitivities to specific environmental processes. Ultimately the data suggest that consideration of individual elements, which are fundamentally interrelated, will oversimplify the environmental effects on the cliff. The extent to which issues over the magnitude and frequency, scale dependency, episodicity and environmental controls on rock cliffs have been addressed has however been partially limited by the nature of the dataset. Whilst the patterns of rockfalls reveal much about geomorphological change undergone by monitored cliffs, a more complete understanding of processes is limited by two aspects of the data. Firstly, despite the high-resolution and extensive spatial coverage achieved, the temporal extent of the record is inadequate to assess the medium to long-term evolution of the cliffs. Secondly, the volumetric losses can only be tentatively associated with the mechanisms of change, such as overhang failure, by the dataset which is predominantly descriptive. More definitive conclusions on the nature of rock slope change, alluded to by the monitoring results, can now be considered with the use of numerical modelling.

Chapter 7
Understanding cliff evolution

7.1 Introduction

The changes recorded in monitored sections of hard rock coastal cliffs have provided new insights into the processes that influence contemporary behaviour, but are limited in understanding the mechanisms driving cliff response. This chapter uses numerical models to address questions raised over the development of slopes, which could not answered by the quantification of short-term changes alone (refer back to the left side of Figure 4.1). The aim of the chapter is to investigate further the nature of rock slope responses, which often involve time periods longer than the extent of the monitoring records. A hybrid element code able to model both discontinuous element interactions and intact material fracture has been used to simulate failure events from their initiation through to their conclusion. The new application of the code required it first to be validated against proven approaches to rock slope analysis before its combined element properties could be used to explore the mechanisms and thresholds governing cliff responses monitored in the field. The models reveal aspects of the controls on slope behaviour, with specific reference to the magnitude, frequency, scale and timing of failures, in addition to the interactions between *in situ* conditions and environmental processes that determine rock slope form.

7.2 The drivers of rock slope change

Recording cliff alterations over time provides insufficient information on the internal mechanisms to gain a more complete understanding of the drivers of landform response: for this rock slope models are required. Many types of rock slope model exist for the purpose of explaining landform change. Most attempts to interpret model output with reference to actual rock slopes have been limited by the type of analysis, which means that modelled failures are governed either by the movement of predefined blocks (discrete analyses) or the initiation of weaknesses (finite analyses). Much of the real-world monitoring data suggest that failure in rock slopes may involve complex and progressive processes, and an appreciation of both aspects of change may need to be considered within the same simulation. The use of numerical model simulations in this study has been driven by several of the key questions over the nature of rock slope change, which remain unanswered from the monitoring analysis (Table 7.1). To address these issues the selection of a modelling code capable of simulating the processes of failure from initiation through to the release and deposition of material from the slope was required. The recent development and application of a combined finite/discrete element code, Elfen (Rockfield, 2001), now offers the potential to incorporate both material fracturing and discrete body interactions within the same problem domain (Eberhardt *et al.*, 2001), although it has yet to be applied in the context of rock cliffs.

Table 7.1: Key questions to be addressed by the modelling investigation. Each question is referred to by number through the course of the chapter.

1. Can the mechanisms behind rock cliff behaviour be better understood with numerical models and used to explain aspects of the changes recorded?
2. What are the generic bounding conditions to failure in rock cliffs?
3. To what extent do the structural weaknesses throughout a rock slope determine its behaviour?
4. How important is material fracture in governing slope development?
5. What are the mechanisms behind the relationship between failures of different magnitudes and frequency of occurrence?
6. Are the mechanisms controlling rock cliff behaviour scale dependent?
7. Is long-term cliff behaviour episodic or continuous?
8. Are cliff forms determined predominantly by subaerial or marine processes, or a combination of the two?
9. Is it appropriate to view long-term cliff recession as a constant process?

7.3 The Elfen code

The application of every model to geomorphological systems is limited by the accuracy of its inputs and the adequacy of its solution in representing reality (Pyle and Richards, 1997). The resultant trade-off between model performance and complexity requires model type to be carefully selected (Cojean, 1995). Elfen is a finite element system able to simulate both the processes within an intact rock mass and the interactions surrounding discontinuous material (Rockfield, 2001). It uses an explicit central difference algorithm to solve applications, allowing finite elements within the continuum to fracture when stressed beyond their relevant failure criterion (Figure 7.1). It has been selected for this study because the progressive nature of failure indicated by the analysis of contemporary rock slope change may cause exclusively discrete or finite models to misrepresent the mechanisms of slope behaviour.

Elfen provides two plasticity models of material response, a Rankine fracturing model, or a Mohr-Coulomb shear model which can be additionally modelled with a Rankine tensile cut-off to model both brittle tensile axial fractures and more ductile shear (Crook *et al.*, 2003). Elfen has been used to examine the initiation and progressive failure of the Randa rockslide, Switzerland (Eberhardt *et al.*, 2004). The hybrid approach successfully modelled the multiple stage slide event in 1991, developing a failure band as the load carrying capacity is reduced over time. The model shifted from continuum to discontinuum analysis as fractures develop and spread in accordance with deviatoric stresses concentrations. The analysis indicated ultimate shear failure only initiates when the surface is nearly fully developed and tensile fracturing has led to significant cohesion loss (Eberhardt *et al.*, 2004). The potential of Elfen to account for the progressive nature of rock failure has therefore already been promoted, but its validation and application remain limited.

Developed since 1986, Elfen is a modular package requiring the manual input of mesh geometry, applied loadings and constraints, material and mesh properties. Its functionality is based around a graphical interface that allows for model definition, implicit and explicit analyses, and post processing facilities. This automates much of the modelling process, shifting the emphasis from the operator to the powerful software algorithms. It should be noted that Elfen cannot currently simulate fracture propagation in three dimensions, and hence its use in the investigation into rock slope mechanisms has been restricted to two-dimensional projects. Although this limits the application of numerical models to solid cliffs, two-dimensional model meshes generate consistently lower stability values than three-dimensional approaches, suggesting the results can be viewed as conservative estimates of stability.

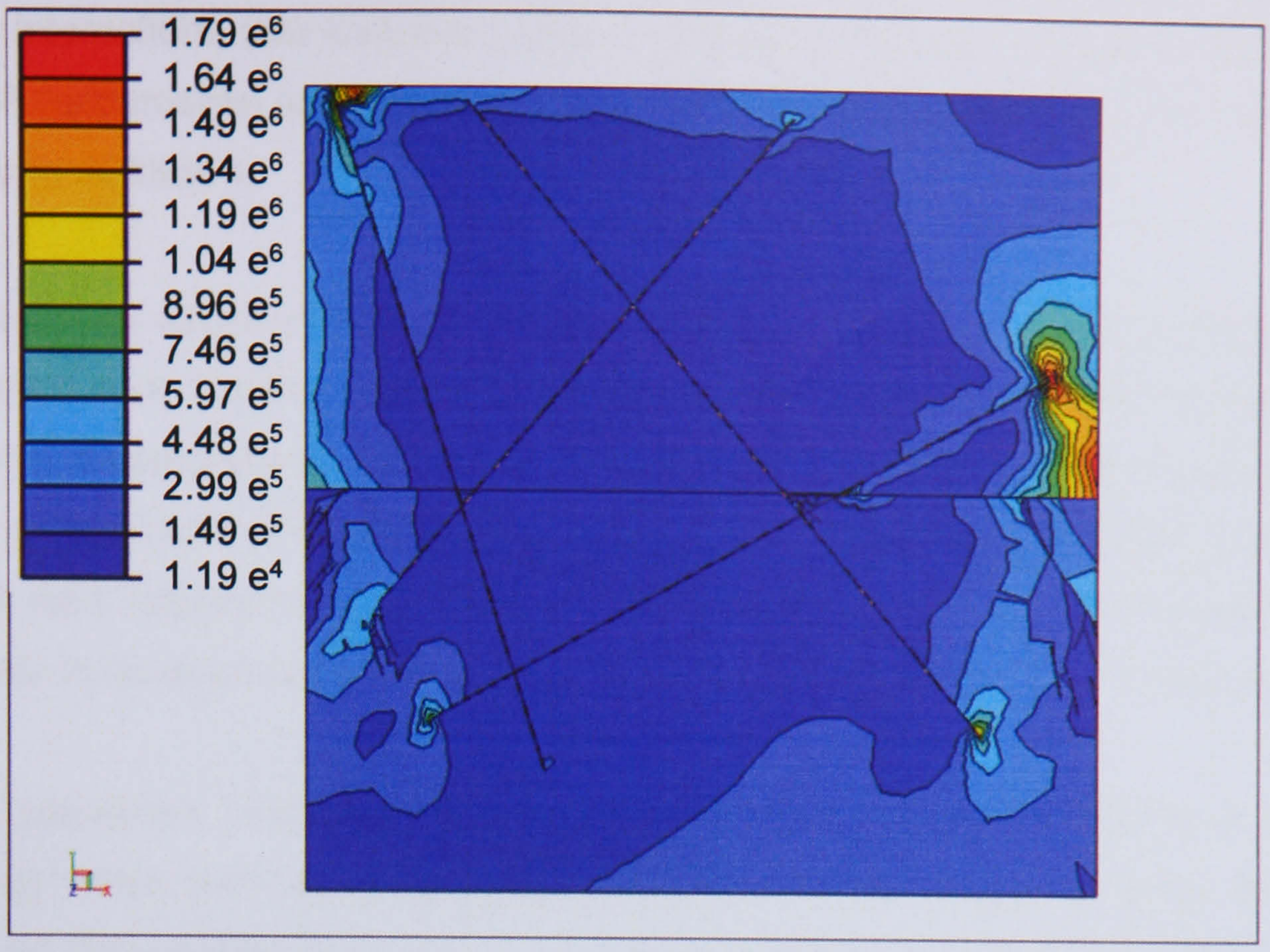

Figure 7.1: The Elfen code has demonstrated the ability to model fracturing through a material, highlighting its potential for the study of rock slope mechanics. Here two rectangular layers,5 m thick, with predefined joints are settled under gravity causing stress concentrations and fracturing towards the edges. Contours denote effective stress.

The Elfen code has not been explored with regards to coastal cliffs, although its potential has been acknowledged (Stead *et al.*, 2004). It is essential then that state-of-the-art, highly automated analytical tools such as Elfen are applied critically and appropriately, following defined numerical modelling practices (Coggan *et al.*, 1998). There is, for instance, a pressing need to establish the relative importance of code parameters such as geometrical changes, boundary and stress conditions and discontinuity properties (Eberhardt *et al.*, 2001). It is therefore critical that the ability of the Elfen code to respond to different model inputs associated with the range of mechanisms thought to operate in rock slopes is established before it can be applied.

7.4 Validating Elfen for rock mass analyses

The current levels of understanding into stability conditions, potential failure mechanisms and sensitivity to change of rock slopes have been significantly advanced with the use of a series of continuum and discontinuum analyses (Selby *et al.*, 1988; Pitchard and Savigny 1989; Pande *et al.*, 1990; Poisel, 1990; Pan and Reed, 1991; Shi, 1993; Adhikary *et al.*, 1996; Allison and Kimber, 1998; Stead *et al.*, 2001; 2004; Eberhardt *et al.*, 2001). Every numerical modelling code requires verification, although the relation of a simulation to the natural environment is often difficult to achieve (Brown, 1987). Agreement between various numerical models and physical tests has for example been used in order to demonstrate the relevance to reality of modelled

material interactions (Cundall and Strack, 1979; Lemos, 1990; Pritchard and Savigny, 1989). A fundamental concern in the new application of a modelling code is therefore how best to validate it.

It seems apparent that an appropriate model of all but the most perfectly jointed or unjointed rock masses must be capable of accounting for both the formation and interaction of separate blocks within the landform, and progressive weakening and yielding of the constituent materials. The lack of suitable comparisons however, in terms of field, laboratory or numerical models, has required the performance of the Elfen code to be assessed by modelling specific aspects of rock slope behaviour.

Established modelling practice promotes the progressive building in of model complexity within carefully constrained bounding conditions from simplistic theoretical beginnings (Eberhardt *et al.*, 2001). It was decided to examine the sensitivity of the code to relevant parameter changes, which might be expected in the field, on two levels. Firstly, well established and field validated simple failure criteria were considered for a single block inclined on a slope. These simulations recreate one of the earliest and most established attempts to quantify rock failure phenomena by DeFreitas and Watters (1973). The results refer to the general conditions associated with different failure modes that have been applied to a wide variety of rock masses. Secondly, the interactions within specific rock mass structures were modelled. Field validated discrete and finite approaches were used to assess the adequacy of the analysis to account for continuously jointed and weak rock slope behaviour respectively. Such models provide greater levels of detail into the mechanisms of slope change but are restricted in their application to more localised analyses. Ultimately the validation of Elfen required it to demonstrate a responsiveness to material deformation both along existing discontinuities, and within rock stressed beyond relevant yield criteria in order for it to reliably account for the mechanisms of rock slope change (refer back to question 1, Table 7.1).

7.5 Model parameters for failure in a single block

In order to gain a basic quantitative understanding of the failure within rock masses, DeFreitas and Watters (1973) conducted field and laboratory tests on a single rectangular block placed on an inclined surface. The base of the block, b, its height, h, angle of plane inclination, α, and friction angle between the block and at the base, ϕ, were systematically altered to establish criteria for block stability and different failure modes (Table 7.2). The failure conditions were verified against rock mass failures from North Devon, Wales and Scotland. The results demonstrated a transition in block

behaviour from stable through to sliding and toppling failures. The limiting conditions for material with a 40° friction angle can be represented on a graph of base plane angle against base to height ratio (Figure 7.2). The distinct regions illustrate that a mass on a flat plane is more likely to be stable than when inclined on a base of increasing α, and sliding will occur when α exceeds ϕ. Wider, flatter blocks, with a large base to height ratio, are more likely to be stable while taller thinner blocks tend towards toppling or a combination of sliding and toppling failure. The failure mechanisms established for a single block provides a useful starting point for the validation, before more complex interactions are considered.

Table 7.2: Empirical failure conditions for a single block inclined on a plane (after DeFreitas and Watters, 1973).

Boundary Condition	Block Failure Mechanism
$\alpha < \phi$ and $b{:}h > \tan \phi$	Stable
$\alpha > \phi$ and $b{:}h > \tan \phi$	Sliding
$\alpha < \phi$ and $b{:}h < \tan \phi$	Toppling
$\alpha > \phi$ and $b{:}h < \tan \phi$	Toppling and sliding

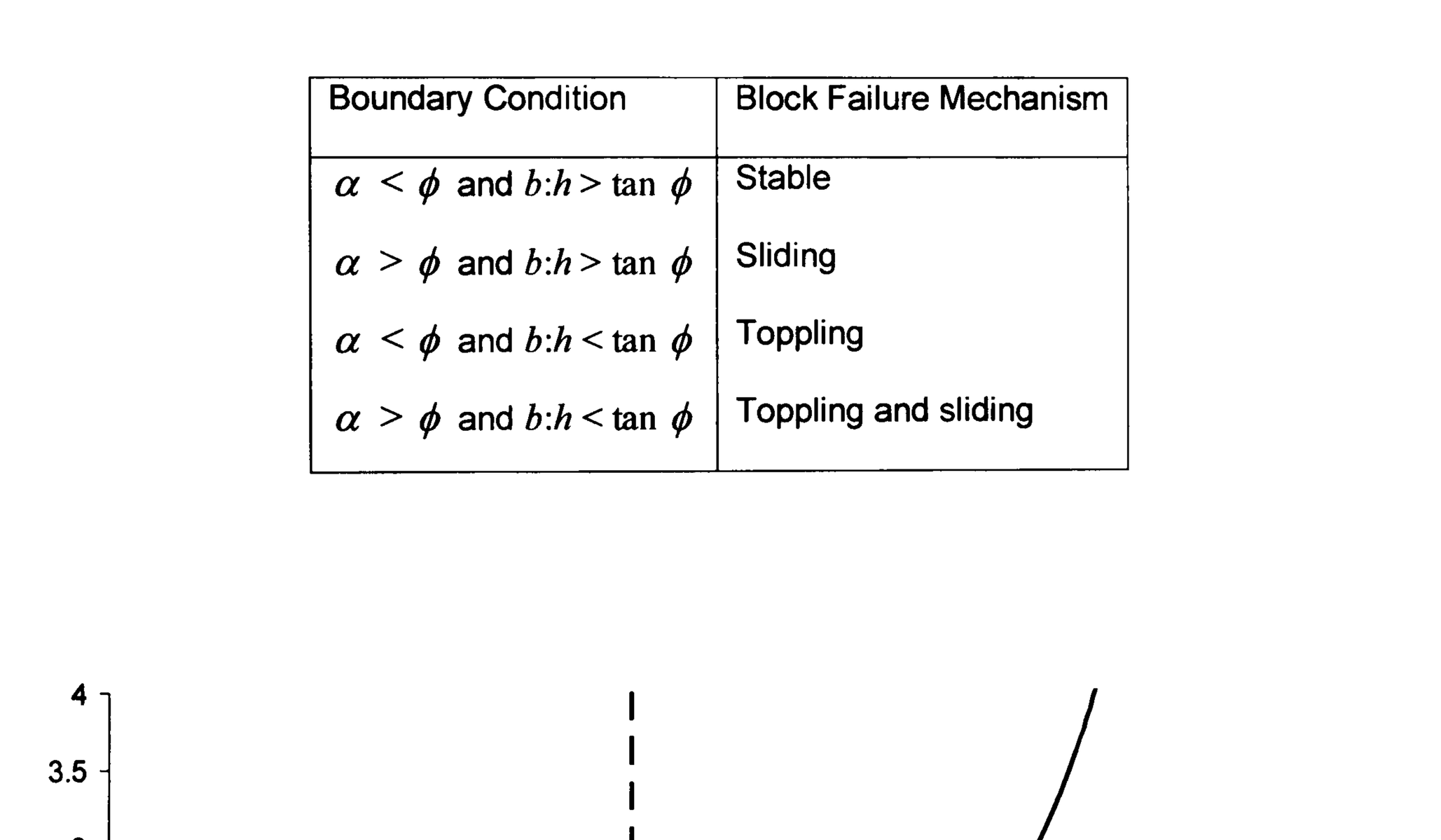

Figure 7.2: Graph of the response of blocks with a 40° friction angle as base to height ratio and base plane angle are altered (DeFreitas and Watters, 1973).

In order to investigate the effect of base plane angles and base to height ratios on modes of block failure, Elfen models were generated to reconstruct the scenarios defined by DeFreitas and Watters (1973). The dimensions of the block and the angle of inclination of the base plane upon which it was placed were varied but the friction angle of the material was kept at 40°. The results show a general agreement with the failure types proposed by DeFreitas and Watters (1973), particularly in the case of stable, toppling and sliding blocks (Figure 7.3). Most significant variability was found in the zone of toppling and sliding failure, which contained both sliding and toppling movements. The angle of internal friction was a strong determinant on the propensity of the block to fail and the coefficient of friction accurately delimited the boundary between stable and toppling conditions, but became slightly more blurred in separating sliding and toppling and sliding movements. The agreement with established failure modes suggests that the algorithms used in Elfen are sufficient to account for varied failure types but raises questions over whether such clear and simple divisions exist in more complex situations. The specific nature of each failure type was examined to reveal the characteristics of different mechanisms of rock slope behaviour.

Example models of each of the three failure types and a stable condition, demonstrate distinct differences in block behaviour despite being located close to the limiting boundary conditions (Figure 7.4). The blocks were initially constrained in horizontally, but allowed to settle vertically under a gravitational force of 9.81 N. The mass was constrained until kinetic energy reached equilibrium, indicating that gravitational stresses had been distributed through the block, and then the horizontal constraints were released. A block inclined on a plane of 39° and with a b:h ratio of 0.7 toppled while increasing the ratio to 1 generated kinematic stability. When the b:h ratio was kept at 1 but the angle of inclination increased to 41° sliding failure was initiated, transferring to sliding and toppling failure when the b:h ratio was reduced to 0.8. The sum of kinetic energy values within each mesh was recorded and plotted, providing an indicator of activity and therefore stability conditions. Although not directly comparable, energy levels up to eight orders of magnitude smaller than masses at the point of failure demonstrated the minimal motion recorded during stable block behaviour. The plot shows an initial decline in energy as the block adjusts to the force of gravity, before the horizontal constraints were released causing a second peak in energy. The energy within the free block is then seen to decline over time. Each of the three failure mechanisms demonstrated similar patterns in their initial phases but rather than level off, the energies within the unstable masses increased exponentially once the constraints were released. The models therefore demonstrate that when a situation in a rock mass exists which is kinematically unstable, failure is inevitable, even under

stabilised *in situ* stresses. Despite the highly simplistic nature of the simulations, similar conclusions have been reached in much more complex, real examples of landslides (Petley, 1994), perhaps suggesting that certain aspects of the failure process may be common to rock forms in general (question 2, Table 7.1).

The models were able to reveal new details about the behaviour of blocks classed as undergoing 'sliding and toppling' failure. A mass with a b:h ratio of 0.9, inclined on a plane of 42° is located on the border between sliding and sliding and toppling failure. The vectors of model displacement were seen to fluctuate between rotational or toppling movements and plane-parallel or sliding movements (Figure 7.5). Indeed during toppling phases the backwards edge of the base of the block momentarily lifted, reducing friction between the block and the base plane to permit sliding. As the sliding movement phase progressed the raised corner was brought once more into contact with the base, increasing friction and reverting movement from sliding back to toppling failure. A graph of the kinetic energy within the block conveyed this interplay between the two failure modes (Figure 7.6). The resultant stick-sliding movement illustrates that even within the most simplistic conceptual models of rock mass behaviour different controlling mechanisms may interact over time. The transitional behaviour demonstrated raises important questions over whether the interaction between different failure modes is actually critical to understanding the nature of failure in rock slopes. It has been common practice in slope analysis to attribute failure 'events' to certain mechanisms such as toppling (Pritchard and Savigny, 1989), sliding (Goodman, 1980) or falling failures (Hantz *et al.*, 2003). Little is known however about the interaction between different modes of slope change, and whether such rigid boundaries adequately describe the way in which natural rock slopes evolve.

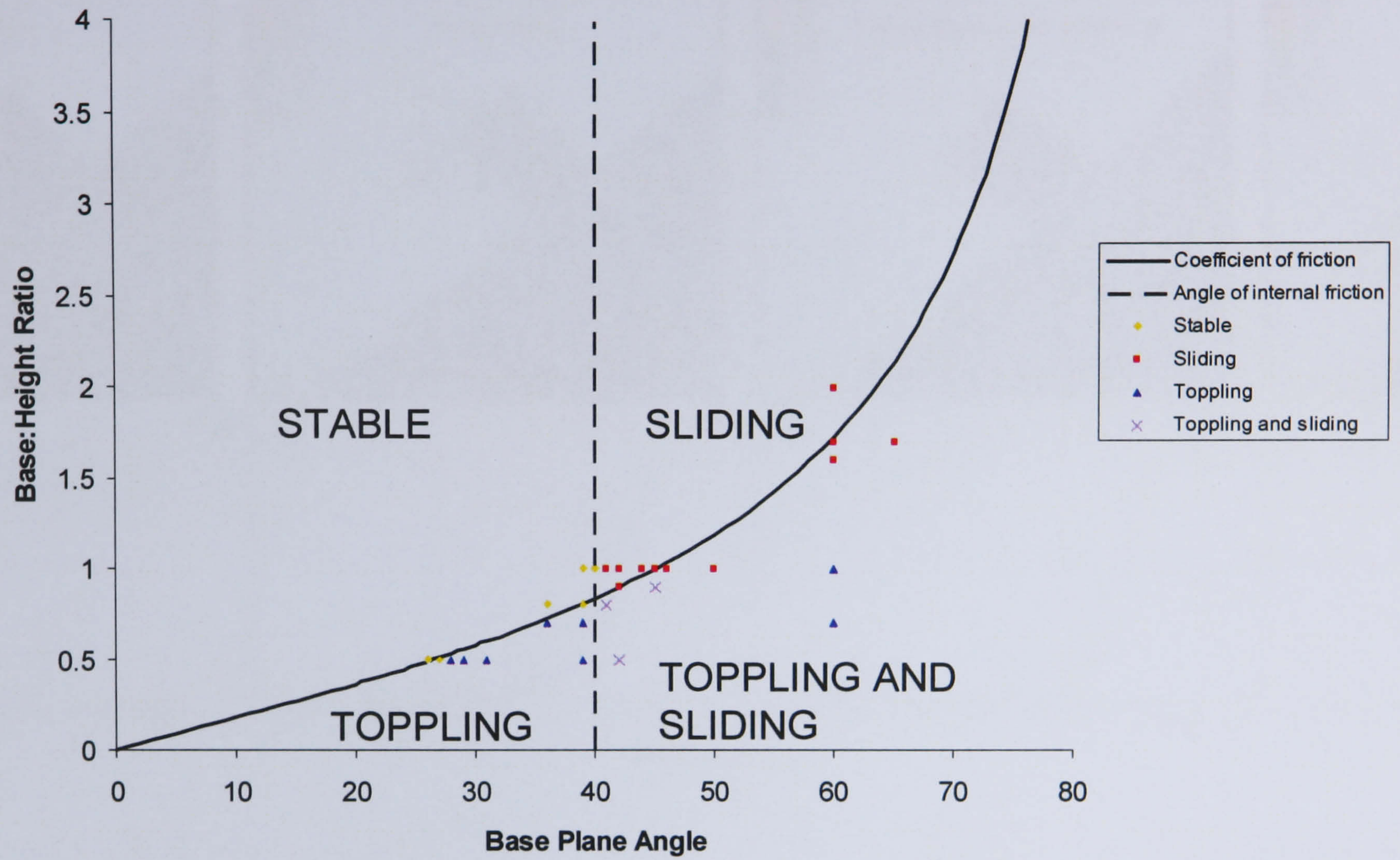

Figure 7.3: Elfen validation of stable, sliding and toppling failure modes in a single block, inclined on a surface. The stable, sliding and toppling boundaries provided strong controls on model behaviour. In agreement with other numerical models of the same scenarios (Kimber, 1998), the toppling and sliding condition recorded a mix of both toppling and sliding failures with increasing base to height ratios, although Elfen also demonstrated a mechanism which involved both toppling and sliding motion in the same simulation, not recorded by Kimber (1998).

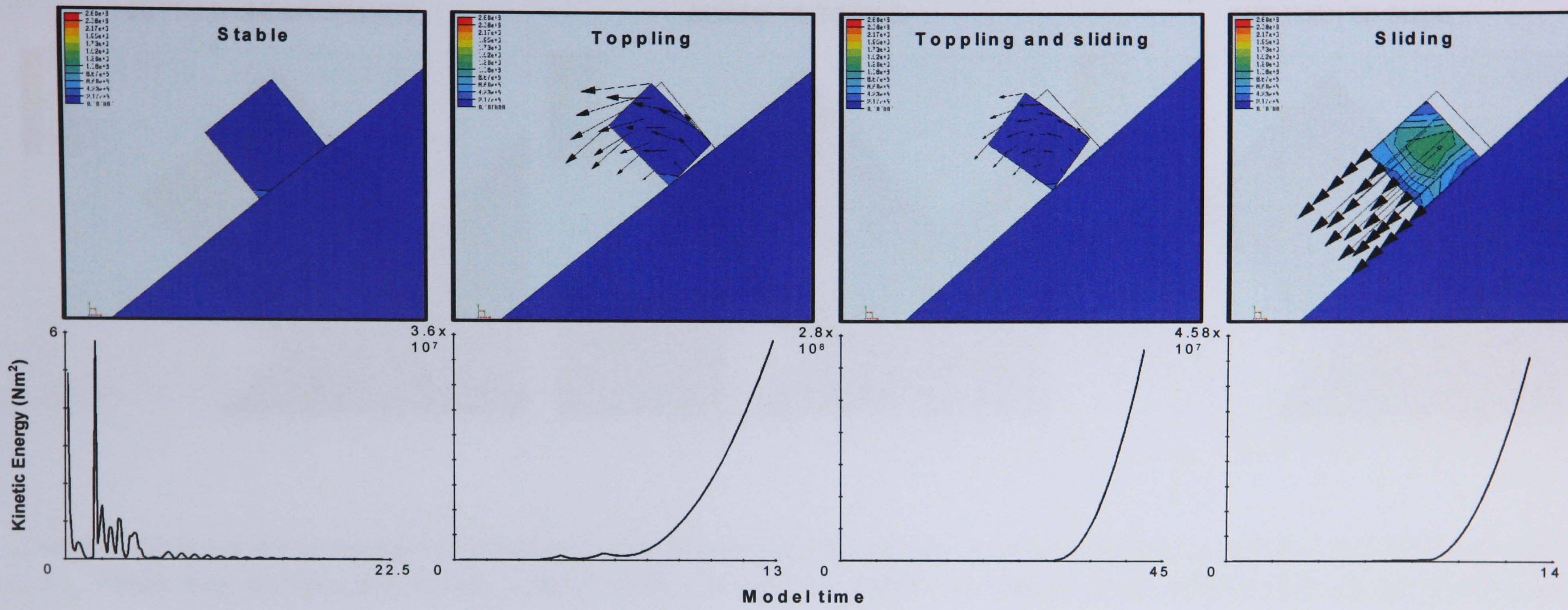

Figure 7.4: Example models and kinetic energy graphs for a single metre thick block inclined on a surface. The contours denote effective stresses within the block and an outline of the original block position is given to indicate the manner of the movement at the point of failure.

SETTLED UNDER GRAVITY

BEGINS TO TOPPLE

AND THEN TO SLIDE

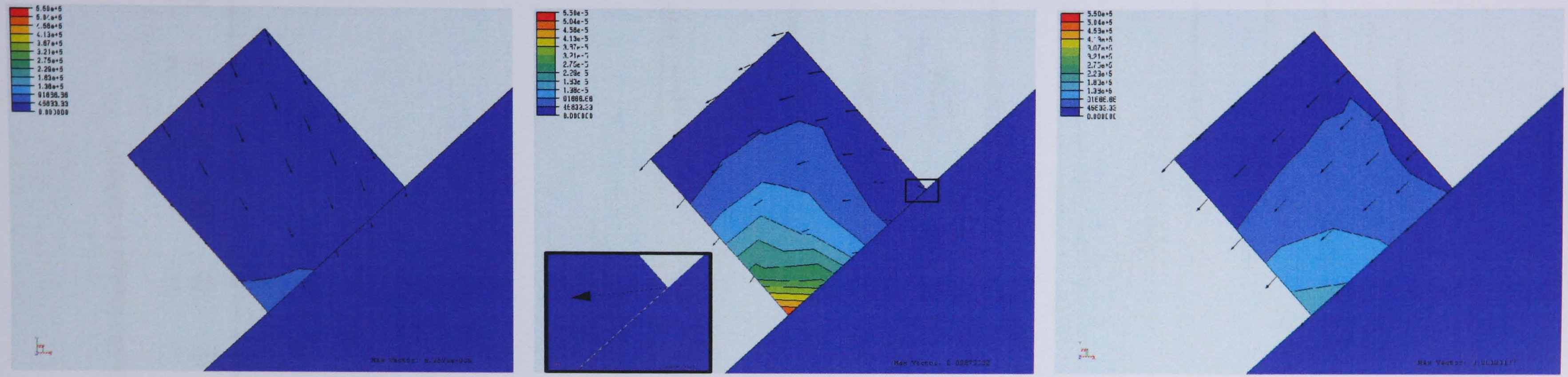

Figure 7.5: Toppling and sliding mechanism in a block inclined on a base plane. This example of a truly transitional mode of failure, bordering classic sliding and toppling motions raises questions over the way in which failures are currently classified. The contours denote effective stress and the vectors represent displacement.

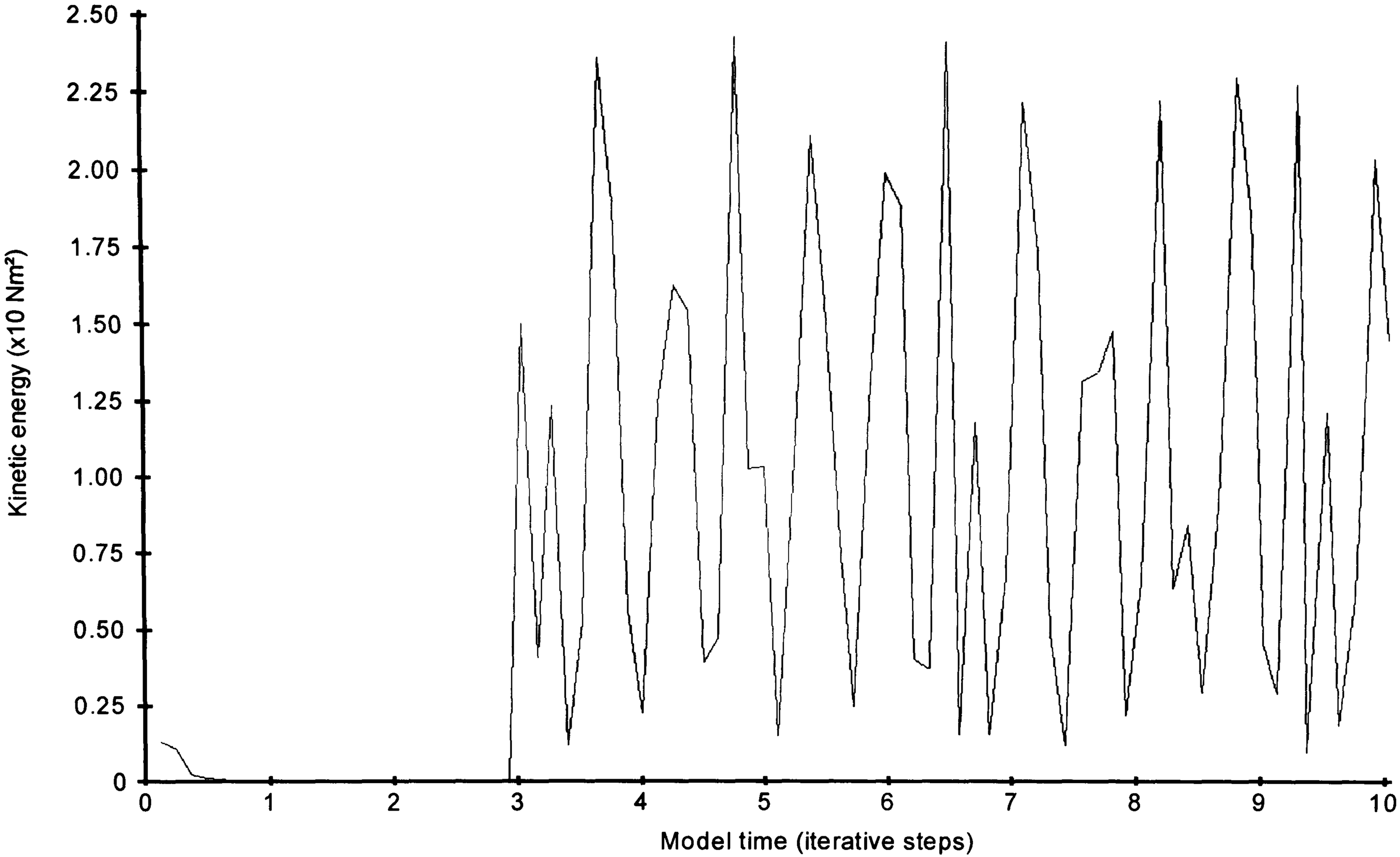

Figure 7.6: The kinetic energy within a block undergoing toppling and sliding failure. The cyclical tilting and sliding movement can be clearly seen in the fluctuations between motion and stability.

7.6 Multiple rectangular block interactions

While single block models demonstrate Elfen's ability to simulate the major failure mechanisms associated with rock slope change, the actual behaviour of the slope is governed by multiple blocks interacting over time. In addition to the properties of the failing material, the displacement of any single element within a rock mass is also a function of applied stresses caused by surrounding blocks. The occurrence of a particular failure type may therefore be controlled not by the kinematics of individual blocks, but by the slope height, layer thicknesses, intact material strength and discontinuity properties (Goodman and Bray, 1976). In order to advance the validity of model performance in accounting for the behaviour of actual rock slopes more testing was evidently required.

Kimber (1998) reconsidered the proposals of DeFreitas and Watters (1973) for kinematic limiting conditions for the failure of a single block, investigating failure modes within a rock mass with the use of the Universal Distinct Element Code (UDEC). The models subdivided the rock masses with regularly spaced bedding planes, again inclined by an angle α, and cross cutting joints, used to set the b:h ratio of the rectangular blocks. The input parameters were kept constant, but the b:h ratio was systematically altered by adjusting the spacing between the vertical joint set, and/or the bedding dip, α, such that the sensitivity of theoretical rock masses could be explored. The geometrical pattern of discontinuities was used to define new failure boundaries for rock masses (Figure 7.7). Through this approach it was seen that the interactions within surrounding rocks make rock masses considerably less stable than single blocks, displaying a significantly larger range of criteria in which failure can occur. For example a single block with a b:h of 3 and α of 35° was seen to be kinematically stable, but the dynamic stresses within a mass of such blocks fails through toppling.

Rock slope models require that once separate elements have developed they should act in a manner appropriate to the kinematic conditions within the landform. In order for the relative influence of discontinuities on rock slope behaviour to be accounted for it was therefore necessary for Elfen to display the different failure types within masses of interacting blocks. Attempts to use Elfen to explore Kimber's (1998) bounding conditions for rock mass behaviour were limited by the input of problem geometries which must entered manually using a combination of pre-defined entities to form the model mesh. This process severely limits the design complexity of the simulated rock mass. The code has however been designed to read geometrical data generated in CAD packages. An AutoCAD customisation was written for the

generation of meshes identical to those produced by Kimber (1998). The script allows the creation of any Elfen geometry mesh, based on standard modelling parameters including block base height and width, mass base height and width, angle of repose of the slope face, bedding angles and joint spacing (Figure 7.8). The system allowed multiple Elfen meshes to be created through the alteration of parameters, saving many hours of manual geometry definition.

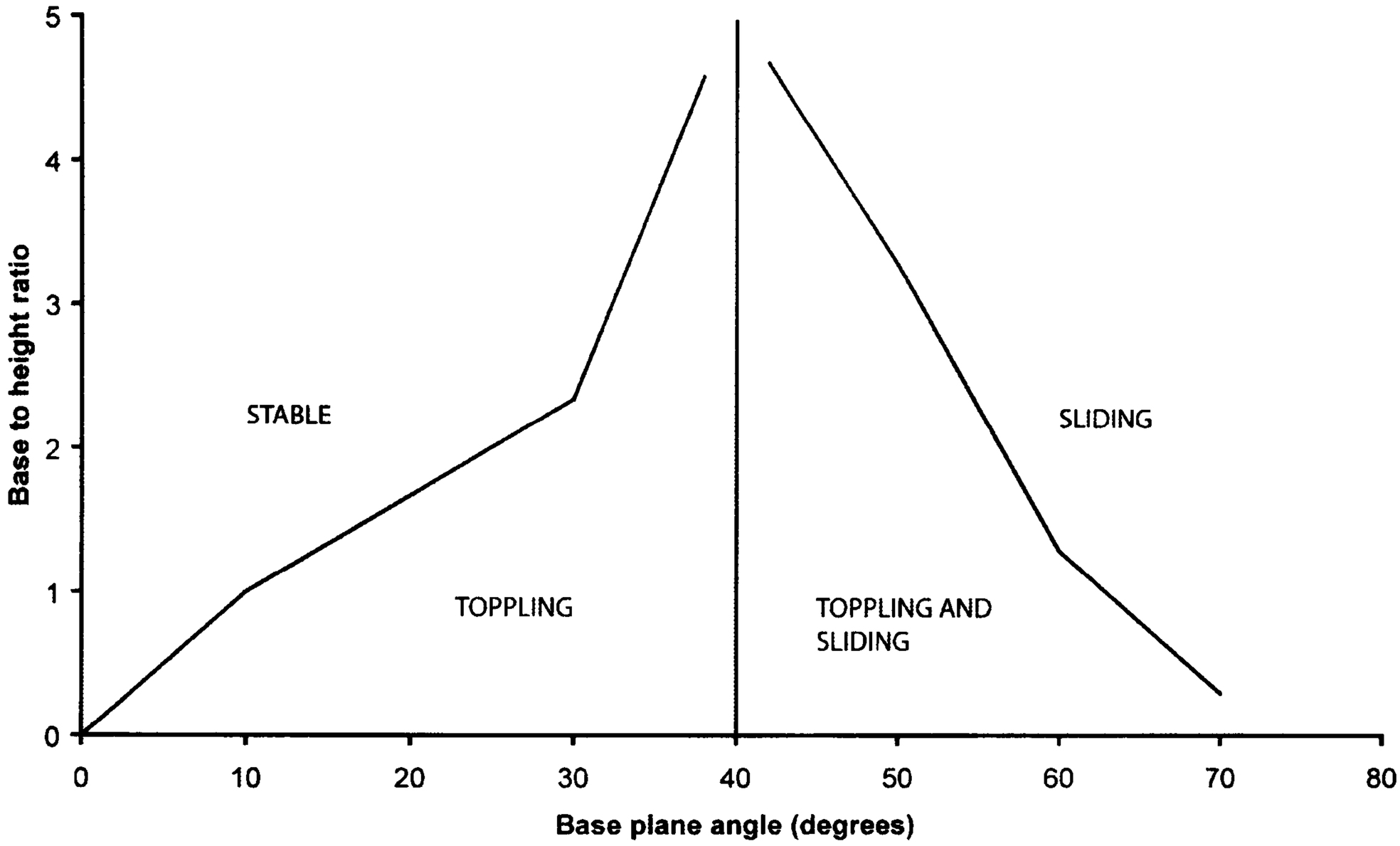

Figure 7.7: Rock mass failure boundary conditions (Kimber, 1998). The zone of toppling and sliding was reduced from that of a single block by the heightened tendency for sliding within masses as blocks were prevented from rotating.

The Elfen projects were defined as discrete in order to generate behaviour similar to that of the UDEC simulations. Discrete projects are well adapted to progressive failures directly dependent on discontinuous features, imposing no limit on the displacement and rotation of individual block elements (Cundall, 1971). In accordance with Kimber's (1998) experiments, the rock mass material was attributed the properties of the Portland Limestone from Dorset, UK. Block density was set to 3000 kg m^{-3}, and the internal friction angle, ϕ, was set at 40°. The jointing and bedding patterns were used to subdivide a rock mass 45 metres high and 80 metres wide. The open rock face angle was set to 85° with all other boundaries kept perpendicular. The blocks were located on a base extending 60 m in front of the rock mass and subjected to a force of -9.81 N vertically to represent the effects of gravity. Initially the vertical boundaries were constrained in the horizontal direction to distribute

gravitational stresses throughout the rock mass. This settling stage was run until the kinetic energy fluctuations within the mesh had minimised, before the horizontal constraint on the inclined rock face was released.

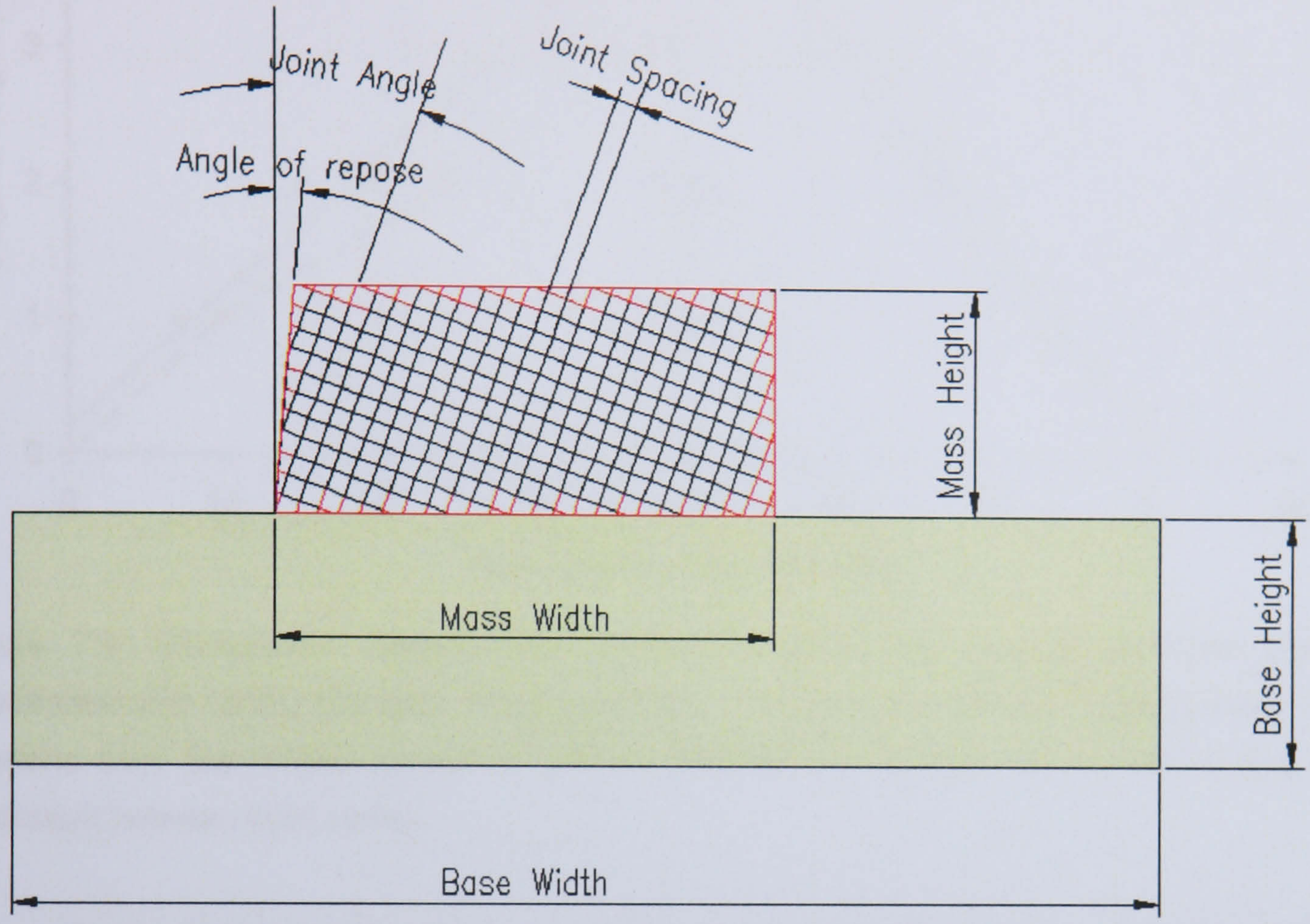

Figure 7.8: Elfen model geometry customisation in AutoCAD. The script enabled the efficient generation of multiple geometry files immediately available for use in Elfen.

The model runs demonstrated sliding, toppling, sliding and toppling and stable rock mass responses (Figure 7.9). The general patterns caused by changes in the base to height ratio and base plane angle were very similar to those registered by Kimber (1998). Subtle differences were recorded between the precise placements of the limiting conditions derived by the two model sets. The Elfen simulations did not display the same inversions in the bounding conditions between either stable and sliding or toppling and sliding and sliding. It is possible that the complex behaviour of masses experiencing instability conditions between multiple failure types causes differences in the computational outcomes of different models. Once again, questions are raised over how adequately fixed classifications of failure type can be used to describe and understand failure mechanisms. The overall correspondence with the extensively applied UDEC code however suggests Elfen's distinct element properties may be an effective tool in the investigation of highly jointed rock masses.

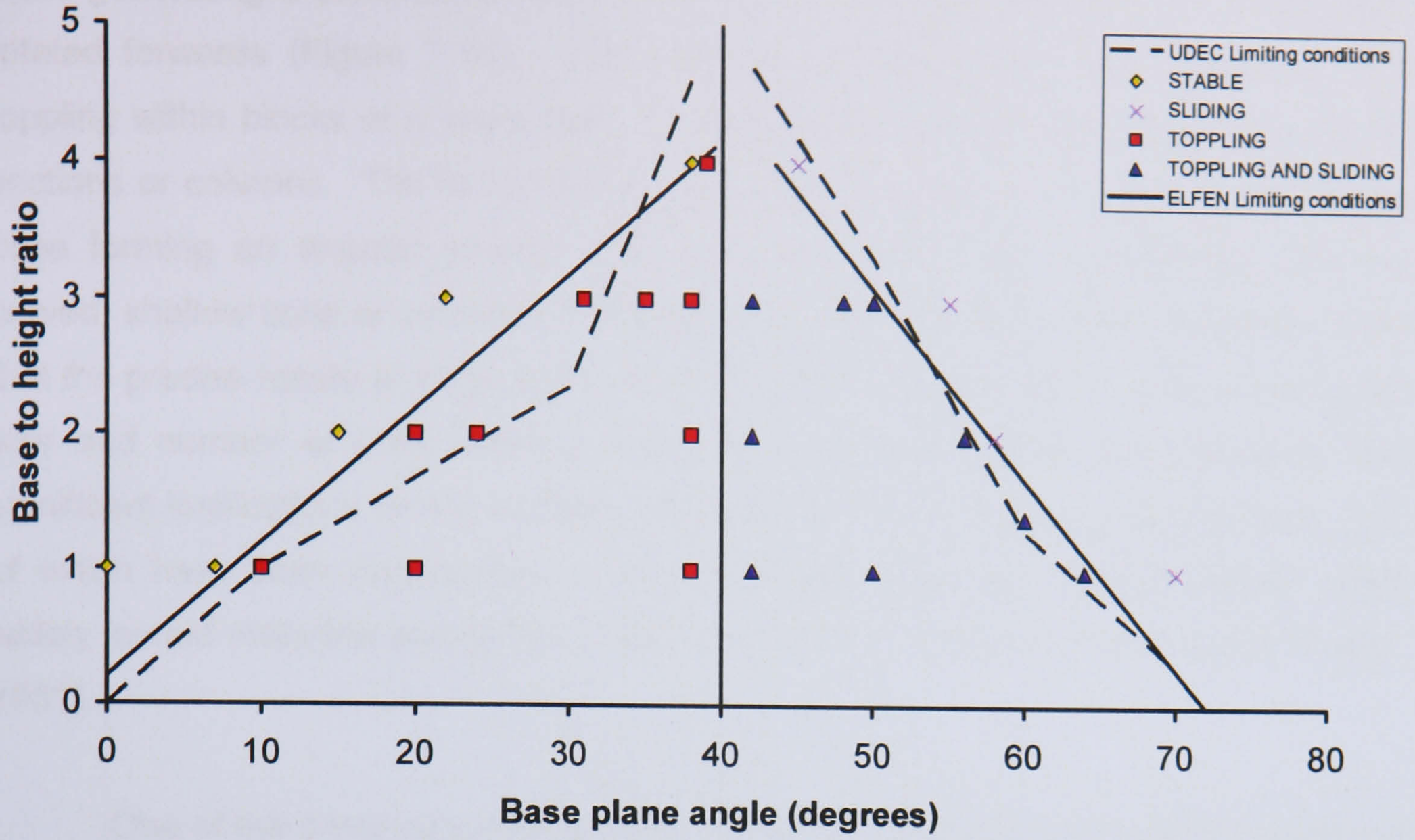

Figure 7.9: Comparison between the limiting conditions for rectangular block masses established with UDEC (Kimber, 1998) and Elfen. The Elfen simulations revealed more linear divisions than the kinked curves of UDEC although the location of the boundaries was consistent between both codes.

Each mode of behaviour recorded can be characterised to understand more about the conditions governing model response. Sliding failures were limited to rock masses with steep bedding dips and high base to height ratios. Relatively larger bases make the blocks more stable in the vertical direction, reducing the likelihood of toppling. Initial movement, denoted by displacement vectors, was parallel to the bedding surface although blocks often rotated and accelerated as the failure progressed and they became detached from the main body of the mass. In accordance with earlier models of single block behaviour, a sharp division was located between the tendency towards either sliding or stability. Beyond the imposed friction angle of 40˚ sliding becomes possible although such failures become increasingly dominated by toppling movements with reducing base to height ratios. Less easily characterised were toppling rock masses, demonstrating complex responses that reflected the transitional nature of the failure mode between sliding and falling movements. With reference to highly jointed rock slopes therefore the internal angle of friction may represent a critical threshold on the occurrence of failure, while the geometry of separate elements exerts greater control over the precise nature of failure.

Toppling movements in blocks with low base to height ratios led to generation of large numbers of elements within the mass. These were seen to deform largely *en*

mass generating a continuous failure surface cambering the slope as the assemblage rotated forwards (Figure 7.10). This flexural bending motion was contrasted with toppling within blocks of a larger base to height ratio which tended to fail as coherent sections or columns. The failure surface penetrated deeper into the rock mass at the base forming an angular junction with the steep back scarp, contrasting with the curved, shallow zone of influence with toppling in flexure. The models therefore imply that the precise nature of slope deformation may reflect scale effects, influenced by the size and number of units within a mass of a set size. Such interpretations hold significant implications for the analysis of block and flexural toppling mechanisms, both of which have been documented in field examples, typically involving harder, more widely jointed materials and softer, highly discontinuous materials respectively (Evans, 1981).

One of the enduring problems with numerical modelling has been the relation of model iterations to real time (Iofis *et al.*, 1990). Rock mass simulations typically progress through a series of explicit time marching solutions causing variations both between modelling packages and within models with different computational requirements. Therefore the contribution of such models to the understanding of rock mass behaviour have typically been restricted to the analysing the spatial phases of landform evolution without quantified temporal constraints. Sliding failures for example have been characterised as a continuum of rapid surging movements separated by less intense activity, contrasting with the more pulse like toppling phases of development (Sijing, 1981; Bovis and Evans, 1996). To investigate temporal differences between the rock mass responses recorded in Elfen, a model was run in which the horizontal constraints on both sides of a mass where released. The front of the mass contained blocks with a b:h was 1 and α of 70˚ and failed through sliding failure. The blocks within the released back slope however were inclined at 20˚ and consequently failed through toppling movements (Figure 7.11). Although both sides were released at the same time, the front of the rock mass showed a consistent phase of activity as blocks slid from the rock mass before accelerating into a falling movement and settling at the slope toe. By contrast the back slope recorded a gradual creep stage until the centre of gravity of the failing mass passed beyond the slope boundary and rapid toppling occurred before a final phase of settling and adjustment. In addition to the temporal extent and sequencing of the two failure types, marked differences were noted in the final run out patterns. The toppled material was conveyed significantly further than the sliding mass even though both events contained material from the top of the mass with the same potential energy stores.

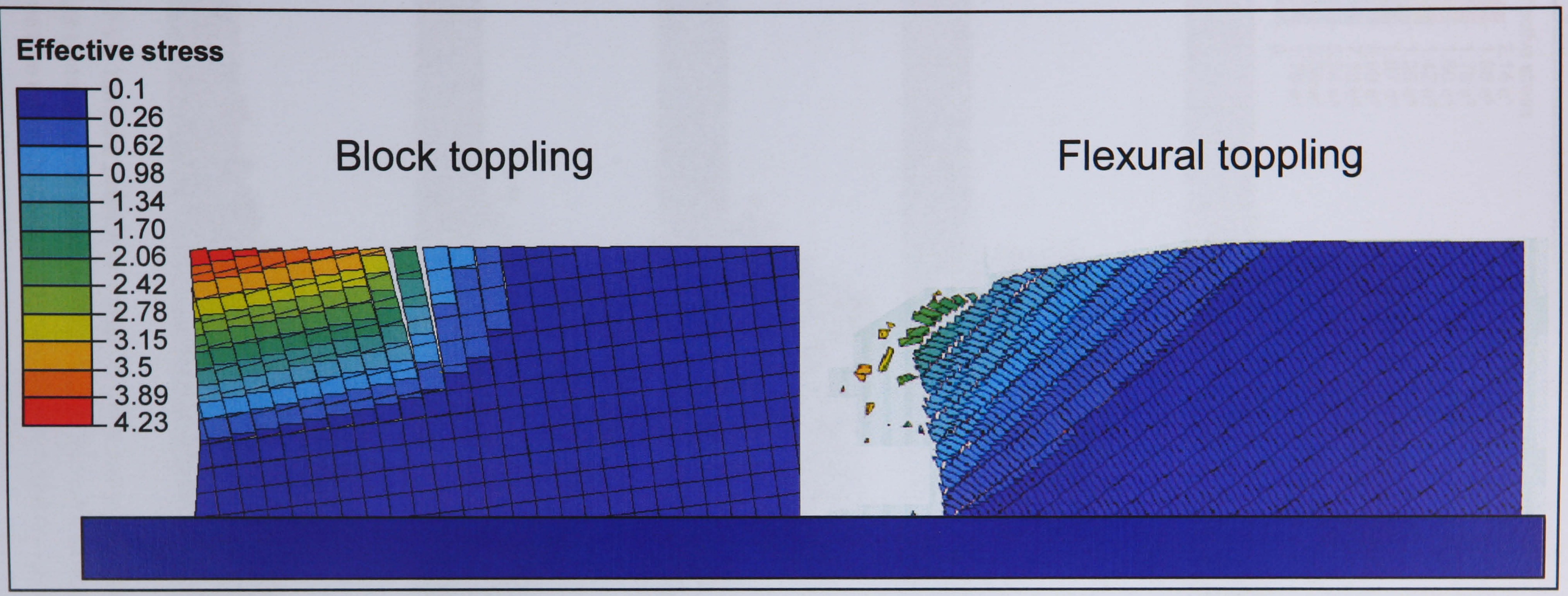

Figure 7.10: Elfen rock mass models displaying the distinction between block and flexural toppling, highlighted in the effective stress contours which reveal the angular and curvilinear failure surfaces of the two toppling modes. Mass height is 40 m.

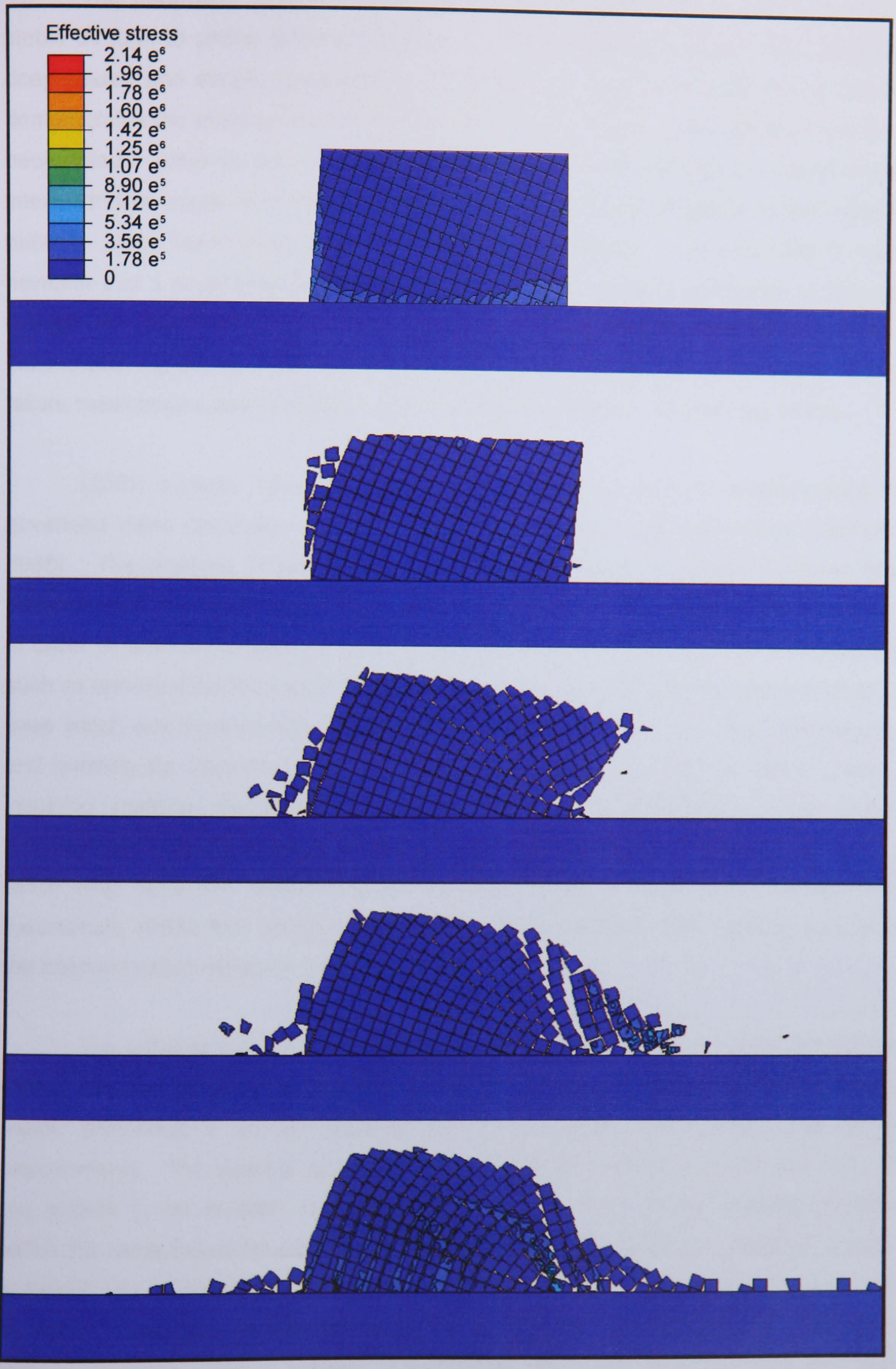

Figure 7.11: Temporal patterns of change in a free rock mass. Sliding movements were more continual contrasting with gradual cambering and then rapid collapse of the toppling face over the same time frame. Contours denote effective stress. Mass height is 40 m.

The parameter sensitivity analysis revealed a continuum of responses from stable through to sliding failures (Figure 7.12). The progression from stable through deep-seated and simple toppling through sliding and toppling to pure sliding failure demonstrates the effect of small perturbations in model inputs. Such effects have also been noted in other studies, Pritchard and Savigny (1989) found that alterations in the internal friction angle, cohesion and tensile strength caused changes in UDEC models between pure, flexural toppling and graben toppling failure. It is important to note however that if small alterations in joint properties can cause a continuum of change through the rock mass profile, it may also do so spatially and temporally in three-dimensional landforms; casting doubt once more on whether the classification of set failure mechanisms are adequate for the variable conditions in natural rock slopes.

UDEC models have demonstrated the importance of joint characteristics in governing mass response, often thought to be the main control on failure (Gerrard, 1988). The analysis of the monitoring data in the previous chapter however has demonstrated the heterogeneity of rock slope response, both spatially and over time. In order to assess the ability of Elfen to account for additional influences on stability such as undercutting the kinematically stable rectangular block model was placed on a base which was incrementally eroded from one side (Figure 7.13). The joint spacing and bedding dip mean that instability from below caused a column to topple forward, involving material throughout the entirety of the exposed face. The model demonstrates Elfen's capacity to simulate wider effects initiated by localised change, which may have the potential to cause large failures even in rock masses with theoretically stable joint configurations. The code is therefore well suited to modelling the interconnected nature of rock slope systems.

The validation of Elfen against more established rock mass analyses such as UDEC has demonstrated a capacity to respond to subtle changes in the predefined mesh, promoting it as an effective tool in simulating well jointed rock slope environments. The discrete approach has enabled the behaviour of different parts of the system to be isolated, revealing sliding, toppling and ultimately falling motions within the same failure for example. Questions have been raised over whether a 'type' of failure can be effectively used to describe such changes, suggesting analysis may be better conducted by viewing failure as a complex multifaceted and continuous process in which different aspects of motion are likely to interact spatially and over time. The interaction of multiple discrete elements has also allowed the processes of rock mass change to be considered over longer time intervals, demonstrating the potential of such models to analyse change beyond the temporal extent of monitoring

records. The *in situ* conditions and forcing processes however mean that in reality the simulated phases within ideal model environments are often recorded out of phase or in combination with other episodes of change in natural rock slopes.

Despite significant advances to rock mass studies made by discrete element models (Cundall and Hart, 1992; Kimber, 1998; Nelis, 2005), questions have been raised over the assumption of complete and continuous networks of joints dividing the landform into separate elements (Eberhardt *et al.*, 2001). The movement of discrete interacting blocks is determined by the defined planes between elements, restricting modelled failures to predetermined surfaces. Many rock masses contain joint sets that are discontinuous both in length and spacing; restricting many discontinuum analyses to idealised, well jointed field examples (Cundall, 1971). Structural complexities are often compounded by material differences within the rock mass, with separate joint characteristics associated with individual layers. When joints are discontinuous, the dominant control on behaviour may switch to the strength of the material (question 3, Table 7.1). Material heterogeneity has been largely avoided by numerical modelling simulations because the consideration of significantly different material properties would require aspects of both finite and discrete element behaviour. For all but the most continuously jointed rock masses, failure surfaces should not be assumed but allowed to initiate and develop according to the interaction between materials, forms and stresses.

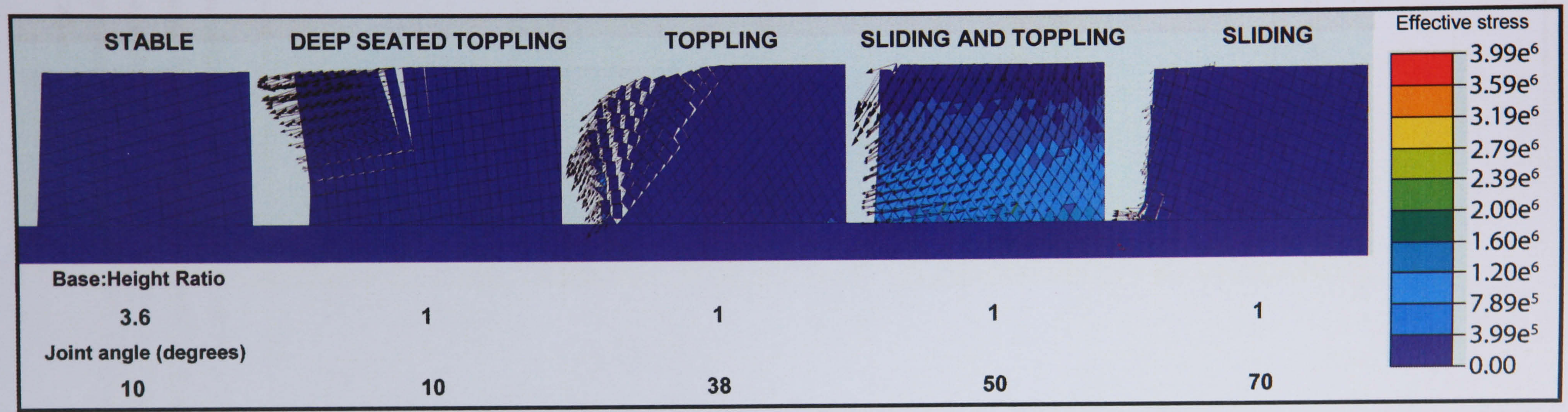

Figure 7.12: Continuum of effects on rock mass failure caused by altering joint characteristics and bedding planes. The transition demonstrates that in complex cliffs for example, where structure and bedding are not uniform, the slope may fail through multiple different modes spatially and over time. Mass height is 40 m.

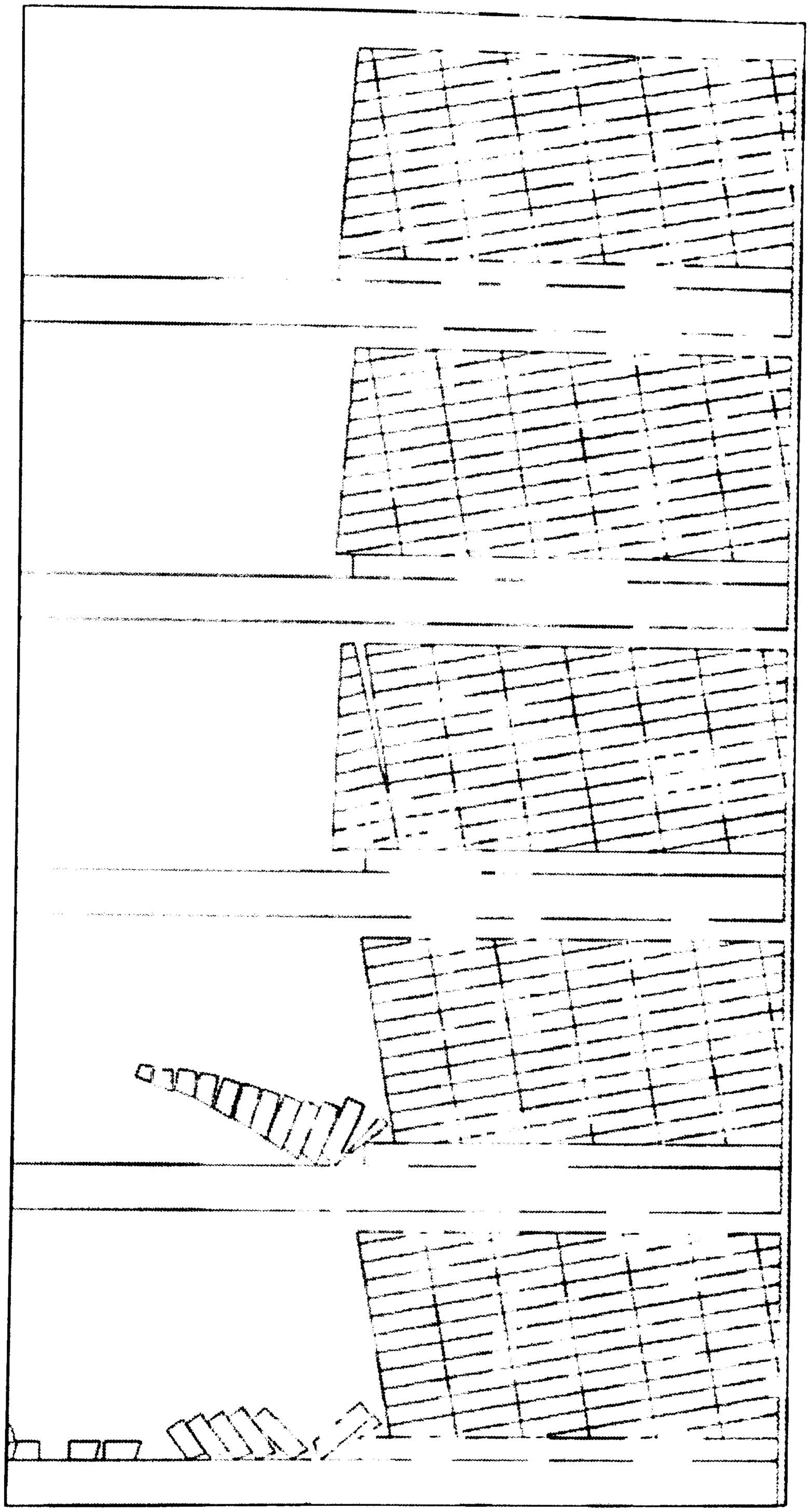

Figure 7.13: Investigating the interconnected response of rock masses with the undercutting of a stable rock mass. It can be seen that a relatively small amount of undercutting in comparison to the size of overlying block length is required to induce instability. What remains to be seen however is the effect when joints do not form continuous division between separate blocks. Mass height is 45 m.

7.7 Rock mass fracturing

The main argument against the application of discontinuum approaches to natural rock slopes is that rock joints are rarely complete planes but commonly separated by intact rock bridges (Stead *et al.*, 2001). The mechanics of fracturing and material yielding associated with the divisions between structural weaknesses is therefore integral to understanding the behaviour of rock masses. The interaction between tension and compression within a rock mass and normal and shear stresses remain poorly modelled and understood (Brunsden, 1999). One of the earliest attempts to account for non-continuity in rock mass joints used limit equilibrium to consider a sliding surface made discontinuous by the presence of rock bridges (Jennings, 1970). The resistance of the slope was calculated relative to the proportion of intact material within the failure surface, eventually shearing when Mohr-Coulomb failure criteria were exceeded. More advanced simulations have taken into account both shear and tension failure to model the interaction between intact rock and discontinuous joints, typically producing a stepped failure surface (Einstein *et al.*, 1983). Such methods are thought to overestimate the strength of the landform because the propensity for material creep and crack propagation has been ignored. Small alterations to discontinuity persistence may therefore result in large changes in the factor of safety derived.

Stresses in jointed rock masses are concentrated towards the ends of discontinuities causing seemingly insignificant loads to give rise to structural changes over time. Tharp's (1984) application of fracture mechanics allowed propagation through simple geometries, although it ignored non-uniform stress states in the slope. Scavia (1995) calculated vertical tensile stress around the crack tip from the stresses at its mid point to show the material at the crack tip deviates away from the theoretically elastic behaviour of the rock mass. When this area was small in comparison to the overall structure size, it was possible to establish a critical value for stress intensity that allowed propagation through the material. Linear elastic fracture mechanics were applied to determine crack growth in brittle rock masses, dependant on both the stress concentration at crack tips and the strength of material divisions. The models assumed initial geostatic stress conditions with all discontinuities compressed and closed. Propagation criterion for models of jointed rock masses were defined for open cracks, responding largely to tensile stresses, closed cracks, under compressive stresses, or a combination of the two (Scavia, 1995). The linear elastic fracture mechanics approach suggests that discontinuities within a slope are more likely to propagate when crack spacing, friction angle, tensile strength and slope height are reduced. Discontinuities dipping out of the rock slope were seen to propagate from the slope toe where stress intensity was highest, forming a complete failure surface over time, although little was

revealed about the nature of the failure once a continuous plane had developed (Figure 7.14).

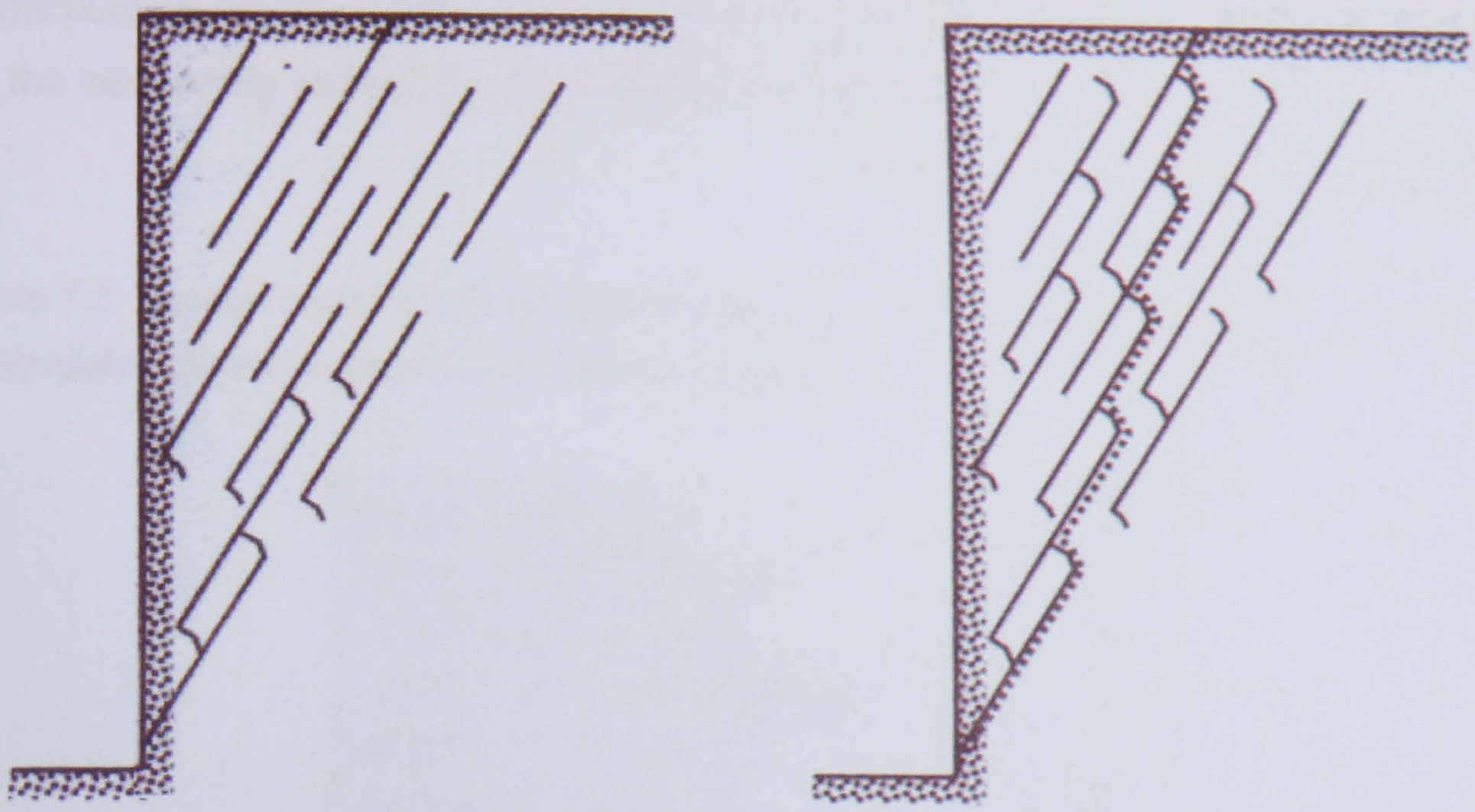

Figure 7.14: Numerical simulation of rock structure propagation in a hypothetical rock slope using linear elastic fracture mechanics (Scavia, 1995). The dotted line denotes the complete failure surface, initiated from the toe. Mass height is 50 m.

The ability of Elfen to accurately model fracture propagation and failure surface development was an essential requirement for its use in the exploration of rock slope mechanics. The slope failure was therefore recreated in Elfen based on values approximated from Scavia (1995) (Table 7.3). A Rankine fracture model was assigned to the rock mass material, which causes it to fail when stressed beyond its tensile limit. The Rankine fracture model is a pressure dependent elasto-plastic material formula that represents the evolution of anisotropic damage by degrading the elastic modulus according to the major principle stress invariant. The extent of the damage caused by discontinuity propagation is dependent on the energy released during fracturing. In accordance with Scavia's (1995) findings, the slope failure was seen to initiate from the slope toe, propagating through a series of steps linking adjacent cracks (Figure 7.15). A complete failure plane was evident by stage 4, although the Elfen mesh demonstrated greater sensitivity to stresses within the rock mass. The discontinuities near the free slope face in particular showed a propensity to propagate, subdividing the rock into increasingly smaller elements as the mass failed. The slide itself caused discontinuities to extend beyond the failing mass into the intact rock, leaving a fractured slope inclined close to the original joint angles of 60° and armoured by substantial

amounts of failed material. The possibility that the influence of the failure may cause weakening beyond the failure plane generates strong linkages with suggestions earlier in the analysis that failure in rock slopes are not discrete 'events' but represent a continuum of development. The nature of future rock failures will evidently be altered by the weakening caused by the present form changes.

Table 7.3: General model geometry and material properties for the assessment of Elfen's ability to simulate fracture propagation and failure evolution.

Slope height (m)	50
Slope angle of repose	90°
Crack spacing (m)	2
Length of rock bridges (m)	4
Length of cracks (m)	15
Inclination of joints	60°
Friction angle of discontinuities	25°
Elastic modulus (MPa)	15000
Poisson's ratio	0.33
Bulk density (Kg m^{-3})	3750
Tensile strength (MPa)	1.5
Fracture energy (Nm^2)	1

The model has demonstrated both the ability of Elfen to account for the development and propagation of failure surfaces and that the progressive fracturing and interaction of material is a critical factor in certain morphological changes (refer back to question 4, Table 7.1). The growth of fractures during failure does not appear to be constant but rather increases through time, due to the energy released as material deforms and yields. The development phase of a failure surface, after it has begun to propagate, may form relatively rapidly, emphasising both the difficulty of predicting actual failures and the importance of obtaining the correct material properties for the analysis. Indeed a limitation of this rapid propagation is apparent in that although a continuous failure surface had developed by stage 4, material was not released from the slope until stage 7 by which time fractures had propagated throughout the mass. The calculation of both material response and discrete body motion within the same model iterations therefore restrict temporal and therefore certain spatial elements to slope change in highly weak or brittle rock.

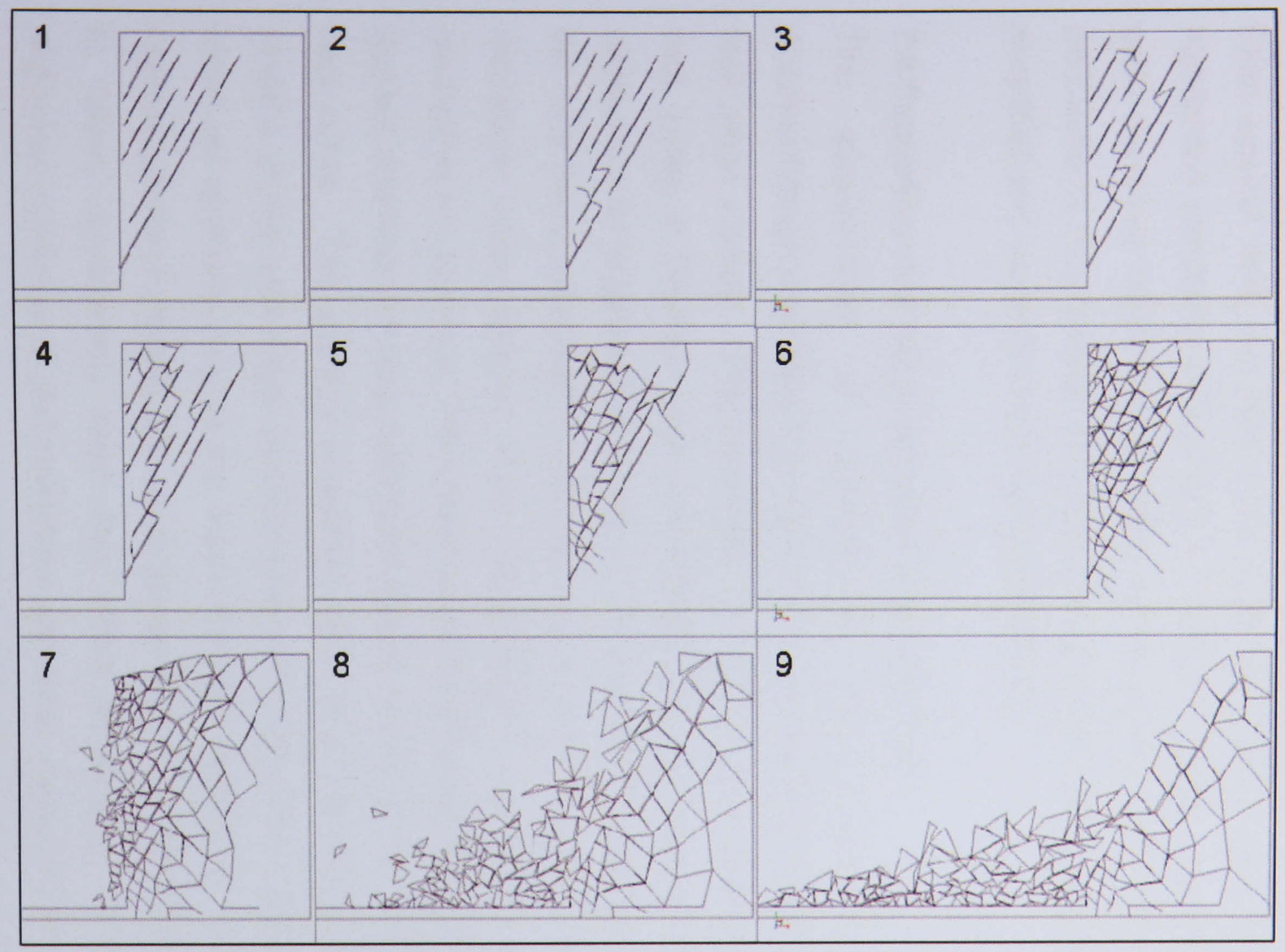

Figure 7.15: Key stages in the development of a failure modelled in Elfen. The original joints were defined using Elfen's rock fracture mesh assignment, causing all joints to be open and hence a conservative estimate of stability to be reached. The progressive growth of fractures initially follows a path very similar to that of Scavia's (1995) predictions. The fractures continue to grow, responding dynamically to material yielding and energy release even before failed blocks can be released from the slope, demonstrating a limitation of the model in the consideration of such weak material. Mass height is 50 m.

A complete description of the processes and mechanisms that interact to determine slope form in complex coastal environments may not be achievable. Improvements in understanding therefore rely on investigations into simplified aspects of change. The ability of the Elfen code to simulate the initiation and progressive development of multiple modes of failure has been demonstrated. It has also proven capable of accounting for processes acting beyond the developing shear plane, such as strength degradation and internal mass deformation; recently shown to be critical preconditions to some large scale failures (Eberhardt *et al.*, 2004). The performance of Elfen against field and laboratory validated discrete and finite element models has highlighted sensitivity of the nature of failure to small changes to model inputs. The code therefore holds the potential to investigate the more specific aspects of the mechanisms that dictated the changes recorded across monitored rock slopes, within simplified and carefully constrained conditions.

7.8 Exploring rock slope mechanisms with Elfen

The incorporation of geotechnical and engineering considerations into geomorphological studies has improved understanding into the mechanics that govern rock slope change. The properties of the four main material constituents within the rock mass at Staithes were established with the use of triaxial compression tests carried out by engineers at Cleveland Potash Ltd. (Table 7.4). The tests revealed that the rock mass contained a complex mix of rock strengths with peak strengths at the mudstone base, weaker shale mid portions and more competent siltstone and sandstone top sections. The shale displayed the weakest and most plastic response to applied stresses, forming materially distinct behaviour to that of the other, more brittle rock types. The material properties have been used to form inputs into numerical models of the rock slope mechanisms but it should be noted that laboratory testing forms an estimate only of the intact material behaviour. Rock material exposed to coastal agents of degradation such as rain and wave action is stressed and weakened to values considerably lower than those established from cut rock cores. The additional influence of discontinuities and other imperfections may further reduce the competence of the rock slope by up to 70% (Pinto Da Cunha, 1990). The following models should therefore be considered estimates of maximum rock slope stability within the boundaries of which failure is likely to occur.

Initial stress ratios have been shown to be important influences on modelled rock slope failures (Stead and Eberhardt, 1997), and may ultimately control the direction of failure surfaces (Chowdhurry, 1978). Therefore all applied models have been settled under gravity, constrained horizontally but not vertically, until kinetically

stable. Once the rock mass has stabilised the relevant horizontal constraints were released to ensure the slope changes form in response to material instabilities rather than the redistribution of stresses in the early stages of simulation. Simplified models have been run in an attempt to gain further information on the mechanisms governing the slope responses highlighted in the previous chapter, with particular reference to the four key hypotheses considered. An example of typical model parameters can be seen in Appendix 2.

Table 7.4: Rock material properties from Staithes, North Yorkshire, used for the input of model parameters for the investigation into the mechanisms governing coastal rock slope behaviour. Source: Cleveland Potash Ltd.

	Elastic Modulus (MPa)	Bulk density (Kg m^{-3})	Poisson's ratio	Tensile strength (MPa)	Uniaxial compressive strength (MPa)
Sandstone	3480.5528	2583	0.3	3.01916	34.21489
Siltstone	2206.324	2492	0.23	1.72369	30.19906
Shale	2137.3764	2486	0.4	3.033695	16.685325
Mudstone	4126.3338	2513	0.28	3.482373	41.544835

7.8.1 The mechanisms behind magnitude-frequency relations

Brunsden (1999) warned against focussing on large scale, infrequent geomorphological change at the expense of more common but less perceptible changes. The analysis of the previous chapter concluded that although a continuum of change was detected the material contribution was biased towards the two extremes of scale; the largest and to a lesser extent the smallest changes were more significant than intermediate sized losses. The monitoring study was unable to reveal any detail on the mechanisms that caused such a pattern, although the process of incremental erosion of basal layers and overhang collapse was suggested by protrusions in the cliff faces. To investigate the mechanics of such a failure a multistage model was constructed with two 5 m thick shale layers located on a fixed platform, with the bottom layer gradually eroded by 0.2 m increments (Figure 7.16). Each time the basal layer was eroded the kinetic energy within the rock mass was allowed to return to equilibrium before the removal of further material from the base.

The undercut model corresponded well with the results from recorded cliff processes. When the upper layer had been destabilised by the removal of 5 m of rock a continuous tension crack appeared causing rapid toppling failure, indicating that once a threshold has been crossed slope failure may develop relatively quickly in response to material yielding. The nature of the failure supports the analysis of the temporal sequence of the toppling mechanism which were seen to fail in a single pulse of activity immediately after initiation (refer back to Figure 7.11). Although the retreat of the upper 5 m of rock failed when undermined by the same distance, the material lost exceeded

that of the incrementally retreating base layer. The evidence that large scale failures may account for greater volumes than the total of more frequent small scale losses was in agreement with the monitoring conclusions, suggesting that undercutting may be an important mechanism in both the occurrence of large failures and the wider changes in slope form over time. Overhang failure therefore provides a viable mechanism by which to link the continuum of changes recorded (question 5, Table 7.1), and further indicates that large scale losses cannot be viewed independently from the less dramatic iterations to slope form.

Although undercutting failure provides one possible explanation for the bias of material losses towards very large and very small failures, questions were raised over the quantitative predictions generated. The 0.2 m recession rate of the basal layer was used to demonstrate the effect of undercutting but the actual rates of annual retreat were typically less than half this value. On a temporal scale therefore the preconditions for the undercutting mechanisms would have taken over 50 years to accumulate the required level of instability in all but the most rapidly eroding sites. Perhaps more significantly only the very largest failures, which were few in number, occurred from an area of protrusion approaching 5 m. Many of the smaller failures detected were located on less prominent areas of protrusion, implying that it was more common for failure to occur earlier than predicted by the idealised model scenario. Few of the monitored sites contained continuous jointing but all contained significant structural weaknesses which may have pre-empted more large scale material losses.

To investigate the impact of simple jointing on the mechanics of undercutting the model was rerun with two incomplete discontinuities dipping out of the rock mass (Figure 7.17) and then dipping into the rock mass (Figure 7.18). The discontinuities dipping out of the rock mass had a significant effect on undercutting, causing failure to initiate after only 2.8 m of basal erosion, with the shear plane becoming complete when undercut by 3 m. Tension failure in the material at the top of the most outward discontinuity caused a small degree of fracturing although no losses were incurred until further erosion had taken place. The model therefore demonstrated the complex nature of cliff failures which may fail progressively in response to ongoing processes. The landward discontinuity also formed a complete failure surface but its release from the rock mass via sliding was prevented by the basal layer which had yet to erode sufficiently. It is therefore important to reiterate that the effects of such failures may extend beyond the immediate loss of material to generate the necessary preconditions to further failures over time.

Noticeable differences were seen in slope response when the discontinuities were orientated dipping into the slope. The more stable configuration caused failure to initiate only after 3.2 m of undercutting. Both models demonstrate that the material simulations without structural weaknesses generally overestimate rock mass strength. Once again the failure began with tension fractures at the top of the most outward discontinuity and led to the rotation and shear failure of the material about a pivot point near the face of the eroding base layer. Both models therefore contrast with the behaviour of a large mass of homogeneous material in which the stresses concentrated at the toe of the slope initiate failure (refer back to Figure 7.15). A difference has therefore been demonstrated between the nature of failures originating from within the deforming layer and those caused by external influences such as undercutting.

The failure was seen to occur more rapidly once initiated, forming a complete failure surface with no further destabilisation required before the release of material. The implication is therefore that although rock with more stably aligned discontinuities may take longer to reach the critical conditions for failure, the nature of the slope change may ultimately be more rapid. In both models the discontinuities form part of the eventual failure plane and hence it may be possible to identify characteristic planes exposed within rock slopes to aid analysis of future behaviour. Further consideration of the future development of the hypothetical rock slopes can be made from the failure profiles. When discontinuities dip out of the slope the tendency will be for the material above a zone of active undercutting to recede from the cliff base, forming slopes with protruding toes such as the type A slopes noted during the site selection (refer back to Table 3.4). Depending on the angle of repose the critical conditions for large magnitude failures may never be reached or take a particularly long time to accumulate. By contrast undercut rock masses with discontinuities dipping into the rock mass, conventionally viewed as structurally more stable in engineering analyses, tended towards steep, overhanging failure surfaces. Such profiles were more representative of type B slopes with overhanging upper sections. Less basal erosion would therefore be required before further large magnitude failures could occur. It is therefore essential that the response of rock slopes to both forcing processes such as undercutting and *in situ* conditions such as joint orientation viewed holistically, as a continuous system of interconnected changes.

Aspects of the interconnected nature of rock slope change were noted at several of the monitored sites, such as at Site 3 where successive failure surfaces

amalgamated or at Site 4 where losses from the mid portion of the cliff caused impacts and losses from the material below (refer back to Figure 5.10). In an attempt to account for the interplay between different layers within the rock slope a further model was run with two additional layers above, one of which was eroded at the same rate of the basal layer (Figure 7.19). This four layered rock slope was more applicable to the monitored rock slopes which generally consisted of an undercut basal layer below a protruding toe with a reclining mid portion associated with the Liassic shales and a protruding top section of more competent siltstone and sandstones. The bottom two layers were assigned with mudstone material properties, overlain by a shale and then a sandstone band. The basal mudstone and shale layers were then eroded at constant rates leaving the upper mudstone and sandstone protruding. No discontinuities were attributed to the material in order to isolate idealised material behaviour. Both the sandstone and the mudstone were capable of supporting greater protrusions than the shale used in earlier models, failing only after 7 m of supporting material had been removed. The marginally weaker sandstone failed before the mudstone band although fracturing had already begun from the upper join with the rest of the rock mass. The failing sandstone collided with the mudstone protrusion below causing fracturing in both layers. Although the impact was concentrated towards the outward extreme of the protrusion, the weight of the additional material caused the mudstone to form a complete fracture through the layer at the junction with the retreating layers. The result was a cliff profile that was once again in general overall alignment. The model illustrates one mechanism for the entire cliff profile to appear to retreat consistently and yet be governed by a combination of large occasional and small but frequent material losses. No protrusions of 7 m from the base level of the cliff were recorded during monitoring, indicating that material and structural weaknesses may play a major role in initiating failures and reducing the magnitude of individual losses.

Ultimately the interrelated nature of the rock slope systems was clearly an important aspect in generating the patterns of different magnitude losses detected throughout the monitoring period. Different areas attributed with specific material and structural properties will become subject to processes of operation that will cause localised responses which may or may not lead to wider slope change. The models therefore support the conceptualisation of the slopes as deforming meshes in which all changes can be related over time. The suggestion made in the previous chapter that the most appropriate scale at which to monitor cliff behaviour is that of the entire slope is also confirmed with activity in the lower cliff influencing mechanisms above; and the changes in upper cliff also impacting on layers below.

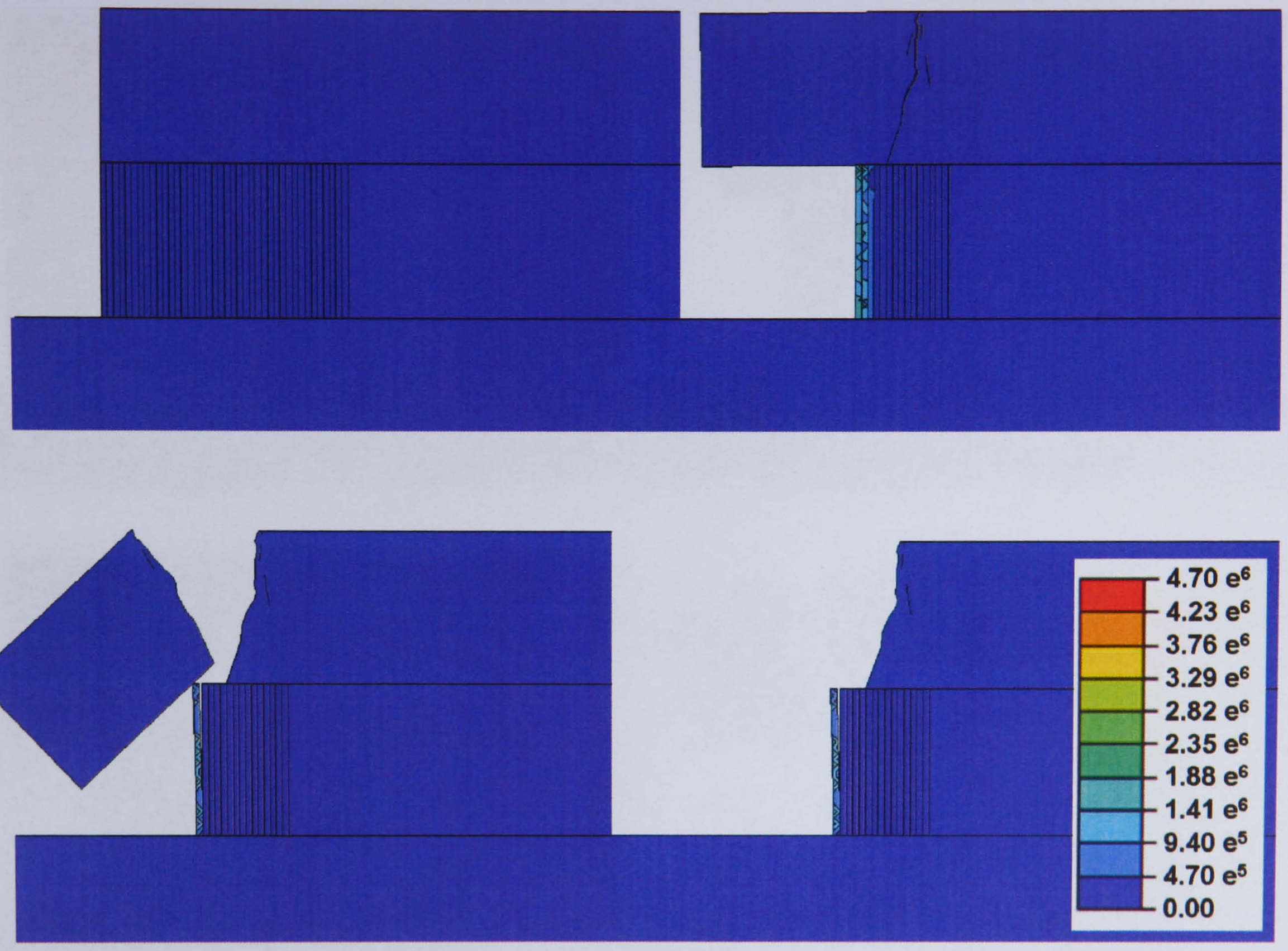

Figure 7.16: Elfen analysis of the mechanisms governing the interaction between high magnitude, low frequency and small, constant changes to the rock slope. Incremental retreat of a supporting layer gradually increases the effective stresses in the layer above until a continuous tension crack behind the line of retreat is formed and toppling failure occurs. Contours denote effective stress. Mass height is 10 m.

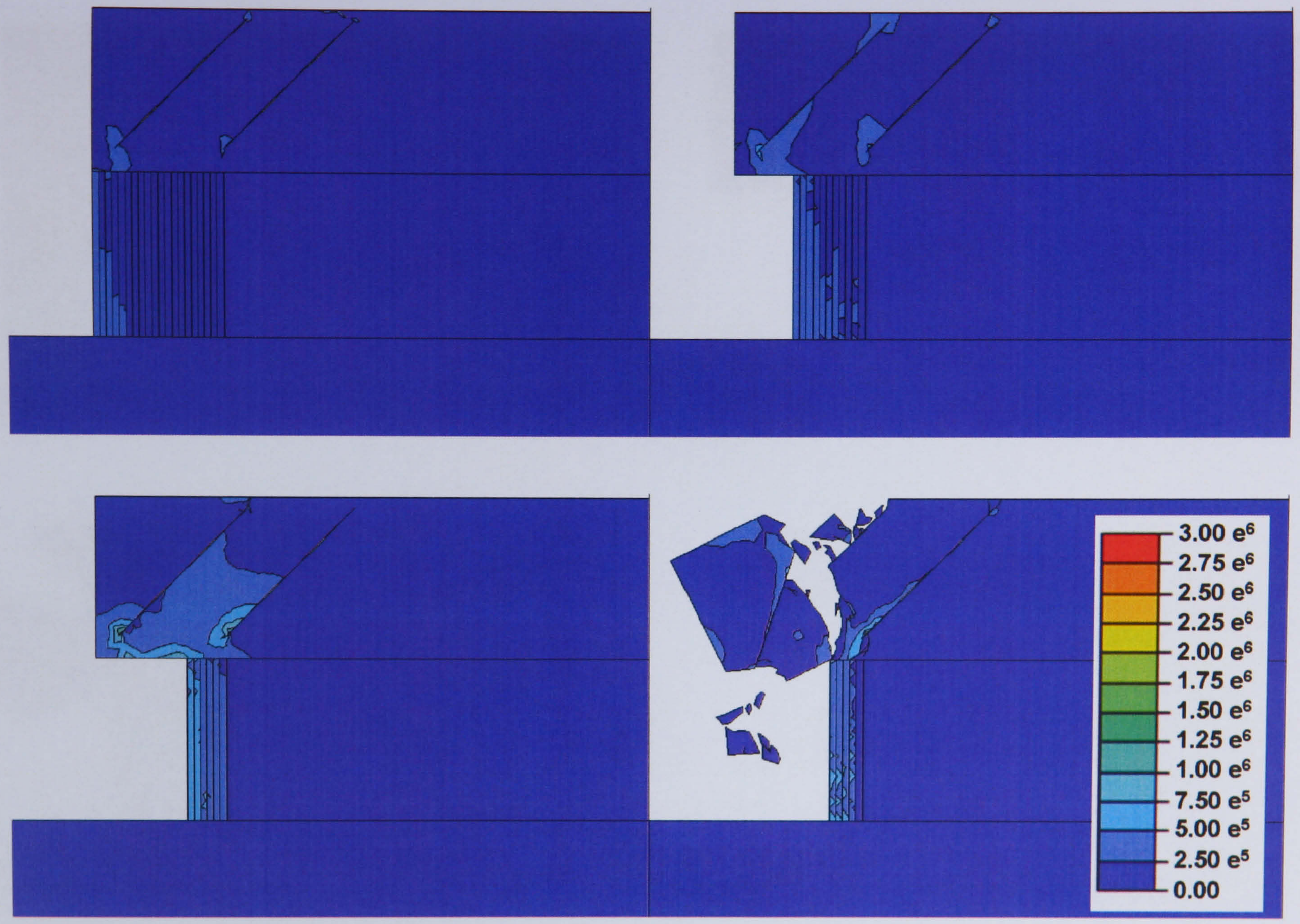

Figure 7.17: Undercutting mechanisms in a 5 m thick rock layer weakened by non-continuous discontinuities dipping 45° out of the slope. Contours denote effective stresses which were seen to be concentrated towards the ends of the joints. Mass height is 10 m.

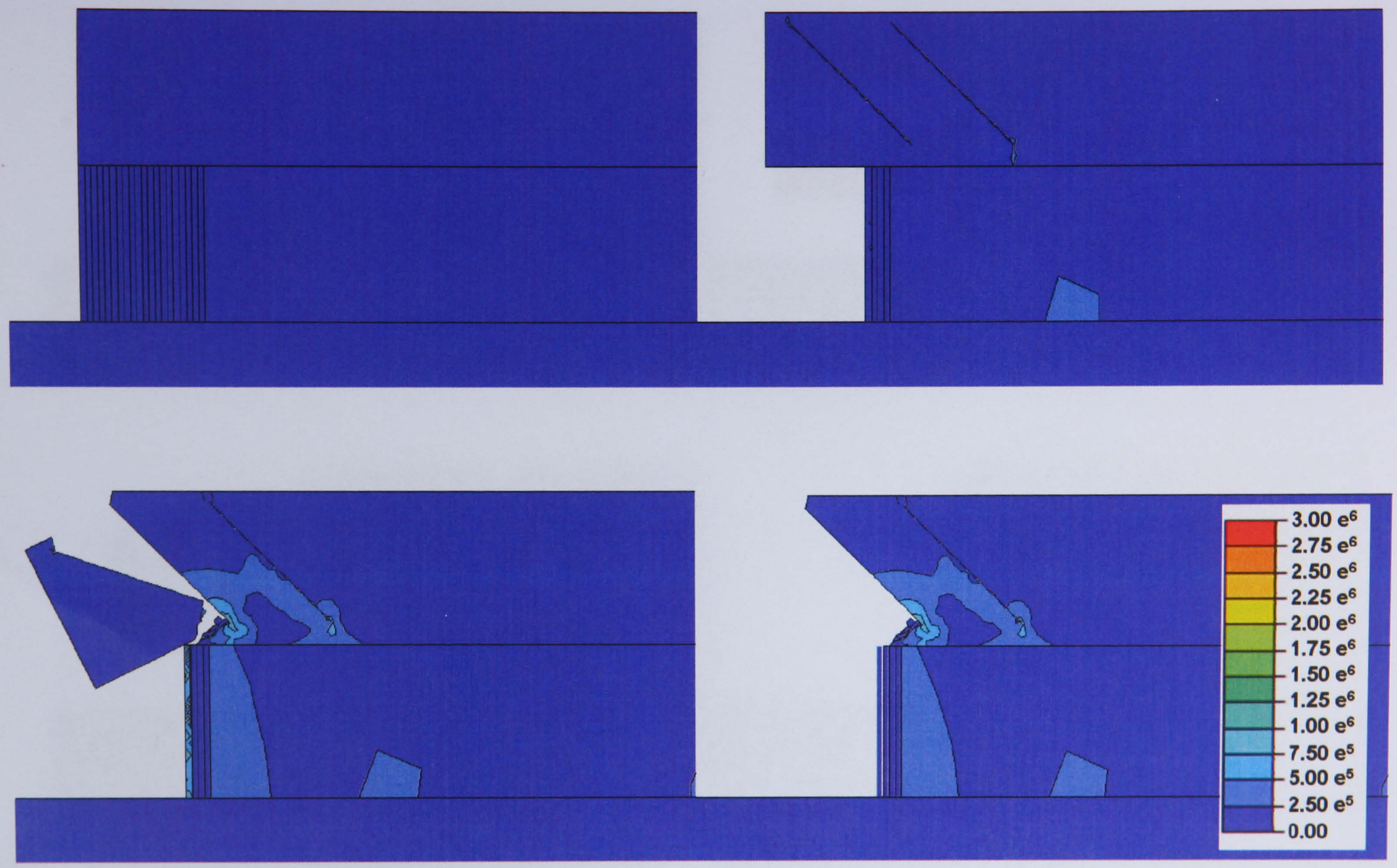

Figure 7.18: Undercutting mechanisms in a 5 m thick rock layer weakened by non-continuous discontinuities dipping 45° in to the slope. Contours denote effective stresses which were seen to be concentrated towards the ends of the joints. Mass height is 10 m.

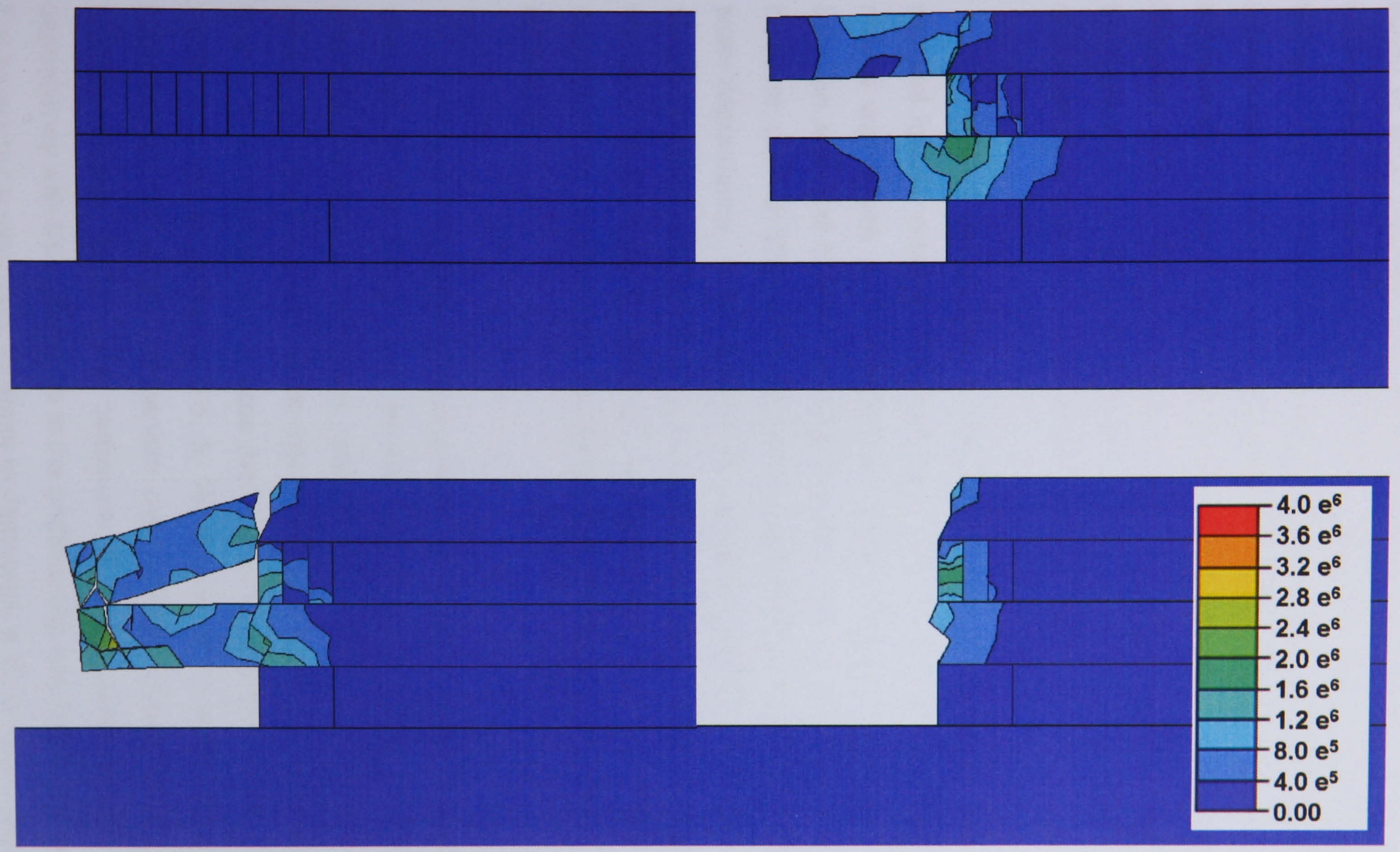

Figure 7.19: Model of a cliff with two mudstone layers at the base overlain by shale and sandstone layers. Weaker rock bands or those exposed to more active environmental forces erode incrementally with constant small scale change leaving more competent layers protruding from the slope which ultimately fail to form a more uniform profile. Ultimately the omission of any material imperfections cause unrealistically rigid behaviour raising questions over the validity of such simplistic applications. Contours denote effective stress and failed material has been deleted for clarity. Mass height is 10 m.

7.8.2 Scale dependency in rock slopes

Rock mass analyses are essentially a product of scale. The choice of modelling package for example, conventionally between finite and discrete element approaches, is typically decided by the resolution of interest. Discrete element simulations are best suited to large outcrops divided by many structural weaknesses (Palmström, 2000), while finite analyses tend to be used for smaller, more continuous slopes (Hicks and Samy, 2002). A recent study used the height of the rock mass and the joint spacing to classify scale effects on rock slopes (Nelis, 2005). Correlations have also been made between the height of the outcrop and the magnitude of failure events (Hermanns and Strecker, 1999). Many of the mechanisms associated with rock slope change have been shown to be scale dependent, causing important implications for the occurrence of failures (e.g. Coulthard *et al.*, 1992; Sjöberg, 1996).

Through the analysis of monitoring data it was found that the continuum of material losses, ranging from sub-metre through to volumes over a thousand cubic metres was largely scale independent; with all subset scales recording relationships between size and frequency of occurrence. The precise nature of this relationship however, such as the concentration and distribution of failures, did exhibit elements of scale dependency. It was concluded that certain processes governing the form of the monitored cliffs were sensitive to the scale at which they are analysed. A key question therefore remains as to whether the dominant failure mechanisms are truly scale dependent or whether the variations detected were a product of the monitoring technique.

Undercutting has been acknowledged as a significant mechanism by which sheer-sided rock slopes can evolve (Hantz *et al.*, 2002), but few studies have attempted to gain a quantitative understanding the processes involved. In order to assess the extent to which scale determines the nature of undercutting, a single shale layer was situated on a 5 m base that was progressively eroded from one end. The model was run for layers of 0.5, 5, 10, 20 and 30 m thicknesses to determine the behaviour of the failure mechanism over scales representative of those found at Staithes (Figure 7.20). The continuum of scales demonstrates a positive scale dependency with little difference in the undercutting required to cause failure in 0.5 and 5 m layers but a significant increase to destabilise a 10 m shale layer. The transition to 10 m and above appears to represent a threshold for the modelled shale in which the thickness of the band provides sufficient competence to withstand disproportionately greater loss of support. The undercutting required for failure then converges towards a direct correlation with increasing band thickness until, at 30 m, fractures occur earlier

due to the weight of material involved. The behaviour of the layer of greatest thickness is in stark contrast to that of the thinnest layer which is able to withstand undercutting over nine times its depth because its limited weight causes lower stresses to accumulate.

The models suggest that, ignoring the influence of discontinuities, there is a greater propensity for thicker rock layers to resist failure from undercutting and therefore to form larger protrusions within the rock slope (see question 6, Table 7.1). In order to assess the extent to which layer thickness exerted a control on actual protrusion and therefore the propensity for larger failures, the monitoring dataset was re-examined. A graph of protrusion against shale band thicknesses for areas which recorded losses demonstrates that the model predictions perform relatively well for layers up to 5 m thick, with one loss detected from a 5.3 m band associated with a protrusion of 4.6 m (Figure 7.21). The increasing divergence of maximum protrusions from the model estimates generated by thicker layers and the presence of many failures from less pronounced localities demonstrate controls other than material competence determined many monitored losses. The most likely explanation for the divergence from model predictions is the presence of material and structural imperfections in the rock mass. The increasing scale of the bands generates a greater likelihood for the rock to incorporate significant structural weaknesses (Adey and Prusch, 1999), causing it to fail earlier and behave more like a thinner layer of material. Extrapolation of the bounding conditions modelled by thinner layers better constrain the monitored results. It may also be possible to elucidate a link between protrusion thresholds and episodic behaviour. At sites where layer thickness is large in comparison to its discontinuities, increased competence may result in a longer period within which the material can resist change, although the resultant protrusion consequently causes a higher magnitude loss when it does occur.

Consideration of the mechanics of slope behaviour at different scales has allowed new understanding to be gained into the evolution of rock slopes. Although the models provide only very simplistic material interactions, further investigation into the competence of undercut layers of different materials and structural weaknesses may be used to determine areas of actual slopes which are nearing the limits of their capacity to support overhangs. Such datasets may hold the potential to change the way rock slope change is viewed, moving away from probabilistic calculations based on past rockfall inventories, towards a more mechanically based assessment of calculated failure criteria.

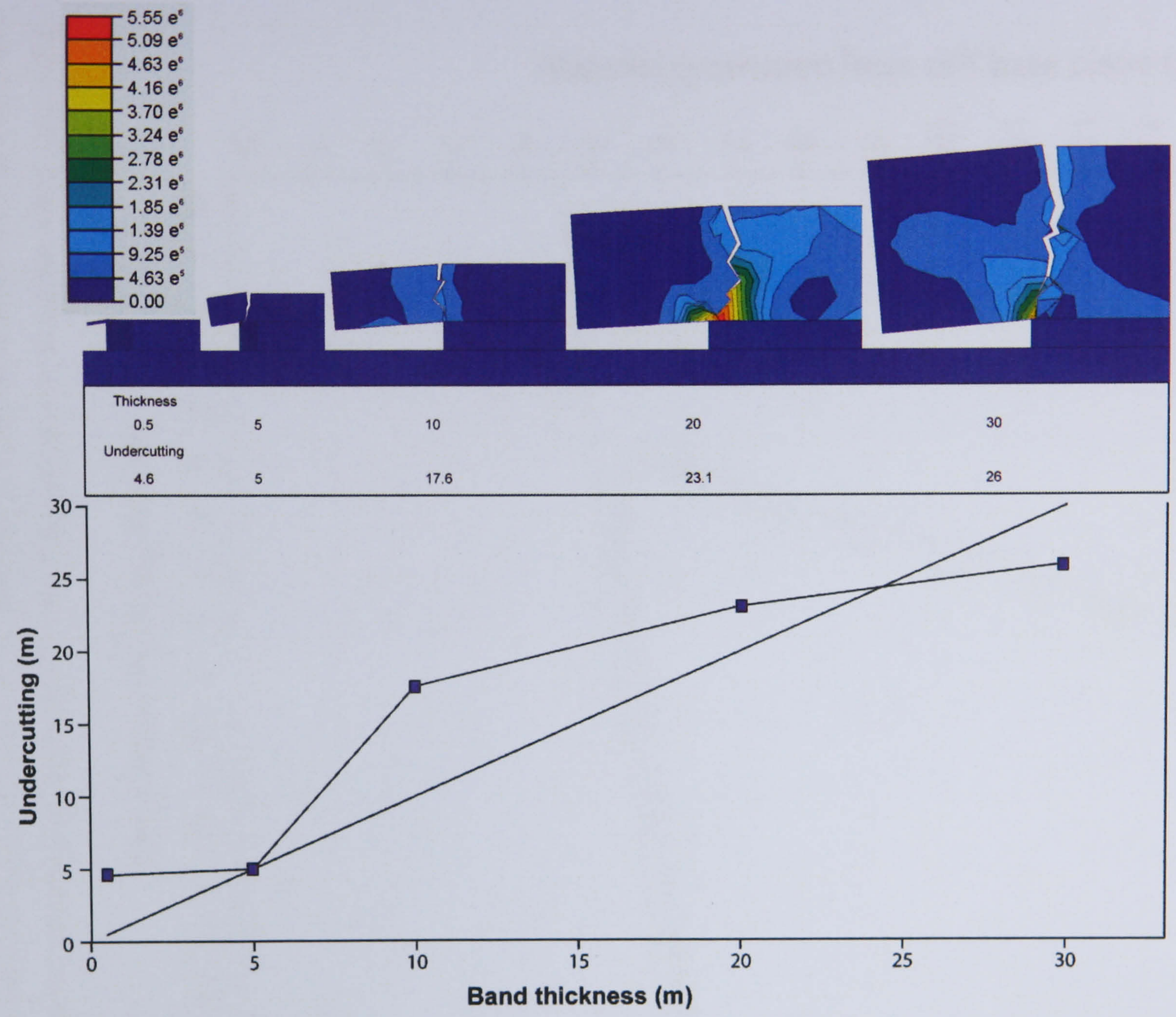

Figure 7.20: Scale effects on undercutting failure. Despite indications that it may fundamentally govern cliff evolution little quantitative analysis has been carried out on the mechanism itself. Contours denote effective stress.

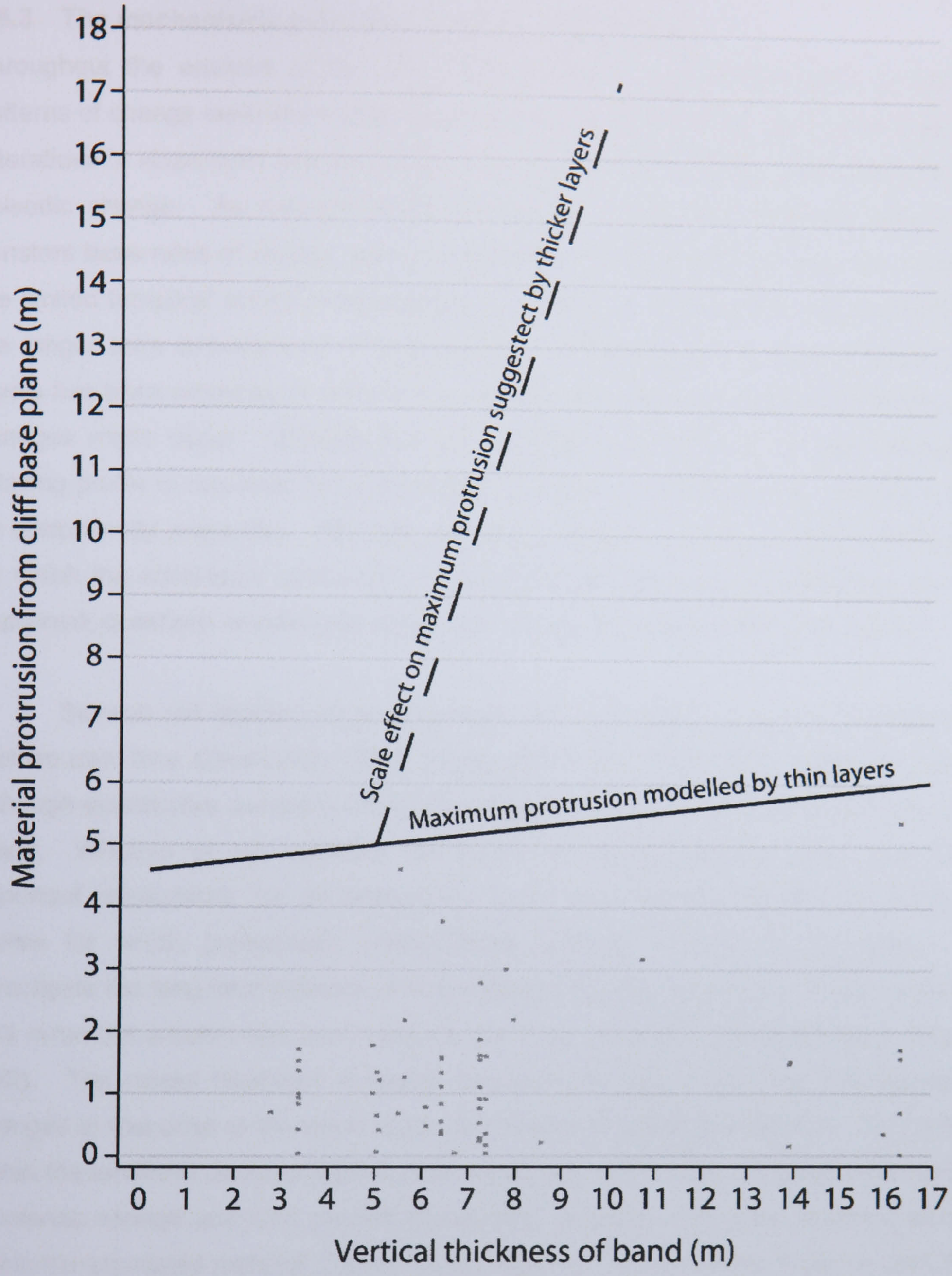

Figure 7.21: Scale effects on monitored shale layers of varied thicknesses across all sites. The data reveal that the scale dependency suggested in the models increasingly overestimates the ability of the slope to support outcrops above 5 m thick. The maximum predictions generated by the thinner layers however provided much closer maximum failure criterion, suggesting the modelled scale effects are prevented in natural slopes, possibly by the presence of discontinuities dividing layers into thinner elements.

7.8.3 The mechanisms governing long-term episodicity

Throughout the analysis of the monitoring dataset it was evident that the spatial patterns of change were intrinsically linked to the temporal development of rock slopes. Alterations in slope form over time were seen to exhibit elements of both continual and episodic change. As material losses increased in size they departed from more constant base rates of change and occurred at increasingly irregular intervals. Due to the limited temporal extent of the dataset however little interpretation was possible of the longer term development of rock slopes. Destabilisation of more coherent rock layers has been promoted in the previous models as a likely mechanism by which such changes might occur. Whether the slope angle tends towards an overhanging or relaxing profile in response to such failures was seen to be influenced, at least in part, by discontinuity properties. Although overhang collapse provides a useful mechanism by which the short-term continuum of magnitude and frequency relationships can be explained, questions remain over longer term, more significant slope development.

Several cliff studies have suggested that rock slopes return to characteristic profiles over time (Zenkovich, 1967; Emery and Kuhn, 1980; 1982; Trenhaile, 1987), although quantitative assessments of the mechanisms driving such changes are rarely made. Whether or not repeated cliff forms are indeed assumed over time holds important implications for understanding future slope developments over temporal scales for which probabilistic assessments become increasingly unreliable. To investigate the long-term patterns of slope change the previous model of cliff behaviour was rerun but erosion was continued into the rock mass after the initial failure (Figure 7.22). The model displayed a typical sequence of high magnitude, low frequency changes in response to the small scale incremental processes of erosion. The activity within the landform demonstrated a clear episodicity, alternating between brief periods of intense change and long periods of inactivity; depicted in a graph of kinetic energy within the simulated material (Figure 7.23). From the energy levels it can be seen that the eight main episodes of change were not separated by regular intervals, nor were the magnitudes of energy involved consistent over time. The model stages 1 and 6 involved noticeably higher levels of energy than the other phases of slope change, implying different scales of slope change may occur despite the relatively continuous processes. It is therefore likely over the longer term, that relatively significant failures occur with comparative regularity, reflective of a continuum response while only the largest scale changes occur more rarely and episodically (refer back to question 7, Table 7.1). Ultimately it is evident that the large scale, long-term processes of change

cannot be appropriately understood without consideration on the more frequent, smaller processes of change.

The debris of failed material was left undeleted as the model continued to run to illustrate the temporal sequence of slope changes. The presence of debris at the base of the slope however is an important factor in the continued development of the slope. Indeed Sheppard and Grant (1947) suggested that the protection against marine activity afforded by talus accumulation was the defining control on the episodic nature of coastal cliffs. Emery and Kuhn (1982) also classified the long-term development of coastal cliffs into inactive slopes which are defended by talus and active slopes where the sea comes into direct contact with the cliff base. Therefore, in reality the continual erosion of the cliff base would be temporarily halted until the debris of failed material had been removed sufficiently to expose the cliff base to wave attack. Under such circumstances it is likely that the slope will recline from its base as subaerial weathering of the mid and upper portions of the slope continues.

From the profiles immediately after large episodes of change it is evident that cliff slopes tend towards a sheer-sided rock face after such events. Similar results were found in much of the monitoring analysis at all scales where the failure of material brought the specific area with which it was associated closer to the overall base line of the cliff. The most notable example was the largest failure recorded, that involved the movement of material in excess of 2000 m^3 but left a failure plane in general alignment with the wider rock face. From the model it was also noted that whilst the large scale losses adjusted the slope towards the more constantly retreating layers, the changes often left a jagged profile with either the upper or lower layer still protruding. Such protrusions may consequently result in smaller scale material losses. Although the precise configuration of the failure surfaces was determined by the meshed elements, the uneven profiles left by modelled mechanisms allows for diverse of slope forms to be assumed over time. The complexity of slope response will ultimately depend also on the weaknesses within the rock mass.

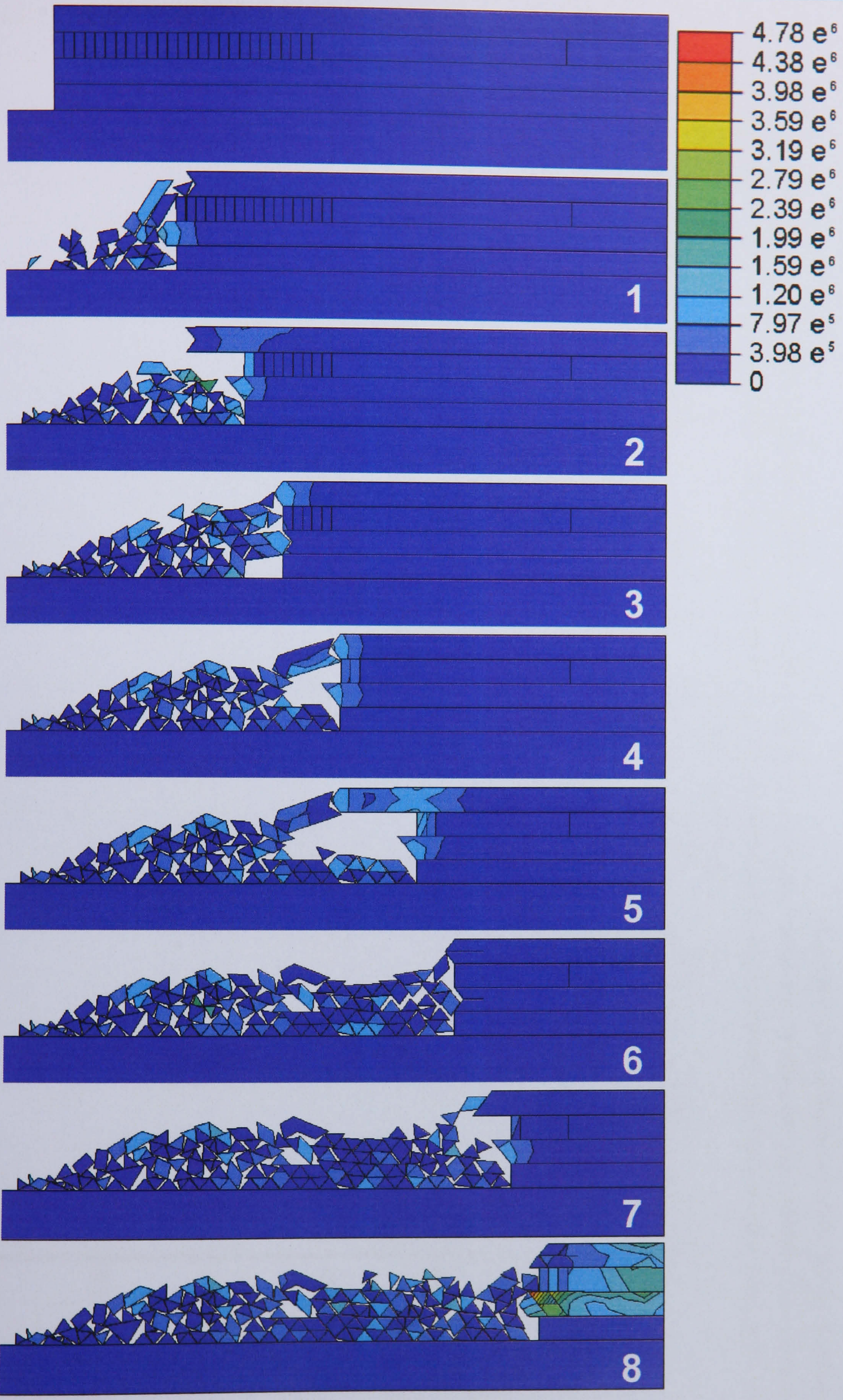

Figure 7.22: The long-term behaviour of a cliff comprising of 5 m thick layers including two mudstones, a shale and a capping sandstone. The model stages refer to the cliff profile following high magnitude losses. Contours denote effective stress. Mass height is 20 m.

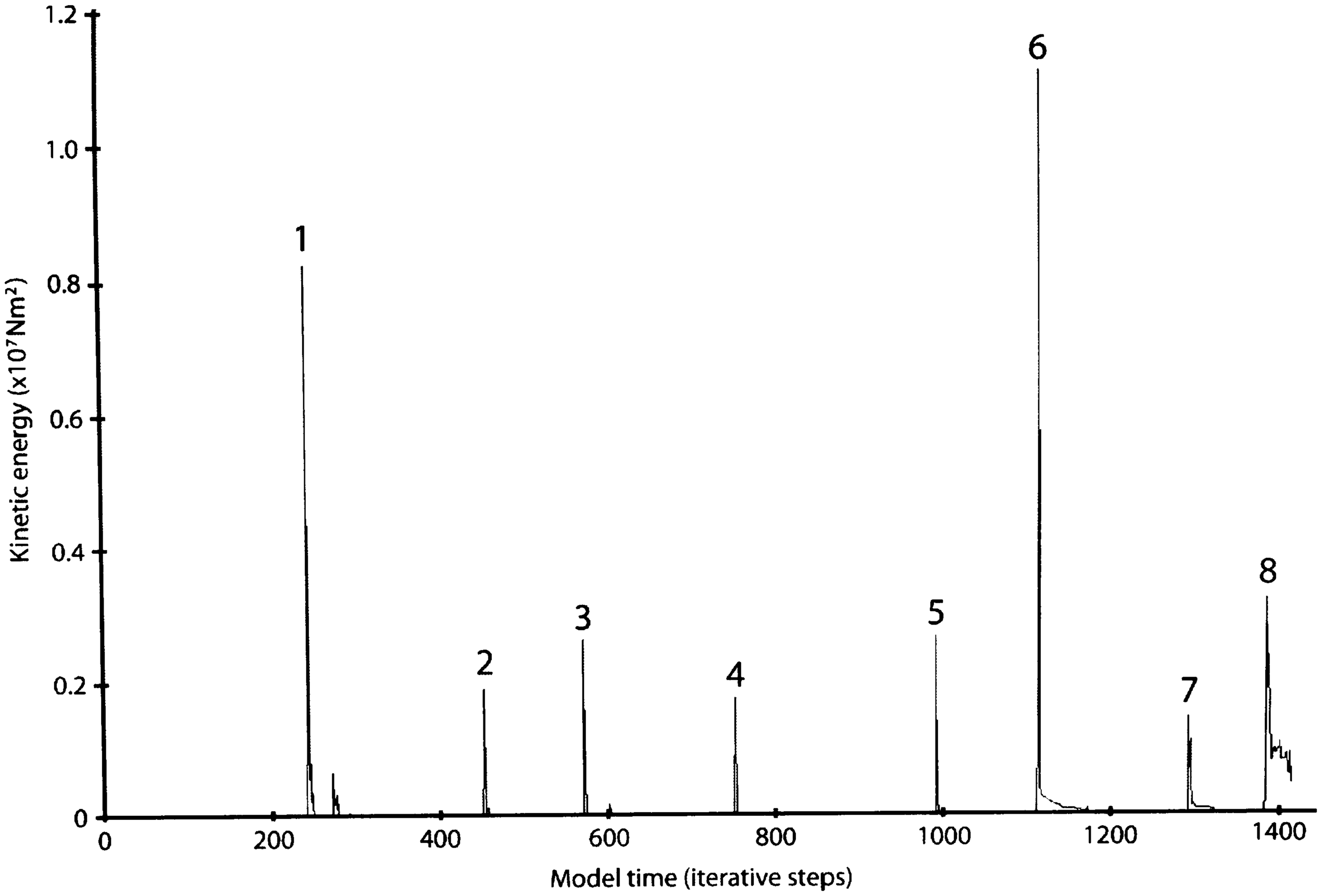

Figure 7.23: Peaks of activity within the long-term behaviour of a hypothetical rock slope (Figure 7.22). The 8 major changes in kinetic energy levels correspond to large failures in overhanging material. Little regularity or consistency was seen in the high magnitude changes although the total amount of erosion accounts for a period of time in the order of 500 years according to monitored rates.

7.8.4 The effect of environmental processes on slope form

Fresh insights into the spatial and temporal aspects of the mechanisms governing the changes in the monitored rock slopes have been revealed with the use of simple applied models. Many of the problems considered thus far have assumed that the changes in rock slopes are driven by a combination of two main sources: subaerial and marine erosion. Although supported by the monitoring data, such characterisations conflict with several classic models of coastal cliff change that suggest slope form is governed almost exclusively by marine activity. One of the most commonly referred to models of cliff development is that of Sunamura's (1992) intermittent basal undercutting (refer back to Figure 2.10). The extent to which the changes detected are a product of either marine and subaerial erosion, or whether they can indeed be solely attributed to marine action therefore remains to be determined. The use of numerical models to determine the effect environmental processes on slope form requires a balance to be achieved between distinguishing between subaerial and marine influences and accounting for the interrelated nature already demonstrated by the system.

A key question in the consideration of the effect of environmental processes has been whether the changes in slope form can be attributed exclusively to subaerial or marine factors. To assess the impact of a cliff subjected only to subaerial processes, the previous model simulating the long-term behaviour of a hypothetical cliff was rerun with erosion occurring only in the weaker shale in the mid portion of the rock mass (Figure 7.24). The overall behaviour of the landform demonstrated significant differences with the previous model in which marine activity was accounted for. No change was recorded in the base layer which became armoured by increasing amounts of debris from the failing layers above. The initial failure of the upper sandstone layer caused the profile of the rock slope to recede from the toe which was left protruding. The resultant cliff form was very similar to that found at the monitored Site 1, categorised as a type A slope with a protruding toe (refer back to Figure 3.5). After stage 4 the limitations of the model became evident with the shale layers continuing to erode although largely protected by accumulated debris which in reality would limit the continued retreat of the cliff until removed. Therefore it seems likely that cliffs governed largely by subaerial processes would typically assume more relaxed profiles, remaining stable for longer periods of time. A graph of the energy levels during the model iterations reveals episodic behaviour with sporadic high magnitude changes associated with the undercut upper layer (Figure 7.25). Episodicity in coastal rock slopes has largely been attributed to marine processes during storm events but the models have shown that such behaviour may also result from continual and progressive low magnitude changes.

Figure 7.24: Long-term subaerial effects on a hypothetical rock slope. The cliff face tilts back over time generating a stable, weathered slope. Contours denote effective stress. Mass height is 20 m.

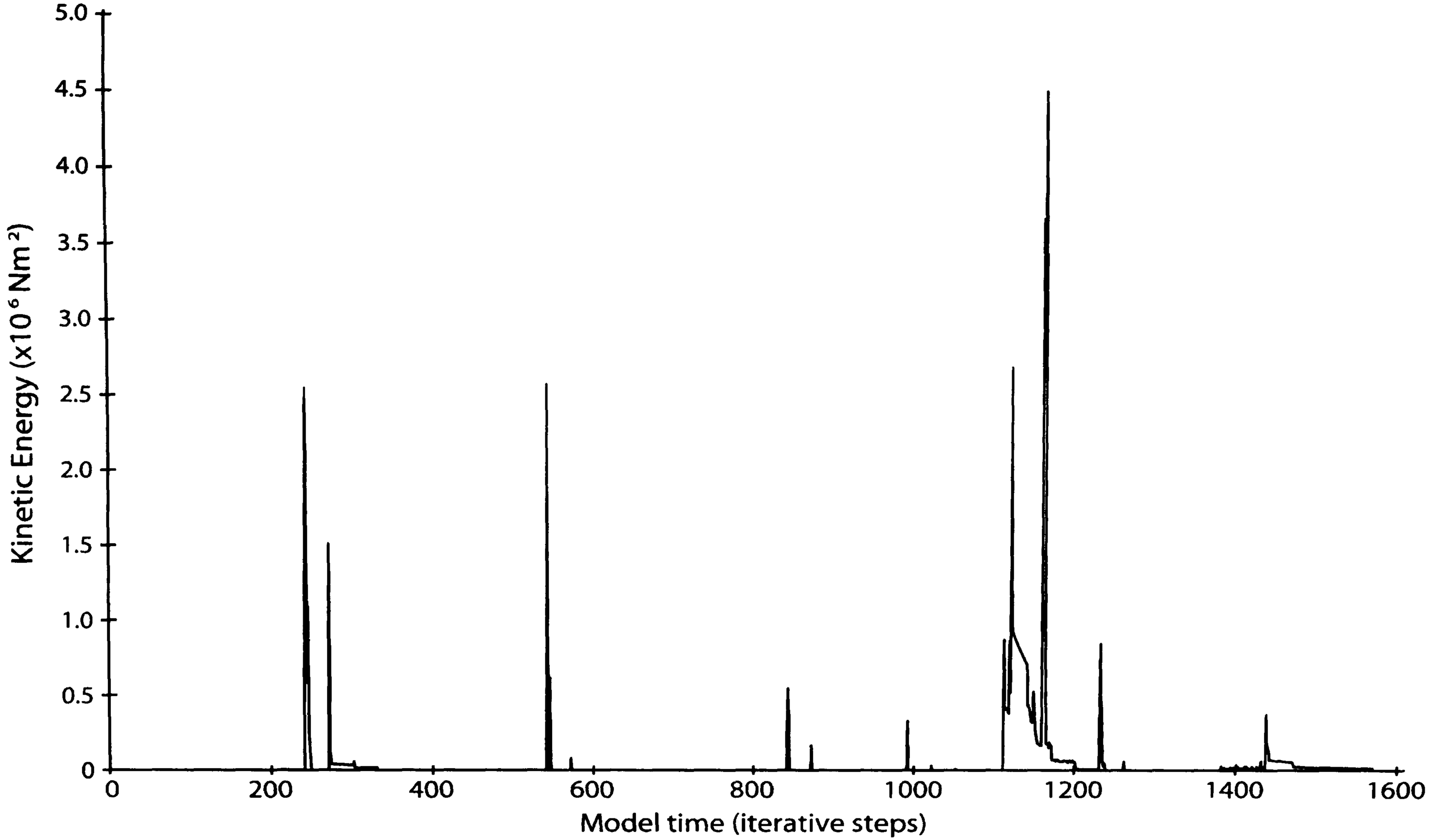

Figure 7.25: The modelled rock mass subject exclusively to subaerial processes demonstrated episodic behaviour, characteristic of undercutting failure. The model supports the findings of the monitoring that multiple controls may cause the changes to slope form recorded.

The effect of marine activity on the overall form of the cliff was then examined by considering a cliff subject exclusively to erosion at the toe of the slope (Figure 7.26). In contrast to the previous model, at no point during the simulation did the retreating slope tilt back from the toe, with upper layers protruding from the toe at all times. Episodes of change were preceded by large overhangs comprising of all cliff material above the retreating base. The cliff profiles were therefore more similar to the type B monitored slopes which displayed overhanging mid and upper portions. When failures did occur the change in form typically involved the whole slope with all layers above the base incurring significant losses. In reality such wide scale change was only seen at one site, Site 3, which recorded the most active loss of material from any of the monitored slopes. An episodic pattern of behaviour was recorded in a graph of kinetic energy fluctuations during the simulation, characteristic of cliff models governed by undercutting failure (Figure 7.27). The larger scale changes caused by basal undercutting produced greater levels of energy than those associated with subaerially influenced slopes, but fewer periods of change were recorded, suggesting that perhaps distinct aspects of change may be attributed to specific environmental drivers. Although the overall performance of the modelled rock slope was similar to that of Sunamura's (1992) results, the top sandstone layer was seen to protrude from the slope even after large scale failure. Differences were also noted in the general failure surface which Sunamura (1992) suggested was angled back from the cliff base. The configuration of the materially complex layers within the cliff must be considered an important factor in the nature of slope response to environmental processes.

The models above have demonstrated that different environmental processes may lead to distinct cliff forms. Whilst the form of cliffs that are repeatedly subject to high energy marine activity may predominantly reflect such influences, it is evident that models that ignore other processes neglect important mechanisms of slope change. In instances where the cliff is based in competent, sparsely jointed rock, the slope profile may be more reflective of subaerial processes. This appears to be the case at Site 1, and despite artificial subsidence of up to 0.35 m since 1973, the weathered reclining slope and minimal material losses confirm the slope was relatively stable during the monitoring period. It thus seems unlikely that even the most active rock slopes in the area are controlled exclusively by marine undercutting, but rather reflect a more complex systemic response to multiple influences (question 8, Table 7.1). This conclusion is supported by the two models in which the subaerial response involved lower magnitude changes than the marine failures which were less frequent. Even in simplistic models such as these the importance of the interaction between environmental processes is evident.

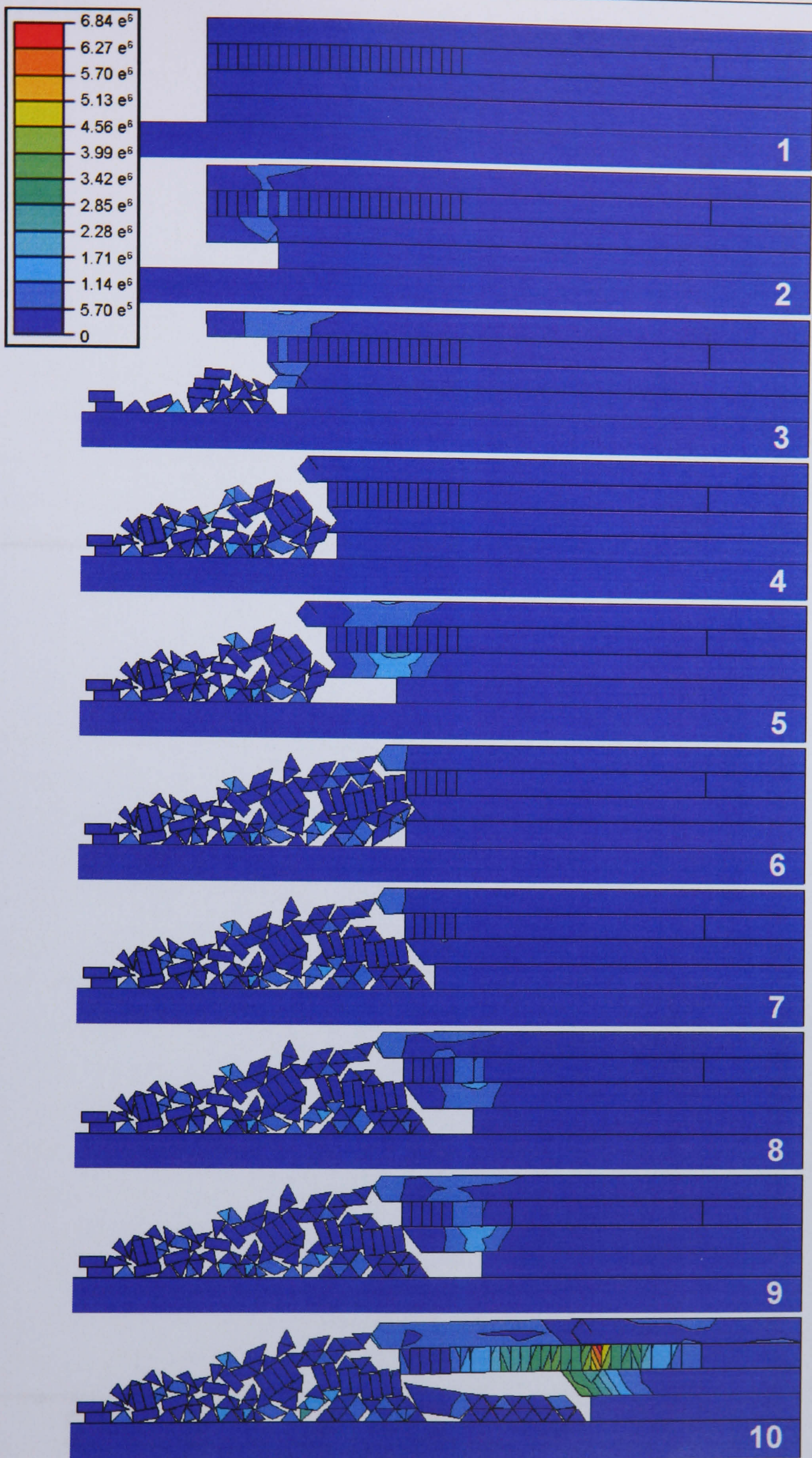

Figure 7.26: Long-term marine effects on a hypothetical rock slope. The cliff profile remains perpetually overhanging over time generating unstable conditions, and increased potential for large magnitude changes. Contours denote effective stress. Mass height is 20 m.

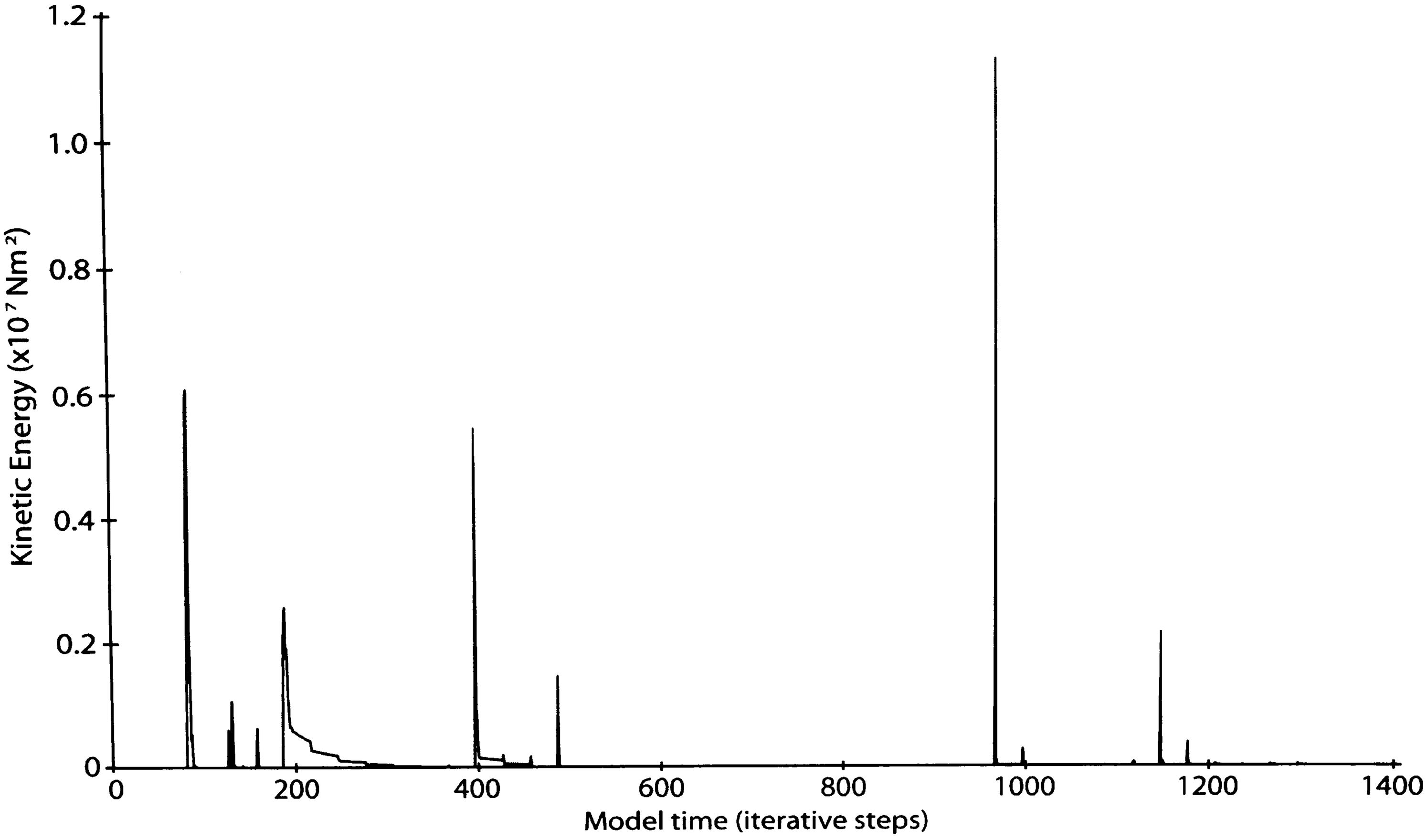

Figure 7.27: The rock mass subject exclusively to basal undercutting demonstrated similar patterns to the behaviour exhibited under subaerial conditions although fewer episodes of change were recorded and larger magnitudes were involved.

Simple numerical models have provided useful tools for the analysis rock slope mechanics. The application of such models to the complex behaviour of systems such as rock slopes however requires the limitations to be carefully considered. The models for example have taken little account of the effects of discontinuities and material weakening over time on the strata, which have often been found to dominate behaviour in well jointed landforms (DeFreitas and Watters, 1973; Brunsden and Lee, 2004). Many of the modelled mechanisms are, in reality, likely to become complicated or even prevented by failures responding directly to *in situ* conditions. In addition to the effect of structural weaknesses on rock slope response to environmental processes, which have been well documented (Lemos, 1990; Pritchard and Savigny, 1989; Kimber, 1998), the monitored rock slopes are materially complex. Material complexity in rock slopes remains poorly understood, despite the widespread occurrence of such landforms in coastal areas (Davies *et al.*, 1998).

In order to aid analysis the previous models have generalised the rock mass into four layers of even thickness: a basal mudstone subject to wave impacts, overlain by a mudstone, a weaker shale and a sandstone above tidal influence. The monitored cliffs at Staithes actually contained four different rock types and were comprised of up to 15 distinct lithological bands of varying thickness. A final model was generated of a rock mass which included all of the monitored layers, taking the average vertical depth of each across all sites. Rather than assume the dominance of concentrated areas of erosion, a retreat rate for each individual layer was calculated by averaging the annual rates of change detected across all sites where the band was present. An initial vertical slope was again considered and subsequently eroded by increments equivalent to 10 years of the change recorded within each layer. The simulation was run for 10 such periods of erosion, to gain an impression of the changes undergone by a generic section of the cliffs at Staithes over 100 years (Figure 7.28). Falling blocks were deleted from the model if they exceeded a velocity of 2 m s^{-1}. The deletions were necessary for running the model but also reduced the debris armouring the slope toe, enabling simulations closer to reality in which much fallen material was removed by the sea. The effect of material complexity on slope form was evident as the slope altered from a linear form to an undulating surface with marked protrusions. By the end of the simulation approximately 180 m^2 of material protruded from the average base of the cliff suggesting failures of this magnitude may take 100 years or more to develop. The model also generated failures in two of the layers beyond the extent of 100 years of retreat. The failure of the intact material implies that the mechanisms operating in rock

slopes cannot be assumed to be consistent over time (refer back to question 9, Table 7.1), and raises serious questions over the use of average retreat rates for the interpretation of cliff behaviour.

A graph of the kinetic energy levels against model iterations demonstrates notable differences with previous long-term simulations (Figure 7.29). The fluctuations were significantly more progressive than those of longer term model runs, increasing to a maximum before declining to stability. The flashy nature of the slope behaviour reflected the imposed model sequence of erosion followed by a period of stability allowed for slope adjustment. In reality the environmental drivers of change are likely to have been more iterative over time, generating a more continuous distribution of failures. The peak level of activity corresponds to a mass which toppled from the upper section of the cliff after the equivalent of 40 years of erosion. The interaction between a continuum of changes is therefore evident with slope behaviour governed by changes at a range of scales even over a 100 year period. Whilst it should be noted that model time steps do not directly refer to actual years of erosion, the more detailed analysis of short-term cliff behaviour has highlighted the importance of considering the appropriate temporal resolution from which to make adequate assessments of slope change.

The numerical models used to aid interpretation of the monitoring data have reduced rock slope behaviour to base elements which have been allowed to interact within carefully constrained boundaries. A hierarchical approach has been adopted from the investigation of wide scale generic principles of failure types, through general field models of discontinuous and fracturing rock masses to the site specific consideration of the mechanics behind cliff behaviour at Staithes. The models have indicated that one of the principal mechanisms governing change in the monitored rock slopes is undercutting; although other mechanisms such as sliding may become more important over time according to the alignment of discontinuities. Furthermore the models have demonstrated that the rock slopes respond to multiple mechanisms on a variety of scales at any one time. In many instances large scale failures, which are less easily interpreted through monitoring studies, appear fundamental in shaping the overall form of the slope in the longer term, demonstrating episodic behaviour as a result of the time taken for appropriate conditions to accumulate. The balance and interconnections between the small scale continual changes seen from the monitoring study to govern short-term cliff behaviour and less frequent slope scale change considered through numerical simulations hold important connotations for the future of rock slope studies.

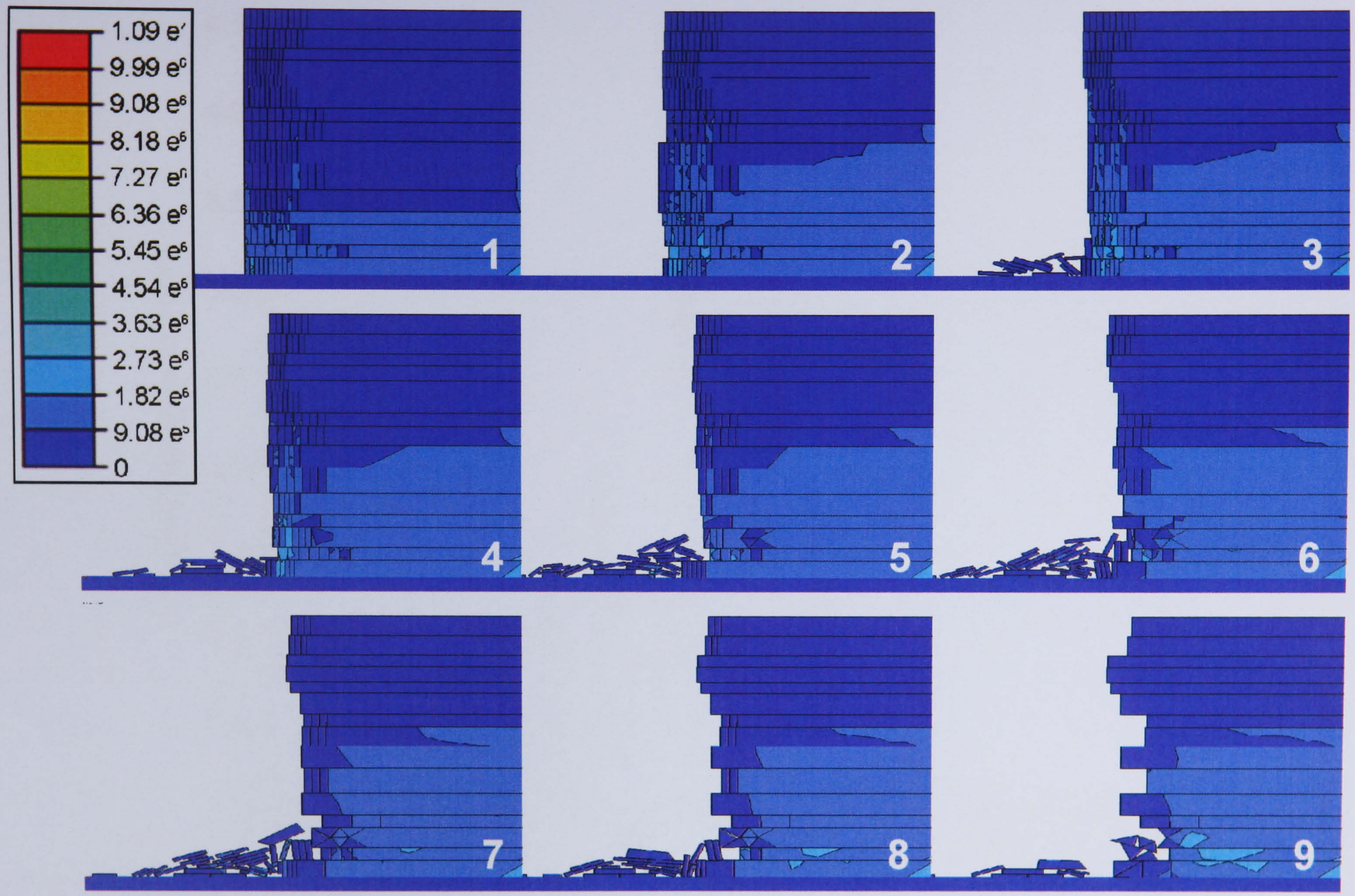

Figure 7.28: Generic model of the cliffs at Staithes, North Yorkshire, over a 100 year period. The stages refer to slope stability following phases of significant change. Although consistently eroded, the configuration of the layers generated a complex response causing fracturing in several layers beyond the material limits predicted for 100 years. Contours denote effective stress. Mass height is 60 m.

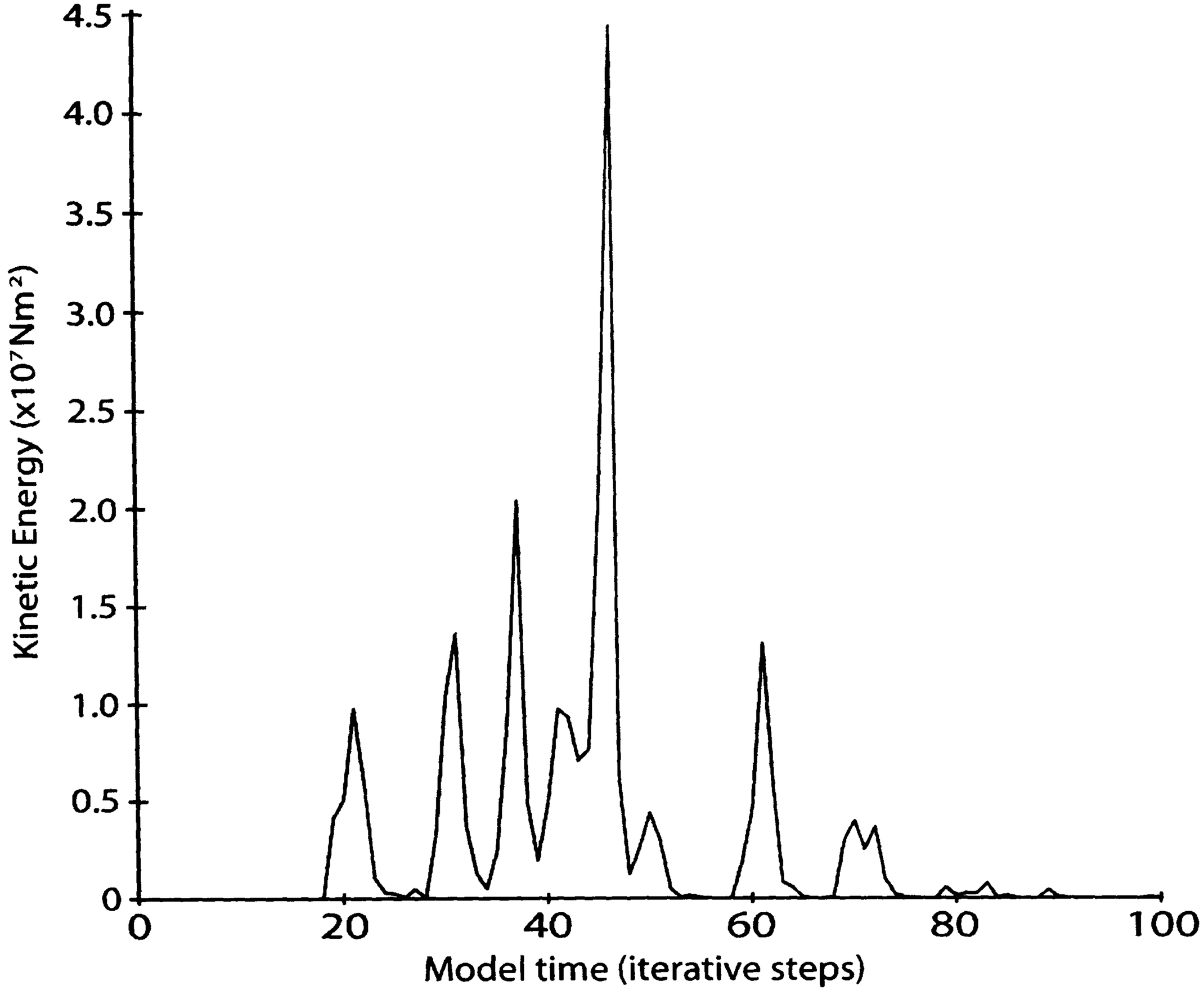

Figure 7.29: The temporal patterns of activity within the generic model of the cliffs at Staithes. The periods of slope change are more progressive and continuous in nature contrasting with the behaviour of cliffs modelled over longer time frames. The peaks refer to periods of instability following the erosion of material.

7.9 Summary

This chapter has used the Elfen numerical modelling code as a tool to better understand the mechanisms and longer term processes associated with the monitored behaviour of the hard rock cliffs at Staithes, North Yorkshire. The new application of the code to coastal cliffs required it first to be validated against established models of rock slope behaviour previously verified against field examples. Elfen was able to account for a variety of mechanical interactions, and in doing so raised important questions over the way in which failure is viewed, and whether certain phases of activity can adequately be described by a failure 'type'. Once validated, applied models were used to address problems of magnitude and frequency, scale dependency, episodicity and the environmental controls on slope behaviour raised in the previous chapter. The models, applied under simplistic and carefully constrained bounding conditions, demonstrate the inadequacy of assuming constant rates of retreat, even over longer term considerations.

Chapter 8
Discussion and conclusions

8.1 Introduction

Despite recent technological advances, many questions persist in understanding coastal geomorphological systems such as cliffs (Stephenson and Brander, 2003). This investigation into coastal cliffs has used tools such as high-resolution monitoring and combined finite/discrete element numerical models with the aim of progressively building a better picture of the relationship between process and form in coastal rock cliffs. Aspects of slope behaviour such as concepts of magnitude and frequency, scale dependency, episodicity and environmental drivers of change have been considered, with implications for both future analyses of coastal cliffs and the wider discipline of rock slope geomorphology in general. The findings of this study can be considered on three levels:

1. The processes and mechanisms governing lithologically complex cliff forms
2. Practical implications for coastal cliff studies
3. Understanding wider issues of rock slope geomorphology

8.2 The processes and mechanisms governing lithologically complex cliff forms

The study site of Staithes, North Yorkshire, was selected for its high, sheer-sided and materially complex cliffs. The Liassic rock from which they are composed provides moderate to strong resistance, commonly forming competent cliff sections (Williams and Davies, 1987). Little is understood about the short-term development of such coastlines, with interpretation predominantly based on long-term records of variable quality or qualitative assessments. The quantitative analysis of selected sites has revealed the diversity of cliff responses, with detectable influences on slope behaviour from a wide variety of controls from morphology, materials and structure to environmental drivers such as rain intensity and wave regimes. Interpretation of these effects in addition to field observations has enabled conclusions to be drawn over the evolution of lithologically complex coastal cliffs.

The monitored cliffs were not dominated exclusively by either a few very large failures or many very small losses. Instead a continuum of change was recorded from each rock type across all sites, during every month. Although the volumetric contributions were often seen to be biased towards either particularly large or very small changes, distinct patterns involving the whole continuum of material sizes were detected. The occurrence of relatively small to medium scale failures, involving volumes less than 100 m^3, are typically assumed to be random and superficial to the rock slope (Matsuoka and Sakai, 1999; Brunsden and Lee, 2004). Analysis of several cliff sections suggested that supposedly insignificant scale losses can be attributed to specific processes and mechanisms. At Site 2, for example, smaller scale losses were noted to have been concentrated upon arched failures within the cliff, with episodes of progressive change associated with the horizontal propagation of the arches. A study of cliff evolution which might have concentrated on the large scale changes which Brunsden (1999) refers to as 'formative' events, would have missed important aspects of slope behaviour. Indeed the release of material from joints parallel to the slope face recorded from several of the arched failures demonstrates strong similarities with stress-release jointing noted in other steep-sided coastal cliffs (Sitar and Clough, 1983).

Changes in slope form occur on multiple spatial and temporal scales. The use of new monitoring and modelling techniques reveals distinct signals between slope changes of different scales and at different times. The findings of the study have been used to form a generalised model of cliff behaviour in composite material (Figure 8.1). As with many conceptualisations of cliff behaviour, each phase of cliff development will not necessarily evolve into the next. The tendency towards particular forms is merely

the reflection of changing conditions over time. The importance of the location and time at which different failures occur in determining their significance to slope behaviour, has been a recurring theme throughout much of the analysis. Nevertheless, the five phases appear to reflect monitored cliff behaviour in the area, seen in the correspondence with laser scanned profiles. The phases provide a useful model to help explain the complexities of the coastal cliff system.

Cliff phase 1: steep slope face. Few truly vertical cliff sections are present within the study area. Most were complicated by a reclining or overhanging upper slope or a protruding toe. This suggests that such a phase may reflect a balance between *in situ* conditions and marine and subaerial processes that is easily disturbed by changing conditions. Where steep cliffs were recorded, they typically display fresh, angular faces with evidence of active spalling throughout the slope. When exposed to marine activity, the base of the cliff is often eroded at a faster rate than the rest of the slope causing a transition to a new characteristic form.

Cliff phase 2: overhanging slope profiles. Overhanging cliffs are relatively rare, although most cliff sections contain some degree of overhanging material. The monitoring data suggest that the more protruded parts of the cliff are most likely to fail. The majority of the failures occur as coherent blocks, often propagating instability upwards from undercut lower layers. The form of the cliff face generates the potential for the failure of exceptionally large volumes, relative to the size of the landform. When such a loss occurs it marks a change to a new phase of development.

Cliff phase 3: overhanging layers from the mid and upper portions of the cliff fall into line with the overall plane of the cliff face. The scale of the slope failure(s) from above the wave cut notch varies significantly across the study site from tens to thousands of cubic metres. The most significant aspect to the new phase is seen as the accumulation of material at the foot of the cliff. Whilst the volumes of material are often insufficient to halt the contact between the cliff base and the sea, several examples were recorded where the slope toe became protected by a debris apron. Immediately after a rockfall much of the peripheral talus is removed by the sea. The debris becomes steepened by a positive feedback between increased erosion and surface exposure of material to further erosive processes, a mechanism that has been noted elsewhere (Emery and Kuhn, 1980). In some instances a densely packed core of material of various sizes provides greater resistance to marine erosion, causing a decline in the rates of change in the deposit, which continues to armour the cliff base long after the initial failure. The reason for the persistence of such a feature may be

twofold. Firstly, much of the fallen cliff material in the area typically comprises elongated slabs. In several instances along the coastline such rocks have been seen to interlock forming a semi-permanent structure on the foreshore capable of withstanding significantly greater marine forces than individual blocks (Robinson, 1977). Secondly, the material from the largest falls consists of a matrix of till and rock fragments. The cohesive properties of the deposit were demonstrated at Site 2 (refer back to Figure 3.16), and appear able to form enduring features even within the coastal environment (Dalrymple *et al.*, 1986).

New insights into the nature of large scale failures were gained from the loss of over 2000 m^3 of material from the cliff section at Site 3 on 29th December, 2004. Although the change in slope form extended beyond the limit of the monitoring area for the site, an early laser scan captured during initial site surveys enabled a difference model to be constructed of the whole failure (Figure 8.2). The analysis reveals the extensive outline of the failure surface, which could not be determined from visual inspection due to the seepage of till, caused by the winter storms, which discoloured the fresh rock exposures ('A' in Figure 8.2). The difference in cliff slope position as a result of the change, approximately 6 m of landward recession in places, is visible by the western extremity of the scar, which is bordered by material that remained protruded. The edge of the failure coincides with a sub-vertical tension crack which runs through the entire rock mass at this point. Indeed, the selection of Site 3, with its strongly jointed characteristics, was based on two similar structures to the east (refer back to section 3.5.3). Site reconnaissance revealed several such weaknesses within rock immediately to the west, which protrude to a similar degree ('B' in Figure 8.2). The model suggests that the potential exists for further failures of comparable magnitude as the cliff adjusts to a new, landward position. Questions remain as to the effect of such a large change to the long-term development of the cliff. It has yet to be determined whether the time taken for rockfall debris to be removed and renewed marine erosion to occur, causes the retreat due to large failures to become comparable to the less dramatic but more constant rates of slope recession. While the catastrophic failure of overhanging cliffs has the potential to influence cliff form for many years, the occurrence of such events were relatively rare and the cliffs at Staithes more commonly developed through less noticeable alterations to form.

The natural defence of the slope toe is most obvious in the accumulation of large debris cones. Similar effects are caused when the slope is based on more competent, sparsely jointed material, such as the basal mudstones at Site 1 and Site 4. Whether the effect of marine activity on the cliff is limited by either a physical barrier, or

the enhanced resistance of the slope itself, a new cliff phase of development often occurs.

Cliff phase 4: protruding slope toe. Although the first 3 phases have largely attributed the main driver of change to marine processes, it must be remembered that the interaction of the slope with subaerial factors continued throughout all phases and may well have a critical influence in the precise nature of change. The magnitude and timing of large failures during cliff phase 3, for example, may be governed not just by protrusion but also loading of the slope by saturated till and material weakening due to internal hydraulic pressure fluctuations. In phase 4, marine processes are reduced to such a degree that subaerial processes become the main controls on slope development. This cliff phase therefore represents a significant departure from previous models of hard rock cliff development (such as Sunamura's (1992) model) in which change is governed exclusively by marine undercutting. When the toe of the slope is held against the processes of retreat for a sufficient period of time the mid and upper portions of the slope continue to weather and fail, relaxing back to leave the toe protruding. The development of slopes with protruding toes reflects a more stable cliff formation, demonstrated in Site 1, for which little significant change was recorded throughout the monitoring period (refer back to Figure 5.2). Instead change becomes dominated by small scale detachments which tend not to propagate.

Cliff phase 5: undercut slope toe. Over time the ability of the slope toe to withstand the erosive force of the encroaching sea will inevitably weaken, causing the cliff base to retreat once more. The time taken for the transition to cliff phase 5 is dependent on the balance between the resistance of the toe material and the effectiveness of the eroding waves. Other studies have considered the factors that influence the interaction. The competence of the toe is a function of material conditions such as mechanical strength and structure (Sunamura, 1977), but the destabilising impact of wave energy remains poorly understood. Assailing waves generate hydraulic processes such as compression, stressing and tension (Longwell *et al.*, 1969), as well as less obvious abrasive effects (Davies, 1972). The effect of marine action is therefore complicated by the availability of material on the foreshore. Many studies have focussed on the protective effects of beach material in dissipating wave energy before it reaches the cliff (Osborne *et al.*, 1989; Everts, 1991; Best and Griggs, 1991; Galster and Schwartz, 1990; Diener, 2000; Mickelson *et al.*, 2002; Runyan and Griggs, 2003), while others have noted the contrasting effect of heightened activity linked to the supply of artillery material to the waves, increasing their erosive capabilities (Robinson, 1977; Neves and Pereira, 1999).

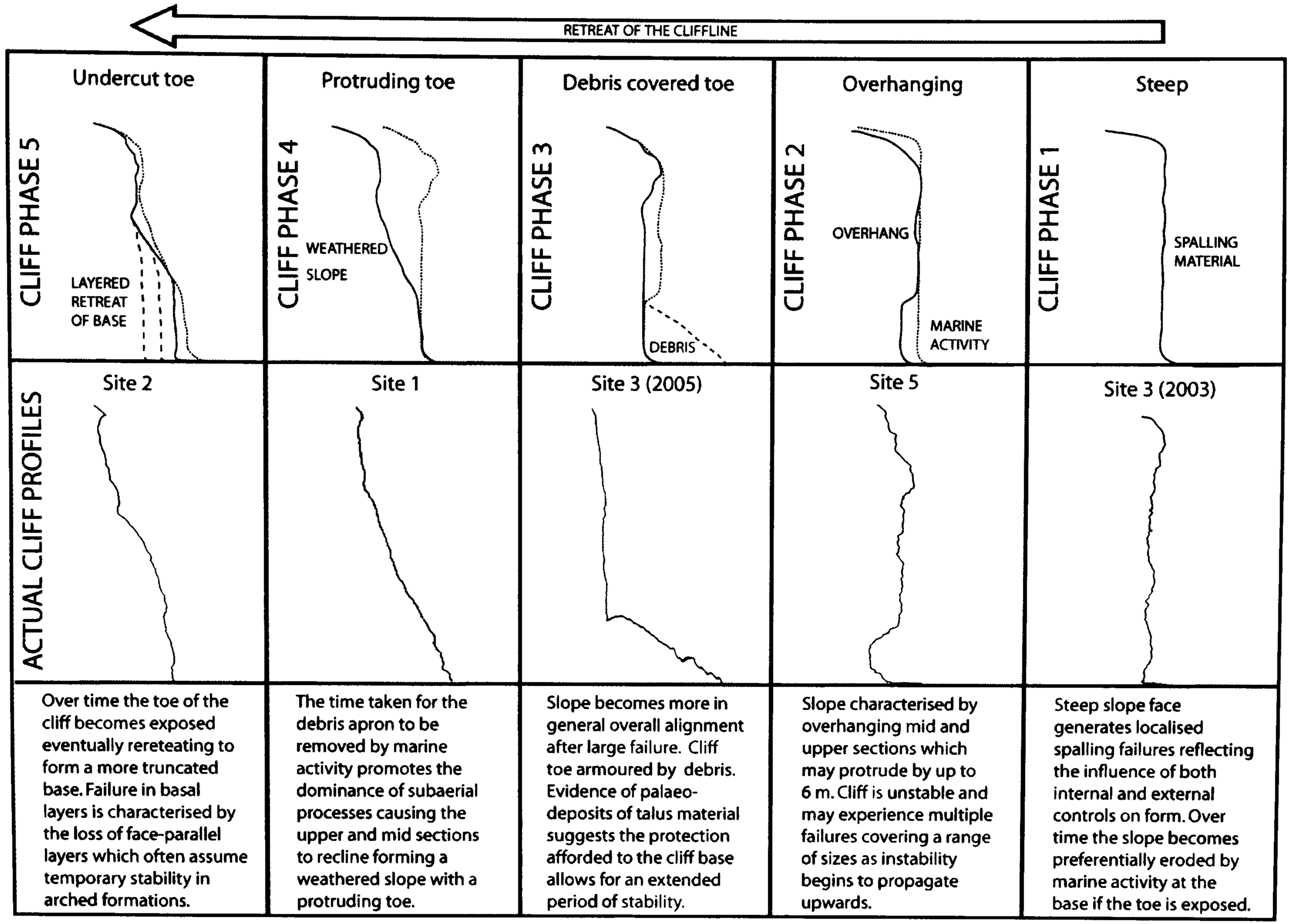

Figure 8.1: Generic model of lithologically complex cliff behaviour. Examples of characteristic phases of slope development were seen throughout the study area but site specifics meant successive slope forms did not always follow in sequence.

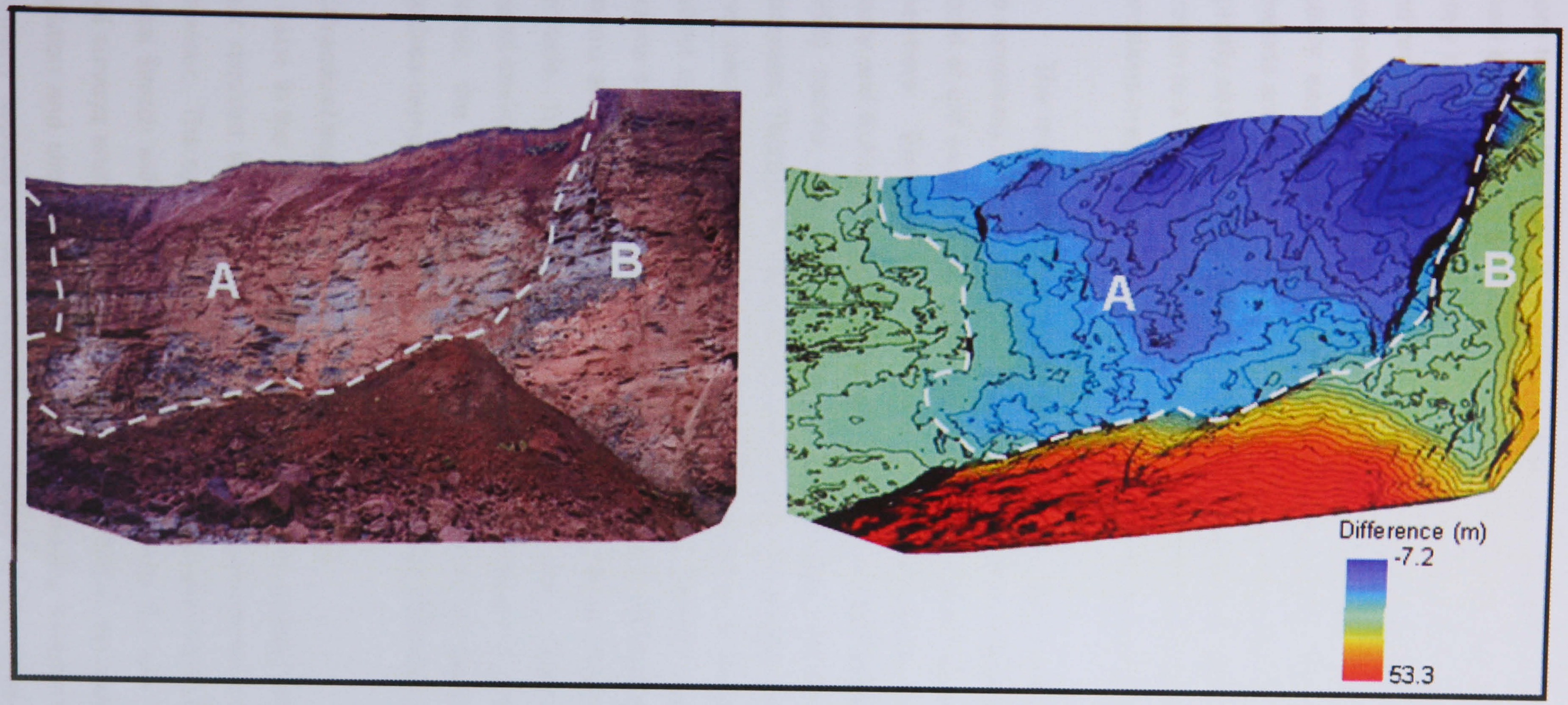

Figure 8.2: Photograph and difference model of the largest failure recorded during the monitoring period. The ability to accurately capture the changes undergone by the cliff during such large scale adjustment in high-resolution is essential in improving understanding of the long-term evolution of the coastline in the area. The rock cliff at this section is 38 m high, capped with 10 m glacial till.

The time scale over which the protruding toe of the cliff slope may regress to a more truncated profile will depend on local site specifics. The landward recession of basal slope sections often occurs as layers parallel to the cliff face. Although failure rarely occurs as coherent sheets, more commonly releasing shallow angular blocks and reaching temporary stability in arched formations, the loss of successive foliations generates characteristic sequences of slope behaviour. When undercut by marine activity each vertical layer, defined by slope parallel tension cracks, propagates upwards and outwards until it reaches less well jointed slope material. Adjacent arches typically coalesce horizontally until the layer has been removed. This process leads to a return to a vertical cliff, completing a cyclical pattern of slope behaviour, although site conditions may cause the slope to revert to any of the previous stages.

The results from the analysis of monitoring and modelling approaches reveal the complexity of processes operating within hard rock coastal cliff systems. A general model of cliff evolution demonstrates many slope responses similar to those detailed elsewhere. Elements of Sunamura's (1977) undercutting and overhang collapse, Emery and Kuhn's (1980) accelerating retreat of rockfall debris, Neves and Pereira's (1999) marine and subaerial process interactions, Robinson's (1977) foreshore processes, Terzaghi's (1962) arched formations and several other coastal cliff studies have been required to form a coherent appreciation of process-form relationships. Distinct cycles of alterations to slope form cause spatially specific cliff responses to become superimposed over different periods of time, generating multiple and complex patterns similar to those noted in other coastal systems (Trenhaile, 1987; Griggs and Trenhaile, 1994; Pethick, 1996; Mottershead, 1997). Whilst the dynamics of the coastal environment cause every cliff section to behave in a very localised and specific manner, the internal mechanisms and/or external processes which drive slope response demonstrate many parallels with aspects of cliff behaviour elsewhere.

8.3 Practical implications for coastal cliff studies

An issue in the study of coastal cliffs concerns the appropriate spatial and temporal cover required to achieve an adequate and representative understanding of slope behaviour. The spatial scale at which cliffs are usually monitored is that of the entire coastal stretch within which they are located. Whilst the use of techniques such as aerial surveys enables large reaches of coastal cliffs to be analysed, the inconsistent resolution and simplistic and occasionally misleading interpretations limit knowledge into many aspects of cliff behaviour. Analysis of the influence of spatial scales presented in this study demonstrates that the complete cliff slope is indeed the

appropriate scale at which to assess landform change. Doubts are raised over the validity of studies which consider large sections of cliff, often generalised into single figures of retreat. Emery and Kuhn (1982) recognised that sea cliffs cannot be expected to demonstrate the same profiles over large areas. Consequently the different patterns and processes of change associated with specific slope types, identified in this study, are ignored by general retreat rates. A management assessment of the coast at Staithes, for example, classed the general susceptibility of the cliffs as moderate, suggesting changes in the cliff are likely to be 'significant' in the intermediate-term (Mouchel Associates Limited, 1996). Such approaches can give little practical, quantitative indication of the current or future processes and mechanisms operating on cliff sections. Spatial differences resulting from material and structural properties are major determinants in cliff steepness (Hampton *et al.*, 2004). More specifically, the analysis presented here shows that factors such as the lithological sequence, failure history and the cumulative and extreme environmental conditions are all capable of influencing localised behaviour.

This study highlights the inadequacies of investigations which use historical maps to generate long-term recession values, in order to calculate annual rates of retreat. Whilst current estimates for cliff retreat in the area performed relatively well for certain areas, many of the monitored sites which show below or more commonly above average changes deviated significantly from the long-term predictions. The poorest performance in the predicted rates of retreat were generated for cliffs that show either stable or rapidly changing behaviour, which are the most significant to concerns of both geomorphological understanding and coastal management. Perhaps more importantly, the complexity of cliff change can not be conveyed in a single set of figures, with the form of the slope changing through time in addition to its seaward position. The historical predictions recorded similar processes of cliff development throughout the coastline, with different rates predicted for the cliff top and more dynamic toe (Agar, 1960). From the present day cliff forms it is clear that such a relationship does not persist through time. More detailed, multiphase conceptualisations are required to better explain the nature of cliff behaviour.

The combined terrestrial laser scanning and photogrammetric monitoring approach has allowed the significance of smaller scale changes to cliff form to be recorded, assessed and validated. The importance of such contributions to slope form suggests that rock cliff studies which consider only the larger, more noticeable changes, ignore important aspects of landform behaviour. Where marine erosion of slope bases is limited by material competence, or imposed barriers such as rockfall

material or sea defences the retreat of the cliff may be predominantly governed by wide scale, less dramatic processes. The ability to accurately quantify small, iterative changes to cliff form is a key consideration in the spatial coverage and resolution that must be achieved in assessing rock cliff behaviour.

The results of this study demonstrate the importance of using volumetric considerations in order to analyse spatial change in rock cliffs. Whilst in some instances relatively accurate, albeit overvalued, patterns of change may be generated through area calculations, other studies have drawn caution over the extrapolation of volumes from two-dimensional analyses. Luckman (1988) concluded that many such techniques overestimate the volumes of material involved. Direct, volumetric measurements of rockfall patterns are rare with most of those that have been attempted relying predominantly on the physical collection of failed material at the base of slopes (Rapp, 1960; Fahey and Lefebure, 1988). The ability to accurately record three-dimensional change is fundamental to better understanding the nature of cliff behaviour (Hapke *et al.*, 2004; Lim *et al.*, 2005). The vast majority of changes detected would not have been recorded by even frequent site visits, casting much doubt over the usefulness of any monitoring of cliff behaviour which relies on qualitative assessments. Many of the concepts embedded within coastal cliff studies, which have led to the notion that rock cliffs can be effectively monitored by recording wherever a noticeable change has occurred, have been drawn into question by this study. The data suggest that a switch is required, particularly in landforms with complex lithology, away from how best to establish the most accurate rates of overall retreat within coastal cliffs to how best to record, analyse and interpret localised changes in the cliffline. The diverse forms throughout most coastlines indicate that behaviour is not uniform spatially or over time. It is only through the identification of specific processes, mechanisms and slope responses that cliff behaviour can be better understood and predicted.

The nature of change in coastal cliffs is complicated by the environment within which they are located. In an attempt to isolate certain aspects of cliff change this study made the distinction between marine and subaerial environmental influences on slope form. The development of coastal rock slopes can not be explained by marine activity alone, but rather reflects the interaction between subaerial and marine processes and mechanisms governed by *in situ* conditions. The findings suggest that an improved understanding of coastal cliffs requires consideration of the system within which they are situated. The importance of both subaerial and marine drivers of change in governing coastal cliff development is increasingly becoming recognised (Neves and Pereira, 1999), suggesting that coastal slopes may vary in their sensitivity

to environmental processes spatially as well as over time. The analysis of coastal cliffs as part of a dynamic system causes other factors to become relevant such as orientation with regard to storm tracks, prevailing and maximum wind directions, foreshore topography and sediment supplies. This study has highlighted the multifaceted nature of cliff response to changes to the coastal system. The influence of anthropogenically driven subsidence in the study area was assumed to be a major control on slope behaviour prior to monitoring. The area of peak subsidence however was later determined to be the most stable site monitored. The effect of alterations to the processes operating on coastal cliffs do not therefore equate to simple reactions in slope form. Cliff studies should consider the potential for landform response in addition to environmental process which may ultimately drive change.

Quantifying the effect of specific environmental processes remains problematic. The impact of waves on the cliff base for example is determined not just by the tidal height, fetch, wind direction and velocity of the waves, but also by the near shore bathymetry, shore platform, coastal configuration and sediment content of the water. Analysis of marine influence is complicated by site conditions that alter through space and over time, making the accurate quantification of the erosive effect on cliffs particularly difficult (Battjes and Groenendijk, 2000). Much further investigation into the quantitative effects of environmental factors such as wave erosion is required to explain cliff behaviour.

Studies of coastal cliffs must also account for temporal aspects to change. The timescale over which the evolution of cliffed coastlines are analysed is a key determinant of the manner in which recession processes appear to operate (Brunsden and Lee, 2004). The time period considered for the evaluation of slope development for example influences the significance of the recorded changes (Schumm and Lichty, 1965). Short-term alterations in coastal cliff form are usually considered over yearly intervals, and concern the transition from stable through marginally stable to unstable and active behaviour. They are often assumed to be random, gaining significance only when collated over longer periods when natural variations become more generalised (Brunsden and Lee, 2004). Emphasis has also been taken away from short-term considerations of cliffs by the realisation that multiple elements of the system operate over different timescales (Brunsden and Jones, 1980). The monitoring study presented here demonstrates that despite limited temporal extents, in the order of a few years, important advances can be made through analysis of high-resolution data.

Failure in coastal cliffs has been largely associated with longer term development, from several to tens of years, because this is both the timescale over which most significant changes are considered to occur and the temporal resolution for which many coastal records exist. Although many concerns have been raised over the validity of long-term datasets, they continue to dominate the basis for contemporary understanding into coastal cliff behaviour. The most widely adopted approach to cliff behaviour, based on long-term records, is that of probabilistic modelling. The data presented here highlight many of the limitations of approaches which use past occurrences to predict future change. Aside from the issues of the validity of the datasets, discussed in Chapter 2, the monitored processes and modelled mechanisms have shown that cliff slopes cannot be assumed to continue to develop as they have in the recent past. Instead a more informed approach using actually monitored slope changes and carefully constrained model simulations capable of inferring mechanisms of change over longer than monitored periods has been promoted. In addition to presenting a greater level of understanding into the nature of cliff changes, the approach developed can be used to analyse recession processes for areas of coastline for which no records exist prior to monitoring.

The techniques used in the study of the hard rock coastal cliffs at Staithes, North Yorkshire, have significant implications for future research into coastal cliffs. The spatial and temporal extent and resolution required to gain an adequate measure of the process of cliff change are essential in determining both the method of analysis as well as an appropriate application. In addition to promoting greater awareness of issues such as applicability and required resolutions, the data produced within the study have also drawn into question several concepts that have become entrenched not just in coastal cliff studies but in rock slope geomorphology in general.

8.4 Understanding wider issues of rock slope geomorphology

Theories of rock slope evolution are as diverse as the landforms themselves, encompassing all scales within the landscape over timeframes ranging from geological epochs to instantaneous rockfalls. Certain recurrent themes presented in this study relate to key aspects of rock slope geomorphology concerning landform behaviour. Concepts of magnitude and frequency for example have become central to many geomorphological studies. During the course of landform development over time, changes from within and outside the system may cause it to respond and adjust. The larger the magnitude of the perturbation the greater the potential for landform change. Many geomorphologists have attempted to establish relationships between the magnitude of the event and the temporal patterns over which changes occur (Whalley,

1984). Concepts such as reaction times, referring to the lag between changes in destabilising influences and landform response (Guzzetti *et al.*, 2002), and relaxation times, or the time over which landform change occurs (Brunsden, 1999), have been applied to relate magnitude and frequency of occurrence. It is often implied that if the reaction time of particular geomorphological systems can be established for events of a certain magnitude, the physical response of the landform can be predicted and remedial action implemented where necessary. Questions remain over the nature of the relationships associated with landform response and whether concepts such as reaction and relaxation times can be reliably applied to natural rock slope systems.

Whether coastal cliffs are dominated by large-scale catastrophic events, whether they are progressive in development, propagating instabilities, or whether they adjust gradually through small scale movements are considered key aspects to rock slope evolution but have remained poorly addressed by existing approaches. Much of the current understanding into the relationships that govern rock slope behaviour has been advanced by landslide studies. Guthrie and Evans (2004) demonstrated a good fit between magnitude-cumulative frequency data and a power law curve for landslides above a certain size. A rollover effect has been found in many records where the distribution of recorded events falls below model predictions (Guzetti *et al.*, 2002). This has largely been attributed to a reduced ability to reliably resolve smaller scale changes (Hungr and Evans, 1996; Stark and Hovius, 2001; Brardinoni and Church, 2004). Brardinoni *et al.* (2003) for example suggested that 85% of landslides in the Capilano basin, British Columbia, were below 650 m^2, the minimum reliable scale for landslide detection. The contribution of these small scale events was thought to have been 30% of the total landslide debris, although a re-evaluation by Bradinoni and Church (2004) suggested this may have been as little as 2.7%. Ambiguity surrounding the quantification of both very small and very large failures highlights the problems of establishing patterns relating to the impact and influence of changes of different magnitudes on landform development from limited datasets (Hinchcliffe and Ballantyne, 1999).

An improved understanding into the manner in which rock slopes change lies in the ability to quantify the relative contributions of large but rare events, frequent small scale changes and everything in between (Guzzetti *et al.*, 2002). The very small or large scales at which many patterns and processes are perceived to occur have long defied physical description and explanation in slope studies (Pelletier *et al.*, 1997; Dussauge-Peisser *et al.*, 2002; Martin *et al.*, 2002). More recently however, with improved datasets, material explanations such as the physical constraints of the slope

have been identified to explain process-form relationships (Guzzetti *et al.*, 2004). New analyses such as these, capable of reliably interpreting a wider spectrum of change, raise important questions over the processes that govern slope geomorphology. It is evident that the geomorphologist must be aware of imposing divisions and concepts during landform analyses, such as hierarchical divisions in magnitude-frequency analysis (DeBoer, 1992), which have resulted from previous assumptions of development. This study for instance has confirmed the potential of both small and intermediate scale failures to drive landform change in some instances.

Notions of episodicity have become well established in rock slope geomorphology (Brunsden and Chandler, 1996). The distinction is often made between temporal and spatial episodicity (Stephenson and Brander, 2003). Most references to episodicity regarding rock slope change relate to temporal occurrence (Hapke and Richmond, 2002; Sallenger *et al.*, 2002), although some studies have attempted to account for the spatial dimension to episodic behaviour. Moore and Griggs (2002) for example generated statistical predictions of the spatial distribution of coastal cliff retreat. Areas that experienced failure over a 40 year measurement period were assumed to be least likely to fail again over the next 40 years. By contrast, the data presented in this study questions the supposition that areas having recently failed will then remain stable for an extended period. Rock failures or episodes of morphological change are not necessarily isolated events.

Previous models concerning rock slope evolution, such as magnitude-frequency relations (Brardinoni *et al.*, 2003), spatially episodic behaviour (Moore and Griggs, 2002), direct environmental triggers (Hapke and Richmond, 2002) and probabilistic failure-no failure predictions (Hall *et al.*, 2002) provide poor explanations for the study findings. The inadequacy of existing concepts has been due to the complexities detected in slope responses not previously accounted for:

1. Weak direct relationships exist between environmental processes and rockfall occurrence in hard rock coastal cliffs.
2. Failures may occur at any given time with no clear triggering factor.
3. Geological controls exert detectable effects on failure patterns.
4. Past failures do not prevent recurrence of failure processes at any given location on the rock face.
5. The evidence suggests failure propagation and spatial and temporal linkages are needed to understand landform behaviour.

The spatial and temporal resolutions of the data collected in this study suggest that failure in rock slopes is neither an independent event, nor is it an end point in landform development. Information has been revealed on the effects of interconnectivity, continual processes, protruding material and environmental factors in governing rock slope behaviour. The response of the cliff is inevitably influenced by all of these aspects, raising questions over how they might be drawn together to improve understanding of rock slope behaviour. The majority of rock slope studies focus on the effects of stress leading to failure (for example Hoek and Bray, 1981), but the changes recorded in the field reflect material strain. Therefore, the theory of strain displacement within rock slopes has been tentatively developed in this study, providing an alternative explanation to the random failure of distinct cliff sections. The theory can be represented conceptually by simplifying the cliff face into a two-dimensional mesh, for which a set of rules can be established. The whole cliff face is affected by subaerial processes while the layers at the slope base are additionally influenced by marine factors, although the responses of distinct areas may interact (Figure 8.3).

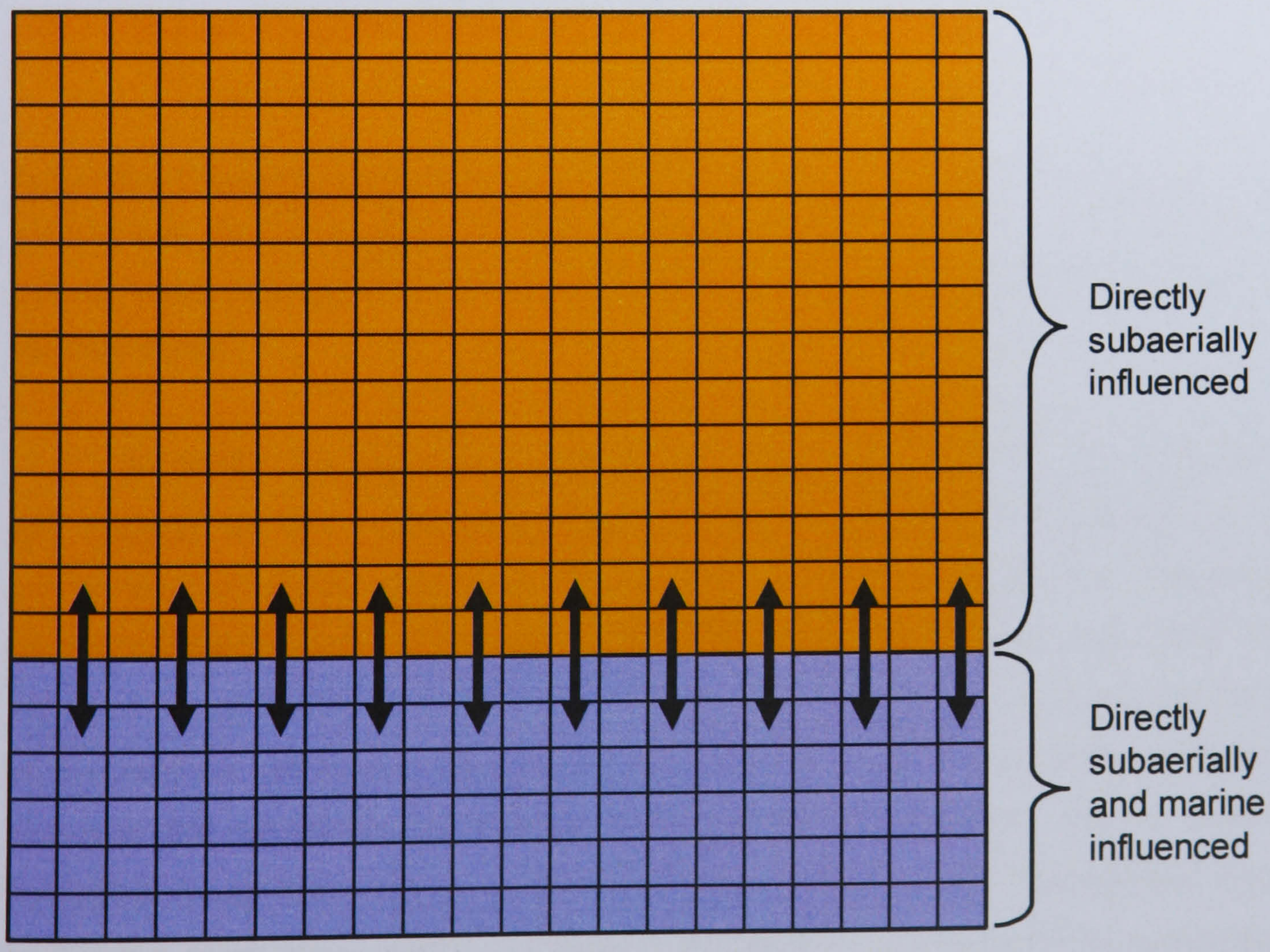

Figure 8.3: Spatially distinct influences on coastal cliff material. Although the base of the cliff is often exposed to the additional force of waves, the interconnectivity of the landform means material responses can be transmitted to other areas. Most notably strain responses may cross the maximum physical extent of marine influence denoted by dashed line, indicated by the crossing arrows.

Environmental agents have the potential to alter the levels of strain in the cliff, and, as Sunamura (1992) suggested, failure will occur when the assailing forces exceed the resisting forces of the cliff material (refer back to Figure 2.5). The material history, geotechnical competence and structural properties all vary spatially and over time causing different sensitivities within the same landform. In order to explain the interrelations between failure processes, strain resulting from environmental forcing may propagate to other connected areas within the mesh (Figure 8.4). Due to the force of gravity, strain effects are most likely to be conveyed upwards and outwards through the connecting rock. Potentially, strain displacement may be transmitted through the rock mass affecting large areas over successive time intervals (Figure 8.5).

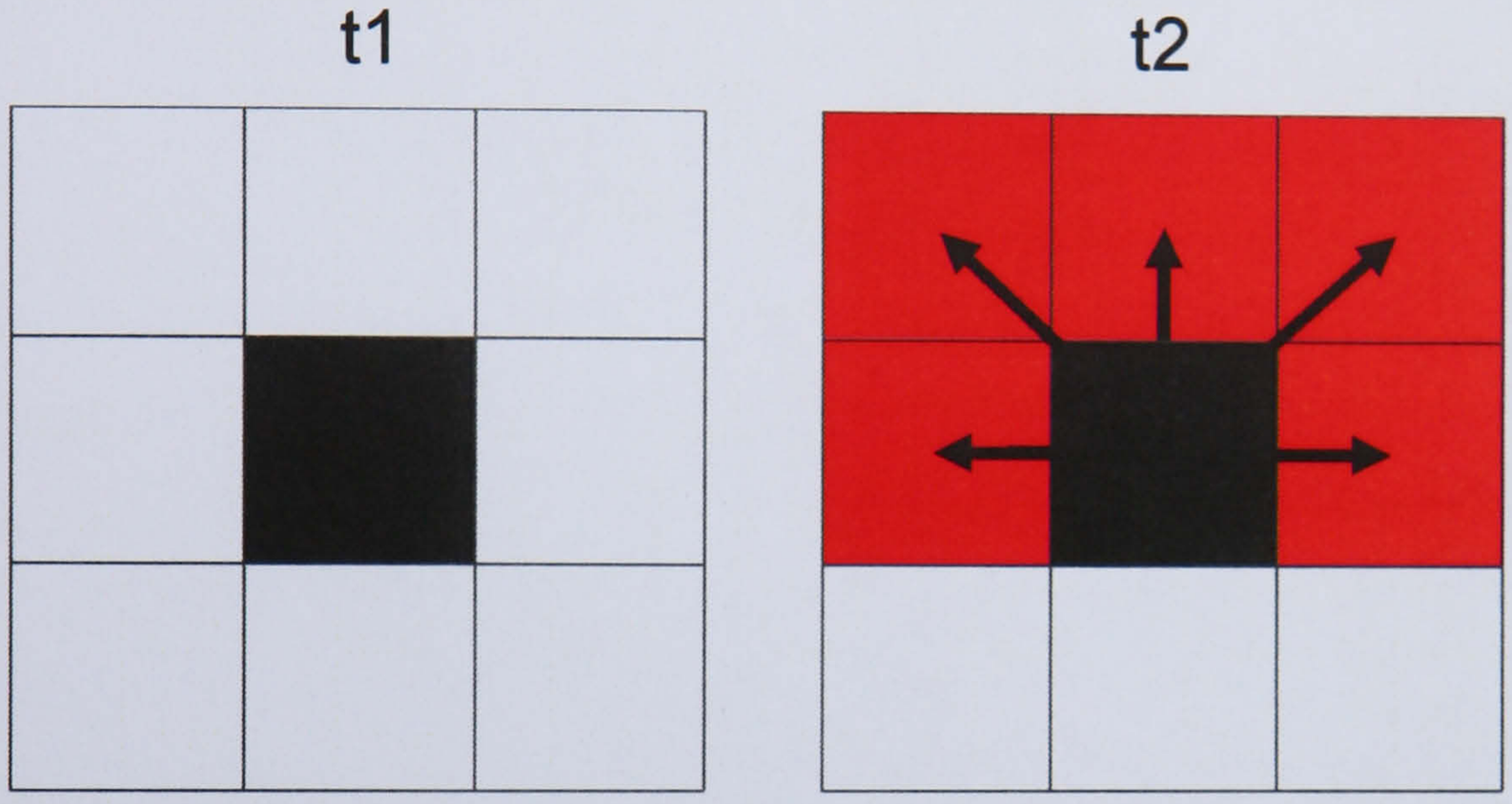

Figure 8.4: Propagation of strain from the central block (in black) with heightened strain rates in the first time step (t1) to peripheral blocks in the following time step (t2). The downward pull of gravity means propagation is most likely to occur upwards and outwards to the bordering cells denoted in red.

In reality, the rate and extent of the strain transferral from the displaced block will depend on the connectivity within the mesh, which is influenced by *in situ* properties such as the degree of jointing and brittleness of the material. Superimposed on the spatial divisions in the cliff caused by environmental processes (refer back to Figure 8.3) are the lithological and structural properties which determine the sensitivity of the mesh or cliff face to change. In sedimentary rocks such as those at Staithes for example the sensitivity to change is complicated by bedding planes which alter behaviour away from cliffs of simpler composition (Figure 8.6). Additionally, any other part of the mesh may experience heightened strain generating complex spatial patterns of change. The probability of transferral of displacement is therefore space and time dependent and ultimately reflects the specific balance between strain and material competence.

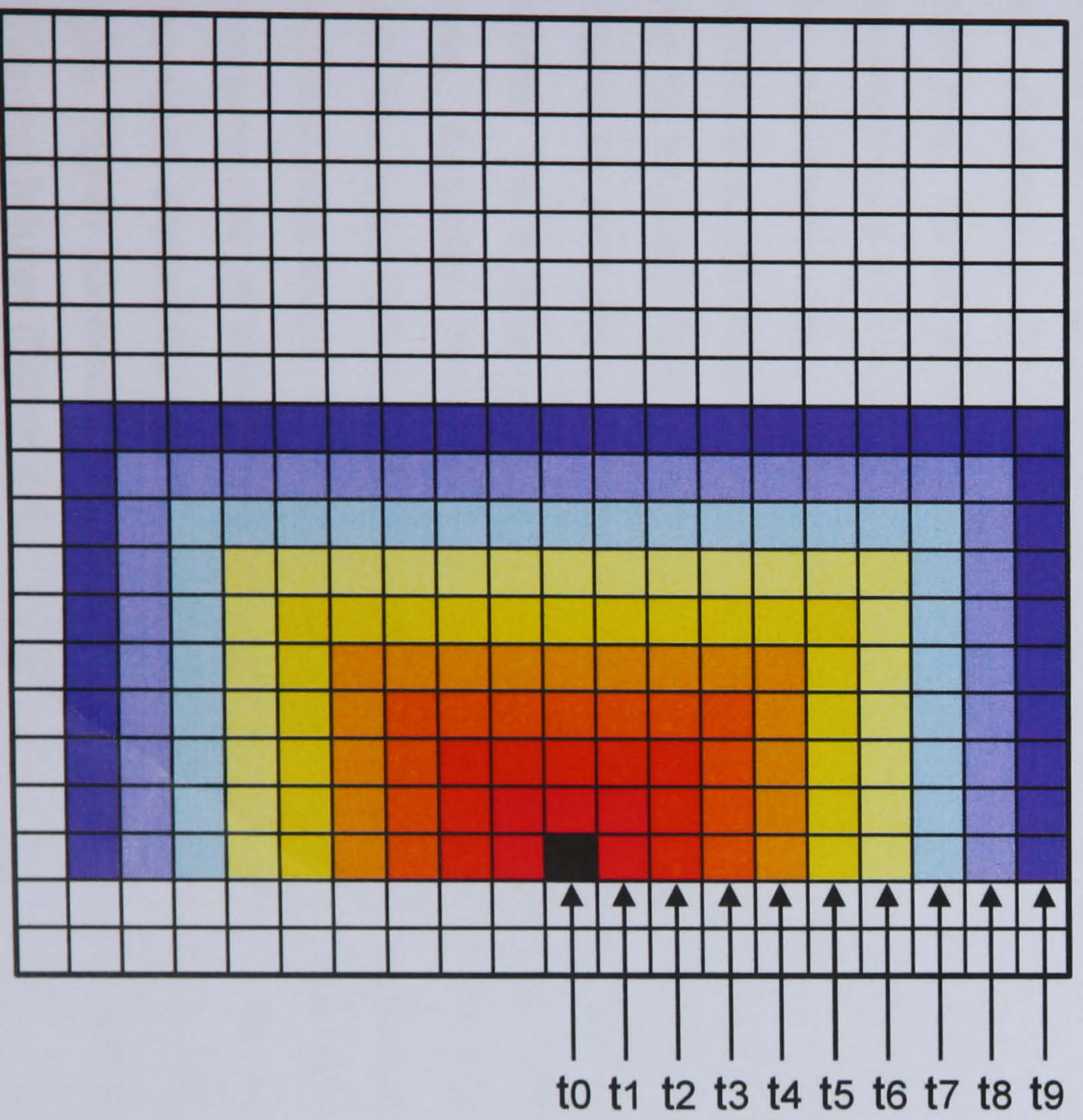

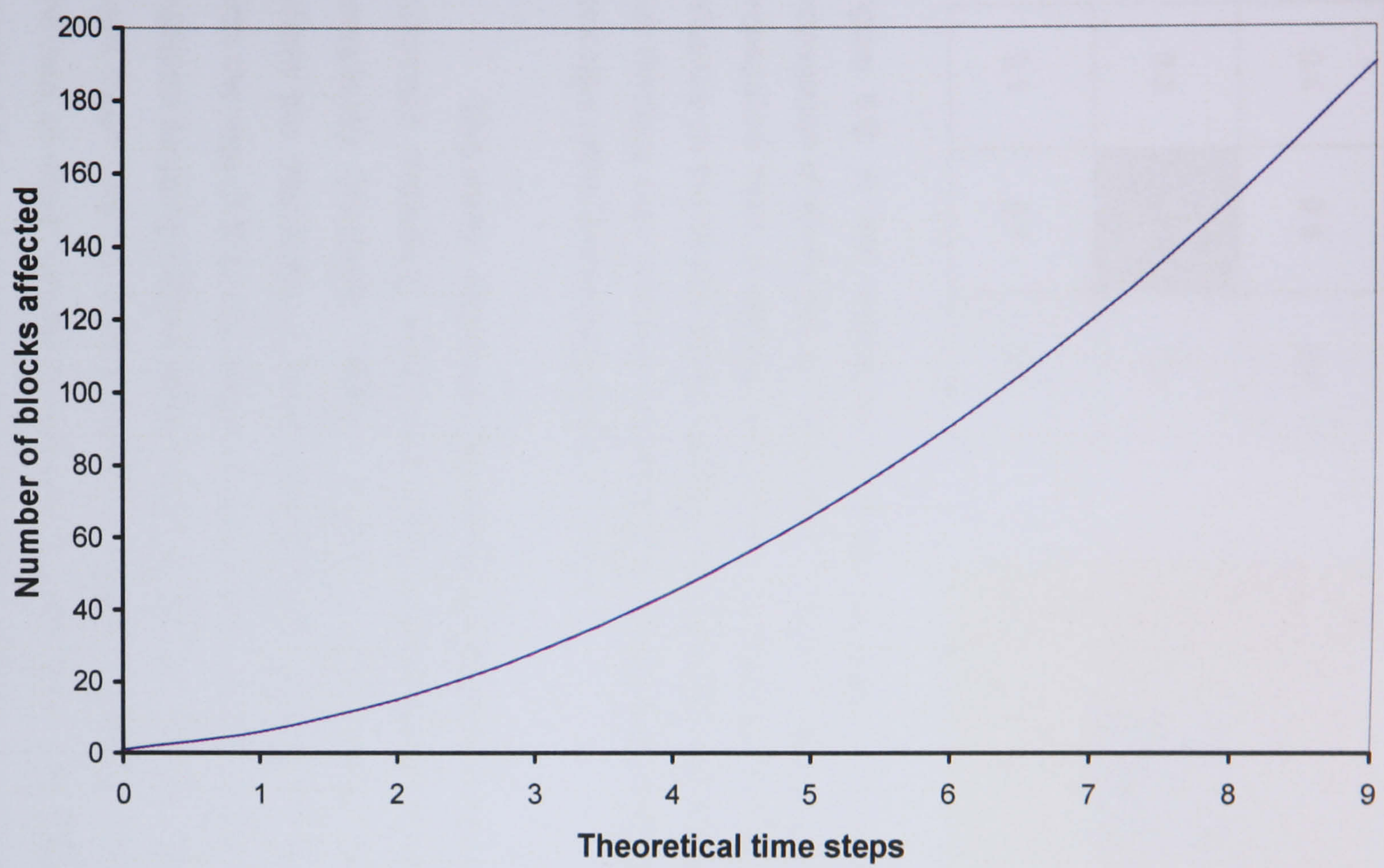

Figure 8.5: Potential propagation through a rock mass from a single cell experiencing high strain rates. Strain may be conveyed directly or dampened as it moves out from the displaced block over successive time intervals from t_0 to t_9. The graph demonstrates that if the rock slope is particularly susceptible, for instance if the material is particularly brittle and/or uniform, an increasing area may become affected generating the potential for large scale failures.

Figure 8.6: *In situ* conditions such as lithological complexities influence the most likely propagation of strain through the mesh. The left cluster represents theoretical probabilities for propagation from a central cell (black) undergoing heightened strain, with the most likely influence on the blocks above, although all may potentially be affected. The right cluster shows that lithology may produce a tendency for strain to be propagated outwards within the same rock type rather than across bedding planes.

The strain displacement model presented is based on the principles of cellular automata modelling which has been successfully used elsewhere to model natural complexity (Wolfram, 1984). Failure occurs when material reaches critical strain, where the destabilising forces exceed the capacity of the material to remain coherent with the rest of the rock slope (Petley *et al.*, 2005). In terms of the mechanical process, material passing critical levels of strain moves beyond its elastic limit. Similar concepts have been used to define the occurrence in landslides where failure is inevitable when the rate of strain displacement enters a tertiary creep phase (Saito, 1969). Whether or not the failure of the block causes wider influences spatially or over time will depend on the efficiency in which strain displacement is transferred through the mesh. A theoretical development over time can be hypothesised to simulate how strain accumulations may lead to sporadic failure within a continuum (Figure 8.7). As seen in the monitored sites, the model reflects a propensity for deformations to be concentrated towards the base and horizontally associated with different lithologies (see for example Figures 5.2 and 5.4). The theory of strain displacement is able to account for both frequent, iterative slope changes and also occasional, large coherent failures. For a large failure to occur, increasing levels of strain must build in the rock mass. Logically, when the interaction between the cliff and its environment allows strain to accumulate through time, an increasing proportion of the slope is likely to pass its critical stain levels. The theory therefore implies that prior to a large scale failure an increasing rate of activity may be recorded. Although the model currently remains a theoretical explanation for the patterns and processes governing the monitored rock slopes, higher numbers of rockfall above 0.001 m^3 were detected in the months prior to the largest failures (Figure 8.8).

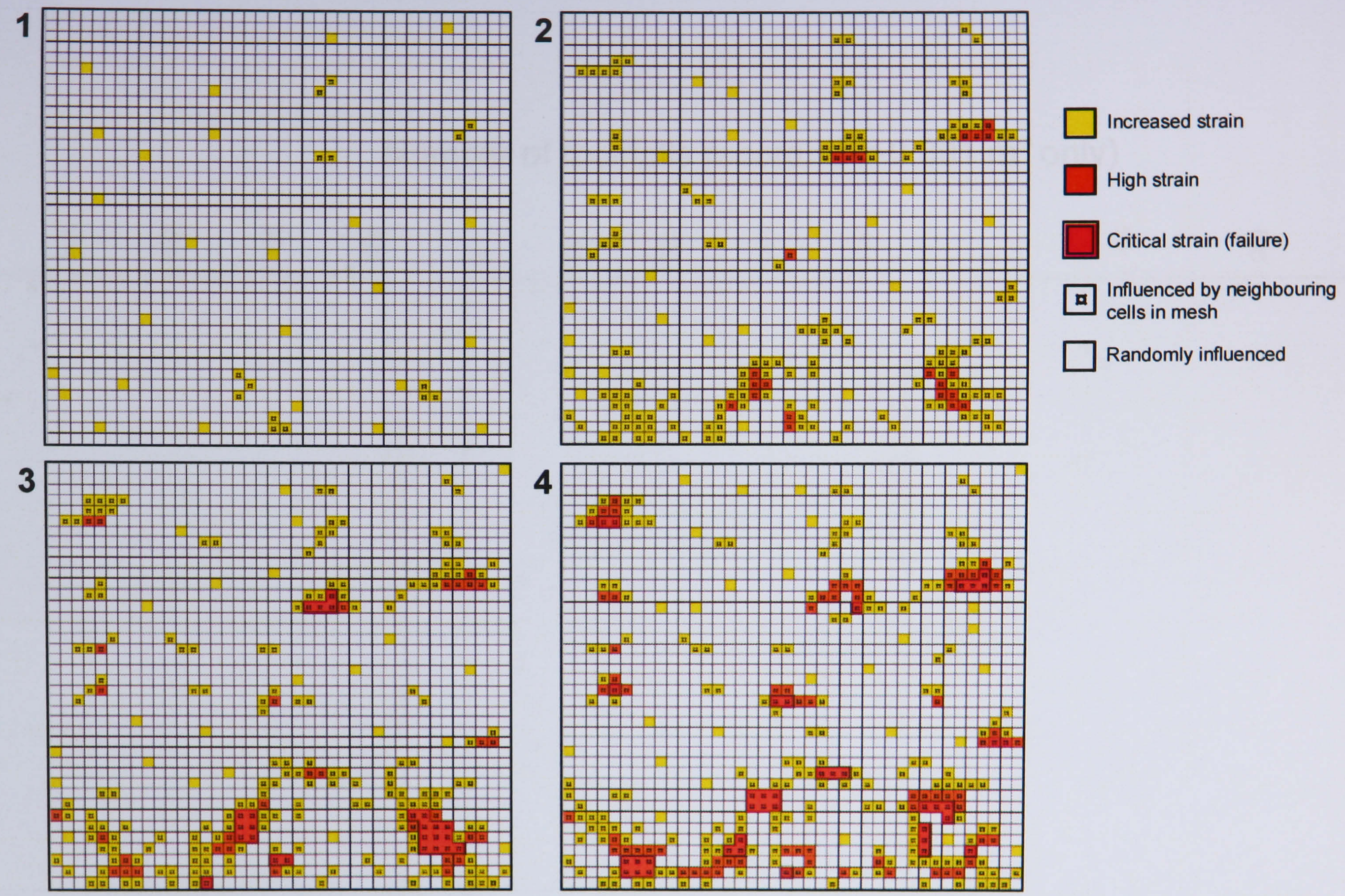

Figure 8.7: Strain displacement theory of failure development. Increases in strain may be randomly caused by internal and external processes but the interconnected nature of the rock face means that changes in the mesh often effect peripheral areas, both directly through material deformation and indirectly by causing protrusions and overhangs following failure. The four stage sequence shows the theoretical propagation as strain concentrations grow. Further investigation of the patterns of strain in rock cliffs and increasingly high-resolution monitoring may ultimately be used as a predictive tool if pre-failure displacements can be identified.

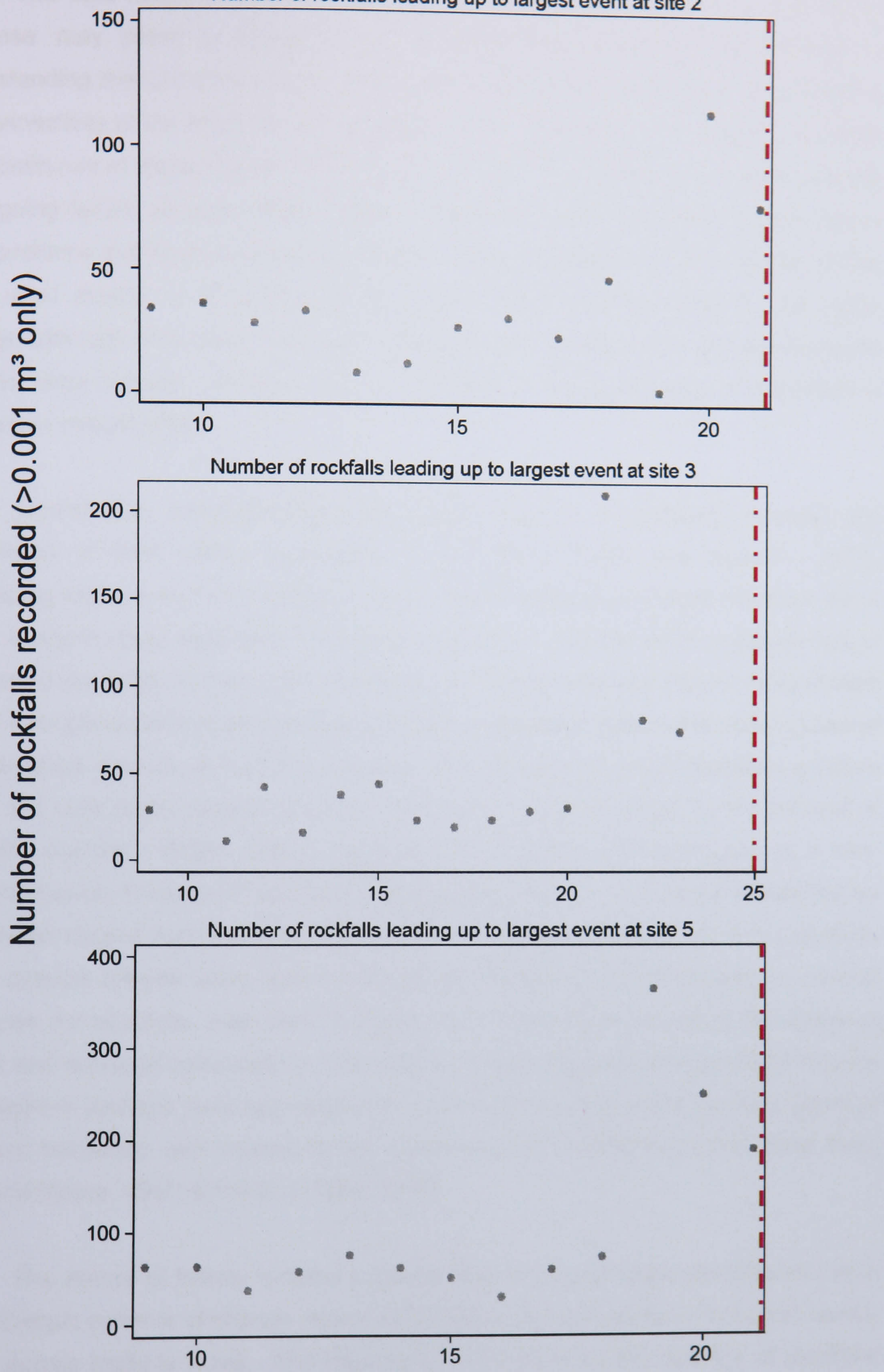

Figure 8.8: The number of rockfalls recorded prior to the largest failure at sites which recorded particularly large volumetric losses during the monitoring period. The red dashed line denotes the occurrence of the largest loss. In every case, although the trend is not linear, heightened numbers of rockfall occur in the months before the failure.

The data recorded in this study suggest that strain propagation and landform response may prove a powerful tool in addressing some of the shortfall in understanding that currently exists in the development of slope failures. Emphasising the connectivity of the landform allows failure to be considered as a progressive stage in a continuum of slope change. Hence any one part of a selected rock slope may be undergoing failure, or peak strain rates, in response to the local balance between *in situ* conditions and environmental processes. The association of strain with failure has been used mostly as a conceptual aid to improving understanding of rock slope change, although links were made with protrusion from a base plane and activity levels prior to large failures. Further work is required in the exploration of deformation analysis in coastal cliffs.

Quantitative measurements have been used to successfully forecast the occurrence of rock slides (Kalaugher *et al.*, 2000; Crosta and Agliardi, 2003), suggesting that a switch from stress to strain based analyses may hold the potential to better interpret other aspects of rock slope behaviour. Critical strain is transferred or dampened according to the *in situ* conditions and hence adjacent material may remain stable throughout several phases of adjustment or respond dynamically, forming part of a wider scale process of landform change. The importance of not considering failure within the rock slope system to be an end point is demonstrated in the concept of landslide capture. Petley (1994) suggested that failures may propagate in a non-uniform manner if 'captured' by other mechanisms. Failure of material should not be considered distinct from the overall response of the slope, demonstrated in this study when multiple failures were seen to be connected spatially or temporally in several instances (for example, refer back to Figure 5.7). The results question the nature of spatial and temporal episodicity in rock slopes. Whilst elements of episodicity may be recorded it is perhaps more appropriate to consider the spatial and temporal aspects of landform behaviour with respect to the processes and mechanisms that drive them (Lee and Moore, 1991; Brunsden, 1993; 1996).

The nature of failure remains a critical aspect to rock slope development over time. Certain patterns of change repeat according to specific scales in time and space, acting across multiple forms. The importance of interpreting the diversity of landform change has been noted elsewhere such as along the Dorset coastline where the patterns recorded within a slope complex at Stonebarrow Hill could only be explained as part of an integrated system of dynamic equilibrium disturbed by local imbalances (Brunsden and Jones, 1980). Although such analyses presented significant advances to rock slope studies by causing landforms to be viewed as interrelated systems rather

than static features governed by failure or stability, questions have been raised in this study over the usefulness of concepts such as dynamic equilibrium in slopes. Dynamic equilibrium has become a fundamental concept in geomorphology but the manner of slope retreat established for Staithes suggests that changes in slope form may not necessarily drive it towards an equilibrium condition. Supposedly transitional and unstable phases of slope behaviour may persist in the landscape indefinitely according to the shifting balance between internal and external controls. The complexities in slope response caused by lagged effects, *in situ* conditions and precursory and trigger events suggest that rather than attempting to establish when a landform is in equilibrium with the influences acting on it, it is preferable to view it as a constantly adjusting and evolving system. It therefore seems logical to assume that for every locality for which the sensitivity to the rock can be assumed to be constant, a unique but interconnected response pattern will be formed over time (Brunsden and Lee, 2004).

For over 50 years the parallel retreat of rock cliffs has formed the basis of many concepts of coastal evolution (King, 1953). Although the emphasis of change has become more process orientated, the concepts of enduring forms in the landscape remain (e.g. Sunamura, 1977; 1999). Such studies have been limited in their validity because of the complexity of the problem (Selby, 1980). Mark (1980) proposed that there was a dichotomy in geomorphological studies between landscape scale and process scale, raising questions over the appropriate level at which to consider cliffed coastlines. Andrle (1996) used characteristic models associated with different scales to investigate how complexity changes continuously with scale in coastal geomorphology. A balance must therefore be set in rock slope studies between the need to establish workable and effective classifications and the limitations of imposing such divisions on dynamic landforms.

The potential of similar landforms, or indeed the same landform viewed at different time periods, to respond to the same imposed change in different ways is reflected in the concept of landform sensitivity. The application of the term has however been diluted by rock slope studies which have tended to characterise highly sensitive cliffs, retreating in short, regular events that cause iterative changes in form and insensitive cliffs retreating through irregular patterns, responding only to rare and extreme events (Brunsden, 1999). The supposedly 'insensitive' cliffs at Staithes have demonstrated diverse and dynamic patterns of change reflected in landform responses over a continuum of scales. The continuum approach to the scales of consideration has long been effectively used in fluvial geomorphology; Hey (1979) for example

promoted a continuous mathematical relation between channel response and development. Ultimately, change in rock slopes reflects the superimposition of periods of critical strain within a constantly deforming landform in which the responses are displayed on a variety of levels. It is not the recurrence of repetitive forms over time which should emphasised but the manner in which they are reached through continual landform adjustment which is required to further advance rock slope geomorphology.

The analysis presented in this study calls for a re-evaluation of the way in which cliffs are perceived to evolve. Consequently, the findings hold far reaching implications for how rock slopes should be studied. A general model of slope evolution in complex coastal cliffs has been presented and strain propagation used as a method to explain the failure patterns. Monitored data provide a physical link between the generalised stages of cliff evolution (refer back to Figure 8.1) and the strain accumulation and propagation required prior to failures (refer back to Figure 8.8).

8.5 Conclusions

The results of this study can be summarised by revisiting the research objectives identified in Chapter 1.

1. To establish an accurate way to measure changes occurring on hard rock coastal cliffs.

A new high-resolution dataset has been established, encompassing the complete range of scales over which hard rock coastal cliffs change. Of primary importance in fulfilling this objective is the ability to validate the three-dimensional change recorded. This has been achieved through the combination of the accuracy of terrestrial laser scanning and the precision and qualitative detail of digital photogrammetry.

2. To assess the validity of current predictions of coastal cliff retreat rates.

The study has cast doubt on the validity of using retreat rates for understanding coastal cliff changes. The new data were compared with the current rates of retreat established for the coastline. The existing rates of retreat are poor approximations of contemporary patterns of change, although the long-term averages of the recorded changes appeared to converge towards the rates generated from aerial perspectives. Whilst this convergence suggests some degree of agreement between the datasets, it is evident that restrictions on the spatial and temporal resolution of aerial mapping techniques have limited the sensitivity of records of slope changes; preventing more detailed analysis of the processes of change.

3. To examine in detail the magnitude and frequency of rockfall activity.

The spatial and temporal scales of data derived from aerial surveys proved inadequate to resolve much of the detail of the way in which coastal cliffs retreat. This leaves much uncertainty over the significance of certain failures to overall slope development. The terrestrial dataset of the changes across cliff faces has allowed the relative contribution of different sized losses to be quantified. The occurrence of large scale losses has the greatest effect on landform change. The reduced impact of smaller losses is not linear, rather the smallest losses accounted for more of the total volumetric changes than failures of more intermediate sized material. More importantly, the data stress the linkages between different sized changes, suggesting for example that the largest failures could only be better understood by the consideration of smaller scale losses.

4. To investigate the effects of spatial scale on cliff change.

Scale is a fundamental consideration in the study of earth surface systems. The geomorphological processes governing monitored rock cliffs exhibit both elements of scale dependency and relationships independent of scale. With regards to the practicability of cliff studies the appropriate scale of analysis is that of the whole landform, raising serious questions over the use of 'representative' subsections and profiles of the cliff face used by many existing analyses.

5. To examine the temporal aspects of rock cliff change.

Understanding of the temporal nature of coastal cliff evolution has been mainly based on inadequate datasets or qualitative interpretations. Few quantitative analyses exist of rock cliff changes through time. This study has analysed in detail the short-term processes of cliff change discovering elements of both episodic and continual behaviour. Episodicity has become an accepted term in the temporal evolution of coastal cliffs but its usefulness was also questioned in the longer term assessments of change provided by numerical modelling. The results of this study indicate that it is more beneficial to consider landform change as continuous and interlinked, complicated by variable rates of activity.

6. To assess spatial and temporal aspects of rock cliff behaviour with regard to environmental processes.

The process of cliff recession is complicated by the coastal environment. The findings of the study suggest that a complete understanding of rock cliff evolution requires that the whole suite of factors influencing the rock material be considered. Many past studies have tended to concentrate on the effect of marine erosion as the sole cause of

large scale change. The results of the monitoring analysis indicate that for certain cliff sections, with more competent or protected cliff toes, the more subtle influence of subaerial processes may dominate slope form. Furthermore, the data indicate that a better understanding of the relationship between slopes and their environment may be achieved with a change in emphasis away from general base-levels in individual processes to more extreme occurrences in compound measurements such as climatic indices or cumulative lags.

7. To investigate the material interactions driving rock cliff response.

Recent developments in numerical modelling were used to develop the measured results in order to explore the mechanisms driving rock cliff response. The models suggest that rock cliff development cannot be understood without the capacity to account for both discrete block interactions and internal material yielding and fracture. The dominant mechanism in the monitored cliff faces was determined to be overhang collapse on a variety of scales, confirming the need to consider the whole continuum of change in order to understand landform behaviour. Further work into the more subtle mechanisms behind cliff behaviour, particularly in landforms with complex lithologies, is still required.

8. To develop a model to better understand cliff development through time.

The findings of the study were combined into a new model of cliff development in complex material, with each cliff phase reflective of a particular set of conditions. The importance of localised analysis has been demonstrated in the development of certain cliff forms, which contrasted with several previous models of coastal cliff evolution. Despite the site-specific elements of the model stages, much of the behaviour noted within the monitored cliff systems is found to be similar to processes noted elsewhere. This suggests that while analysis must be tailored to each individual cliff section, common theories on certain aspects of development may ultimately be established.

This study has considered the nature of hard rock coastal cliff evolution. From the development, implementation and analysis of a new high-resolution monitoring approach and the validation and application of a hybrid element numerical modelling code several conclusions can be drawn. Current approaches used to assess coastal cliff recession are inadequate. Existing methodologies produce inaccurate and often misleading results which have hindered the investigation of cliff behaviour. Key concepts of the way in which cliffs change, which have become synonymous with rock slope studies have been questioned by the new dataset. Several important aspects of the contemporary understanding of how cliffs and rock slopes in general are perceived

to evolve have been re-evaluated. New, more detailed and explanatory forms of analysis have been promoted as effective answers to the challenges of interpreting change in complex coastal cliff systems.

8.6 Original contribution to knowledge

This study has attempted to contribute to the knowledge of rock slope systems by challenging existing assumptions on hard rock coastal cliff evolution. An extensive high-resolution dataset has been collected on rock cliff behaviour through the investigation and integration of new developments in digital photogrammetry and terrestrial laser scanning. The combination of the consistent accuracies provided by time-of-flight point clouds with the precision and visual qualities of orthorectified images provide an effective answer to the problem of deriving high quality information from sheer-sided, high cliffs with inter-tidally exposed bases. Several technological and software based innovations have been required to achieve such a dataset from planning through data collection to processing and analysis. Ultimately a new tool for geomorphological research has been developed (Lim *et al.*, 2005).

The geomorphology of hard rock coastal cliffs is highly complex, with behaviour patterns that often cannot be adequately explained by established notions of slope evolution. Many studies to date have approximated cliff retreat from alterations in the cliffline over time. The variety of changes recorded at monitored sites were seldom reflected by responses at the cliff toe or cliff top, and thus even improvements in spatial resolution brought by aerial photogrammetric and LiDAR surveys will provide little benefit to understanding of geomorphological change in this environment. It is suggested that the limited temporal resolution at which aerial surveys can be conducted has hindered understanding of the more frequent iterations undergone by rock slopes and forced concepts of evolution to rely on generalised annual rates of retreat. Furthermore, cliff retreat has typically become synonymous with cliff erosion. From the results in this study however it is evident that there are important differences between the two. The simple planimetric landward retreat of the cliffline, currently relied upon by many coastal planning and management organisations to measure change, generated very poor interpretations of landform behaviour. In order to improve understanding into monitored slope behaviour records must account for three-dimensional changes occurring over time. Comparisons between one, two and three-dimensional data on cliff changes reveal the importance of viewing landform development as a volumetric process. The study findings show that the majority of techniques currently used to understand rock slopes are inadequate, not just in terms of spatial and temporal resolution, but also in the type of data they seek to collect.

The findings hold implications for many of the analytical approaches which have been developed on cliffline measurements. Probabilistic analyses have attempted to account for the large uncertainty within such datasets by calculating the statistical likelihood of recurrence intervals. The results of high-resolution cliff face monitoring suggest that neither rates of retreat, nor the occurrence of losses of particular sizes can be considered consistent over time. Instead failures appear to be linked through more complex relationships and the loss of any size of material may contribute to further changes of similar or different scales. Landform responses have been seen to diverge over time rather than to recur in a predictable manner. This divergence is evident in the performance of probabilistic predictions against actual monitored results with increasing disparities linked to the magnitude of the failure and time of consideration. Current attempts to account for uncertainties caused by gaps in knowledge over the way in which cliffs evolve may provide inaccurate estimates of future cliff developments. Improvements to knowledge can only be gained from investigating carefully defined aspects of the complexities involved rather than assuming any uniformity of response.

One of the key concepts underpinning current knowledge of rock slope evolution has been the relationship between the frequency of occurrence and different magnitude events. It is commonly thought that hard rock cliffs evolve through large but infrequent changes, with smaller losses rarely significant in the shaping of the overall landform. This has been due to both an inability to quantify smaller changes from cliff sections and a tendency to focus on the more obvious and easily identified large scale events. The monitoring results reveal a continuum of change from small pebble-sized losses to failures which incorporated the entire cliff section. Similar relationships were seen at all sites, in all material types and for every month of monitoring. Although magnitude-cumulative frequency distributions appear to be generic across different cliff sections, the relative contributions of the different magnitude events to landform development are less simple. Overall, the total volume of smallest losses is found to be greater than that of the more intermediate scale failures which occurred less often. Large events cannot be understood without a consideration of the preconditions leading to their initiation, which often involve more constant small scale changes generating overhangs. Past investigations that have focused on interpretation of larger failures at the expense of the more common and continual slope alterations have therefore limited knowledge, not just into small scale processes but also of larger slope alterations.

A wide variety of types and patterns of rock cliff behaviour have been identified. Scale exerts a strong influence on many elements of coastal cliff knowledge, from the scale of the slope and its associated processes to the scales of investigation, analysis and interpretation. A key question over many aspects of cliff behaviour has been whether they are scale dependent. Many studies have attempted to analyse cliff behaviour using sample areas or points considered representative of the wider landform. The results of different scale analysis in this study reveal the inadequacy of point, line, profile and subset area extrapolations in accounting for temporally diverse changes in form. Indeed any dataset which does not consider the rock slope as a whole is likely to generate an incomplete or misleading perception of the changes that govern the landform. The processes of slope change interact between scale dependent and independent operations. Whilst localised processes are clearly sensitive to the scale at which they were analysed for example, the overall magnitude-frequency relationship is scale independent above 100 m^2. The continuum of changes is increasingly stepped below the 100 m^2 threshold where the complete range of failure magnitudes cannot be sufficiently recorded. The recognition that certain processes may dominate localised areas of change and yet remain apparently insignificant to the behaviour of the landform as a whole reiterates the importance of achieving appropriate monitoring extents and resolutions to record change. Improvements to understanding of coastal cliff evolution must therefore account for the multiple and interacting scales at which the processes, mechanisms and materials operate within a rock slope system.

This study has reconsidered the temporal nature of cliff change. Many analyses of rock slopes describe the episodic evolution of the landform over time, with long periods of inactivity punctuated by phases of rapid and dramatic change. The occurrence of large scale failures over time is, by their very nature, infrequent and therefore irregular. The time taken for the appropriate preconditions to failure and the necessary *in situ* characteristics mean that large losses will inevitably be less predictable than smaller changes. The results of this study question the usefulness of the concept of episodicity, which has long been associated with the temporal development of rock slopes. Apparently random large scale 'events' can be set within a wider continuum of rock slope alterations which is better suited to explain the phases of landform change. The switch away from viewing failure as 'an event' towards more continual notions of failure as an ongoing process is promoted by conceptualising the slope as a deformable mesh with failures representing critical stain periods. Placing the emphasis of analysis on strain deformations rather than stress accumulations enables each loss of material to be related to subsequent changes as the mesh adjusts

over time. Therefore analyses which assume activity is least likely where recent failures have occurred are inappropriate and when viewed as part of a continual process, failures can reveal significantly more about the response of the wider landform than just a single isolated material loss.

The continuous, strain dependent nature of failure in rock cliffs is supported in positive correlations of material losses with protrusion from the average cliff face and accelerated rockfall activity prior to large failures. It is common for rock slope analyses to assess failure in terms of stability, whether a slope will or will not fail. Some attempts have been made to account for the complex nature of failure by subdividing slopes into stable, unstable and those undergoing progressive instability. If failure is indeed a continuous and responsive process, all rock slopes are progressively unstable and apparent stability simply reflects a period of minimal deformation. Furthermore, standard Factor of Safety measurements are of limited use unless able to respond dynamically to a constantly changing set of failure criteria. Evidence of both episodic and continual behaviour were detected and determined to be essential in explaining rock slope evolution. The static conditions for large scale failures can only be understood in the context of more continual changes. The study promotes a re-evaluation of the way in which failure in rock slopes is viewed and a movement of emphasis away from static to more dynamic and progressive forms of analyses for rock slope behaviour.

One of the most complicating factors in understanding the behaviour of coastal cliffs is the environment within which they are situated. Studies to date have failed to satisfactorily relate specific rock slope changes to all but the most extreme environmental processes. Although recent attempts have been made to attribute soft cliff responses to El Nino phenomena (Sallenger *et al.*, 2003), understanding into the interaction between coastal processes and hard rock cliff response has remained largely theoretical. The study demonstrates that commonly used distinctions between marine and subaerial processes are overly simplistic and that the marine influence may extend significantly beyond the area directly impacted by waves. The interrelationships between various factors means it is preferable to consider suites of processes rather than to identify the effect of individual conditions. The contributions of subaerial processes to slope change match the effects of marine activity in some instances, demonstrating that influencing factors should not be assumed but carefully measured. The susceptibility of the cliff may for example mean that despite being located within higher energy marine conditions, the basal layers of a cliff section prove more competent than weaker material subjected only to subaerial weathering.

The data generated on coastal cliff behaviour provide a previously unreported level of detail on slope changes. The nature of change highlights the complex behaviour of sheer-sided, hard rock coastal cliffs. Similarities between the patterns of change across different sites, specific sensitivities to material properties, slope type and environmental controls and consistencies between failure magnitudes and amount of protrusion all contribute to knowledge of coastal cliff evolution. The thresholds to failure in coastal rock masses have been further investigated with the use of advanced numerical models, allowing conclusions to be drawn on future cliff developments. A significant contribution of this study has been to demonstrate that the technology now exists to collect new detailed records of inaccessible landforms, which, when carefully constrained within error margins, may be used to re-evaluate many critical aspects of geomorphological understanding.

8.7 Recommendations for further research

It is possible to make recommendations for further research into the nature of hard rock coastal cliff evolution. One of the limitations to this study has been the temporal length of the record. New, carefully planned and consistently maintained high-resolution data should be collected for further advances to be made in understanding coastal cliff behaviour. The original intention of the study was to begin monitoring every month and then to establish a suitable, less intensive monitoring framework once the level of changes were established for each site. It was subsequently discovered that the most appropriate sampling interval was at least monthly with every collection at every site detecting some form of slope change. One appropriate direction for further research will therefore involve the investigation of slope changes at higher temporal resolution, perhaps looking at alterations between individual tidal cycles.

In addition to establishing the most appropriate frequency of data collection, spatial issues in monitoring coastal cliff faces should be further considered. Modern remote sensing technologies are continuing to develop and the scope now exists for new systems to monitor larger cliff sections with the techniques used in this study, generating a wider perspective of the evolution of the coast. The development of the monitoring technique required resolution to be maximised at all times, although this limited the coverage achieved and generated large datasets. The trade-off between data quantity and quality could be assessed to establish the most effective resolution at which to monitor cliffs.

The potential now exists to generate and compare detailed records of coastal cliff behaviour. Comparisons could be made between the Liassic rock coasts of North Yorkshire and west Dorset for example. In addition to improving understanding into the way in which different cliffs behave through time, the establishment of such datasets would support the movement away from simple concepts of cliff retreat rates to more informed considerations of cliff behaviour.

An improved understanding of coastal cliff behaviour requires further investigation into the environmental processes acting on the rock material. For example, it has been suggested that the ability to record the seismic shaking of the rock mass induced by wave impact might be used to relate marine processes to rockfall activity (Adams *et al.*, 2002; Busby *et al.*, 2002). By combining quantitative datasets such as accurate rockfall volumes and direct wave impacts, measured through rock material vibrations, the role of marine influences on slope development may be more clearly defined.

The computer modelling used in this study has inevitably simplified the contributing factors to cliff development. The tentative links between the monitored changes and the modelled cliff mechanisms require further investigation and the building in of complexity to increase their relevance to actual cliff development. The Elfen code can, for example, directly import laser scanned profiles which could then be used to look at the precise effects of form on slope behaviour. Advances to the study would be the progression from two- to three-dimensional modelling codes and the ability to temporally constrain model stages, possibly with the development of more long-term high-resolution monitoring datasets.

This study provides a contribution to the ongoing research into the nature of coastal cliff behaviour. It is a first attempt to address the shortage of high-resolution, accurate data on the changes occurring over sheer-sided hard rock coastal cliffs. Through the synoptic advances in remote sensing and combined element modelling, key aspects regarding the evolution of hard rock cliffs have been reconsidered. Continued investigation of coastal cliff behaviour with the use of increasingly advanced methods of data capture and analysis will continue to reveal details which will cause geomorphologists to further question the way in which such landforms are currently perceived to evolve. The conclusions from the study may ultimately influence the direction of future research into coastal cliff geomorphology and hold resonance within wider considerations of earth surface systems.

PHOTOGRAMMETRIC TECHNICAL DETAILS

The calibration procedure was undertaken by Alex Koh at Bath Spa University (01/07/2003). It involved the collection of two sets of images of a testfield containing 111 targets from convergent stations. The image sets were converged at a range of angles from 0° to 60°, ensuring that a minimum of 66% of the control targets were covered by each image. The camera was rolled though 90° clockwise and anticlockwise and focused at infinity throughout. The targets were surveyed to millimetre accuracy in three dimensions and used analyse the interior orientation parameters of focal length, principal point offset, radial lens distortion (k_1, k_2, k_3) and tangential distortion. The technical details used in the photogrammetric setup have been summarised in the following table.

Camera calibration statistics		
Camera	Kodak Pro 14n	
Lens	Nikkor468225	
Focal length (mm)	28.719	
Imaging array (pixels)	4536 x 3024	
Pixel size (mm)	0.008467	
Principal point offsets (mm)	X_p	0.0362
	Y_p	1.2924
Radial distortion (mm)	K_0	1.85E-04
	K_1	4.90E-07
	K_2	-4.12E-09
Field setup		
Maximum distance to cliff		70 m
Maximum station separation		54.4 m
Maximum angle of inclination		15°
Typical convergence angle		20°
Number of control points		50

SUMMARY OF MODELLING PARAMETERS

Example model parameters		
Global discrete properties	Damping	0.1
	Field	0.2
	Normal penalty (N m^2)	1.00E+10
	Tangental penalty (N m^2)	1.00E+09
	Zone	2
	Smallest element	1
	Friction	0.2
	Cohesion	0
	Contact damping type	Velocity/Momentum
	Contact type	Node-Edge
Time steps	Initial time step	1
	Maximum time step	1
	Factor of critical time step	0.9
Termination data	Maximum number of time step	100000000
	Termination time	10
	Minimum time step	0

ABRAHAMS, A. D. and PARSONS, A. J., 1987. Identification of strength equilibrium rock slopes: further statistical considerations. *Earth Surface Processes and Landforms*, 12, 631-635.

ADAMS, J. C. and CHANDLER, J. H., 2002. Evaluation of LIDAR and medium scale photogrammetry for detecting soft-cliff coastal change. *Photogrammetric Record*, 17(99), 405-418.

ADAMS, P. N., ANDERSON, R. S. and REVENAUGH, J., 2002. Microseismic measurement of wave-energy delivery to a rocky coast. *Geological Society of America*, 30(10), 895-898.

ADEY, R. A. and PUSCH, R., 1999. Scale dependency in rock strength. *Engineering Geology*, 53(3), 251-258.

ADHIKARY, D. P., DYSKIN, A. V. and JEWELL, R. J., 1996. Numerical modelling of the flexural deformation of foliated rock slopes. *International Journal of Rock Mechanics and Mining Sciences & Geomechanical Abstracts*, 33, 595-606.

AGAR, R., 1960. Post-glacial erosion of the North Yorkshire coast from the Tees Estuary to Ravenscar. *Proceedings from the Yorkshire Geological Polytechnic Society*, 32, 409-428.

AGLIARDI, F. and CROSTA, G. B., 2003. High resolution three-dimensional numerical modelling of rockfalls. *International Journal of Rock Mechanics & Mining Sciences*, 40, 455-471.

AHMON, J., 2004. The application of short-range 3D laser scanning for archaeological replica production: the Egyptian tomb of Seti I. *Photogrammetric Record*, 19(106), 111-127.

AHNERT, F., 1988. Modelling landform change. In: Anderson, M. G. (Ed.), Modelling geomorphological systems. John Wiley & Sons, Chichester, 375-400 pp.

ALLAN, J. C. and KOMAR, P. D., 2002. Extreme storms on the Pacific Northwest Coast during the 1997-98 El Nino and 1998-99 La Nina. *Journal of Coastal Research*, 18, 175-193.

ALLISON, R. J., 1993. Slopes and slope processes. *Progress in Physical Geography*, 17(1), 92-101.

ALLISON, R. J., 1994. Slopes and slope processes. *Progress in Physical Geography*, 18(3), 425-435.

ALLISON, R. J., 1996. Slopes and slope processes. *Progress in Physical Geography*, 20(4), 453-465.

ALLISON, R. J. and KIMBER, O. G., 1998. Modelling failure mechanisms to explain rock slope change along the Isle of Purbeck coast, UK. *Earth Surface Processes and Landforms*, 23, 731-750.

ALLISON, R. J., 1989. Rates and mechanisms of change in hard rock coastal cliffs. *Zeitschrift für Geomorphologie, Supplementband*, 73, 125-138.

ALLISON, R. J. and BRUNSDEN, D. In press. Mass Movement. In: *The history of the study of landforms*.

ANDERS, F. J. and BYRNES, M. R., 1991. Accuracy of shoreline change rates as determined from maps and aerial photographs. *Shore and Beach*, 59(1), 17-26.

ANDRLE, R., 1996. Complexity and scale in geomorphology: statistical self-similarity vs. characteristic scales. *Mathematical Geology*, 28(3), 275-293.

ATTEWELL, P. B. and FARMER, I. W., 1976. *Principles of engineering geology*. John Wiley & Sons, New York, USA, 1045 pp.

AYDAN, Ö., SHIMIZU, Y. and ICHIKAWA, Y., 1989. The effective failure modes and stability of slopes in rock mass with two discontinuity sets. *Rock Mechanics and Rock Engineering*, 22, 163-188.

BACON, S. and CARTER, D. J. T., 1991. Wave climate changes in the north Atlantic and North Sea. *International Journal of Climatology*, 11, 545-558.

BAILEY, B., COLLIER, P., FARRES, P., INKPEN, R. and PEARSON, A., 2003. Comparative assessment of analytical and digital photogrammetric methods in the construction of DEMs of geomorphological forms. *Earth Surface Processes and Landforms*, 28, 307-320.

BALTSAVIAS, E. P., FAVEY, E., BAUDER, A., BOSCH, H. and PATERAKI, M., 2001. Digital surface modelling by airborne laser scanning and digital photogrammetry for glacier monitoring. *Photogrammetric Record*, 17(98), 243-274.

BARKER, R., DIXON, L. and HOOKE, J., 1997. Use of terrestrial photogrammetry for monitoring and measuring bank erosion. *Earth Surface Processes and Landforms*, 22, 1217-1227.

BARTON, N. R., 1974. Engineering classification of rock masses for design of tunnel supports. *Rock Mechanics*, 6, 189-236.

BARTON, N. R., 2002. Some new Q-value correlations to assist in site characterisation and tunnel design. *International Journal of Rock Mechanics and Mining Sciences*, 39, 185-216.

BARTON, N. R., LIEN, R. and LUNDE, J., 1974. Engineering classification of rock masses for the design of tunnel support. *Rock Mechanics*, 6, 189-236.

BATTJES, J. A. and GROENENDIJK, H. A., 2000. Wave height distributions on shallow foreshores. *Coastal Engineering*, 40, 161-182.

BENSON, M. A., 1960. Characteristics of frequency curves based on a theoretical 1,000-year record. In: Dalrymple, T. (Ed.), *Flood frequency analyses: U.S. Geological Survey Water-Supply Paper 1543-A*, 1-80 pp.

BENUMOF, B. T. and GRIGGS, G. B., 1999. The dependence of seacliff erosion rates on cliff material properties and physical processes; San Diego County, California. *Shore and Beach*, 67(4), 29-41.

BEST, T. C. and GRIGGS, G. B., 1991. A sediment budget for the Santa Cruz littoral cell, California. In: Osborne, R. H. (Ed.), *From shoreline to abyss; contributions in marine geology in honour of Francis Parker Shepard*. Society of Economic Paleontologists and Mineralogists Special Publication no. 46, 35-50.

BIENIAWSKI, Z. T., 1973. Engineering classification of jointed rock masses. *The Civil Engineer in South Africa*, 15, 335-334.

BIENIAWSKI, Z. T., 1978. Determining rock mass deformability: experience from case histories. *International Journal of Rock Mechanics and Mining Sciences*, 15(5), 237-247.

BIENIAWSKI, Z. T., 1984. *Rock mechanics design in mining and tunnelling*. A. A. Balkema, 272.

BIRD, E. C. F., 1969. *Coasts*. MIT Press, Cambridge, Massachusetts, 246 pp.

BIRD, E. C. F., 2000. *Coastal Geomorphology: An introduction*. John Wiley & Sons, West Sussex, England, 322 pp.

BJERRUM, L., 1967. Engineering geology of Norwegian normally consolidated marine clays as a related to settlements of buildings. *Geotechnique*, 17(2), 81-118.

BLÖSCHL, G. and SIVAPALAN, M., 1995. Scale issues in hydrological modelling – A review. *Hydrological Processes*, 9(3-4), 251-290.

BOGGETT, A. D., MAPPLEBECK, N. J. and CULLEN, R. J., 2000. South Shore Cliffs, Whitehaven – geomorphological survey and emergency cliff stabilization works. *Quarterly Journal of Engineering Geology and Hydrogeology*, 33, 213-226.

BOVIS, M. J. and EVANS, S. G., 1995. Rock slope movements along Mount Currie 'fault scarp', southern Coast Mountains, British Columbia. *Canadian Journal of Earth Sciences*, 32, 2015-2020.

BOVIS, M. J. and EVANS, S. G., 1996. Extensive deformations of rock slopes in southern Coast Mountains, south-west British Columbia, Canada. *Engineering Geology*, 44, 163-182.

BRADINONI, F. and CHURCH, M., 2004. Representing the landslide magnitude-frequency relation: Capilano River Basin, British Columbia. *Earth Surface Processes and Landforms*, 29, 115-124.

BRADINONI, F., SLAYMAKER, O. and HASSAN M. A., 2003. Landslides inventory in a rugged forested watershed: a comparison between air-photo and field survey data. *Geomorphology*, 54, 179-196.

BRADY, B. H. G., HSIUNG, S. H. and PHILIP, J., 1990. Verification studies on the UDEC computational model of jointed rock. In: Rossmanith, H. P. (Ed.), *Mechanics of jointed and faulted rock*. A. A. Balkema, Rotterdam, 551-558 pp.

BRAISINGTON, J., LANGHAM, J. and RUMSBY, B., 2003. Methodological sensitivity of morphometric estimates of coarse fluvial sediment transport. *Geomorphology*, 53, 299-316.

BRAY, M. J. and HOOKE, J. M., 1997. Prediction of soft-cliff retreat with accelerating sea-level rise. *Journal of Coastal Research*, 13(2), 453-467.

BROMHEAD, E.N., IBSEN, M.-L., PAPANASTASSIOU, X. and ZEMICHAEL, A.A., 2002. Three-dimensional stability analysis of a coastal landslide at Hanover Point, Isle of Wight. *Quarterly Journal of Engineering Geology and Hydrology*, 35, 79-88.

BROWN, E. T., 1987. Introduction. In: Brown, E. T. (ed.), *Analytical and Computational Methods in Engineering Rock Mechanics*. Allen and Unwin, London, 1-31 pp.

BRUNSDEN, D., 1984. Mudslides. In: Brunsden, D. and Prior, D., B. (Eds.) *Slope Instability*. John Wiley & Sons, Chichester, 363-410 pp.

BRUNSDEN, D., 1993. The persistence of landforms. *Zeitschrift für Geomorphologie, NE Supplementband*, 13-20.

BRUNSDEN, D., 1996. Geomorphological events and landform change: The centenary lecture to the Department of Geography, University of Heidelberg. *Zeitschrift für Geomorphologie, NF Supplementband*, 40(3), 273-288.

BRUNSDEN, D., 1999. Some geomorphological considerations for the future development of landslide models. *Geomorphology*, 30, 13-24.

BRUNSDEN, D. and CHANDLER, J. H., 1996. Development of an episodic landform change model based upon the Black Ven Mudslide, 1946-1995. In: Anderson, M. G. and Brooks, S. M. (Eds.), *Advances in Hillslope Processes*. John Wiley & Sons, Chichester, 869-896 pp.

BRUNSDEN, D. and JONES, D. K. C., 1980. Relative time scales and formative events in coastal landslide systems. *Zeitschrift für Geomorphologie, NF Supplementband*, 34, 1-19.

BRUNSDEN, D. and LEE, E. M. (Eds.), 2004. Behaviour of coastal landslide systems: an inter-disciplinary view. *Zeitschrift für Geomorphologie Supplementband*, 134, 112 pp.

BRUNSDEN, D. and THORNES, J. B., 1979. Landscape sensitivity and change. *Transactions of the Institute of British Geographers*, 4, 463-484.

BRUUN, P., 1988. The Bruun Rule of erosion by sea level rise. *Journal of Coastal Research*, 4, 627-648.

BRYAN, W. B. and STEPHENS, R. S., 1993. Coastal bench formation at Hunauma Bay, Oahu, Hawaii. *Geological Society of America Bulletin*, 105, 377-386.

BUCKLEY, S. and MILLS., J. 2000. GPS and the wheel - how integrating the world's greatest inventions is helping to monitor coastal erosion. *Surveying World*, 9(1), 1-41.

BUSBY, J., CHRISTOPHE GOURRY, J., SENFAUTE, G., PEDERSEN, S. and MORTIMORE, R., 2002. Can we predict coastal cliff failure with remote, indirect measurements? In: McInnes, R. G. and Jakeways, J. (Eds.), *Instability: Planning and Management*. Proceedings of the international conference. Thomas Telford, Ventnor, Isle of Wight, UK, 203-208 pp.

BUTLER, J. B., LANE, S. N. and CHANDLER, J. H., 1998. Assessment of DEM quality for characterising surface roughness using close range digital photogrammetry. *Photogrammertic Record*, 16(92), 271-291.

BYRNE, J. V., 1963. Coastal erosion, northern Oregon. In: *Essays in marine geology in honour of K. O. Emery*. University of Southern California Press, Los Angeles, 11-33 pp.

BYRNES, M. R. and HILAND, M. W., 1994. Shoreline position and nearshore bathymetric change. In: Kraus, N. C., Gorman, L. T. and Pope, J. (Eds.), *Kings Bay Coastal and Estuarine Physical Monitoring and Evaluation Program: Coastal Studies.* Army Corps of Engineers Technical Report CERC-94-9.

CAMBERS, G., 1976. Temporal scales in coastal erosion systems. *Transactions of the Institute of British Geographers*, 1, 246-256.

CAMERON-CLARKE, I. S. and BUDVARI, S., 1981. Correlation of rock mass classification parameters obtained from borecore and in situ observations. *Engineering Geology*, 17, 19-53.

CARSON, M. A. and KIRKBY, M. J., 1972. *Hillslope Form and Process*. Cambridge University Press, Cambridge, 475 pp.

CARTER, R. W. G., 1988. *Coastal Environments: An Introduction to the Physical, Ecological and Cultural Systems of Coastlines*. Academic Press, London, 614 pp.

CHANDLER, J. H. and BRUNSDEN, D., 1995. Steady state behaviour of the Black Ven mudslide: the application of archival analytical photogrammetry to studies of landform change. *Earth Surface Processes and Landforms*, 20, 255-275.

CHANDLER, J. H. and BRUNSDEN, D., 1996. Development of an episodic landform change model based upon the Black Ven mudslide, 1946- 1995. In: Brooks, S. and Anderson, M., (Eds.) *Advances in Hillslope Processes*. John Wiley & Sons, London, 869-898 pp.

CHANDLER, J. H. and MOORE, R., 1989. Analytical photogrammetry: a method for monitoring slope instability. *Quarterly Journal of Engineering Geology*, 22(2), 97-110.

CHANDLER, J. H. and PADFIELD, C. J., 1996. Automated digital photogrammetry on a shoestring. *Photogrammetric Record*, 15(88), 545-560.

CHANDLER, J. H., 1999. Effective application of automated digital photogrammetry for geomorphological research. *Earth Surface Processes and Landforms*, 24, 51-63.

CHANDLER, J. H., BUFFIN-BÉLANGER, T., RICE, S., REID, I. and GRAHAM, D., 2003. The accuracy of a river bed moulding/casting system and the effectiveness of a low-cost digital camera for recording river bed fabric. *Photogrammetric Record*, 18(103), 209-223.

CHEESEMAN, J. E. and CUTLER, M. E. J., 1999. *Evaluation of a DEM error descriptor method*. GIS Research UK 7th Annual Conference (GISRUK '99), Southampton, UK.

CHEFFINS, O. W. and RUSHTON, J. E. M., 1970. Edinburgh castle rock: a survey of the north face by terrestrial photogrammetry. *Photogrammetric Record*, 63(35), 417-433.

CHOWDHURRY, R. N., 1978. *Slope analysis*. Elsevier, Amsterdam.

CIRIA, 1999. *Glacial till*. CIRIA Report C504, 252 pp.

CLARK, A.R. and GUEST, S., 1991. The Whitby cliff stabilisation and coast protection scheme. In: Chandler, R. J. (Ed.), *Slope stability engineering*. Thomas Telford, 283-290 pp.

CLOWES, M., 1999. Digital photogrammetry at English Heritage: a pictorial review of projects to date. *Photogrammetric Record*, 17(99), 441-452.

COGGAN, J. S., STEAD, D. and EYRE, J., 1998. Evaluation of techniques for quarry slope stability assessment. *Transactions of the Institute of Mining & Metallurgy Section A*, 107, 139-147.

COJEAN, R., 1995. Influence of geological structures in slope stability analysis for open cast mining and quarry excavations. In: Eddleston, M. (Ed.), *Engineering Geology of Construction*. Geological Society, London, 321-334 pp.

COOPER, M. A. R., 1998. Datums, coordinates and differences. In: Lane, S. N., Richards, K. S. and Chandler, J. H. (Eds.), *Landform Monitoring, Modelling and Analysis*. John Wiley & Sons, Chichester, 21- 36 pp.

CORDING, E. J. and DEERE, D. U., 1972. Rock tunnel support and field measurements. *Proceedings of the Rapid Excavation Tunnelling Conference, AIME, New York*. 601-622 pp.

COTTON, C. A., 1951. Atlantic gulfs, estuaries and cliffs. *Geological Magazine*, 88, 113-128.

COTTON, C. A., 1969. Marine cliffing according to Darwin's theory. *Royal Society of New Zealand Transactions, Geology*, 6, 187-208.

COULTHARD, M. A., JOURNET, N. C. and SWINDELLS, C. F., 1992. Integration of stress analysis into mine excavation design. In: Tillerson, J. R. and Wawersik, W. R. (eds.), *Rock mechanics, Proceedings of the 33rd U.S. Symposium, Santa Fe NM 3-5 June 1992*. A. A. Balkema, Rotterdam, 451-461 pp.

CROOK, I., WILSON, S., YU, J. G. and OWEN, R., 2003. Computational modelling of the localised deformations associated with borehole breakout in quasi-brittle materials. *Journal of Petroleum Science & Engineering*, 31(3-4), 177-186.

CROSTA, G. B. and AGLIARDI, F., 2003. Failure forecast for large rock slides by surface displacement measurements. *Canadian Geotechnical Journal*, 40, 176-191.

CROWELL, M. and LEATHERMAN, S. P., 1999. Coastal Erosion Mapping and Management. *Journal of Coastal Research Special Issue No.* 28, 121-139.

CROWELL, M., LEATHERMAN, S. P. and BUCKLEY, M. K., 1991. Historical shoreline change: Error analysis and mapping accuracy. *Journal of Coastal Research*, 7(3), 723-744.

CRUDEN, D. M. and EATON, T. M., 1987. Reconnaissance of rockslide hazards in Kananaskis County, Alberta. *Canadian Geotechnical Journal*, 24, 414-429.

CRUDEN, D. M. and HU, X., -Q., 1994. Topples on underdip slopes in the Highwood Pass, Alberta, Canada. *Quarterly Journal of Engineering Geology*, 27, 57-68.

CRUDEN, D. M. and HU, X., -Q., 1996. Hazardous modes of rock slope movement in the Canadian Rockies. *Environmental and Engineering GeoSciences*, 2(4), 507-516.

CUNDALL, P. A., 1971. *A Computer Model for Simulating Progressive Large-Scale Movements in Blocky Rock Systems*. Symposium on Rock Fracture, Nancy, France, October 1971, Section 2-8.

CUNDALL, P. A. and HART R. D., 1992. Numerical modelling of Discontinua. In: Owen, D. R. and Hinton, E. (Eds.), *Engineering Computations*. Pineridge Press, 101-113 pp.

CUNDALL, P. A. and STRACK, O. D. L., 1979. A discrete numerical method for granular assemblies. *Géotechnique*, 29, 47-65.

DABROWSKA-ZIELINSKA, K., KOGAN, F., CIOLKOSZ, A., GRUSZCZYNSKA, M. and KOWALIK, W., 2002. Modelling of crop growth conditions and crop yield in Poland using AVHRR-based indices. *International Journal of Remote Sensing*, 23(6), 1109-1123.

D'ALESSANDRO, L., GENEVOIS, R., BERTI, M., URBANI, A. and TECCA, P. R., 2002. Geomorphology, stability analyses and stabilisation works on the Montepiano Travertinous Cliff (central Italy). In: Allison, R. J. (Ed.), *Applied geomorphology*. John Wiley & Sons, Chichester, West Sussex, 21-38 pp.

DALRYMPLE, R. A., BRIGGS, R. B., DEAN, R. G. and WANG, H., 1986. Bluff recession rates in Chesapeake Bay. *Journal of Waterway, Port, Coastal and Ocean Engineering*, ASCE, 112(1), 164-168.

DAVIDSON, C. and ARNOTT, R. G. D., 1986. Rates of erosion of tills in the nearshore zone. *Earth Surface Processes and Landforms*, 11, 53-58.

DAVIDSON, C., ARNOTT, R. G. D. and Law, M. N., 1996. Measurement and prediction of long-term sediment supply to coastal foredunes. *Journal of Coastal Research*, 12, 654-663.

DAVIES, J. L., 1972. *Geographical variation in coastal development*. Oliver and Boyd, New York, 204 pp.

DAVIES, P., WILLIAMS, A. T. and BOMBOE, P., 1998. Numerical analysis of coastal cliff failure along the Pembrokeshire Coast National Park, Wales, UK. *Earth Surface Processes and Landforms*, 23, 1123-1134.

DAVIS, W. M., 1912. A geographical pilgrimage from Ireland to Italy. *Association of American Geographers Annals*, 2, 73-100.

DAVIS, W. M., 1922. Faults, under-drag and landslides of the Great Basin Ranges. *Bulletin of the Geological Society of America*, 33, 92-96.

DEBOER, D. H., 1992. Constraints on spatial scale transference of rainfall-runoff relationships in semiarid drainage basins drained by ephemeral streams. *Hydrological Sciences Journal*, 37, 491-504.

DE FREITAS, M. H. and WATTERS, R. J., 1973. Some field examples of toppling failure. *Geotechnique* 23(4), 495-514.

DE FREITAS, M. H., 1972. Some examples of cliff failure in South West England. *Proceedings of the Ussher Society*, 2(5), 388-397.

DEERE, D. U., 1989. *Rock Quality Designation (RQD) after Twenty Years, U. S. Army Corps of Engineers Contract Report GL-89-1, waterways Experiment Station.* Viksburg, MS, 1-67 pp.

DEERE, D. U., MERRIT, A. H. and CROON, R. F., 1969. *Engineering Classification of in situ Rock*. Technical Report, AWFL-TR-67-144, Air Force Weapons Laboratory, Kirtland Air Force Base, New Mexico.

DEFRA (Department for Environment, Food and Rural Affairs), 2001. *National Appraisal of Assets at Risk from Flooding and Coastal Erosion, including the potential impact of climate change*. Final report, July 2001. Flood Management Division, London, 1-64 pp.

DENNESS, B., 1971. The reservoir principle of mass movement. Report from the Institute of Geological Sciences, 72(7), 1-13.

DERSHOWITZ, W. S. and EINSTEIN, H. H., 1988. Characterizing rock joint geometry with system models. *Rock Mechanics and Rock Engineering*, 21, 21-51.

DESMOND, L. G. and BRYAN, P. G., 2003. Recording architecture at the archaeological site of Uxmal, Mexico: a historical and contemporary view. *Photogrammetric Record*, 18(102), 105-130.

DETOLEDO, P. E. C. and DEFREITAS, M. H., 1993. Laboratory testing and parameters controlling the shear strength of filled rock joints. *Géotechnique*, 43, 1-19.

DIAS, J. M. A. and NEAL, W. J., 1992. Sea cliff retreat in southern Portugal: profiles, processes, and problems. *Journal of Coastal Research*, 8(3), 641-654.

DICKSON, M. E., KENNEDY, D. M. and WOODROFFE, C. D., 2004. The influence of rock resistance on coastal morphology around Lord Howe Island, southwest Pacific. *Earth Surface Processes and Landforms*, 29, 629-643.

DIENER, B.G., 2000. Sand contribution from bluff recession between Point Conception and Santa Barbara, California. *Shore and Beach*, 68(2), 7-14.

DONG, J. -J. and PAN, Y. -W., 1996. A hierarchical model of rough rock joints based on micromechanics. *International Journal of Rock Mechanics and Mining Sciences & Geomechanical Abstracts*, 33, 111-123.

DOUGLAS, W. G. R., 1980. Magnitude-frequency study of rockfall in Co. Antrim, N. Ireland. *Earth Surface Processes and Landforms*, 5, 123-130.

DUARTE, C. A., BABUŠKA, I. and ODEN, J. T., 2000. Generalized finite element methods for three-dimensional structural mechanics problems. *Computers and Structures*, 77, 215-232.

DUNCAN, J. M., 1996. State of the art: limit equilibrium and finite-element analysis of slopes. *Journal of Geotechnical Engineering*, ASCE 122(7), 577-597.

DUPERRET, A., DE POMERAI, M. R., GENTER, A., MORTIMORE, R. N. and DELACOURT, B., 2002. Coastal rock cliff erosion by collapse at Puys, France: the role of impervious marl seams within chalk of NW Europe. *Journal of Coastal Research*, 18, 52-61.

EASTMAN, J. R. and MCKENDRY, J. E., 1994. *Change and time series analysis. Explorations in GIS technology, volume 1*. UNITAR, Geneva, Switzerland, 78 pp.

EBERHARDT, E., STEAD, D. and COGGAN, J. S. 2004. Numerical analysis of initiation and progressive failure in natural rock slopes – the 1991 Randa rockslide. *International Journal of Rock Mechanics and Mining Sciences*, 41, 69-87.

EBERHARDT, E., WILLENBERG, H., LOEW, S. and MAURER, H., 2001. Active rockslides in Switzerland – understanding mechanisms and processes. In: *International Conference on Landslides – Causes, Impacts and Countermeasures*. Dacos, 25-34 pp.

EINSTEIN, H. H., VENEZIANO, D., BAECHER, G. B. and O'REILLY, K. J., 1983. The effects of discontinuity persistence on rock slope stability. *International Journal of Rock Mechanics & Mining Sciences & Geomechanical Abstracts*, 20(5), 227-26.

ELSINGHORST, C., GROENEBOOM, P., JONATHAN, P., SMULDERS, L. and TAYLOR, P. H., 1998. Extreme value analysis of North Sea storm severity. *Journal of Offshore Mechanics and Arctic Engineering*, 120(3), 177-183.

EMERY, K.O., 1941, Rate of surface retreat of sea cliffs based on dated inscriptions. *Science*, 93, 617-618.

EMERY, K. O. and KUHN, G. G., 1980. Erosion of rock shores at La Jolla, California. *Marine Geology*, 37, 197-208.

EMERY, K. O. and KUHN, G. G., 1982. Sea cliffs: their processes, profiles, and classification. *Geological Society of America Bulletin*, 93, 644-654.

EMERY, K. O. and MILLIMAN, J. D., 1978. Suspended matter in surface waters: influence of river discharge and of upwelling. *Sedimentology*, 25, 125-140.

EMERY, K. O., 1960. *The sea off southern California: A modern habitat of petroleum*. John Wiley & Sons, New York, 366 pp.

ERDAS, 2001. *Imagine OrthoBASE User's Guide*. Erdas Incorporated, 524 pp.

ESTRIN, Y. and BRECHET, Y., 1996. On a model of friction sliding. *Pure and Applied Geophysics*, 147, 745-762.

EVANS, R., 1981. An analysis of secondary rock failures - the stress redistribution method. *Engineering Geology*, 14, 77-86.

EVANS, R., VALLIAPPAN, S., MCGUCKIN, D., and RAJA SEKAR, H. L., 1981. *Stability analysis of a rock slope against toppling failure*. Proceedings, 3rd International Symposium on Weak Rock, Tokyo, 665-670 pp.

EVENDEN, G. I., 1990. *Cartographic projection procedures for the UNIX environment - a user's manual*. Geological Survey Open-File Report No.91-57, Woods Hole, Massachusetts, U.S., 1-63 pp.

EVENDEN, G. I., 1991. *Notes on a method to transform digitized coordinates to geographic coordinates*. U. S. Geological Survey Open-File Report No. 91-57, Woods Hole, Massachusetts, U.S., 1-53 pp.

EVERTS, C. H., 1991. Seacliff retreat and coarse sediment yields in Southern California. In: *Coastal Sediments '91. Proceedings of the Speciality Conference on Quantitative Approaches to Coastal Sediment Processes*. Seattle, Washington, 25-26 June 1991, 1586-1598 pp.

FAHEY, B. D. and LEFEBURE, T. H., 1988. The freeze-thaw weathering regime at a section of the Niagra Escarpment on the Bruce Peninsula Southern Ontario, Canada. *Earth Surface Processes and Landforms*, 13, 293-304.

FARDIN, N., STEPHANSSON, O. and JING, L., 2001. The scale dependence of rock joint surface roughness. *International Journal of Rock Mechanics and Mining Sciences*, 38(5), 659-669.

FERREIRA, J. A. and GUEDES SOARES, C., 2000. Modelling distributions of significant wave height. *Coastal Engineering*, 40(4), 361-374.

FISHMAN, K. L., DERBY, C. W. and PALMER, M. C., 1991. Verification for numerical modelling of jointed rock mass using thin layer elements. *International Journal for Numerical and Analytical Methods in Geomechanics*, 15, 61-70.

FLEMMING, C. A., 1965. Two-storied cliffs at the Auckland Islands. *Royal Society of New Zealand Transactions*, 3, 171-174.

FLICK, R. E., 1998. Comparison of tides, storm surges, and mean sea level during he El Nino Winters of 1982-83 and 1997-98. *Shore and Beach*, 66(3), 7-17.

FOX, A. J. and GOOCH, M. J., 2001. Automatic DEM generation for Antarctic terrain. *Photogrammetric Record*, 17(98), 275-290.

FRASER, C. S., 1997. Digital camera self-calibration. *ISPRS Journal of Photogrammetry and Remote Sensing*, 52, 149-159.

FRUNEAU, F., ACHACHE, J. and DELACOURT, C., 1996. Observation and modelling of the Sant-Etienne-de-Tinee landslide using SAR interferometry. *Tectonophysics*, 265, 181-190.

FRYER, J. G., 1995. Camera calibration. In: Atkinson, K. B. (Ed.), *Close Range Photogrammetry and Machine Vision*. Whittles Publishing, Edinburgh, Scotland, 156-179.

GALSTER, R. W. and SCHWARTZ, M. L., 1990. Ediz Hook - a case history of coastal erosion and rehabilitation. In: Schwartz, M. L. and Bird, E. C. F. (Eds.), Artificial beaches. *Journal of Coastal Research Special Issue*, 6, 103-113.

GARDNER, J., 1970. Rockfall; a geomorphic process in high mountain terrain. *Albertan Geographer*, 6, 15-20.

GARDNER, J., 1977. High magnitude rockfall-rockslide: frequency and geomorphic significance in the Highwood Pass area, Alberta, Great Plains - Rocky Mountain. *Geographical Journal*, 6, 288-238.

GELINAS, P. J. and QUIGLEY, R. M., 1973. *The influence of geology on erosion rates along the north shore of Lake Erie*. Proceedings of the Sixteenth Conference of the International Association of Great Lakes Research, 421-430 pp.

GENOVOIS, R., GALGARO, A. and TECCA, P. R., 2000. Image analysis for debris flow properties estimation. *Physics and Chemistry of the Earth*, 26(9), 623-631.

GERRARD, J., 1988. *Rocks and landforms*. Allen and Unwin Incorporated, Wellington, New Zealand, 319 pp.

GOOCH, M. J. and CHANDLER, J. H., 2000. Failure prediction in automatically generated digital elevation models. *Computers and Geosciences*, 27(8), 913-920.

GOOCH, M. J., CHANDLER, J. H. and STOJIC, M., 1999. Accuracy assessment of digital elevation models generated using the Erdas Imagine Orthomax digital photogrammetric system. *Photogrammetric Record*, 16(93), 519-531.

GOODMAN, R, E., 1980. *Introduction to Rock Mechanics*. John Wiley & Sons, New York, 242 pp.

GOODMAN, R. E. and BRAY, J. W., 1976. Toppling of rock slopes. In: American Society of Civil Engineers, *Rock Engineering for Foundations and Slopes*. University of Colorado, Boulder, Colorado, 201-234 pp.

GORMAN, L., MORANG, A. and LARSON, R., 1998. Monitoring the coastal environment; part IV: mapping, shoreline changes, and bathymetric analysis. *Journal of Coastal Research*, 14(1), 61-92.

GRAHAM, R. W. and MILLS, J. P., 2000. Digital cameras for aerial survey: where are we now? *Photogrammetric Record*, 16(96), 905-909.

GRAINGER, P. and KALAUGHER, P. G., 1987. Intermittent surging movements of a coastal landslide. *Earth Surface Processes and Landforms*, 12, 597-603.

GRAINGER, P. and KALAUGHER, P. G., 1988. Hazard zonation of coastal landslides. In: Bonnard, C. (Ed.), *Landslides*. Proceedings of the 5th International Symposium on Landslides. A. A. Balkema, Rotterdam, 1169-1174 pp.

GRIFFITHS, J. S., 2004. Geomorphological mapping. In: Goudie, A. S. (Ed.), *Encyclopedia of Geomorphology*. Routledge, London, 427-428 pp.

GRIGGS, G. B., 1994. California's coastal hazards. *Journal of Coastal Research, Special Issue* 12, 1-15.

GRIGGS, G. B. and JOHNSON, R. E., 1983. The impact of the 1983 storms on the coastline of northern Monterey Bay. *California Geology*, 36, 163-174.

GRIGGS, G. B. and SAVOY, L., 1985. *Living with the California coast*. Duke University Press, Durham, North Carolina, 393 pp.

GRIGGS, G. B. and TRENHAILE, A.S., 1994. Coastal cliffs and platforms. In: Carter, R. W. G. and Woodroffe, C. D. (Eds.), *Coastal evolution; Late Quaternary shoreline morphodynamics*. Cambridge University Press, Cambridge, 425-450 pp.

GROVE, J. M., 1972. The incidence of landslides, avalanches and floods in western Norway during the Little Ice Age. *Arctic and Alpine Research*, 4, 131-138.

GUTHRIE, R. H. and EVANS, S. G., 2004. Magnitude and frequency of landslides triggered by a storm event, Loughborough Inlet, British Columbia. Natural *Hazards and Earth System Sciences*, 4, 475-483.

GUY JR., D. E., 1999. Erosion hazard area mapping, Lake County, Ohio. *Journal of Coastal Research, Special Issue*, 28, 185-196.

GUZZETTI, F., MALAMUD, B. D., TURCOTTE, D. L. and REICHENBACH, P., 2002. Power-law correlations of landslide areas in central Italy. *Earth and Planetary Science Letters*, 195, 169-183.

HALL, D. B., 1996. Modelling the failure of natural rock columns. *Geomorphology*, 15, 123-134.

HALL, J. W., MEADOWCROFT, I., LEE, E. M. and VAN GELDER, P. H. A. J. M. 2002. Stochastic simulation of episodic soft coastal cliff recession. *Coastal Engineering*, 46, 159-174.

HAMPTON, M. A., 2002. Gravitational failure of sea cliffs in weakly lithified sediment. *Environmental and Engineering Geosciences*, 8(3), 175-191.

HAMPTON, M. A., GRIGGS, G. B., EDIL, T. B., GUY, D. E., KELLY, J. T., KOMAR, P. D., MICKELSON, D. M. and SHIPMAN, H. M. (Eds.), 2004. *Formation, evolution, and stability of coastal cliffs – status and trends*. U.S. Geological Survey Professional Paper 1693, 1-129 pp.

HANSEN, M. J., 1984. Strategies for classification of landslides. In: Brunsden, D. and Prior, D. B. (Eds.), *Slope Instability*. Landscape Systems. John Wiley & Sons, Chichester, 1-23 pp.

HANSOM, J. D., 2001. Coastal sensitivity to environmental change: a view from the beach. *Catena*, 42(2), 291-305.

HANTZ, D., VENGEON, J. M. and DUSSAGUE-PEISSER, C., 2003. An historical, geomechanical and probabilistic approach to rock-fall hazard assessment. *Natural Hazards and Earth System Science*, 3, 693-701.

HAPKE, C. J. and RICHMOND, B. M., 2002. The impact of climatic and seismic events on the short-term evolution of seacliffs based on 3-D mapping - Northern Monterey Bay, California. *Marine Geology*, 187(3-4), 259-278.

HAPKE, C. J. and GRIGGS, G. B., 2002. Long-term volumetric sediment contribution from landslides; Big Sur coastline, California. In: Ewing, L., and Wallendorf, L. (Eds.), *Proceedings Solutions to Coastal Disasters '02*. ASCE, 652-663 pp.

HAPKE, C., 2005. Estimated material yield from coastal landslides based on historical digital terrain modeling, Big Sur, California. *Earth Surface Processes and Landforms*, 30, 679-697.

HARP, E. L. and SAVAGE, W. Z., 1997. *Landslides triggered by the April 1997, tropical storms in Pohnpei*. Federated States of Micronesia, U.S. Geological Survey Open-File Report 97-696, 1-10 pp.

HART, R. D., 1993. An introduction to distinct element modelling for rock engineering. In: Hudson, J. A. (Ed.), *Comprehensive Rock Engineering*. Pergamon Press, Oxford, Volume 2, 245-261 pp.

HASLETT, S. K., 2000. *Coastal Systems*. Routledge, London, 218 pp.

HEALY, T., 1991. Coastal erosion and sea level rise. *Zeitschrift für Geomorphologie*, 81, 15-29.

HEIPKE, C., 1999a. Automatic aerial triangulation: results of the OEEPE-ISPRS test and current developments. In: Fritsch, D. and Spiller, R. (Eds.), *Photogrammetric week '99'*. Wichmann Verlag, Heidelberg, 177-191 pp.

HEIPKE, C., 1999b. Digital Photogrammetric Workstations. *GIM International*, 1(13), 1-81.

HEIPKE, C. and EDER, K., 1999. *Performance of tie point extraction in automatic aerial triangulation*. OEEPE Official Publications No. 36, 125-185 pp.

HEIPKE, C., 1995. State-of-the-art of digital photogrammetric workstations for topographic applications. *Photogrammetric Engineering and Remote Sensing*, 61(1), 49-56.

HENCHER, S. R., LIAO, Q.-H. and MONAGHAN, B. G., 1996. Modelling of slope behaviour for open pits. *Transactions of the Institution of Mining and Metallurgy – Section A*, 105, A37-A47.

HERMANNS, R. L. and STRECKER, M. R., 1999. Structural and lithological controls on large Quaternary rock avalanches (sturzstroms) in arid northwestern Argentina. *Journal of Geology*, 108, 35-52.

HERVÁS, J., BARREDO, J. I., ROSIN, P. L., PASUTO, A., MANTOVANI, F. and SILVANO, S., 2003. Monitoring landslides from optical remotely sensed imagery: the case history of Tessina landslide, Italy. *Geomorphologie*, 45, 63-75.

HEUZE, F. E., 1979. Scale effects in the determination of rock mass strength and deformability. *Rock Mechanics*, 12, 167-192.

HEY, R. D., 1979. Causal and functional relations in fluvial geomorphology. *Earth Surface Processes*, 4, 179-182.

HICKS, M. and SAMY, K., 2002. Influence of heterogeneity on undrained clay slope stability. *Quarterly Journal of Engineering Geology and Hydrology*, 35, 41-49.

HIGH-POINT RENDEL, 1999. *Cowbar Coastal Protection and Cliff Stabilisation*. Strategic Study Report produced by High-Point Rendel for Scarborough Borough Council, 1-40 pp.

HIGH-POINT RENDEL, 2002. *Coastal Mining Environmental Impact Statement*. Consultation Document for Scarborough and Redcar and Cleveland Borough Council.

HINCHCLIFFE, S. and BALLANTYNE, C. K. 1999. Talus accumulation and rockwall retreat, Trotternish, Isle of Skye, Scotland. *Scottish Geographical Journal*, 115, 53-70.

HOEK, E., 1983. Strength of jointed rock masses. *Géotechnique*, 33, 187-223.

HOEK, E. and BRAY, J. W., 1981. *Rock Slope Engineering*, (3rd Edition). The Institution of Mining and Metallurgy, London, 358 pp.

HOEK, E., BRAY, J. W. and BOYD, J.M., 1973. The stability of a rock slope containing a wedge resting on two intersecting discontinuities. *Quarterly Journal of Engineering Geology*, 6, 1-55.

HOEK, E., KASIER, P. K. and BAWDEN, W. F., 1995. *Support of underground excavations in hard rock*. A. A. Balkema, Rotterdam, 215 pp.

HORN, B. K.P., 1987. Closed-form solution of absolute orientation using unit quaternions. *Journal of the Optical Society of America A, Optics and Image Science,* 4(4), 629-642.

HOSKING, A. and MCINNES, R., 2002. Preparing for the impacts of climate change on the central south coast of England: a framework for future risk. *Journal of Coastal Research Special Issue,* 36, 381-389.

HOUGHTON, J. T., DING, Y., GRIGGS, D. J., NOGUER, M., VAN DER LINDEN, P. J., DAI, X., MASKELL, K. and JOHNSON, C. A. (Eds.), 2001. *Climate change 2001: The Scientific Basis. Contribution of Working Group I to the Third Assessment Report of the Intergovemmental Panel on Climate Change*. Cambridge University Press, Cambridge, 881 pp.

HOWARD, A. S., 1985. Lithostratigraphy of the Staithes Sandstone and Cleveland Ironstone Formations (Lower Jurassic) of north-east Yorkshire. *Proceedings of the Yorkshire Geologists Society*, 45, 261-275.

HOWARD, A. D. and MCLANE III, C. F., 1988. Erosion of cohesionless sediment by groundwater seepage. *Water Resources Research*, 24, 1659-1674.

HOWARTH, M. K., 1992. The ammonite family Hildoceratidae in the Lower Jurassic of Great Britain. Monograph of the Palaeontographical Society, London, 586, 1-106.

HOWELL, H. H. and BARROW, G., 1888. *North Cleveland*. Eyre and Spottiswoode, London, 102 pp.

HSIA, J. S. and NEWTON, I., 1999. A method for the automated production of digital terrain models using a combination of feature points, grid points and filling back points. *Photogrammetric Engineering and Remote Sensing*, 65(6), 713-719.

HUA, T. C. and FAIRBAIRN, D., 2000. Change detection in aerial imagery assisted by GIS for topographic dataset revision. *The Malaysian Surveyor*, 35(2), 14-26.

HUANG, Y. D., 2000. Evaluation of information loss in digital elevation models with digital photogrammetric systems. *Photogrammetric Record*, 16(95), 781-791.

HUDSON, J. A. and HARRISON, J. P., 1997. *Engineering Rock Mechanics: An Introduction to the Principles*. Elsevier Sciences, Oxford, 444 pp.

HUMPHRIES, L., 2001. A review of relative sea level rise caused by mining-induced subsidence in the coastal zone: some implications for increased coastal recession. *Climate Research*, 18, 147-156.

HUNGR, O. and EVANS, S.G., 1996. *Rock avalanche runout prediction using a dynamic model.* Proceedings from the 7th International Symposium on Landslides, Trondheim, Norway, 233-238 pp.

HUNTING GEOLOGY AND GEOPHYSICS LIMITED, 1969. *Report on the geology of an offshore area between Cowbar Nab and Boulby Scar, Staithes, Yorkshire.* Prepared for Cleveland Potash Limited by Hunting Geology and Geophysics, Herts, 1-5 pp.

HUTCHINSON, I., JAMES, T. S., CLAGUE, J. J., BARRIE, J. V. and CONWAY, K. W., 2004. Reconstruction of late Quaternary sea-level change in southwestern British Columbia from sediments in isolation basins. *Boreas*, 33, 183-194.

HUTCHINSON, J. N., 1973. The response of London Clay cliffs to differing rates of toe erosion. *Geologia Applicata e Idrogeologia*, 8, 221-239.

HUTCHINSON, J. N., 1984. Landslides in Britain and their countermeasures. *Journal of the Japan Landslide Society*, 21, 1-24.

HUTCHINSON, J. N., CHANDLER, M. P. and BROMHEAD, E. N., 1981. *Cliff recession on the Isle of Wight, SW coast.* Proceedings of the 10th international conference of the soil mechanics and foundation engineering, Stockholm, 429-434 pp.

HUTCHINSON, J. N., CHANDLER, M. P. and BROMHEAD, E. N., 1985. *A review of current research on the coastal landslides forming the undercliff of the Isle of Wight, with some practical implications.* Proceedings of the Conference on Problems Associated with the Coastline, Isle of Wight, 1-16 pp.

IOFIS, I. M., MAKSIMOV, A. V. and MIRONOV, V. V., 1990. Some practical aspects of numerical simulation of jointed rock mass by distinct element method. In: *Proceedings International Conference of Mechanics of Jointed and Faulted Rock, Vienna, 18-20 April.* A. A. Balkema, Rotterdam, 479-486 pp.

ISRM, 1988. Suggested methods for determining the fracture toughness of rock. *International Journal of Rock Mechanics and Mining Sciences, Geomechanics Abstracts*, 25(2), 71-96.

ITASCA, 2000. *UDEC – Universal Distinct Element Code.* Itasca Consulting Group, Minneapolis.

JACOBSEN, K. and WEGMANN, H., 1998. *Experiences with Automatic Aerotriangulation.* Proceedings of ASPRS-RTI Annual Convention, Tampa, USA, March 30 - April 3.

JAEGER, J. C., 1969. *Behaviour of closely jointed rock.* Proceedings 11th Symposium of Rock Mechanics, 57-68 pp.

JAEGER, J. C., 1972. *Rock Mechanics and Engineering.* Cambridge University Press, London, 417 pp.

JELGERSMA, S. and TOOLEY, M. (Eds.), 1992. *Impacts of sea-level rise on European coastal lowlands.* Blackwell, Oxford, 267 pp.

JENNINGS, E. B., 1970. *A mathematical theory for the calculation of the stability of slopes in open cast mines*. Proceedings of open pit mining symposium, Johannesburg. A. A. Balkema, Cape Town, 87-102 pp.

JENNINGS, S., ORFORD, J. D., CANTI, M., DEVOY, R. J. N. and STRAKER, V., 1998. The role of relative sea-level rise and changing sediment supply on Holocene gravel barrier development: the example of Porlock, Somerset, UK. *The Holocene*, 8(2), 165-181.

JIANG, Y., NEGATOMI, M. and OKADA, T., 1995. Studies on toppling failure mechanisms of slope in discontinuous rockmass. In: Rossmanith, H. P. (Ed.), *Mechanics of jointed and faulted rock*. A. A. Balkema, Rotterdam, 605-610 pp.

JING, L., 2003. A review of techniques, advances and outstanding issues in numerical modelling for rock mechanics and rock engineering. *International Journal for Rock Mechanics and Mining Sciences*, 40, 283-353.

JOHANNESSEN, C. L., FEIEREISEN, J. J. and WELLS, A. N., 1982. Weathering of ocean cliffs by salt expansion in a mid latitude coastal environment. *Shore and Beach*, 51, 26-34.

JONES, D. K. C. and LEE, E. M., 1994. *Landsliding in Great Britain*. London, HMSO, 396 pp.

JONES, D. G. and WILLIAMS, A. T., 1991. Statistical analysis of factors influencing cliff erosion along a section of the west Wales coast. *Earth Surface Processes and Landforms*, 16, 95-111.

KAKANI, D. L. and PITEAU, D. R., 1976. Finite element analysis of toppling at Hell's Gate Bluffs, British Columbia. *Bulletin of the Association of Engineering Geologists*, 13, 315-327.

KALAUGHER, P. G., HODGSON, R. L. P. and GRAINGER, P., 2000. Pre-failure strains as precursors of sliding in a coastal mudslide. *Quarterly Journal of Engineering Geology and Hydrology*, 33, 325-334.

KAMPHUIS, J. W., 1987. Recession rate of glacial till bluffs. *Journal of Waterway, Port, Coastal and Ocean Engineering*, 113(1), 60-73.

KÄSER, C., CZAKA, T. and KUNZ, T., 1999. *Digital aerotriangulation for map revision with Match AT*. Proceedings OEEPE Workshop on Automation in digital photogrammetric production. Paris, June 22-24, 1999.

KENT, P. E., 1980. *Eastern England from the Tees to the Wash. British Regional Geology*. HMSO, London, 155 pp.

KERSTEN, T., STERNBERG, H., MECHELKE, K. and ACEVEDO PARDO, C., 2004. Terrestrial laser scanning system MENSI GS100/GS200 – accuracy tests, experiences and projects at the Hamburg University of Applied Sciences. In: Maas, H. -G. and

Schneider, D. (Eds.), *Panoramic Photogrammetry Workshop*. Proceedings of the ISPRS working group V/I, Dresden, Germany, February 19-22.

KIMBER, O. G., 1998. *Mechanisms of failure of jointed rock masses and the behaviour of steep slopes*. Ph.D. Thesis, University of Durham, Durham, 601 pp.

KIMBER, O. G., ALLISON, R. J. and COX, N. J., 1998. Mechanisms of failure and slope development in rock masses. *Transactions of the Institute of British Geographers*, 23, 353-370.

KIMBER, O. G., ALLISON, R. J. and COX, N. J., 2002. Rates and mechanisms of change of hard rock steep slopes on the Colorado Plateau, USA. In: Allison, R. J. (Ed.), *Applied Geomorphology*. John Wiley & Sons, Chichester, 65-90 pp.

KING, L. C., 1953. Canons of landscape evolution. *Geological Society of America Bulletin*, 64, 721-751.

KOLDITZ, O., 1995. Modelling flow and heat transfer in fractured rocks: conceptual model of a 3-D deterministic fracture network. *Geothermics*, 24(3), 451-470.

KOMAR, P. D. and MCDOUGAL, W. G., 1988. Coastal erosion and engineering structures: The Oregon experience. *Journal of Coastal Research, Special Issue*, 4, 77-92.

KOMAR, P. D. and SHIH, S. M., 1993. Cliff erosion along the Oregon coast: a tectonic sea level imprint plus local controls by beach processes. *Journal of Coastal Research*, 9(3), 747-765.

KRAUS, N. C., 1988. The effects of seawalls on the beach: an extended literature review. *Journal of Coastal Research Special Issue*, 4, 1-28.

KRUPNIK, A., 2003. Accuracy prediction for ortho-image generation. *Photogrammetric Record*, 18(101), 41-58.

KUHN, G. G. and SHEPARD, F. P., 1979. Accelerated beach-cliff erosion related to unusual storms in southern California. *California Geology*, 32(3), 58-59.

KUHN, G. G. and SHEPARD, F. P., 1984. *Sea cliffs, beaches, and coastal valleys of San Diego County*. University of California Press, Berkeley, California, 193 pp.

LAJTAI, E. Z., 1969. Strength of discontinuous rock in direct shearing. *Géotechnique*, 19(2), 218-233.

LANARO, F., JING, L., STEPHANSSON, O. and BARLA, G., 1997. DEM modelling of laboratory tests of block toppling. *International Journal of Rock Mechanics and Mining Sciences*, 34(3-4), 506-507.

LANE, S. N., JAMES, T. D. and CROWEL, M. D., 2000. Application of digital photogrammetry to complex topography for geomorphological research. *Photogrammetric Record*, 16(95), 793-821.

LANE, S. N., JAMES, T. D., PRITCHARD, H. and SAUNDERS, M., 2003. Photogrammetric and laser altimetric reconstruction of water levels for extreme flood event analysis. *Photogrammetric Record*, 18(104), 293-307.

LANE, S. N., RICHARDS, K. S. and CHANDLER, J. H. (Eds.), 1998. *Landform Monitoring, Modelling and Analysis*. John Wiley & Sons, Chichester, 454 pp.

LEATHERMAN, S. P., 1983. Shoreline mapping: A comparison of techniques. *Shore and Beach*, 51, 28-33.

LEE, E. M., 1997. *Investigation and management of soft rock cliffs*. Proceedings of the MAFF Conference of River and Coastal Engineers, 32nd, Keele, England, 1997, B1.1-B1.12 pp.

LEE, E. M., 2001. Living with natural hazards: the costs and management framework. In: Higgett, D. and Lee, E. M. (Eds.), *Geomorphological processes and landscape change: Britain in the last 1000 years*. Blackwell, London, 237-268 pp.

LEE, E. M., 2005. Coastal cliff recession risk: a simple judgement-based model. *Quarterly Journal of Engineering Geology and Hydrology*, 38, 89-104.

LEE, E. M. and CLARK, A. R., 2002. *Investigation and Management of soft rock cliffs*. Thomas Telford Publishing Ltd, Heron Quay, London, 382 pp.

LEE, E. M. and JONES, D. K. C., 2004. *Landslide risk assessment*. Thomas Telford Limited, London, 404 pp.

LEE, E. M. and MOORE, R., 1991. *Coastal landslip potential assessment: Isle of Wight Undercliff, Ventnor*. Geomorphological Services Limited.

LEE, E. M., MEADOWCROFT, I. C., HALL, J. W. and WALKDEN, M., 2002. Coastal landslide activity: a probabilistic simulation model. *Bulletin of Engineering Geology and the Environment*, 61, 347-355.

LEE, J. S., VENEZIANO, D. and EINSTEIN, H. H., 1990. Hierarchical fracture trace model. In: Hastrulid, W. and Johnson, G. A. (Eds.), *Rock Mechanics Contributions and Challenges*. Proceedings of the 31st US Rock Mechanics Symposium. A. A. Balkema, Rotterdam.

LEE, L., PINCKNEY, C., and BEMIS, C., 1976. *Seacliff base erosion*. ASCE National Water Resources and Ocean Engineering, San Diego, California, 1976, Conference Proceedings, 1-14 pp.

LEMOS, J. V., 1990. A comparison of numerical and physical models of a blocky medium. In: Rossmanith, H. P. (Ed.), *Mechanics of jointed and faulted rock*. A. A. Balkema, Rotterdam, 509-514 pp.

LEUNG, C. F. and KHEOK, S. C., 1987. Computer aided analysis of rock slope stability. *Rock Mechanics and Rock Engineering*, 20, 111-122.

LI, Z., 1988. On the measure of digital terrain model accuracy. *Photogrammetric Record*, 38, 1117-1126.

LI, Z., 1993. Mathematical models of the accuracy of digital terrain model surfaces linearly constructed from square gridded data. *Photogrammetric Record*, 14(82), 661-674.

LIANG, T. and HEIPKE, C., 1996. Automatic relative orientation of aerial images. *Photogrammetric Engineering & Remote Sensing*, 62(1), 47-55.

LICHTI, D. D. and HARVEY, B. R., 2002. *The effects of reflecting surface material properties on time-of-flight laser scanner measurements*. Symposium on Geospatial Theory, Processing and Applications, Ottawa, 1-9 pp.

LILLESAND, T. M. and KIEFER, R. W., 2000. *Remote Sensing and Image Interpretation*, (4th Edition). John Wiley & Sons, New York, 724 pp.

LIM, M., PETLEY, D. N., ROSSER, N. J., ALLISON, R. J., LONG, A. J. and PYBUS, D., 2005. Combined digital photogrammetry and time-of-flight laser scanning for monitoring cliff evolution. *Photogrammetric Record*, 20(110), 109-129.

LIN, D. and FAIRHURST, C. 1988. Static analysis of the stability of three-dimensional blocky systems around excavations in rock. *International Journal of Rock Mechanics & Mining Sciences & Geomechanical Abstracts*, 25, 139-147.

LIVINGSTONE, D., RAPER, J. and MCCARTHY, T., 1999. Integrating aerial videography and digital photography with terrain modelling: and application for coastal geomorphology. *Geomorphology*, 29, 77-92.

LONGWELL, C. R., FLINT, R. F. and SANDERS, J. E., 1969. *Physical geology*. John Wiley & Sons, New York, 685 pp.

LOODTS, J., 1996. Logistics and integration of the system: the eurosense experiences. *Applications of Digital Photogrammetric Workstations*. Proceedings OEEPE Workshop, Lausanne, Switzerland.

Luckman, B. H., 1988. Debris accumulation patterns on talus slopes in Surprise Valley, Alberta. *Géographie Physique et Quaternaire*, 42, 247-278.

LUCKMAN, B. H., 1976. Rockfalls and rockfall inventory data: some observations from Surprise Valley, Jasper National Park, Canada. *Earth Surface Processes*, 1, 287-298.

MALET, J.-P., REMAÎTRE, A., MAQUAIRE, O., ANCEY, C. and LOCAT, J., 2003. Flow susceptibility of heterogeneous marly formations. Implications for torrent hazard control in the Barcelonnette basin (Alpes-de-Haute-Provence, France). In: Rickenmann, D. and Chen, C.-L. (Eds.), *Proceedings of the Third International Conference on Debris-Flow Hazard Mitigation: Mechanics, Prediction and Assessment*. Davos, Switzerland, 1-12 pp.

MAQUAIRE, O., 1992. The Bessin cliffs. In: Flageolett, J. C. (Ed.), *Prevention of coastal erosion and submersion risks*. CERG, 85-92 pp.

MARK, D. M., 1980. On scales of investigation in geomorphology. *Canadian Geographer*, XXIV, 1, 81-82.

MASSONNET, D. and FEIGL, K. L., 1998. Radar interferometry and its application to changes in the earth's surface. *Reviews of Geophysics*, 36(4), 441-500.

MATSUOKA, N. and SAKAI, H., 1999. Rockfall activity from an alpine cliff during thawing periods. *Geomorphology*, 28(3-4), 309-328.

MATZNETTER, K., 1956. Der Vorgang der Massenbewegungen an Beispielen des Lostertales in Vorarlberg. *Geographie Jahresber aus Österreich*, 25, 1-108.

MAY, V. J. and HANSOM, J. D., 2003. *Coastal geomorphology of Great Britain*. Joint Nature Conservation Committee, Peterborough, 737 pp.

MAY, V. J. and HEEPS, C., 1985. The nature and rates of change on chalk coastlines. *Zeitschrift für Geomorphologie NF Supplement Band*, 57, 81-94.

MAY, V. J., 1966. A preliminary study of recent coastal changes and sea defences in south east England. *Southampton Research Series in Geography*, 3, 3-24.

MCBRIDE, R. A., 1989. Accurate computer mapping of coastal change: Bayou Lafourche shoreline, Louisiana, USA. In: Magoon, O. T. (Ed.), *Coastal Zone '89*. ASCE, New York, 707-719 pp.

MCCULLAGH, M. J., 1998. Quality use and visualisation in terrain modelling. In: Lane, S. N., Richards, K. S. and Chandler, J. H. (Eds.), *Landform Monitoring, Modelling and Analysis*. John Wiley & Sons, Chichester, 95-117 pp.

MCDOUGAL, W. G., Sturtevant, M. A. and Komar, P. D., 1987. Laboratory and field investigations of the impact of shoreline stabilization structures on adjacent properties. In: *Coastal Sediments 1987*. ASCE, 961-963 pp.

MICKELSON, D. M., BROWN, E. A., EDIL, T. B., MEADOWS, G. A., GUY, D. E., LIEBENTHAL, D. L. and FULLER, J. A., 2002. Comparison of sediment budgets of bluff/beach/nearshore environments near Two Rivers, Wisconsin, on Lake Michigan, and at Painesville, Ohio, on Lake Eerie. *Geological Society of America Abstracts with Programs*, 34(2), A-12.

MIKHAIL, E. M., BETHEL, J. S. and MCGLONE, J. C., 2001. *Introduction to modern photogrammetry*. John Wiley & Sons, New York, 479 pp.

MILLER, M. C. and AUBREY, D. G., 1985. *Beach Changes on Eastern Cape Cod, Massachusetts, From Newcomb Hollow to Nauset Inlet, 1970-1974*. U.S.A.C.E., Coastal Engineering Research Center, Vicksburg, MS, CERC-MP-85-10, 1-58 pp.

MILLS, J. P., BUCKLEY, S. J., MITCHELL, H. L., CLARKE, P. J. and EDWARDS, S. J., 2005. A geomatics data integration technique for coastal change monitoring. *Earth Surface Processes and Landforms*, 30(6), 651-664.

MILLS, J. P., PEIRSON, G. C., NEWTON, I. and BRYAN, P. G., 2000. Photogrammetric investigation into the suitability of desktop image measurement software for architectural recording. *International Archives of Photogrammetry and Remote Sensing*, 32(B5), 525-532.

MILLS, J. P., NEWTON, I. and PEIRSON, G. C., 2001. Pavement deformation monitoring in a rolling load facility. *Photogrammetric Record*, 17(97), 7-24.

MITCHLEY J. and MALLOCH, J. C., 1991. *Sea Cliff Management Handbook for Great Britain*. University of Lancaster and Joint Nature Conservation Committee, Peterborough, 125 pp.

MOORE, I. D., GRAYSON, R. B. and LADSON, A. R., 1991. Digital terrain modelling: a review of hydrological, geomorphological and biological applications. *Hydrological Processes*, 5(1), 3-30.

MOORE, L. J., 2000. Shoreline mapping techniques. *Journal of Coastal Research*, 16, 111-124.

MOORE, L. J. and GRIGGS, G. B., 2002. Long-term cliff retreat and erosion hotspots along the central shores of the Monterey Bay National Marine Sanctuary. *Marine Geology*, 181, 265-283.

MOORE, L. J., BENUMOF, B. T. and GRIGGS, G. B., 1999. Coastal Erosion Hazards in Santa Cruz and San Diego Counties, California. *Journal of Coastal Research Special Issue No.* 28, 121-139.

MORGAN, R. P. C., 1986. *Soil Erosion and Conservation*. Longman, London, 298 pp.

MOTTERSHEAD, D., 1997. *Classic Landform Guide: South Devon Coast*. The Geographical Association, 50 pp.

MOUCHEL ASSOCIATES LIMITED, 1996. Shoreline Management Plan – Huntcliffe to Flamborough Head – Sub-cell 1d.L. G. Mouchel.

MULLER, L. 1959. The European approach to slope stability problems in open pit mines. Proceedings on the 3rd Symposium on Rock Mechanics. *Colorado School of Mines Quarterly*, 54(3), 116-133.

NAGIHARA, S., MULLIGAN, K. R. and XIONG, W., 2004. Use of a three-dimensional laser scanner to digitally capture the topography of sand dunes in high spatial resolution. *Earth Surface Processes and Landforms*, 29, 391-398.

NAIRN, R. B., 1997. Cohesive shores. *Shore and Beach*, 65(2), 17-21.

NASH, D., 1987. A comparative review of limit equilibrium methods of stability analysis. In: Anderson, M. G. and Richards, K. S. (Eds.), *Slope Stability*. John Wiley & Sons, Chichester, 11-75 pp.

NELIS, S. B., 2005. *Modelling rock slope behaviour and evolution with reference to Northern Spain and southern Jordan*. Ph.D. thesis, Department of Geography, University of Durham, 312 pp.

NEVES, M. and RAMOS PEREIRA, A., 1999. The interaction between marine and subaerial processes in the evolution of rocky coasts: The example of Castelejo (southwest Portugal). *Boletín Instituto Español de Oceanografía*, 15, 1-4, 251-258 pp.

NICHOL, S. L., HUNGR, O. and EVANS, S. G., 2002. Large-scale brittle and ductile toppling of rock slopes. *Canadian Geotechnical Journal*, 39, 773-788.

NICHOLLS, R. J. and SMALL, C., 2002. Improved estimates of coastal population and exposure to hazards released. *EOS Transactions*, 83(2), 301-305.

NIETO, J. C., ALFONSO, M. and SANZ, R., 1995. Reliability of measured Sea states using radar system on shore. In: Guedes Soares, C. E. (Ed.), *Proceedings of the 14th International Conference on Offshore Mechanics and Artic Engineering*, 63-70 pp.

NORRIS, R. M. and BACK, W., 1990. Erosion of seacliffs by groundwater. In: Higgins, C. G. and Coates, D. R. (Eds.), *Groundwater Geomorphology; the role of subsurface water in earth-surface processes and landforms*. Geological Society of America Special Paper 252, 283-290 pp.

OKA, N., 1998. Application of photogrammetry to the field observation of failed slopes. *Engineering Geology*, 50, 85-100.

OSBORNE, R. H., FOGARTY, T. M. and KUHN, G. G., 1989. A quantitative comparison of course-grained sediment yield from contributing cliffs and associated rivers; southern Orange and San Diego Counties, California. *Geological Society of America, Cordilleran Section, Abstracts with Programs*, 21(5), 1-126.

PAILLARD, M., PREVOSTO, M., BARSTOW, S. F. and GUEDES SOARES, C., 2000. Field measurements of coastal waves and currents in Portugal and Greece. *Coastal Engineering*, 40(4), 285-296.

PALMSTRÖM, A., 1982. *The volumetric joint count – A useful and simple measure of the degree of jointing*. IVth Int. Congress IAEG, New Dehli, V221 – V228 pp.

PALMSTRÖM, A., 1995. *Characterising the strength of rock masses for use in design of underground structures*. Proceedings Conference on the Design and Construction of Underground Structures. New Delhi, 43-52 pp.

PALMSTRÖM, A., 2000. Recent developments in rock support estimates by the RMi. *Journal of Rock Mechanics and Tunnelling Technology*, 6(1), 1-19.

PAN, X. D. and REED, M. B., 1991. Coupled distinct element-finite element method for large deformation analysis of rock masses. *International Journal of Rock Mechanics and Mining Sciences & Geomechanical Abstracts*, 28, 93-99.

PANDE, G. N., BEER, G. and WILLIAMS, J. R., 1990. *Numerical methods in rock mechanics*. John Wiley, Chichester, 327 pp.

PAUSKA, J. C., MOORE, I. D. and KRAMER, L. A., 1991. Terrain analysis: integration into the Agricultural Nonpoint Source Pollution (AGNPS) model. *Journal of Soil and Water Conservation*, 46(1), 59-64.

PENCK, W., 1924. Die morphologische analyse: Ein kapitel der phyialischen geologie. *Geographische Abhandlungungen*, 2, 1-283.

PETHICK, J., 1996. Coastal slope development: Temporal and spatial periodicity in the Holderness cliff recession. In: Anderson, M. G. and Brooks, S. M. (Eds.), *Advances in hillslope processes*. John Wiley & Sons, Chichester, 897-917 pp.

PETLEY, D. N., 1994. *The deformation of mudrocks*. Ph.D. Thesis University of London, 310 pp.

PETLEY, D. N., 2004. The evolution of large slope failures: mechanisms of rupture propagation. *Natural Hazards and Earth System Science*, 4.1, 147-152.

PETLEY, D. N., MANTOVANI, F., BULMER, M. H. and ZANNONI, A., 2005. The use of surface monitoring data for the interpretation of landslide movement patterns. *Geomorphology*, 66(1-4), 133-147.

PHILPOTT, K. L., 1984. Comparison of cohesive coasts and beach coasts. *Proceedings Coastal Engineering in Canada*, 227-244 pp.

PILKEY, O. H., YOUNG, R. S., RIGGS, S. R., SMITH, A. W. S., WU, H. and PILKEY, W. D., 1993. The concept of shoreface profile of equilibrium: a critical review. *Journal of Coastal Research*, 9(1), 255-278.

PINTO DA CUNHA, A., 1990. *Scale effects in rock masses*. Proceedings of the first international workshop of scale effects in rock masses, Loen, Norway, June 7-8. A.A. Balkema, Rotterdam.

PITEAU, D. R., STEWART, A. F., MARTIN, D. C. and TRENHOLME, B. S., 1985. A combined limit equilibrium and statistical analysis for design of high rock slopes. In: *Rock masses: modelling of underground openings/probability of slope failure/fracture of intact rock*. Proceedings Symposium Geotechnical Engineering Division, A.S.C.E., Denver, April 29-30, 93-105 pp.

POISEL, R., 1990. The dualism-continuum of jointed rock. In: Rossmanith, H. P. (Ed.), *mechanics of jointed and faulted rock*. A. A. Balkema, Rotterdam, 41-50 pp.

PREVOSTO, M., KROGSTAD, H.E. and ROBIN, A., 2000. Probability distributions for maximum wave and crest heights. *Coastal Engineering*, 40, 329-360.

PRICE, D. G., 1993. A suggested method for the classification of rock mass weathering by a ratings system. *Quarterly Journal of Engineering Geology*, 26, 69-76.

PRIEST, G. R., 1999. Coastal shoreline change study, northern and central Lincoln County, Oregon. *Journal of Coastal Research, Special Issue*, 28, 140-157.

PRIEST, S. D. and HUDSON, J. A., 1981. Estimation of discontinuity spacing and trace length using scan line surveys. *International Journal of Rock Mechanics and Mining Sciences & Geomechanics Abstracts*, 18, 183-197.

PRIOR, D. and RENWICK , W. H., 1980. Landslide morphology and processes on some coastal slopes in Denmark and France. *Zeitschrift für Geomorphologie Supplement Band*, 34, 63-86.

PRITCHARD, M. A. and SAVIGNY, K. W., 1989. Numerical modelling of toppling. *Canadian Geotechnical Journal*, 27, 823-834.

PROUDMAN OCEANOGRAPHIC LABORATORY, 1997. *Natural Environmental Research Council Open Report No. 123,* 1-19 pp.

PURRER, W., 1997. Geotechnical based procedures in tunnelling. *Felsbau*, 15, 222-224.

PYLE, C. J., RICHARDS, K. S. and CHANDLER, J. H., 1997. Digital photogrammetric monitor of river bank erosion. *Photogrammetric Record*, 15(89), 753-764.

QUIGLEY, R. M., GELINAS, P. J., BOU, W. T. and PACKER, R. W., 1977. Cyclic erosion-instability relationships; Lake Erie north shore bluffs. *Canadian Geotechnical Journal*, 14, 310-323.

RAMAMURTHY, T. and ARORA, V. K., 1994. Strength predictions for jointed rocks in confined and unconfined states. *International Journal of Rock Mechanics and Mining Sciences & Geomechanical Abstracts*, 31, 9-22.

RAPP, A., 1960. Recent development of mountain slopes in Kärkevagge and surroundings, Northern Scandinavia. *Geografiska Annaler*, 42, 73-200.

RAWSON, P. F. and WRIGHT, J. K., 2000. *The Yorkshire Coast*. The Yorkshire Coast Geologists' Association Guide No. 34, Geologists' Association, London, 117 pp.

REES, S., 2002. Restoration of natural processes and biodiversity to soft cliffs. *Littoral 2002: The Changing Coast*. EUROCOAST/EUCC, Portugal, 6 pp.

RESEARCH MACHINES PLC., 2003. Average climate conditions, northeast United Kingdom. BBC website: www.bbc.co.uk/weather/world/city_guides, last viewed on 17/10/2005.

RICHARDS, K., ARNOLD, N., LANE, S., CHANDRA, S., EL-HAMES, A. and MATTIKALLI, N., 1995. Numerical landscapes: static, kinematic and dynamic process-form relations. *Zeitchrift für Geomorphologie Supplement Band*, 101, 201-220.

RICHARDS, K. S. and LORRIMAN, N. R., 1987. Basal erosion and mass movement. In: Anderson, M. G. and Richards, K. S. (Eds.), *Slope stability*. John Wiley & Sons, New York, 331-357 pp.

RITTER, D. F., 1986. *Process geomorphology*. Wm. C. Brown, Dubuque, Iowa, 579 pp.

ROBERTSON, A. M., 1970. *The interpretation of geological factors for use in slope theory*. Proceedings Planning Open Pit Mines, Johannesburg, 55-71 pp.

ROBINSON, C., MONTGOMERY, B. and FRASER, C., 1995. The effects of image compression on automated DTM generation. In: Fritsch, D. and Hobbie, D. (Eds.), *Photogrammetric week '95'*. Wichmann Verlag, Heidelberg, 1995.

ROBINSON, L. A. 1974. *Towards a process response model of cliff retreat – the case of North East Yorkshire*. Ph.D. Thesis, University of Leeds, 401 pp.

ROBINSON, L. A., 1977. Marine erosive processes at the cliff foot. *Marine Geology*, 23, 257-271.

ROCKFIELD, 1999. *ELFEN User Manual, Version 2.8*. Rockfield Software Limited, Prince of Wales Dock, Swansea.

ROCKFIELD, 2001. *ELFEN User Manual, Version 3.0*. Rockfield Software Limited, Prince of Wales Dock, Swansea.

ROSIN, P. L., 2001. Unimodal thresholding. *Pattern Recognition*, 34(11), 2083-2096.

ROTT, H., SCHEUCHL, B., SIEGEL, A. and GRASEMANN, B., 1999. Monitoring very slow slope movements by means of SAR interferometry: a case study from a mass waste above a reservoir in The Otztal Alps, Austria. *Geophysical Research Letters*, 26, 1629-1632.

RUNYAN, K. B. and GRIGGS, G. B., 2003. The effects of armoring seacliffs on the natural sand supply to the beaches of California. *Journal of Coastal Research*, 19(2), 336–347.

SAITO, M., 1969. Forecasting time of slope failure by Tertiary creep. *Proceedings of the 7th International Conference on Soil Mechanics and Foundation Engineering*, 2, 677-683.

SALEH, R. A., 1996. Photogrammetry and the quest for digitisation. *Photogrammetric Engineering and Remote Sensing*, 62(6), 675-678.

SALLENGER, A. H. Jr., KRABILL, W., BROCK, J., SWIFT, R., MANIZADE, S. and STOCKDON, H., 2002. Sea-cliff erosion as a function of beach changes and extreme wave runup during the 1997-1998 El Niño. *Marine Geology*, 187, 279-297.

SCAVIA, C., 1990. Fracture mechanics approach to stability analysis of rock slopes. *Engineering Fracture Mechanics*, 35, 899-910.

SCAVIA, C., 1995. A method for the study of crack propagation in rock structures. *Géotechnique*, 45(3), 447-463.

SCAVIA, C., 1996. The effect of scale on fracture toughness: a fractal approach. *Géotechnique*, 46(4), 683-693.

SCHENK, T., 1997. Towards automatic aerial triangulation. *ISPRS Journal of Photogrammetry and Remote Sensing*, 53, 110-121.

SCHENK, T. and TOTH, C., 1991. Reconstructing visible surfaces. *SPIE*, 1526, 78-89.

SCHUMM, S. A. and LICHTY, R.W., 1965. Time, space and causality in geomorphology. *American Journal of Science*, 263, 110-119.

SCHUMM, S. A., 1991. To interpret the earth: ten ways to be wrong. Cambridge University Press, Cambridge, 180 pp.

SELBY, M. J., 1980. A rock-mass strength classification for geomorphic purposes: With tests from Antarctica and New Zealand. *Zeitschrift für Geomorphologie*, 24, 31-51.

SELBY, M. J., 1987. *Hillslope Materials and Processes*. Oxford University Press, Oxford, 451 pp.

SELBY, M. J., AUGUSTINUS, P., MOON, V. G. and STEVENSON, R. J., 1988. Slopes on strong rock masses: modelling and influences of stress distributions and geomechanical properties. In: Anderson, M. G. (Ed.), *Modelling Geomorphological Systems*. John Wiley & Sons, 341-374 pp.

SEN, Z. and KAZAI, A., 1984. Discontinuity spacing and RQD on estimates from finite length scanlines. *International Journal of Rock Mechanics and Mining Sciences & Geomechanical Abstracts*, 21, 203-212.

SENSENY, P. E. and SIMONS, D. A., 1994. Comparison of calculational approaches for structural deformation in jointed rock. International Journal for Numerical and Analystical Methods in Geomechanics, 18, 327-344.

SERAFIM, J. L. and PEREIRA, J. P., 1983. *Considerations of the geomechanics classification of Bieniawski*. International Symposium on Engineering Geology for Underground Construction, LNEC, Lisbon, Volume 1, India, 486-492 pp.

SHALOWITZ, A. L., 1964. *Shore and Sea Boundaries (Vol. 2)*. U.S. Coast and Geodetic Survey, U.S. Department of Commerce, 420 pp.

SHARMA, S., RAGHUVANSHI, T. K. and ANBALAGAN, R., 1995. Plane failure analysis of rock slopes. *Geotechnical and Geological Engineering*, 13, 105-111.

SHENNAN, I., 1989. Holocene crustal movements and sea level changes in Great Britain. *Journal of Quaternary Science*, 4, 77-89.

SHENNAN, I. and HORTON, B. P., 2002. Holocene land- and sea-level changes in Great Britain. *Journal of Quaternary Science*, 17(5-6), 511-526.

SHEPARD, F. P. and GRANT. U. S., 1947. Wave erosion along the southern California coast. *Geological Society of America Bulletin*, 58, 919-926.

SHI, G. -H., 1993. *Block System Modeling by Discontinuous Deformation Analysis*. Computational Mechanics Publications, London, England, 209 pp.

SHI, G. -H. and GOODMAN, R. E., 1984. *Discontinuous Deformation Analysis*. *Proceedings of the 25th U.S. Symposium on Rock Mechanics*, 269-277.

SIJING, W., 1981. On the mechanism and process of slope deformation in an open pit mine. *Rock Mechanics*, 13, 145-156.

SINGH, B. and GOEL, R. K., 1999. *Rock Mass Classification: A Practical Approach in Civil Engineering*. Elsevier, Oxford, 267 pp.

SITAR, N. and CLOUGH, G. W., 1983. Seismic response of steep slopes in cemented soils. *Journal of Geotechnical Engineering*, 109(2), 210-227.

SITAR, N. and MACLAUGHLIN, M. M., 1997. *Kinematics and discontinuous deformation analysis of landslide movement*. Keynote Lecture, 2nd Panamerican Symposium on Landslides, Rio de Janeiro, Nov. 10-14th, 1997, 1-9 pp.

SJÖBERG, J., 1996. *Large scale slope stability in open pit mining - a review*. Division of Rock Mechanics - Technical Report 1996: 10T, Luleå University of Technology, Luleå.

SLAMA, C. C. (Ed.), 1980. *Manual of photogrammetry. American Society of Photogrammetry (4th ed)*. Falls Church, Virginia, 1056 pp.

SMALL, C., GORNITZ, V. and COHEN, J. E., 2000. Coastal hazards and the distribution of human population. *Environmental Geoscience*, 7, 3-12.

SMITH, M. J. and SMITH, D. G., 1996. Operational experiences of digital photogrammetric systems. *International Archives of Photogrammetry and Remote Sensing*, 31(B2), 357-362.

SMITH, M. J., SMITH, D. G. and WALDRAM, D. A., 1996. Experiences with analytical and digital seteroplotters. *Photogrammetric Record*, 15(88), 519-526.

ST. JOHN, C. M., 1971. *Three dimensional analysis of jointed rock slopes*. Proceedings of the International Symposium of Rock Fracture, Nancy, France, Paper II-9.

STAFFORD, D. B., 1971. *An aerial photographic technique for beach erosion surveys in North Carolina*. Technical Memorandum No. 36, U.S. Army Engineer Waterways Experiment Station, Vicksburg, MS, 122 pp.

STARFIELD, A. M. and CUNDALL, P. A., 1988. Towards a methodology for rock mechanics modelling. *International Journal of Rock Mechanics and Mining Sciences & Geomechanics Abstracts*, 25(3), 99-106.

STANIFORTH, A., 1993. Geology of the North York Moors. North York Moors National Park, 40 pp.

STARK, C. P. and HOVIUS, N., 2001. The characterization of landslide size distributions. *Geophysical Research Letters*, 28, 1091-1094.

STEAD, D. and EBERHARDT, E., 1997. Developments in the analysis of footwall slopes in surface coal mining. *Engineering Geology*, 46(1), 41-61.

STEAD, D., COGGAN, J. S. and EBERHARDT, E., 2004. Realistic simulation of rock slope failure mechanisms: the need to incorporate principles of fracture mechanics. *International Journal of Rock Mechanics and Mining Sciences*, 41(3), 1-6.

STEAD, D., EBERHARDT, E., COGGAN, J. and BENKO, B., 2001. *Landslides - Causes, Impacts and Countermeasures*. UEF Proceedings, 17-21 June 2001, Davos, Switzerland, 615-624 pp.

STEPHENSON, W. J. and BRANDER, R. W., 2003. Coastal geomorphology into the twenty-first century. *Progress in Physical Geography*, 27(4), 607-623.

STEPHENSON, W. J. and BRANDER, R. W., 2004. Coastal geomorphology. *Progress in Physical Geography*, 28(4), 569-580.

STONE, J. L. and CLOWES, M., 2004. Photogrammetric recording of the Roman earthworks "Cawthorn Camps", North Yorkshire. *Photogrammetric Record*, 19(106), 94-110.

STORLAZZI, C. D. and GRIGGS, G. B., 1998. The 1997-98 El Nino and erosion processes along the central coast of California. *Shore and Beach*, 66(3), 12-17.

SUMNER, P. and NEL, W., 2002. The effect of rock moisture on Schmidt hammer rebound: tests on rock samples from Marion Island and South Africa. *Earth Surface Processes and Landforms*, 27, 1137-1142.

SUNAMURA, T., 1976. Feedback relationship in wave erosion of laboratory rock coast. *Journal of Geology*, 84, 427-437.

SUNAMURA, T., 1977. A relationship between wave-induced cliff erosion and erosive force of waves. *Journal of Geology*, 85, 613-618.

SUNAMURA, T., 1980. *A laboratory study of offshore transport of sediment and a model for eroding beaches*. Proceedings, 17th International Conference of Coastal Engineering, ASCE, 920-938 pp.

SUNAMURA, T., 1988. Projection of future coastal cliff recession under sea-level rise induced by the greenhouse effect: Nii-jima Island, Japan. *Transactions of the Japanese Geomorphological union*, 9(1), 17-33.

SUNAMURA, T., 1992. *Geomorphology of rocky coasts*. John Wiley & Sons, Chichester, 302 pp.

SYNDER, J. P., 1987. *Map projections – A working manual*. U.S. Geological Society Professional Paper 1395, Washington, DC, 383 pp.

TEIXEIRA, J. A., ABREU, M. P. and GUEDES SOARES, C., 1995. Uncertainty of ocean wave hindcasts due to wind modelling. *Journal of Offshore Mechanics and Arctic Engineering*, 117, 294-297

TERLEIN, M. T. J., ASCH, T. W. J. and WESTERN C. J., 1995. Deterministic modelling in GIS-based landslide hazard assessment. In: Carrar, A. and Guzzetti, F. (Eds.), *Geographical information systems in assessing natural hazards*. Kluwer, London, 57-77 pp.

TERZAGHI, K., 1946. *Rock defects and loads on tunnel supports*. Publications from the Graduate School of Engineering, Harvard University, 418, Soils and Mechanics Series, 25, 1-95 pp.

TERZAGHI, K., 1950. *Mechanisms of landslides*. Geological Society of America, Berkely Volume: 83-123.

TERZAGHI, K., 1962. Stability of steep slopes on hard unweathered rock. *Géotechnique*, 12, 251-270.

THARP, T. M., 1984. *Stability of slopes in discontinuity jointed rock*. Proceedings 25th US Symposium on Rock Mechanics, 891-898 pp.

THORNES, J. B., 1978. The character and problems of contemporary theory in geomorphology. In: Embleton, C., Brunsden, D. and Jones, D. K. C. (Eds.), *Geomorphology, present problems and future prospects*. Oxford University Press, London, 14-24 pp.

THORNTON, E. B., MCGEE, T., TUCKER, S. P. and BURYCH, D. M., 1987. *Predicting erosion on the recessive Monterey Bay shoreline*. Proceedings of the Coastal Sediments Conference, New Orleans, 1809-1824 pp.

TRENHAILE, A. S., 1987. *The geomorphology of rock coasts*. Oxford University Press, Oxford, 384 pp.

TRENHAILE, A. S., 2002. Rock coasts, with particular emphasis on shore platforms. *Geomorphology*, 48, 7-22.

TUCKER, G. E. and SLINGERLAND, R. L., 1994. Erosional dynamics, flexural isostasy, and long-lived escarpments: A numerical modeling study. *Journal of Geophysical Research*, 99, 12229-12243.

TURNER, R. J., 1981. *Ground water conditions in Encintas, California as they relate to sea cliff stability*. Master of Science Thesis, Fullerton, California State University, 81 pp.

U.S. ARMY CORP OF ENGINEERS, 1985. *Shoreline movement data report, Portugese Point to Mexican Border (1852-1982)*. Coastal Engineering Research Centre, Vicksburg, Mississippi, 1-49 pp.

VALLEJO, L. E. and DEGROOT, R., 1988. Bluff response to wave action. *Engineering Geology*, 26, 1-16.

VAN RIJN, L. C., 1998. *Principles of coastal geomorphology*. Aqua Publications, Amsterdam, 730 pp.

VARNES, D. J., 1978. Slope movements and types and processes. In: Schuster, R. L. and Krizek, R. J. (Eds.), *Landslides: analysis and control*. National Academy of Sciences, Transportation Research Board Special Report, Washington D.C., 12-33 pp.

VAUGHAN, T. W., 1932. Rate of sea-cliff recession on the property of the Scripps Institution of Oceanography, La Jolla, California. *Science*, 75, 250.

VIETMEIER, J., WAGNER, W. and DIKAU, R., 1999. *Monitoring moderate slope movements (landslides) in the southern French Alps using differential SAR interferometry*. Proceedings 2nd International Workshop on ERS SAR Interferometry "FRINGE'99". Liege, Belgium.

WALDER, J. S. and HALLET, B., 1985. A theoretical model of the fracture of rock during freezing. *Geological Society of America Bulletin*, 96, 336-346.

WALDER, J. S. and HALLET, B., 1986. The physical basis of frost weathering, toward a more fundamental and unified perspective. *Arctic and Alpine Research*, 18(1), 27-32.

WANG, Y., 1996. Structural matching and its applications for photogrammetric automation. *International Archives of Photogrammetry and Remote Sensing*, 31(B3), 918-923.

WANG, Y., 1998. Principles and applications of structural image matching. *ISPRS Journal of Photogrammetry and Remote Sensing*, 53(3), 154-165.

WANG, Y., YANG, X., STOJIC, M. and Skelton, B., 2002. *A new digital photogrammetric system for GIS professionals*. IAPRS, Volume XXIV, Part 2, Commission II, Xi'an, 2002.

WARBURTON, P. M., 1981. Vector stability analysis of an arbitrary polyhedral block with any number of free faces. *International Journal of Rock Mechanics and Mining Sciences & Geomechanical Abstracts*, 18, 415-427.

WEST, T. R., 1996. The effects of positive pore pressure on sliding and toppling of rock blocks with some considerations of intact rock effects. *Environmental and Engineering Geosciences*, 2(3), 339-353.

WHALLEY, W. B., 1984. Rockfalls. In: Brunsden, D. and Prior, D. B. (Eds.), *Slope Instability*. Landscape Systems. John Wiley & Sons, Chichester, 217-256 pp.

WICKENS, E. and BARTON, N. R., 1971. The application of photogrammetry to the stability of excavated rock slopes. *Photogrammetric Record*, 7(37), 46-54.

WILCOX, P. R., MILLER, D. S., SHEA, R. H. and KERKIN, R. T., 1998. Frequency of effective wave activity and the recession of coastal bluffs; Calvert Cliffs, Maryland. *Journal of Coastal Research*, 14(1), 256-268.

WILLIAMS, A. T. and DAVIES, P., 1987. *Rates and mechanics of coastal cliff erosion in Lower Lias rocks*. Proceedings Coastal Sediments 87, 1855-1870 pp.

WILLIAMS, A. T., DAVIES, P. and BOMBOE, P., 1993. Geometrical simulation of coastal cliff failures in Liassic strata, South Wales, U.K. *Earth Surface Processes and Landforms*, 18, 703-720.

WILLIAMS, D. J., STOLBERG, D. J., SOOLE, P. and POROPAT, G., 2002. *Monitoring erosion off unvegetated mine tailings facilities and natural slopes using high-resolution, digital stereo-photogrammetry*. 4th International conference on environmental geotechnics, Brazil 2002.

WOLF, P. R. and DEWITT, B. A., 2000. *Elements of photogrammetry with applications in GIS*, (3rd Edition). McGraw-Hill Incorporated, New York.

WOLF, P. R., 1983. *Elements of photogrammetry*. McGraw-Hill, New York, 628 pp.

WOLFRAM, S., 1984. Cellular automata as models of complexity. *Nature*, 311(4), 281-312.

WOOD, W. L., STOCKBERGER, M. T. and MADALON, L. J., 1994. Modeling beach and nearshore profile response to lake-level change. *Joumal of Great Lakes Research*, 20(1), 206-214.

WOODWORTH, P. L., TSIMPLIS, M. N., FLATHER, R. A. and SHENNAN, I., 1999. A review of trends observed in British Isles mean sea level data measure by tide gauges. *Geophysical Journal International*, 136, 651-670.

WYLLIE, D. C. and WOOD, D. F., 1983. Stabilisation of toppling rock slope failures. In: Haynes, L. (Ed.), *Engineering Geology and Environmental Constraints*. Colorado Geological Survey, Colorado, 103-115.

WYLLIE, D. C., 1980. Toppling Rock Slope Failures: Examples of Analysis and Stabilization. *Rock Mechanics*, 13, 89-98.

ZANBAK, C., 1983. Design charts for rock slopes susceptible to toppling. *Joumal of Geotechnical Engineering*, 109(8), 1039-1062.

ZHANG, B. and MILLER, S., 1997. Adaptive automatic terrain extraction. Integrating photogrammetric techniques with scene analysis and machine vision III. *SPIE*, 3072, 27-36.

ZHANG, W. and MONTGOMERY, D. R., 1994. Digital elevation model grid size, landscape representation and hydrologic simulations. *Water Resources Research*, 30(4), 1019-1028.

ZENKOVICH, V. P., 1967. *Processes of coastal development*. Oliver and Boyd, London, 738 pp.

ZIENKIEWICZ, O. C., 1977. The Finite Element Method in Engineering Sciences, (3rd edition). McGraw-Hill, London, 787 pp.

ZVIELY, D. and KLEIN, M., 2004. Coastal cliff retreat rates at Beit-Yannay, Israel, in the 20th century. *Earth Surface Processes and Landforms*, 29, 175-184.